DISCLAIMER NOTICE

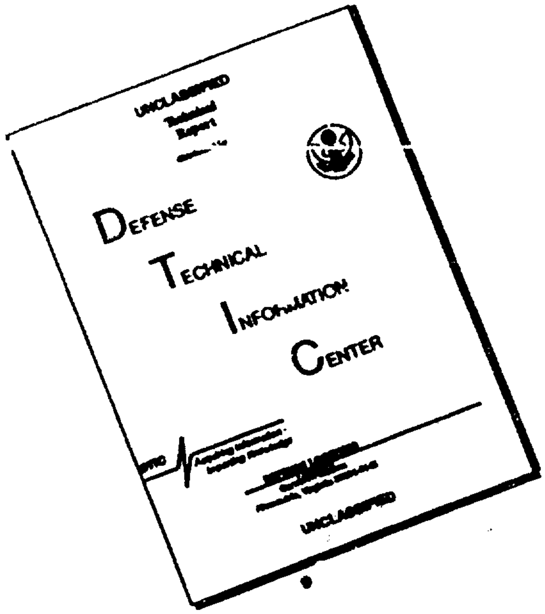

THIS DOCUMENT IS BEST QUALITY AVAILABLE. THE COPY FURNISHED TO DTIC CONTAINED A SIGNIFICANT NUMBER OF PAGES WHICH DO NOT REPRODUCE LEGIBLY.

IASA Contractor Report 187081

ADVANCED EXPANDER TEST BED PROGRAM

PRELIMINARY DESIGN REVIEW REPORT

Pratt & Whitney
Government Engines & Space Propulsion
P.O. Box 109600
West Palm Beach, Florida 33410-9600

May 1991

Prepared for:
Lewis Research Center
Under Contract NAS3-25960

National Aeronautics and
Space Administration

CONTENTS

FOREWORD

This technical report summarizes the results of the Advanced Expander Test Bed preliminary design as presented at the Preliminary Design Review held at the NASA-Lewis Research Center (NASA-LeRC) on 29–31 January 1991. The work was conducted by the Pratt & Whitney (P&W) Government Engines & Space Propulsion division of the United Technologies Corporation for NASA-LeRC under Contract NAS3–25960. Effort under this contract started on 27 April 1990.

Mr. Wiliam K. Tabata is the NASA program manager, and Mr. James R. Brown is the P&W program manager.

SECTION I
INTRODUCTION

NASA mission studies have identified the need for one or more new space engines. The new propulsion systems are to be oxygen/hydrogen expander cycle engines of 7,500 to 50,000 pounds thrust or more; and must achieve high performance through efficient combustion, high combustion pressure, and high area ratio exhaust nozzle expansion. The engines will feature a wide degree of versatility in terms of throttleability, operation over a wide range of mixture ratios, autogenous pressurization, in-flight engine cooldown and propellant settling. Other engine requirements include: long life, man-rating, reusability, space-basing, and fault tolerant operation.

The Space Chemical Engine Technology (SCET) Program is charged with developing the technology base for the design and development of these new space engines. The Advanced Expander Test Bed (AETB) will support this objective by providing a vehicle for the following:

- Validation of the high-pressure expander cycle concept
- Investigation of the system interactions, transients, dynamics, control functions, and health monitoring techniques
- Verification of design and analysis codes to assure scalability and minimize the risk associated with space engine development
- Investigation of throttling and high mixture ratio operation
- Testing of advanced, mission-focused components made available from other SCET contracts
- Evolution into NASA's Focused Test Bed Engine.

To satisfactorily perform these functions the AETB must challenge technology limits while providing a high degree of flexibility and rugged, reliable, low-maintenance operation. The AETB engine requirements are summarized in Table 1. A nominal operating thrust of 20,000 pounds has been selected.

Table 1. AETB Requirements

Propellants	Oxygen/Hydrogen
Cycle	Expander
Thrust	>7500 lb (20,000 lb Selected)
Pressure	Nominal 1200 psia
Mixture Ratio	6.0 ± 1.0 (Optional Operation at 12.0)
Throttling	20% Minimum (5% Desirable)
Propellant Inlet Conditions:	
Hydrogen	38 R, 70 psia
Oxygen	163 R, 70 psia
Idle Modes	Tankhead (Nonrotating Pumps) Pumped (Low-NPSH Pumping)
Life	100 Starts 2 Hours (5 Hours Desirable)

The AETB is being designed using the latest component technologies and design and analysis methods. Although similar to the SCE concepts, the AETB will differ in the following important areas:

- Current technology will be used, whereas the SCE could use technology developed over the next few years.

- The AETB will be designed for sea level testing; therefore, will not require a high area ratio nozzle.

- Relatively high-pressure pump inlet conditions are supplied to simulate boost pump discharge pressures.

- Component designs will be flight-type, but not flight-weight.

- Components will be arranged to simulate expected flight engine line volumes, pressure drops, and other factors affecting engine response; however, accessibility and interchangeability will be emphasized, rather than working to specific envelope limitations.

- Extensive instrumentation will be provided for control and validation of engine operation. Limited health monitoring diagnostic instrumentation will be available, however, provisions will be made for special instrumentation and evaluation of advanced diagnostic techniques.

The AETB design is based on current technology; however, there are some areas where the stringent requirements of the AETB (such as adequate chamber pressure to realistically evaluate advanced system interactions) introduce some uncertainty into applications of this technology. The results of ongoing Pratt & Whitney (P&W) test programs will provide component and subcomponent verification prior to engine fabrication to minimize this risk. These Independent Research & Development (IR&D) programs are aimed at extending the high-pressure engine technology base to include space engine requirements. The subcomponent tests consist of:

- Full-scale combustion tests with prototype hardware to measure total thrust chamber heat flux, heat flux profile and combustion efficiency

- High-speed cryogenic bearing tests to confirm bearing life

- Oxygen turbopump interpropellant seal tests and hydrogen turbopump brush seal tests to confirm seal durability and leakage

- Turbine airflow testing to confirm turbine aerodynamics and predicted leakage losses.

The preliminary design of the AETB began on 27April 1990 and was completed in January 1991. The preliminary design review was held 29-31 January 1991 at the NASA Lewis Research Center (LeRC). This report is a summary of the preliminary design and of the information presented at the review.

SECTION II
SUMMARY

A. Design Approach

The Advanced Expander Test Bed (AETB) operates on oxygen/hydrogen propellants and has a nominal operating point of 20,000 pounds thrust, 1200 psia chamber pressure and a mixture ratio of 6.0. The AETB design approach is focused on achieving high chamber pressure with adequate cycle and component design margins and on providing a high degree of flexibility. The flexibility will consist of: (1) the ability to operate over a wide range of conditions, (2) the ability to easily interchange components, and (3) a versatile control system that can accommodate changes in operating conditions, incorporate additional engine diagnostics and accommodate new components.

Five unique features of the design contribute to achieving the desired flexibility: (1) the split expander cycle, (2) a 25 percent cycle and component uprated design margin, (3) dual-orifice injection to facilitate throttling and high mixture ratio operation, (4) a dual-shaft fuel pump for rotordynamic stability, and (5) use of a proven advanced electronic brassboard controller design approach.

In the split expander cycle shown in Figure 1, a portion of the first-stage fuel pump discharge flow is routed directly to the injector. The remainder of the fuel passes through the second and third stages of the pump and is used to cool the thrust chamber assembly and drive the turbopumps. The two fuel streams are mixed prior to injection. The split expander cycle reduces the energy needed to drive the fuel turbopump and allows a higher combustion chamber pressure to be achieved. A major advantage of the split expander cycle is that controlling the flow split between the thrust chamber cooling flow and the bypass flow benefits engine throttling and high mixture ratio operation. At these conditions the fraction of fuel passing through the thrust chamber cooling jacket can be increased, resulting in lower turbine inlet temperatures and lower thrust chamber wall temperatures. The AETB split expander cycle has the further advantage that it can be operated as a full expander cycle.

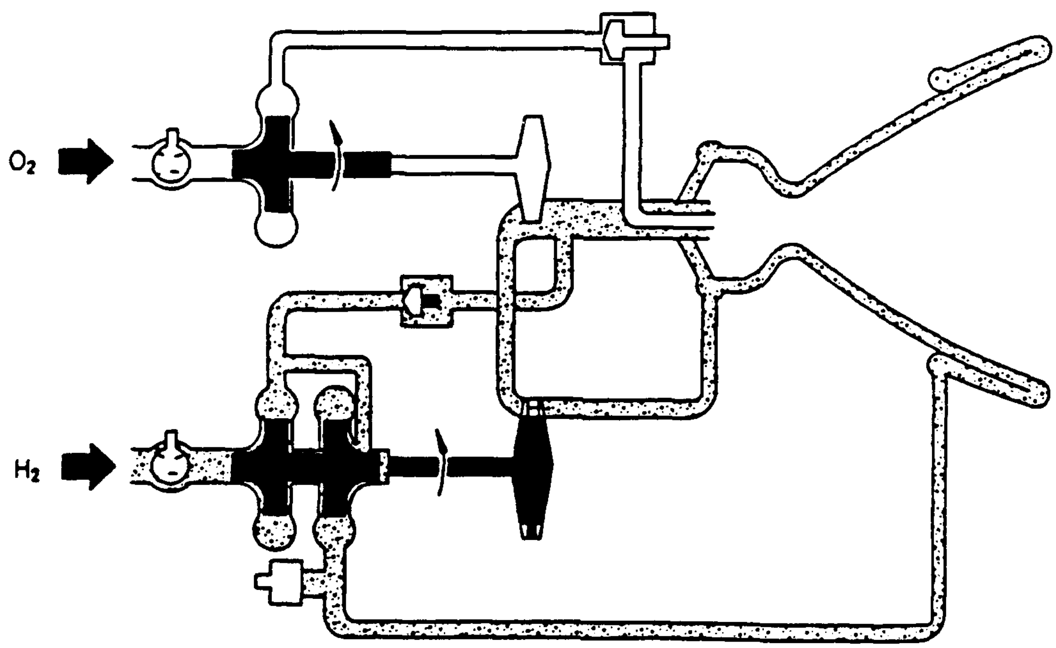

Figure 1. Split Expander Cycle

B. Operating Cycles

The AETB is being designed for 1500 psia chamber pressure and 25,000 pounds vacuum thrust, 25 percent above the normal operating level. This approach builds in component design margin, and adds flexibility for operating at off-design conditions when testing non-Test Bed, focused technology components. In addition, high mixture ratio operation can be demonstrated and the AETB can be run as a full expander cycle. Table 2 lists some of the cycle key parameters at the design thrust level, the normal operating point, a five-percent throttled level, a full expander operating point, and the high mixture ratio operating point. The engine can also be run in a pumped idle mode.

Table 2. AETB Cycle Conditions

	Normal Operating Point	Uprated Design Point	5% Thrust	Full Expander Cycle	High Mixture Ratio
Thrust, lbf (Vacuum Equivalent)	20,000	25,000	1,000	16,400	17,000
Chamber Pressure, psia	1,200	1,500	65	980	1,000
Mixture Ratio	6.0	6.0	3.5	6.0	12.0
Nozzle/Chamber Coolant Exit Temperature, °R	957	1,020	750	1,000	805
Fuel Pump Speed, RPM	87,700	99,200	18,900	90,000	79,000
Fuel Pump First-Stage Discharge Pressure, psia	1,640	1,920	103	1,840	1,490
Fuel Pump Third-Stage Discharge Pressure, psia	3,500	4,500	251	3,300	2,670
Fuel Turbopump Horsepower	1,670	2,520	22	1,690	966
Oxidizer Pump Speed	42,500	48,900	8,240	38,300	40,100
Oxidizer Pump Discharge Pressure, psia	1,900	2,360	154	1,630	1,500
Oxidizer Turopump Horsepower	348	530	4	296	362

C. Oxygen Turbopump

The oxygen pump is a single-stage centrifugal pump powered by a single-stage, full-admission turbine. The pump discharge pressure is 1900 psia and pump speed is 42,500 rpm at the normal operating point. Primary subcomponents include a three-blade inducer designed for pump stability, a high-efficiency, single-stage pump with a shrouded impeller, an interpropellant seal package to separate the liquid oxygen and gaseous hydrogen turbine drive fluid, a single-stage, full-admission turbine, two 35-mm ball bearings and a 27-mm roller bearing. Attention is given to leakage control through careful seal placement, configuration selection and design. A cross section of the turbopump showing the basic features is shown in Figure 2.

The oxygen turbopump hydrodynamic design emphasizes attainment of stable operation over a wide flow range and achievement of cycle performance objectives. Moderate suction specific speed requirements have been selected to avoid pump induced instabilities. The inlet-to-discharge diameter ratio of the impeller, a critical factor with regard to instabilities, has also been limited within successfully demonstrated levels for the suction specific speed selected. The impeller is shrouded and has a low discharge blade angle.

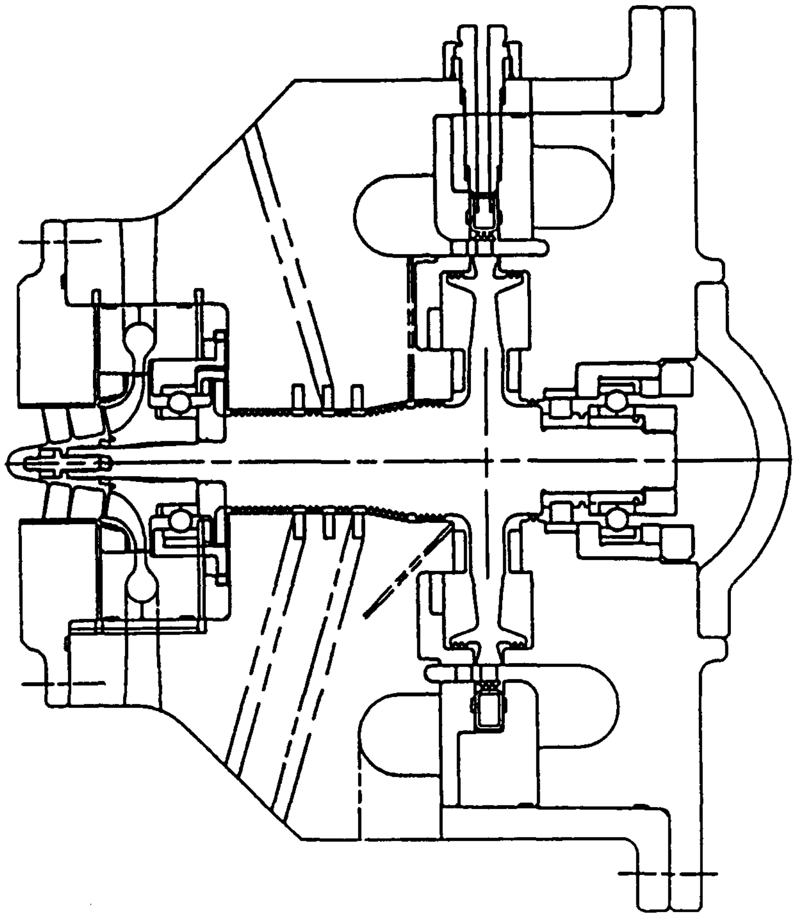

Figure 2. Oxygen Turbopump

The turbopump interpropellant seal package is based on use of knife-edge seals and gaseous helium to purge the seal cavities. The helium purge is required only for ground testing. The seals ensure separation of the oxygen used as bearing coolant from hydrogen leakage through the thrust piston, and restricts propellant overboard leakage. Knife-edge seals work best when they are sealing a fluid in the gaseous state. A radially slotted rotating slinger/vaporizer is located between the pump ball bearing and helium dam to vaporize any liquid oxygen leakage.

The oxygen turbopump turbine is a conventional single-stage, full-admission, turbine. The turbine is predicted to attain a stage efficiency of 82 percent.

D. Hydrogen Turbopump

The main hydrogen pump is a dual-shaft, three-stage centrifugal pump with the first stage and inducer driven by a single-stage, full-admission turbine and the second and third stages driven by a second one-stage turbine as shown in Figure 3. At the operating point, the fuel pump runs at 87,700 rpm to provide a discharge pressure of 3,500 psia.

Approximately 50 percent of the hydrogen exits the pump after the first stage and flows through a control valve, bypassing the coolant jacket, and flowing into a mixer downstream of the turbines. The remaining hydrogen proceeds through the final two stages of the high-pressure pump and is used to cool the thrust chamber assembly.

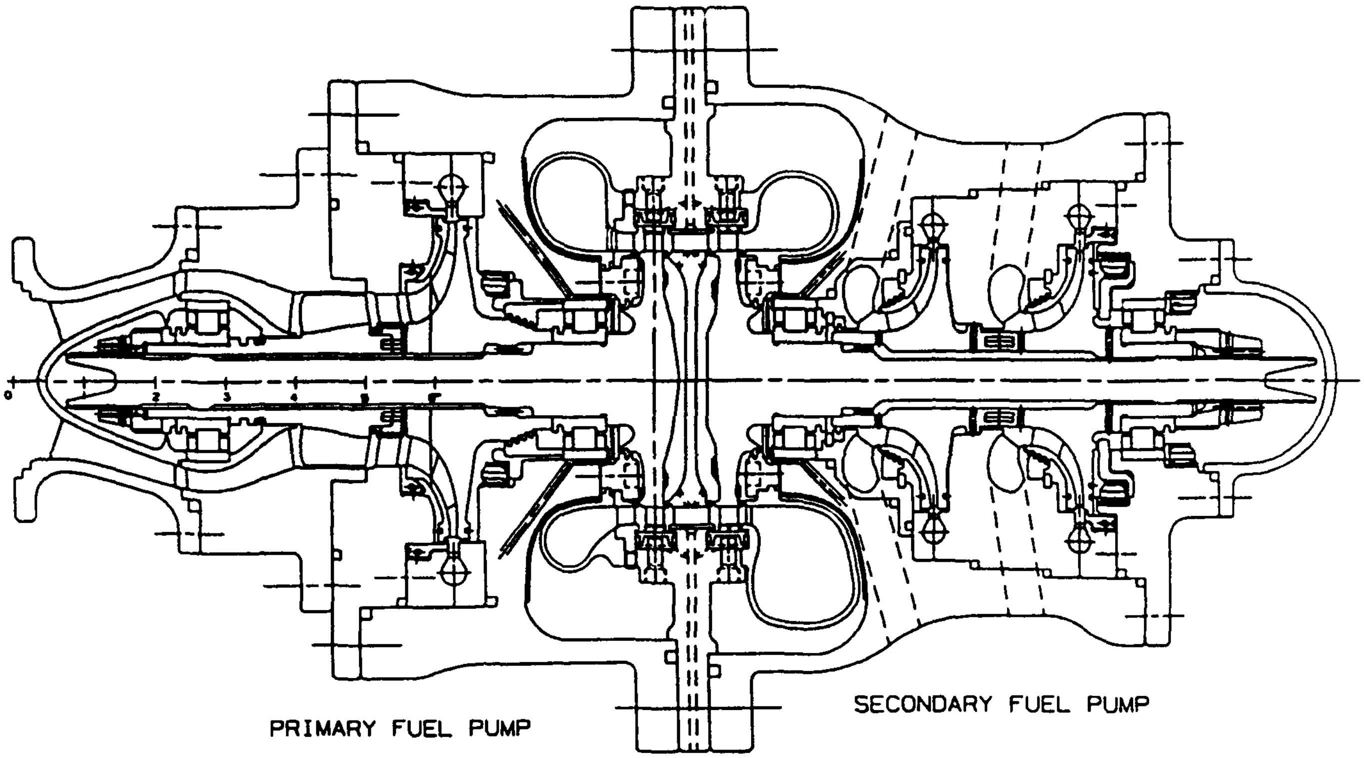

Figure 3. Dual-Shaft Hydrogen Turbopump

Particular emphasis is placed on achieving stable pump operation over a wide range of throttle ratios and mixture ratios, as well as meeting cycle performance requirements. The pump inlet configuration shown was selected primarily to provide adequate bearing support to meet rotordynamic requirements. The inlet struts also serve to minimize induced pre-swirl during throttling conditions to improve pump stability.

All three stages of the fuel turbopump employ shrouded impellers and low discharge blade angles to maximize efficiency and provide steep head-flow characteristics for improved off-design stability. The second and third-stage impellers are configured in an in-line arrangement to minimize leakage between stages.

The dual-shaft fuel pump is driven by two single-stage, counter-rotating turbines. Stage efficiencies are 82 percent for the primary turbine and 84 percent for the secondary turbine. The fluid velocity leaving the first-segment turbine exits in the same direction as the counter-rotating second-segment turbine, thereby significantly improving the efficiency of the second stage by eliminating the second-vane gas turning losses found in typical co-rotating, multi-stage turbines. Both stages are high efficiency, high reaction stages. The back-to-back, single-stage turbines eliminate the large overhung mass of a multi-stage turbine, a major driver in achieving subcritical rotordynamics.

The primary fuel turbopump rotor is supported by two 27-mm roller bearings. A second set of roller bearings supports the rotor of the secondary fuel turbopump. Roller bearings provide the high radial stiffness, 3.0+ million lb/in., necessary to achieve adequate critical speed margin. The fuel turbopump roller bearings operate at a DN of 2.37 million at the nominal operating speed of 87,700 rpm and at a DN value of 2.7 million at the design operating speed of 100,000 rpm.

Nozzle-Thrust Chamber Assembly

The nozzle-thrust chamber assembly consists of: (1) a dual-orifice injector for high combustion efficiency l wide range throttling, (2) a conventional torch igniter, (3) a milled channel copper thrust chamber capable achieving adequate cooling with 50 percent fuel flow, and (4) an extended length tubular 7.5:1 area ratio level nozzle extension capable of providing total heat transfer rates equal to a high altitude nozzle, Figure The operational flexibility comes from use of the dual-orifice injection concept to provide good atomization l flow stability over the range of combustion pressure and mixture ratio desired, and a thrust chamber coolant wpath geometry that provides adequate cooling with 50 percent fuel flow at the 1500 psia design point. The percent fuel cooling capability is an outgrowth of the split expander cycle requirements, but has the added iefit of allowing substantial overcooling when desired.

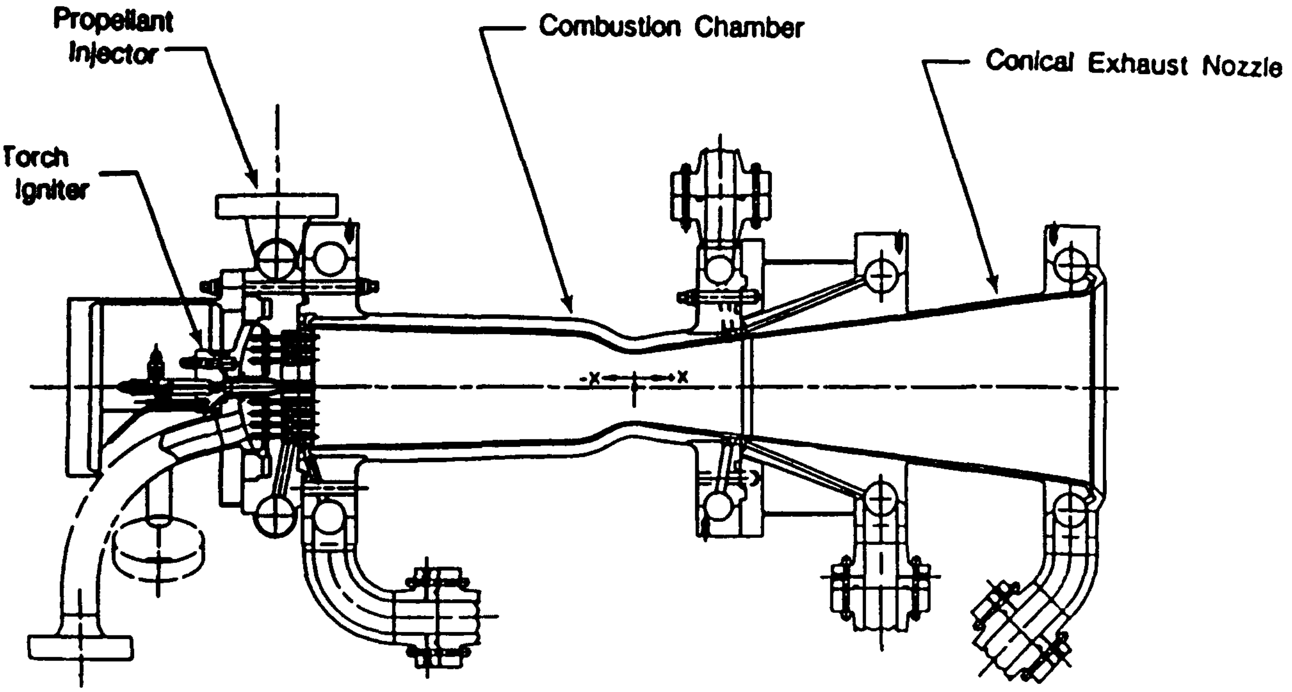

ure 4. Thrust Chamber Assembly

The combustion chamber has a contraction ratio of 3:1 (chamber area-to- throat area) and a combustion mber length of 15 inches to provide an optimum trade-off between heat pickup to drive the cycle, coolant ssure drop, and combustion efficiency. A thrust chamber length of 12.0 inches is predicted to be sufficient to iieve over 99 percent combustion efficiency; however, the 15.0-inch length was selected to provide additional lrogen heating for cycle power.

The chamber cooling configuration consists of 120-milled passages sized to maintain a maximum wall iperature of 1460 R without exceeding the cycle allow- able coolant pressure drop. At the normal operating nt the maximum wall temperature is 1390 R. Closing the jacket bypass valve as the engine is throttled uces thrust chamber wall temperature at low thrust. Closing the jacket bypass valve also produces low wall iperatures with high mixture ratio operation. At an oxidizer-to-fuel ratio of 12:1 and 1000 psia chamber ssure, the predicted wall temperature is 1160 R, low enough to prevent oxidation of the copper walls.

A conical tubular exhaust nozzle is used to duplicate the cycle thermodynamics of a flight engine with a high area ratio cooled exhaust nozzle. Typical flight engine configurations studied in the past have 1000:1 area ratio exhaust nozzles regeneratively cooled to an area ratio of approximately 200:1. The conical tubular nozzle is 16.25 inches long and provides expansion from the thrust chamber exit area ratio of 2:1 to an area ratio of 7.5:1. The nozzle design is single pass, parallel flow tubular construction. The nozzle divergence angle is 7.5 degrees off the centerline.

F. Control System

The AETB control schematic is shown in Figure 5. The primary control points are: (1) the fuel jacket bypass valves (FJBV) for thrust and chamber coolant flow control, (2) the secondary oxidizer control valve (SOCV) for mixture ratio control and control of injector primary pressure drop, and (3) the main turbine bypass valve (MTBV) for additional thrust control.

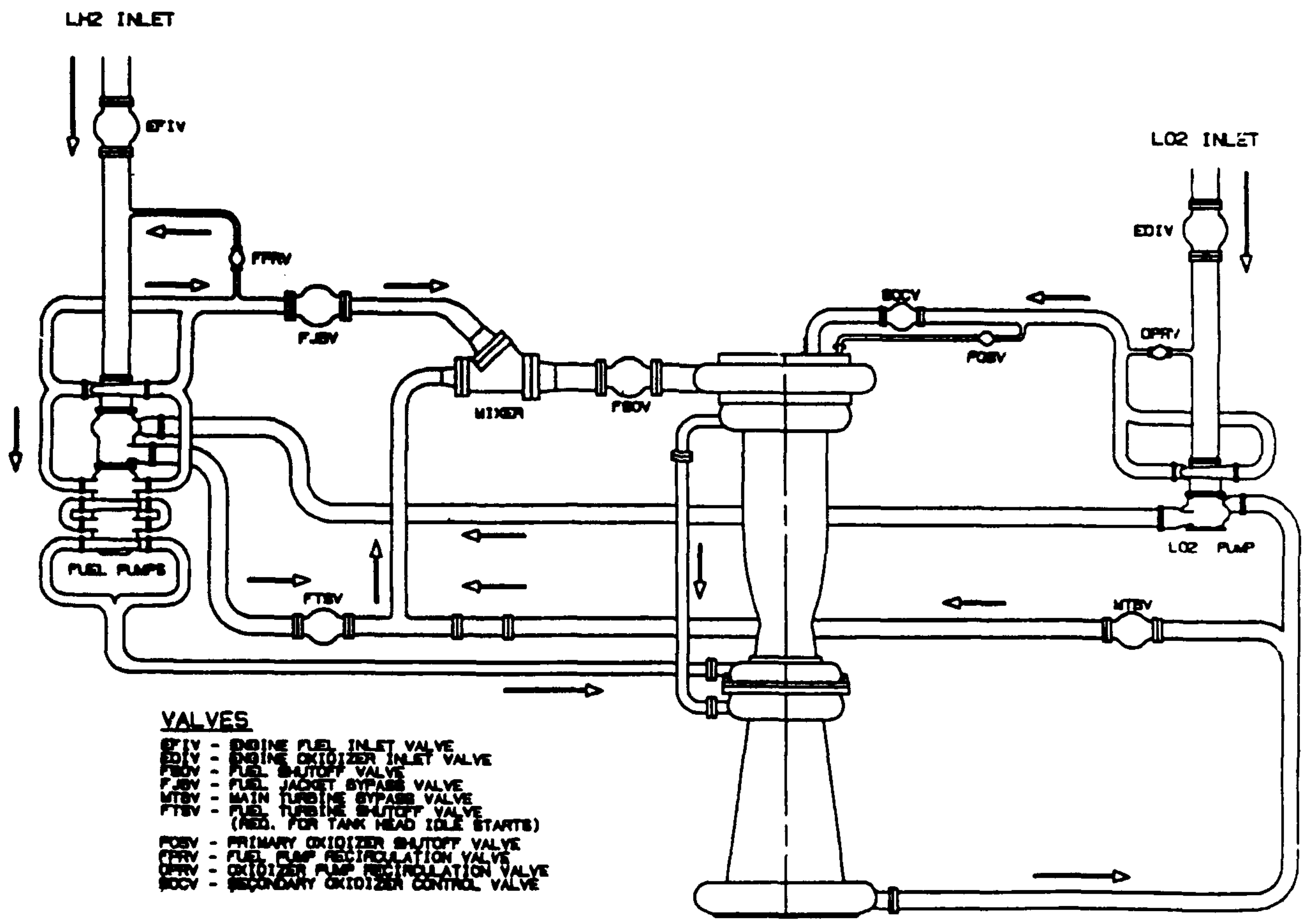

Figure 5. AETB Simplified Flow Schematic

The selection of the baseline control system for a throttleable split expander cycle with dual-orifice injection is relatively straightforward. The jacket bypass valve is required to control the coolant jacket flow for throttled and high mixture ratio operation. The oxidizer secondary control valve is required to control the oxidizer flow split during throttling. These two valves alone provide adequate control for mixture ratio variation between 5.0

and 7.0 and thrust control between 125 and 75 percent power. For thrust control below 75 percent, an additional means of relieving turbine flow is required.

The control system is designed to allow control points and control function to be readily changed throughout the test program. Optional control features consist of: a second turbine bypass valve, a line between the two turbines to the turbine bypass line, spool pieces that allow either one or two turbine bypass valves to be placed in any of four locations, and fuel and oxidizer recirculation valves that can be used if necessary in throttling tests. These optional features provide enhanced flexibility to investigate various control modes.

Other control options may be desirable for off-design operation. Control of the power split between the fuel and oxidizer turbines appears to be necessary for high oxidizer-to-fuel operation ratios, i.e., 12.0. This control is provided by using a second turbine bypass valve or by moving the turbine bypass valve so that it reduces the fuel turbine-to-oxygen turbine power ratio.

Full expander cycle operation up to 750 psia can be achieved simply by closing the jacket bypass valve. Operation to 980 psia as a full expander cycle is possible with minor engine modifications. Tank head idle operation is achieved by moving one of the turbine bypass valves to a location to cut off the flow through the turbines, and inserting a blank-off plate in the common turbine line.

Recirculation of fuel and oxidizer may be desirable as a means of investigating pump stability. The planned approach is to design the turbopumps so that recirculation is not required, but to provide recirculation valves for later investigations.

Tank head idle starting may be the normal operating mode for applications in space. While the AETB will have the ability to start in tank head idle, less complicated starting is planned for most testing. Liquid hydrogen and liquid oxygen will be supplied to the AETB at pressures simulating operation with boost pumps. Cooldown valves will be provided for pre-cooling of the lines and turbomachinery.

The AETB brassboard controller will be an electronic rack mounted system. The engine test schematic shown in Figure 6 includes the AETB, the controller brassboard and a monitor system. The brassboard controller functions as a full authority controller during pre-run checks, cooldown, start, throttling, steady-state operation and shutdown. The monitor system is used to simulate the vehicle interface, down-load programs to the brassboard, control execution, record data and analyze data.

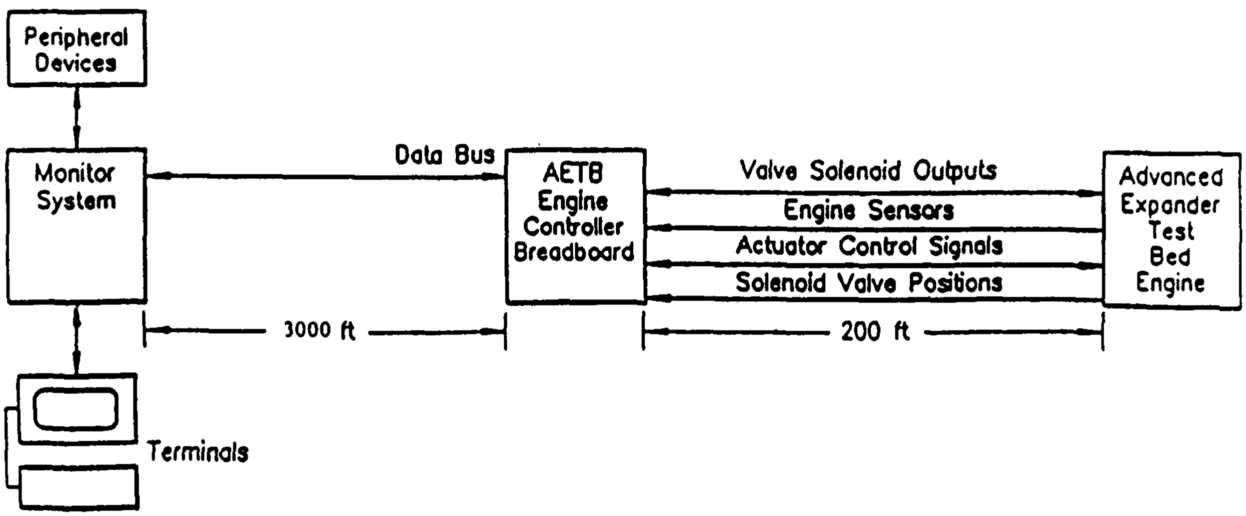

Figure 6. AETB Breadboard Control Schematic

A device termed "EMPRESS" (Experimental Multiprocessing Real Time Engine Simulation System) will be used to facilitate software control development and system and engine checkout. EMPRESS has been used extensively as a simulation tool for advanced gas turbine and National Aero-Space Plane (NASP) testing. In the software test environment, EMPRESS is used in place of the engine. Tests that would normally require an engine are performed with EMPRESS, thereby reducing test requirements and reducing the risk associated with first-time use of new software prior to engine test. Engine anomalies experienced during an engine test can be simulated without jeopardizing hardware, and in most cases, the anomalies can be diagnosed with electronic simulation.

G. Integrated System

The integrated AETB system is shown conceptually in Figure 7. The relatively small size is driven by the use of a sea level conical nozzle rather than a high area ratio bell nozzle. The nozzle is designed to provide a heat flux equivalent to a high area ratio nozzle so that cycle energy requirements will be met while allowing sea level testing. The engine can be throttled to 15 percent thrust without nozzle separation. Testing below 15 percent without separation can be accomplished by removing the conical nozzle, or by testing in an altitude facility..

The integrated system is configured to provide a high degree of operational flexibility and ease of maintenance while meeting the test bed requirements of providing a close simulation of line lengths, pressure drops, critical thermal masses, and valve responses.

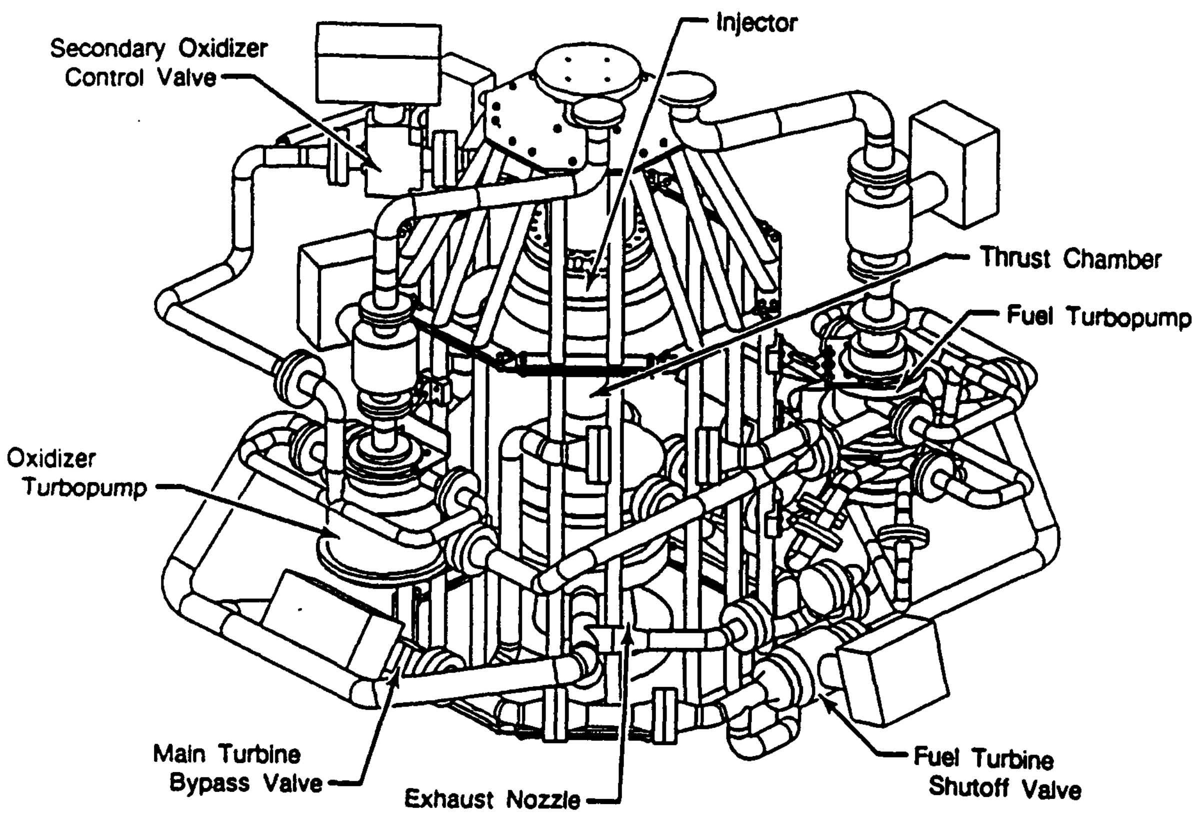

Figure 7. AETB Assembly

SECTION III
ENGINE CYCLES AND OPERATION

The Advanced Expander Test Bed (AETB) engine is a hydrogen/oxygen split expander cycle engine designed for a thrust level of 25,000 pounds and a mixture ratio of 6.0. The engine has a normal operating thrust of 20,000 pounds and is being designed to operate over a throttling range of 20 to 1 and at mixture ratios between 5.0 and 7.0. With minor hardware relocations, the engine can also operate as a full expander cycle and at a mixture ratio of 12.0. A simplified flow schematic of the test bed configured in the split expander mode of operation is shown in Figure 8. The control system, described in more detail in Section IV, allows closed-loop control of chamber pressure and open-loop control of mixture ratio. The main turbine bypass valve (MTBV) is the primary control point for thrust control.

The secondary oxidizer control valve (SOCV) is used to control the oxidizer flow split, thereby maintaining adequate injector pressure loss during throttling, and is the primary mixture ratio control valve. The fuel jacket bypass valve (FJBV) controls the coolant jacket flow to maintain a turbine temperature below 1060 R during throttling. Selected key parameters are presented in Figure 9 for the normal operating level.

The hydrogen pump (primary and secondary) is a twin-shaft, three-stage, centrifugal pump with the first stage and inducer driven by a single-stage, full-admission turbine and the second and third stages also driven by a one-stage, full-admission turbine. At the normal power level and a mixture ratio of 6.0, the fuel pump operates at 87,700 rpm to provide the required hydrogen pressure level of 3489 psia. Approximately 45 percent of the hydrogen exits the pump after the first stage and flows through a control valve (FJBV), bypassing the coolant jacket and flowing into a mixer downstream of the turbines. The remaining hydrogen proceeds through the final two stages of the high-pressure pump and is used to cool the chamber and nozzle assemblies. From there, most of the hydrogen coolant is used to drive the oxygen turbine and the back-to-back fuel turbines. The turbine drive fluid is routed through the oxygen turbine before the fuel turbine to minimize hydrogen turbine leakage losses. Over 16 percent of the hydrogen coolant flow at the operating point bypasses the turbines through the MTBV which is used for thrust control. The turbine flow then combines with the jacket bypass flow in the mixer and continues to the injector manifold and the combustor chamber.

Below a thrust level of 6,000 pounds, the power split between the turbines is no longer satisfied by the MTBV and SOCV alone. For adequate mixture ratio control below 6000 pounds thrust, the fuel pump must be loaded up via the fuel pump recirculation valve (FPRV), or the fuel turbine power reduced through a second turbine bypass valve (FTBV), Figure 10.

The oxidizer pump is a single-stage centrifugal pump powered by a single-stage, full-admission turbine. To provide the required pump discharge pressure of 1898 psia, the oxidizer pump rotates at 42,500 rpm at the normal operating level. From the pump discharge, the oxygen flow is divided into two separate streams which supply the primary and the secondary manifolds of the dual element injector. As stated earlier, mixture ratio control is achieved with a control valve in the secondary oxidizer flow line. The two oxygen flow streams mix within the injector element and are propelled into the main chamber where combustion with hydrogen takes place.

Operating the engine as a full expander cycle can be achieved simply by closing the FJBV and allowing the entire hydrogen flow to pass through the second and third stages of the fuel pump, the chamber and nozzle cooling passages, and the turbines. The increased coolant flow to the chamber and nozzle assembly results in a large pressure drop and a relatively low chamber pressure. However, if the FJBV is relocated to the position shown in Figure 10 (CCBV), the coolant pressure drop penalty is avoided and the cycle still operates as a full expander. The achievable chamber pressure in this configuration is 981 psia. High mixture ratio (12.0) operation of the engine requires control of the power split between the fuel and oxidizer turbines. This control can be provided by using a second fuel turbine bypass valve (FTBV) as shown in Figure 11. Chamber pressure of 1000 psia can be achieved with this configuration. Figure 12 outlines the AETB operating envelope while Table 3 lists several key operating parameters. Detailed engine cycle sheets are contained in Appendix A for selected operating points.

During the AETB preliminary design phase, both steady-state and transient models were developed using the P&W Rocket Engine Transient Simulation System (ROCETS) developed under NASA Contract NAS8-36944. The models are programed in Fortran 77 and structured in a modular building block configuration which allows easy changeout of component characteristics to evaluate effects on the engine cycle. One feature of the models is an expanded range of component characteristics, allowing simulation of the test bed across the entire operating range, from 0 to 125 percent of normal operating level. Propellant properties are read from tables using the latest sophisticated, high-speed map reader, which greatly enhances the efficiency of the program. The propellant property values are taken from the most recent NBS programs while the combustion properties are based on the NASA-LeRC Chemical Equilibrium computer program. Advanced simultaneous balancing techniques, developed for gas turbine simulations, are used to improve precision and increase program efficiency. The transient model contains all the critical volume dynamics and rotor inertias necessary to simulate test bed ignition and acceleration to any rotating thrust level from 5 to 125 percent thrust.

The engine models were continually used during the preliminary design. The steady-state model can balance to either chamber pressure and mixture ratio, emulating an engine trim test, or to control valve areas. The engine model was used to define the operating envelope discussed earlier, as well as define the effects of increased secondary flows on the engine cycle. The characteristics of component performance variations are also currently being generated. The AETB dynamic model was used to define the engine cycle start and shutdown transient characteristics. The control system requirements have been generated and the engine system abort levels defined with this model. During the final design phase, control valve sensitivity studies will be conducted and the control logic for the real time model formulated. The steady-state and dynamic engine models are deliverable to NASA-LeRC at the Critical Design Review. Subsequently, the models will be updated and verified using test data. Figure 13 presents the information required to validate the engine models and the testing which is scheduled to provide that data. Specific guidelines, as listed below, were followed to maintain structural, aerodynamic or stability design constraints:

- Fuel pump speeds kept below 100,000 rpm — maintains rotordynamic margins
- Maximum turbine inlet temperature set at 1060 R — protects turbine and valve seals
- Oxidizer injector $\Delta p/P_c$ maintained above four percent — ensures stable combustion throughout throttle range
- Valve flow turndown kept below 50:1 — manufacturing limit to provide producibility
- Valves sequenced to: — prevent pump stall during transients, — prevent reverse flow through FJBV, and — maintain the oxidizer-to-fuel ratio (O/F) within flammability limits during start.

The operational phases for the test bed were divided into five sections:

- Prestart — fuel and LO_2 lines purged out, — pump cooldown achieved (controller monitors)
- Start — timed valve movement, — LO_2 lead start using primary injector, — main chamber ignition (controller checks), — accel to mainstage using secondary LO_2 injector
- Mainstage — closed-loop P_c control, — open-loop mixture ratio control

- Shutdown —abort scenario, — valves move to failsafe positions, — propellant injectors purged immediately
- Post-Shutdown — fuel and LO_2 lines purged.

Control logic for each phase will be defined using the engine models. The start and shutdown transients were patterned after RL10 expander cycle engine transients with modifications to allow for the split expander configuration and the dual orifice injector on the oxidizer side. The present start transient accelerates from static conditions to 100 percent power (1200 psia chamber pressure) in four seconds, as shown in Figure 14. The shutdown transient decelerates from 100 percent power and shuts down to 10,000 rpm primary fuel pump speed within two seconds, as shown in Figure 15.

The AETB start transient preliminary valve schedule is shown in Figure 16. The primary oxidizer shutoff valve (POSV) opens first, at a rate of 330 percent per second, to provide LO_2 to the primary LO_2 injector for a LO_2 lead start. A helium supply of 0.01 lbm per second is used to purge the primary LO_2 injector. The primary LO_2 purge is fully on at the closed POSV position and linearly ramps shut at 50 percent POSV position. The fuel shutoff valve (FSOV) begins to open at 0.5 second after the POSV at a rate of 200 percent per second. The FSOV provides fuel to the fuel injector and is purged with 0.01 lbm per second of helium. The purge flow to the fuel injector is fully on at the closed FSOV position and linearly ramps off at 50 percent FSOV position. Once the FSOV is fully open, the upstream fuel valves, the fuel jacket bypass valve (FJBV) and the fuel cool-down valve (FCDV), dictate the amount of fuel flow into the fuel injector. Chamber ignition occurs at 0.6 second as shown in Figure 14. With chamber ignition, the pumps begin to accelerate and the LO_2 primary injector fills at 1.45 seconds. The secondary oxidizer control valve (SOCV) begins to open once the primary LO_2 injector is filled. The SOCV is held at the 15 percent position to limit chamber pressure thereby preventing combustion products from flowing back into the secondary LO_2 injector.

A criterion for the FJBV during start is to prohibit reverse flow of the heated fuel mixer fluid to the secondary fuel pump inlet, possibly causing secondary fuel pump cavitation. After the primary LO_2 injector has filled, the FJBV is opened to increase fuel flow to the chamber, thus increasing the available power. The FCDV allows a path for additional fuel to flow through the pump stage and dump overboard, preventing fuel pump stalls during the acceleration that occurs while the LO_2 injector is filling. The FCDV begins to close at 1.6 seconds, after the primary oxidizer injector has filled. By closing the FCDV, more fuel is passed through the heat exchanger and turbines, and into the chamber, thereby further increasing available power to the turbines. With this increased power, the pumps accelerate further, filling the secondary LO_2 injector at 2.45 seconds. Since the primary fuel pump is designed for twice the flow of the secondary fuel pump, and reverse flow through the FJBV must be avoided, the FCDV must close at a slow rate, i.e., 90 percent per second, to maintain stable pump flow characteristics in the primary fuel pump. Meanwhile, the FJBV cannot open too quickly since this would result in starving the secondary fuel pump of flow, or reversing flow through the FJBV. For primary fuel pump speeds below 12,000 rpm, reverse flow through the FJBV is a concern. For primary fuel pump speeds greater than 12,000 rpm, starving the secondary fuel pump of flow is a concern. Figure 17 shows the stable operation of all pumps for the start transient. At 2.45 seconds, the SOCV can ramp to its 100 percent power position. The main turbine bypass valve (MTBV) is used to trim the power. The MTBV is opened to its 100 percent position once the primary fuel pump speed is within 10 percent of the 100 percent power speed. During mainstage operation, the MTBV maintains a constant chamber pressure level using a closed loop function tied to the brassboard controller. Mixture ratio control is open loop and is set by controlling the SOCV area. The turbine inlet temperature is controlled by setting the FJBV area. The valve areas and the chamber pressure level will be programmed into the controller software prior to the test and will be determined using the engine steady-state model.

The abort shutdown should be the worst case scenario for the components. All valves begin to move at the same time signal, in this case 0.1 second as shown in Figure 18. The POSV closes at a rate of 330 percent per second and the SOCV closes at a rate of 250 percent per second. The oxidizer cool down valve (OCDV) opens fully at a rate of 330 percent per second. At 0.3 second, no more LO_2 will be provided to the LO_2 injectors and the helium purge is activated at 50 percent POSV and 50 percent SOCV positions, using the same ramp as the start transient. The LO_2 injector purge clears the LO_2 injectors of any oxygen. Meanwhile, the FJBV closes at a rate of 330 percent per second and the FSOV closes at a rate of 250 percent per second. The FSOV closes after the SOCV and POSV to provide a fuel-rich, cool shutdown. The fuel injector helium purge is activated at 50 percent FSOV position, using the same ramp as the start transient. The fuel injector purge clears the fuel injector of any fuel. The FJBV closes before the FSOV to prevent reverse flow through the FJBV. The MTBV is opened, at a rate of 310 percent per second, to assist in powering down by bypassing flow around the turbines. The FCDV opens at a rate of 200 percent per second to allow continued flow through the pumps while they are still pumping. The FCDV also provides a bleed path for the turbine and heat exchanger fluids once the FSOV and the FJBV are closed. Figure 19 shows the stable pump operation during the shutdown transient. From Figure 15, it can be seen that both the chamber pressure and turbine inlet temperature drop when the POSV and SOCV are closed, due to the sharp reduction of LO_2 flow to the chamber and the lower mixture ratio. At 0.5 second the chamber pressure drops further and turbine inlet temperature increases as a result of the reduced fuel flow. As the helium purges the injectors of fuel and LO_2, the chamber pressure drops to near static conditions. The primary fuel pump speed powers down to 10,000 rpm in two seconds, at which time there is no more power available through the turbines, and the pumps spool down from this point.

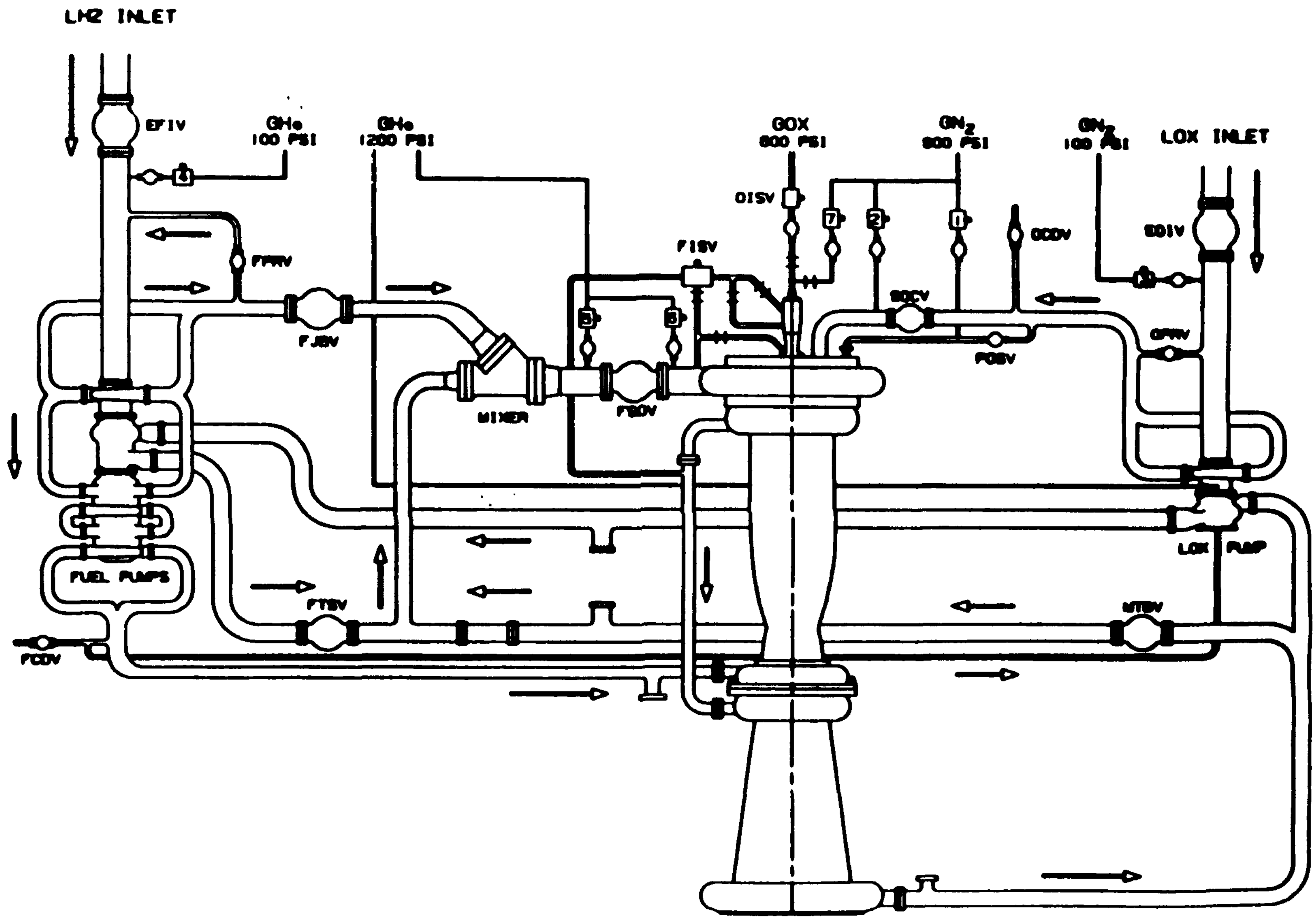

Figure 8. Split Expander Flowpath Schematic for Deep Throttling Capability

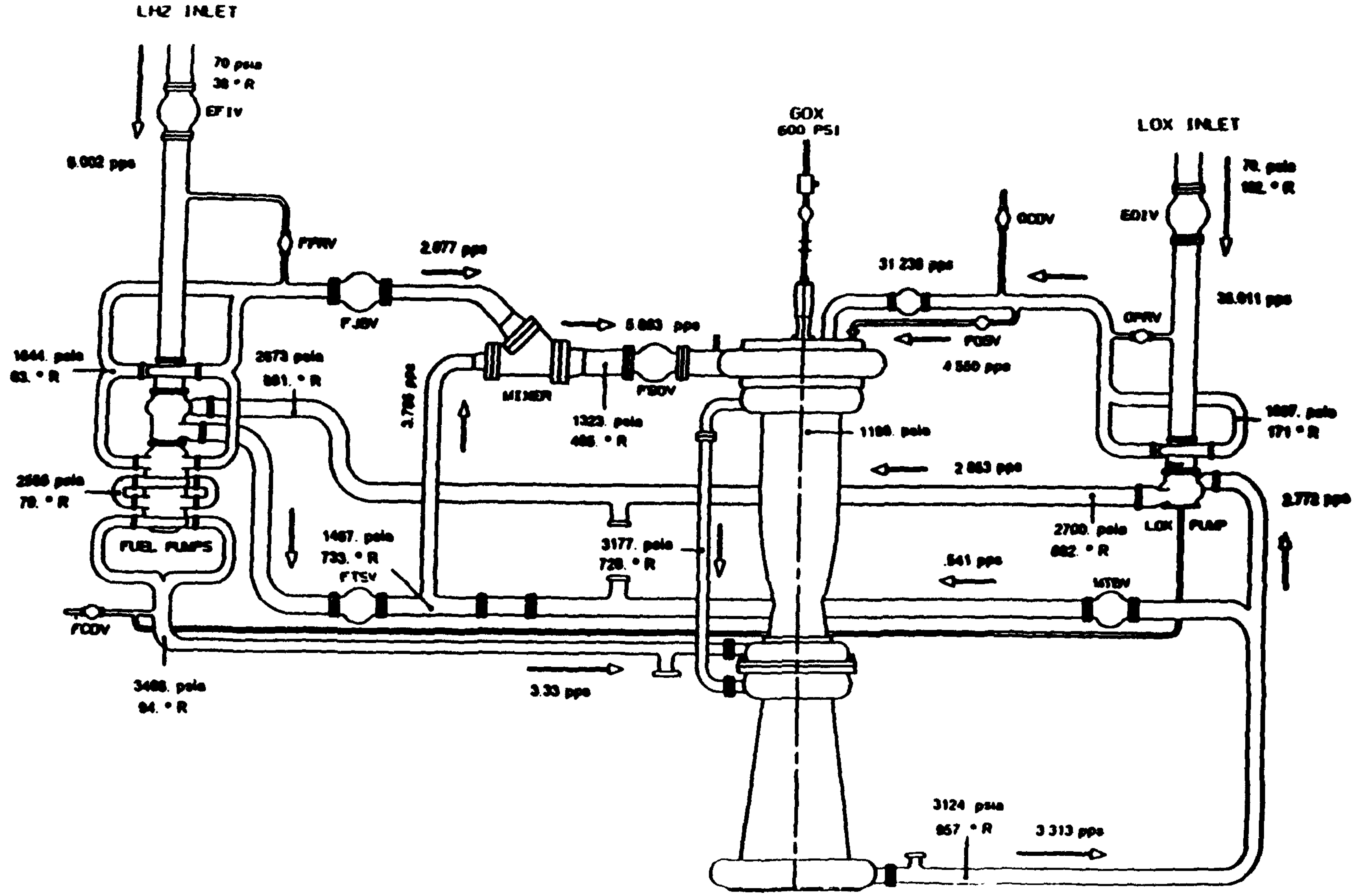

Figure 9. Split Expander Cycle Normal Operating Point Fluid Conditions

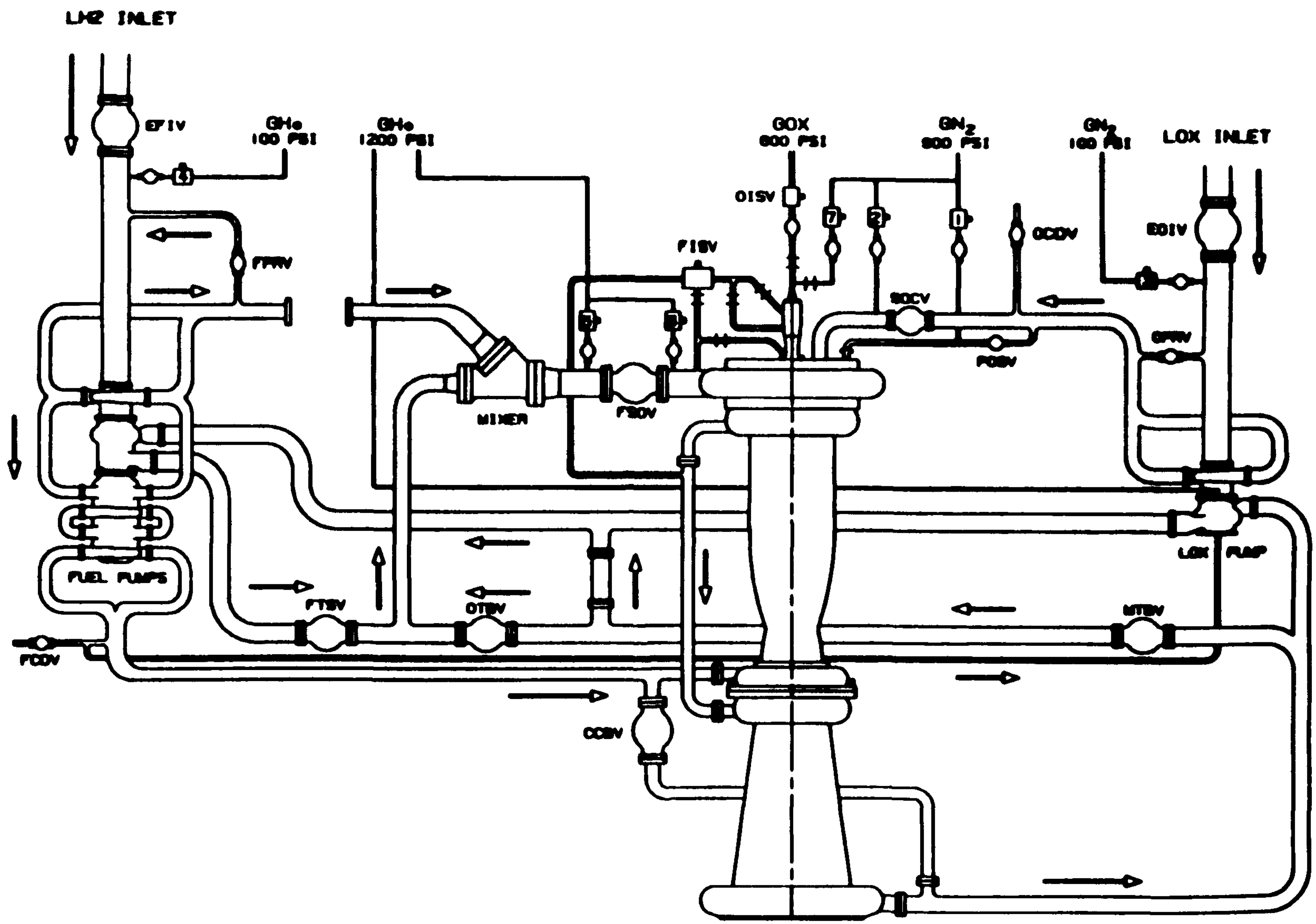

Figure 10. Valve Relocation for Full Expander Operation

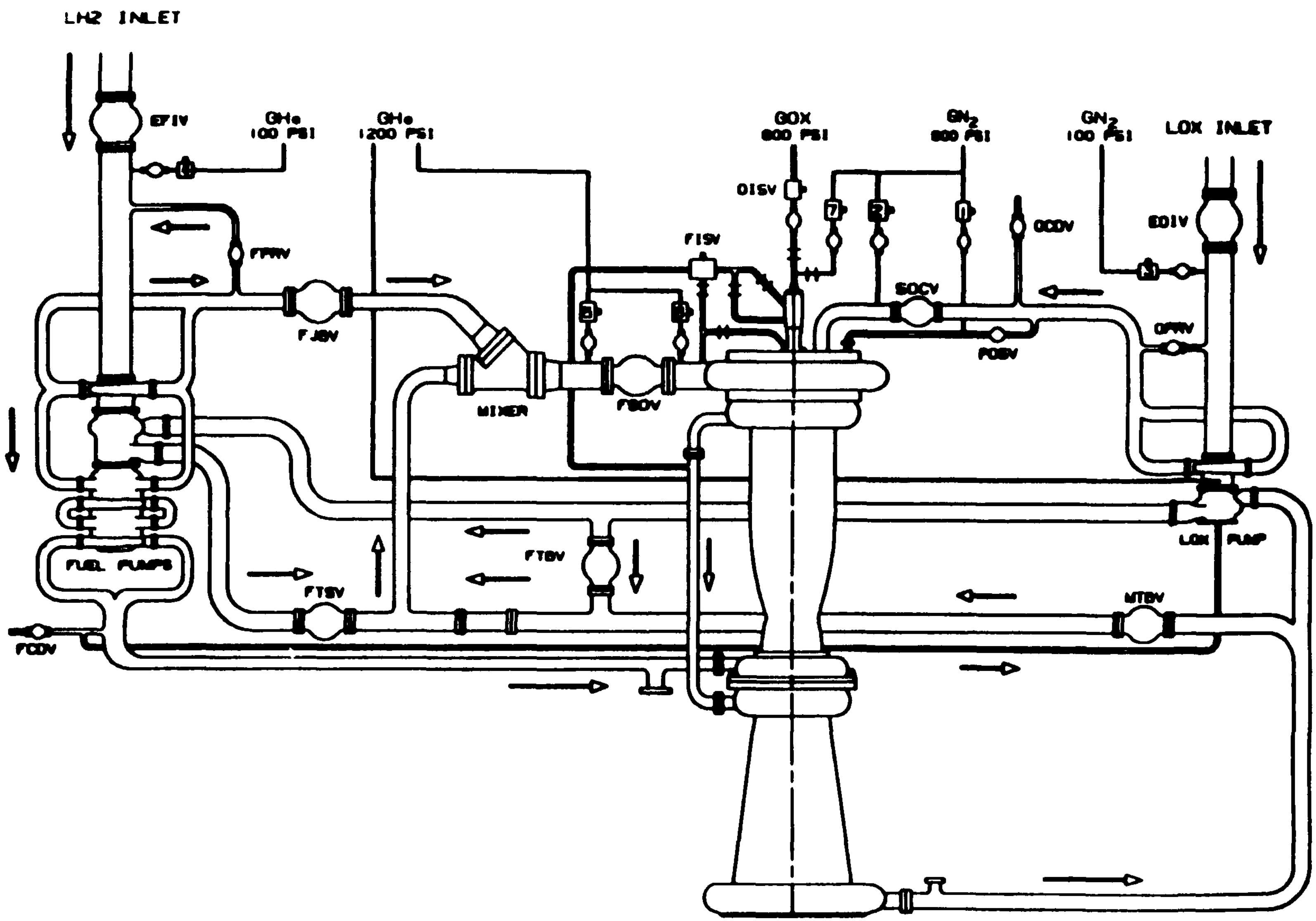

Figure 11. Configuration for High Mixture Ratio Operation (Fuel Turbine Bypass Valve)

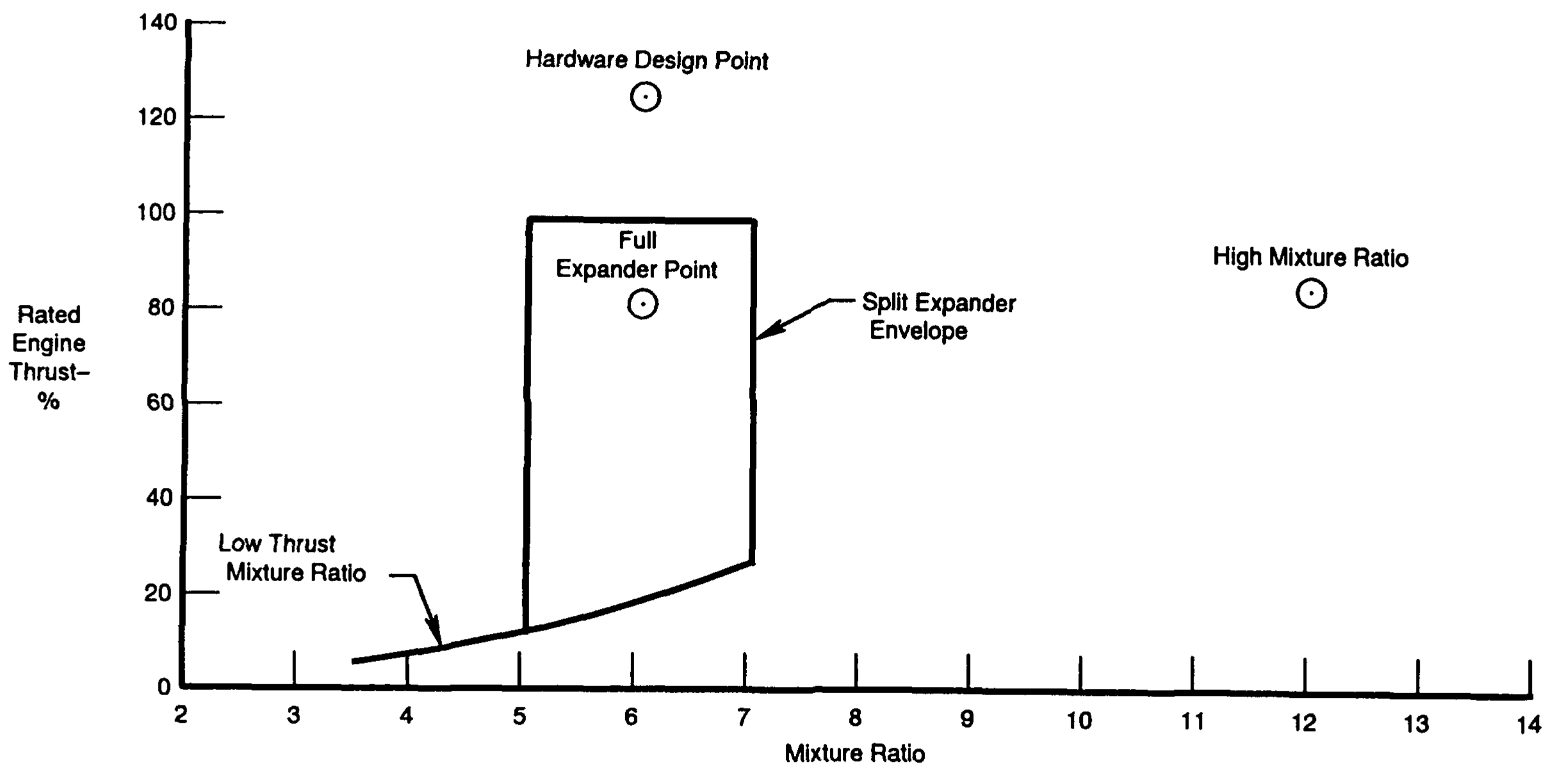

Figure 12. Steady-State Operating Envelope

Table 3. AETB Design Tables

Cycle Parameter		Uprated Design Point	Normal Operating Point	20% Thrust	5% Thrust	Tank Head Idle
Vacuum Thrust (E=1000:1)	lb.	25000	20000	4000	1000	88
Chamber Pressure	psia	1500	1198	238	65	6
Mixture Ratio		6.0	6.0	6.0	3.5	3.5
1st Fuel Pump Speed	rpm	98,240	87,715	34,842	18,921	0
2nd Fuel Pump Speed	rpm	99,221	84,786	33,087	22,275	0
Fuel Pump Disch. Pressure	psia	4503	3489	627	251	19
Oxidizer pump speed	rpm	48,863	42,502	15,411	8,241	0
Oxid Pump Disch. Pressure	psia	2356	1898	355	154	16
Oxid Turb Inlet Temp	deg R	1019	958	887	745	700
Fuel Turb Inlet Temp	deg R	943	882	727	478	700
Chamber/Nozzle ΔP	psid	410	354	120	94	6.5
Chamber/Nozzle ΔT	deg R	907	863	834	698	662
Pri LOX Injector ΔP	psid	181	151	26.2	20.3	7.1
Sec LOX Injector ΔP	psid	180	111	3.3	n/a	n/a
% Turbine Bypass Flow		3.8	16.3	59.8	65.4	100
% Jacket Bypass Flow		41.9	34.6	0	0	0

(Continued) Table 3. AETB Design Tables

Cycle Parameter		Normal Operating Point	Normal Operating Point	Full Expander Cycle	High Mixture Ratio
Vacuum Thrust	lb.	20000	20000	16419	17000
Chamber Pressure	psia	1241	1157	981	1001
Mixture Ratio		5.0	7.0	6.0	12.0
1st Fuel Pump Speed	rpm	89,819	83,868	90,000	79,180
2nd Fuel Pump Speed	rpm	90,799	79,517	84,994	70,346
Fuel Pump Disch. Pressure	psia	3752	3176	3301	2670
Oxidizer pump speed	rpm	45,594	39,460	38,314	40,151
Oxid Pump Disch. Pressure	psia	2273	1539	1628	1498
Oxid Turb Inlet Temp	deg R	907	1060	627	806
Fuel Turb Inlet Temp	deg R	838	969	599	739
Chamber/Nozzle ΔP	psid	345	344	239	272
Chamber/Nozzle ΔT	deg R	807	968	531	719
Pri LOX Injector ΔP	psid	228	77	142	101
Sec LOX Injector ΔP	psid	100	127	71	150
% Turbine Bypass Flow		5.5	24.0	26.4	10.3
% Jacket Bypass Flow		44.8	30.5	0	0

- Turbopump Performance
- Chamber/Nozzle Heat Transfer
- Combustion Performance
- Control Valve Characteristics
- Actuator Hysteresis and Dynamics
- Engine Volumes and Rotor Inertias
- Plumbing Losses/Injector Areas
- Nozzle Performance

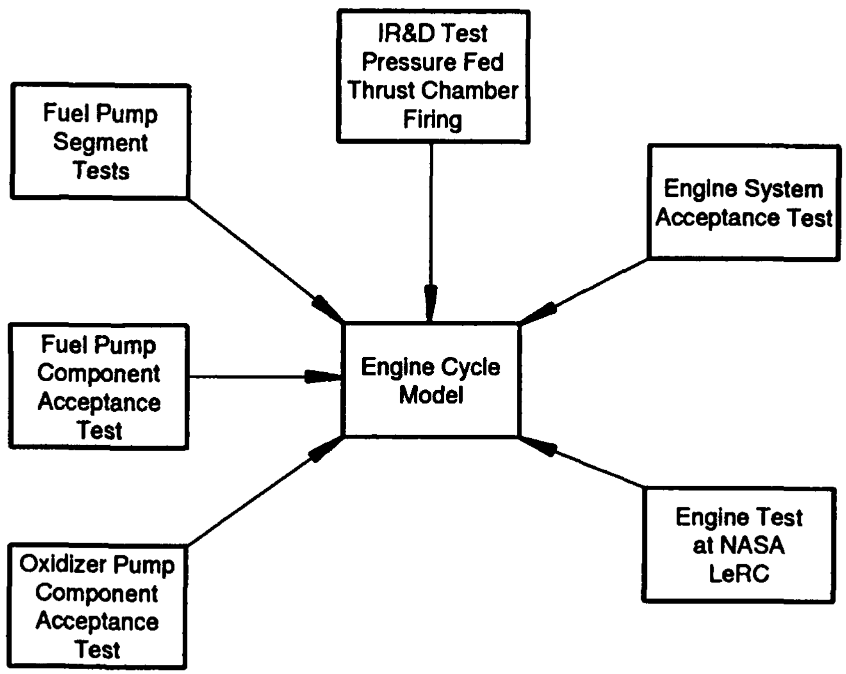

Figure 13. AETB Engine Simulation Validation

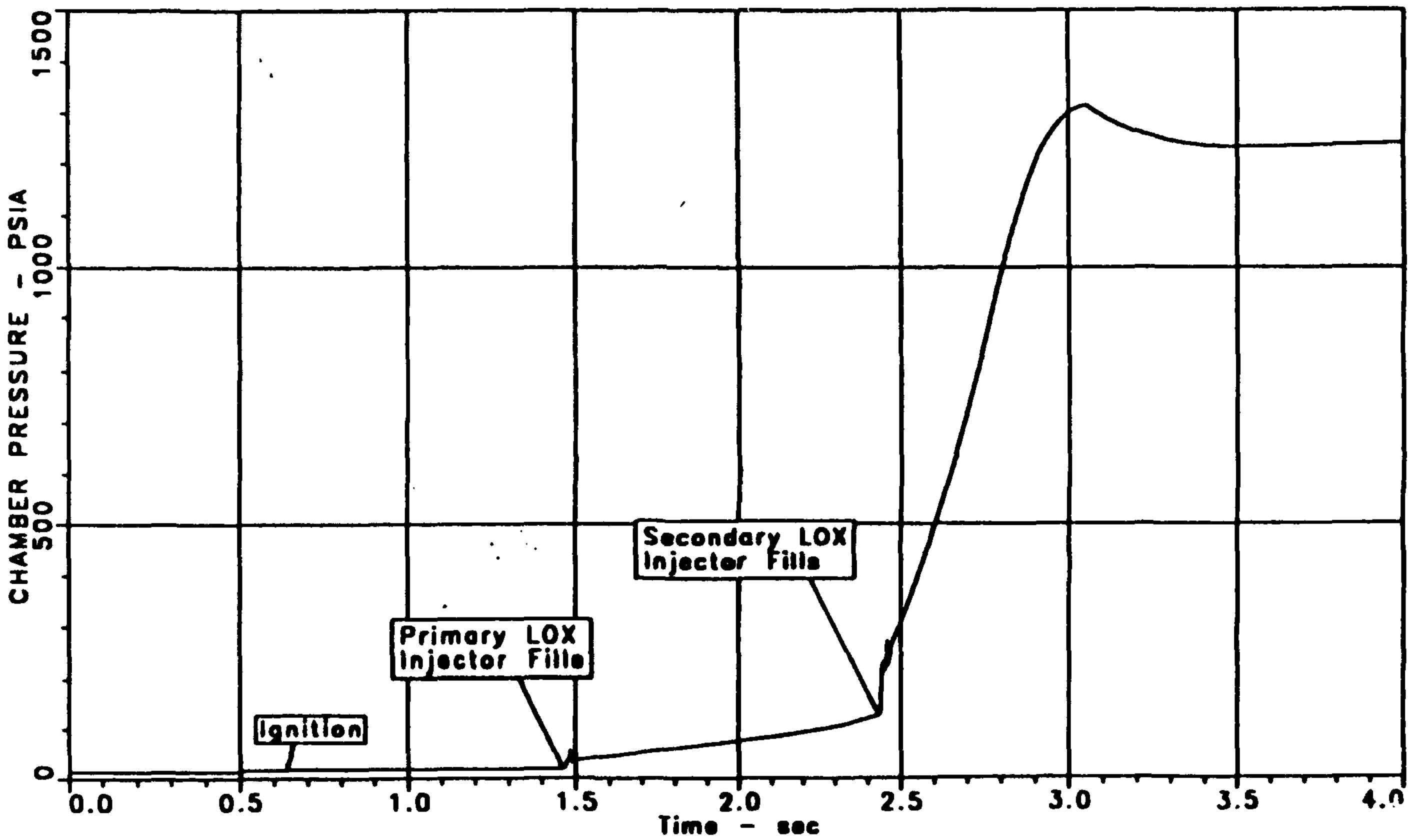

Figure 14. AETB Start Transient

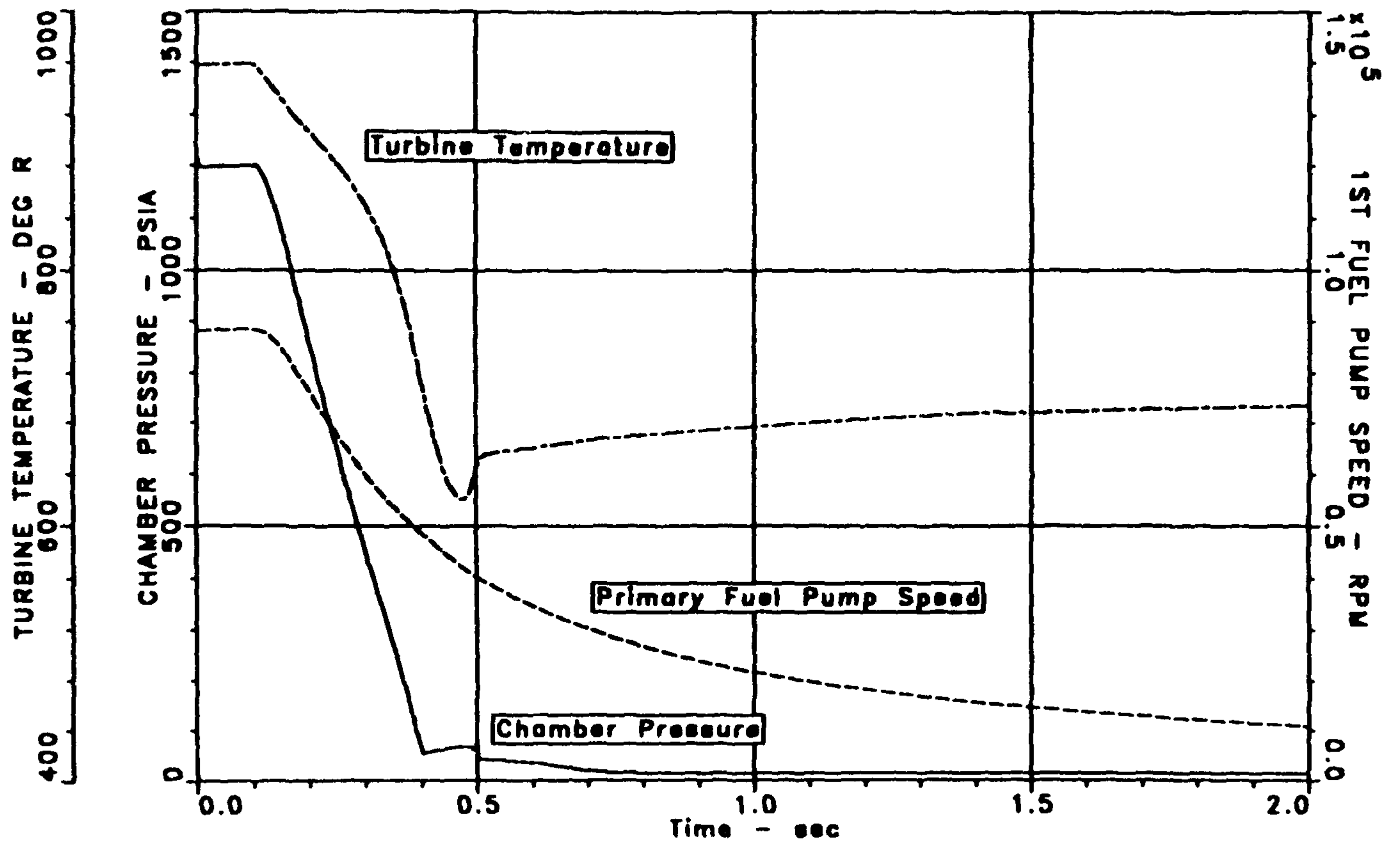

Figure 15. AETB Shutdown Transient

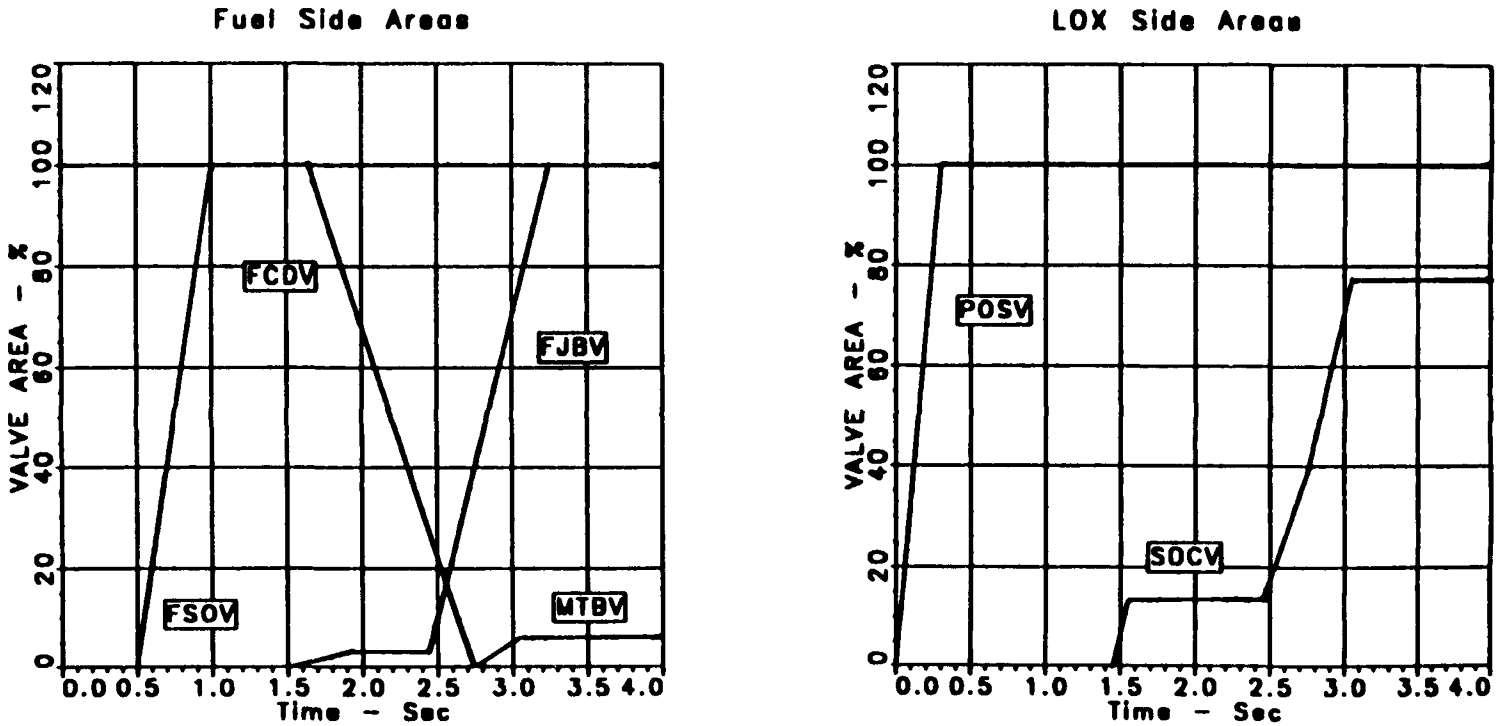

Figure 16. AETB Start Transient Valve Sequence

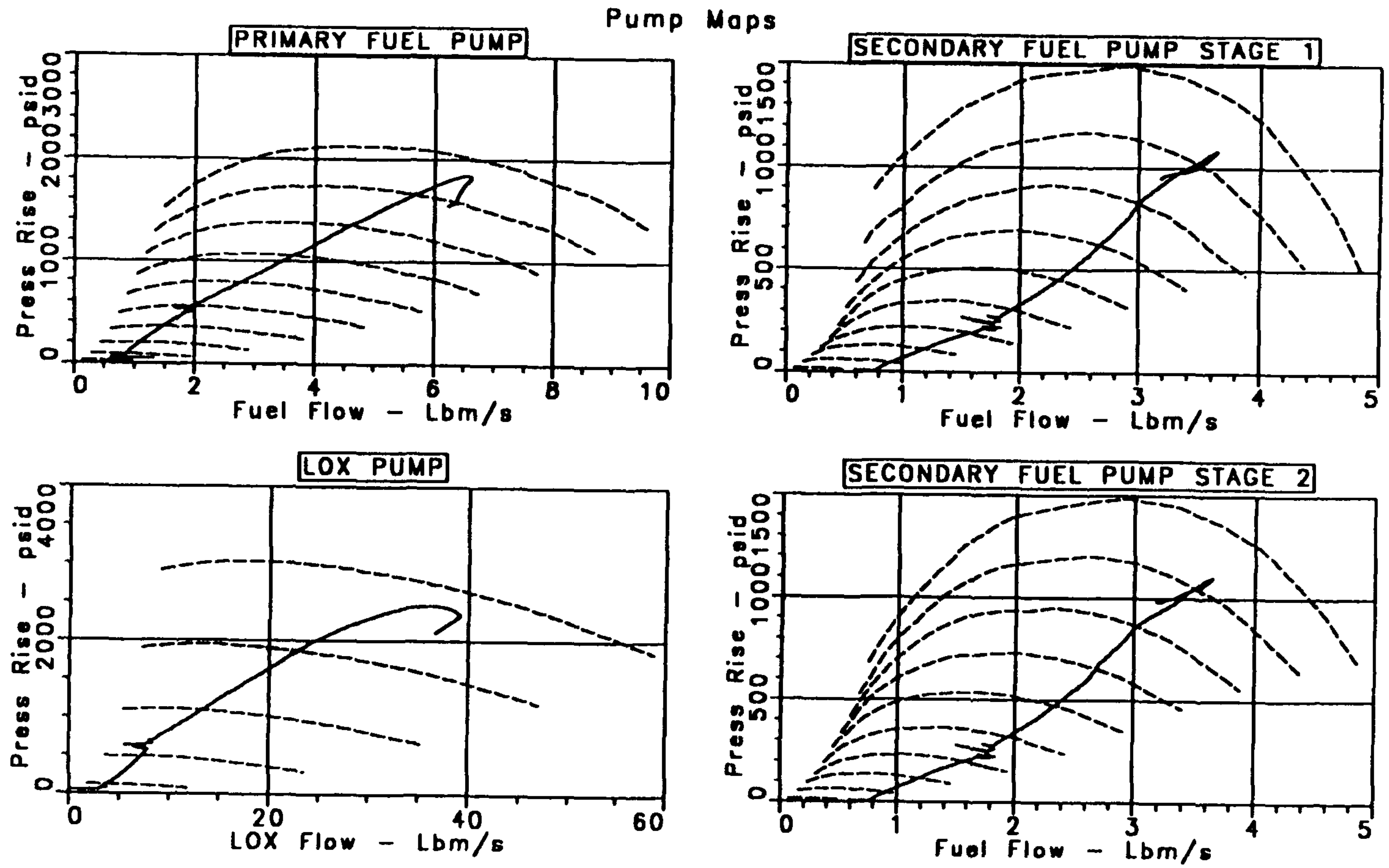

Figure 17. AETB Start Transient — Pump Head Rise

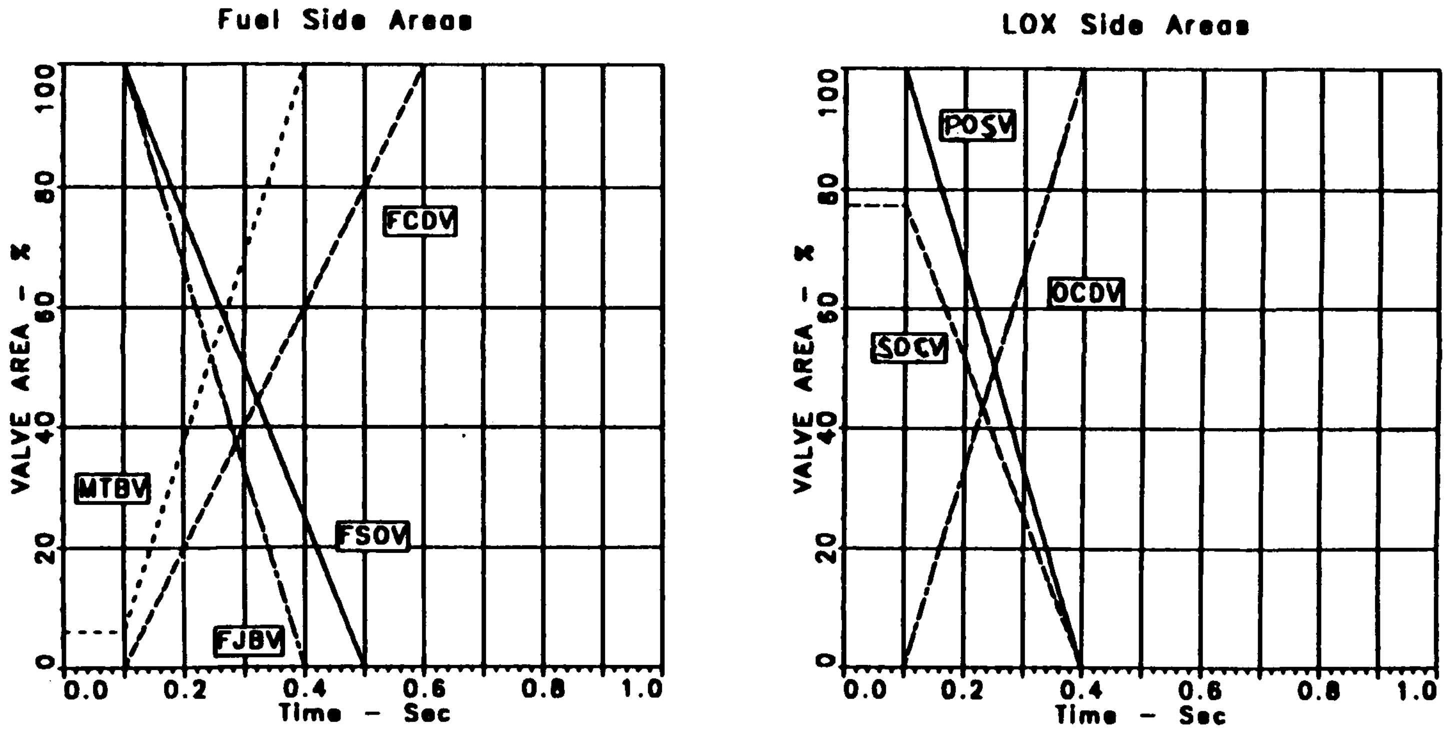

Figure 18. AETB Shutdown Valve Sequence

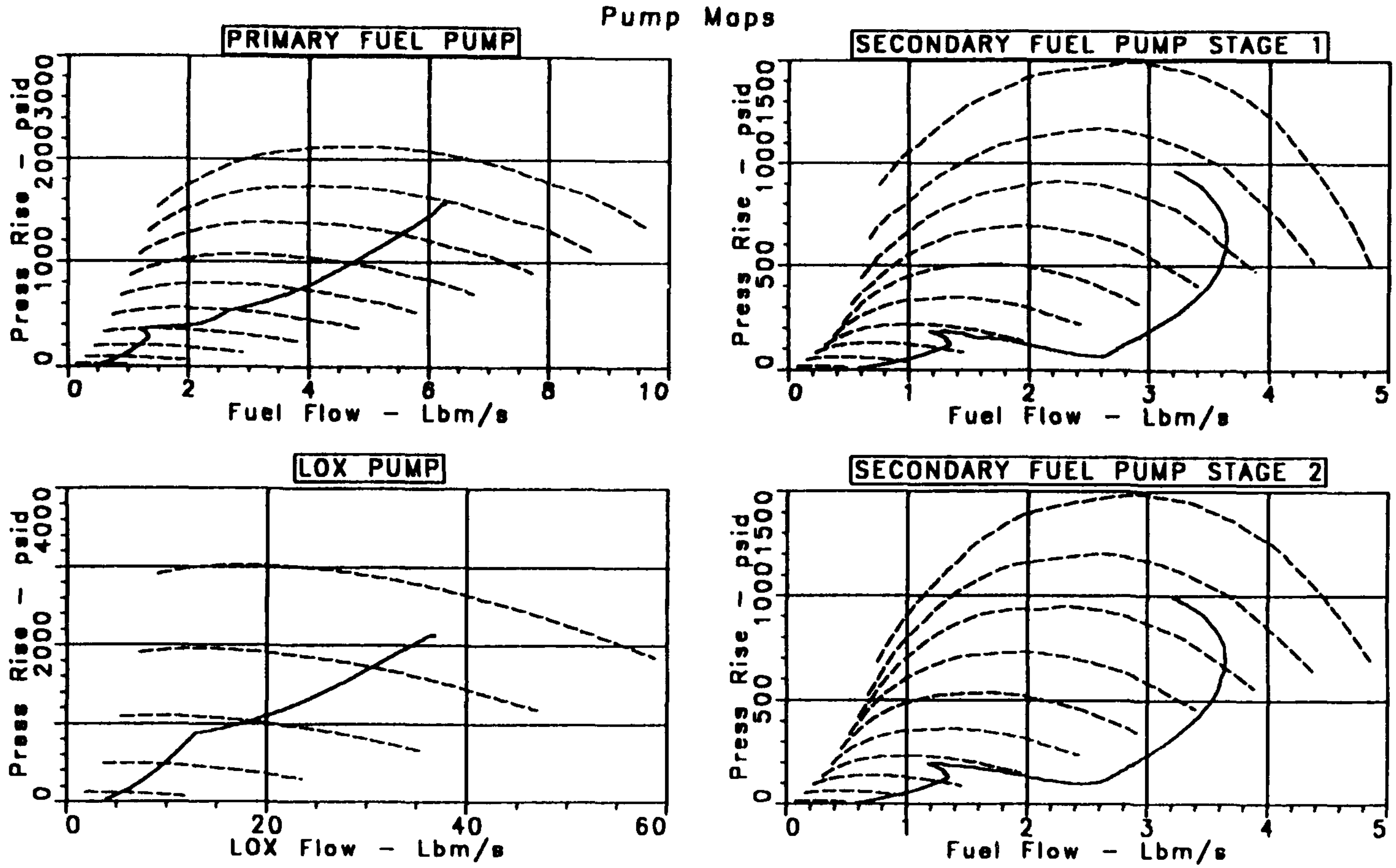

Figure 19. AETB Shutdown Transient — Pump Head Rise

SECTION IV
COMPONENT DESIGN

A. Mechanical Design Requirements

The AETB design requirements include a combination of contract requirements, P&W standard design practice and guidelines established by the unique requirements of the AETB Program.

Table 4 delineates some of the more important of these requirements. A key item to note is the use of a 25,000-pound (25K) thrust design point to ensure safe operating margins at the 20K thrust maximum planned operating point. Also, for life predictions, a cycle is conservatively defined to start at ambient temperature and zero speed/pressure, go to design point speed/temperature/ pressure, and then return to ambient conditions. Another pertinent point is the desired 1000-cycle life goal for all components except the thrust chamber and nozzle. These two components have high thermally induced stresses and will be designed to meet the 100-cycle AETB requirement.

The structural requirements are based on experience and NASA's structural guideline handbook #505B. Table 5 gives the key structural factors of safety. The approach to assuring adequate burst margins is predicated on both jet and rocket engine experience. The burst factor definition for housings is relatively classical; see Table 6. However, the factors for disks are definitely experienced based. For example, for hollow bore disks, empirically obtained "Material Utilization Factors" (MUF) are applied. These factors are simply correction factors for the different disk materials used in disk designs. For solid bore disks another experience-based approach is used, i.e., plastic growth limits at the web or rim (whichever is more limiting) are applied to determine speed limits. Stress related burst factors, which are proportional to speed squared, are always used for consistency.

The approach to rotordynamic design is also based on jet and rocket engine experience. The fundamental approach in the AETB is subcritical operation with a 20 percent speed margin at the highest power point. For the AETB, the goal is 20 percent margin at the design point. Other features important to rotor stability include double pilots for impellers, inducers and turbine rotors, and two-plane balance for impellers and turbine rotors.

Other design requirements include using average dimensions for stress analysis except for:

- Minimum thickness on pressure vessels
- Worst case dimensions for low cycle fatigue (LCF) limited areas
- Minimum dimensions on tiebolts.

Materials property data are based on -3 sigma characterizations taken from approved sources such as MIL-HDBK-5, P&W material manual, and P&W Space Shuttle Main Engine (SSME) Alternate Turbopump Development (ATD) materials manual. Hydrogen and oxygen compatibility are also important in selecting the materials.

All structural analysis is conducted using proven, state-of-the-art procedures. Many of the computer codes employed are off-the-shelf while others are P&W developed proprietary codes. Table 7 depicts some of the key structural codes, types, and uses.

Table 4. Key Engine Requirements

REQUIREMENT	*MUST SATISFY*	*DESIRED*
THRUST	>7.5K LB	20K OPERATING POINT 25K DESIGN POINT
CHAMBER PRESSURE	1200 PSIA	1200 @ OP POINT 1500 @ DESIGN POINT
THROTTLING	5/1	20/1 FROM OP POINT
LIFE *	100 CYCLES ** 2 HOURS	1000 CYCLES *** 5 HOURS
VERSITILITY	REPLACEABLE COMPONENTS	COMPONENTS EASILY ACCESSED/REPLACED
INSTRUMENTATION	MIN FOR PERF/CODE VERIFICATION	ADAPTABLE FOR MORE INSTRUMENTATION
OPERATING MODES	EXPANDER, HIGH O/F	SPLIT EXPANDER, HIGH O/F, EXPANDER

* CALCULATED AT DESIGN (OR MOST LIMITING) POINT
** CYCLE = O TO DESIGN PT TO 0
*** EXCEPT CHAMBER & NOZZLE 100 CYCLES

Table 5. Structural Factors of Safety Requirements

LOADING CONDITION	*YIELD*	*ULTIMATE*
COMBINED LOADS - ALL STRUCTURES	1.1	1.4
PRESSURE LOAD ONLY - ENGINE - VALVES, ETC - LINES < 1.5" DIA	 1.2* 1.5 2.0	 1.5* 2.0 4.0
ROTOR SPEED + THERMALS - ALL ROTATING STRUCTURES	1.2*	1.5*
* PROOF TEST <u>MAY</u> BE AVOIDED	1.8	2.25

Table 6. Burst Factor Definitions

COMPONENT	*BURST FACTOR*	*DEFINITIONS*
HOUSINGS	Sult/Snom	Sult = ULTIMATE TENSILE Snom = AVG TANGENTIAL STRESS
HOLLOW BORE DISKS	MUFXSult/Snom	MUF = MATERIAL UTILIZATION FACTOR
SOLID BORE DISKS	(Nb/Nd)2	Nb = LOWEST SPEED OF 1% WEB PLASTIC OR 0.5% RIM PLASTIC GROWTH Nd = DESIGN SPEED

Table 7. Structural Analysis Codes

CODE	TYPE	ELASTIC	PLASTIC	Kt	LCF	VIBS
NASTRAN	F.E.	X		X		X
MARC	F.E.	X	X	X		
W140*	F.D.	X	X		X	
U553*	MATL DATA				X	
W526*	SHELL	X				X
BEASY	B.E.	X		X		
BEST2D	B.E.	X		X		

* P&W CODES

B. Turbopump Overview

1. Turbopump Design Requirements

The oxygen and hydrogen turbopumps are configured to meet the design requirements stated in Section III, as well as specific requirements for the turbopumps. These requirements include:

- Meeting the requirements of the split expander cycle at the uprated 25,000-pound thrust design point (125 percent of normal operating thrust)

- Providing stable pump operation over the desired throttling range of 5 to 125 percent of normal operating thrust

- Ensuring subcritical rotordynamics by maintaining an adequate margin above the uprated design speed, with a goal of 20 percent margin

- Providing the desired life of five hours and 100 starts without overhaul (required life is two hours).

Specific features included in the oxygen turbopump are as follows:

- A long-life, knife-edge interpropellant seal package

- Stability enhancing features for deep throttling and high mixture ratio operation

- Single-stage, full-admission turbine

- Two ball bearings for rotor transient thrust control and a roller bearing for rotor stiffness

- Ball and roller bearing speeds that are within previous experience

- Control of turbine blade tip clearances

- Proven materials: INCO 718 for liquid oxygen service, A-286 and Super A-286 for warm hydrogen service

- Use of advanced design and analysis tools, including finite element analyses where required.

Figure 20 shows a cross-section of the oxygen turbopump.

The hydrogen turbopump also includes specific features to meet the engine requirements:

- Dual shaft fuel pump for subcritical rotor dynamics

- Two roller bearings on each shaft for rotor stiffness

- Materials and bearing speeds based on Space Shuttle Main Engine – Alternate Turbopump Development (SSME-ATD) experience

- Inlet vanes and interstage struts for enhanced stability

Figure 21 shows a cross section of the hydrogen turbopump.

:. Risk Reduction and Verification Plans

To meet the AETB engine requirements, three areas of component technology should be confirmed. These re impeller producibility, cryogenic brush seals, and high DN (diameter times speed) roller bearings. A brief escription of the technology verification plans is presented below.

- Impeller Producibility — The need to produce a high-performance engine, with deep throttling capability, and within a reasonable time and cost, places conflicting demands on the hydrogen turbopump impellers. High efficiency and a high turndown ratio dictate high-speed operation together with features such as integral shrouds, a large number of thin blades, a large sweep (wrap) angle, and a small discharge angle. This complex geometry and the high operating speed raise stress leve.. to the point where wrought material properties are required. However, this same geometry makes the part very expensive (both in terms of cost and schedule), and quite difficult to produce with conventional fabrication methods. To satisfy these conflicting technical and programatic requirements, P&W is investigating non-conventional fabrication methods. The principal method being pursued is to fabricate the impellers by machining discrete sections, and then joining the sections using a diffusion bonding technique. This effort is underway, and the diffusion bonding trials are expected to be complete by mid-1991.

- Cryogenic Brush Seals — Because of the high turndown ratio required in throttleable engines, control of pump internal flows at low power settings becomes critical. This limitation arises because at low power settings the internal labyrinth seal leakage can become an unacceptably large fraction of the total pump flow. Brush seals have inherently higher pressure drop than labyrinth seals, hence internal flows drop off less rapidly as the engine is throttled. Seal testing in a cryogenic hydrogen bearing rig is planned to confirm the seal design. Metallurgical laboratory evaluation of the properties of the standard brush seal material in cryogenic hydrogen will also be carried out.

- High DN Roller Bearings — The use of negative internal clearance roller bearings in large turbopump applications, such as the XLR129 and the SSME-ATD programs has been demonstrated. An ongoing IR&D program will verify the scalability of the design methods to small, space-engine-size bearings. As part of this same program, ball bearings will be tested up to speeds commensurate with space engine applications.

3. Turbopump Testing

Both sets of oxygen and hydrogen turbopumps will be tested at P&W's E-8 high-pressure test facility prior o installation on the test bed. In addition to acceptance testing to verify that the pumps are ready for installation on the test bed, design methodology verification testing will be carried out. The testing is summarized below.

- Oxygen Turbopump — The acceptance testing will consist of four tests of 20 to 50 seconds duration with each pump. Figure 22 presents a test matrix for the acceptance testing. After the completion of acceptance testing on the second turbopump, design methodology verification testing will be carried out on this unit. Three tests are planned for this purpose; the testing will focus on investigating any performance anomalies identified during acceptance testing. Figure 23 shows the instrumentation planned for acceptance and verification testing.

- Hydrogen Turbopump — The primary and secondary segments of the first unit will be tested independently. This will allow hydrodynamic and aerodynamic performance of the two segments to be evaluated without regard to possible interactions between them. Four speed line and cavitation tests are planned for each segment. The second turbopump will be tested as a complete assembly. An acceptance test program consisting of six speedline and cavitation tests are planned for this unit. A series of three design methodology verification tests is planned to be carried out after completion of acceptance testing. The test matrices for the hydrogen turbopump are shown in Figure 24.

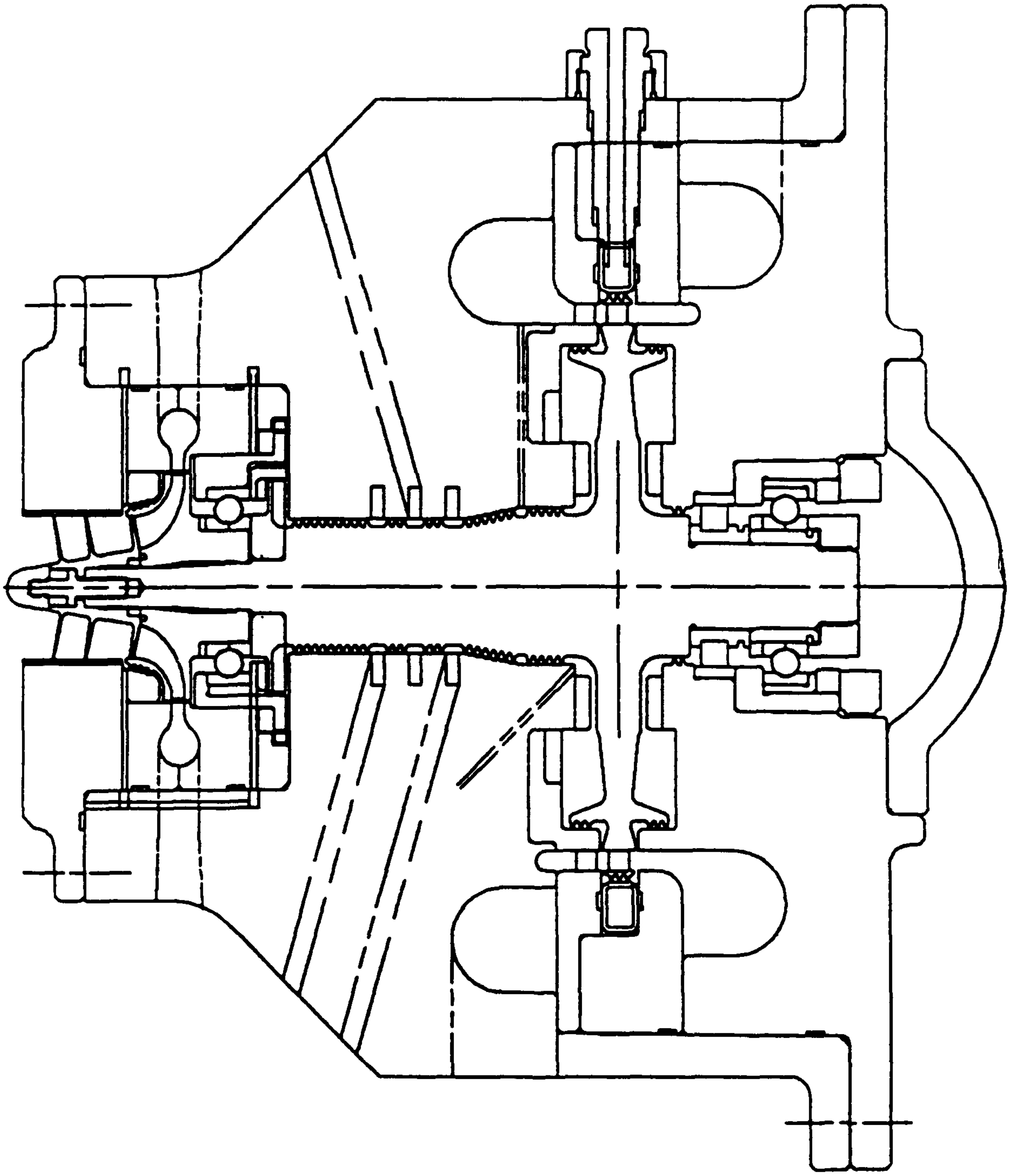

Figure 20. AETB Oxygen Turbopump

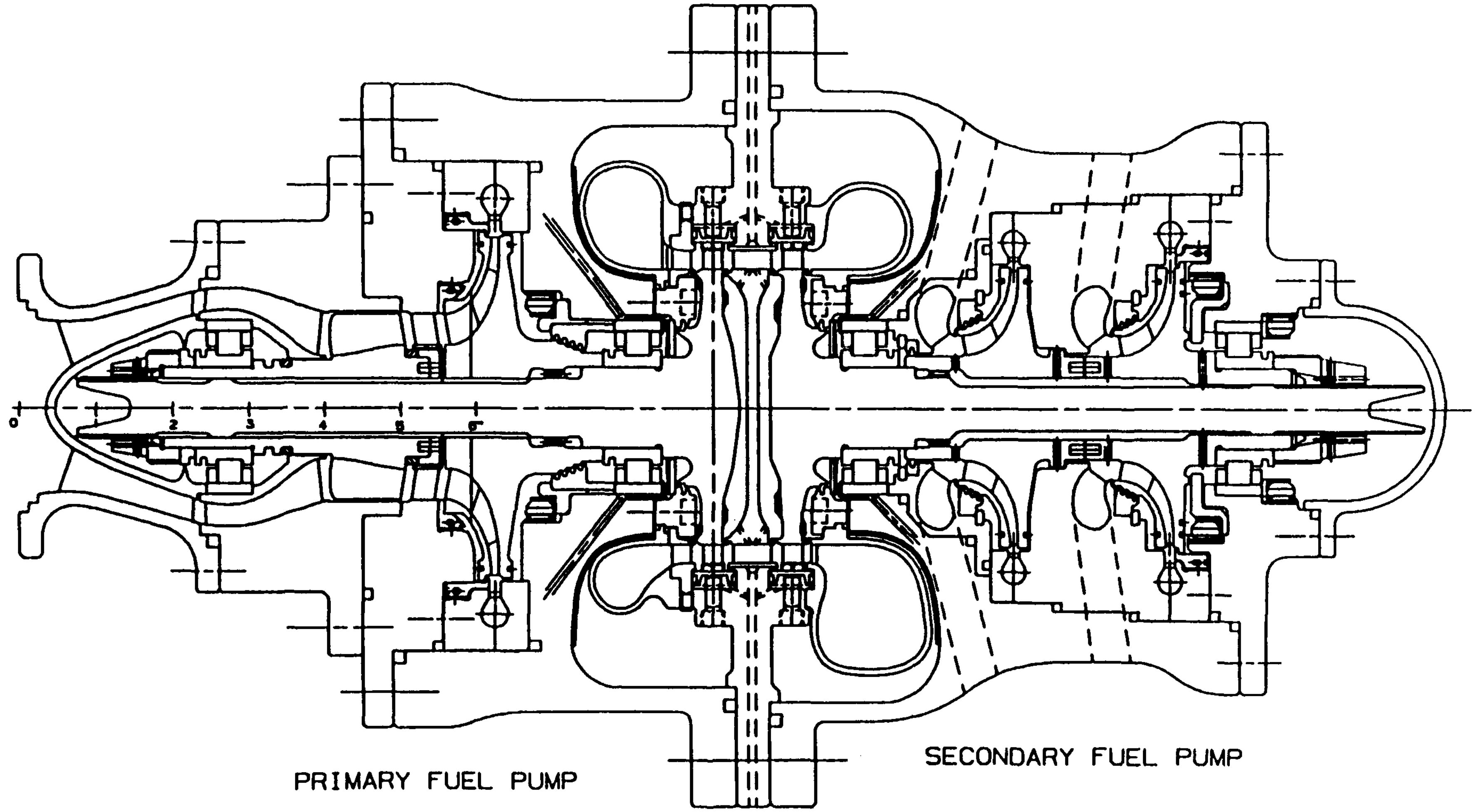

Figure 21. AETB Hydrogen Turbopump

Pump	Test No	Type of Test	Relative* Speed ~%	Relative* Q/N ~%	Equivalent Thrust ~%
1	1	Speedline	20	20-110	5
1	2	Speedline	70	70-110	50
1	3	Speedline	100	90-110	100
1	4	Speedline Overflow	100	100-Overflow Point	100
2	1	Speedline	100	90-110	100
2	2	Cavitation	20	20	5
2	3	Cavitation	70	70	50
2	4	Cavitation	100	100	100

*Relative to Normal Operation Point

R21308/10

Figure 22. Oxygen Turbopump Acceptance Testing

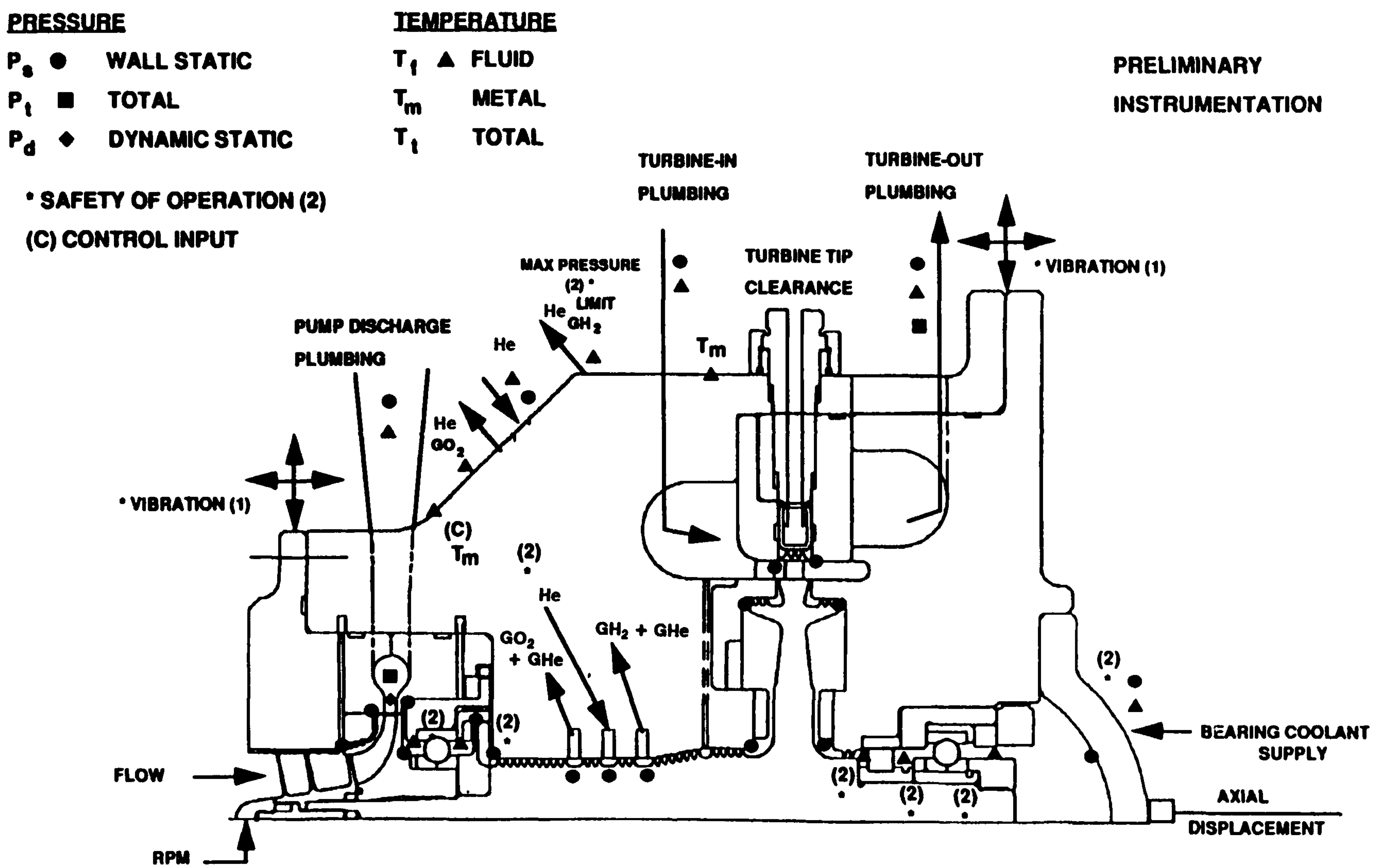

Figure 23. Oxygen Turbopump Instrumentation

TURBOPUMP SEGMENT TEST CONDITIONS

Pump Segment	*Test No*	*Type of Test*	*Relative* Speed ~%*	*Relative* Q/N ~%*	*Equivalent Thrust ~%*
1	1	Speed Line	20	20-110	5
1	2	Speed Line	70	70-110	50
1	3	Speed Line	100	90-110	100
1	4	Cavitation	20	23-110	5
2	1	Speed Line	17	57-110	5
2	2	Cavitation	66	82-110	50
2	3	Speed Line	100	90-110	100
2	4	Speed Line Overflow	100	100-Overflow Point	100

*Relative to Normal Operation Point

R21308/10

COMPLETE TURBOPUMP ACCEPTANCE TEST CONDITIONS

Pump Segment	*Test No*	*Type of Test*	*Relative* Speed ~%*	*Relative* Q/N ~%*	*Equivalent Thrust ~%*
2	1	Speedline	20	20-110	5
2	2	Speedline	70	70-110	50
2	3	Speedline	100	90-110	100
2	4	Cavitation	20	20	5
2	5	Cavitation	70	70	50
2	6	Cavitation	100	100	100

*Relative to Normal Operation Point

Figure 24. Hydrogen Turbopump Test Matrices

C. Oxygen Pump

1. Design Features

The AETB liquid oxygen turbopump shown in Figure 25 is a single-stage, high efficiency, centrifugal type pump. The impeller is driven by a single-stage, integrally bladed, full-admission, reaction turbine that is integral with the rotor shaft. An interpropellant seal package (IPS), separates the turbine hydrogen gas from the oxygen at the pump end of the turbopump.

The hydrodynamic design provides stable pump operation over the entire 20 to 1 throttle range of the test bed engine. An axial screw-type inducer is used to maintain impeller suction properties over this broad operating range. The inducer is close coupled to the impeller to minimize rotor length, loads and flow distortions. The impeller is a low exit angle design with an integral shroud for efficient operation at low pump speeds.

Rotor speed is approximately 49,000 rpm at the test bed design point of 25,000 pounds thrust. Pump flow is 45 lb/sec at a discharge pressure of 2350 psia. The pump discharges into a vaneless double discharge volute, which minimizes hydraulic side loads on the rotor.

The pump end of the rotor is supported by a single, liquid oxygen cooled, ball bearing. Eighty percent of the bearing cooling flow is recirculated to the impeller inlet. Sufficient pressure and temperature margins are maintained with this flow to insure that pump cavitation does not occur. Downstream, a vaporizer is used to reduce the density of the oxygen entering the IPS thereby reducing the amount of oxidizer that is lost overboard through the IPS.

The IPS consists of five sets of labyrinth seals. A helium purge in the center of the seal system is used for ground test to ensure separation of the oxidizer and fuel within the turbopump. Radial clearances have been set at 0.003 inch for the hydrogen side to provide the required sealing capability, and a slightly greater 0.005 inch for the oxygen side of the pump to reduce the risk of rubbing in liquid oxygen.

The turbine disk and blades and the turbopump shaft are machined as one piece. This integral fabrication feature results in a less complex design and provides greater rotor stiffness for increased critical speed margins. Outboard seal wings are used to prevent flowpath gas ingestion or recirculation. Radial location of the wings can be changed if required during the design phase to make small adjustments to rotor thrust balance. The turbine is a single-stage, full-admission, reaction turbine. The reaction of the blades is being adjusted during the design phase to balance the major axial loads on the rotor. The current reaction is approximately 50 percent.

Due to the small size of the turbopump, seal clearances are very important to pump efficiency. Turbine tip clearances are particularly critical in meeting the performance requirements of the turbopump at the design point. Therefore, the turbine tip shroud will be thermally conditioned with liquid hydrogen to limit radial growth and help maintain design tip clearance.

The turbine inlet and exit volutes are a unique design. The radial inlet and axial discharge of the inlet volute (and the axial inlet and radial discharge of the exit volute) allow access from the side of the housing for machining. Without this accessibility, the volutes would be very difficult to produce. The two volutes are constant-area, full-admission configurations that are mirror images of each other and are clocked 180 degrees to reduce rotor side loads.

Rotor critical speeds dictate that the turbine end of the rotor be supported by a roller bearing. A ball bearing is also incorporated on the turbine end of the rotor to take out any axial unbalance during transient or off-design operation. Both bearings are cooled by hydrogen supplied from the third-stage fuel pump discharge.

The turbopump housings are a robust design, providing substantial stiffness for rotor support and sufficient room for plumbing and instrumentation access. The minimal number of components also reduces the risk of troublesome joint leakages.

2. Material Selection

Figure 26 shows the primary material selections for the major components in the LO_2 turbopump. The material selections are based on the fluid and thermal environments. A286 and Super A286 are used for most of the major housing components for strength and resistance to hydrogen embrittlement. The materials selected for LO_2 and GO_2 service are based on NASA material compatibility testing, SSME turbopump material specifications and material strength requirements. Testing of other materials and combinations of materials is ongoing and will be used as appropriate in the critical design phase.

Liquid oxygen bearing material selection (inner and outer races, rolling elements and cage materials) is based on SSME-ATD and RL10 experience. The use of AISI 440C for the pump end bearing inner race, for LO_2 compatibility reasons, results in significant stress levels in the race at room temperature. These stresses can result in a stress corrosion cracking problem in the inner race in a very short time. However, a new heat treat cycle has been developed that dramatically increases inner race shelf life. This improvement allows the use of 440C without a prohibitively low shelf life.

AISI 9310 is used for the races in the hydrogen cooled bearings at the turbine end since LO_2 compatibility is not an issue with these bearings. This material allows greater margins for the radial fits between the bearings and shaft.

The rotor is made of Super A286 to provide resistance to hot hydrogen as well as high strength. The inducer, the impeller and the vaporizer are made from INCO 718, chosen for its strength and the fact that it has a slightly better LO_2 compatibility rating than other high-strength nickel alloys.

At the time of PDR, NASA was planning LO_2 frictional heating tests to evaluate several other alloys. When the data are available from these tests, the LO_2 turbopump materials will be reevaluated to ensure the best selections are made.

3. Liquid Oxygen Turbopump Operating Conditions

Figures 27, 28, and 29 show the LO_2 pump operating conditions at the design point (25,000 pounds thrust), the maximum operating point (20,000 pounds thrust) and the minimum required turn-down thrust (4000 pounds). The figures show pump and turbine inlet and exit flow conditions as well as shaft speed, torques, horsepower and tip speeds. All three figures represent an O/F ratio of 6.0.

Figures 30 and 31 show the internal flows at the 25,000-pound and the 4000-pound thrust levels. Temperatures and pressures are shown for major cavities as well as the mass flow rates. These flows are based on 0.003-inch radial clearances on the hydrogen labyrinth seals and 0.005-inch radial clearances on the oxygen labyrinth seals. Windage heat-up has been accounted for and the vaporizer effectiveness is based on the E727 Vaporizer program developed under the SSME-ATD program.

The rotor has been axially thrust balanced at the design point conditions. Figures 32 and 33 show the rotor thrust balance at the 25,000-pound and the 4000-pound power levels, respectively. The total imbalance is only 40 pounds at the design point and increases to nearly 500 pounds at the 4000-pound thrust level. This load is acceptable because it occurs at relatively low rotor speed. The objective is to minimize the axial loads at higher speeds. Analysis is continuing to determine what the axial imbalance is at other power levels. With this additional analysis, it will be possible to determine how much bias can be applied to the rotor to minimize the bearing axial loads at high speed.

4. Inducer/Impeller

The inducer, shown in Figure 34, is a three-blade design with moderate suction specific speed (N_{ss}) for low-speed performance. The impeller, Figure 35, is a shrouded design with a low discharge blade angle for improved throttleability.

During preliminary design, work focused on defining an impeller configuration that was not only hydrodynamically sound and structurally acceptable but was also practical to produce. Manufacturing capability proved to be the most limiting requirement for the impeller. Fortunately, the design did not have to be compromised for manufacturability and all design hydrodynamic parameters fell well within design experience.

Early in the design phase, IN100 material was thought to be necessary to achieve the required structural margins for LCF life. This material selection was a concern because IN100 did not rate well in oxygen promoted combustion tests. However, preliminary structural analysis shows that INCO 718 will achieve the required structural margins and is currently the material of choice.

Subcritical rotordynamics is a primary design goal. The pump bounce mode is very dependent upon the inducer/impeller length and weight. The latest impeller length is 0.070 inch shorter than the original configuration. The resultant critical speed is 122 percent of the design point speed of 48,863 rpm which falls in what is considered to be the low risk area of Figure 36 based on P&W experience.

Structural analysis of the inducer indicates that the LCF life exceeds the design goal of 1000 cycles. The analysis is based on a geometrically scaled inducer model from an existing design. The model was modified to reflect actual blade thicknesses, and stress concentration factors (K_t) were conservatively established.

Blade vibrational analysis, Figure 37, indicates a 45 percent frequency margin for the blade's first bending mode at 4E. This is conservative, because the analysis did not account for centrifugal stiffening. Figure 38 shows the Campbell diagram for the inducer blade.

The impeller structural analysis was based on a two-dimensional (2D), finite element, body of revolution model with general boundary conditions applied, Figure 39. The analysis indicates that the impeller hub concentrated stresses are acceptable and result in an LCF life greater than 1000 cycles. The stresses, K_t, and the factors of safety are shown in Figure 40.

The impeller blade analysis is based on a modified impeller model. Although the model was geometrically scaled by the tip radius, actual shroud and blade thicknesses were used. The hub was fixed radially. Differences not accounted for include blade wrap angle and the number of blades. Further details are shown in Figure 41.

The results of the impeller blade stress analyses indicate the design is structurally adequate. The principal stresses are 61 ksi and −69 ksi at the trailing edge and hub interface. The factors of safety are 2.56 on yield and 3.19 on ultimate strength. The stress concentration factor for a 1,000 cycle life is 3.4.

Blade HCF capability was predicted using a modified Goodman diagram shown in Figure 42. The Goodman diagram was debited by the maximum allowable K_t of 3.4. At the steady stress of 69 ksi, the maximum allowable vibratory stress is 12.6 ksi. Based on P&W experience, this is adequate margin to proceed with the design. The actual vibratory stresses will be calculated during the final design phase of the program.

. Turbine Blisk and Shaft

The design of the AETB oxygen turbopump features a single-stage, full-admission, 50 percent reaction urbine with a 7.00-inch tip diameter. The preliminary turbine airfoil design is shown in Figure 43. Turbine fficiency is predicted to be 82 percent at the design point thrust of 25,000 pounds. The turbine disk is integral vith the rotor shaft to maintain rotor critical speed margin and IPS clearance control. The turbopump Campbell iagram, Figure 44, shows significant margins for the blade modes.

Turbine blisk analysis shows positive stress margins. A plastic analysis model (PWA deck 5138) was loaded vith cavity pressures, rotor speeds, rim loads, and temperature gradients. Bore stresses are 61 ksi radial resulting n a burst factor of 1.49. Due to time constraints, the disk LCF life has not been calculated, but, based on the ow stress levels, LCF life is not considered to be a problem.

Blade thermal mechanical fatigue is a concern as well as disk axial thermal gradients. For both problems he internal conditioning of the pump prior to engine start, during operation, and at shutdown, must be studied ınd may have to be controlled to meet life requirements.

The LO_2 turbine blades are similar in size and shape to the fuel pump turbine blades and turn at approximately ıalf the speed. Therefore the stresses are expected to be below the fuel pump blade stresses.

i. Interpropellant Seal (IPS)/Vaporizer

The amount of LO_2 leakage in the IPS is driven by the density of the oxygen entering the IPS. Reducing the lensity reduces the oxygen lost overboard. Therefore, a vaporizer, modeled after one that has been successfully lemonstrated in the SSME/ATD LO_2 turbopump vaporizer, is incorporated in the design. Although the vaporizer equires additional turbine power of 38 horsepower (hp), trade studies showed the additional power to be ıcceptable and the oxygen lost overboard was reduced by 90 percent.

Trade studies were conducted to optimize the number of knife edges, diameters, and clearances. The current configuration is a blend of all the beneficial features that could be incorporated without compromising other mportant design features. For instance, the improvement gained from adding one more knife-edge was offset y a decrease in rotor critical speed margin caused by the resultant increase in rotor length. Another example s that the decrease in seal diameter and rotor diameter at the same time would decrease rotor stiffness and lecrease the chances of maintaining tight seal clearances.

The IPS package consists of a helium dam with 11 knife-edges on the hydrogen side and 10 on the oxygen side. Concern about rubbing in LO_2 led to limiting the radial clearances for the oxygen side of the IPS to).005 inch. Leakage control requirements necessitated the use of 0.003-inch radial clearances on the hydrogen side of the IPS.

Additional benefit on the LO_2 side was gained from the incorporation of a stationary vane system upstream f the vaporizer. This vane counteracts the pumping action on the backside of the vaporizer and reduces the lownstream pressure. The lower pressure results in less leakage overboard.

'. Bearings

The first approach to the rotor support design consisted of two 24-mm ball bearings for axial load control ınd a single 27-mm roller bearing for radial stiffness and critical speed margin, Figure 45. Many bearing onfigurations were evaluated. . As the LO_2 turbopump design developed, the rotor size increased, as did the earing loads. To maintain design parameters within current experience levels, the ball bearing size was increased to 35 mm. This bearing design is very similar to a bearing used in the P&W RL-10 rocket engine. The RL-10 test and operating experience adds significant credibility and confidence to the design.

Material selection for each bearing was based on its location. For bearings exposed to liquid oxygen, 440C steel was chosen for the application based on experience and LO_2 compatibility tests. This choice creates a design hardship with the bearing inner races. When the race is installed on the A286 shaft, the required fit for anti-rotation is so tight that the bearing race has a limited shelf life. However, material processing and design changes have improved the life expectancy of the bearing inner race to acceptable levels. Bearing coolant flows are provided through constant area orifices and are sufficient to achieve the desired bearing life of five hours.

8. Housing

The pump housing design features vaneless volutes. The pump discharge volute, shown in Figure 46, is double discharge for reduced radial loads. The turbine inlet and exit volutes, shown in Figure 47, are single inlet and exit to provide high efficiency and low losses. A unique configuration was developed to allow the turbine volutes to be more easily produced. The two volutes are a semicircular design originating at a parting line in the turbine housings. The strategic location of the parting lines allows these volutes to be machined with conventional techniques.

The pump discharge volute is a traditional configuration that will be produced in two halves and welded together. The original concept called for the two halves to be separate pieces and be axially loaded by the housings; however, analysis showed that the pressure and thermal loadings were too high to consider this a viable design.

The major structural housings, Figure 48, are structurally robust, reflecting the test rig approach to the design. The robustness of the housings adds radial and axial stiffness to the rotor, providing increased confidence to critical speed predictions.

The thermal gradients in the housings are significant and preliminary analysis indicates some isolated high-stress areas. Minor configuration changes may be needed during the final design phase. To maximize turbine efficiency, a tip clearance control scheme, shown in Figure 49, has been added to provide thermal conditioning to achieve the required diameter for proper turbine tip clearances. Thermal mechanical fatigue (TMF) is also a consideration in the turbine inlet duct. Super A286 material is used to enhance TMF life.

9. Structural Analysis

Preliminary structural analysis was completed for several of the AETB LO_2 turbopump components. The components analyzed include the inducer blade, the impeller blade and hub, the turbine disk, and the turbine inlet housing.

Structural analysis of the inducer blade included a 2D finite element plate model for blade stresses and vibratory responses. Results indicate that the blade aerodynamic design will meet all structural requirements. Hub analysis is pending.

Analysis of the impeller consisted of a finite element 2D body-of-revolution model for hub stresses and a 2D plate model in space for blade stress estimates. All analyses of the impeller are favorable.

A 2D bending analysis of the turbine disk was completed. Initially, axial thermal gradients caused unacceptable axial deflections, indicating a need to change the internal flow scheme around the turbine. The current flow scheme eliminates the disk axial gradient, and analysis indicates acceptable stresses and deflections. A plastic/residual membrane stress analysis shows adequate burst margin for the disk, Figure 50.

A 2D boundary element analysis program (BEASY) was used to generate thermal gradients for the turbine ılet housing based on predicted surface temperatures and film coefficients. A 2D finite element structural analysis 'as then used to predict the thermal stresses and deflections as shown in Figure 51. The analysis pointed out ne location that was overstressed due to the thermal gradient. A more detailed thermal model is currently being onstructed which will determine the validity of this preliminary analysis. Thermal conditioning of the housings ıay be needed to achieve the desired durability at all locations.

0. Thrust Balance

In an early version of the LO_2 pump design, rotor thrust balance was controlled through the use of a thrust alance piston. This thrust balance piston generated balance loads through the use of high-pressure hydrogen from ıe third-stage fuel pump discharge. Subsequent internal flow and cycle analysis predicted that the flows required) make the thrust piston work would have a significant detrimental effect on cycle efficiencies. Therefore, the ırust balance piston was eliminated and the axial loads are transmitted through the ball bearings.

The axial loads on the LO_2 rotor were balanced at the 25K thrust level by adjusting seal diameters and lightly changing the turbine reaction. Thrust loads have been calculated at the 4K thrust level and are less than 00 lbf. At the 4K thrust level, the rotor rpm and bearing cooling flow rates are such that the ball bearings are apable of operating with the 500 lbf axial load.

1. Instrumentation

A preliminary instrumentation plan has been formulated for the oxygen pump. The plan includes nstrumentation for control, safety, and performance. Figure 52 is an instrumentation schematic for oxygen ump acceptance testing.

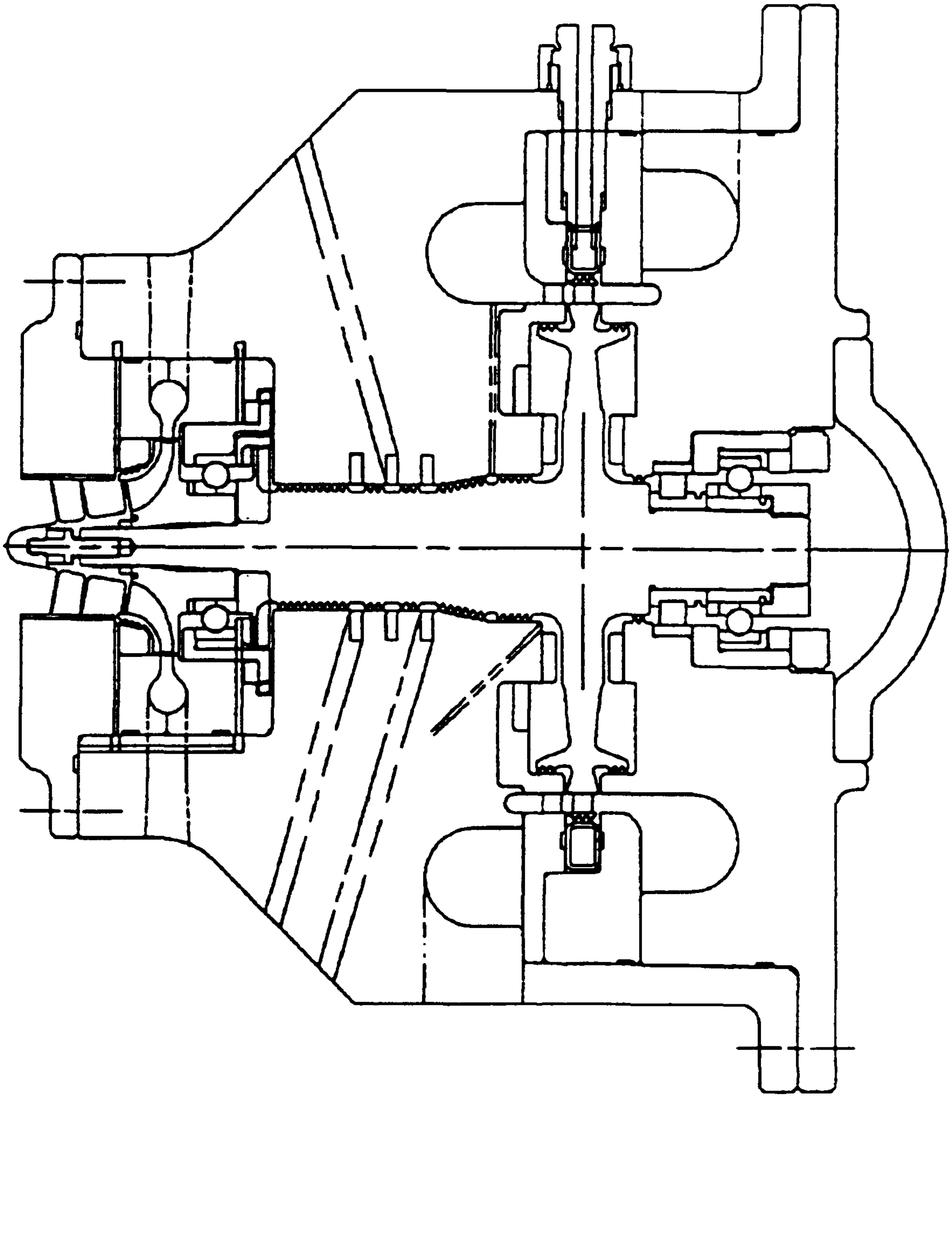

Figure 25. Liquid Oxygen Turbopump

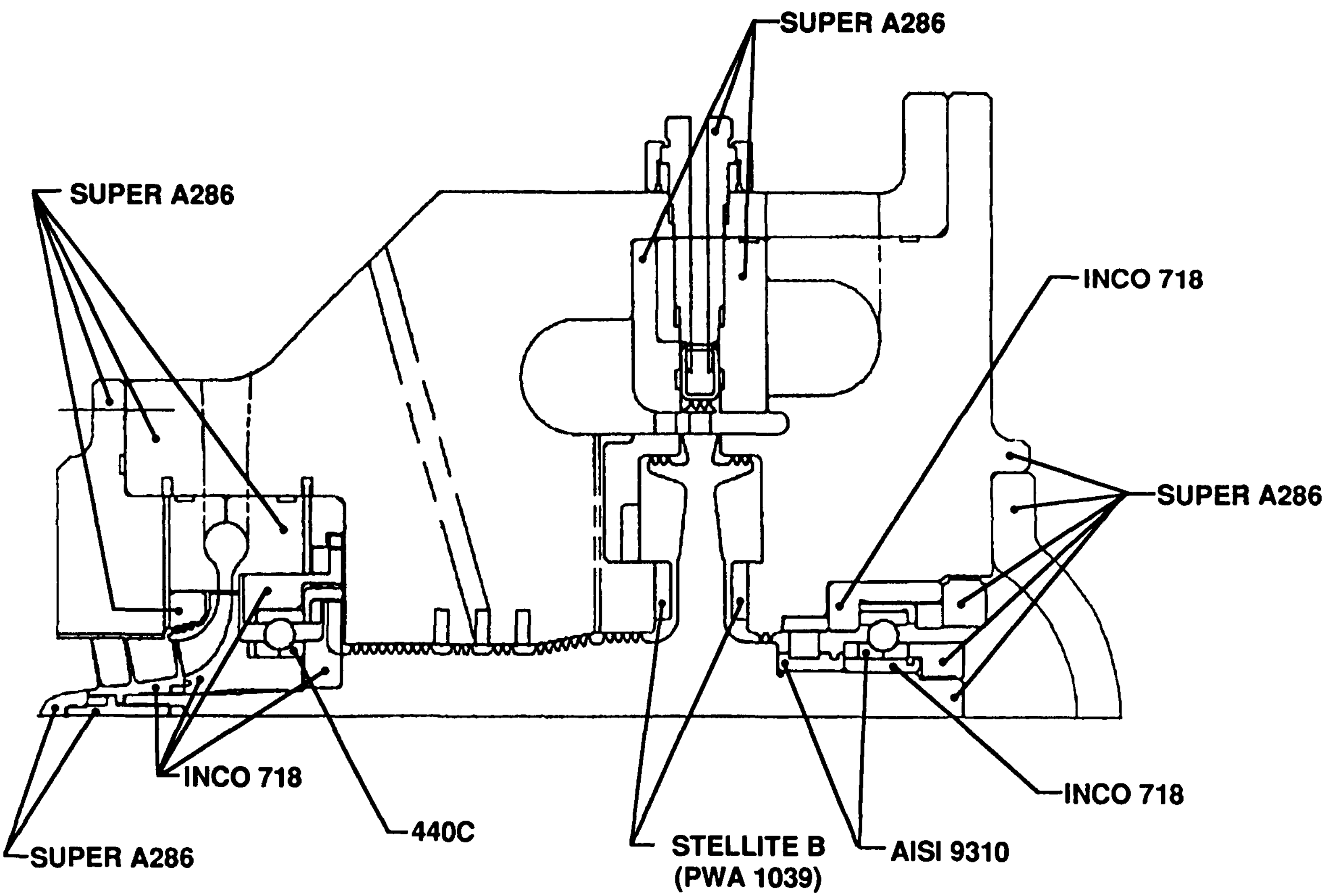

Figure 26. Liquid Oxygen Turbopump Materials

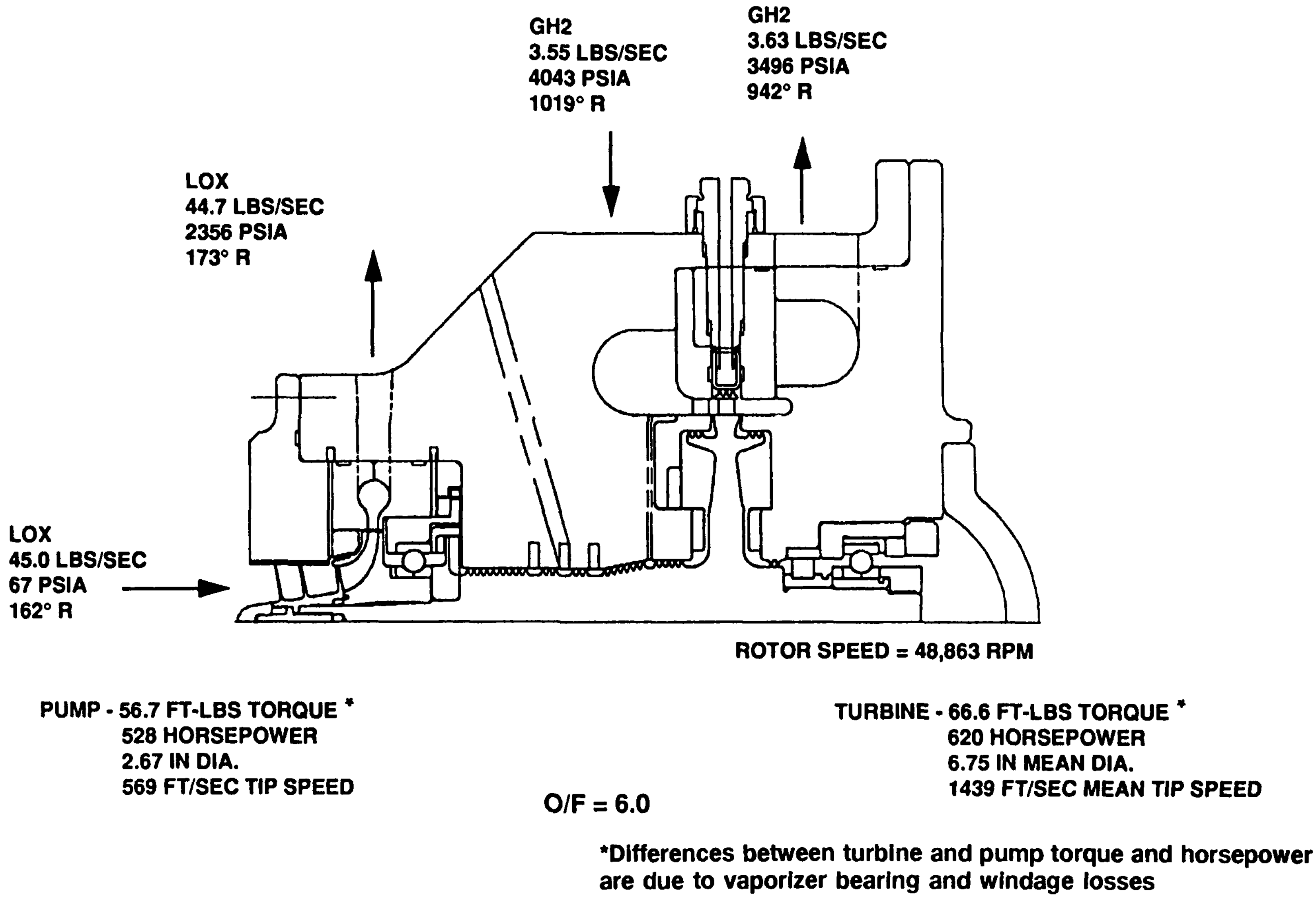

Figure 27. Liquid Oxygen Turbopump Design Parameters

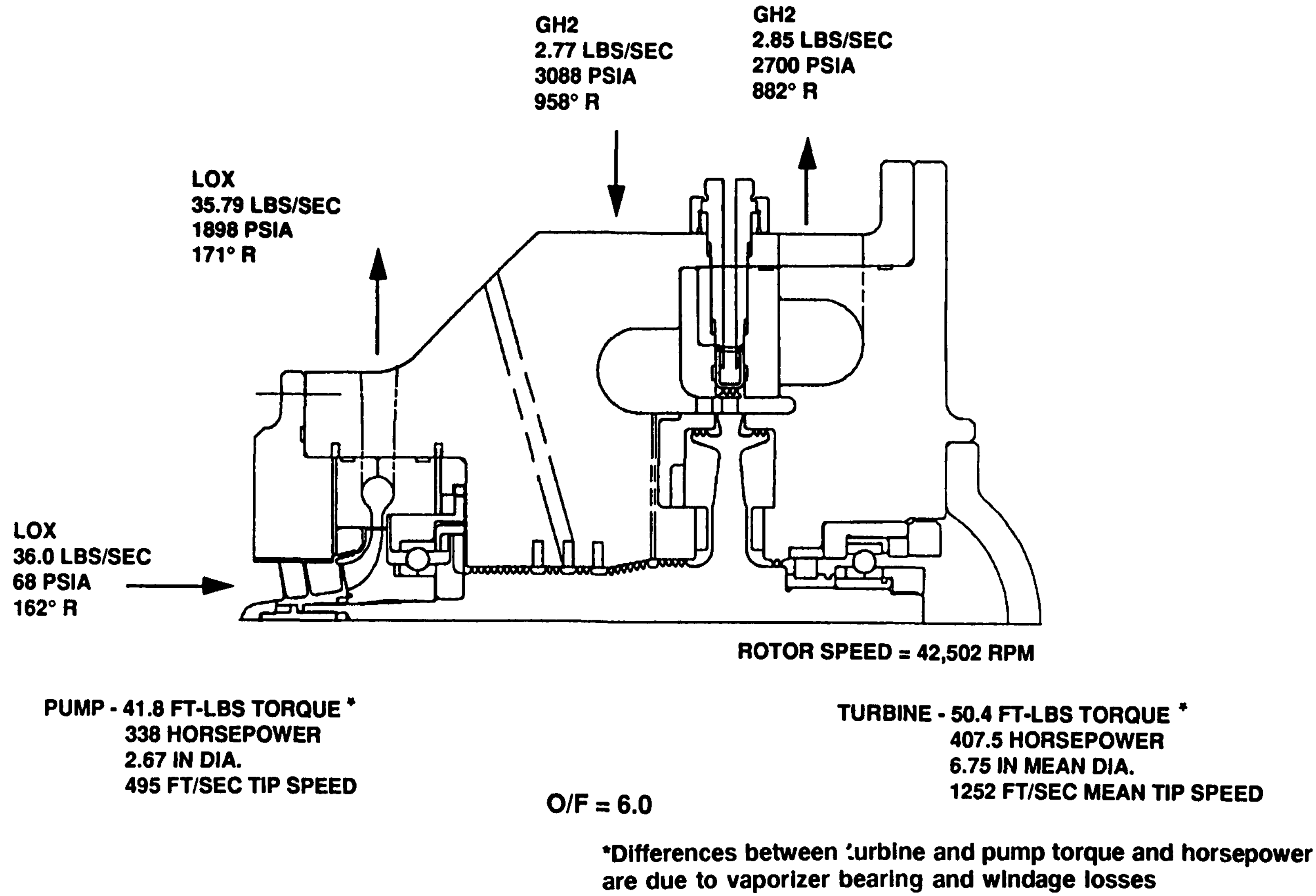

Figure 28. Liquid Oxygen Turbopump Operating Parameters at 20K Thrust

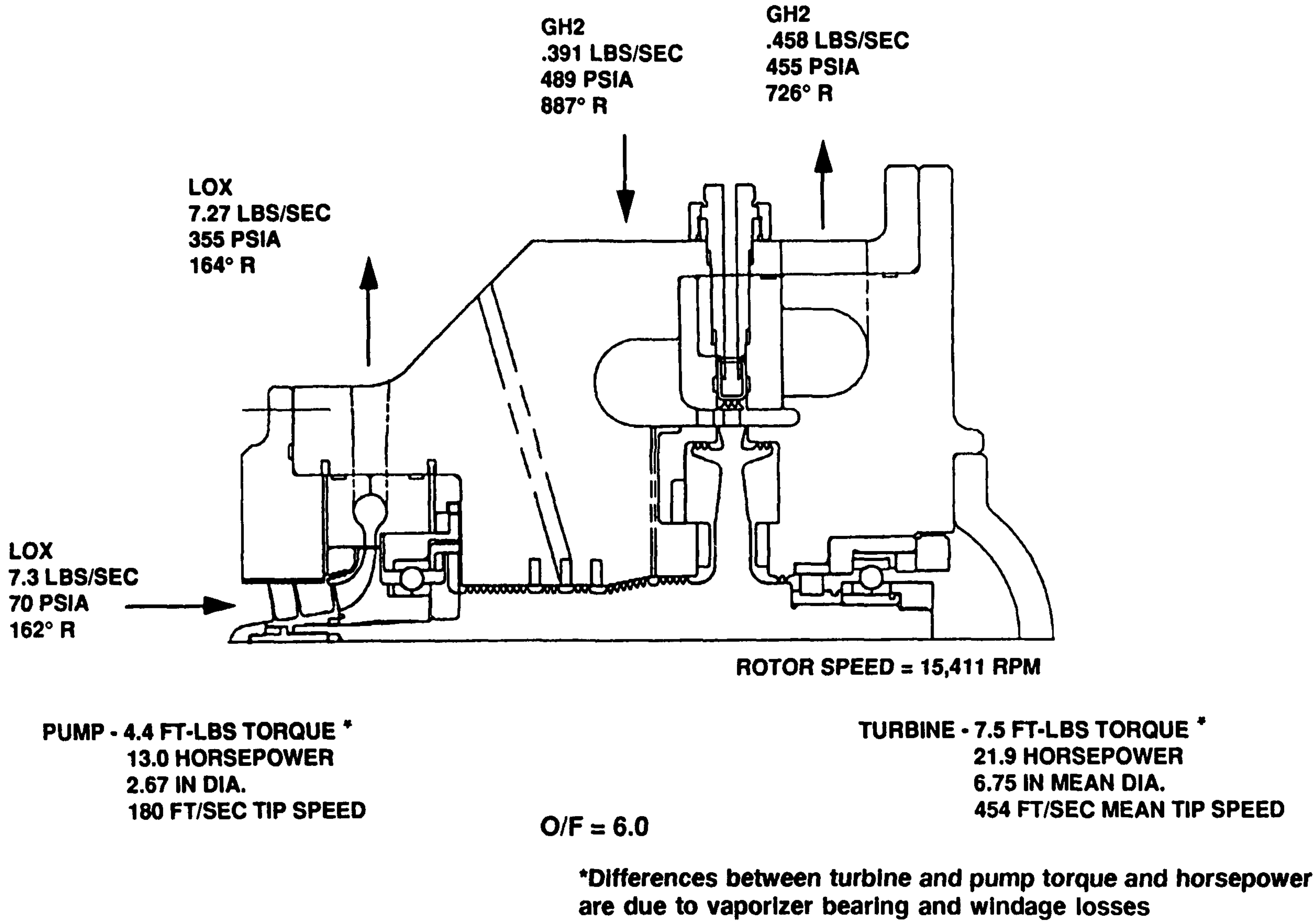

Figure 29. Liquid Oxygen Turbopump Operating Parameters at 4K Thrust

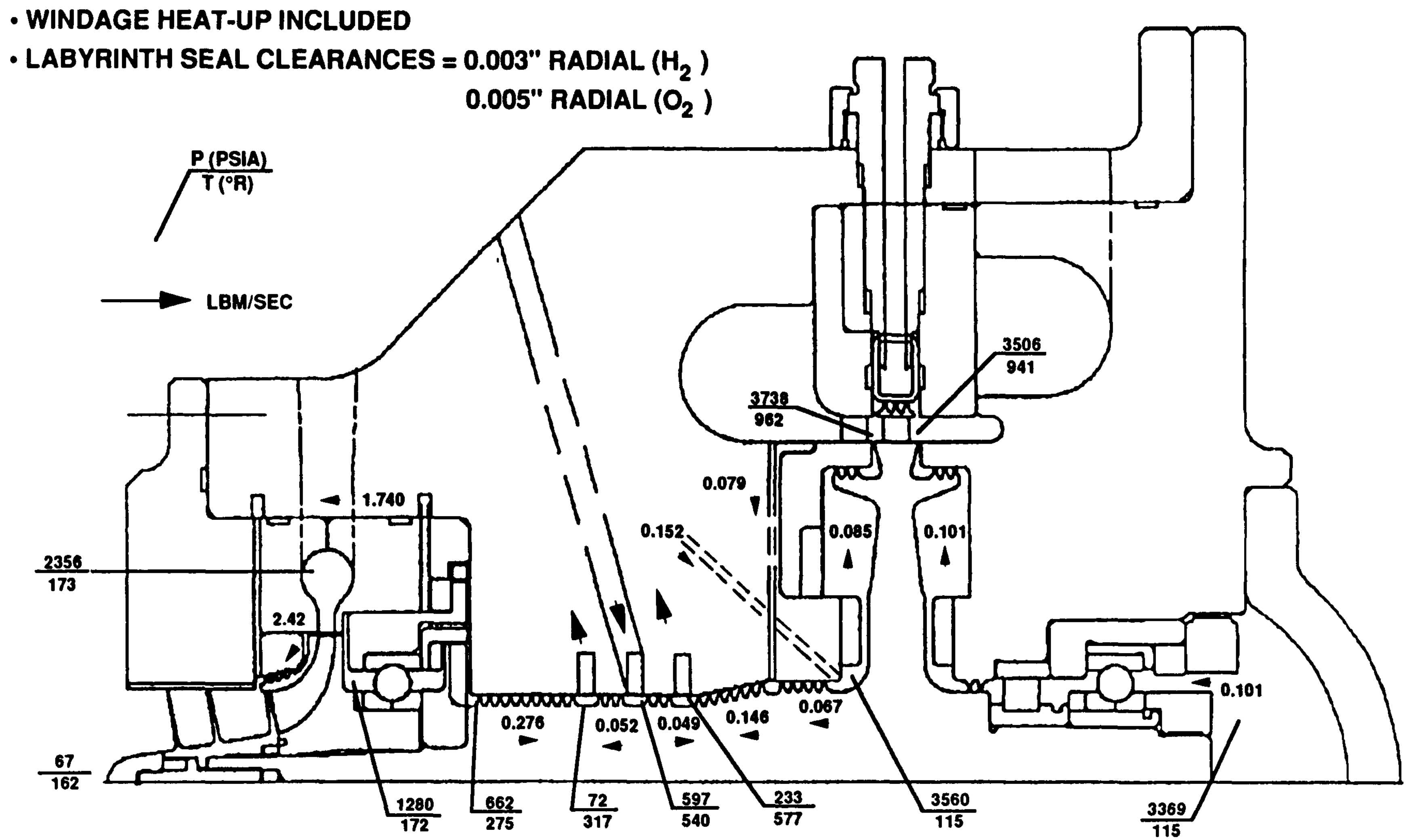

Figure 30. Liquid Oxygen Turbopump Internal Flows at Design Point

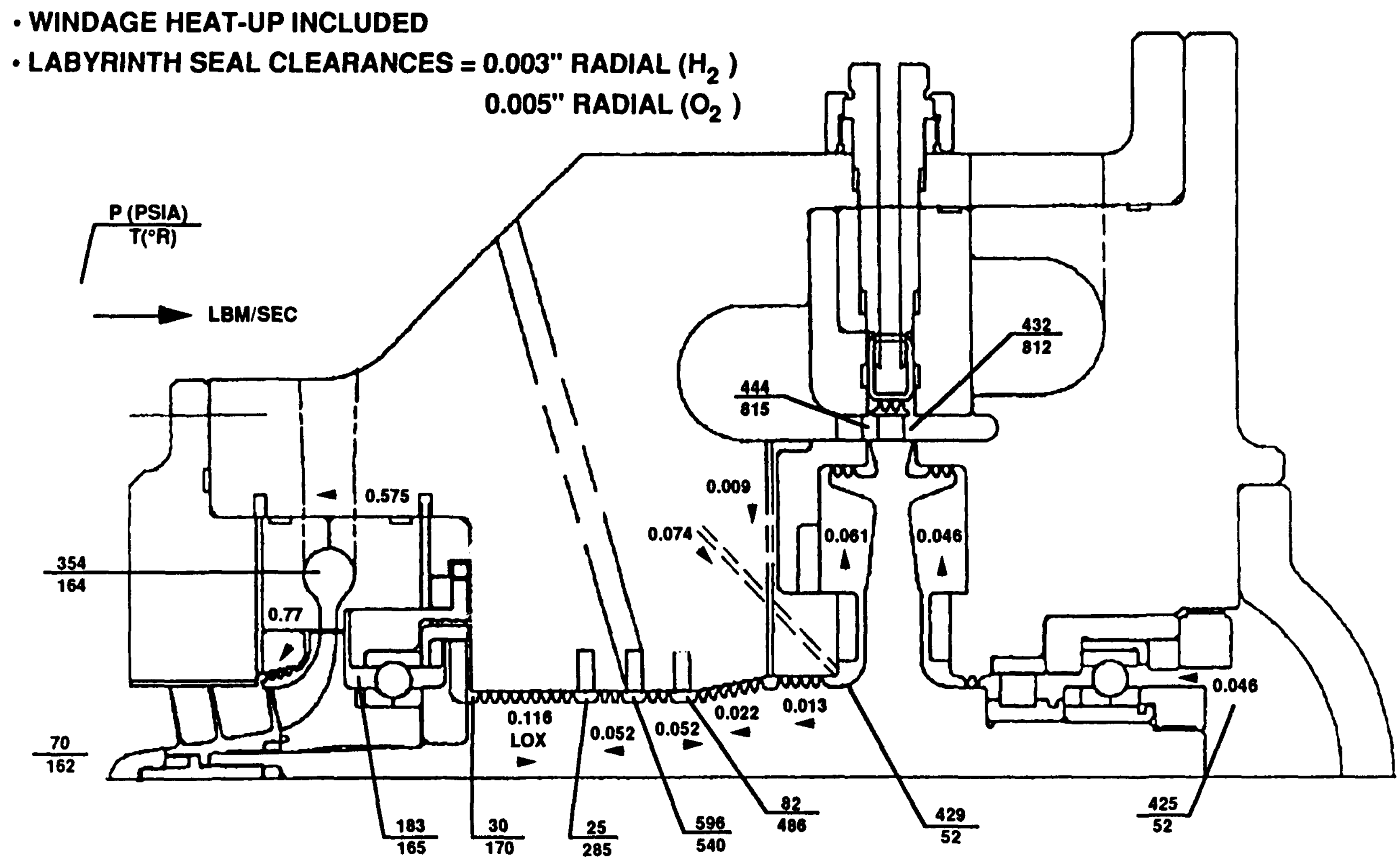

Figure 31. Liquid Oxygen Turbopump Internal Flows at 4K Thrust

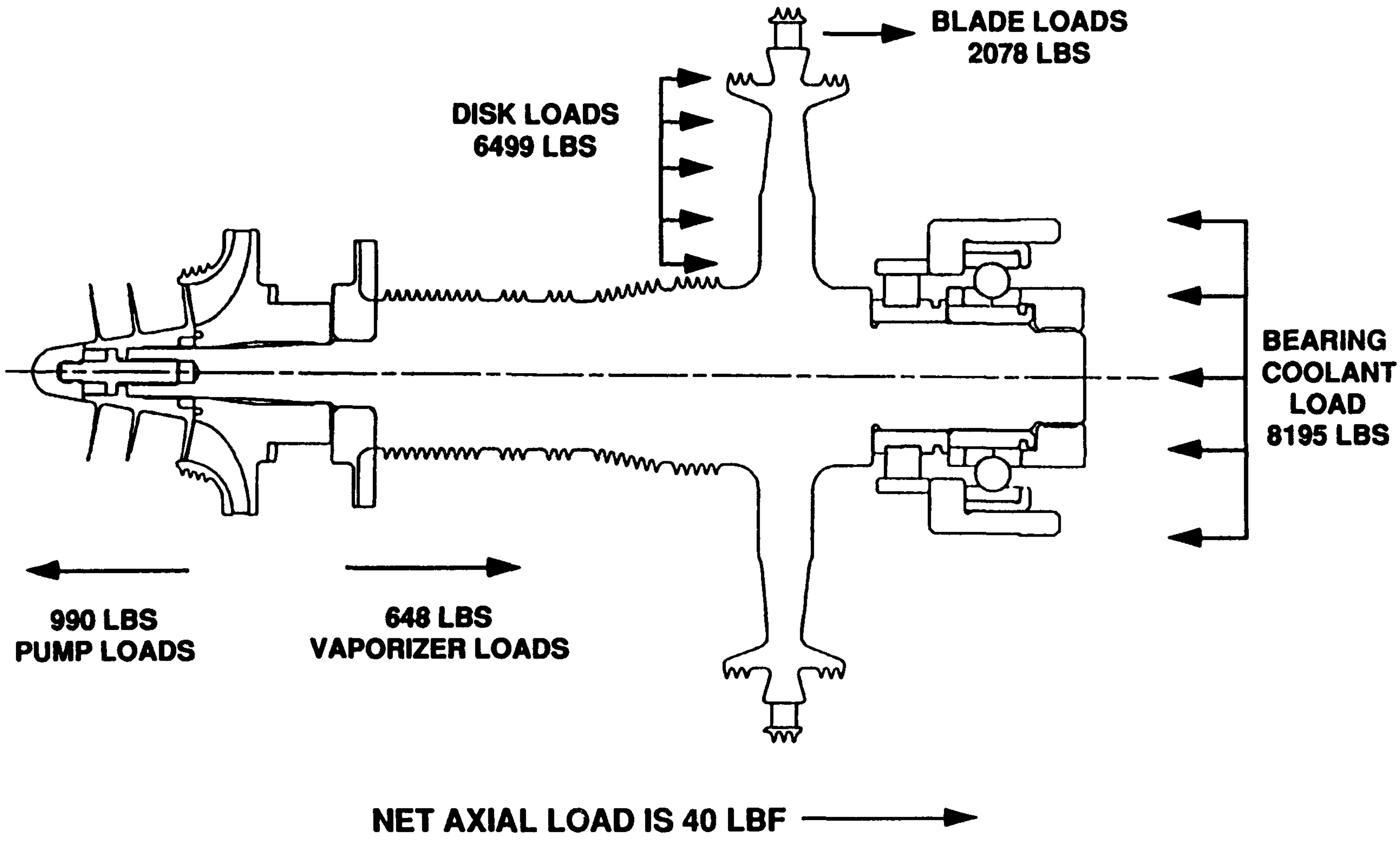

Figure 32. Liquid Oxygen Turbopump Design Point Thrust Balance

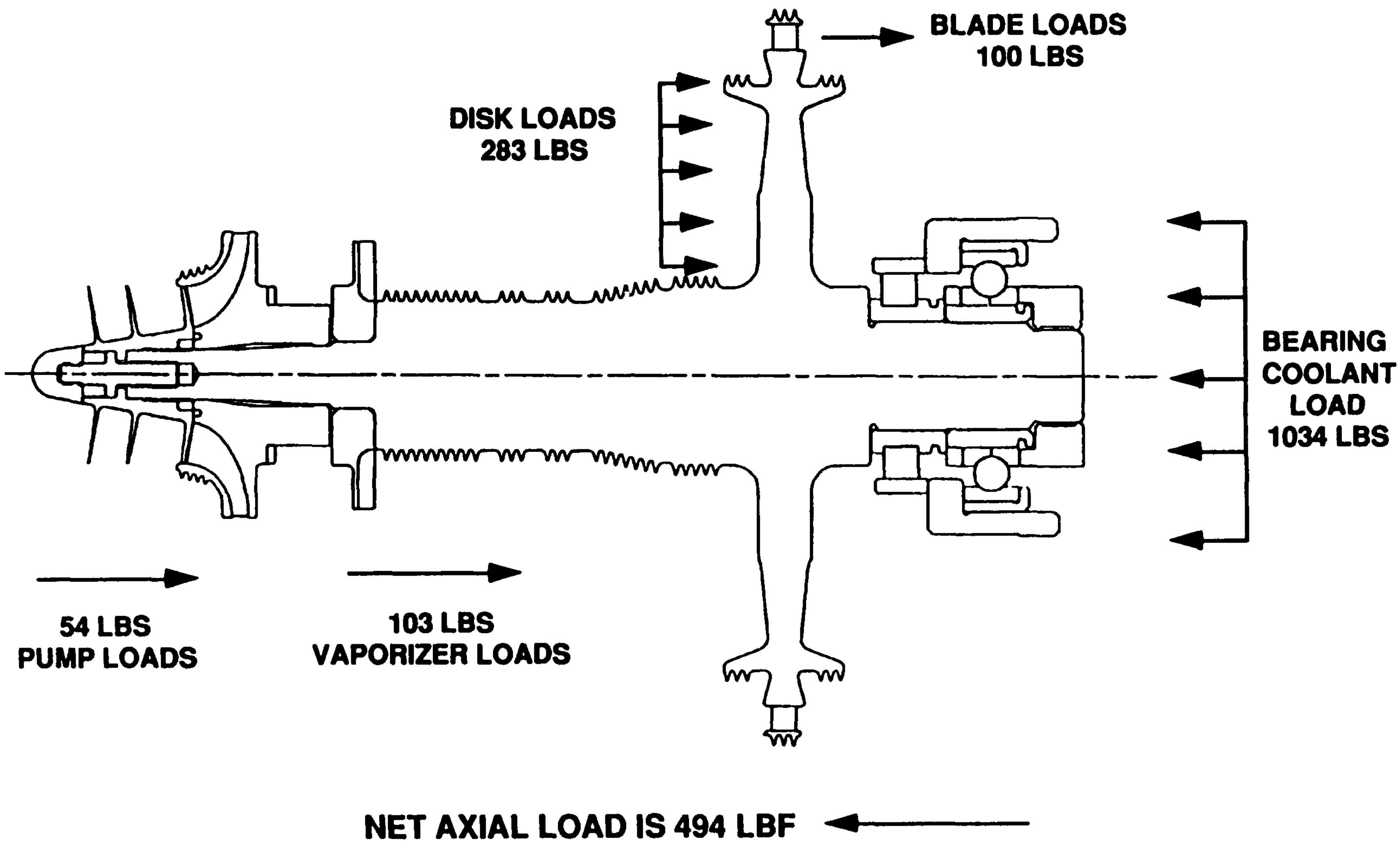

Figure 33. Liquid Oxygen Turbopump Thrust Balance at 4K Thrust

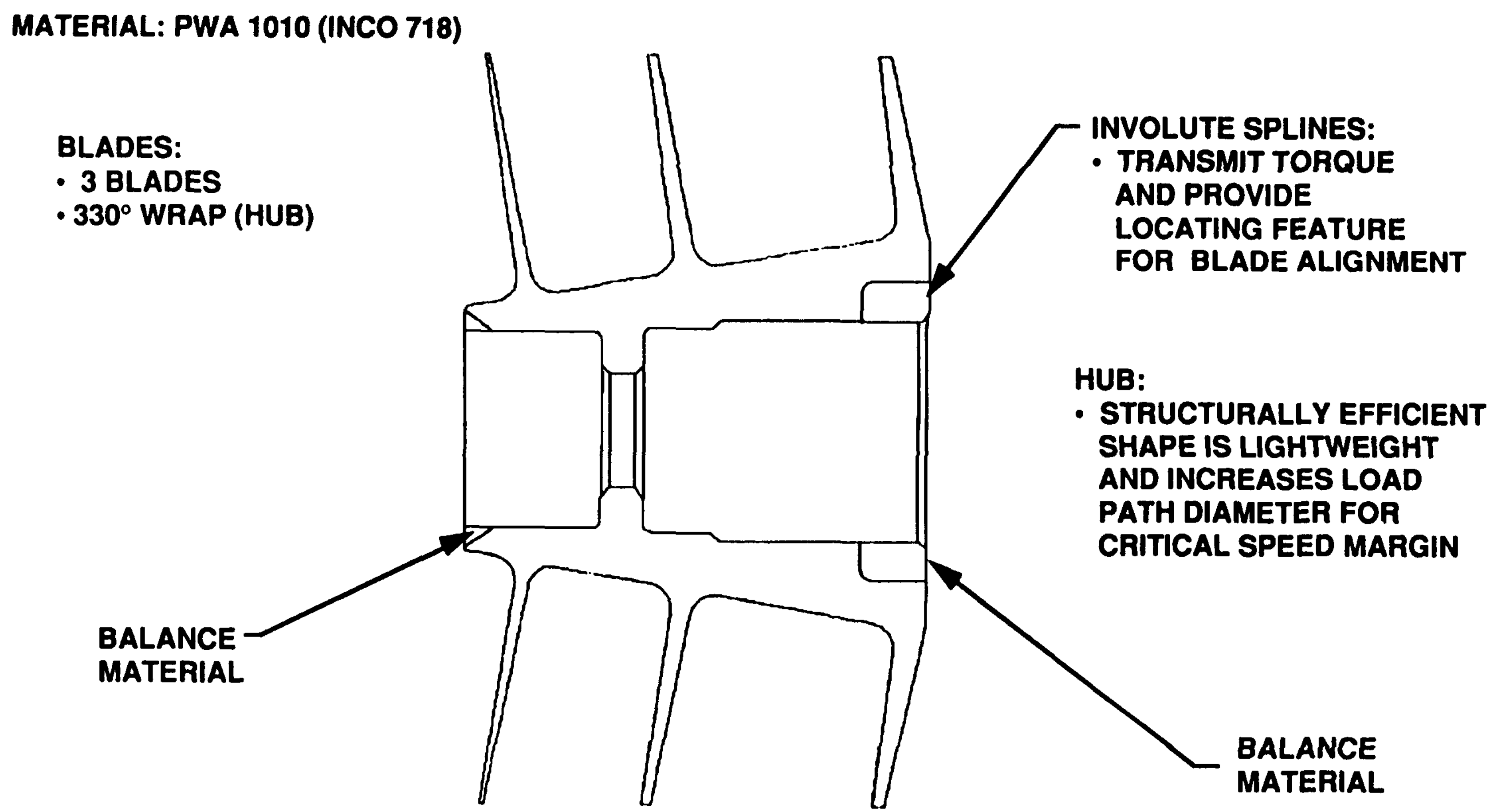

Figure 34. Liquid Oxygen Turbopump Inducer

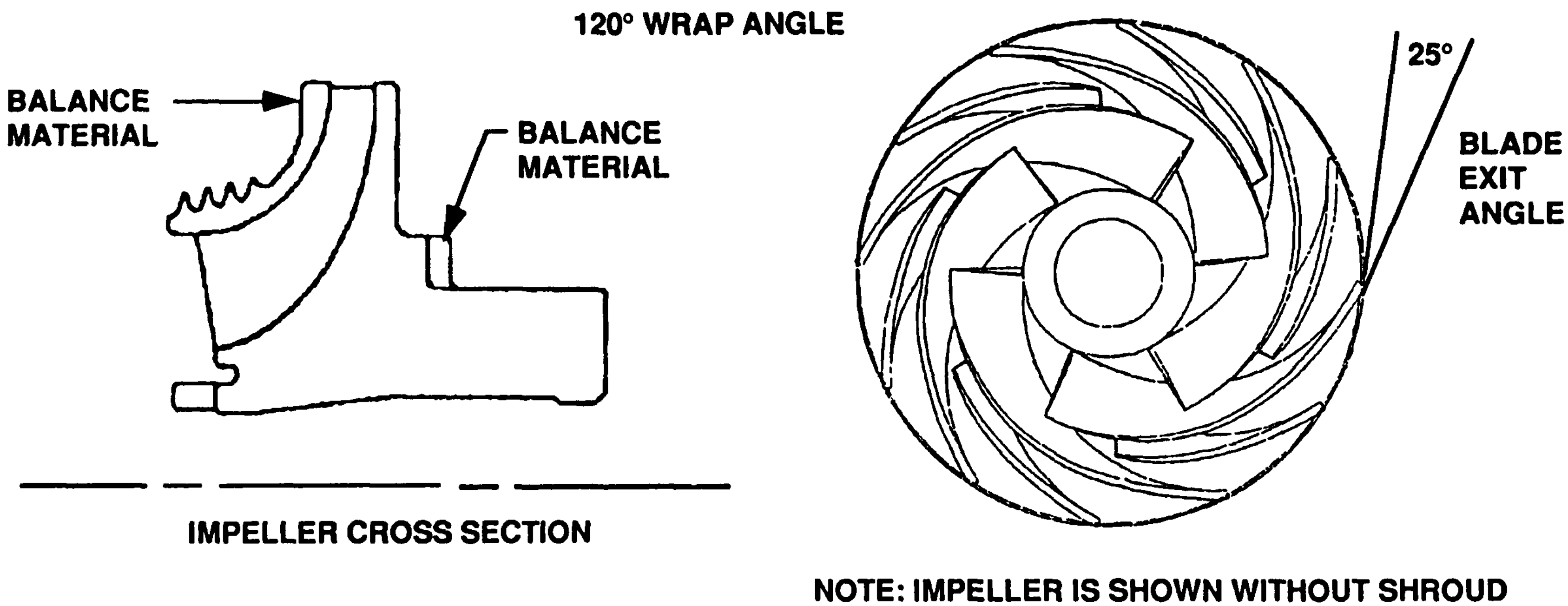

Figure 35. Liquid Oxygen Turbopump Impeller

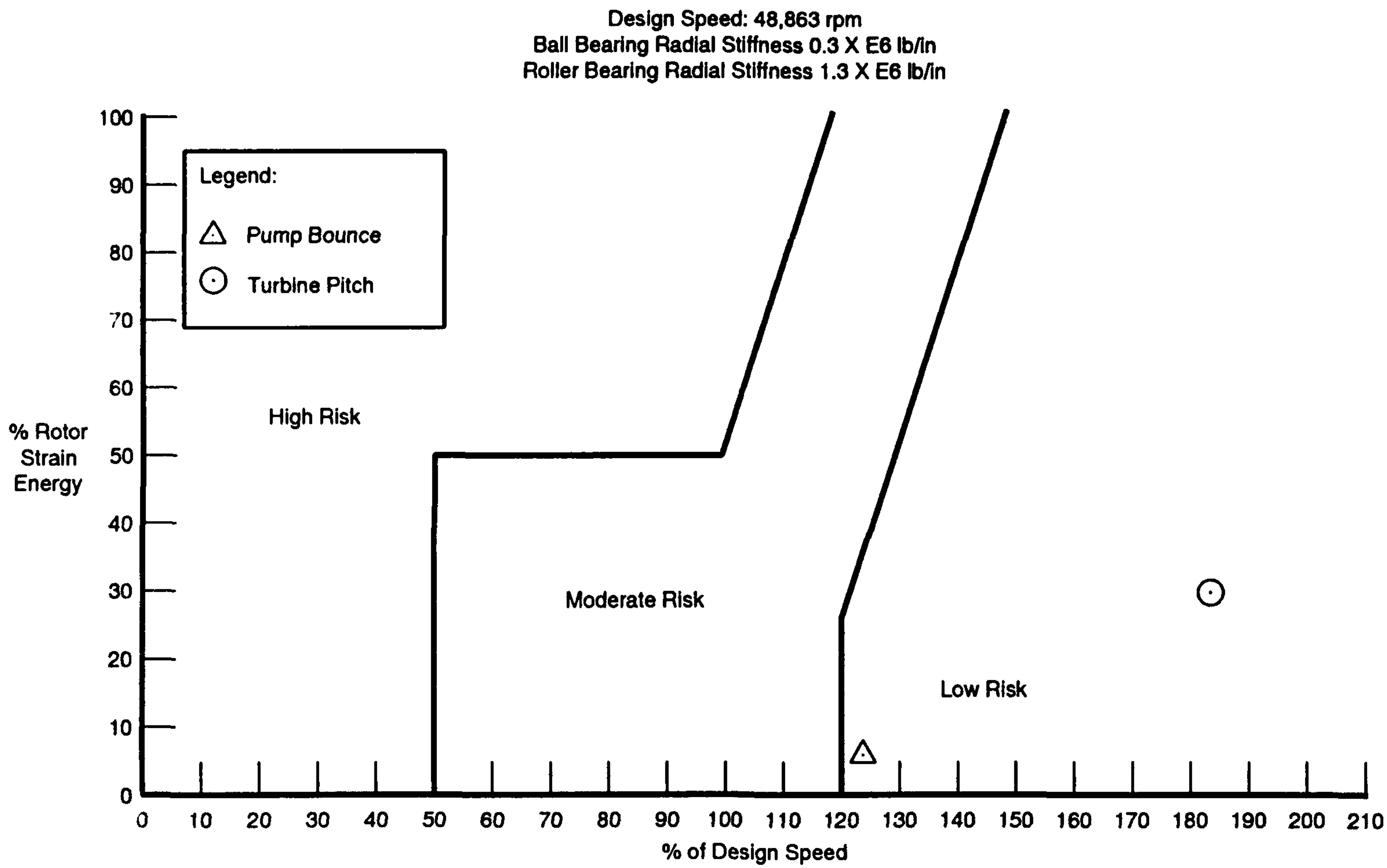

Figure 36. Rotordynamic Analysis

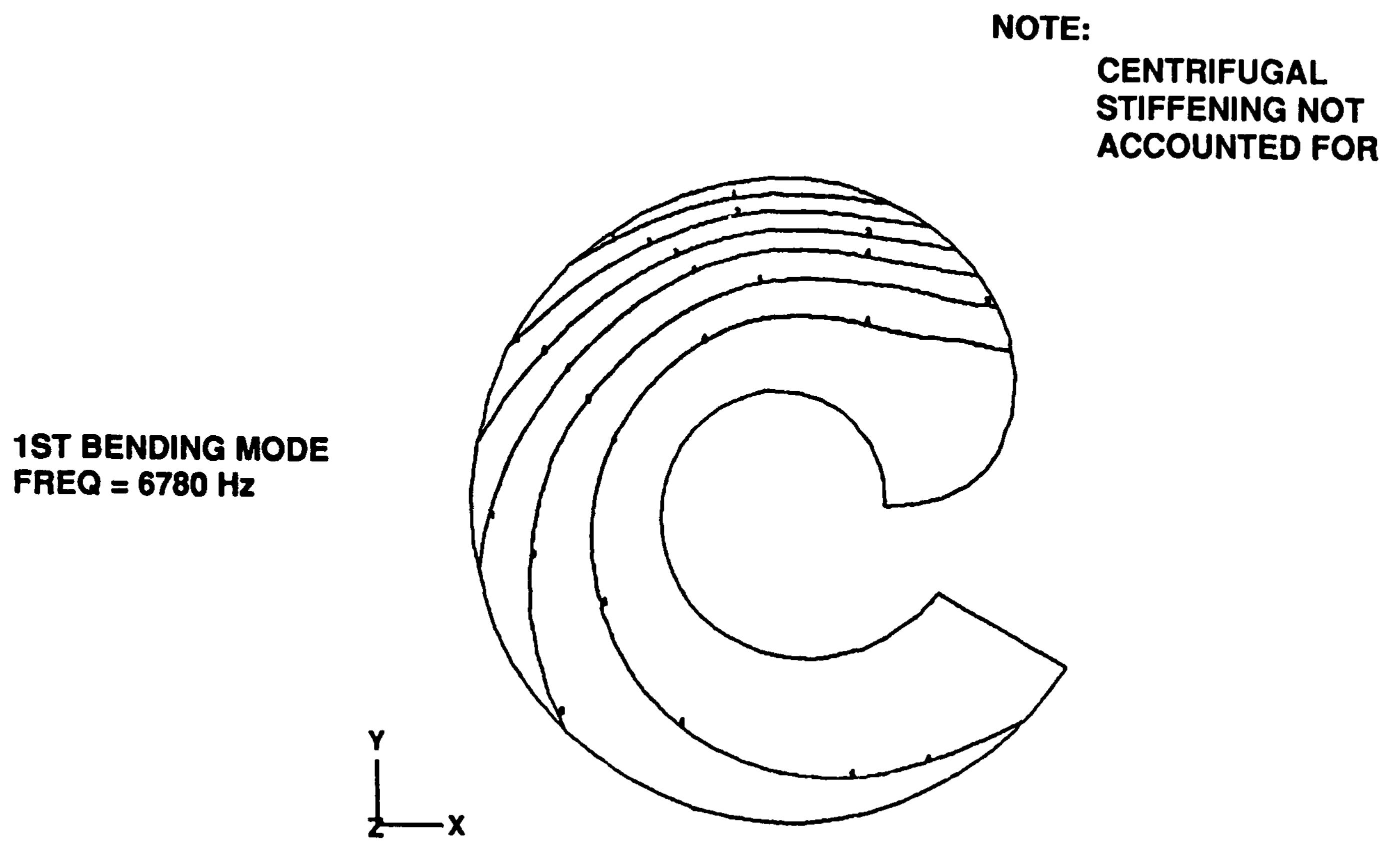

Figure 37. Liquid Oxygen Turbopump Inducer Blade Vibration Analysis Showing Lines of Constant Deflection

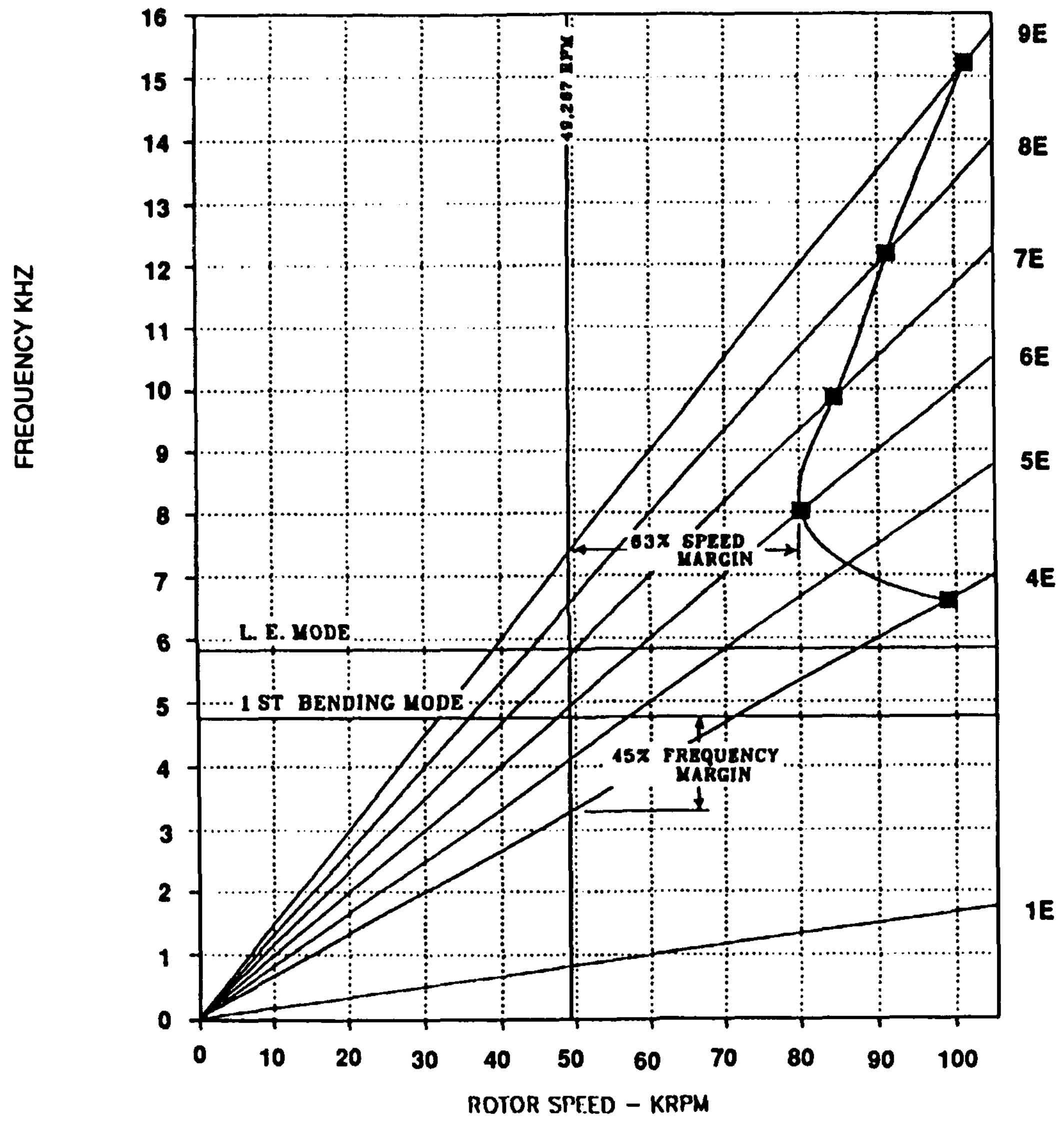

NOTE:
Both centrifugal stiffening and operation in LO_2 accounted for.

Figure 38. Liquid Oxygen Turbopump Inducer Blade Campbell Diagram

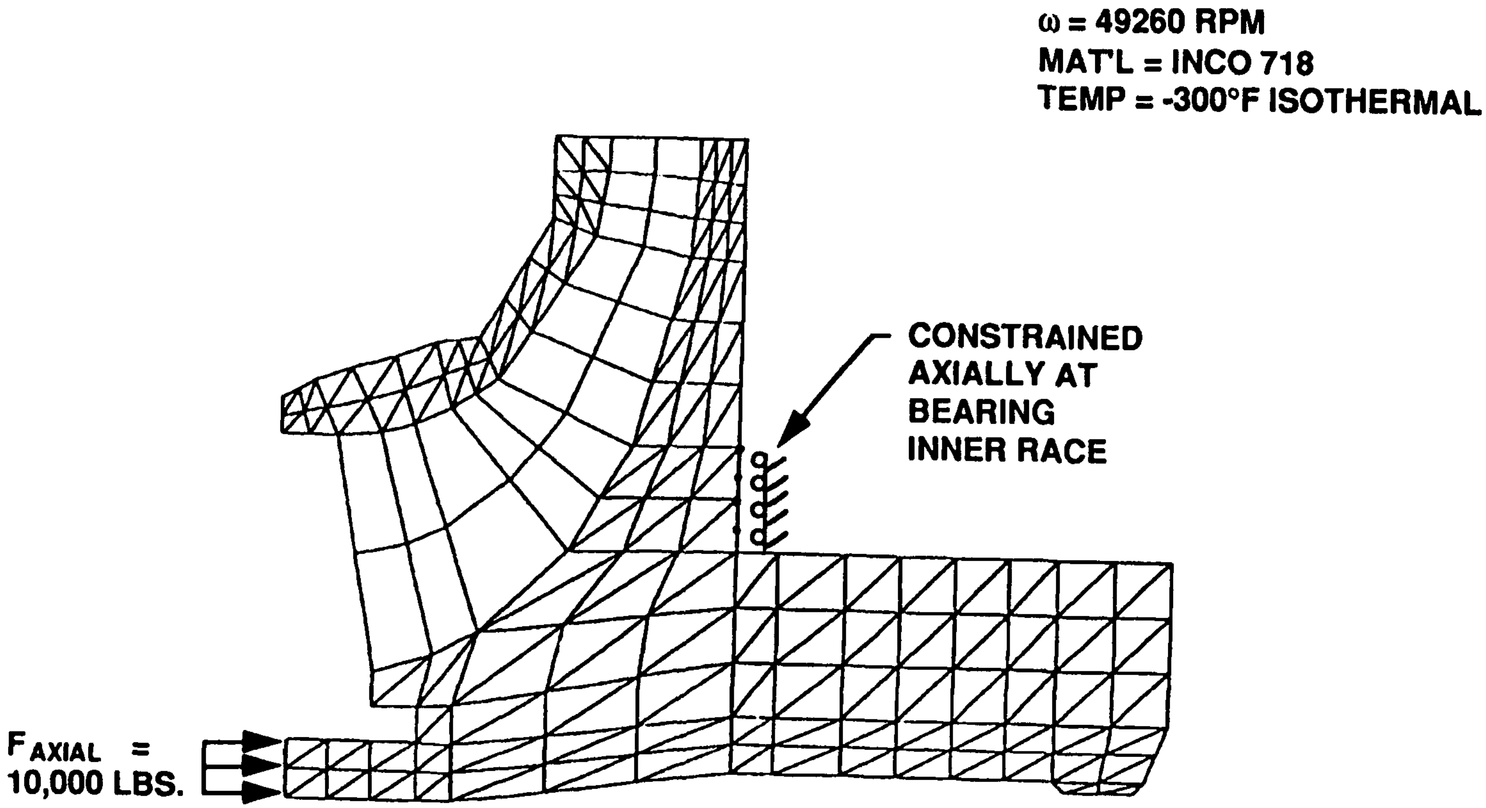

Figure 39. Liquid Oxygen Turbopump Impeller Body of Revolution Hub Model

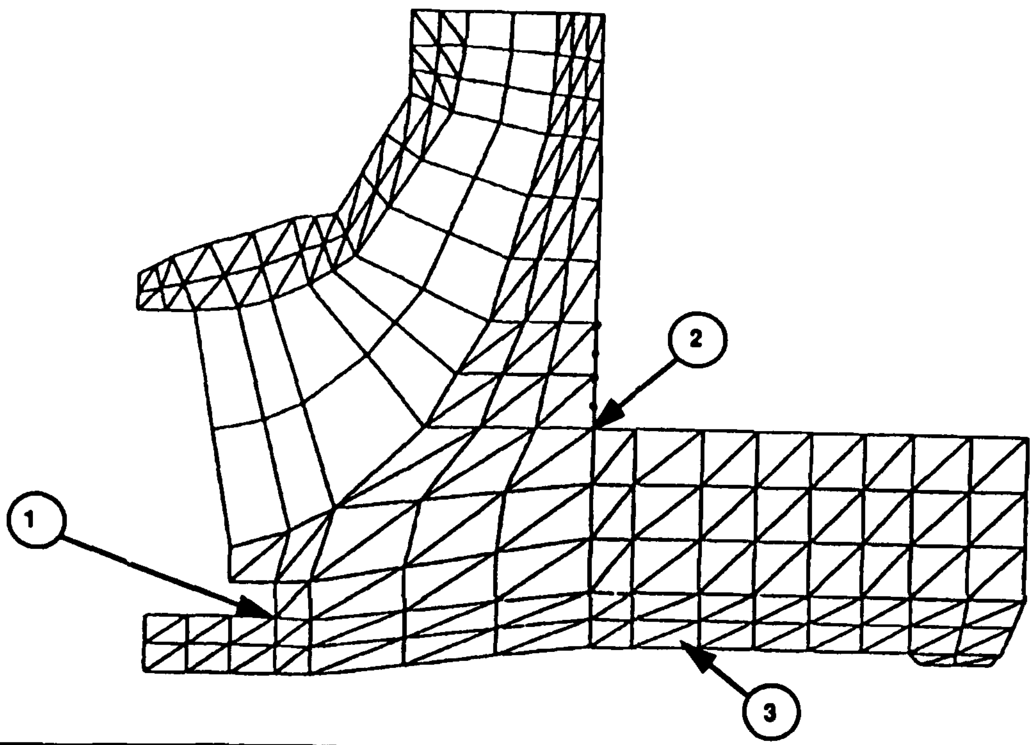

LOC.	σ (Ksi)	TYPES OF STRESS	TEMP (°F)	σ Y	σ ULT	FS_Y	FS_{ULT}	K_T CALCULATED	LCF LIFE (CYCLES)
1	-60	MIN.PRIN.	-300	177	220	2.95	3.67	1.97	>1000
2	32	MAX.PRIN.	-300	177	220	5.53	6.87	2.20	>1000
3	35	VON MISES	-300	177	220	5.06	6.28	1.00	>1000

Figure 40. Liquid Oxygen Turbopump Impeller Body of Revolution Hub Model Results

- ATD IMPELLER PLATE MODEL MODIFIED TO PREDICT STRESSES
  - ATD DIMENSIONS SCALED BY TIP RADIUS
  - SHROUD THICKNESS = .050"
  - BLADE THICKNESS = .050"
  - RPM = 49270
  - FIXED RADIALLY AT HUB

DIFFERENCES NOT ACCOUNTED FOR:

- WRAP ANGLE ATD = 70° AETB = 120°
- # OF BLADES ATD = 4/4 AETB = 6/6

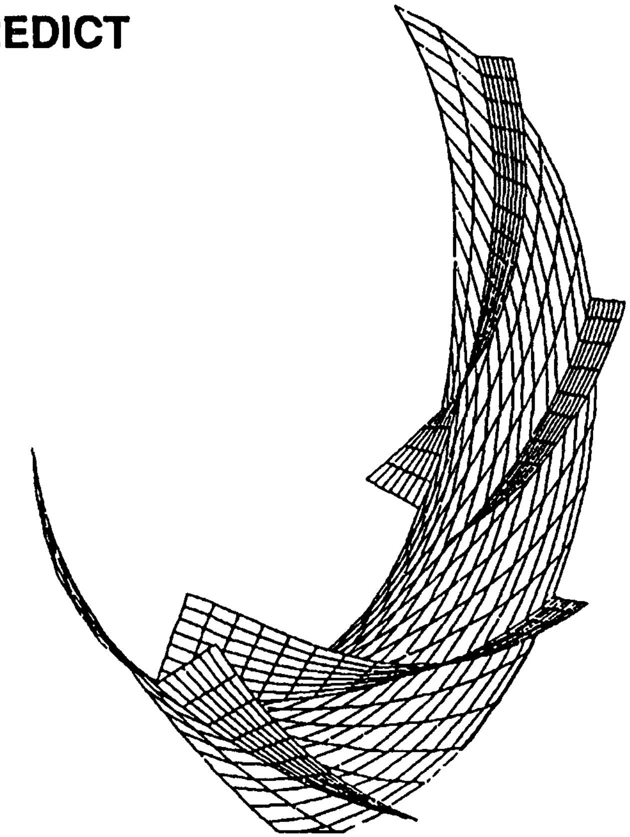

FINITE ELEMENT MODEL

Figure 41. Liquid Oxygen Turbopump Impeller Blade Stress Estimates

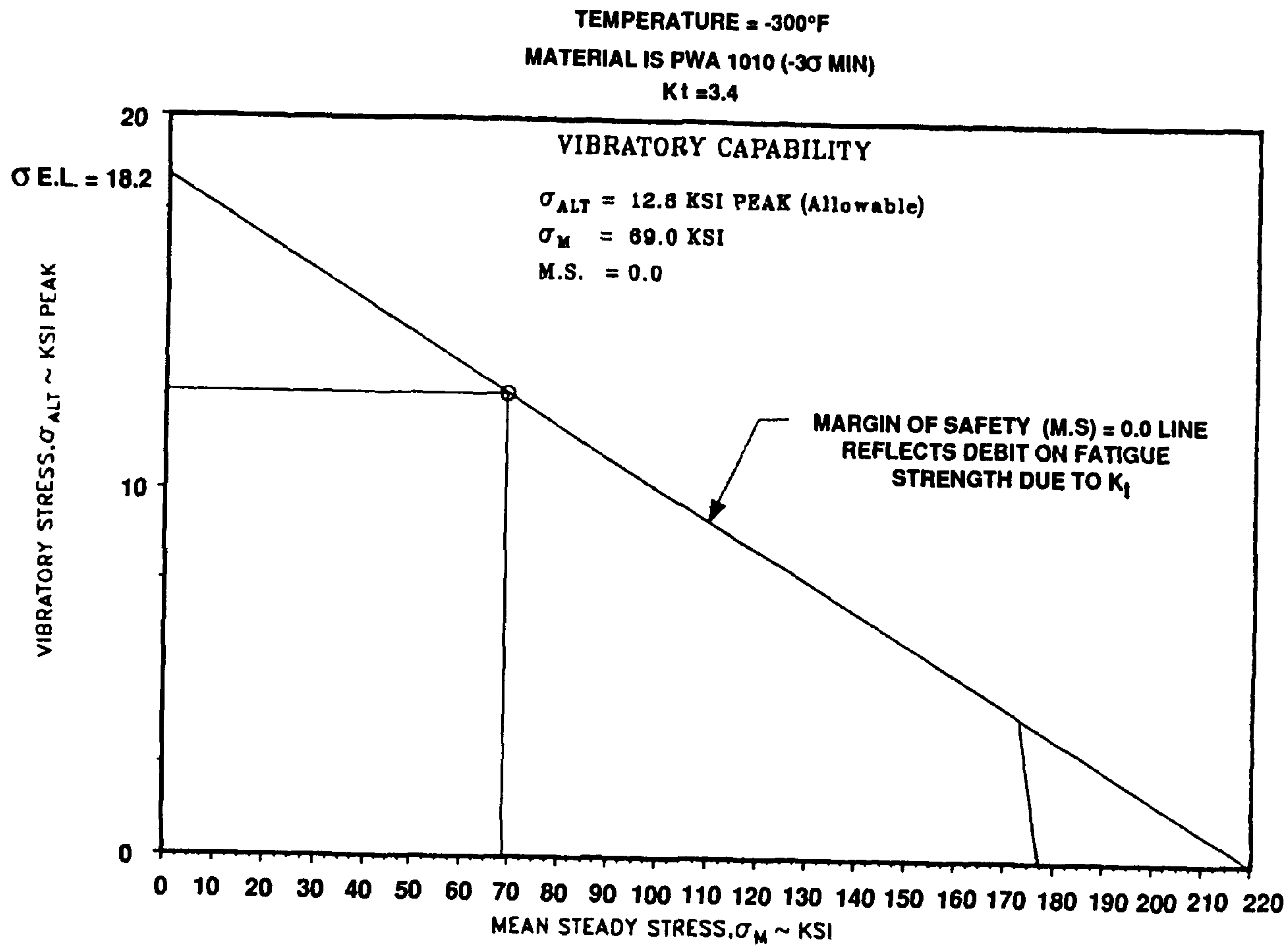

NOTE: IF MARGIN OF SAFETY > 0.0, DESIGN MEETS CRITERIA

Figure 42. Liquid Oxygen Turbopump Impeller Blade Vibratory Stresses

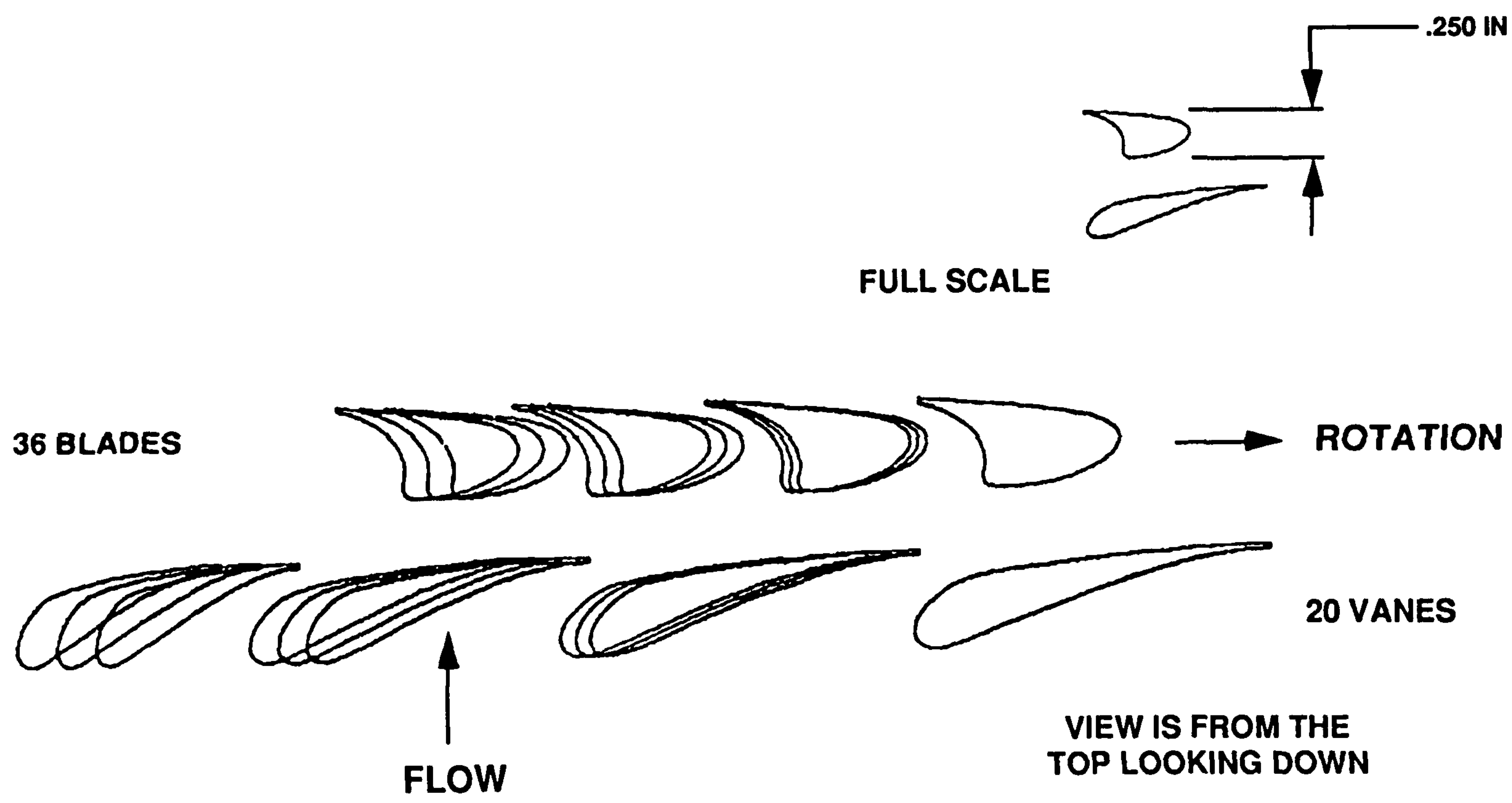

Figure 43. Turbine Airfoils

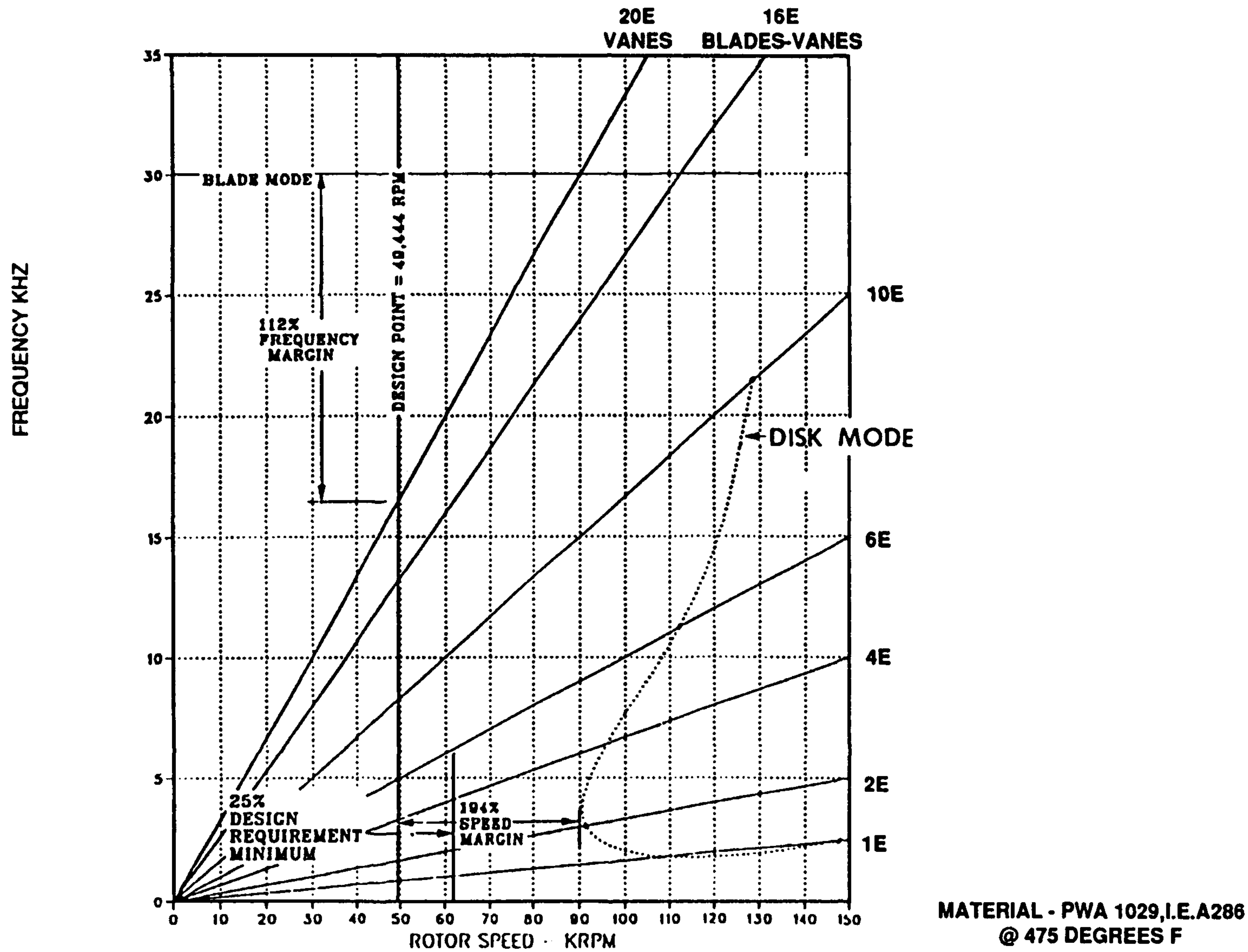

Figure 44. Turbine Disk Campbell Diagram

UTILIZES TWO BALL BEARINGS AND A ROLLER BEARING

LOX PUMP BALL BEARING

- LOX COOLED (2.0 PPS)
- DN 1.75M
- 440C MATERIAL
- BRONZE / PTFE CAGE (SALOX M)

TURBINE ROLLER BEARING

- LH_2 COOLED (0.1 PPS)
- DN 1.35M
- 440C ROLLER
- 9310 RACES
- REINFORCED TFE CAGE (ARMALON)

TURBINE BALL BEARING

- LH_2 COOLED (0.1 PPS)
- DN 1.75M
- 440C ROLLER & OUTER RACE
- 9310 INNER RACE
- RULON CAGE

LOX BEARING DESIGN PARAMETERS
ARE WITHIN ATD LOX PUMP EXPERIENCE

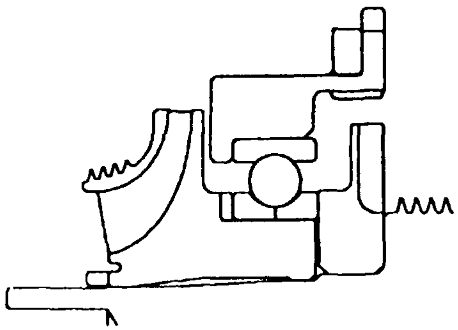

SIGNIFICANT TEST
EXPERIENCE IN LH_2

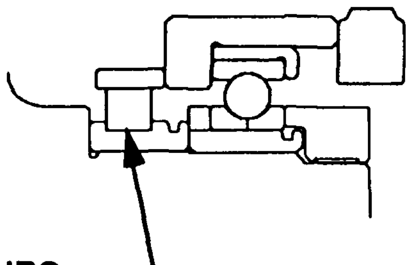

NEGATIVE IRC
FOR IMPROVED
ROLLER STABILITY

Figure 45. Liquid Oxygen Turbopump Bearing Description

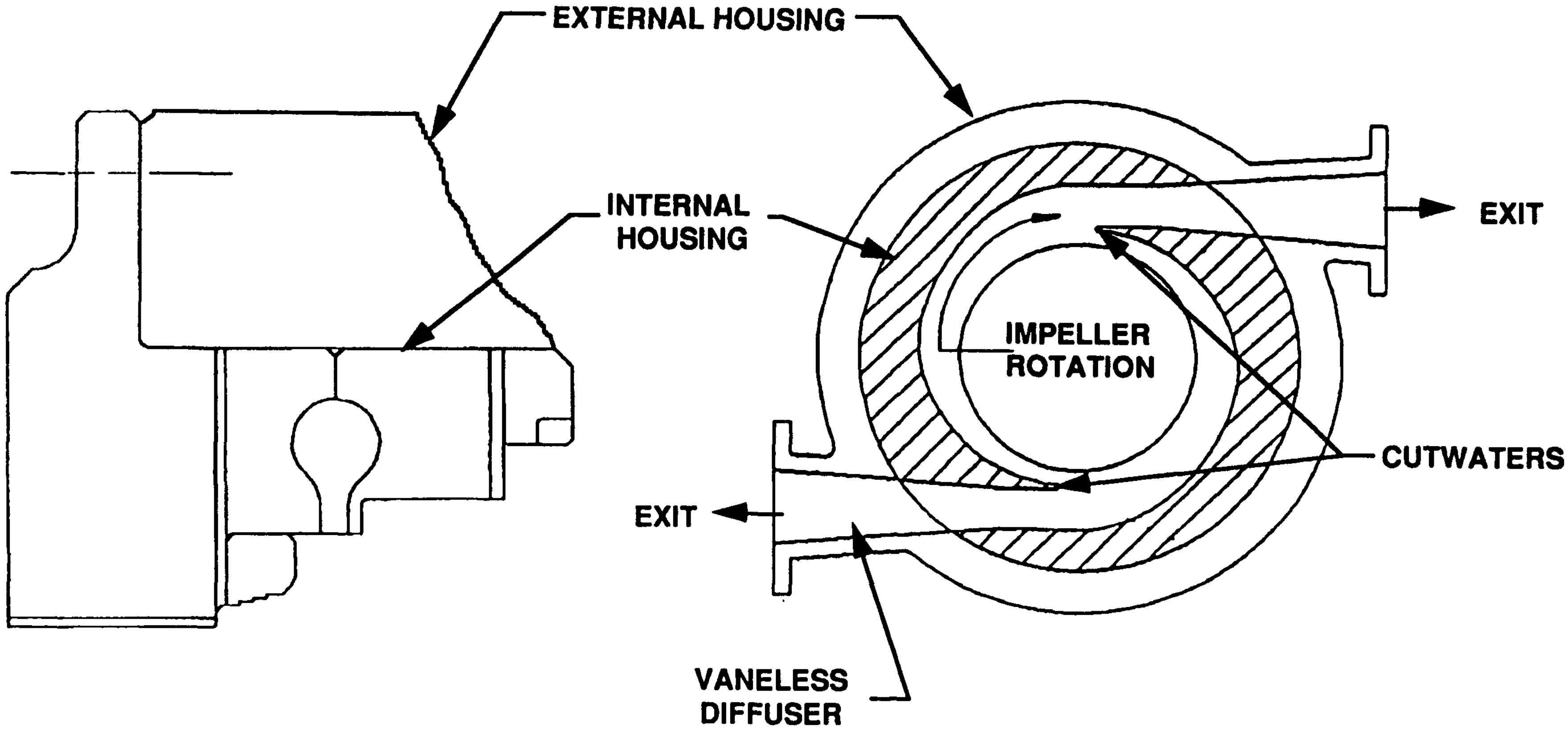

Figure 46. Liquid Oxygen Turbopump Discharge Volute

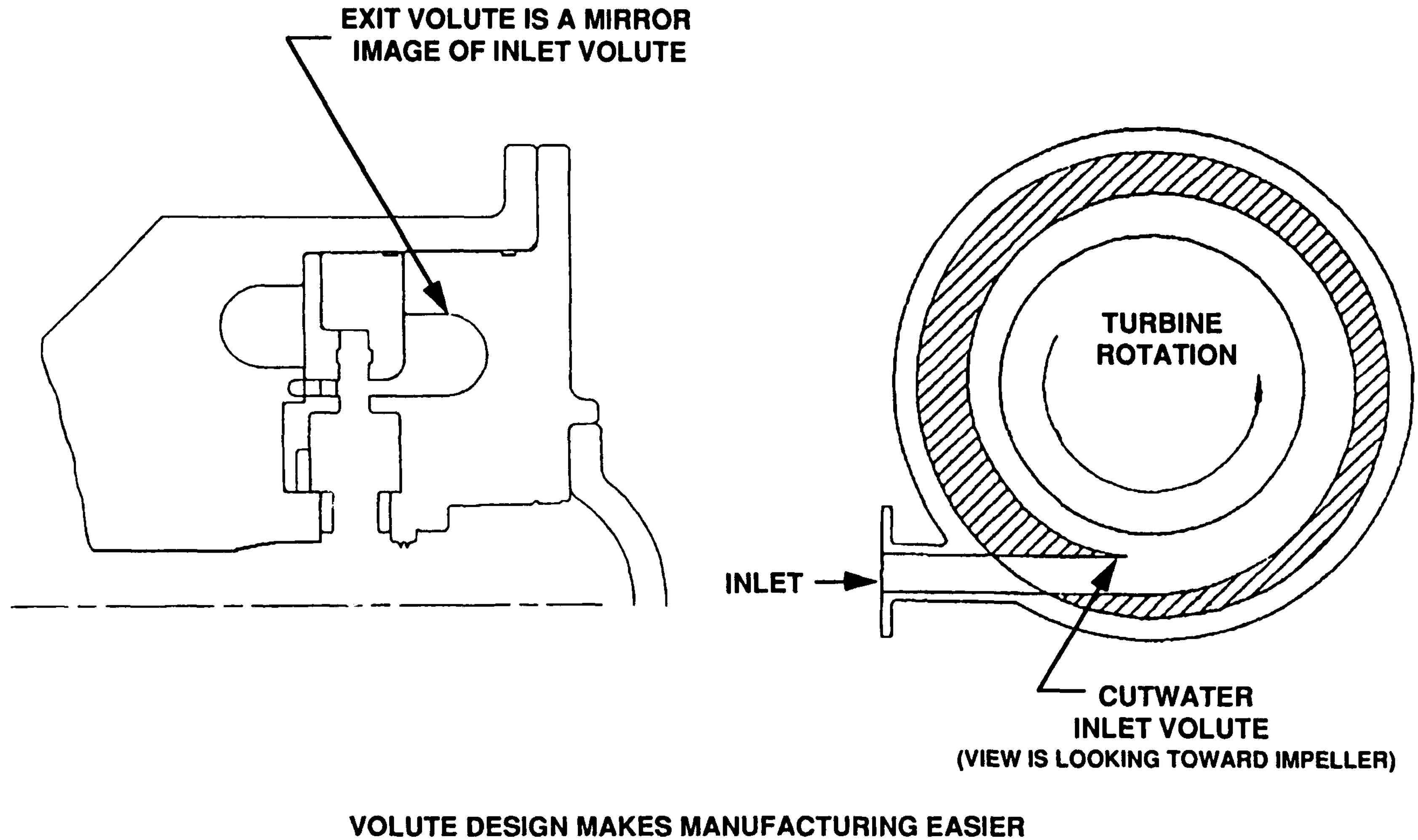

Figure 47. Turbine Volutes

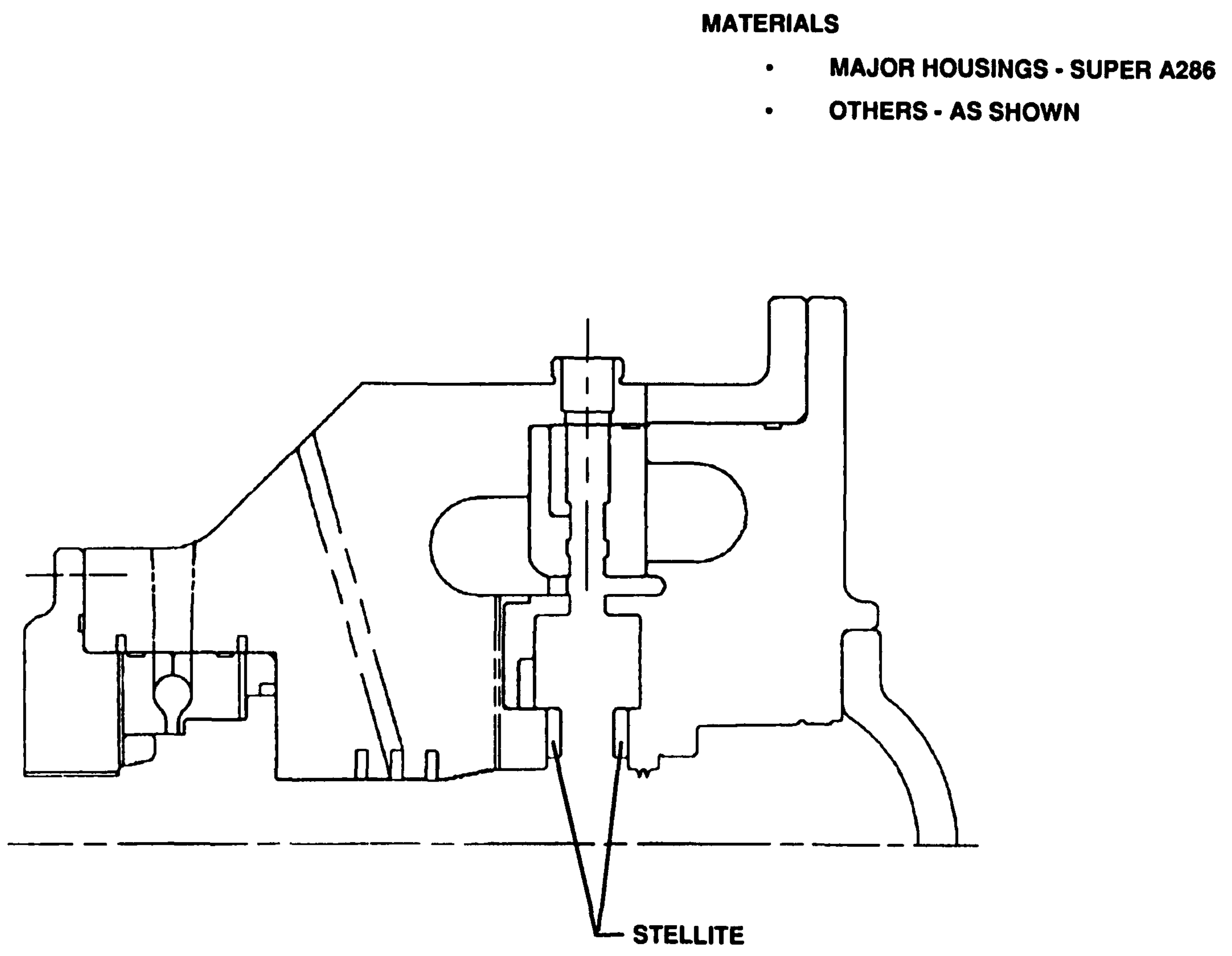

Figure 48. Liquid Oxygen Turbopump Housings

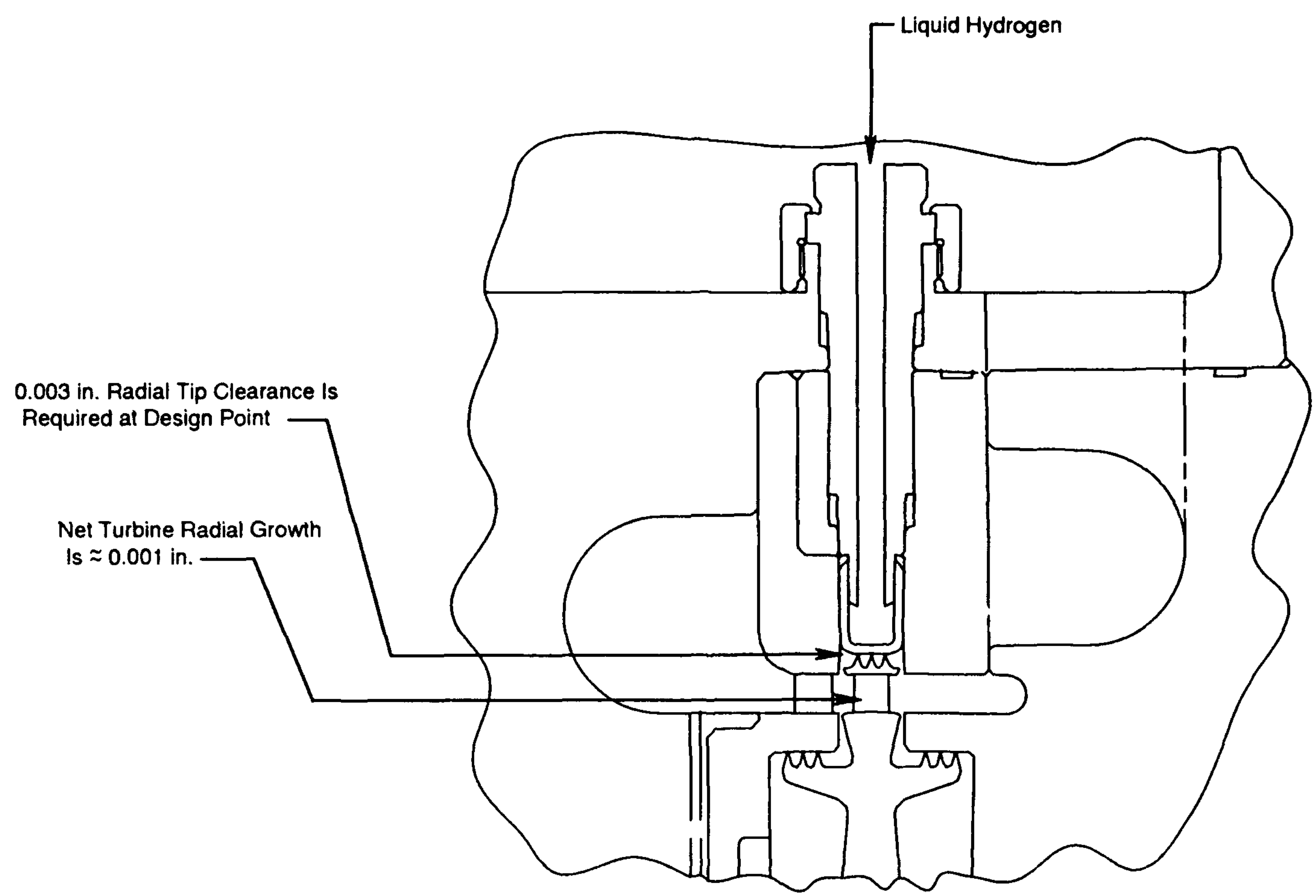

Figure 49. Turbine Tip Shroud Cooling Mechanism

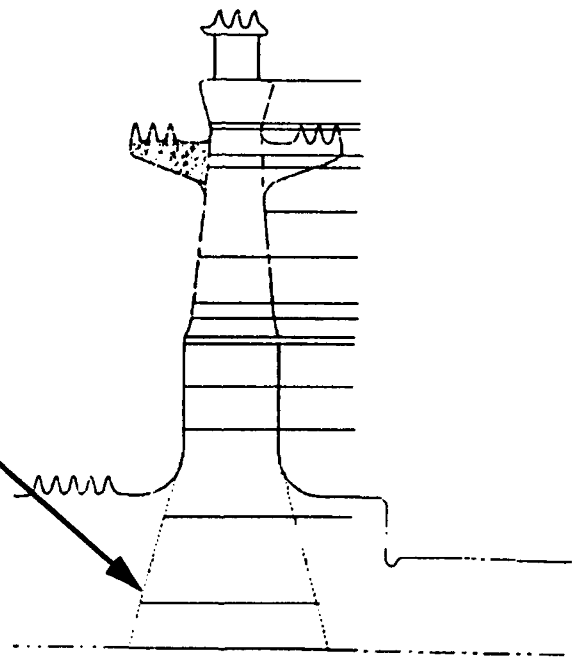

Figure 50. Turbine Disk Stress Analysis

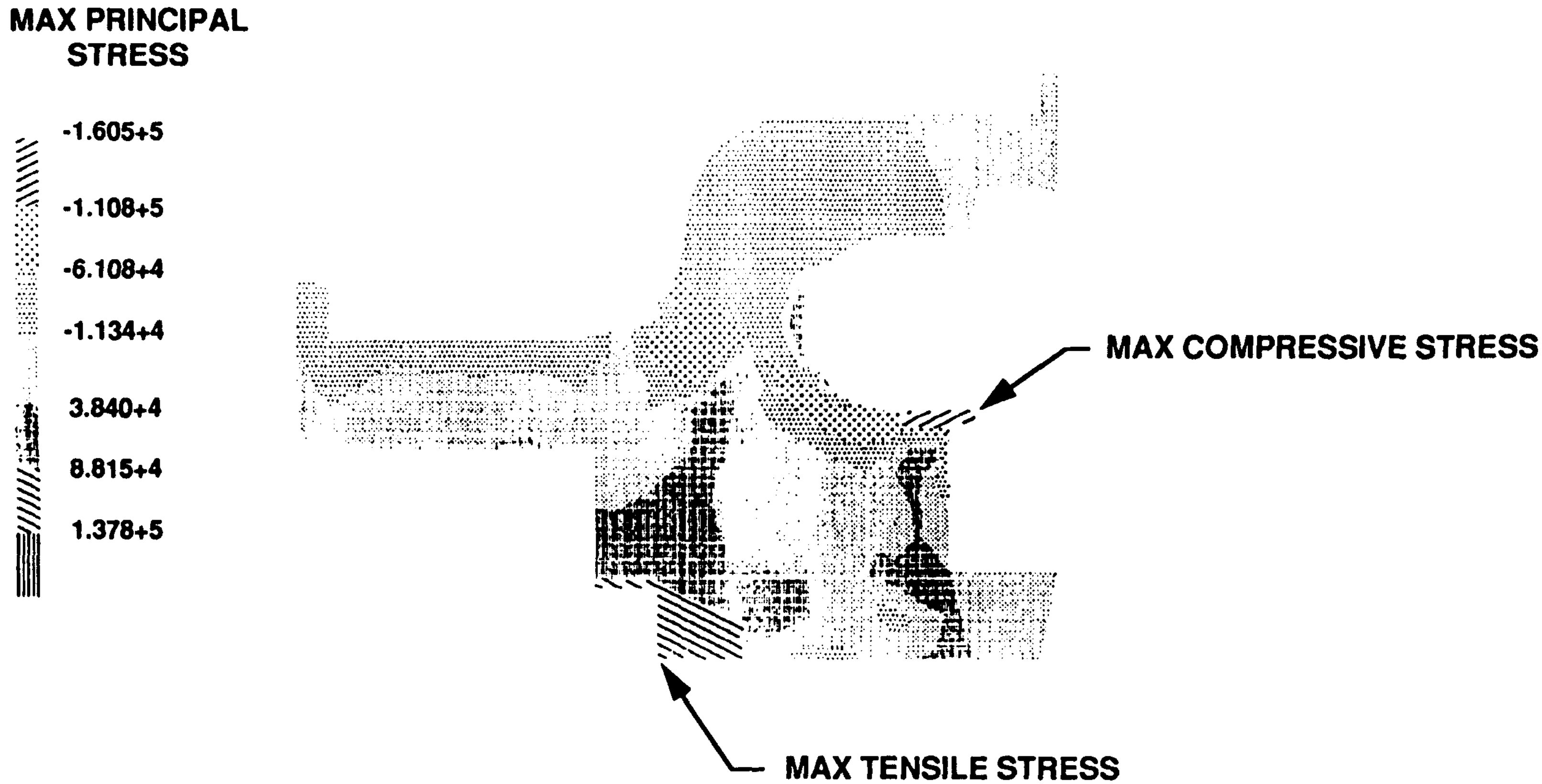

Figure 51. Liquid Oxygen Turbopump Housing Stress Analysis

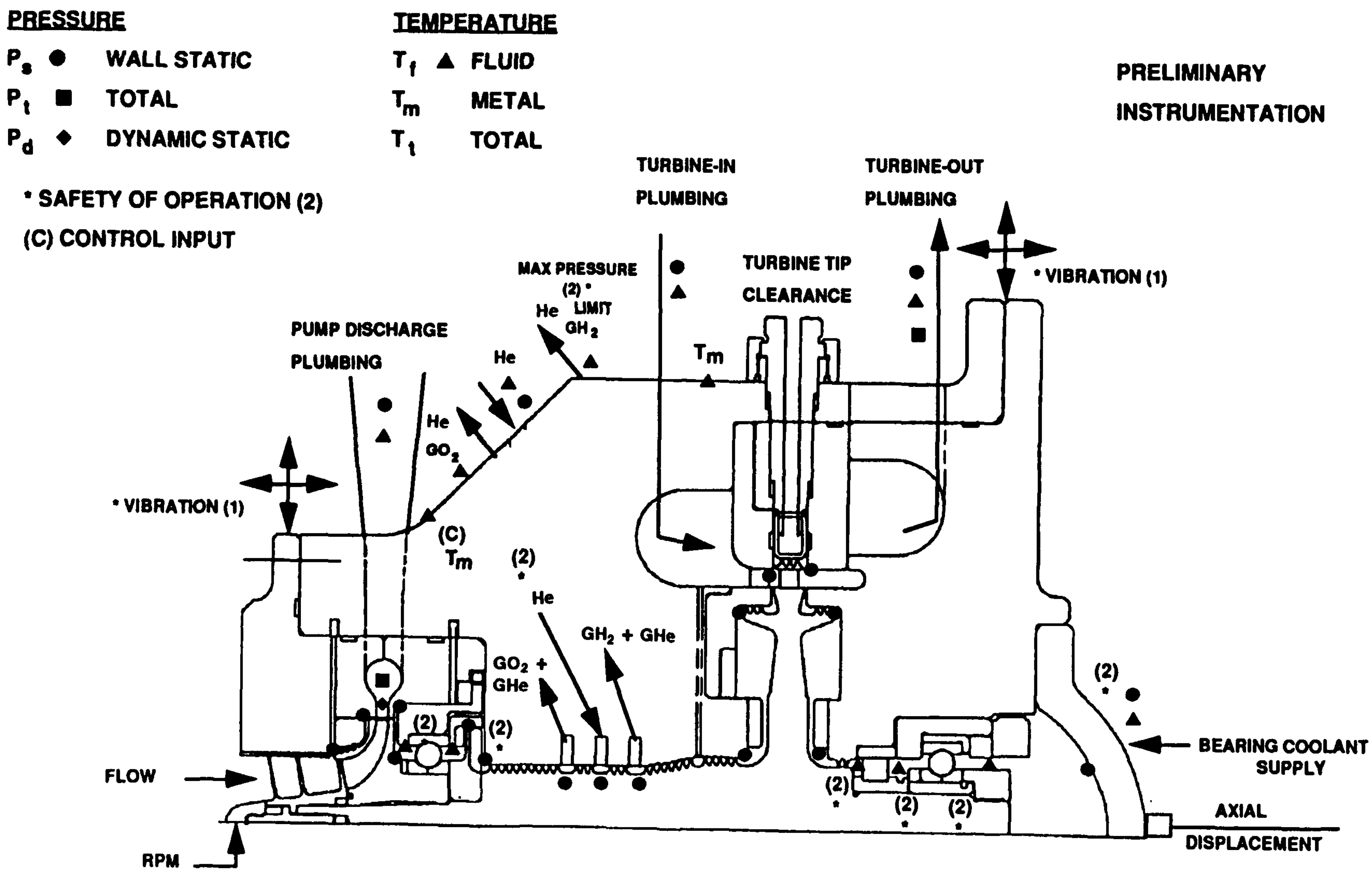

Figure 52. Liquid Oxygen Turbopump Instrumentation

D. Hydrogen Turbopump

1. Design Features

The hydrogen turbopump is a dual-shaft configuration, with counter-rotating primary and secondary turbopump rotors mounted in a common housing. The secondary pump is sized for approximately 60 percent of the primary pump flow. Short, stiff rotors, with two roller bearings on each shaft are used to provide the necessary support for subcritical rotordynamics. In the primary pump, inlet struts upstream of the inducer are incorporated to minimize preswirl, and interstage struts between the inducer and impeller are used to raise shutoff head coefficient, thereby increasing stability. Integral impeller shrouds provide increased efficiency, and multiple blades are used to enhance throttled stability. The full admission turbines provide 2525 hp and feature integrally shrouded rotors to further increase efficiency.

2. Primary Turbopump

The primary turbopump is being designed for operation at 98,240 rpm at the design point. The liquid hydrogen flow rate for this condition is 7.50 lb/sec at an inlet pressure and temperature of 70 psia and 38 R. It is discharged at 1917 psia and 68 R.

The turbine flow rate is 3.85 lb/sec at inlet conditions of 3451 psia and 896 R. It exits the primary turbine at 2507 psia and 815 R. Figure 53 provides more detailed information regarding primary turbopump operating conditions.

The materials used in the primary turbopump have been selected based on the availability of characterized mechanical properties, suitability for the expected operating conditions, and resistance to hydrogen embrittlement. Figure 54 shows the materials selected for the major components.

a. Inducer

The purpose of the inducer is to pressurize the inlet of the impeller to the level required to prevent impeller cavitation. The inducer material is wrought A110 ELI titanium. It has three unshrouded blades, each with a wrap angle of 292 degrees. The maximum blade tip speed is 1065 fps.

Preliminary hydrodynamic design of the inducer blades is complete. The final design work will include additional analysis to finalize blade thickness distribution and blade-to-hub fillet radii. The preliminary hub stress analysis indicates a burst factor of approximately 4.0, which is well in excess of the required 2.25. Figure 55 presents more detailed information about the inducer.

b. First-Stage Impeller

The first-stage impeller will be fabricated from wrought A110 ELI titanium. Hydrodynamic considerations require the incorporation of an integral shroud, a large blade wrap, a large number of blades, a small blade exit angle and a small blade exit height. These features make it impractical to machine the impeller in one piece. A manufacturing development program has been initiated to produce a monolithic structure from multiple concentric rings which can then be machined by conventional methods.

The latest 3D NASTRAN stress analysis of the current impeller indicates its LCF life is near the goal of 1000 cycles at the design point. The peak nominal local stress in the region of the blades is approximately 127 ksi. This would translate into an allowable blade-to-hub fillet K_t of 1.4. The impeller burst factor is estimated to exceed the required value of 1.5 at the design point. More detailed design and structural information is presented in Figures 56 and 57.

c. *Primary Turbopump Housings*

The various materials used for the turbopump housings have been selected on the basis of strength, stiffness, compatibility with the contained fluid, and ease of manufacture. The use of castings was ruled out early in the program due to concerns about their timely availability, as well as the high cost of casting tooling in the context of the small quantity of parts to be fabricated.

The pump inlet duct, which is not in the bearing load path, provides the attachment point for the hydrogen inlet manifold. It will be fabricated from wrought aluminum.

The remaining cold pump-end housings, comprised of the inducer housing/bearing support, the interstage strut housing and the volute collector, will be fabricated from wrought INCO 718 nickel alloy. The inlet struts and the interstage struts help pump stability during throttling operation, while the vaneless, double-discharge volute collector helps pump stability and reduces bearing side loads. The volute collector is made in two mirror-image halves, fully machined except for the cutwaters and conical diffusers. The halves are radially electron-beam welded, then the cutwaters and diffusers are machined. The thrust balance seal stators are machined from wrought cobalt alloy to provide transient contact surfaces compatible with the thrust balance rotor (tungsten carbide coatings on the titanium impeller).

The turbine inlet housing will be fabricated from wrought A-286 steel, selected for its resistance to degradation from exposure to warm hydrogen as well as for its high strength. This housing also contains the discharge portions of the double-conical pump diffusers and the single-tangential entry inlet volute for the full-admission turbine. The inlet volute insulates the inlet housing pressure vessel from large thermal loads.

The turbine inlet volute will be fabricated from A-286 steel alloy. The forward wall of the volute will initially have an access hole to allow tool entry for machining the inner flow passage. A plug will then be welded over the access hole. This inlet volute acts as a heat shield for the turbine inlet housing, since it is subjected to larger thermal gradients and higher temperatures than the inlet housing.

The first-stage turbine stator will be fabricated from A-286 steel alloy to provide resistance to thermal shock and exposure to hot hydrogen. The stator has 14 integrally machined vanes, with a span and an axial chord length of 0.25 inch.

The turbine intermediate housing is comprised of an outer support flange, the second-stage stator, and a diaphragm, all of which will be fabricated from various grades of A-286 steel alloy. The stator has 8 integrally machined vanes, each with a 0.25-inch span and 0.50 inch axial chord length.

The primary and secondary turbine blade tip shrouds are mounted in the intermediate housing. They are machined from wrought A-286 steel alloy for resistance to thermal shock and are held in position by radial pins. The shroud diameters are controlled by admission of high-pressure hydrogen into the intermediate housing. This control method is used to obtain the 0.003-inch radial turbine tip clearance required at the design point. Figures 58 through 63 show more detailed information about the turbopump housings and the turbine airfoils.

d. *Primary Turbine Blisk*

The turbine blisk, with its integral shroud, will be fabricated from wrought A-286 steel alloy. This material was selected for its high strength, thermal shock durability, and resistance to degradation under hot hydrogen exposure. Preliminary analysis indicates a burst factor of approximately 1.82 at the design point, based on the current bore-rim temperature gradient and the criterion of <0.5 percent residual growth at the disk rim. (The required burst factor is 1.5).

The preliminary bore/web/rim axial offsets have been determined using a shell analysis and an initial finite element analysis. The results of these analyses indicate an estimated LCF life that exceeds the required 100 cycle life, and approaches the 1000 cycle goal at the design point.

These analyses will be updated when iterations are complete on the turbine reaction levels needed to optimize axial thrust balance. The temperature distribution associated with that turbine configuration will be used to update the analyses. Figure 64 shows more detailed turbine blisk design information.

e. Shaft/Bearings/Rotordynamics

The shaft is an integral part of the turbine blisk, thus it will also be machined from wrought A-286 steel alloy. The shaft supports and axially preloads the rotor stack, and transmits torque from the turbine to the pump.

At the estimated design point pump torque of 817 in.-lb, the shaft nominal shear stress is 11 ksi; the shear yield strength is 96 ksi. The spline bearing stress is also 11 ksi, well within the design criterion of 20 ksi. The shaft is also the tiebolt for the rotor stack. The tiebolt will apply approximately 20,000 pounds of axial preload to the stack. The preload will prevent the rotor stack from becoming unseated during operation. The rotor uses two roller bearings to provide sufficient rotor support stiffness for subcritical rotor dynamics. They provide a radial springrate of approximately 1.0×10^6 lb/in. at the pump end and 1.5×10^6 lb/in. at the turbine end. The bearings are discussed in more detail in a subsequent section of this report. The latest rotordynamics analysis indicates that the primary turbopump lowest critical speed is 109,500 rpm, a margin of 9.5 percent at the design point. At nominal normal operating point the critical speed margin is 29 percent. Figures 65 through 67 present more detailed information about the shaft, bearings and rotordynamics.

f. Internal Flows

The internal flows are comprised of the bearing coolant flow, turbine conditioning flow, and thrust balance flows. These flows have been minimized to achieve acceptable operation in the split expander cycle.

- Bearing cooling requires a flow rate of 0.20 lb/sec for each bearing at the design point.

- Turbine conditioning flows are required to control turbine blade tip clearance and housing gaps and to minimize axial temperature gradients from one disk face to the other.

  - Turbine disk rim seals are used to reduce hot gas inflow from the main flowpath, thereby minimizing cooling flow requirements.
  - Brush seals are used to reduce the leakage flow from the bearing compartment to the disk rim.
  - Static seals are used upstream and downstream of the turbine tip seal stators to reduce leakage of conditioning fluid.

- Thrust balance flows are minimized by using only single-face thrust balance systems, and by closely controlling thrust balance component tolerances. The values of these secondary flows are shown in Figure 68.

g. Primary Turbopump Thrust Balance

The thrust balance system of the primary turbopump is comprised of a rotor (the front shroud of the impeller) and a stator (the inserts fastened to the housing) with axially variable orifices between them at the shroud OD and ID. These orifices vary as a function of rotor axial displacement from the neutral or null position (equal travel possible in both forward and aft directions) in a way that causes the pressure on the impeller shroud to vary and oppose the displacement.

The rotating componer. projected areas and internal cavity pressures of the pump and turbine, together with the axial forces on the turbine blades are used to calculate the net shaft load in the null position. This net load is then compared to the thrust balance system capability (change in axial force versus displacement from null position at maximum available displacement) to determine the thrust balance margin.

The primary turbopump rotor is balanced within 200 pounds at the design point with an 86 percent reaction turbine. The estimated thrust balance capability at design point is +3700 pounds. Work is in progress for calculation of the net rotor force at the null position and thrust balance capability for other operating conditions including 1, 4, 10, 15 and 20K thrust levels.

Transient rotor axial force unbalance is controlled by contact surfaces in the thrust balance system at the OD and ID of the impeller front shroud. The amount of axial travel possible is set by adjusting the thrust balance seal stators to provide a space 0.016 inch wider than the thrust balance rotor. The design and materials selection for these contact surfaces is similar to P&W's SSME-ATD high-pressure fuel turbopump design, using cobalt alloy stators and tungsten carbide coatings on the titanium rotor. The durability of these components is being characterized in the SSME-ATD program.

3. Secondary Turbopump

The secondary pump segment is similar to the primary pump segment in, many respects. Both have double-discharge volute collectors for the impellers and both use single tangential access turbine discharge and inlet volutes. The secondary pump uses identical roller bearings as the primary, and both the turbine blisk and the impellers are integrally shrouded. Significant differences between the pumps include the following:

- The secondary segment uses two impellers and does not require an inducer. Its capacity is approximately 60 percent of the primary pump.
- The secondary pump impellers have only two sets of blades versus the three sets featured on the primary pump impeller. Both of the secondary pump impellers use the same blade geometry.
- The secondary pump impellers are smaller in diameter than the primary pump impellers, and operate at a lower tip speed with correspondingly lower stresses.
- The secondary turbopump's lowest critical speed occurs at 123,500 rpm, providing a margin of 24.5 percent at the design point and 46 percent at the normal operating point.

Figures 69 through 71 provide more detailed information on the secondary turbopump.

The secondary turbopump is designed for operation at 99,220 rpm at the design point. Liquid hydrogen flows into the pump inlet from the primary pump discharge at a rate of 4.77 lb/sec, and at a pressure of 1912 psia and temperature of 70 R. Flow is discharged from the third-stage impeller at 4503 psia and 111 R.

The pumping elements require 1180 hp, which is supplied by the expansion of gaseous hydrogen through the turbine. The turbine gas comes from the primary turbine at a rate of 3.97 lb/sec at conditions of 2507 psia and 823 R. It exits the secondary turbine at 1843 psia and 745 R. Operating conditions and internal flow parameters for the secondary pump are presented in Figures 72 and 73.

The materials used in the secondary turbopump have been selected based on the availability of characterized material properties, suitability for the expected operating conditions, and resistance to hydrogen embrittlement. Figure 74 shows the materials selected for the major components.

The thrust balance system of the secondary turbopump is comprised of a rotor (the rear face of the third-stage impeller) and a stator (the inserts fastened to the housing) with axially variable orifices between them. Thrust balance is achieved as orifice size varies with rotor axial displacement from the neutral or null position, thereby causing the pressure acting on the impeller to change so that it opposes the displacement.

The rotating component projected areas and internal cavity pressures of the pump and turbine, together with the axial forces on the turbine blades, are used to calculate the net shaft load in the null position. This net load is then compared to the thrust balance system capability to determine the thrust balance margin.

The secondary turbopump rotor is axially balanced within 25 pounds at the design point, with a 57 percent reaction turbine. The estimated thrust balance capability at the design point is + 2000 pounds.

Transient rotor axial force unbalances are controlled by contact surfaces in the thrust balance system at the OD and near the ID of the third-stage impeller rear face. The amount of axial travel possible is set by adjusting the thrust balance seal stators to provide a space 0.016 inch wider than the thrust balance rotor. The design and materials selection for these contact surfaces is similar to P&W's SSME-ATD high-pressure fuel turbopump design, using cobalt alloy stators and tungsten carbide coatings on the titanium rotor. Durability of these components is being characterized in the SSME-ATD program.

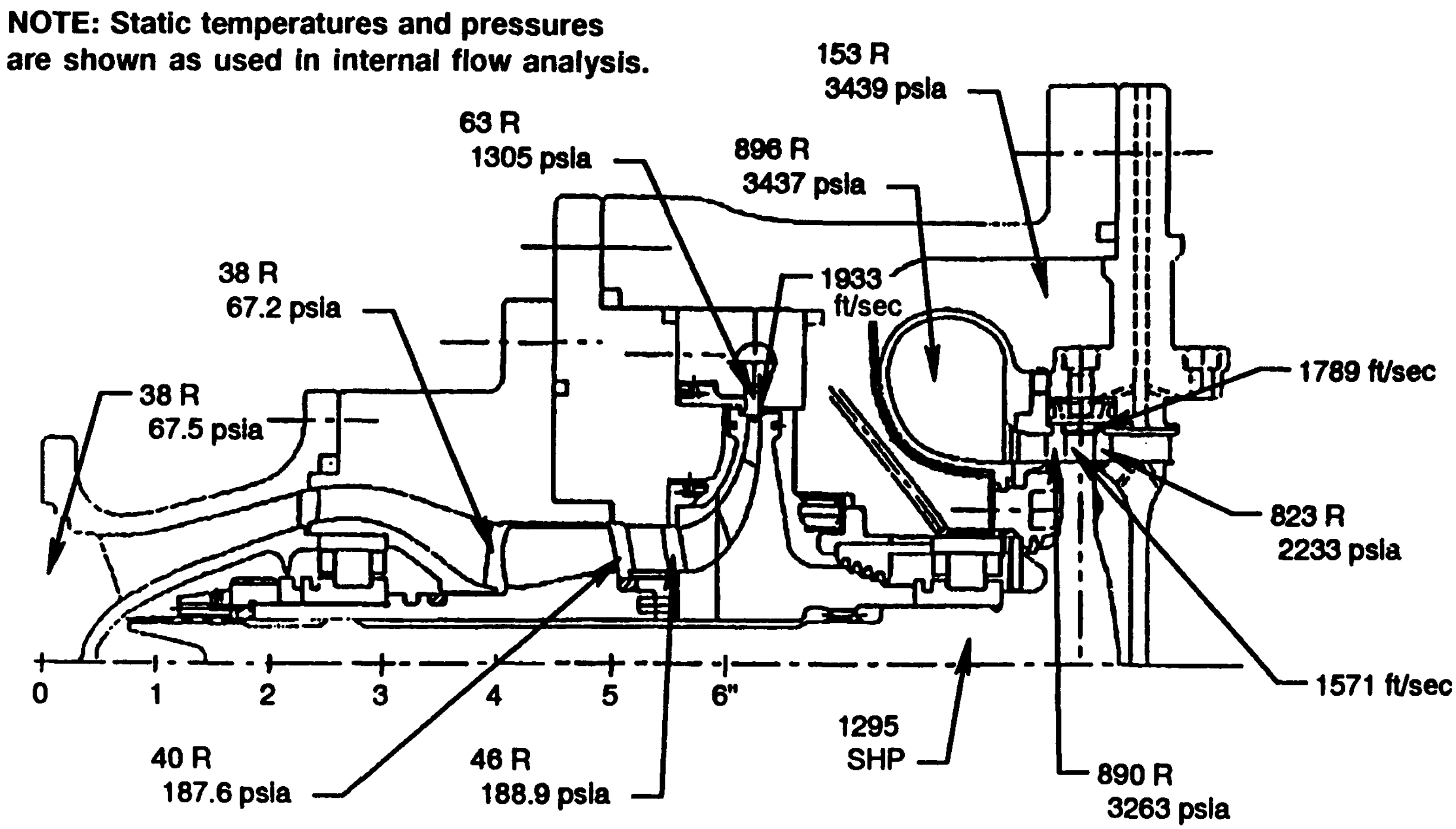

Figure 53. Primary Turbopump Design Point Parameters

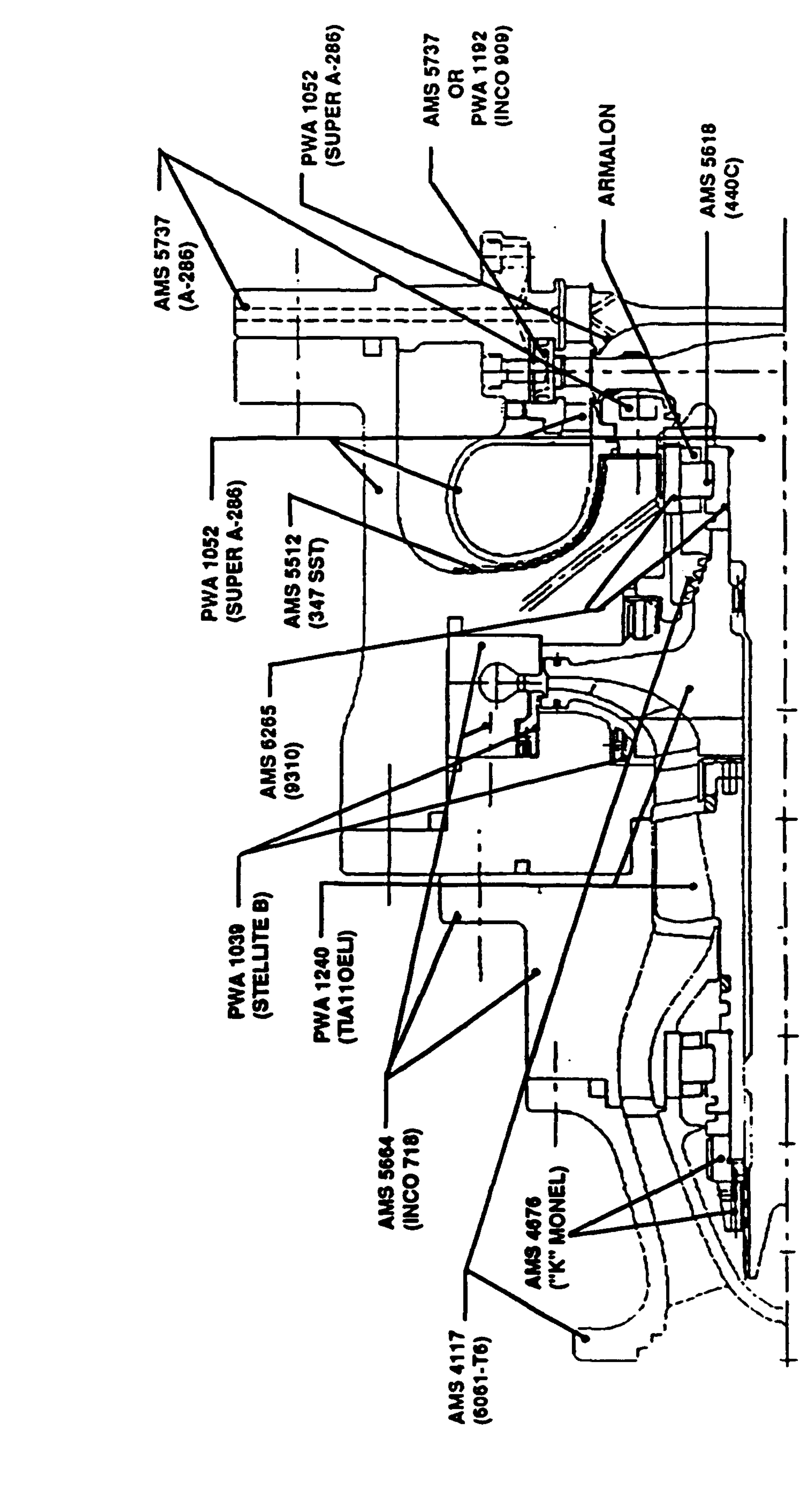

Figure 54. Primary Turbopump Materials

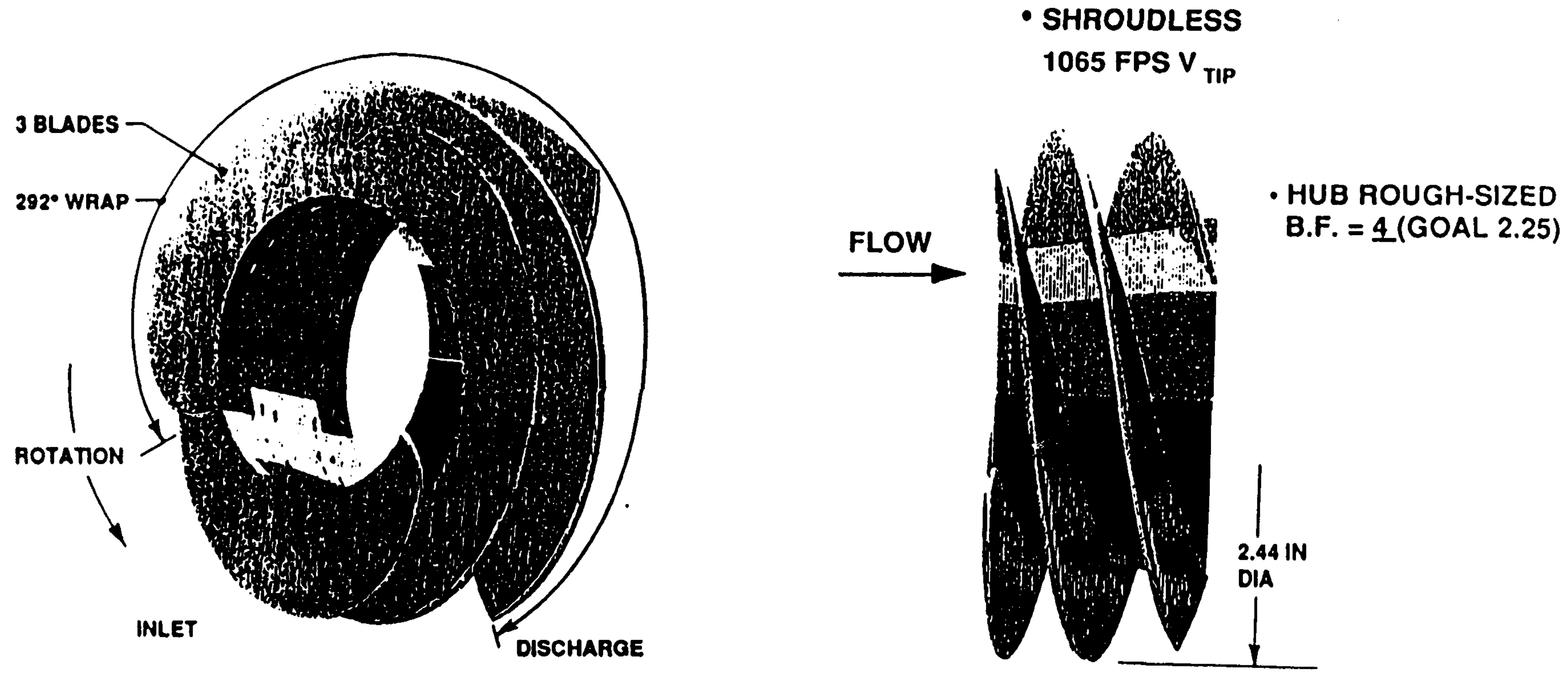

Figure 55. Primary Turbopump Inducer

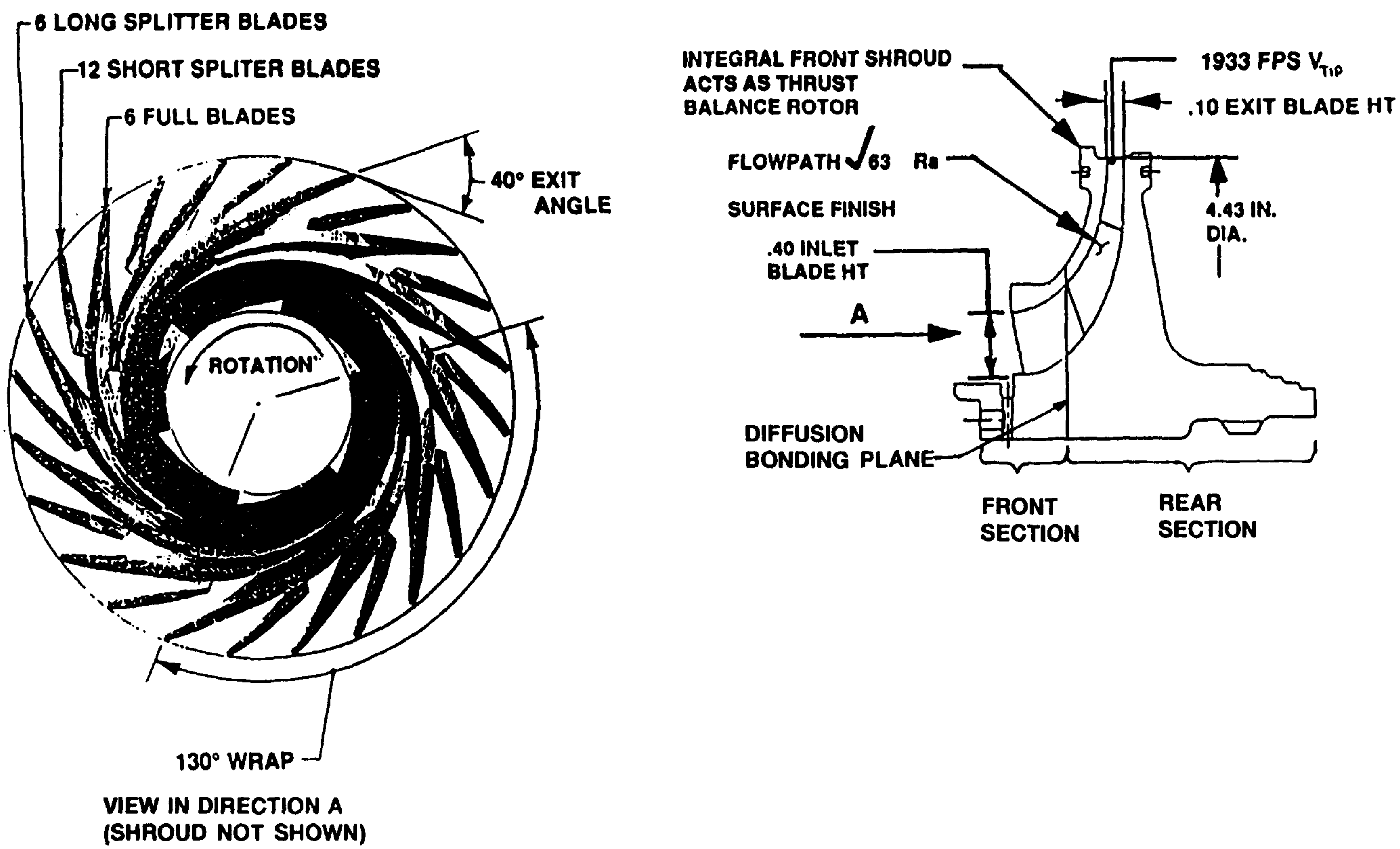

Figure 56. First-Stage Impeller Description

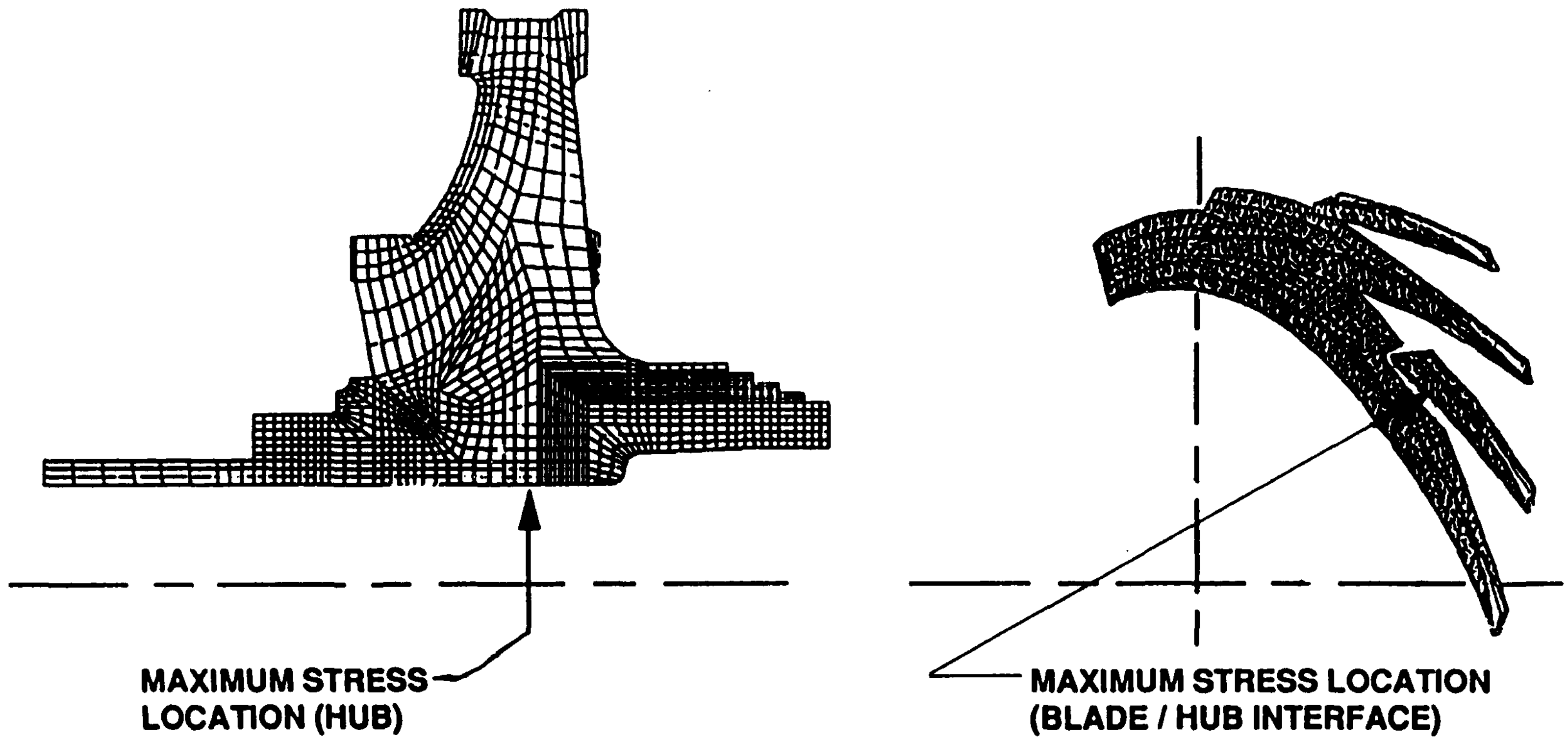

Figure 57. First-Stage Impeller Stress Analysis

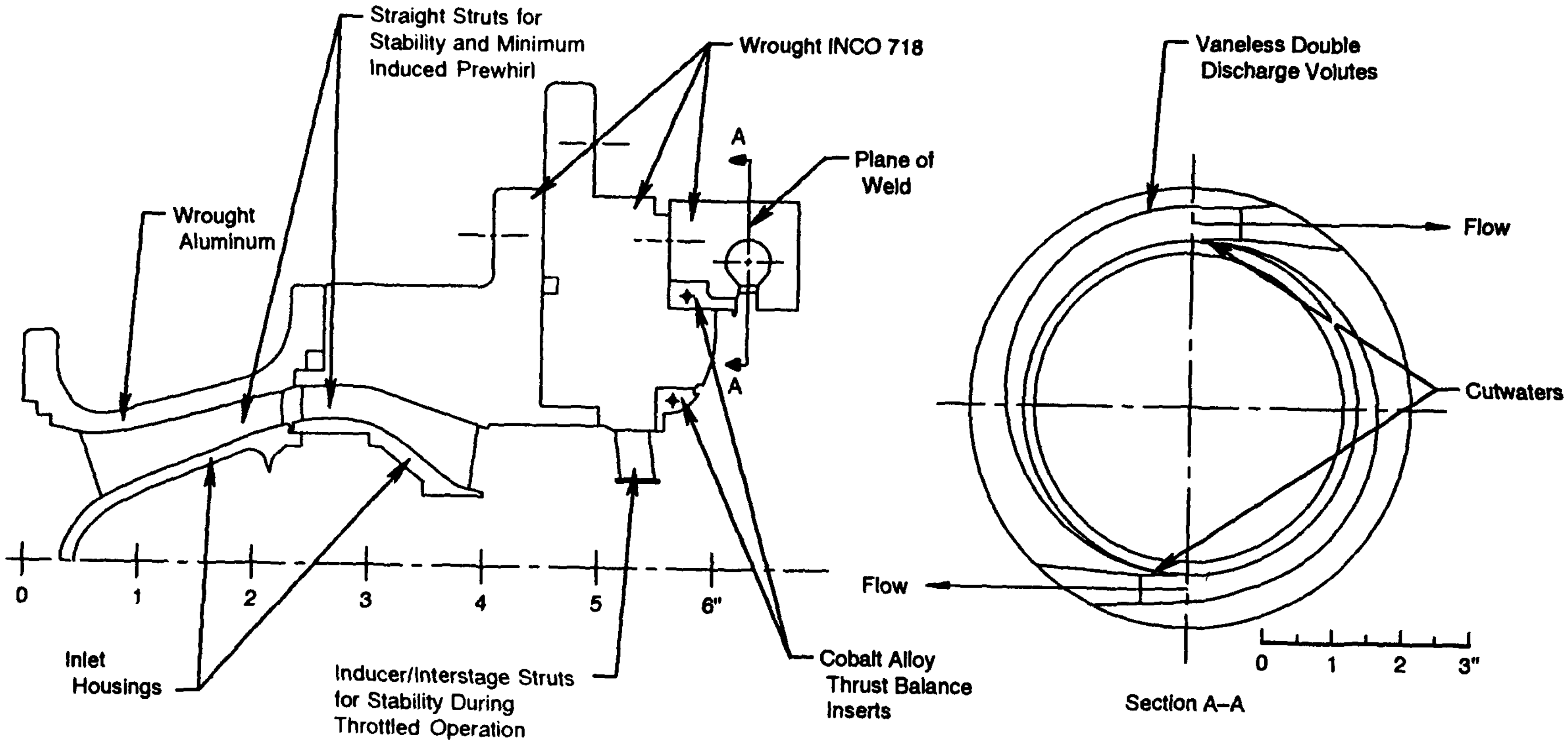

Figure 58. Primary Turbopump Housing Description

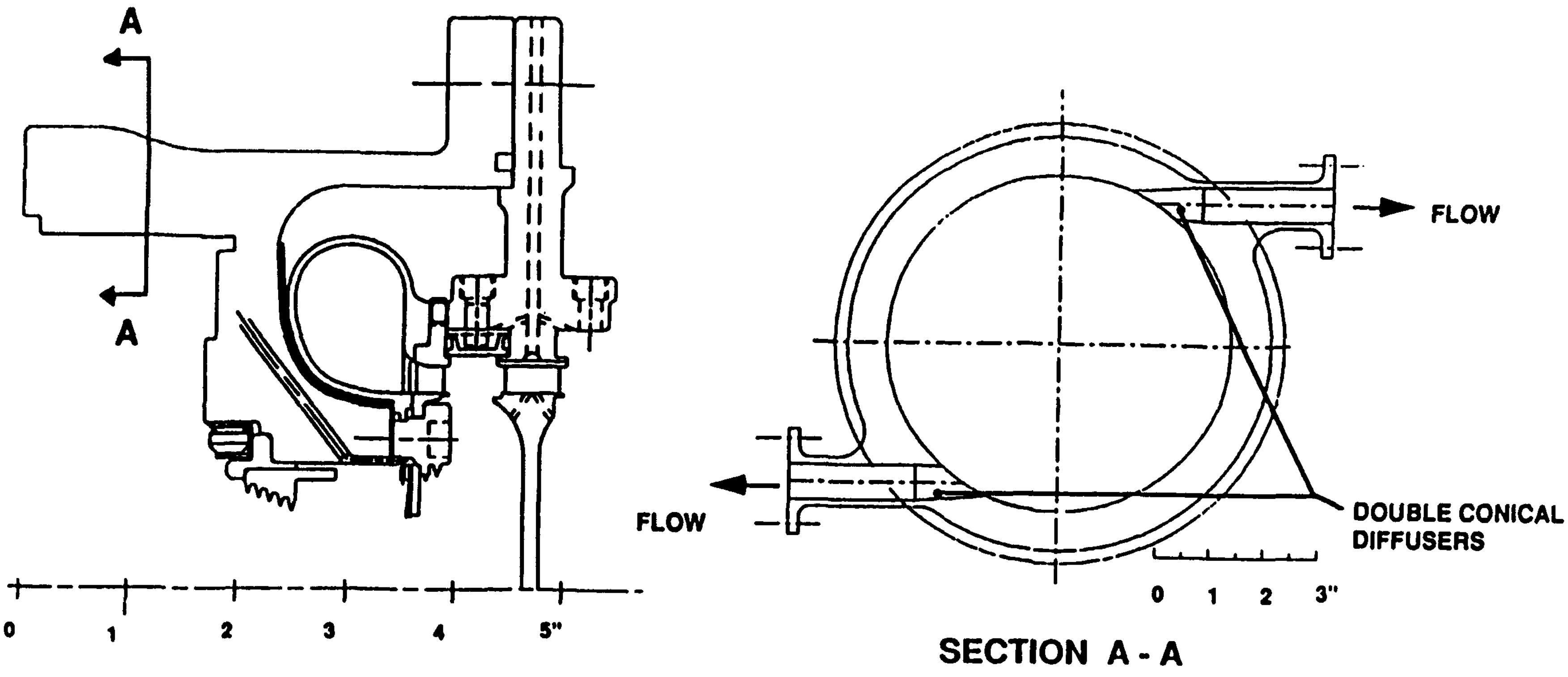

Figure 59. Detail of Primary Turbopump Housing

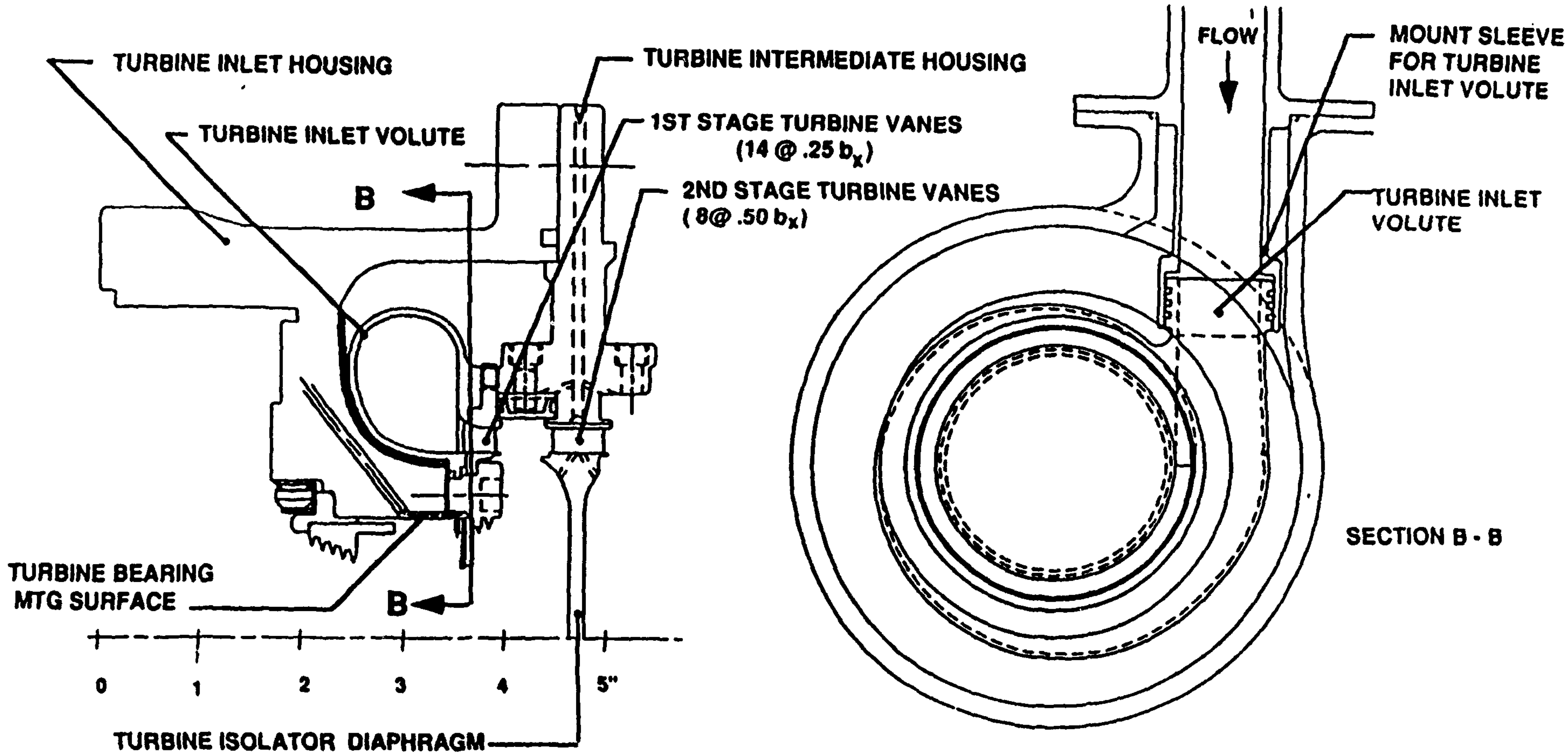

Figure 60. Detail of Turbine Inlet Volute

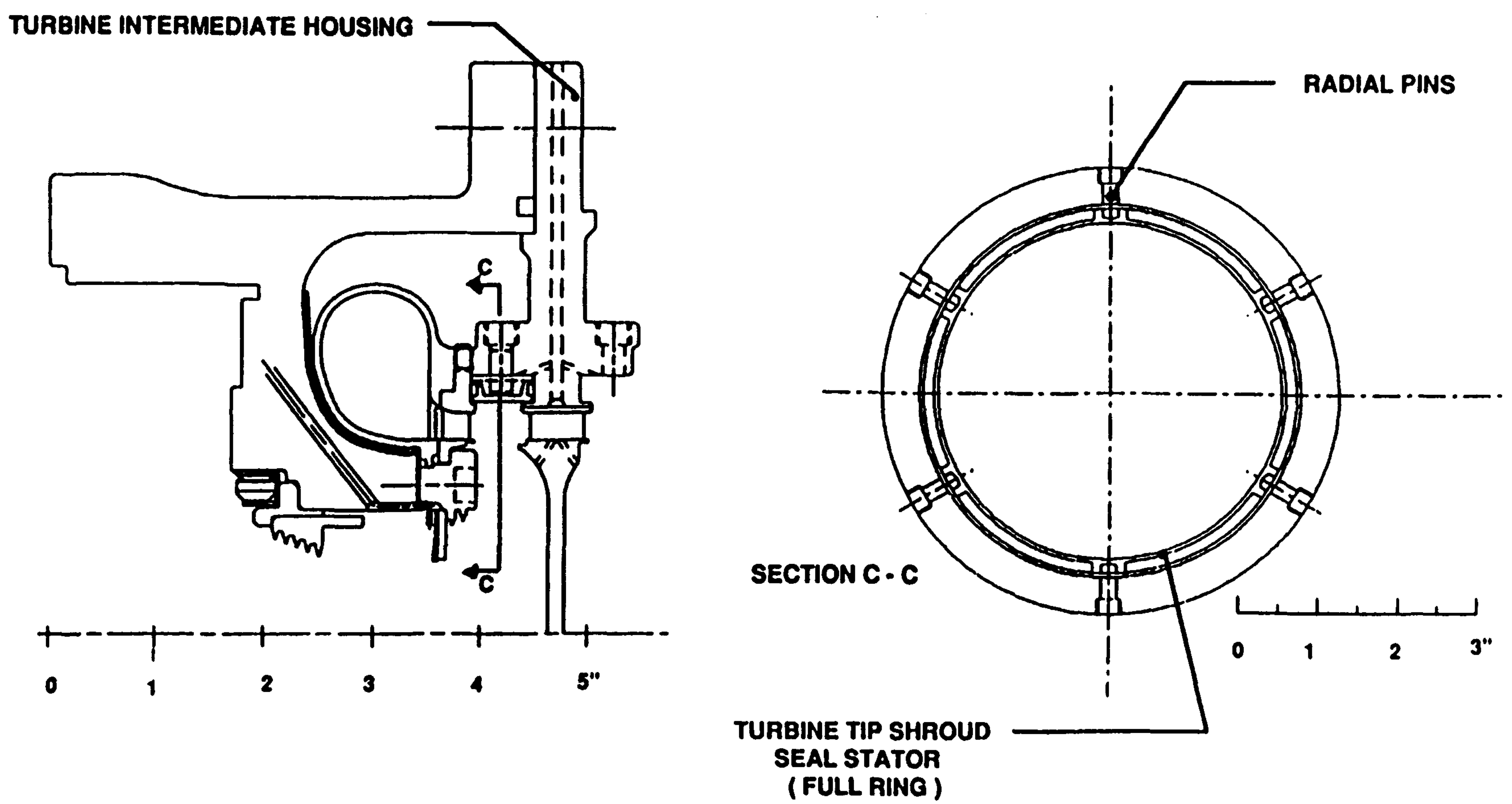

Figure 61. Detail of Turbine Intermediate Housing

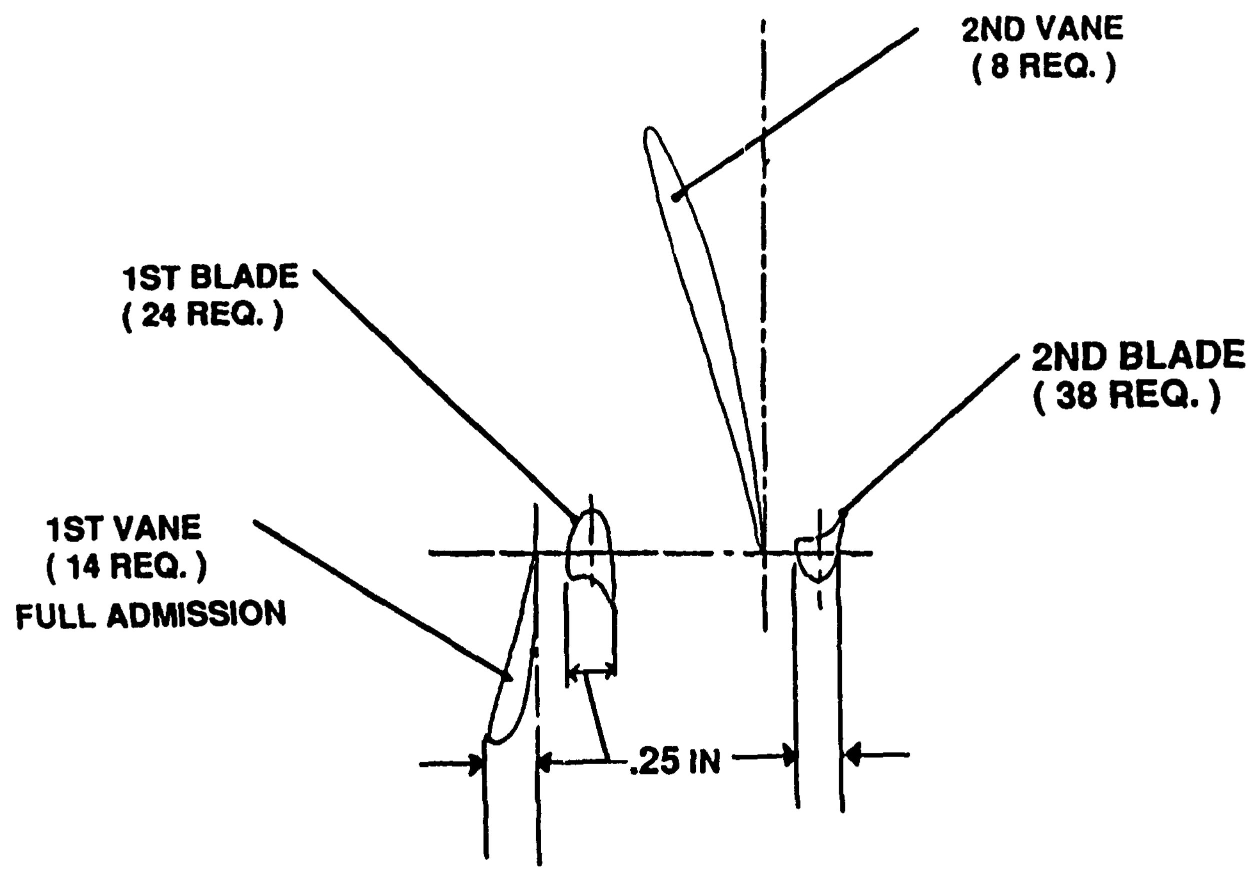

Figure 62. Profile of Turbine Airfoils

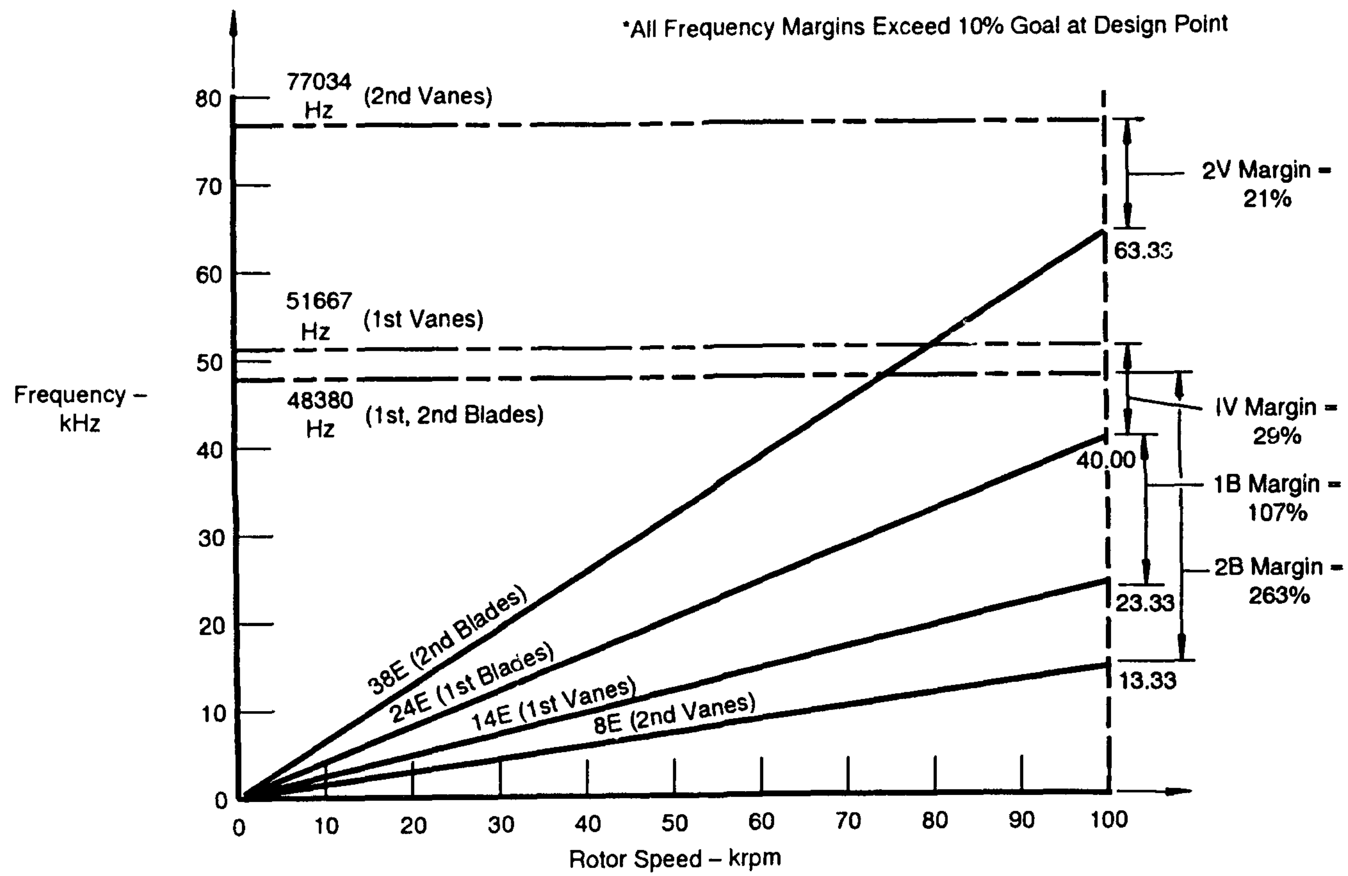

Figure 63. Turbine Airfoil Campbell Diagram

- Approximately 3.85 lb/sec GH_2 Expanded from 3452 psia/896 R to 2507 psia/815 R;1295 hp to Pump
- V Rim 1571 FPS, Vtip 1789
- Disk Sized Using W140 Plastic Analysis/Preliminary ΔT to Growth Criteria
  - Estimated BF = 1.82 (1.5 Acceptable)
  - Further Subjected to Shell Analysis (W526) and Initial Finite Element Analysis (BEASY) to Set Rim/Web/Bore Axial Offsets and Estimate LCF Life. (Predicted LCF Life Approx. 1000 Cycles)
  - Need to Factor in Calculated Temperatures

- Material Super A-286; for High Strength and Resistance to Exposure to Hot Hydrogen (*P&W Experience in ATD Turbopumps*)
- Full Admission Turbine per RL10 Experience to Get Maximum Efficiency and P_C

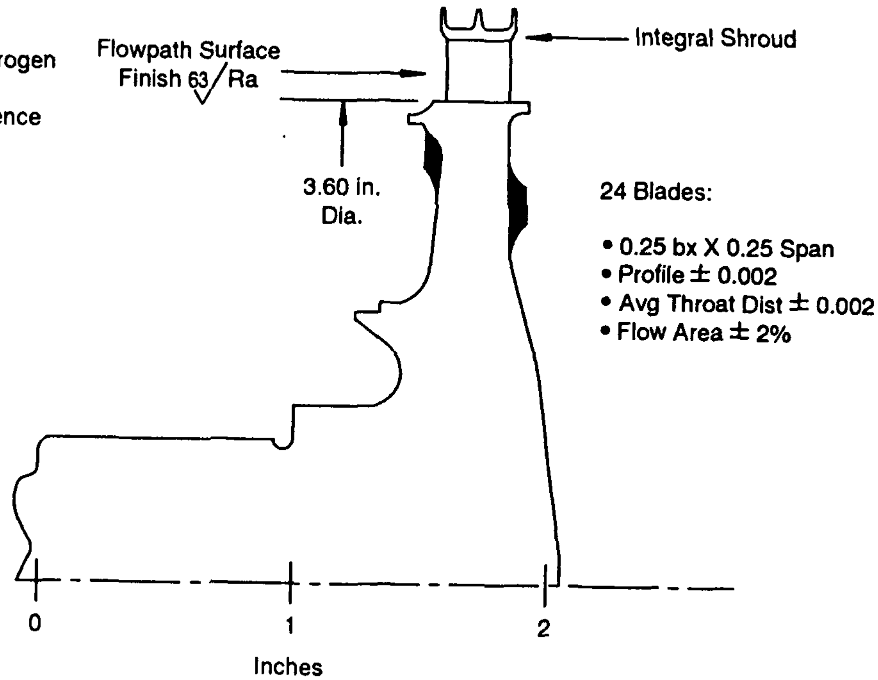

Figure 64. Primary Turbine Blisk

- SHAFT CENTERS AND AXIALLY PRELOADS ROTOR STACK; TRANSMITS TORQUE TO PUMP
  - PRELIMINARY SIZED FOR TORQUE, SPLINE LENGTH, ASSY. PRELOAD
  - GOOD P&W EXPERIENCE WITH THIS TYPE ROTOR STACK

- 27MM BORE DIA ROLLER BEARINGS
  - STIFF RADIAL SPRINGRATE

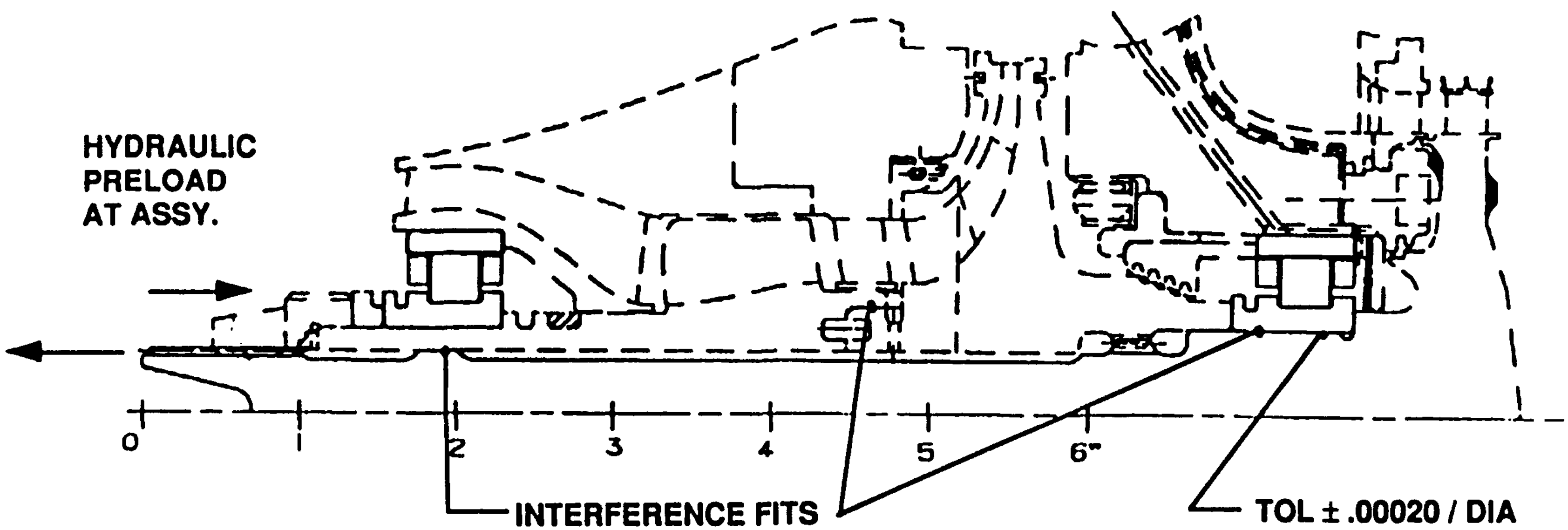

Figure 65. Primary Turbopump Shaft and Bearings

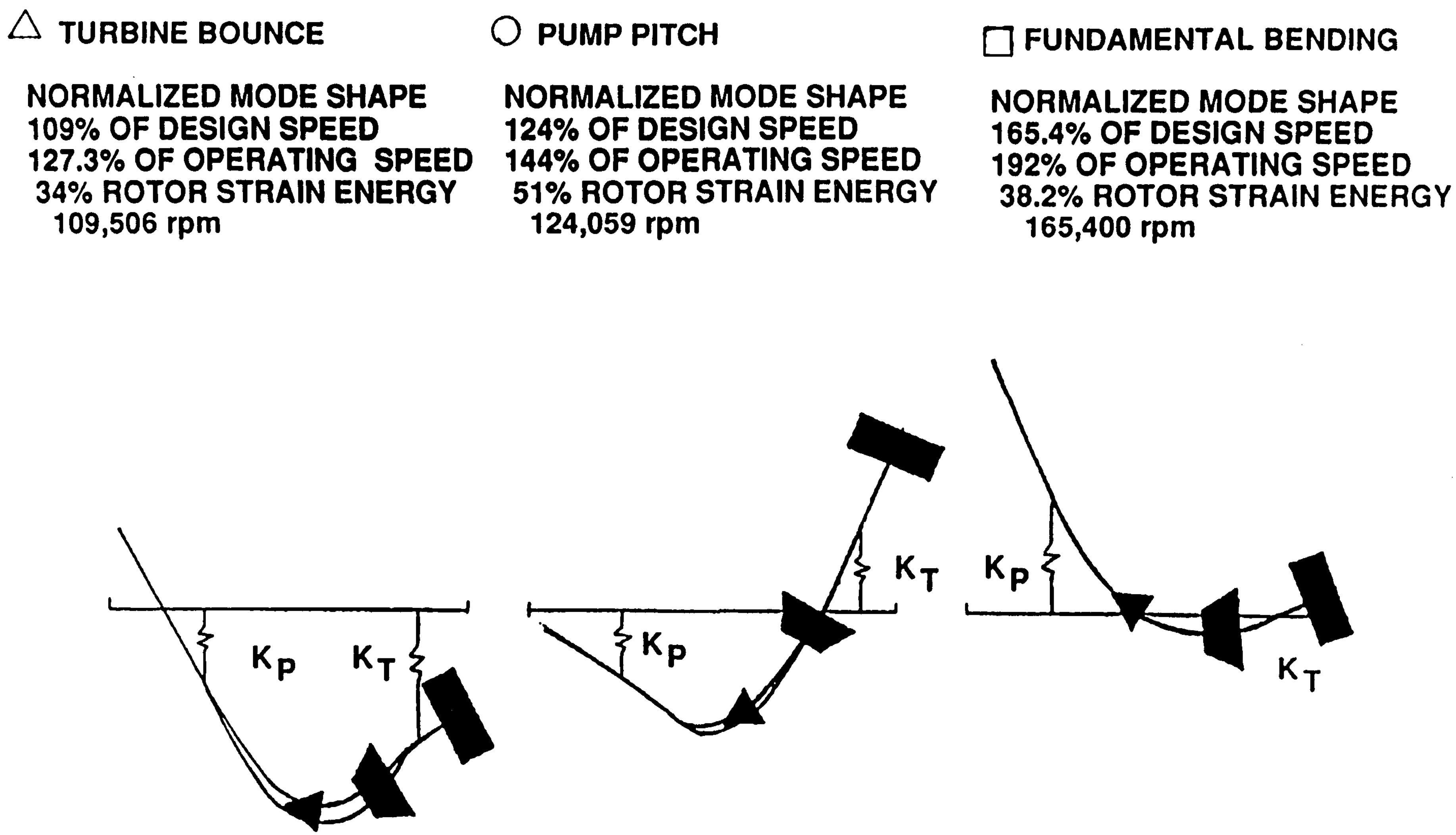

Figure 66. Primary Turbopump Rotordynamics Mode Shapes

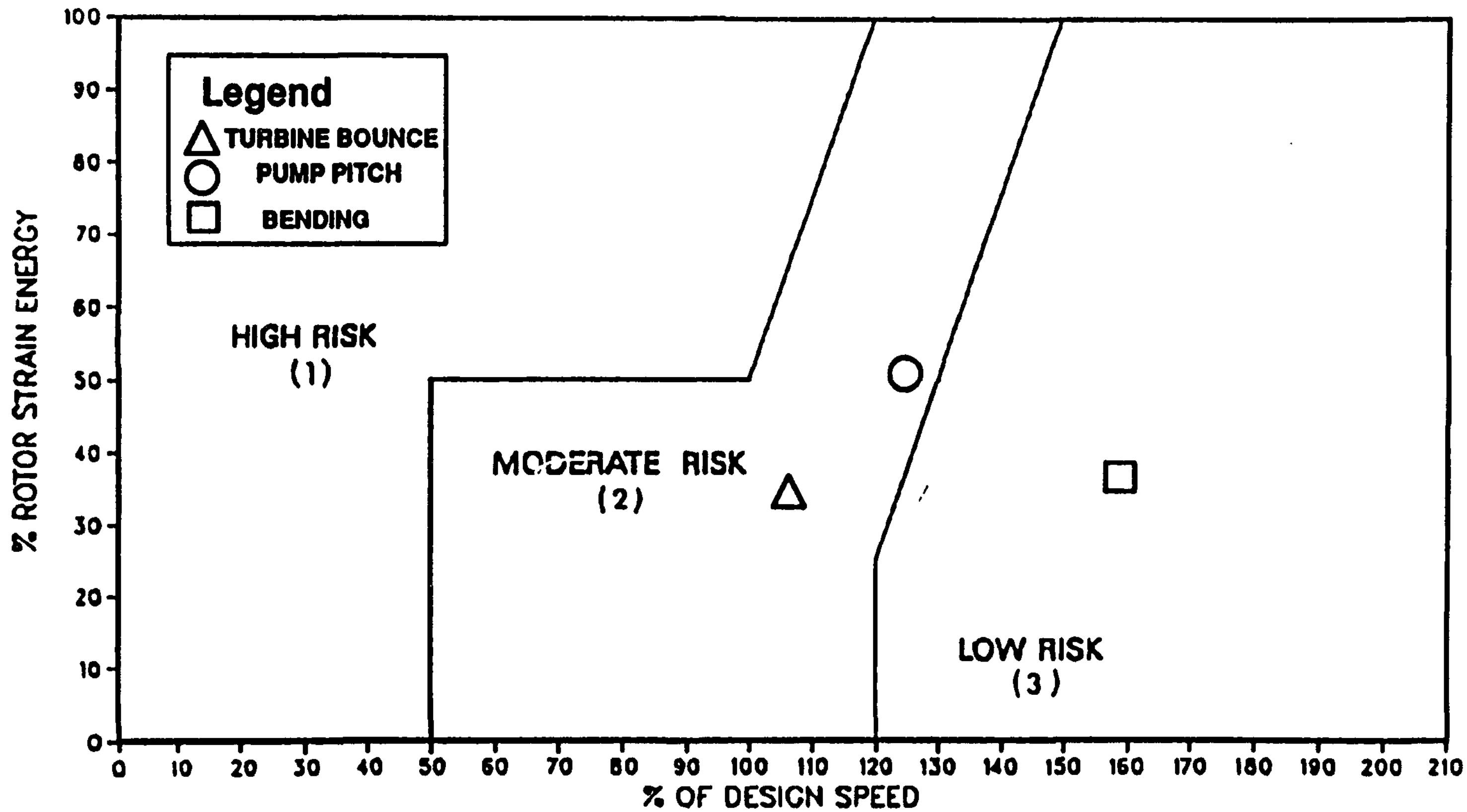

Figure 67. Primary Turbopump Rotordynamics Analysis

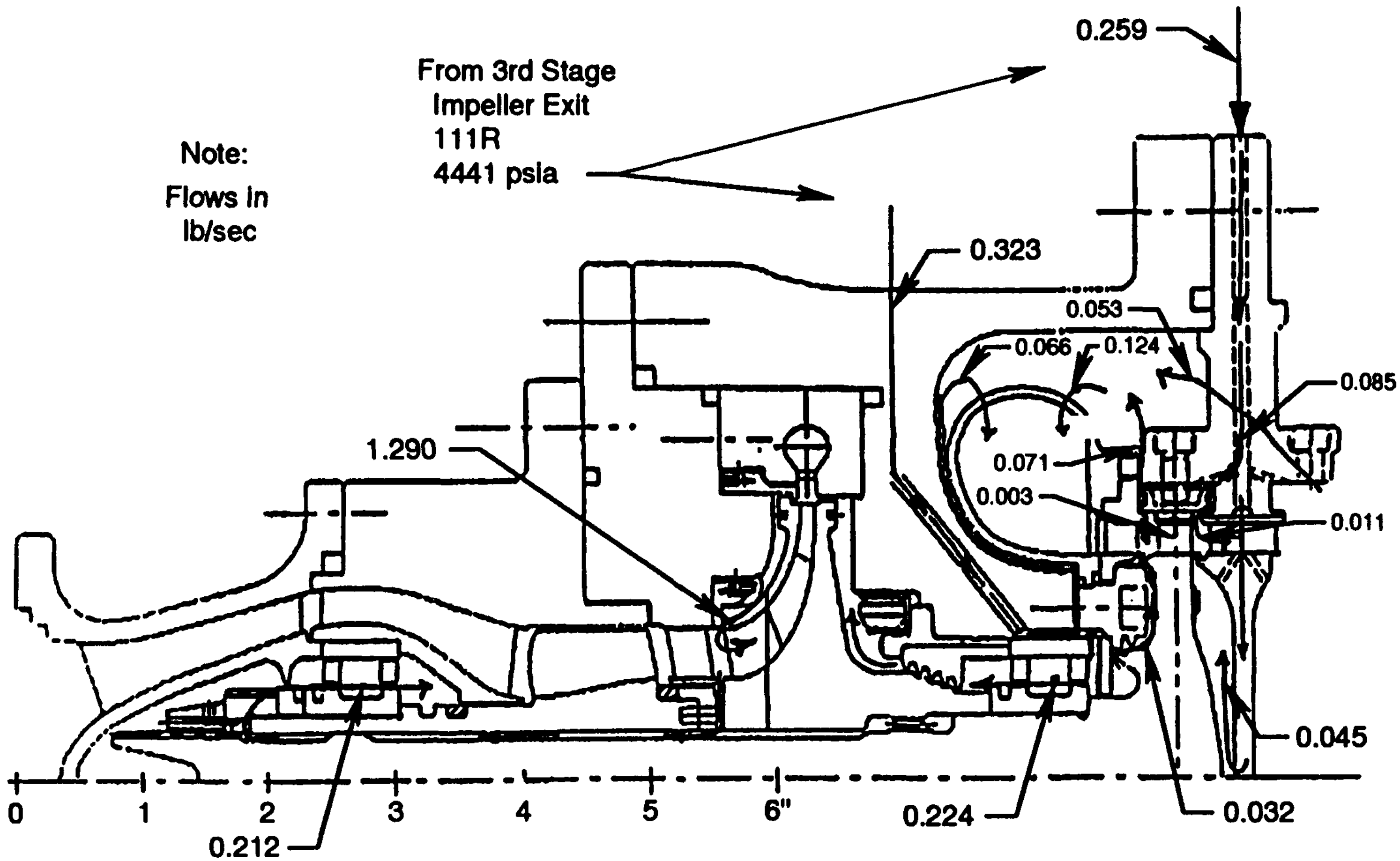

Figure 68. Primary Turbopump Internal Flows

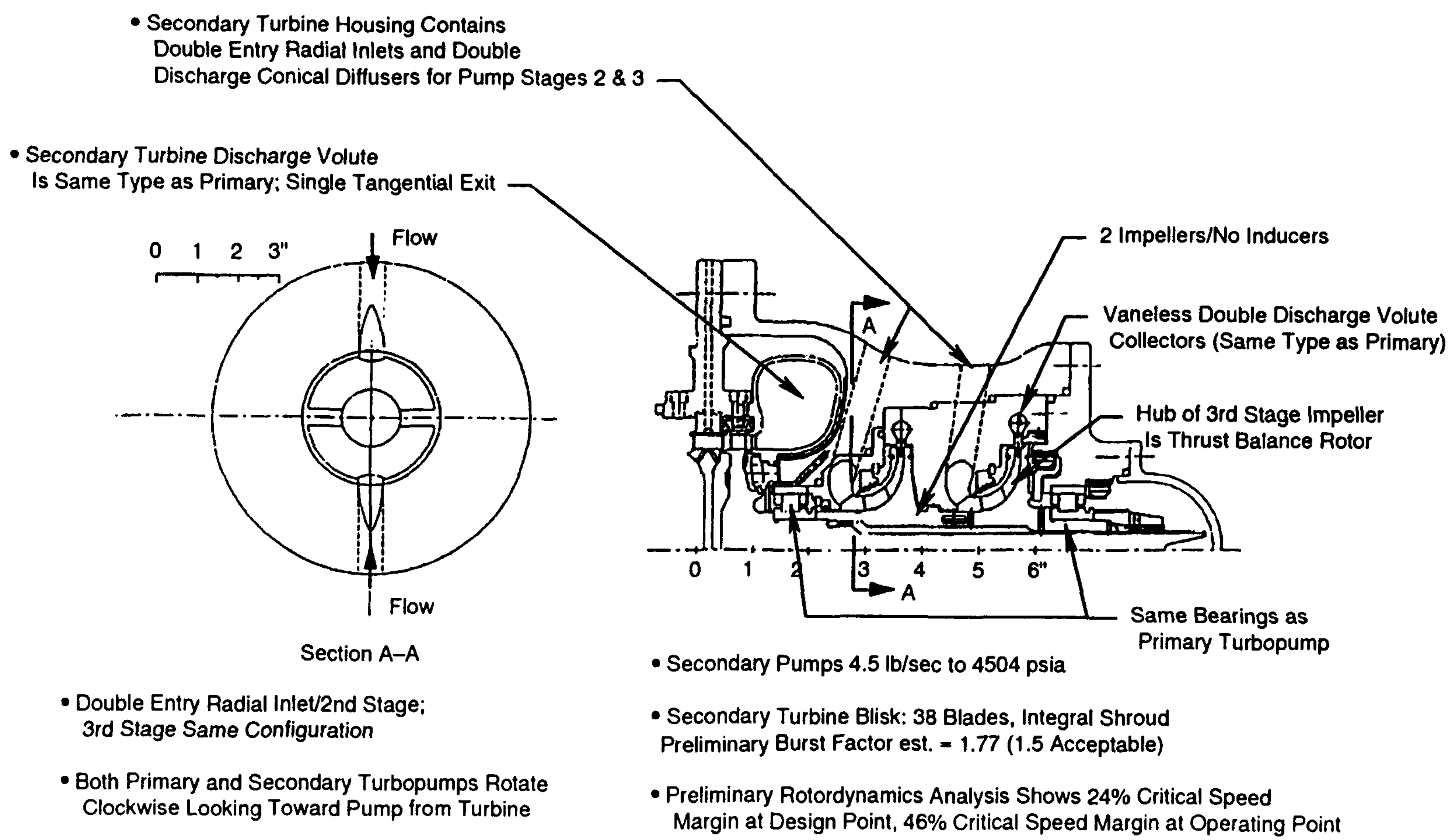

Figure 69. Comparison of Secondary Pump to Primary Pump

TURBINE BOUNCE

NORMALIZED MODE SHAPE
124.5% OF DESIGN SPEED
145% OF OPERATING SPEED
14.2% ROTOR STRAIN ENERGY
124,525 rpm

PUMP PITCH

NORMALIZED MODE SHAPE
136% OF DESIGN SPEED
158% OF OPERATING SPEED
66.4% ROTOR STRAIN ENERGY
136,179 rpm

FUNDAMENTAL BENDING

NORMALIZED MODE SHAPE
176% OF DESIGN SPEED
205% OF OPERATING SPEED
45.4% ROTOR STRAIN ENERGY
176,332 rpm

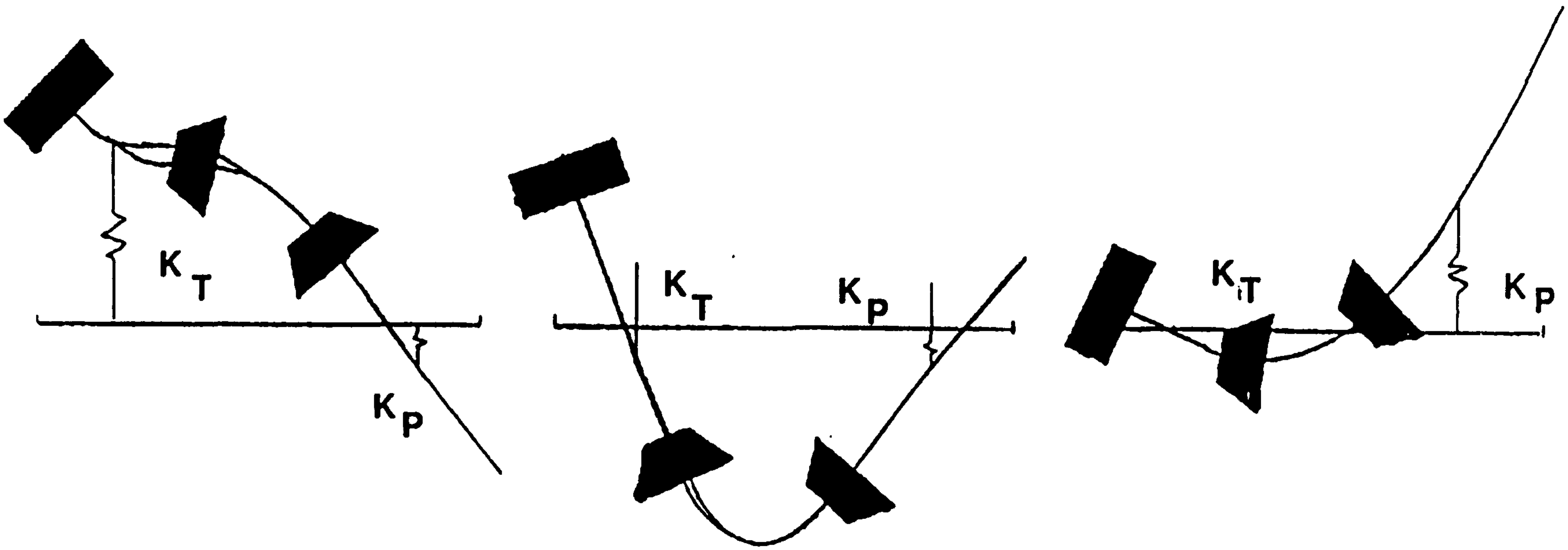

Figure 70. Secondary Turbopump Rotordynamics Modes

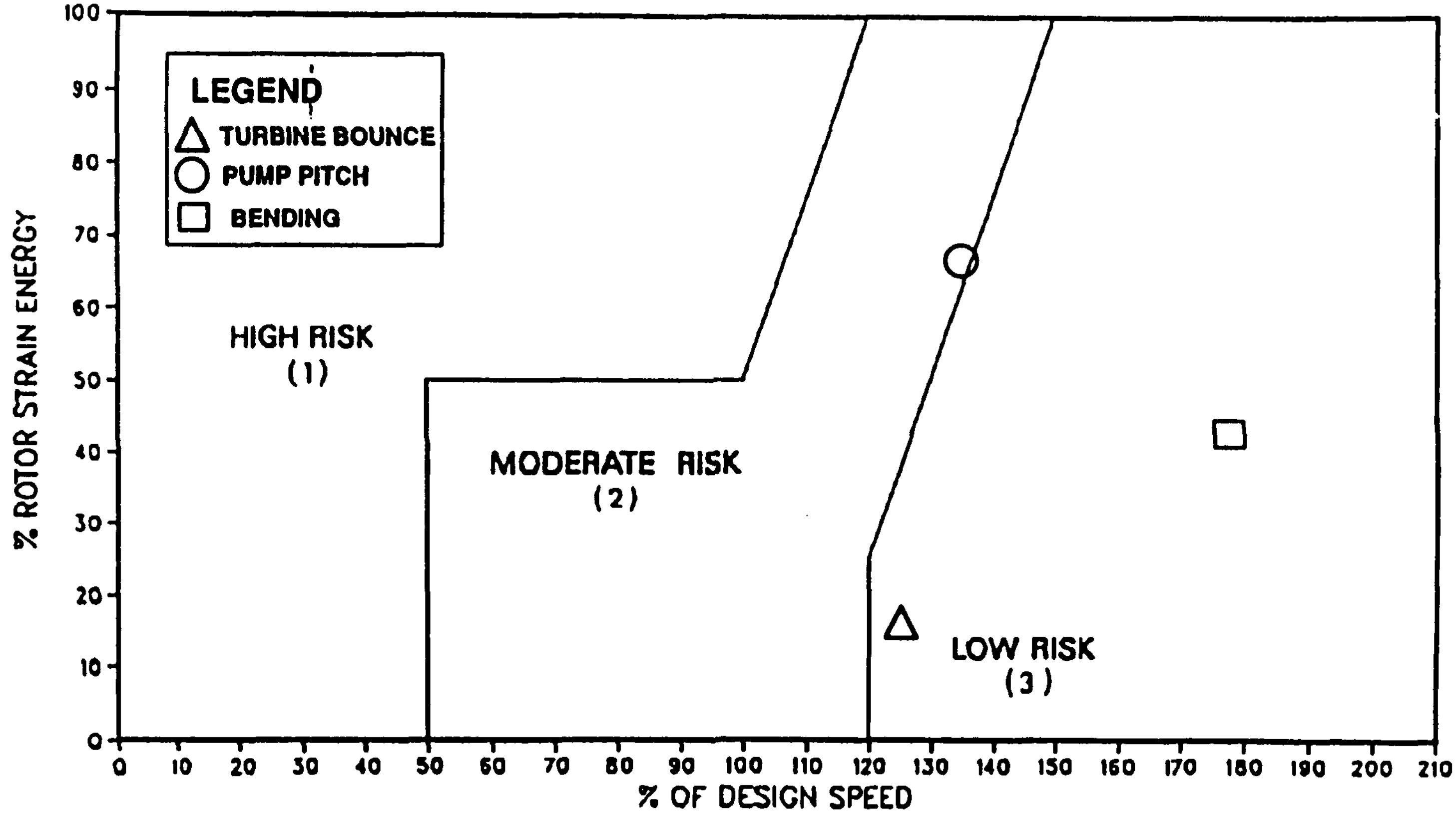

Figure 71. Secondary Turbopump Rotordynamics Analysis

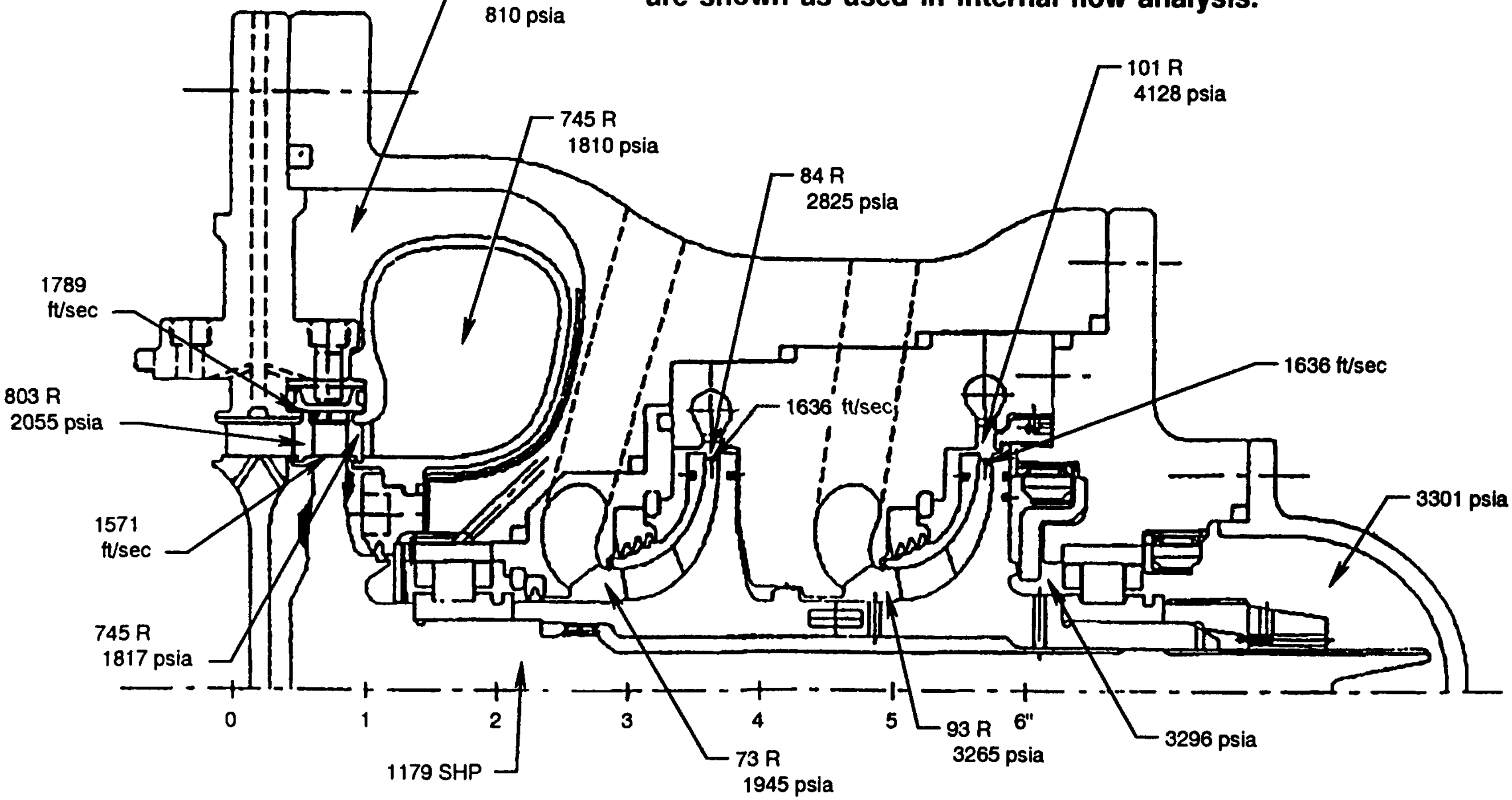

Figure 72. Secondary Turbopump Design Point Parameters

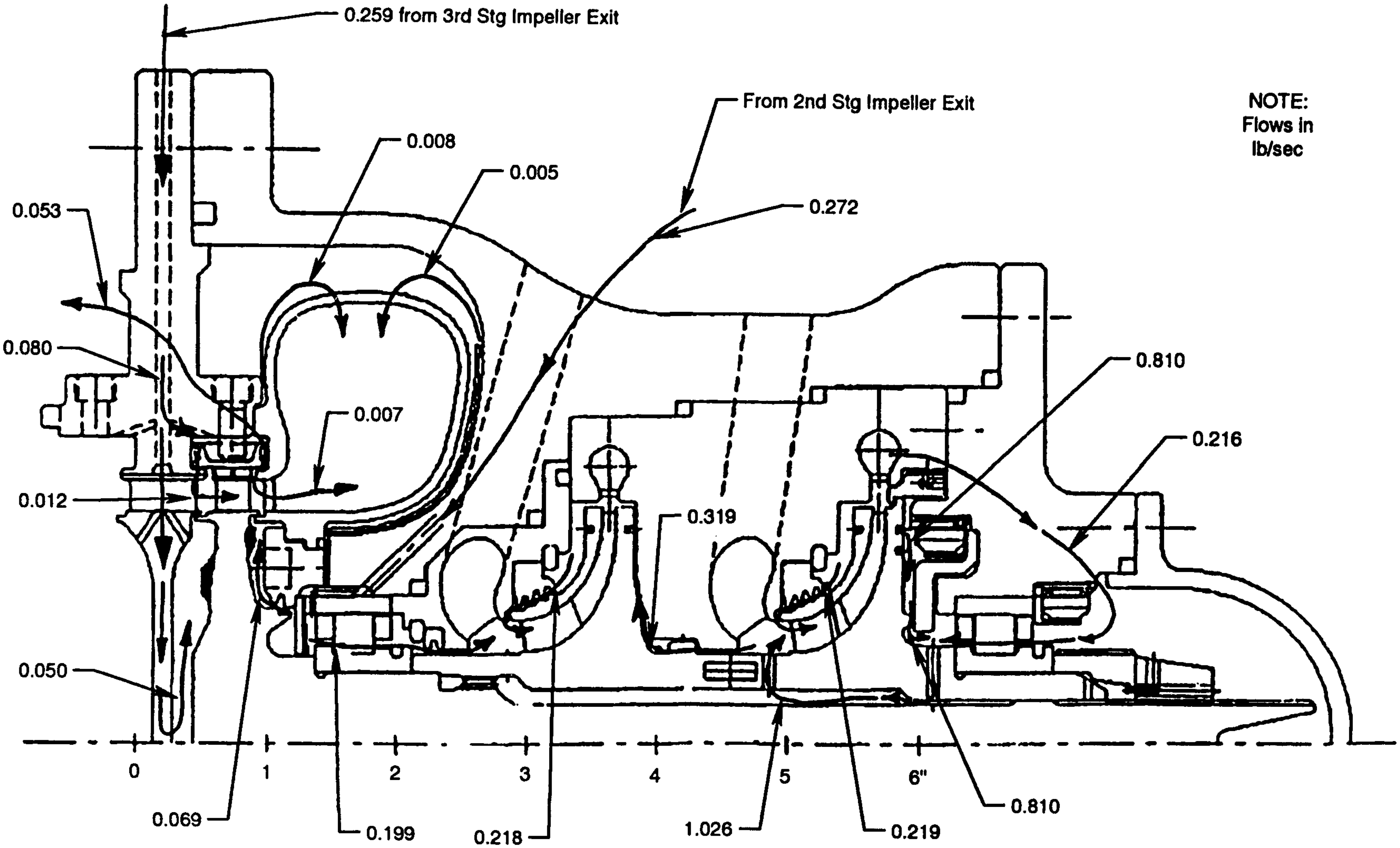

Figure 73. Secondary Turbopump Internal Flows

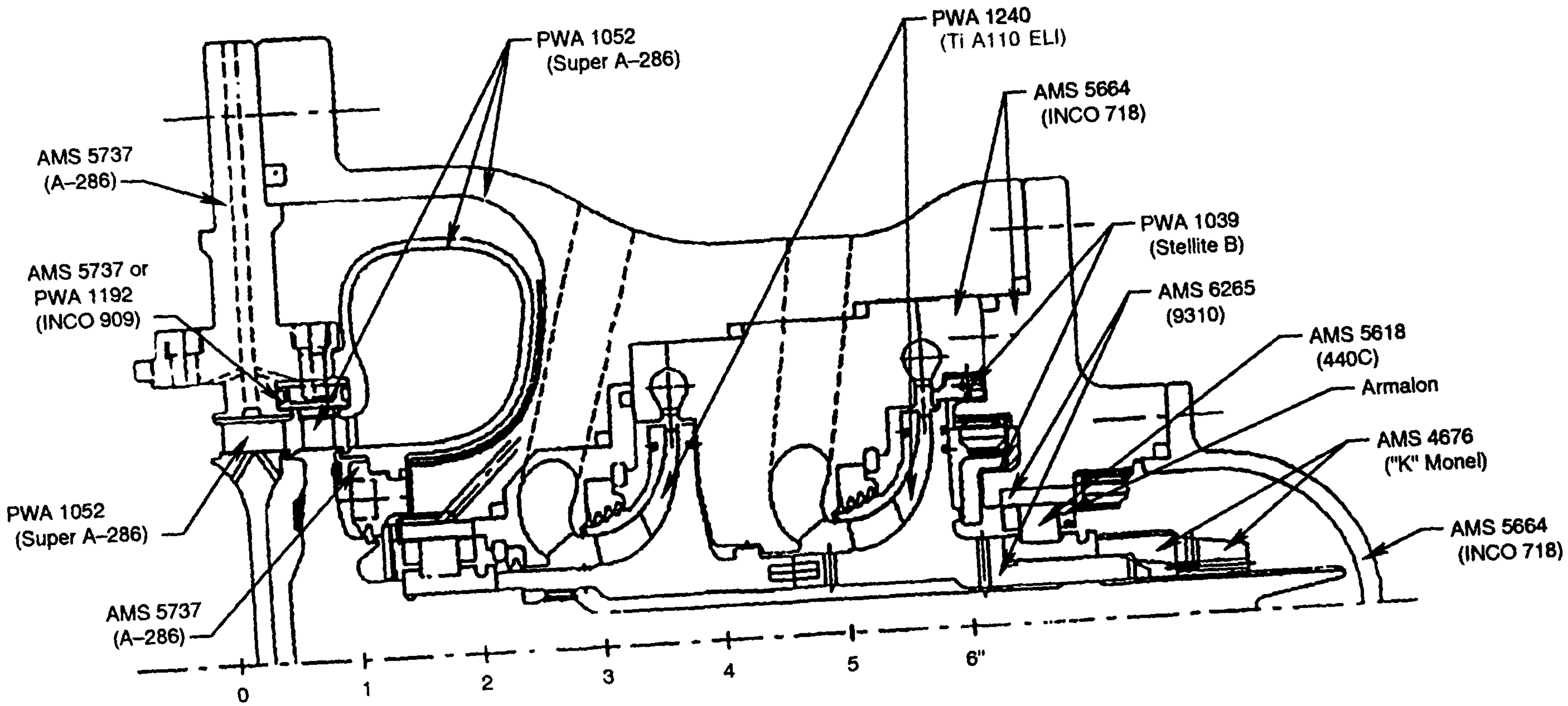

Figure 74. Secondary Turbopump Materials

E. Turbopump Hydrodynamics

1. Hydrodynamic Design Approach

The AETB split expander cycle requires high turbopump efficiency through high pump design speed, stage-headrise and low internal leakage. The AETB is also required to demonstrate a 20 to 1 throttling ratio and high reliability. The combination of these three requirements has not been achieved in any previous rocket engine turbopump design. Also of concern are the performance effects associated with the small size of the pumps requiring tight seal and blade tip clearances, smooth surface finishes, and tight flowpath dimensional tolerances. High reliability will be achieved by designing pumps with adequate hydrodynamic margins for pressure rise, flow capacity, suction performance and stability.

The design methodology applied to AETB turbopump hydrodynamic designs is an iterative process which begins with the engine cycle analysis and proceeds through three design phases: conceptual, preliminary and final, as shown by the schematic in Figure 75. Each phase includes hydrodynamic analyses which are increasingly detailed, proceed from one-dimensional meanline analyses to two- and three-dimensional flow field analyses.

Codes for the analysis of 3D viscous flow fields are now being developed for use in the final design phase. One code developed for this purpose by P&W is the NASTAR program. The ability of NASTAR to model complex, 3D flow fields has been successfully demonstrated on the centrifugal impeller shown in Figure 76. The computational results compared very favorably with test measurements. The NASTAR program will be employed to analyze the AETB first-stage fuel pump impeller flow passages at the 25K design point and at low-power throttle points. Results of these analyses could yield insight into hydrodynamic effects that limit pump throttling range.

2. AETB Oxygen Turbopump

The AETB oxygen turbopump configuration, shown in Figure 77, is a single stage design with an axial flow inlet and inducer and a radial flow impeller. The pump has been designed at a rotational speed that results in a moderate suction requirement for the pump and thus high potential for stability and performance. The inducer serves to allow cavitation to occur in a controlled manner and to gradually collapse any vapor in the inducer blade passages before the flow enters the impeller. The impeller has an integral shroud and features a tight clearance, four-tooth, stepped labyrinth seal for low leakage and high efficiency. The impeller has also been designed with a low discharge blade angle for high efficiency and throttleability. The impeller discharges into a double-discharge collecter, which includes a vaneless diffuser, a double-tongue volute and twin conical discharge diffusers. As in the case of the hydrogen pump stages, this configuration also minimizes radial loads and improves throttleability.

The geometric design parameters for the inducer and impeller are tabulated in Table 8. The oxygen pump inducer features three low-camber blades with a tip solidity of 1.98. The impeller features a 6/6 blading configuration for a total of 12 blades at the discharge. It has a discharge blade height of 0.160 inch and a discharge blade angle of 25 degrees for throttleability.

The hydrodynamic design parameters for the pump are tabulated in Table 9. The pump design speed is 49,400 rpm. This speed resulted from the turbopump meanline analysis, which optimizes speed until specific speed, suction specific speed, head coefficient and impeller diameter ratio are within the experience correlation limits. Subsequent refinements to the engine cycle reduced the pump pressure rise requirements resulting in a lower speed requirement of 47,665 rpm at the 25K thrust point. At this speed, the pump has 39 percent NPSH margin when operating at the required suction specific speed of 22,560. A moderate design point stage-head coefficient was selected to achieve a steep (negative slope) head-flow characteristic essential to high throttleability. Since the axial loads will be controlled by the ball bearings, the pump does not require a thrust balance piston and therefore does not have the attendant leakage and efficiency penalty. The predicted design point efficiency for this pump is 73 percent.

The pump inducer has been designed for an inlet tip flow coefficient of 0.115 as shown in Figure 78. Based on a correlation of rocket turbopump experience for inducer suction capability, the inducer has a design point suction capability parameter of 34,750, taking into account the effects of hub and blade leading edge blockage. For the AETB oxygen pump, the suction specific speed is 28,630. This defines the peak of the predicted suction capability curve at the design flow coefficient shown in Figure 79. The required operating points for the pump illustrate that the pump is predicted to have adequate NPSH margin over the entire engine throttling range, including full-expander operation.

The pump design and off-design headrise requirements and efficiency predictions are presented in Figure 80. The 1K thrust point (20:1 throttling) is the lowest flow coefficient (Q/N) requirement, which is 21.5 percent of the design point value.

The size of the oxygen pump in terms of specific diameter has been optimized in the same manner as described in the hydrogen pump section. Figure 81 shows that for the design specific speed, the oxygen pump has been sized to achieve a near optimum efficiency. This also yields a low stage-head coefficient which is desirable for high throttleability.

Figure 82 compares the pump design point efficiency and stage-head coefficient to the correlations of previous rocket turbopump experience. The efficiency prediction is somewhat lower than the correlation due to the additional leakage (lower volumetric efficiency) requirements of the bearing coolant flow, which is recirculated to the impeller inlet, and inter-propellant seal package over-board leakage. The head coefficient is on the low side of the experience band, but this was intentional in order to achieve high throttleability.

The inducer has been designed in accordance with the incidence and solidity criteria presented in Figure 83. The inducer has an inlet tip blade angle of 11 degrees and a tip solidity of 1.98.

Figure 84 presents the impeller blade angle distribution at the hub, mean and tip streamlines. The impeller has six blades at the inlet and six splitter blades at about 45-percent blade length to contain blade-to-blade loadings within experience levels. Figure 85 presents the design point results of the quasi-3D streamline analysis and shows that the velocity distributions are smooth from the impeller hub to shroud.

The oxygen pump throttle characteristic is presented in Figure 86 and is similar to that presented for the hydrogen pump. At 20:1 throttle ratio (1K thrust), the pump is required to operate at 21.5 percent Q/N, which is close to the points demonstrated by the RL10A-3-1 LO_2 pump and 350K oxygen pump which also demonstrated high throttleability. Based on this experience, the LO_2 pump is expected to achieve its throttling goal of 20:1.

The AETB oxygen pump will be instrumented with sensors in strategic locations from inlet to discharge as shown in Figure 87 to verify the hydrodynamic design methodology. Number, type and location of the sensors have been selected in the same manner as those for the hydrogen pump.

3. AETB Hydrogen Turbopump

The AETB primary hydrogen turbopump configuration, shown in Figure 88, includes several design features that contribute to the achievement of either high performance or high throttleability. The pump features an axial flow inducer and radial flow impeller separated by an interstage strut to enhance throttleability. This feature was demonstrated on the XLR129 fuel pump and showed a significant increase in the shutoff head coefficient, thereby steepening the head-flow characteristic. Inlet struts, a vaneless discharge volute, and a moderate impeller exit blade angle are included in the design to further enhance throttleability. The inlet struts prevent inlet preswirl at off-design or throttle points. Preswirl, if not avoided, reduces the headrise capability of the pump, resulting in a less steep head-flow characteristic. The combination of vaneless diffuser and discharge collector avoids the stall susceptibility of incidence sensitive vaned or airfoil diffuser vane cascades. The moderate impeller blade angle minimizes exit flow recirculations between the collector and impeller discharge at the throttle points, which delays the onset of hydrodynamic pumping instabilities, providing increased operating range.

An impeller shroud has been incorporated to minimize leakage and improve pump efficiency. The shroud face also serves as an integral thrust balance piston. Face seals at the ID and OD of the impeller act in an alternating (open/closed) manner with axial shaft travel, as the controlling orifices between the shroud cavity and the sink (low pressure, impeller inlet) and source (high pressure, impeller exit), respectively, in response to changes in the turbine axial load.

The second and third stages of the secondary hydrogen pump, shown in Figure 89, include several of the same features as the primary pump first stage. Common features include double-discharge collectors and moderate impeller exit blade angles for improved throttleability, and shrouded impellers for increased performance. Four-tooth labyrinth seals with tight clearances are included, along with an in-line impeller arrangement, for reduced leakages and improved efficiency. The stage inlets are of the double side-entry type scaled from the successful XLR129 fuel pump. Like double discharge collectors, double entry inlets also help minimize radial loads. They also minimize inlet preswirl, thereby improving pump throttleability.

The geometric design parameters for the first stage inducer and impeller are tabulated in Table 10. The hydrogen pump inducer features three low camber blades with a moderate solidity of 1.88, as required to control hydrodynamic loadings. The inducer is more than adequate for the required pump suction performance.

The impeller features a 6/6/12 blading configuration for a total of 24 blades at the discharge to reduce flow deviation, or slip, and recirculation at off-design operating points. The discharge blade height is 0.100 inch, which is the desired minimum for producibility. The discharge blade angle is 40 degrees. This angle is higher than the ideal angle for maximum throttleability, but was a compromise to keep impeller steady-state blade stresses within allowable limits and to ensure producibility.

The geometric design parameters for the second and third stage impellers are tabulated in Table 11. The impellers have identical flowpath and blading geometry and feature a 6/6 blading configuration for a total of 12 blades at the discharge. Like the first stage, these impellers have a blade height of 0.100 inch and a 40-degree exit blade angle for structural and producibility reasons.

The hydrodynamic design parameters for the first stage pump are tabulated in Table 12. The first-stage design speed is 100,000 rpm at the 25K thrust point. Higher speeds would be within hydrodynamic experience, however, this speed is the maximum allowable based on the rotordynamic critical speed margin and bearing design requirements. A stage specific speed of 682 derived from the selected speed, pressure rise, and flow rate indicates the pump maximum efficiency potential. After including the additional leakage due to the integral thrust piston, the stage efficiency is predicted to be 60 percent. With the tip speed of 1934 ft/sec set by structural limits and headrise set by the engine cycle, a stage-head coefficient of 0.558 results. The tip speed, along with the rotational speed, also sets the impeller tip diameter of 4.432 inches. With tip diameter, blade height and tip speed determined, the impeller discharge flow coefficient of 0.125 is calculated.

The hydrodynamic design parameters for the second and third stage impellers are tabulated in Table 13. The design rotational speed of the secondary hydrogen pump was also set at 100,000 rpm based on critical speed and bearing considerations. The major hydrodynamic design parameters were determined in a similar manner as the first-stage pump. A stage specific speed of 780 gives these stages a higher efficiency potential.

The second-stage efficiency of 73 percent is higher than the third stage's 65 percent, since it does not have the added leakage of an integral thrust piston.

The first-stage pump inducer has been designed for an inlet tip flow coefficient that provides the pump with the required suction capability including adequate margin. This selection is based on the correlation of suction specific speed versus flow coefficient for previous rocket pumps equipped with inducers, as shown in Figure 90.

The first-stage hydrogen pump design and off-design suction requirements have been analyzed and are all well within the predicted suction capability of the pump, as Figure 91 shows. This provides ample NPSH margin at all the required split-expander cycle operating points from 1K to 25K pounds thrust as well as the full-expander cycle points.

The pump design and off-design headrise requirements and efficiency predictions are presented in Figure 92 for all three pump stages. The plots show that the throttle requirements of the first stage are more severe than those of the second or third stages. The higher shutoff head coefficient of the first stage is a result of the staging of the inducer and impeller at off-design conditions due to the presence of of the interstage strut, which reduces the angular momentum generated by the inducer at the inlet to the impeller.

The sizes of the three pump stages, represented by specific diameter, have been optimized based on their stage specific speeds and the empirical correlations of pump efficiency, Figure 93. Since the second and third stages have higher specific speeds than the first stage, they inherently have a higher efficiency potential as the trend of efficiency islands indicates. The stage specific speed and diameter together explicitly determine the stage-head coefficient.

Figure 94a shows the hydrogen pump design point efficiency predictions compared to previous experience as correlated with specific speed. The stage-head coefficients of all three stages are within experience levels, as shown in the specific speed correlation, Figure 94b.

The incidence of the pump inducer at the tip of the leading edge has been selected based on a correlation of incidence at maximum demonstrated suction specific speed versus inlet tip blade angle. The inlet tip relative flow angle, was determined from a streamline analysis of the inlet and inducer. This analysis indicates the angle is 5.0 degrees at the 25K design point. An inlet tip blade angle of 7.5 degrees, gives an incidence of 2.5 degrees, within previous experience as shown on Figure 95a.

The inducer solidity chosen for the hydrogen pump inducer is within the previous rocket turbopump experience correlation of suction specific speed versus tip solidity as shown in Figure 95b. This ensures that the pump will have adequate suction capability.

Figure 96 presents the impeller blade angle distribution at the hub, mean, and tip stream surfaces for the pump impellers, with the locations of the splitter blade leading edges indicated. The chordwise and spanwise distribution of these blade angles, along with splitter locations, is the result of an iterative design process between the geometry and quasi-3D streamline flow codes to optimize the internal hydrodynamic loadings. Results of the streamline analyses, which include the effects of incidence, deviation (or slip) and hydraulic losses, are presented in Figures 97 and 98 in the form of relative velocity versus percent blade length. Flowpath area distributions and blade contours have been optimized to achieve smooth meanline velocities and diffusion rates.

The first-stage pump inlet is an annular duct which serves to deliver the flow over the No. 1 bearing compartment to the inducer inlet. The axial inlet features two non-turning airfoil strut rows. The first strut has four equally spaced airfoils and provides structural support for the inlet nose cone and inner flowpath wall. The second strut has eight equally spaced airfoils and provides support and stiffness for the bearing. An axisymmetric streamline analysis of the inlet flowpath including strut blockage has been performed. Results of the preliminary inlet design are presented in Figure 99. Hub and tip streamline absolute velocity distributions indicated an excessive wall diffusion loading along the inner flowpath wall of the second strut row leading into the inducer leading edge hub. During the final design phase this loading will be reduced to an acceptable level by increasing the flange inlet area and refining the flowpath area and curvature distributions. The increased inlet area will also minimize the radial flow profile stemming from the inlet flowpath curvature entering the inducer and thereby enhance its suction performance.

The first-stage pump throttle characteristics are presented in Figure 100. Pump throttling is represented by a curve of percent of design flow-to-speed ratio (percent Q/N) as a function of engine vacuum thrust. Engine throttle ratios of 20, 10, and 5:1 have been noted on the x-axis. At 20:1 (1K thrust, 6.0 O/F ratio), the AETB first stage pump is required to operate at 22.7 percent Q/N. The RL10A-3-1 fuel pump, which featured a first-stage impeller with a 50-degree exit blade angle and a second-stage impeller with a 90-degree exit blade angle, demonstrated deep engine throttling with the pump operating down to 24 percent Q/N. Based on this experience, the first-stage fuel pump, with a 40-degree blade angle, is expected to achieve its throttling goal of 20:1.

The AETB hydrogen pump stages will be instrumented with sensors in strategic locations from inlet to discharge as shown in Figure 101 to verify the hydrodynamic design methodology. Static pressure taps along the impeller shrouds and backfaces will provide data for the calculation of pump axial loads. Inlet and discharge pressure and temperature sensors will provide data for the calculation of stage-headrise and efficiency. Dynamic wall static pressures will provide high response data to measure potential pump-induced hydraulic oscillations over the full range of operation.

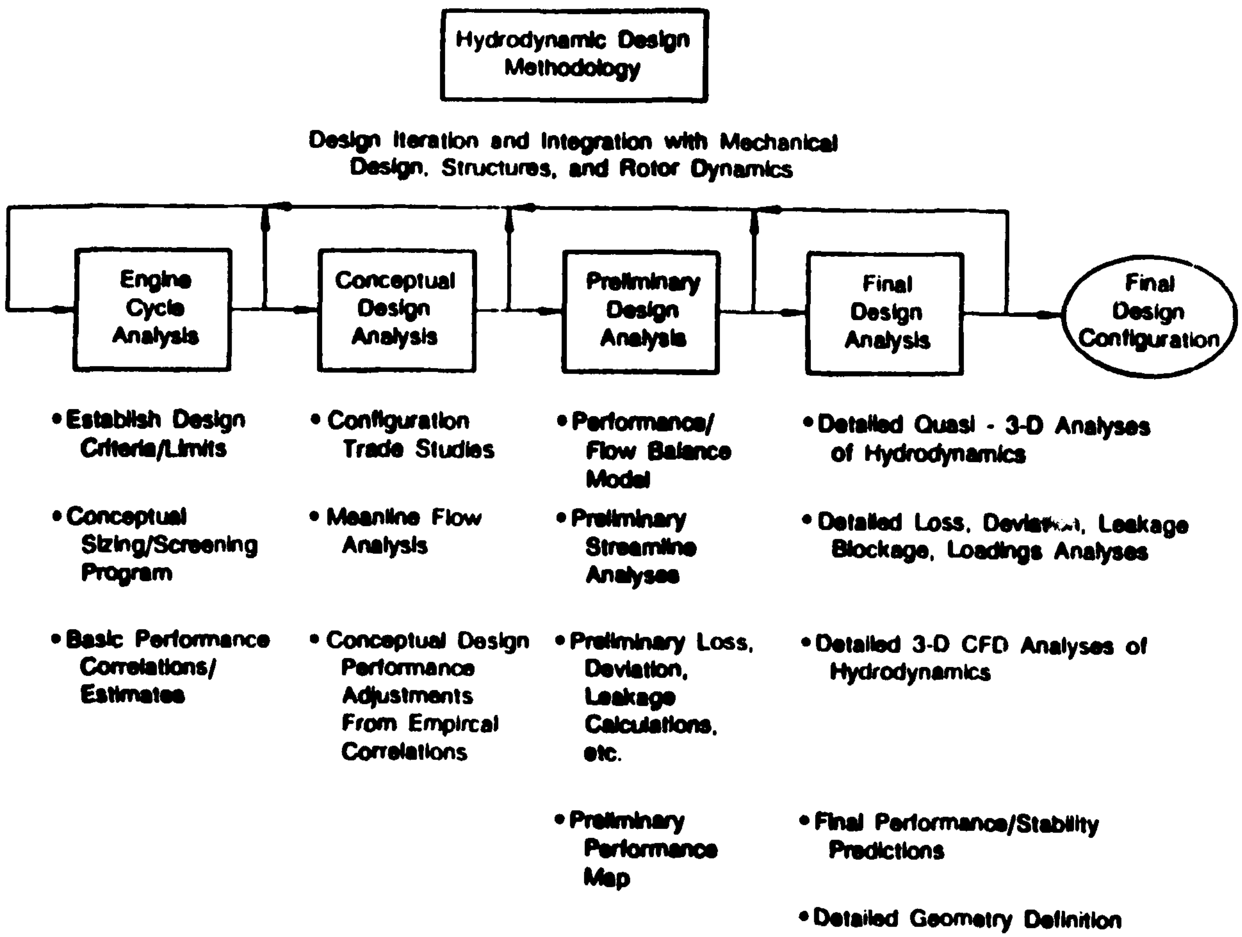

Figure 75. Turbopump Hydrodynamic Design Methodology

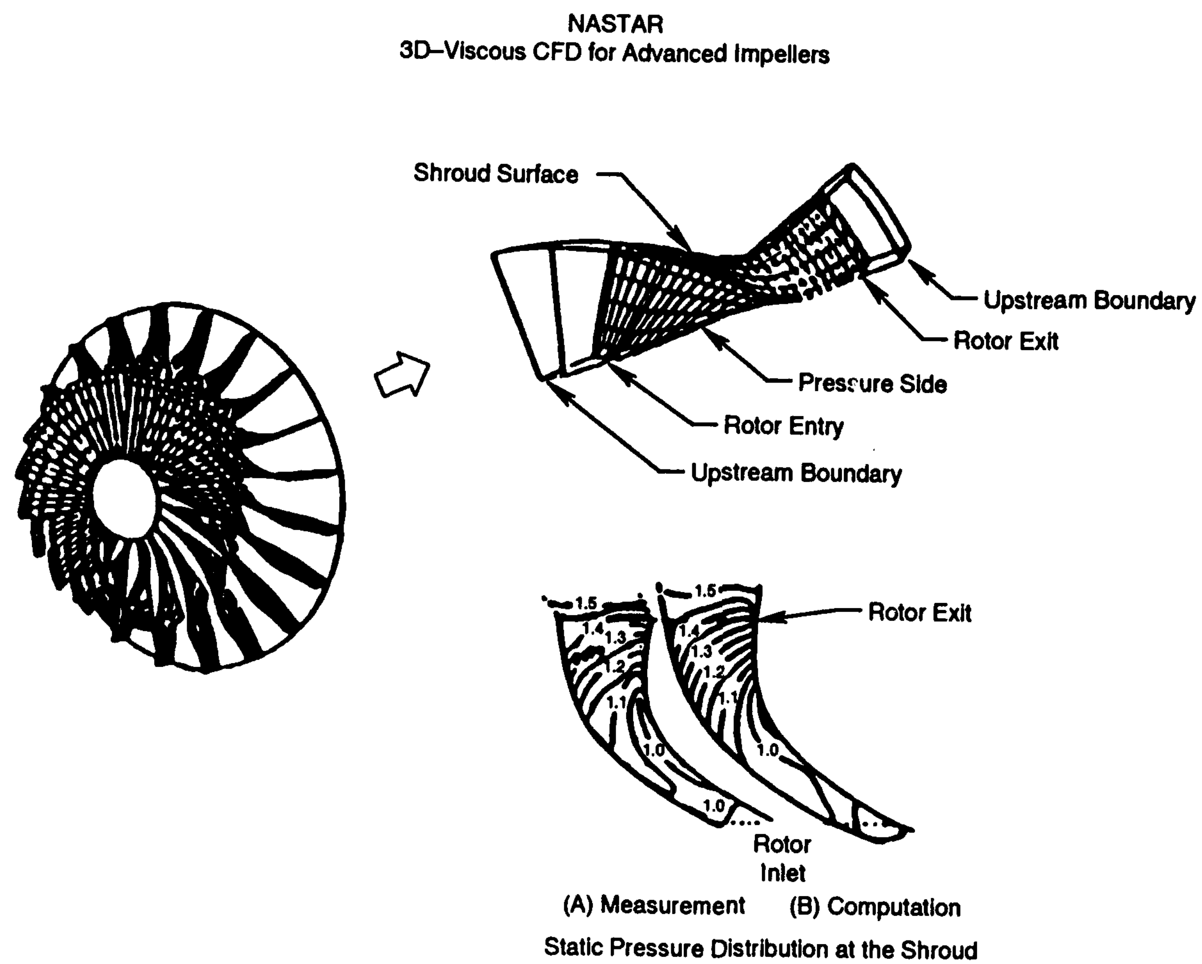

Figure 76. 3D NASTAR for Impeller Flow Analysis

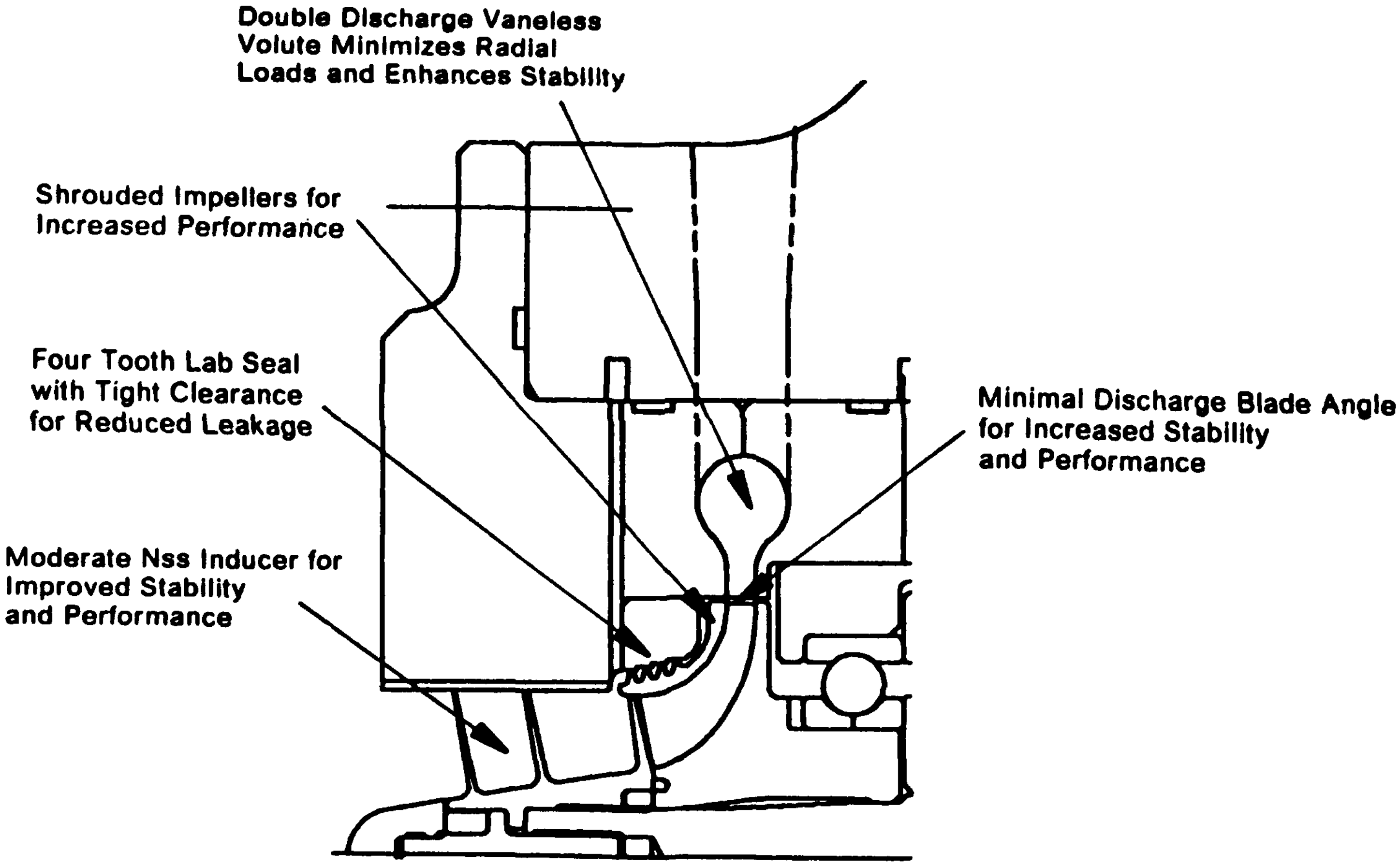

Figure 77. AETB Oxygen Turbopump Features

Table 8. Oxygen Turbopump Geometric Design Parameters

INDUCER

Parameter	Description	Value
D_{1t}	Inlet Tip Diameter (in.)	1.75
D_{1h}	Inlet Hub Diameter (in.)	0.525
$D_{1.5t}$	Exit Tip Diameter (in.)	1.75
$D_{1.5h}$	Exit Hub Diameter (in.)	0.940
β_{1t}^*	Inlet Tip Blade Angle (deg.)	11.0
$\beta_{1.5m}^*$	Exit Mean Blade Angle (deg.)	26.7
σ	Inducer Tip Solidity	1.98
Z	Number of Blades	3

IMPELLER

Parameter	Description	Value
$D_{1.5t}$	Inlet Tip Diameter (in.)	1.75
$D_{1.5h}$	Inlet Hub Diameter (in.)	0.940
D_{2m}	Exit mean Diameter (in.)	2.785
β_{2m}^*	Exit Mean Blade Angle (deg.)	25.0
b_2	Discharge Blade Height (in.)	0.162
Z	Number of Blades	6 + 6

Table 9. Oxygen Turbopump Hydrodynamic Design Parameters

INDUCER

Parameter	Description	Value
W_{in}	Inlet Mass Flow Rate (lbm/sec)	45.0
P_{in}	Inlet Pressure (psia)	67.0
T_{in}	Inlet Temperature (deg R)	162.1
N	Rotational Speed (rpm)	49,400
$NPSH_{Avail}$	Available NPSH (ft)	106.0
$NPSH_{Reqd}$	Required NPSH (ft)	78.9
$N_{ss-Reqd}$*	Suction Specific Speed - Required (rpm $\frac{(gpm)^{1/2}}{(ft)^{3/4}}$)	23,380
N_{ss-Cap}*	Suction Specific Speed - Capability (rpm $\frac{(gpm)^{1/2}}{(ft)^{3/4}}$)	28,630
NPSHM	NPSH margin (percent)	34

STAGE

Parameter	Description	Value
U_{tip}	Impeller Tip Speed (ft/sec)	600
ΔH_{poly}	Stage Head Rise (ft)	4,804
N_s	Stage Specific Speed (rpm $\frac{(gpm)^{1/2}}{(ft)^{3/4}}$)	1,432
ϕ_{2m}	Discharge Flow Coefficient	0.140
ψ_{poly}	Stage Head Coefficient	0.429
η_{poly}	Stage Efficiency (percent)	73

* N_{ss} referenced to water

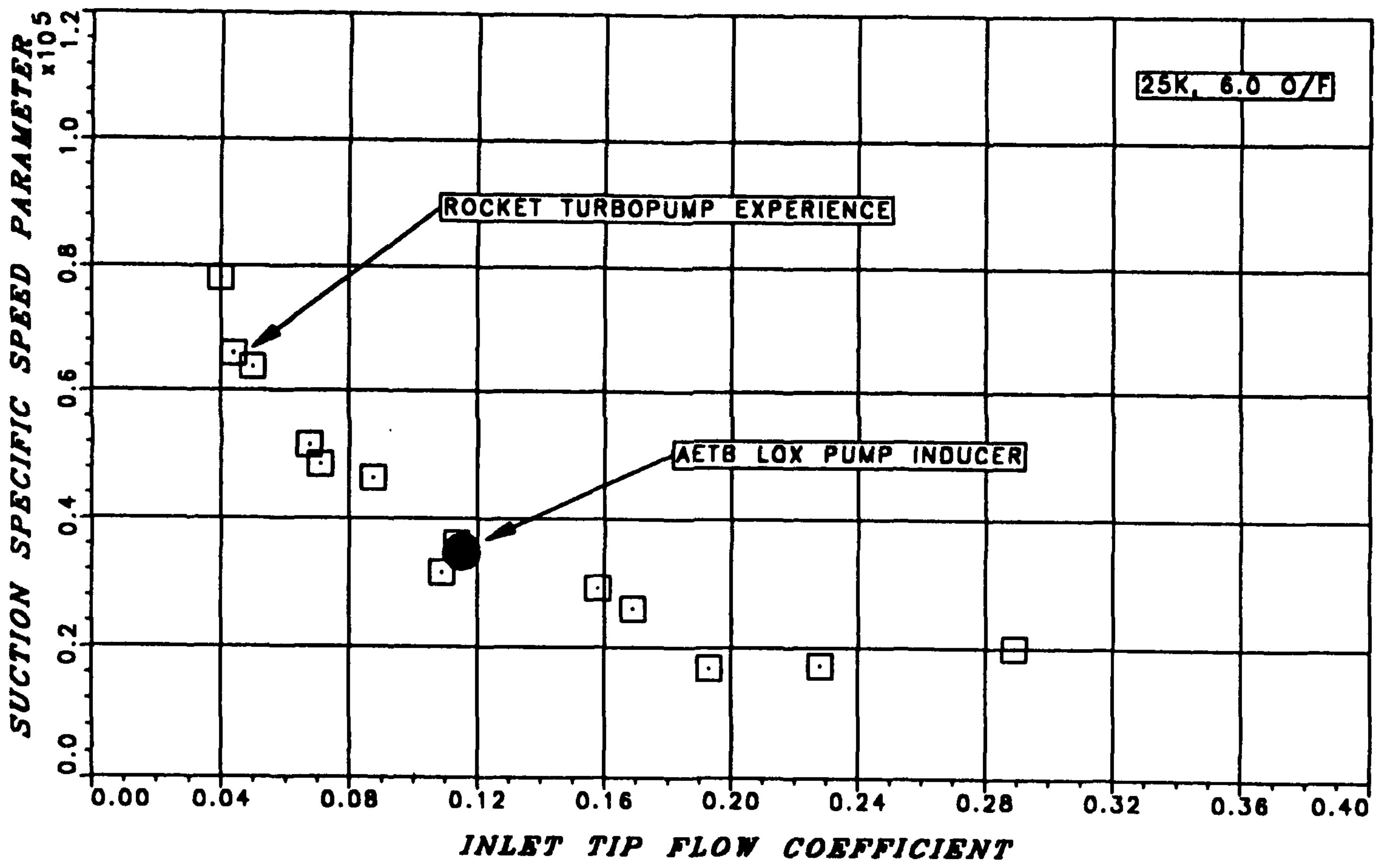

Figure 78. Oxygen Turbopump Inducer Tip Flow Coefficient

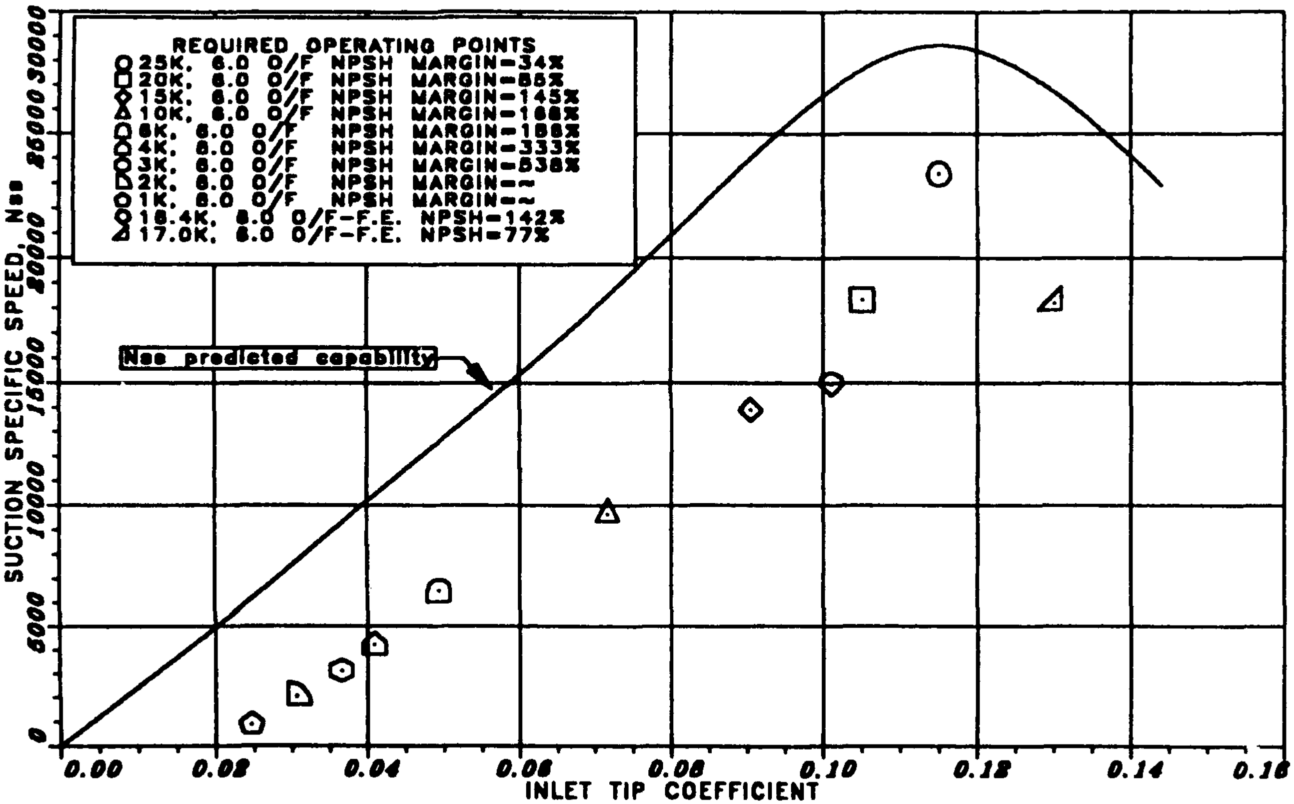

Figure 79. Oxygen Turbopump Suction Performance Characteristics

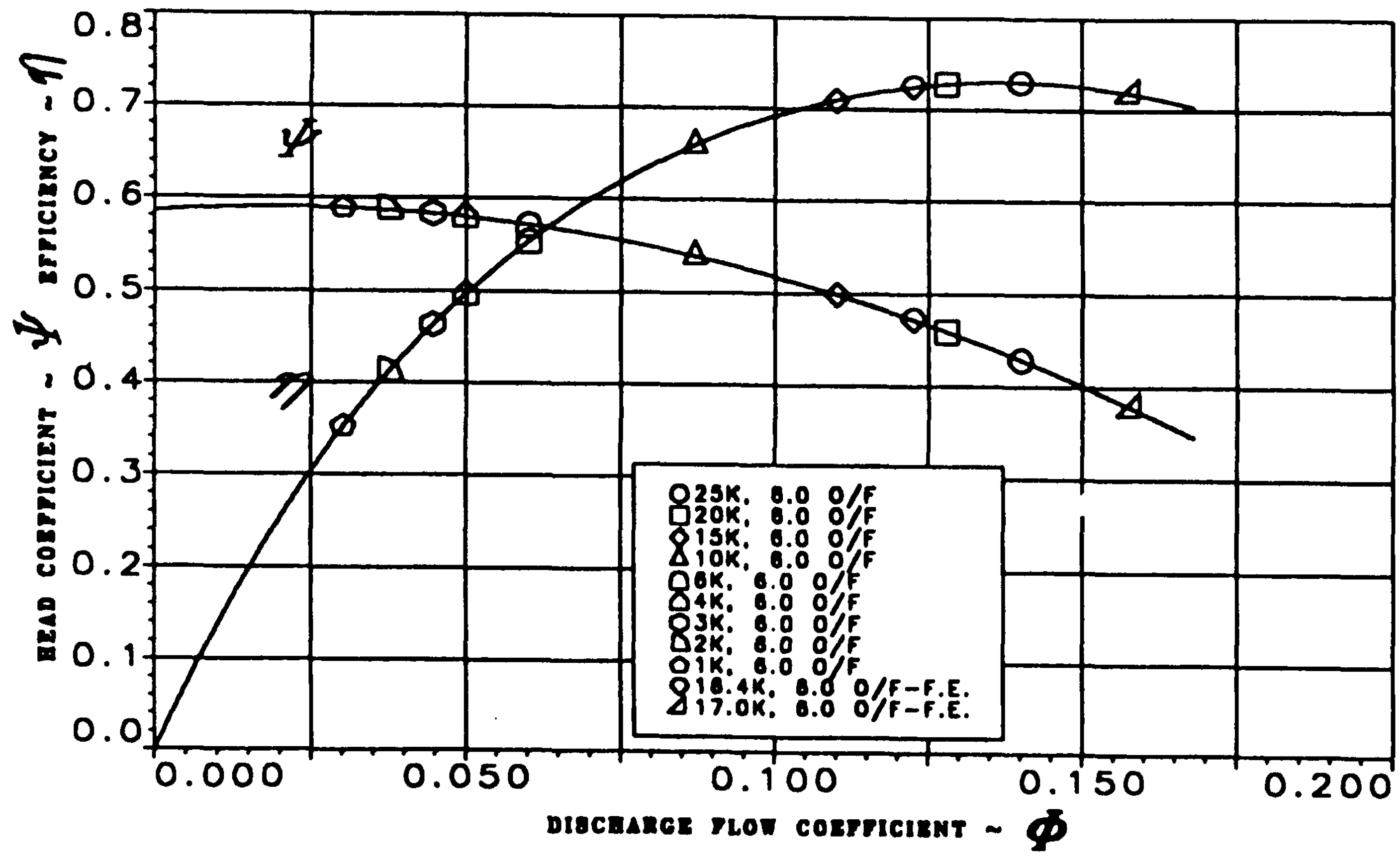

Figure 80. Oxygen Turbopump Stage Performance Characteristics

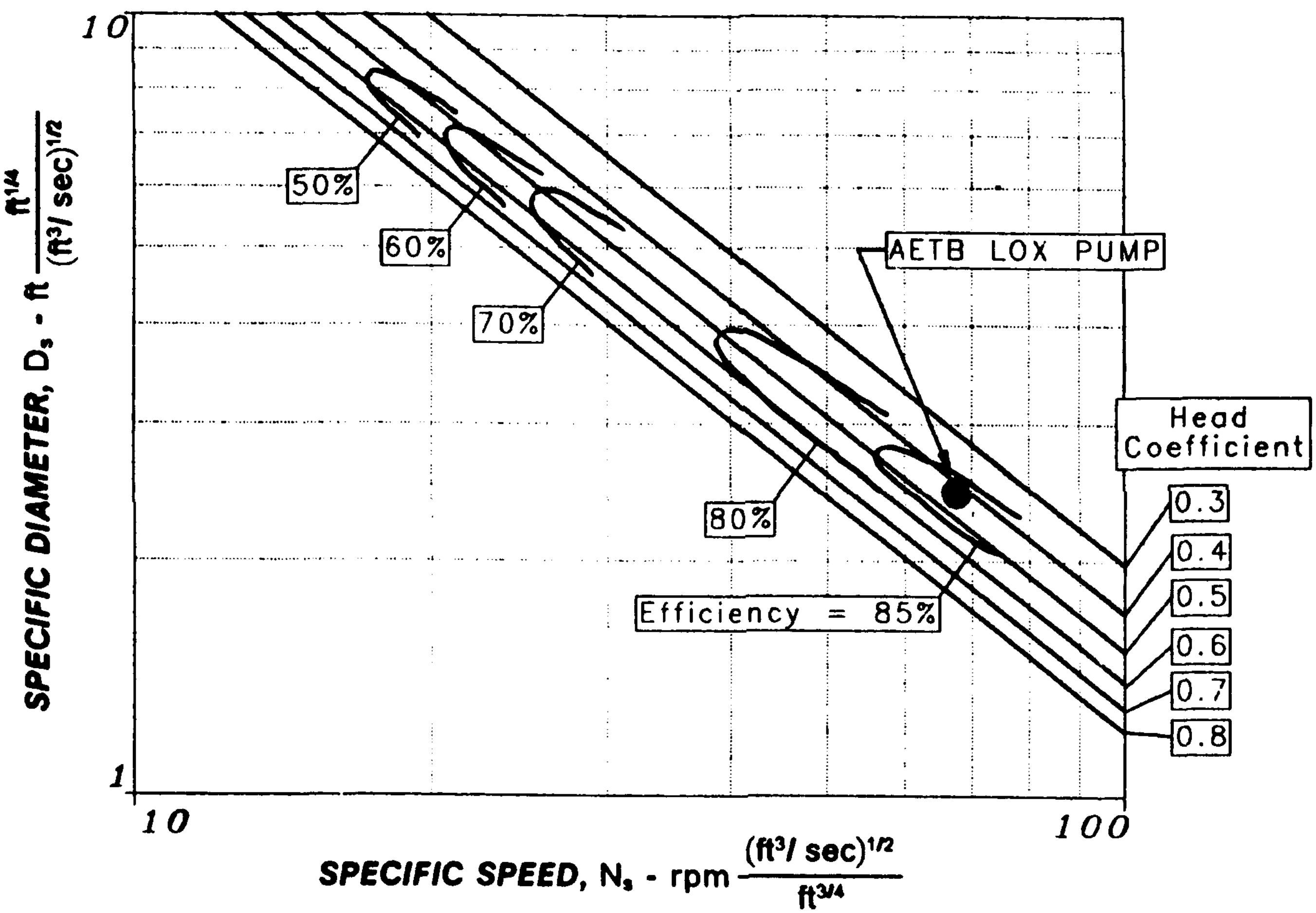

Figure 81. Oxygen Turbopump Specific Diameter versus Specific Speed

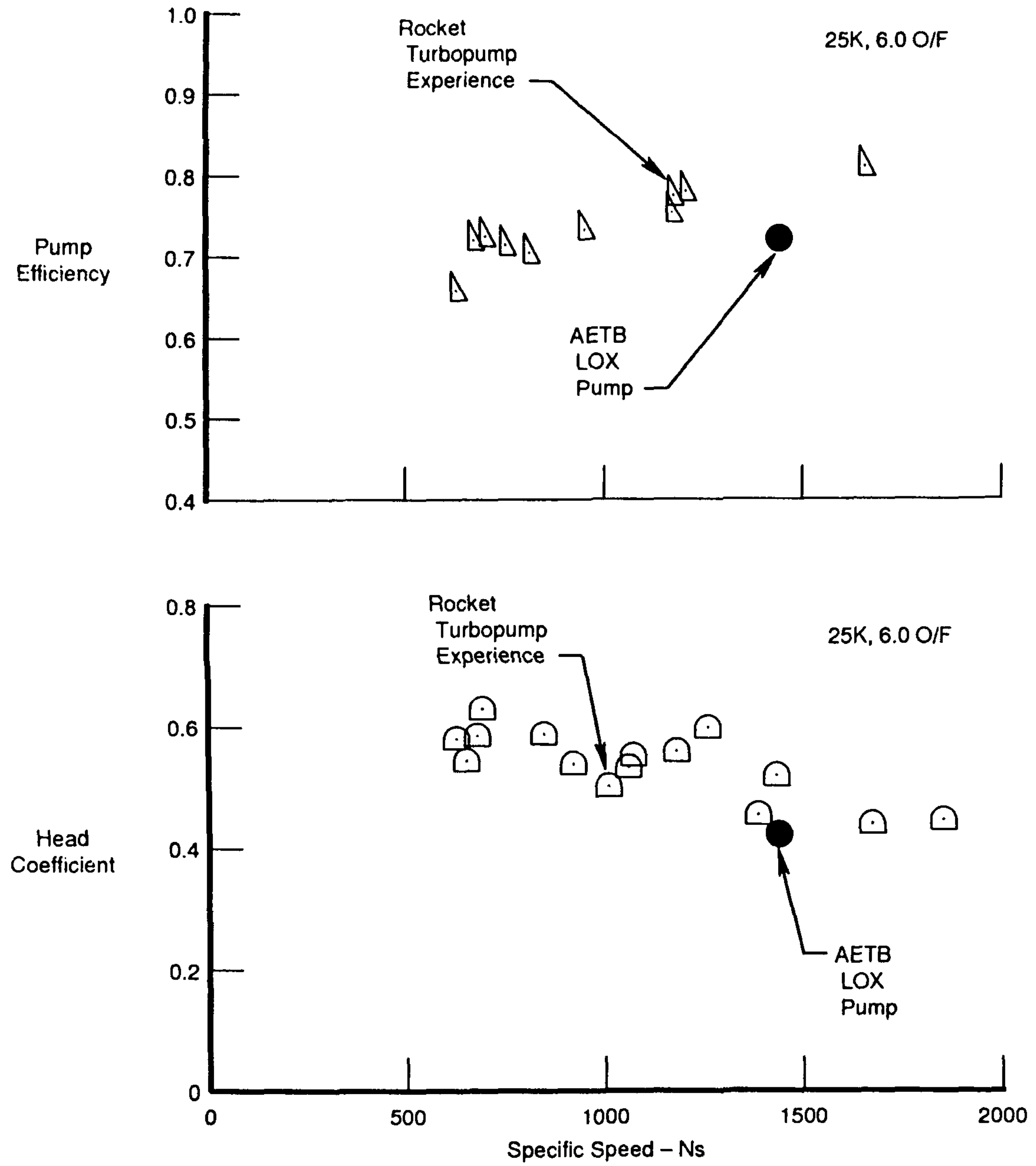

Figure 82. Oxygen Turbopump Efficiency and Head Coefficient Historical Data

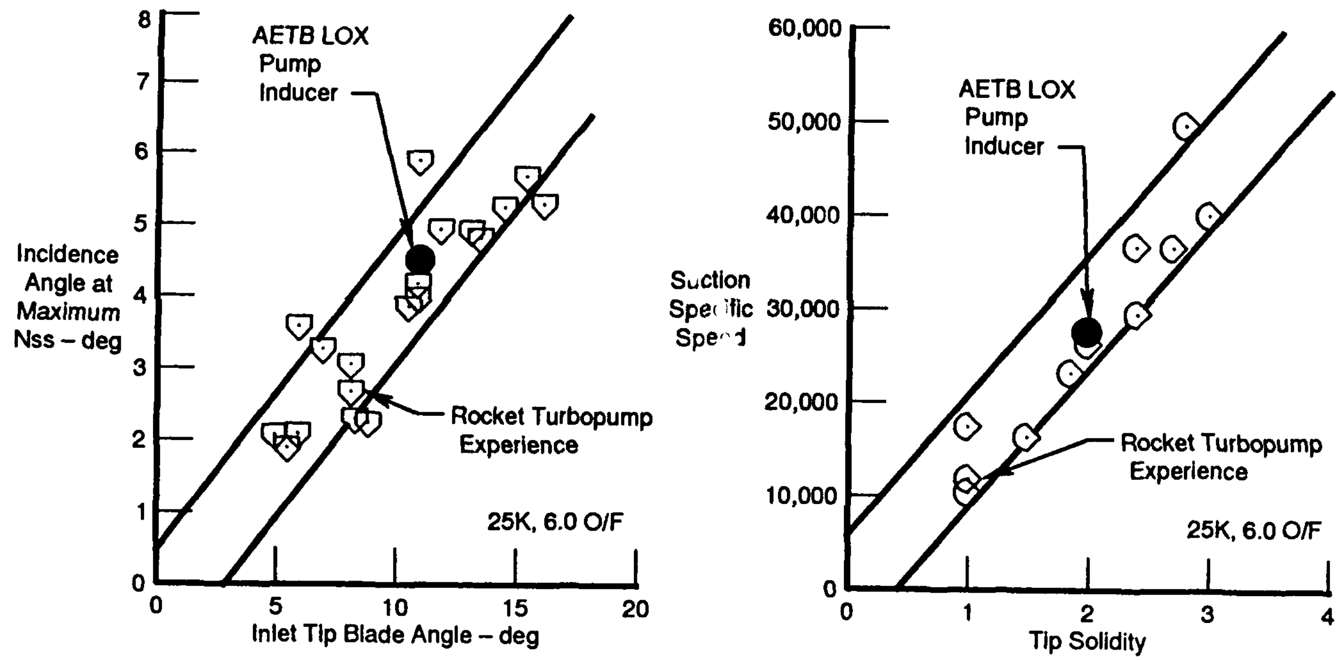

Figure 83. Oxygen Turbopump Inducer Incidence and Solidity

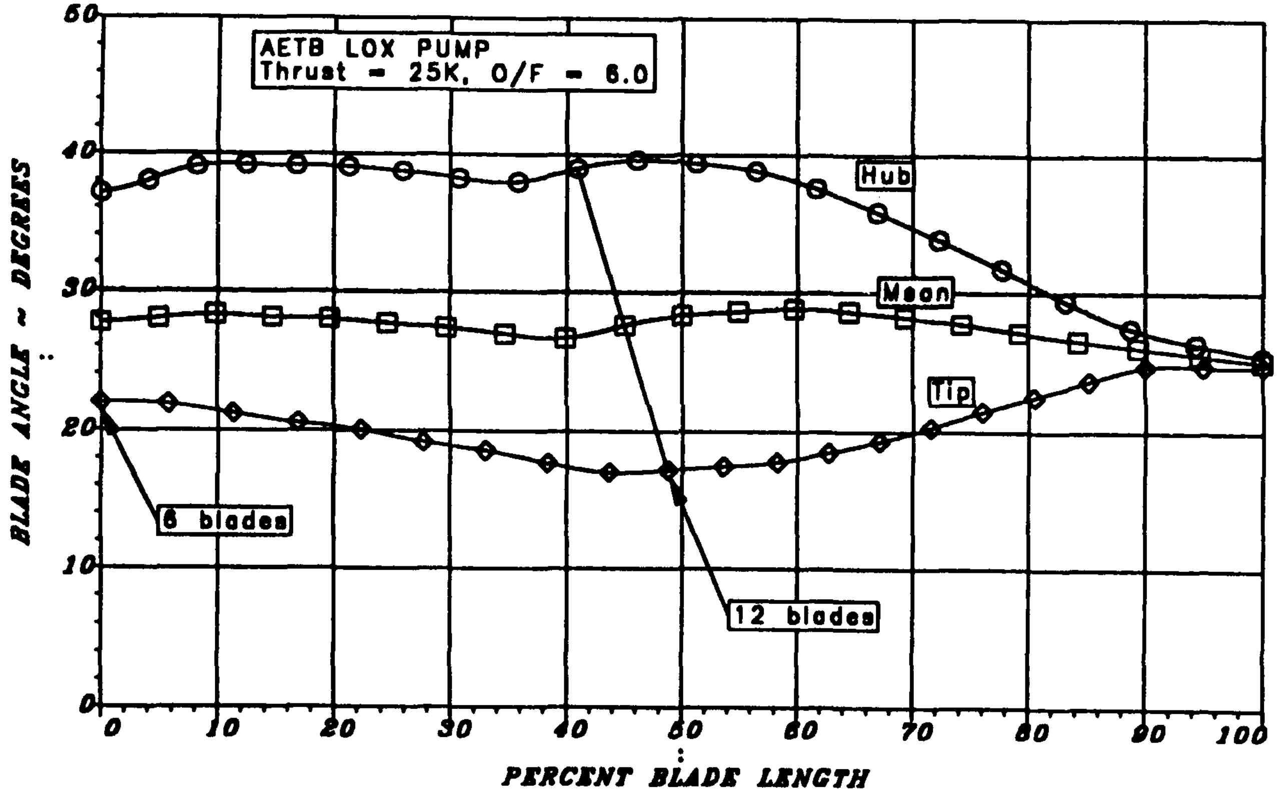

Figure 84. Oxygen Turbopump Impeller Blade Distribution

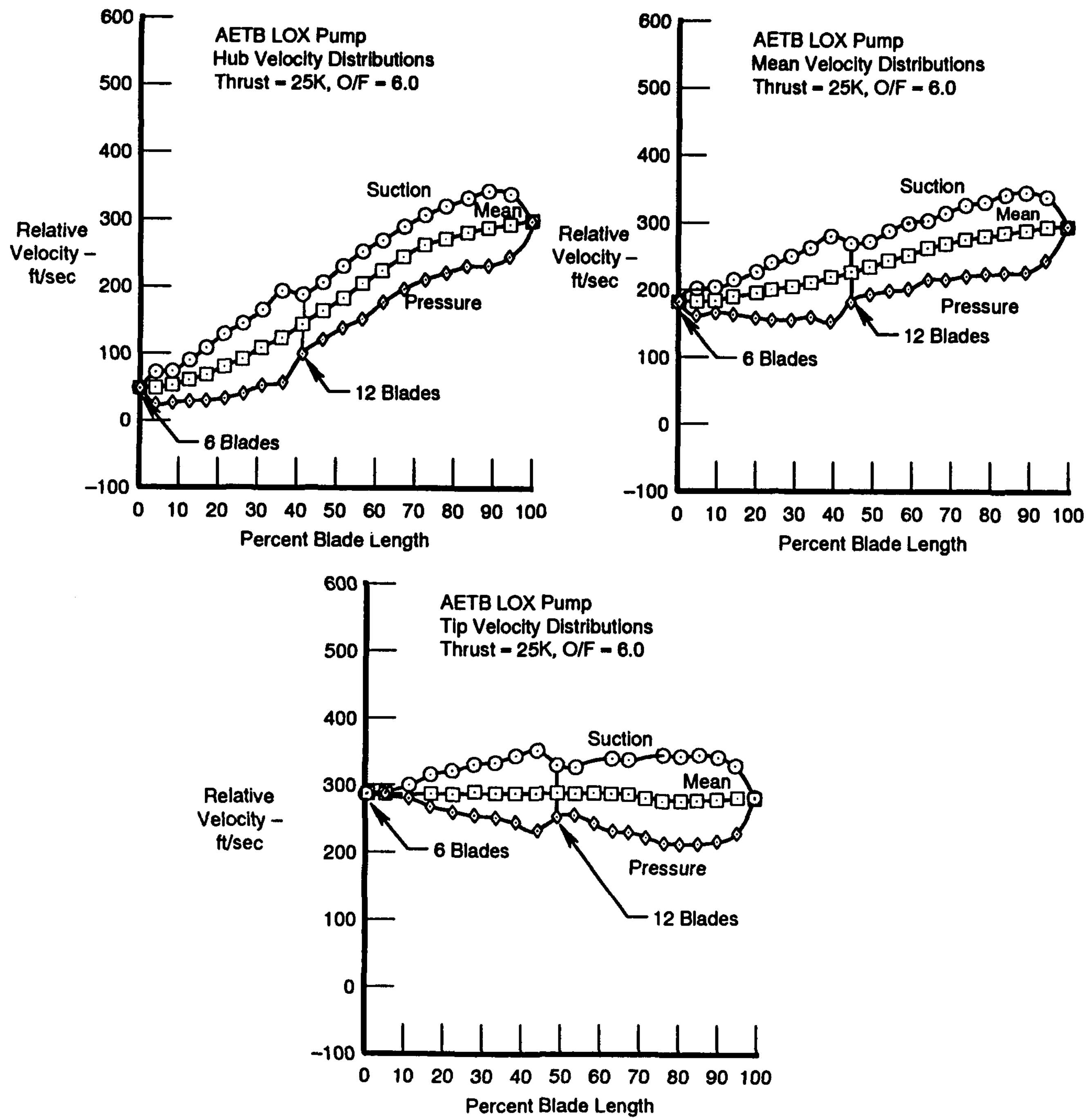

Figure 85. Oxygen Turbopump Impeller Velocity Distributions

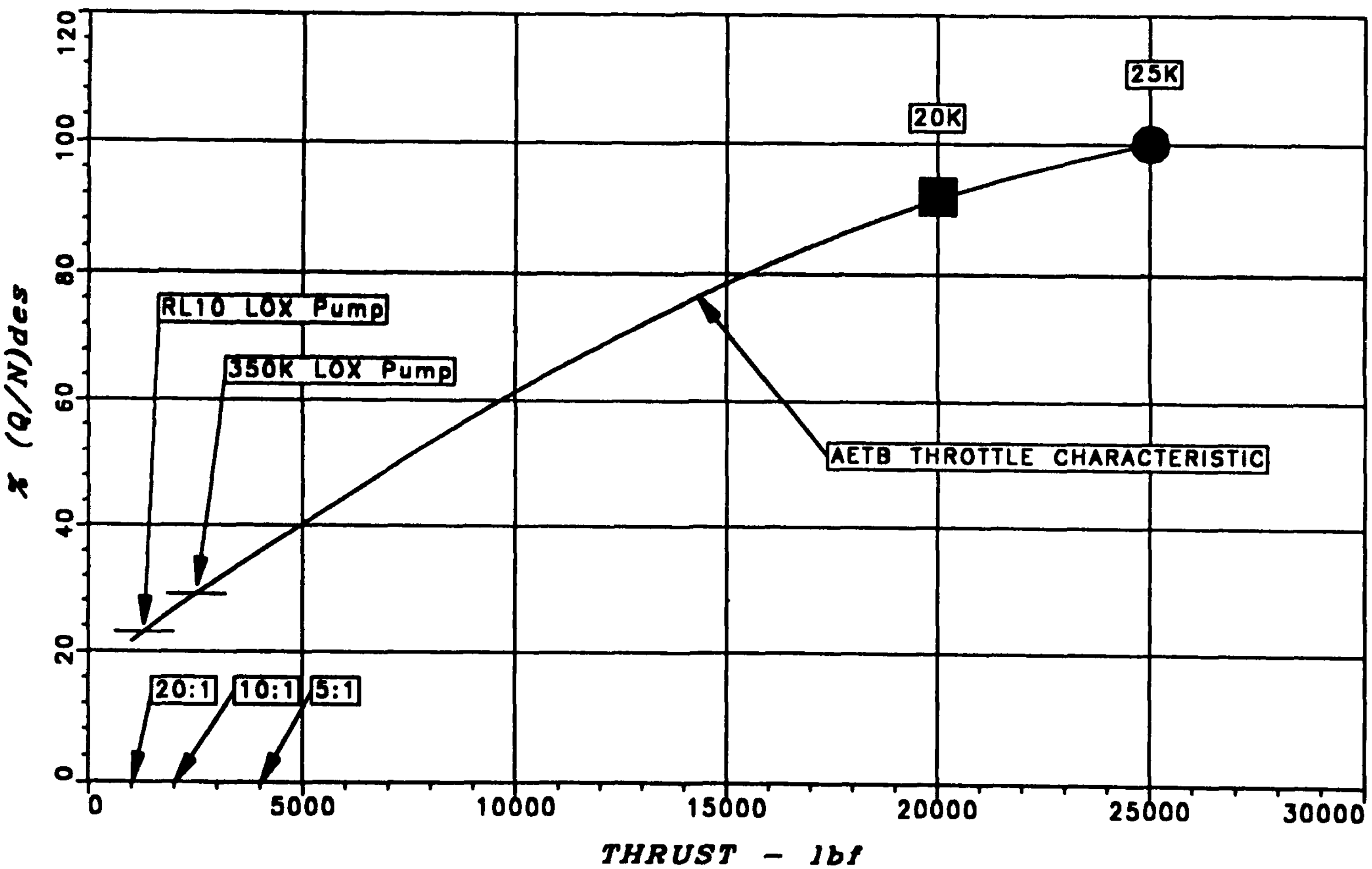

Figure 86. Oxygen Turbopump Throttle Characteristic

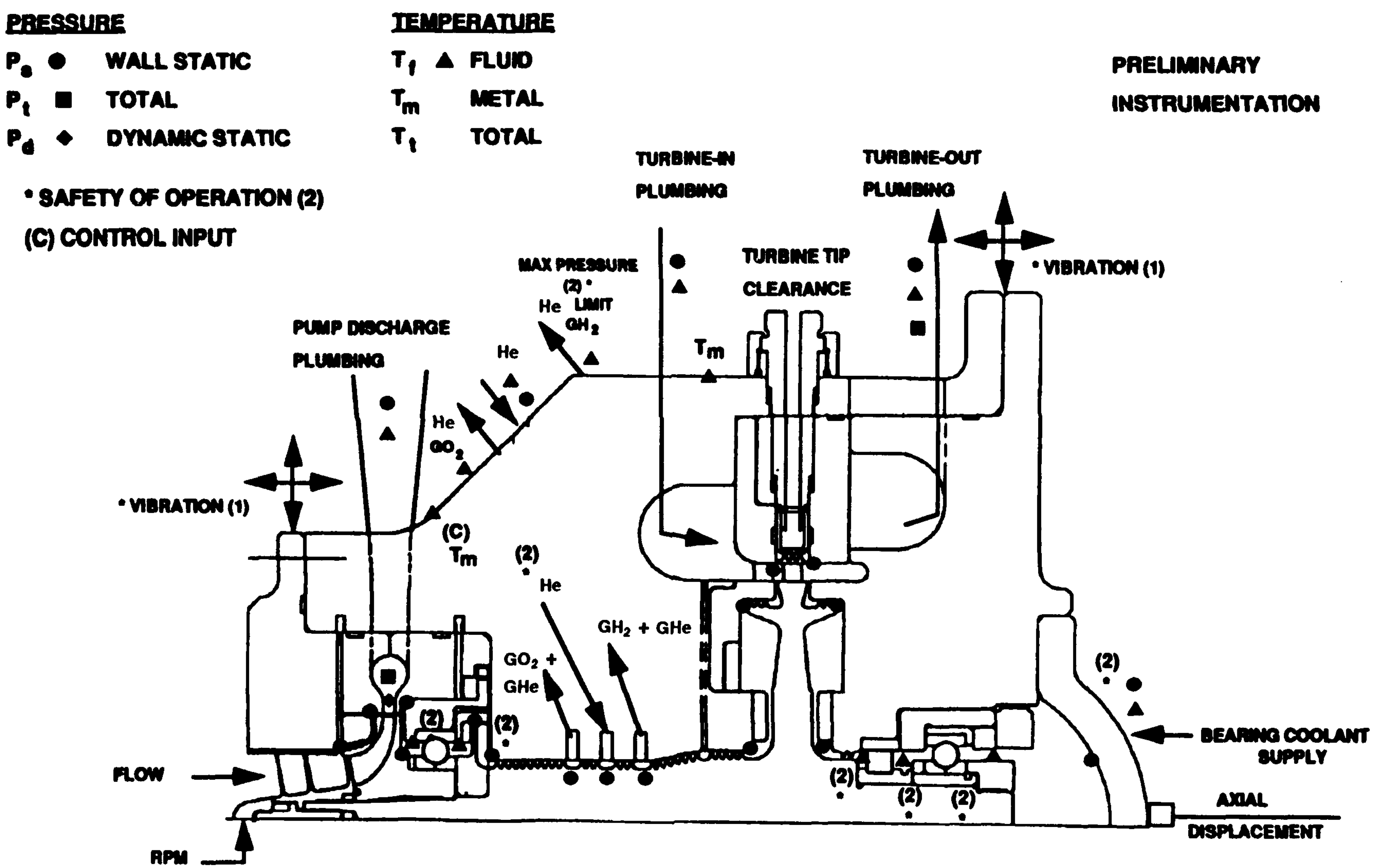

Figure 87. Oxygen Turbopump Instrumentation

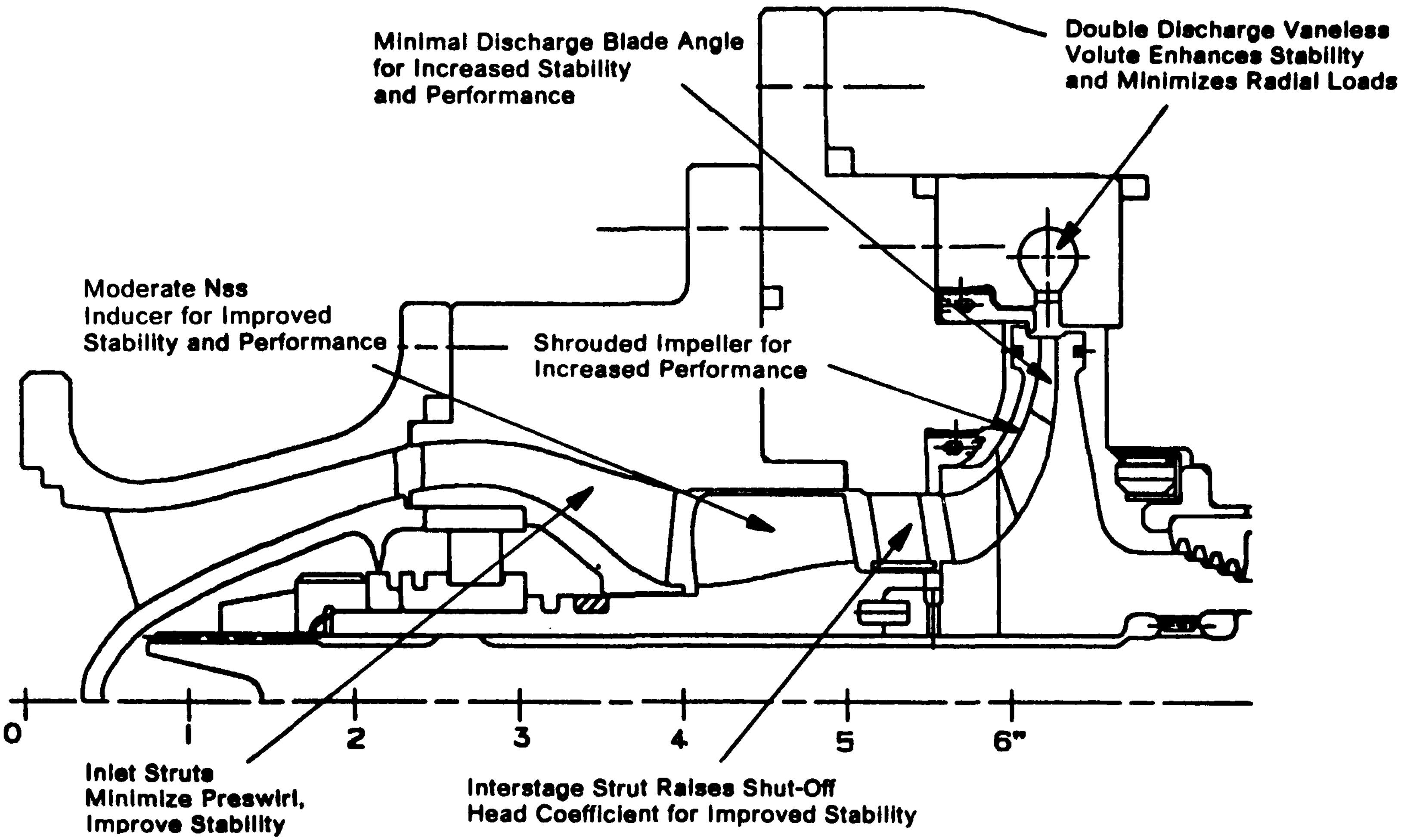

Figure 88. Primary Hydrodynamic Configuration and Features

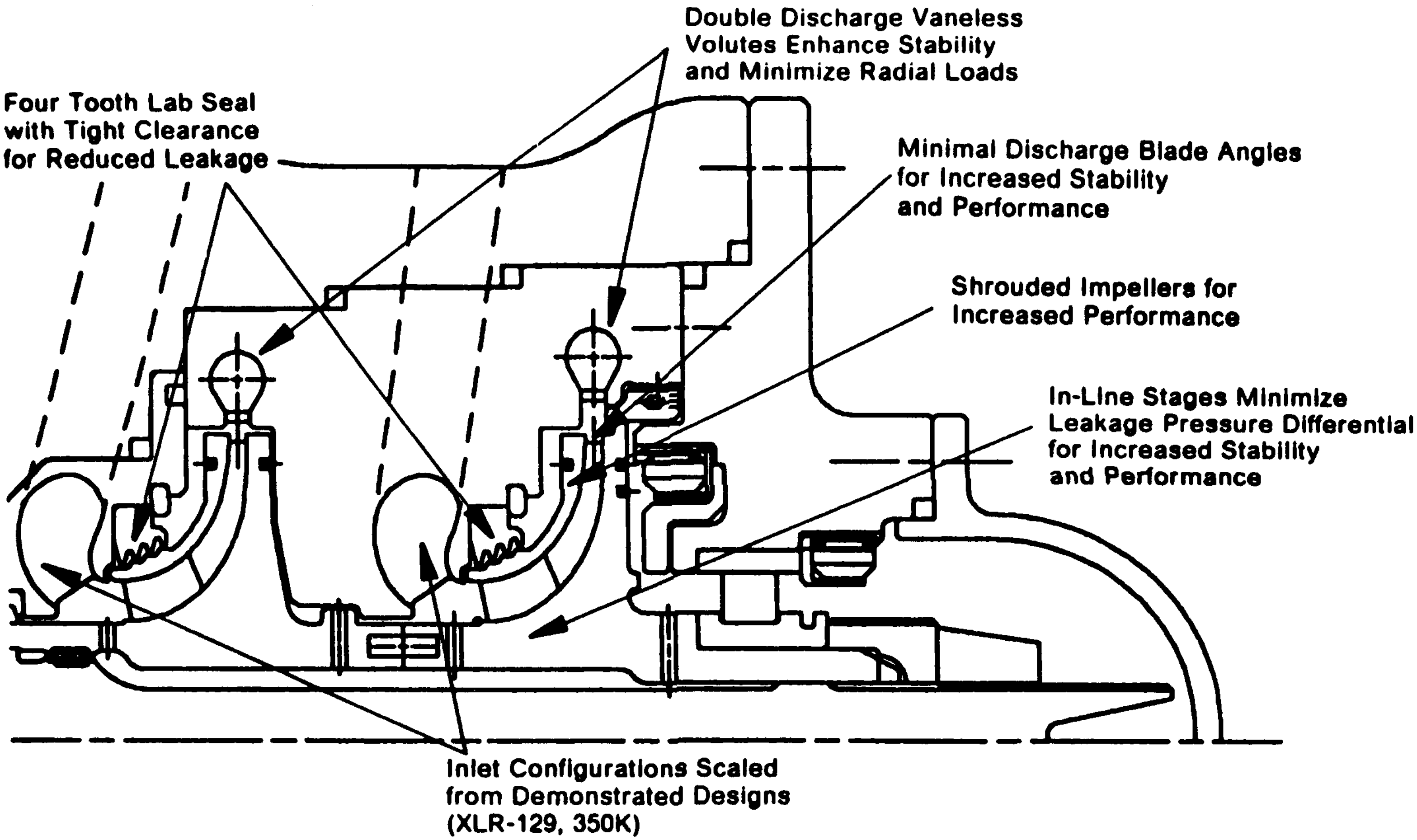

Figure 89. Secondary Hydrogen Pump Hydrodynamic Configuration and Features

Table 10. Primary Hydrogen Turbopump Design Parameters

INDUCER

Parameter	Description	Value
D_{1t}	Inlet Tip Diameter (in.)	2.43
D_{1h}	Inlet Hub Diameter (in.)	1.35
$D_{1.5t}$	Exit Tip Diameter (in.)	2.43
$D_{1.5h}$	Exit Hub Diameter (in.)	1.63
β_{1t}^*	Inlet Tip Blade Angle (deg.)	7.5
$\beta_{1.5m}^*$	Exit Mean Blade Angle (deg.)	13.6
σ	Inducer Tip Solidity	1.88
Z	Number of Blades	3

IMPELLER

Parameter	Description	Value
$D_{1.5t}$	Inlet Tip Diameter (in.)	2.43
$D_{1.5h}$	Inlet Hub Diameter (in.)	1.63
D_{2m}	Exit mean Diameter (in.)	4.432
β_{2m}^*	Exit Mean Blade Angle (deg.)	40.0
b_2	Discharge Blade Height (in.)	0.10
Z	Number of Blades	6 + 6 + 12

Table 11. Secondary Hydrogen Turbopump Geometric Design Parameters

IMPELLER

Parameter	Description	Value
D_{1t}	Inlet Tip Diameter (in.)	1.90
D_{1h}	Inlet Hub Diameter (in.)	1.40
D_{2m}	Exit mean Diameter (in.)	3.579
β_{2m}^{*}	Exit Mean Blade Angle (deg.)	40.0
b_2	Discharge Blade Height (in.)	0.10
Z	Number of Blades	6 + 6

Table 12. Primary Hydrogen Turbopump Hydrodynamic Design Parameters

INDUCER

Parameter	Description	Value
W_{in}	Inlet Mass Flow Rate (lbm/sec)	7.50
P_{in}	Inlet Pressure (psia)	67.5
T_{in}	Inlet Temperature (deg R)	38.0
N	Rotational Speed (rpm)	100,000
$NPSH_{Avail}$	Available NPSH (ft)	1,600
$NPSH_{Reqd}$	Required NPSH (ft)	439.5
$N_{ss-Reqd}$*	Suction Specific Speed - Required $\left(rpm \frac{(gpm)^{1/2}}{(ft)^{3/4}}\right)$	10,500
N_{ss-Cap}*	Suction Specific Speed - Capability $\left(rpm \frac{(gpm)^{1/2}}{(ft)^{3/4}}\right)$	25,000
NPSHM	NPSH margin (percent)	264

STAGE

Parameter	Description	Value
U_{tip}	Impeller Tip Speed (ft/sec)	1,934
ΔH_{poly}	Stage Head Rise (ft)	64,855
N_s	Stage Specific Speed $\left(rpm \frac{(gpm)^{1/2}}{(ft)^{3/4}}\right)$	682
ϕ_{2m}	Discharge Flow Coefficient	0.125
ψ_{poly}	Stage Head Coefficient	0.558
η_{poly}	Stage Efficiency (percent)	60

* N_{ss} referenced to water

Table 13. Secondary Hydrogen Turbopump Hydrodynamic Design Parameters

STAGE

Parameter	Description	2nd Stage	3rd Stage
W_{in}	Inlet Mass Flow Rate (lbm/sec)	4.776	4.776
P_{in}	Inlet Pressure (psia)	1,912	3,197
T_{in}	Inlet Temperature (deg R)	69.7	90.5
N	Rotational Speed (rpm)	100,000	100,000
U_{tip}	Impeller Tip Speed (ft/sec)	1,562	1,562
ΔH_{poly}	Stage Head Rise (ft)	40,550	40,550
N_s	Stage Specific Speed (rpm $\frac{(gpm)^{1/2}}{(ft)^{3/4}}$)	780	780
ϕ_{2m}	Discharge Flow Coefficient	0.115	0.115
ψ_{poly}	Stage Head Coefficient	0.535	0.535
η_{poly}	Stage Efficiency (percent)	73	65

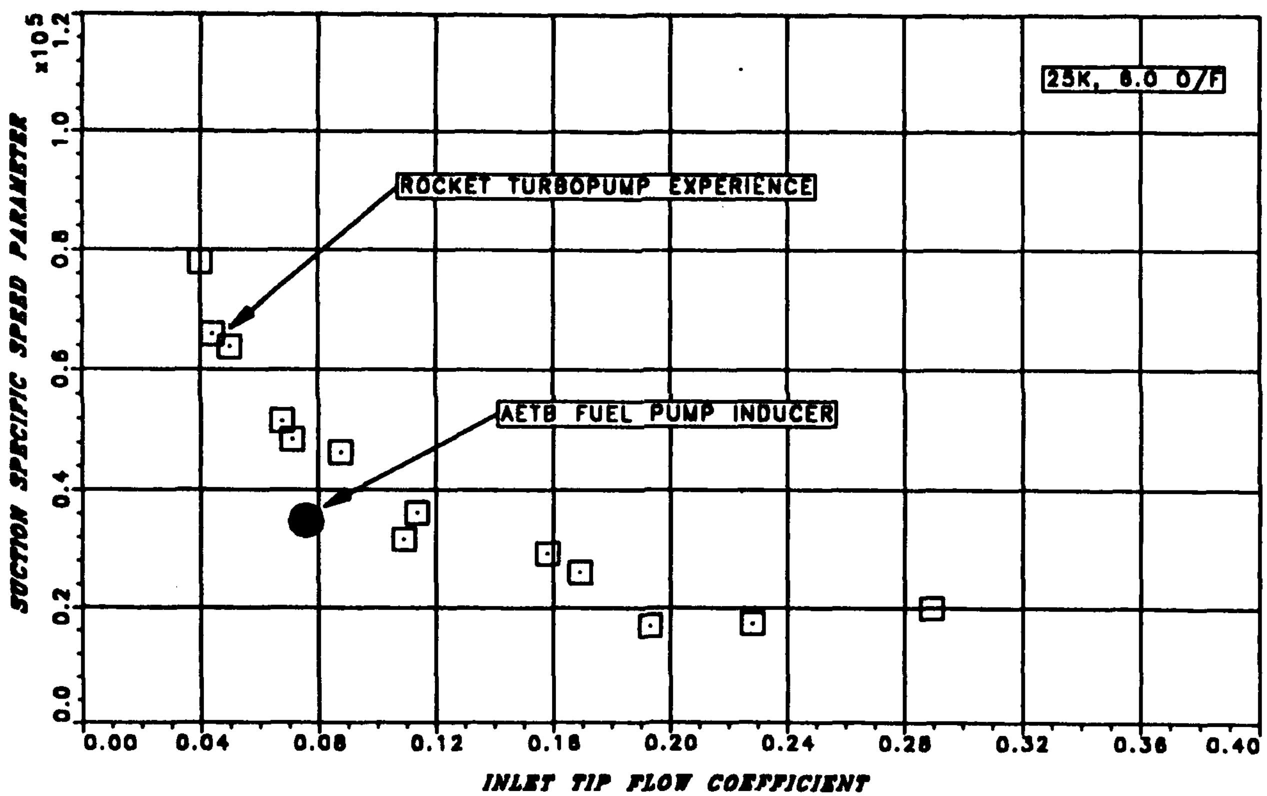

Figure 90. Hydrogen Turbopump Inducer Suction Specific Speed

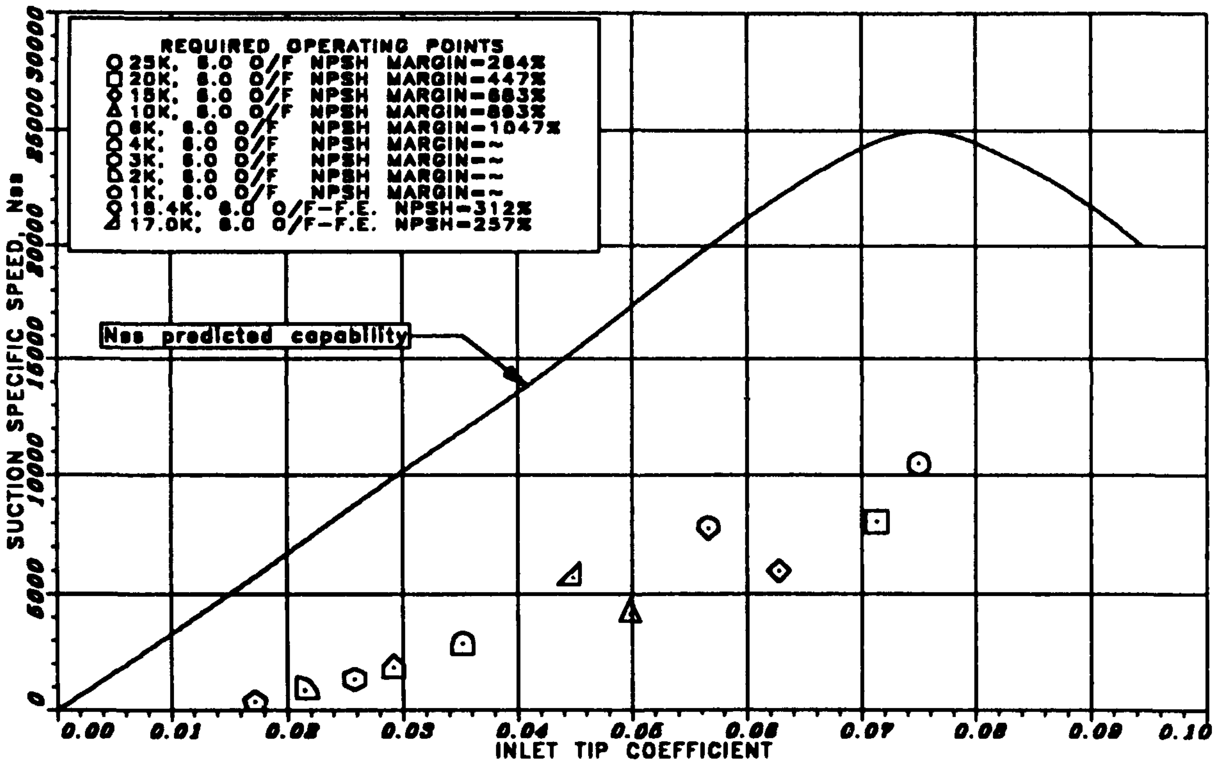

Figure 91. Hydrogen Turbopump Inducer Suction Performance Characteristics

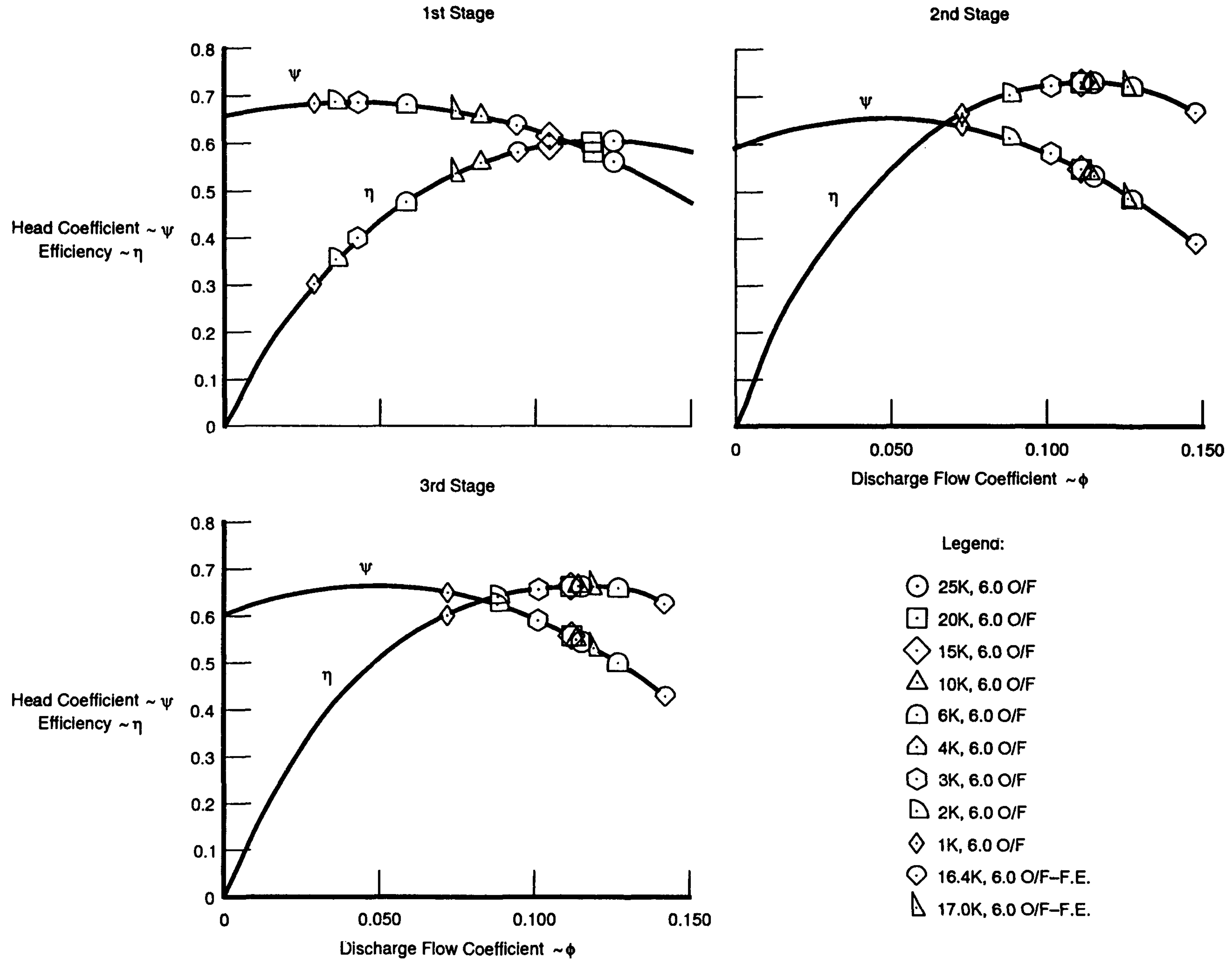

Figure 92. Hydrogen Turbopump Stage Performance Characteristics

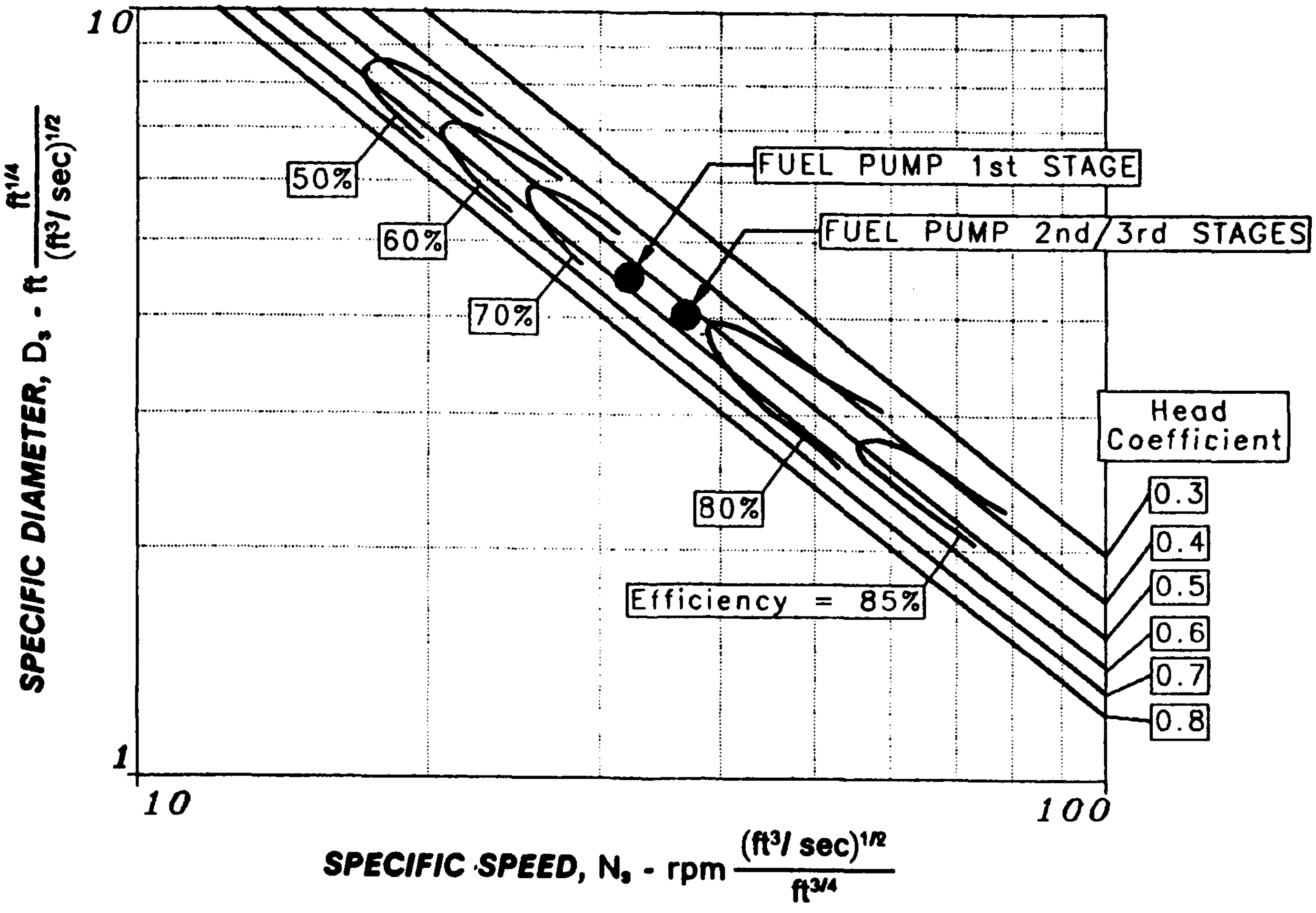

Figure 93. Hydrogen Turbopump Specific Diameter versus Specific Speed

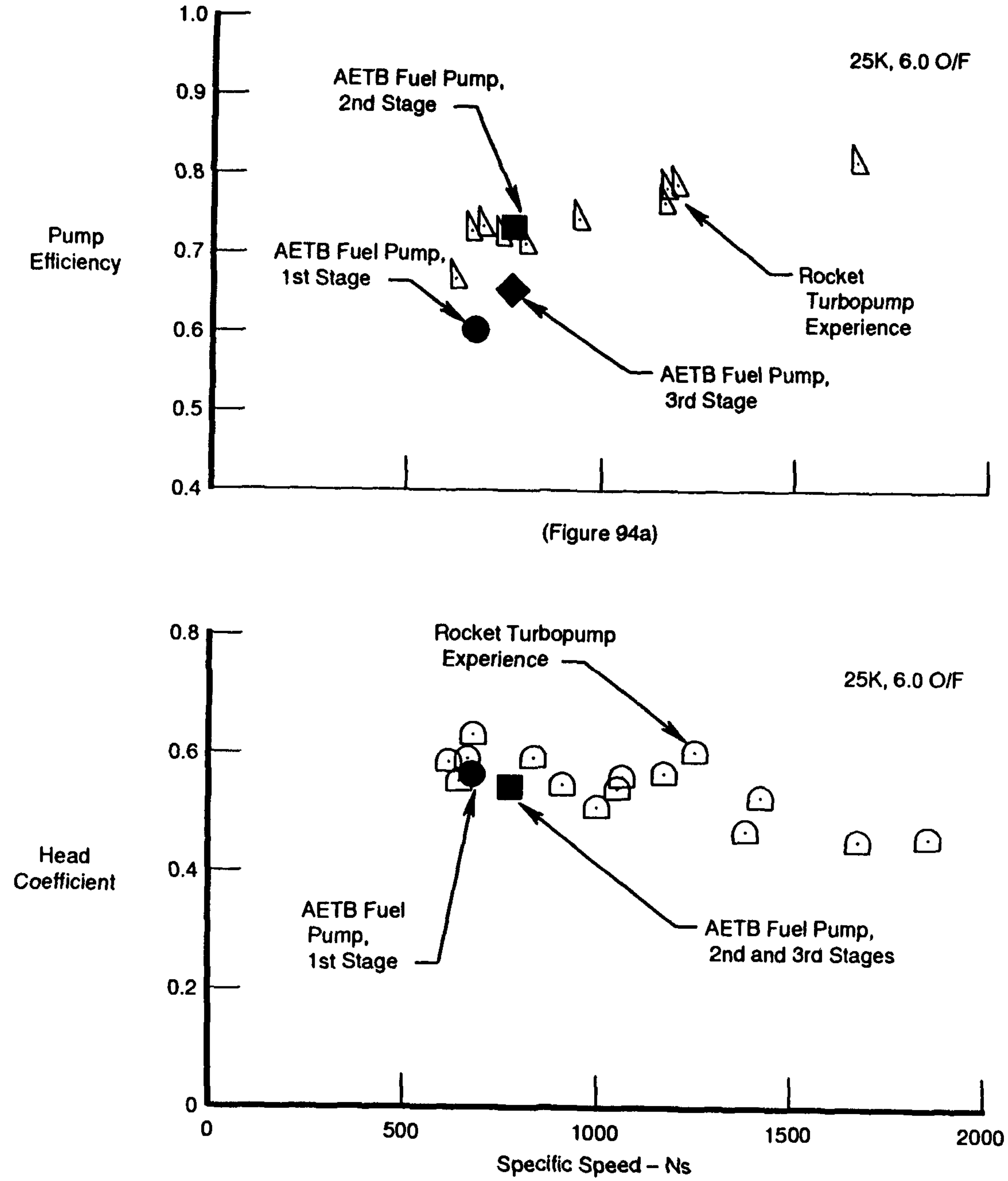

Figure 94. Hydrogen Turbopump Efficiency and Head Coefficient versus Experience

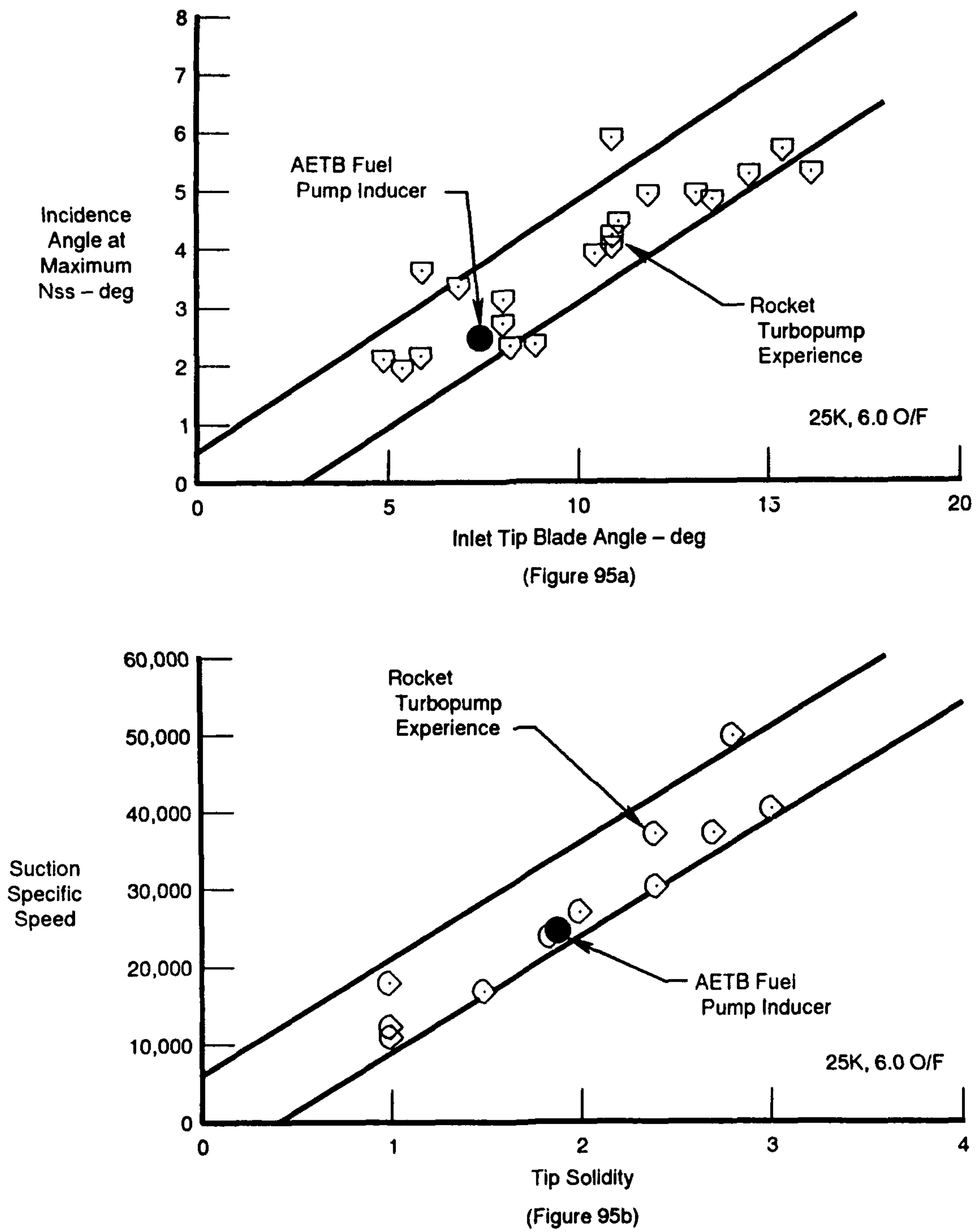

Figure 95. Hydrogen Turbopump Inducer Incidence and Solidity

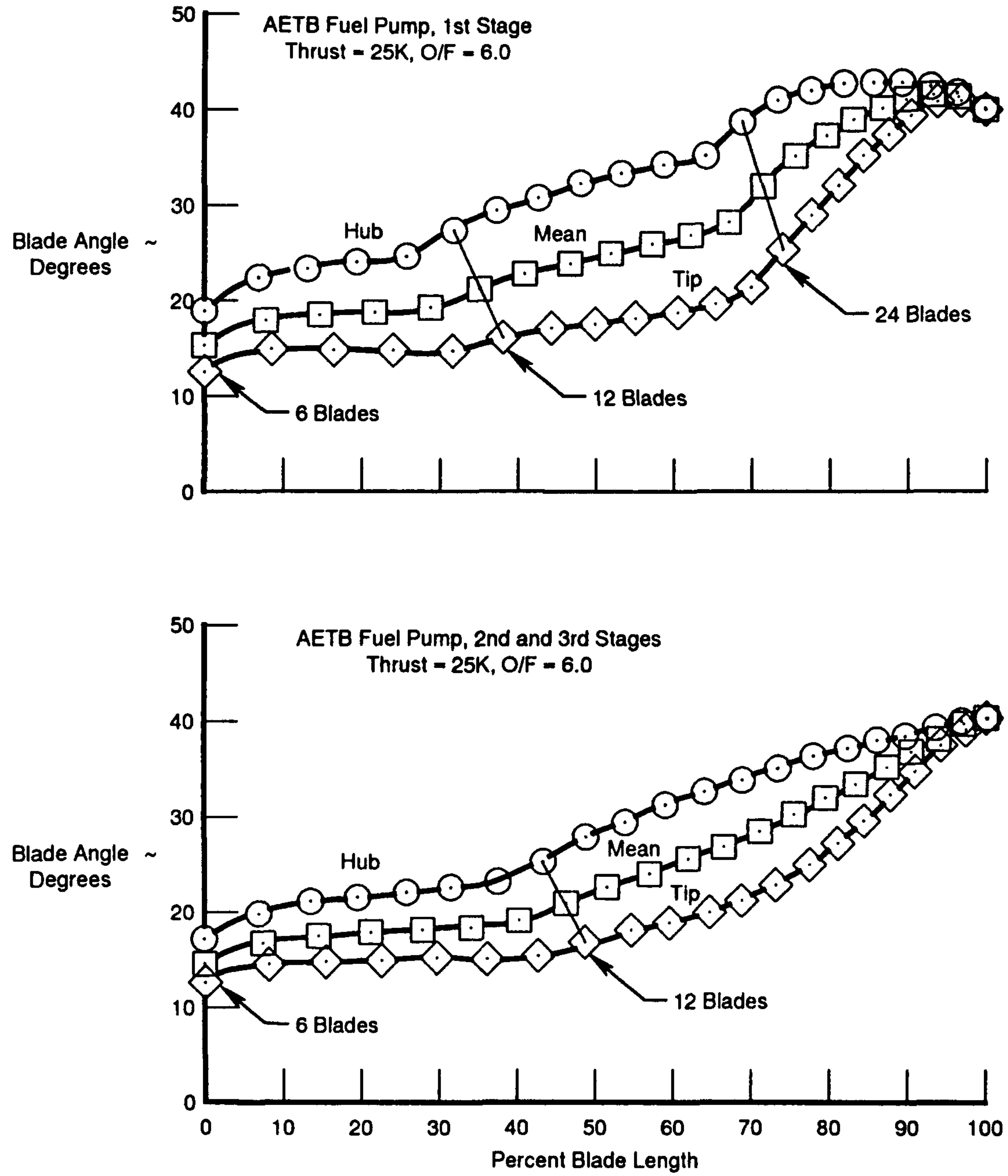

Figure 96. Hydrogen Turbopump Impeller Blade Angle Distributions

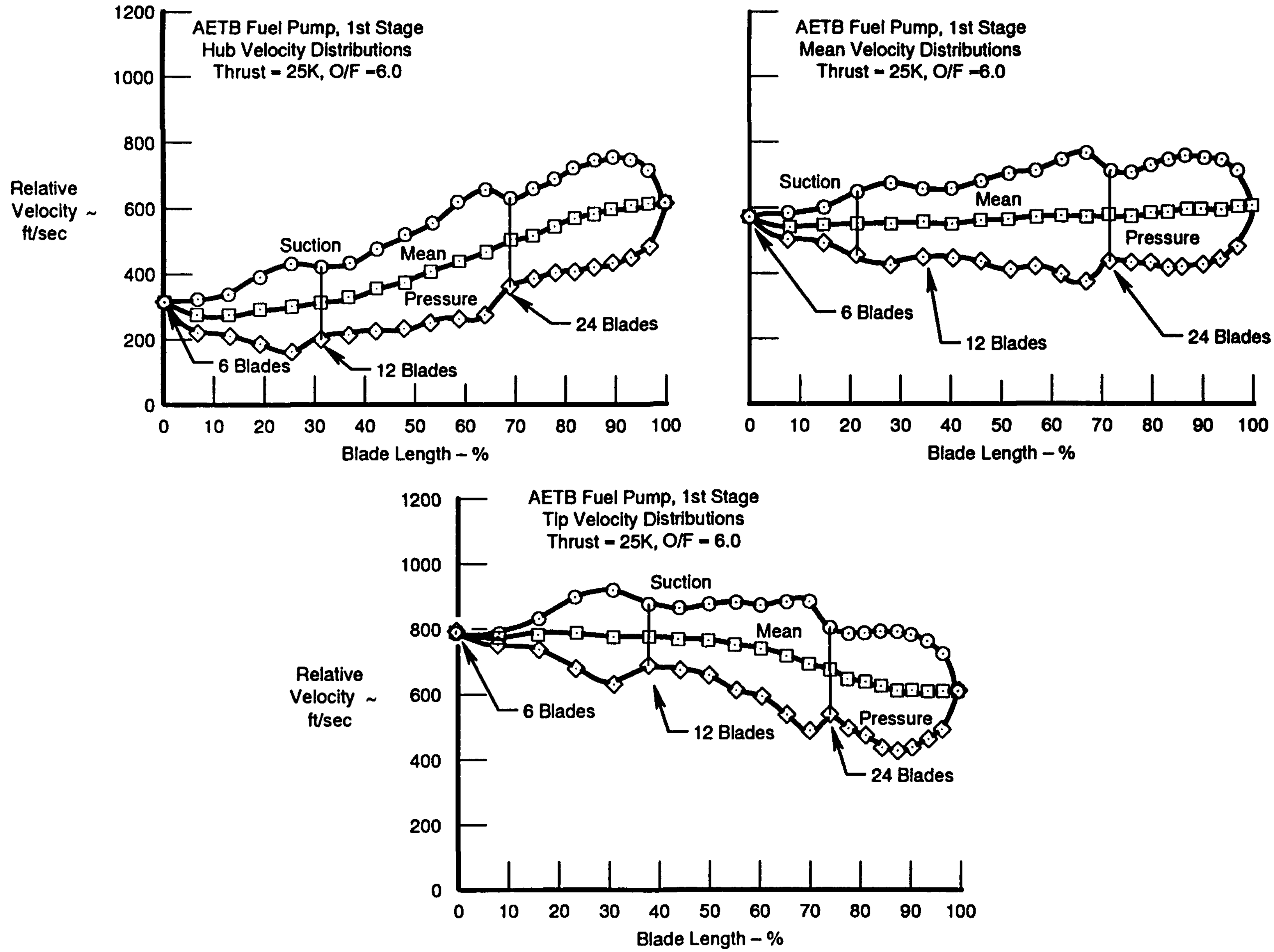

Figure 97. Hydrogen Turbopump First-Stage Impeller Velocity Distributions

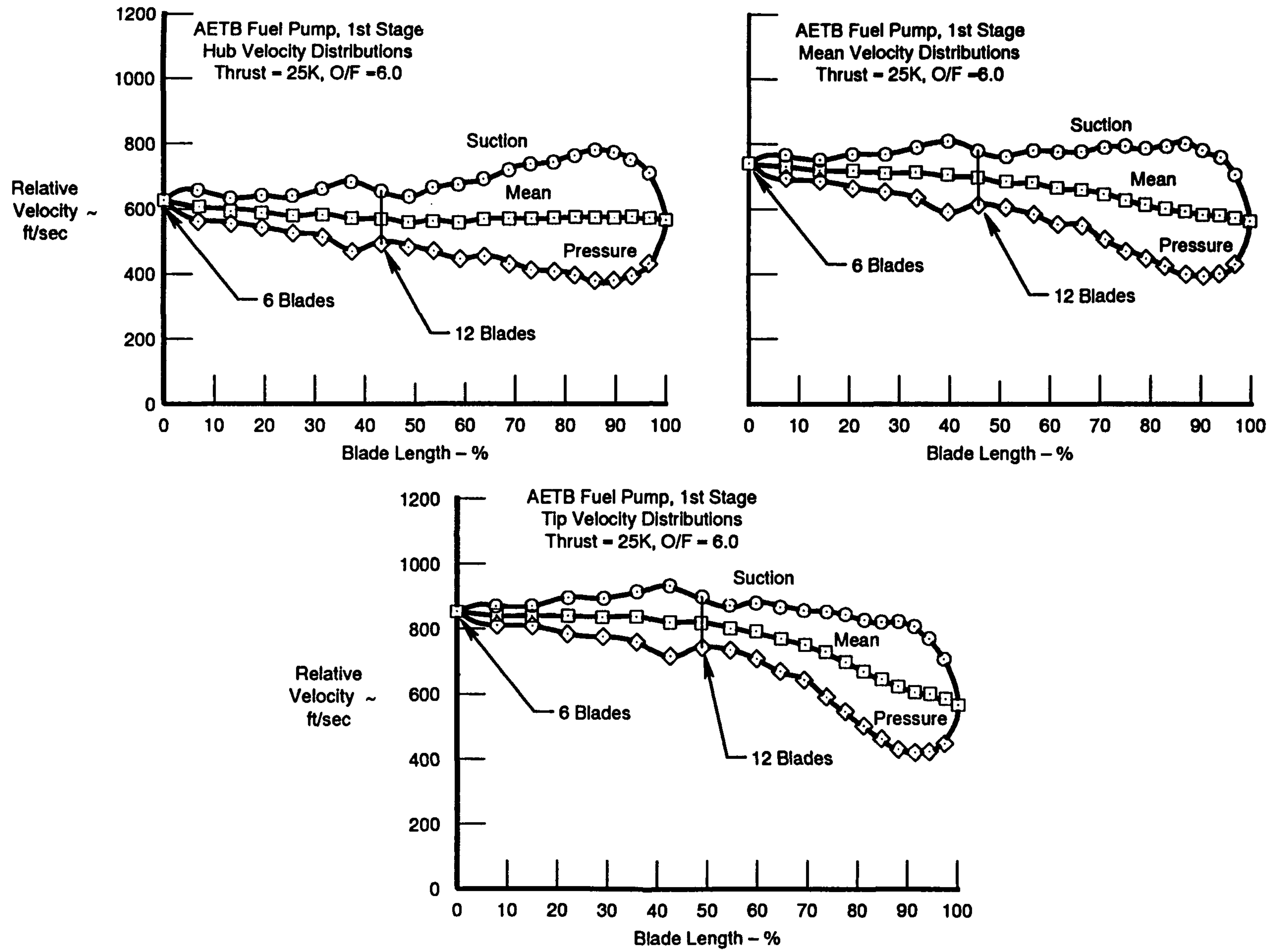

Figure 98. Hydrogen Turbopump Second and Third-Stage Impeller Velocity Distributions

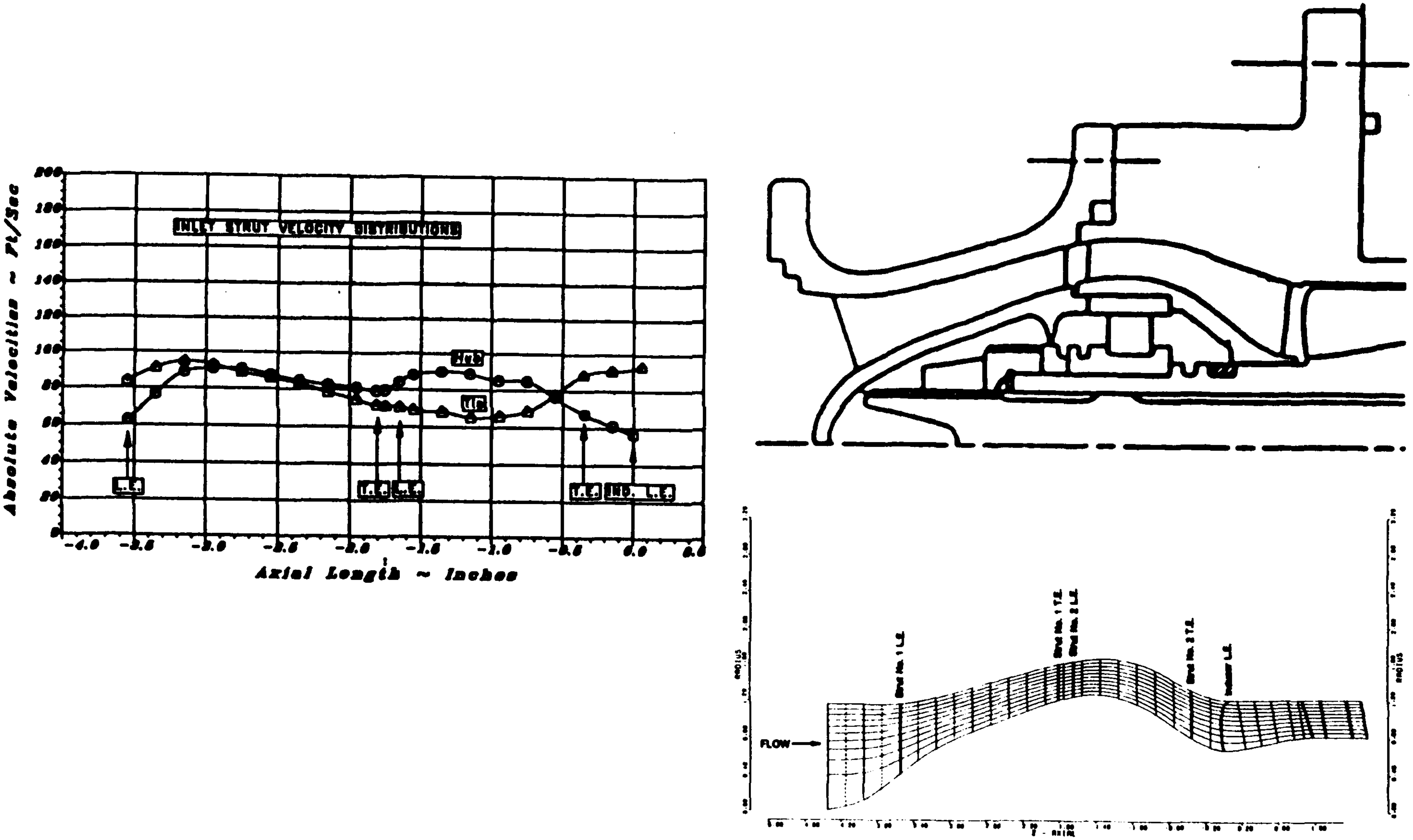

Figure 99. Hydrogen Turbopump Streamline Analysis of Inlet Flowpath

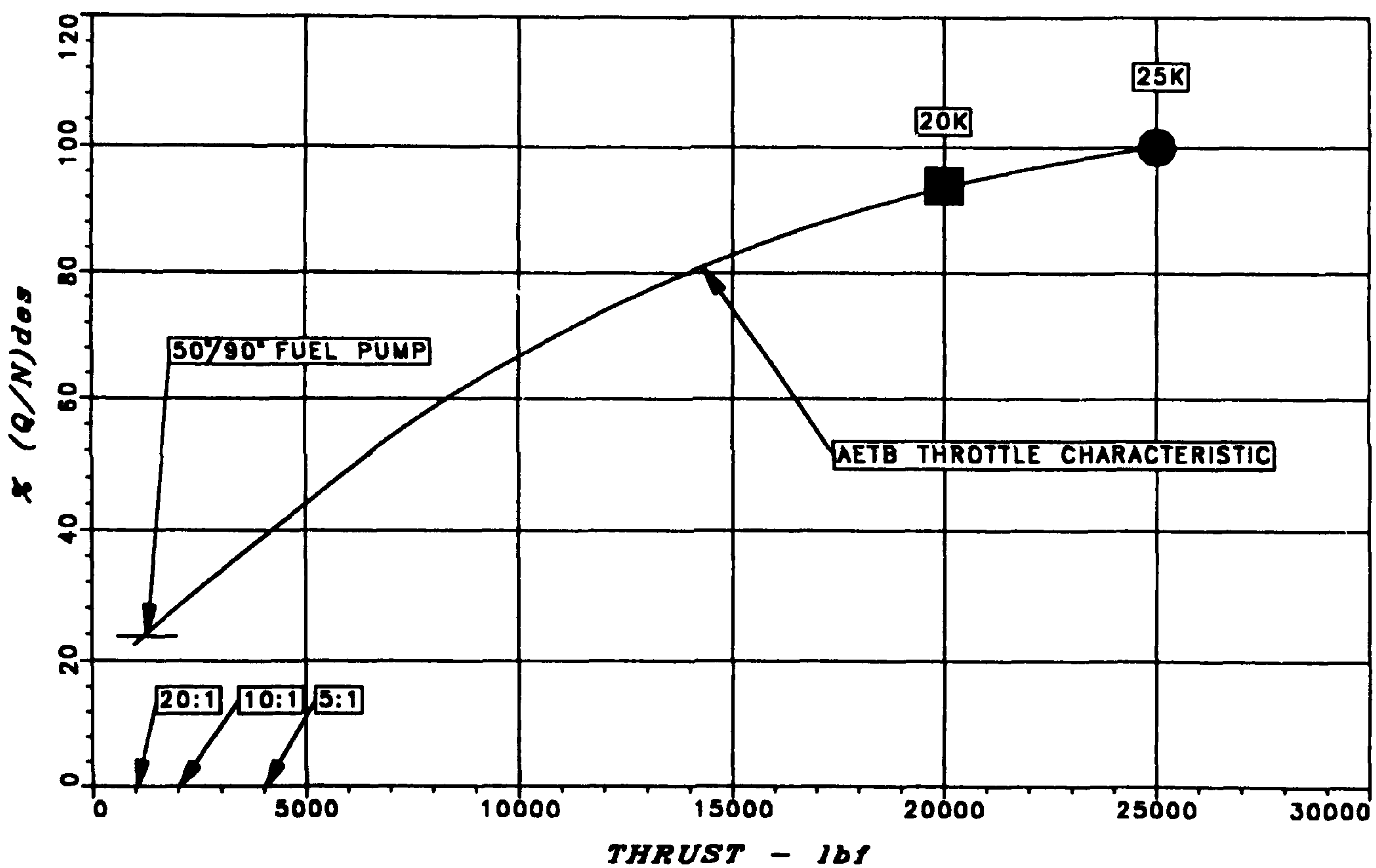

Figure 100. Hydrogen Turbopump First-Stage Throttle Characteristics

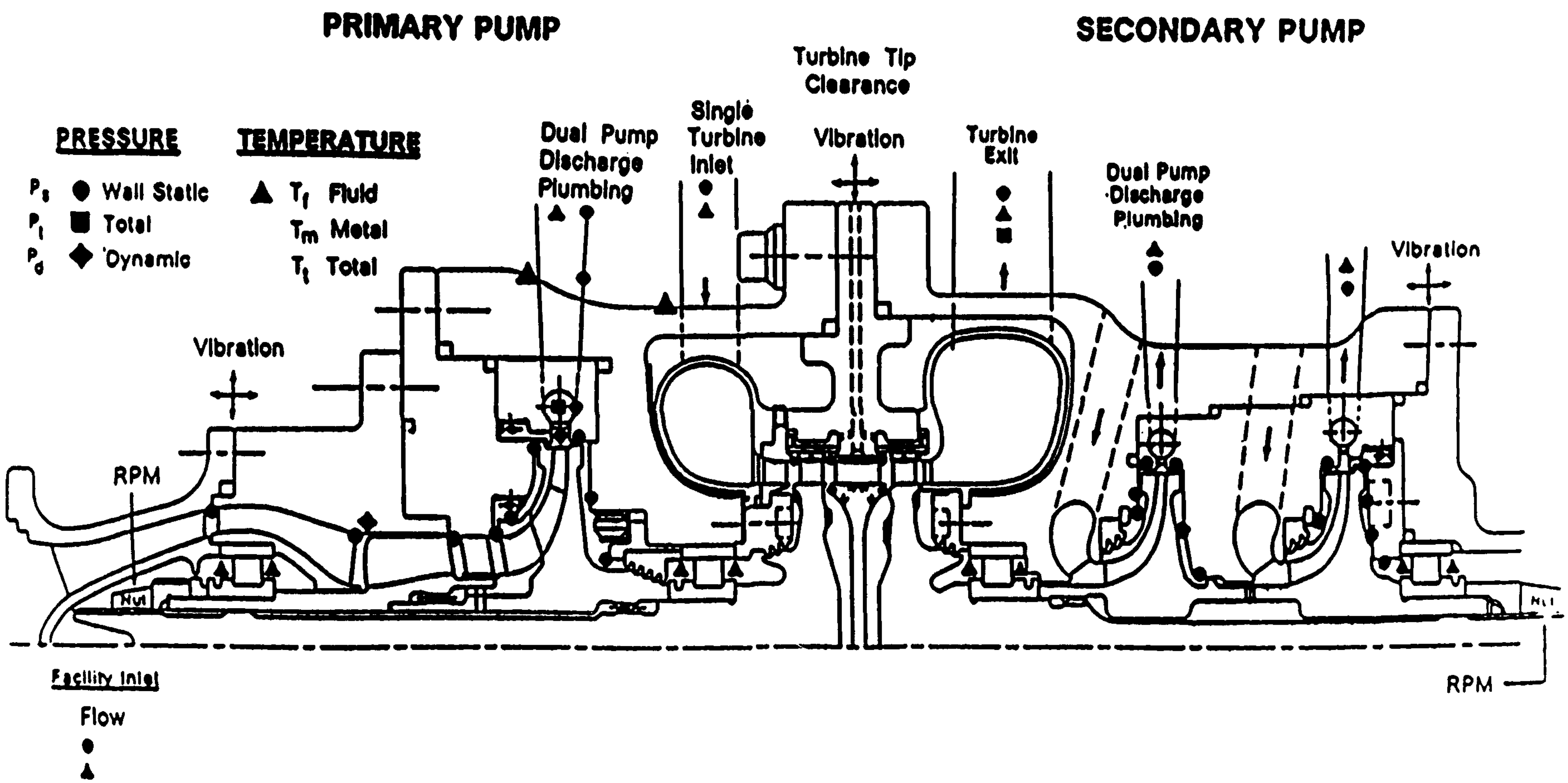

Figure 101. Hydrogen Turbopump Instrumentation

F. Turbine Aerodynamics

1. Turbine Aerodynamic Design Approach

The split expander and expander cycles demand high turbine efficiency to reduce engine size and weight. In addition, stable operation free of high vibratory gas loads that could cause bearing side loads should be attained. A full-admission reaction turbine was chosen to fulfill these requirements because this type of turbine has proven more stable and efficient than partial admission impulse turbines during the development of the RL10 and SSME-ATD turbopumps. Figure 102 shows that the performance characteristics of the AETB turbines fall within the area of demonstrated RL10 and ATD turbine experience.

The turbines are arranged in a back-to-back and counter-rotating configuration in the fuel turbopump to eliminate interturbine pipe losses and significantly reduce the second turbine vane gas turning losses. Low loss inlet and exit volutes are employed to reduce the first vane gas turning losses and eliminate the need for exit guide vanes. A constant static pressure gradient is designed into the volutes to eliminate circumferential pressure gradients that cause bearing side loads.

Mechanical options were chosen for high leakage efficiency and are necessary for low aerodynamic losses. A radial tip clearance of 0.003 inch at the maximum power running condition is the most dominant mechanical option chosen and is necessary to employ reaction turbines to their full efficiency. A passive tip clearance control system, that maintains a cold case that shrinks on a dynamically and thermally growing turbine blade tip, is expected to produce the desired close tip clearance at the full power design point. A thermal tip clearance that controls the tip shroud radial position by using cold impinging hydrogen will back up the passive system.

The integral bladed disk and shroud will reduce parasitic leakage flows around the root attachment and over the blade tips. The delicate machining of these blade flow channels will also allow 0.010-inch blade trailing edge thicknesses with a channel dimensional tolerance of +0.002 inch within a 0.050-inch throat gaging dimension.

2. Oxygen Turbine Description

The oxygen turbine elevation is shown in Figure 103 along with its design parameters. It is a conventional single-stage reaction turbine with a volute inlet and discharge. The inlet volute flow enters the first vane tangentially, and reduces the first vane gas turning losses, as shown in Figure 104. The low axial velocity through this blading annulus, coupled with modern small blade manufacturing methods that allow small gaging gaps of 0.059 inch, trailing edge thicknesses of 0.010 inch, and exit gas angles of 4.8 degrees, enables this relatively low specific speed design to have high efficiency in this application. The tight tolerance control is made possible with the advanced blade gas path machining capabilities being applied. The blading also has an integrally machined shroud for low leakage and strength as a result of this machining process.

3. Hydrogen Turbine Description

The hydrogen turbine elevation is shown in Figure 105 along with its design parameters. It has conventional single-stage reaction turbines with a volute inlet and discharge. The counter-rotating secondary turbine is mounted back-to-back in a manner conventional to current advanced fighter engine dual spool turbines. The reaction level of the primary turbine is high enough to provide enough residual velocity from its blading to power the second-stage blade without any significant acceleration through the second vane. The angle of flow into the second vane varies very little over the operating range as shown in Figure 106 so that efficiency varies only eight percent over this range. The high reaction first blade has a significant change in inlet angle but its inlet Mach number is so low that no significant inlet loss occurs nor is there any inlet separation. Initial computational fluid dynamics (CFD) analysis has shown this to be true and it will be confirmed as the final design is developed and tested. The blades have an integrally machined shroud for low leakage losses and for shroud strength at high wheel speeds.

4. Turbine Methodology and Verification

The turbine aerodynamic methodology and design codes employed are listed in Figure 107. Analysis during the preliminary design progressed through the meanline analysis. During the analysis, overall engine performance was traded with overall turbopump size, cost and reliability. The efficiency, number of stages, diameter, airfoil stress and pull on the disk were selected in conjunction with the needs of the engine cycle. Once the engine cycle is finalized, the output of the meanline analysis will be used as input to the streamline analysis which defines the turbine radial flow, pressure and temperature maps for the case and disk structural analysis. The streamline analysis will provide the airfoil gas dynamic environment and lead to the design of the airfoil cross-section contours. These contours will be radially faired and the detailed analysis of the airfoil stress and pull will be performed to confirm that the initial estimates of disk stress, reliability and airfoil endwall compatibility were maintained.

Of primary concern is dependence on turbine mechanical and manufacturing techniques which need to be verified in the test bed engine to support the turbine performance goals. Blade tip clearance control during engine acceleration transients, turbine tip shroud strength and integrity at full speed and temperature, the control of parasitic leakages, and the manufacturing of small blade gaps and tolerances will be verified during component and engine testing.

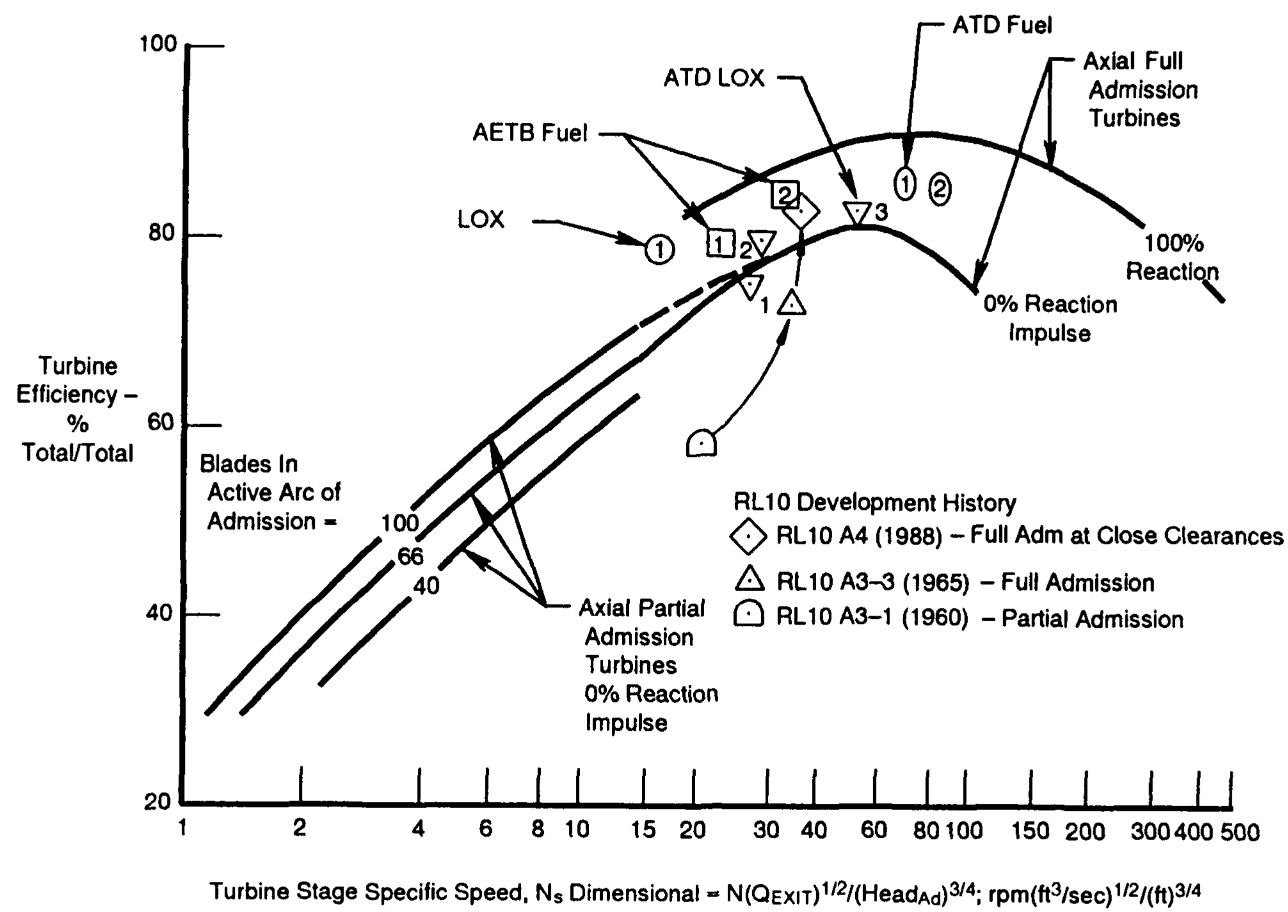

Figure 102. Turbine Efficiency versus Stage Specific Speed

Horsepower	620
Efficiency T/T	.822
ΔH (BTU/lb)	124.3
Velocity Ratio (Ideal)	.5228
Gamma	1.398
Flow Parameter	.0276
Pressure Ratio	1.152
P IN (psia)	4043.9
P Discharge	3496.6
T IN (R°)	1018.7
T Discharge	942.3

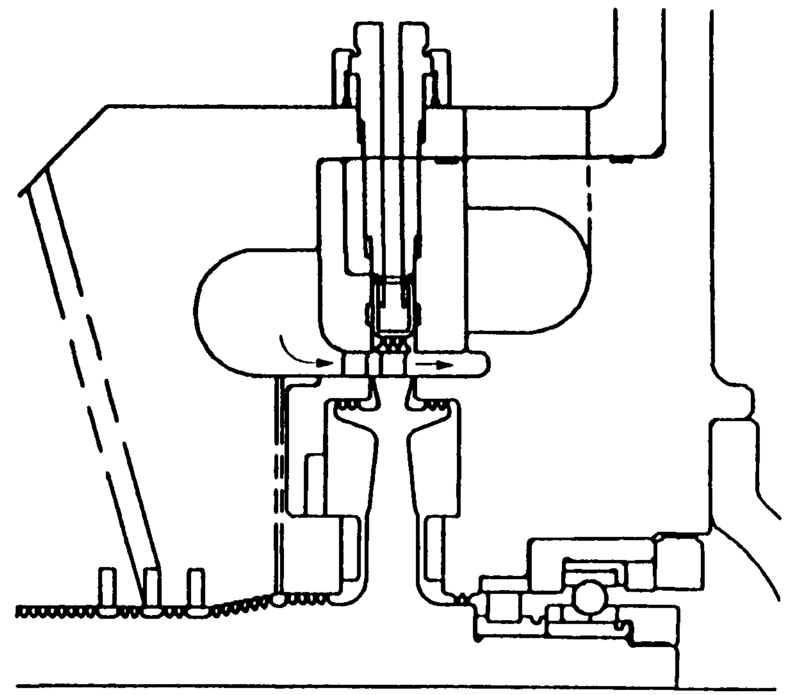

Figure 103. Oxygen Turbopump Turbine Design Parameters

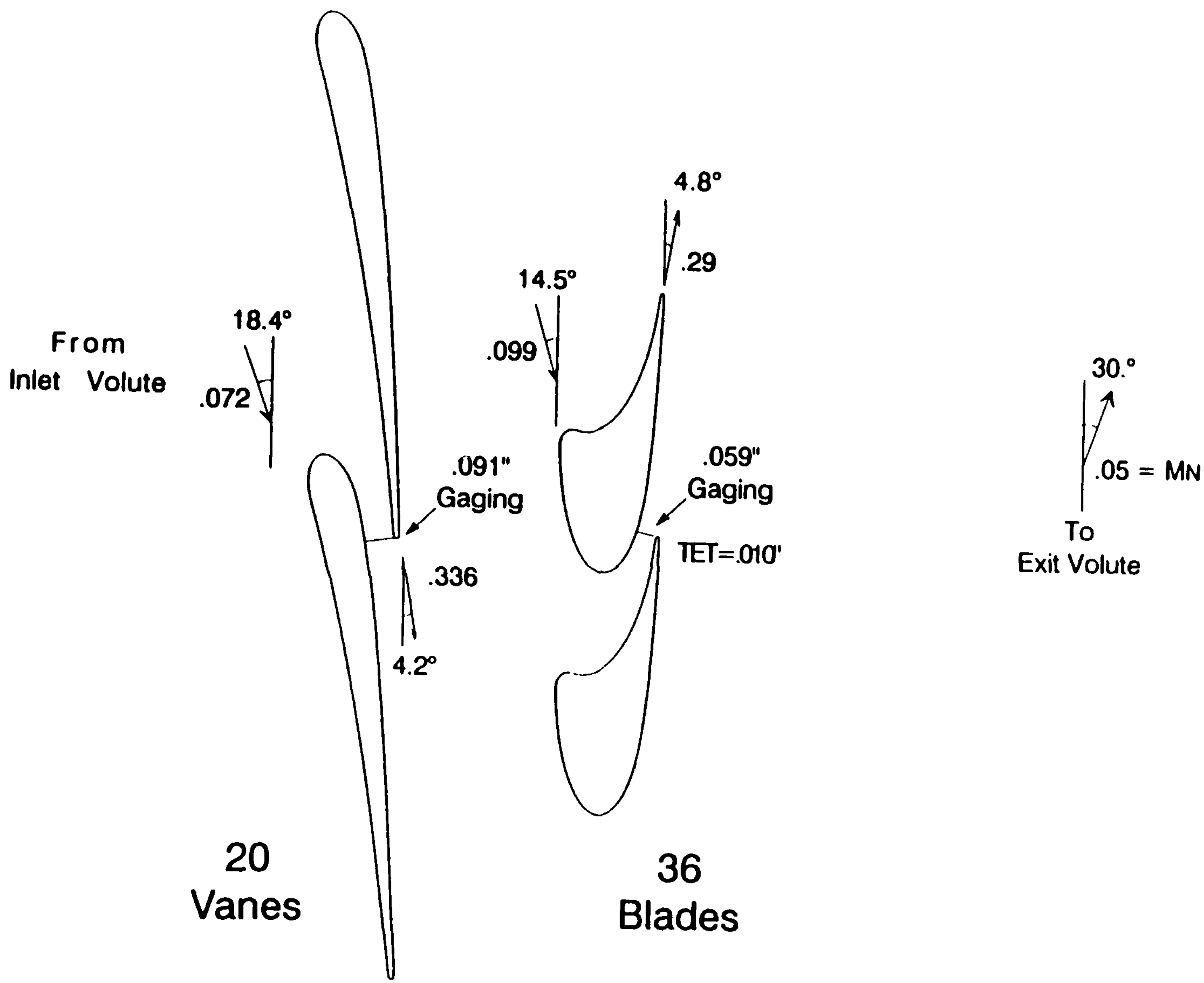

Figure 104. Oxygen Turbopump Turbine Geometry

	Primary	Secondary
Horsepower	1315	1210
Efficiency T/T	.816	.843
Velocity Ratio (Ideal)	.4285	.4659
ΔH (BTU/lb)	241.5	215.5
Gamma	1.398	1.398
Flow Parameter	.0334	.0452
Pressure Ratio	1.377	1.360
P IN (psia)	3460.2	2507.3
P Discharge	2507.3	1843.1
T IN (R°)	942.5	815.1
T Discharge	815.1	744.7

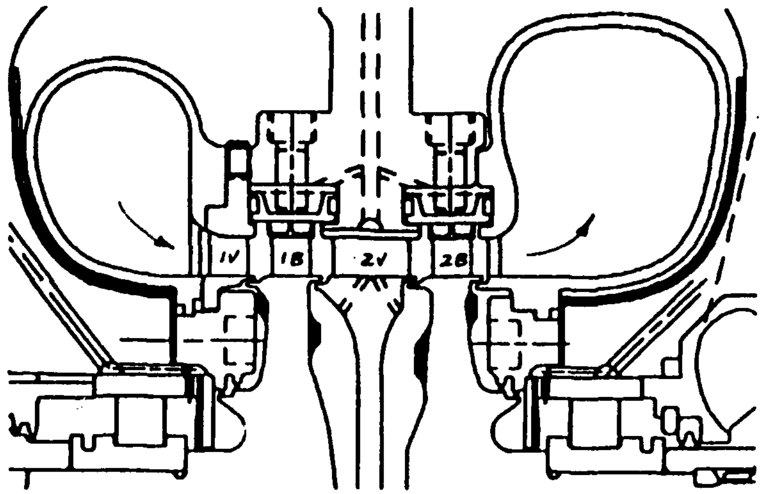

Figure 105. Hydrogen Turbopump Turbine Design Parameters

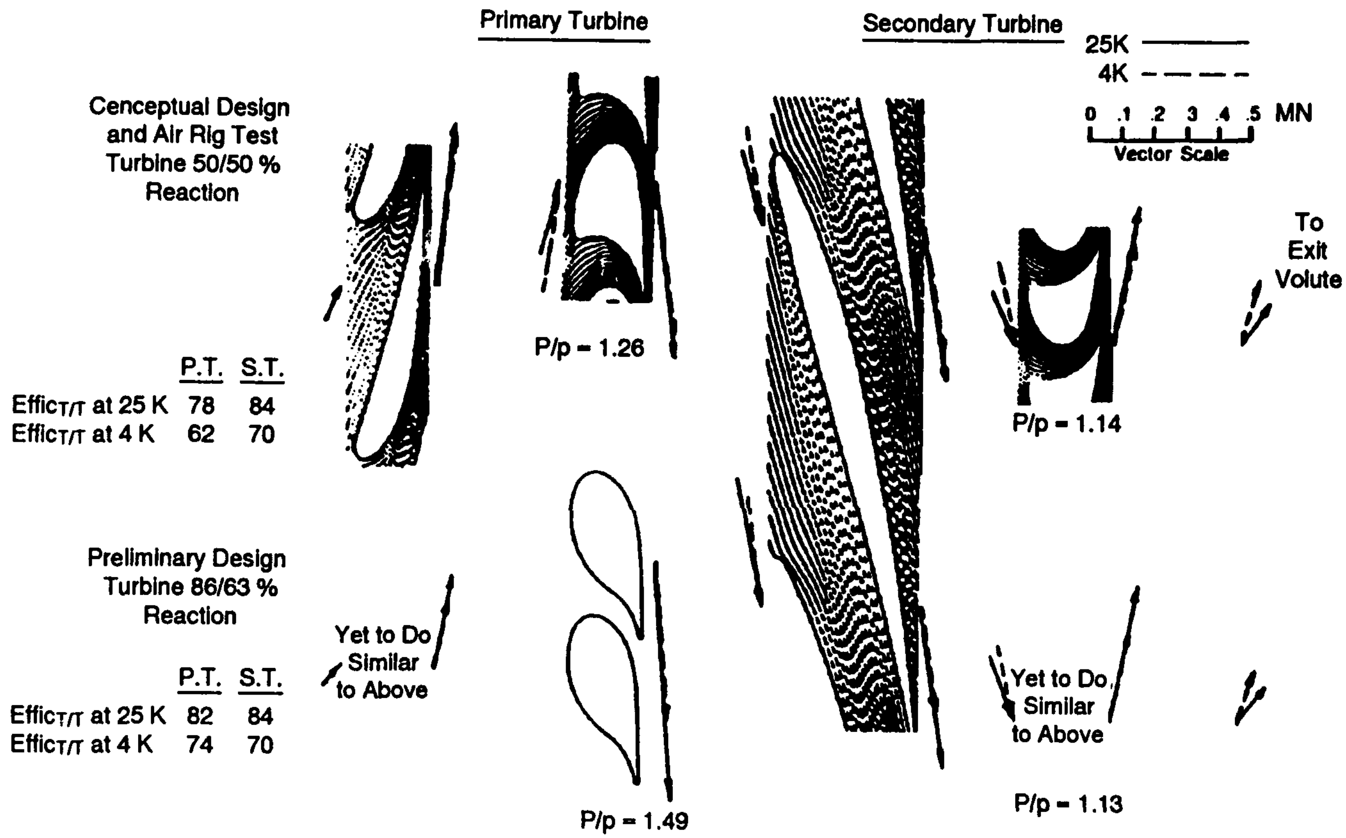

Figure 106. Hydrogen Turbopump Turbine Geometry

Code	Title	Description
E83A	Meanline Design, TSOD	To define the turbine flowpath elevation, design point performance and average gas conditions. Parametric study varying turbine geometry (diameter, blade height, chord, etc.), stage work split, and row static pressure drop. Calculations done at flowpath midspan using empirical airfoil loss correlations.
W677	Streamline Design	Spanwise definition of gas velocity triangles. Spanwise curvature analysis used to select spanwise swirl, reaction and work distributions. Complete definition of flow field through the turbine
M905	Airfoil Cross-Section Design	Generation of airfoil contours meeting aerodynamic and durability requirements. Interactive design program used to generate and analyze airfoil contours. Three to six airfoil contours designed from root to tip. Each section must have acceptable static pressure and boundary layer characteristics and geometry compatible with structural requirements (root contour compatible with attachment, airfoil dimensions consistent with cooling and manufacturing limitations).
V581	Airfoil Fairing	Geometric definition of complete airfoil. Synthesis of the airfoil by radially fairing the external and internal airfoil contours. Calculation of basic pull and bending stresses including effect of blade tilt.
V310	Multi-Stage 3D Flow Analysis	Refine and optimize the entire flowpath configuration, including airfoils and endwalls. Assess the effects of airfoil curvature, thickness, lean and sweep distributions, and endwall convergence/divergence and curvature distributions to provide absolute controlled diffusion flow passages.

Figure 107. Turbine Methodology and Design Codes

G. Bearings

1. Design Conditions

The rotor support system for the oxygen turbopump includes two ball bearings and one roller bearing. The ball bearings are axially preloaded with 300 pounds by means of springs to prevent skidding and provide radial stiffness at the pump end of the rotor. Two ball bearings were selected to provide transient axial load capability in either direction. The ball bearings are designed to carry transient loads up to 2500 pounds. The roller bearing uses negative internal clearance to prevent skidding and provide roller guidance. The roller bearing provides high radial stiffness to the turbine end of the rotor for increased critical speed margin. The roller bearing design is identical to the fuel turbopump roller bearings. The pertinent boundary conditions used to design the oxygen turbopump bearings are provided in Figure 108. The rotor support systems for the primary and secondary hydrogen turbopumps include two roller bearings on each rotor. Roller bearings were selected primarily based on the high radial stiffness requirements. The roller bearings have been designed to carry radial loads up to 350 pounds; the maximum expected load is 163 pounds. The roller bearings use negative internal clearance to prevent skidding and provide roller guidance. The pertinent boundary conditions used to design the hydrogen turbopump bearings are provided in Figure 109.

2. Nomenclature and Background Information

The AETB bearings have been designed to meet or exceed the conventional Pratt & Whitney (P&W) bearing design guidelines, and cryogenic specific guidelines that have been established under the SSME-ATD, RL10, and XLR129 programs. The major guidelines are listed below.

a. Ball Bearings

Internal Radial Clearance (IRC) (total clearance between the rolling elements and the races) — The internal radial clearance of a ball bearing sets the contact angle between the balls and the races.

Hertzian Contact Stress (load deformation at the ball to race contact forms an elliptical pressure area.) — Based on 15 hours of SSME-ATD testing in LO_2, the maximum steady contact stress should be limited to 388 ksi. The limit for liquid hydrogen (LH_2) use is based on five hours of testing at 483 ksi with RL10 bearings. For transient axial load capability, the SSME-ATD program has demonstrated 60 cycles at 665 ksi in LH_2.

Stress Velocity (SV) value (the product of the contact stress times the ball slip velocity, and a measure of the application severity at the ball-to-race contact.) — Based on SSME-ATD LO_2 and LH_2 experience, the SV value should be less than 2.0M psi-fps to minimize wear and heat generation.

Ball Excursion (the distance a ball attempts to move circumferentially from the cage pocket center, where the cage speed is the average ball orbital speed.) — A ball bearing operating under combined axial and radial load will have a variation in ball-to-race contact angle around the circumference. Since ball orbital speed is related to contact angle, a ball will undergo an orbital speed variation as it travels around the circumference. This, in turn, varies ball-to-ball spacing. As ball excursion increases, ball-to-cage interaction loads and cage-to-cage guide land loads increase. In a cryogenic bearing, moderate ball excursions are desirable since the ball-to-cage interaction is the mechanism for lubricating the bearing. The maximum ball excursion should be less than two times the ball pocket clearance.

B1 Life (the number of hours that 99 percent of the bearings in a given application will operate without exhibiting a rolling contact fatigue failure of subsurface origin.) — The calculation is based on the Lundberg-Palmgren life theory. The life theory does not directly apply to a properly lubricated cryogenic bearing, since wear or surface initiated distress are the predominant distress modes. Also, the calculated life is conservative since the life theory is based on test data and materials and manufacturing technology from the 1930's.

Figure 110 provides graphical representation of the ball bearing nomenclature described above.

b. Roller Bearing

Internal Radial Clearance (the total clearance between the rolling elements and races.) — The roller bearing uses negative internal clearance for preloading the rollers.

Contact Stress (stress due to interaction between the rolling elements and the races.) — The undeflected contact between a cylinder and a surface is a line. The load deformation creates a rectangular pressure area. The SSME-ATD program demonstrated 18 hours of operation with a contact stress of 300 ksi.

Edge Loading (stress caused by interaction between the roller corners (edges) and the races.) — High stresses result when the roller is loaded at the edge. Edge loading is reduced or eliminated by crowning the roller. Based on the XLR129 15-hour durability demonstration, edge stresses should be less than 200 ksi.

Minimum Roller Preload — In a cryogenic bearing, roller guidance is controlled with roller preload. The roller preload is obtained with negative IRC. The roller preload required to keep the rollers stable is determined empirically. Based on SSME-ATD and XLR129 experience, the minimum roller preload for the AETB should be 220 pounds.

Figure 111 provides graphical representation of the roller bearing nomenclature described above.

c. Cryogenic Bearing Experience at P&W

A broad experience base has been accumulated in the development of cryogenic bearings. Figures 112 through 114 summarize the pertinent P&W cryogenic bearing experience gained through rig testing in the RL10, 350K, XLR129, and SSME-ATD programs.

3. Design Description and Trade Studies

a. Ball Bearings

An extensive trade study was performed to ..ct the configuration. The trade study included bearing size, rolling element size and quantity, race curvatures, and IRC. The study also included the existing RL10 bearing to determine if it was suitable for the AETB. Figure 115 shows the contact stress and SV value for a 27x58-mm bearing and the 35x62-mm RL10 bearing. With the expected radial load of about 50 pounds, both contact stress and the SV value are within experience guidelines. As shown in Figure 116, the existing RL10 bearing had advantages over a new design and was, therefore, selected for the AETB.

The RL10 bearing is suitable for LH_2 use only and requires modification for LO_2 use. The cage was redesigned with LO_2 compatible materials. The LO_2 bearing cage will use Salox-M bronze-filled teflon inserts and a K-Monel shroud, a design proven in the SSME-ATD program. The inserts provide a transfer film lubricant, and the shroud provides a structural support element which is tolerant of rubbing in LO_2. For the LH_2-cooled bearing, the inner ring material will be AISI 9310, which has better fracture toughness than the AISI 440C it replaces. The AISI 9310 also provides increased stress corrosion cracking resistance over AISI 440C. The LO_2-cooled bearing must use AISI 440C instead of AISI 9310 for the inner ring due to LO_2 compatibility concerns. Promoted combustion testing in the SSME-ATD program has shown that AISI 9310 is not suitable for use in a LO_2 environment. Concerns of AISI 440C are discussed in the risk assessment section. The materials selected for the ball bearings are listed in Figure 117.

Bearing temperature control is vital to success because it assures stable operation and prevents localized surface distress at the ball to race contact points. To assure this temperature control and establish an adequate coolant flow rate, bearing heat generation must be known. Analytical heat generation techniques have been verified during the SSME-ATD program. Figure 118 shows the predicted fluid temperature rise across the bearings at various LO_2 coolant flow rates. Note the selected flowrate of 2.0 pps in relation to the knee of the curve. This clearly defines the safe operating area. Similar analysis on the LH_2-cooled ball bearing was conducted and a coolant flowrate requirement of 0.1 pps LH_2 was established. Detailed thermal analysis is planned during the final design to show load and flow margins and transient behavior of the bearings. The thermal modelling is based on a NASA approach using the SINDA Heat Transfer Code.

A design summary of the LO_2 turbopump ball bearings is provided in Figure 119. Experience guidelines are also provided to show design margins. Final verification of the ball bearing design will come under an IR&D program. A rig test will be performed simulating AETB operating conditions to demonstrate bearing durability. In the test rig, both the LO_2-cooled and LH_2 bearings are tested along with the interpropellant seal. The rig is shown in Figure 120.

b. Roller Bearings

A detailed trade study was performed to optimize the rolling element size and geometry for the AETB operating conditions. Figure 121 shows the effects of radial load and negative IRC on contact stress and minimum roller preload for the nominal geometry of the selected configuration. The XLR129 and SSME-ATD test data were used to establish a safe minimum roller preload for the AETB. Specifically, the minimum roller preload was selected based on a ratio of roller energy of the proven designs to the AETB condition. From this approach, a minimum roller preload of 220 pounds was selected to ensure adequate roller guidance. For the worst case design radial load of 163 pounds, the minimum roller preload is greater than 270 pounds and the maximum contact stress is 358 ksi. Although the contact stress is above the previous test experience of 200 ksi, the AETB life goal of five hours is far less than the 18-hour life demonstrated at 300 ksi. The negative internal clearance could be reduced to decrease the contact stress but this would reduce the minimum roller preload margin.

Material selection for the roller bearing was based on the SSME-ATD program. AISI 9310, the race material, has excellent fracture toughness compared to through hardened steels. Figure 122 shows the superior fracture toughness of AISI 9310 compared to AISI 440C. Armalon was chosen for the cage material, again based on previous roller bearing experience. Armalon is a glass fabric laminate filled with Teflon. The glass fabric provides the structural integrity, while the Teflon provides the lubrication.

Roller bearing coolant flow requirements were selected using the same methodology as the ball bearings. For the design point in the hydrogen turbopump, a coolant flow requirement of 0.2 pps was selected. For the oxygen turbopump, a coolant flow requirement of 0.1 pps was selected. Cooling curves for both turbopump roller bearings are provided in Figure 123.

A summary of key roller bearing design parameters is provided in Figure 124. Final verification of the roller bearing design will be provided under an IR&D rig test program. A cross section schematic of the test rig is provided in Figure 125. The test rig will simulate turbopump operating conditions and verify the bearing life. Three bearings are tested simultaneously; the center bearing reacts 100 percent of the applied radial load while the other two bearings react 50 percent of the load. Axial thrust balance control is provided by a thrust piston.

4. Bearing Methodology and Verification

Negative internal radial clearance provides the restraining force to provide roller stability. The negative clearance produces additional load between the roller and the races, which increases contact stress. For the AETB roller bearing design, the small size and high speed requirements necessitate heavy internal preload. The resultant contact stress can be as high as 359 ksi or approximately 20 percent above SSME-ATD experience. Roller stability margin also needs to be addressed since the required roller preload was determined empirically. A dynamic model is currently being modified under a NASA-MSFC contract to analyze negative internal clearance roller bearings. This model can be used to verify roller stability. The ultimate verification will be provided under the IR&D rig testing.

High assembly hoop stresses in cryogenic bearing inner rings can cause stress corrosion cracking (SCC) failures. AISI 440C has excellent general corrosion resistance but is susceptible to stress corrosion cracking. Figure 126 shows the contributors to SCC and steps taken to minimize the risk. Testing at P&W's Materials Engineering and Technology Laboratory has compared an AETB (RL10) AISI 440C inner ring to early ATD AISI 440C inner rings. Although this test is still underway, the data presented below shows a substantial difference in AISI 440C processing.

	Stress	Time to Failure
AETB 440C	35 ksi	255 days (still testing, no failures)
Non-Optimized 440C	35 ksi	19 days
AETB 440C	50 ksi	255 days, still testing, no failures)
Non-Optimized 440C	50 ksi	<1 day

By maintaining hoop stresses below 25 ksi, the SCC risk is very small.

Figure 127 shows various computer models used in the design of cryogenic rolling element bearings. Methodology verification of some of these models has been carried out under the SSME-ATD program. For the AETB, all of the models will be anchored or verified under the IR&D rig test program.

Design Speed: 49,000 rpm
Operating Speed: 42,000 rpm

		Pump-End Ball	Turbine-End Roller	Turbine-End Ball
DN	- Design Speed	1.7×10^6 mm-rpm	1.3×10^6 mm-rpm	1.7×10^6 mm-rpm
	- Operating Speed	1.5×10^6 mm-rpm	1.1×10^6 mm-rpm	1.5×10^6 mm-rpm
Loads	- Radial	48 lbs	31 lbs	nil
	- Axial (Steady)	300 lbs	N/A	300 lbs
Coolant	- Type	LOX	LH_2	LH_2
	- Pressure	1280 psia	3370 psia	3370 psia
	- Temperature	172 R	120 R	115 R

Figure 108. Oxygen Turbopump Bearing Design Conditions

Design Speed: 100,000 rpm
Operating Speed: 88,000 rpm

		Primary Fuel Pump		Secondary Fuel Pump	
		Inducer End (#1)	Turbine End (#2)	Turbine End (#3)	Inducer End (#4)
DN	- Design Speed	2.7×10^6 mm-rpm	2.7×10^6 mm-rpm	2.7×10^6 mm-rpm	2.7×10^6 mm-rpm
	- Operating Speed	2.4×10^6 mm-rpm	2.4×10^6 mm-rpm	2.4×10^6 mm-rpm	2.4×10^6 mm-rpm
Loads	- Radial	72 lbs	163 lbs	40 lbs	64 lbs
Coolant	- Type	LH_2	LH_2	LH_2	LH_2
	- Pressure	138 psia	3271 psia	1961 psia	3348 psia
	- Temperature	42 R	116 R	91 R	114 R

Figure 109. Hydrogen Turbopump Bearing Design Conditions

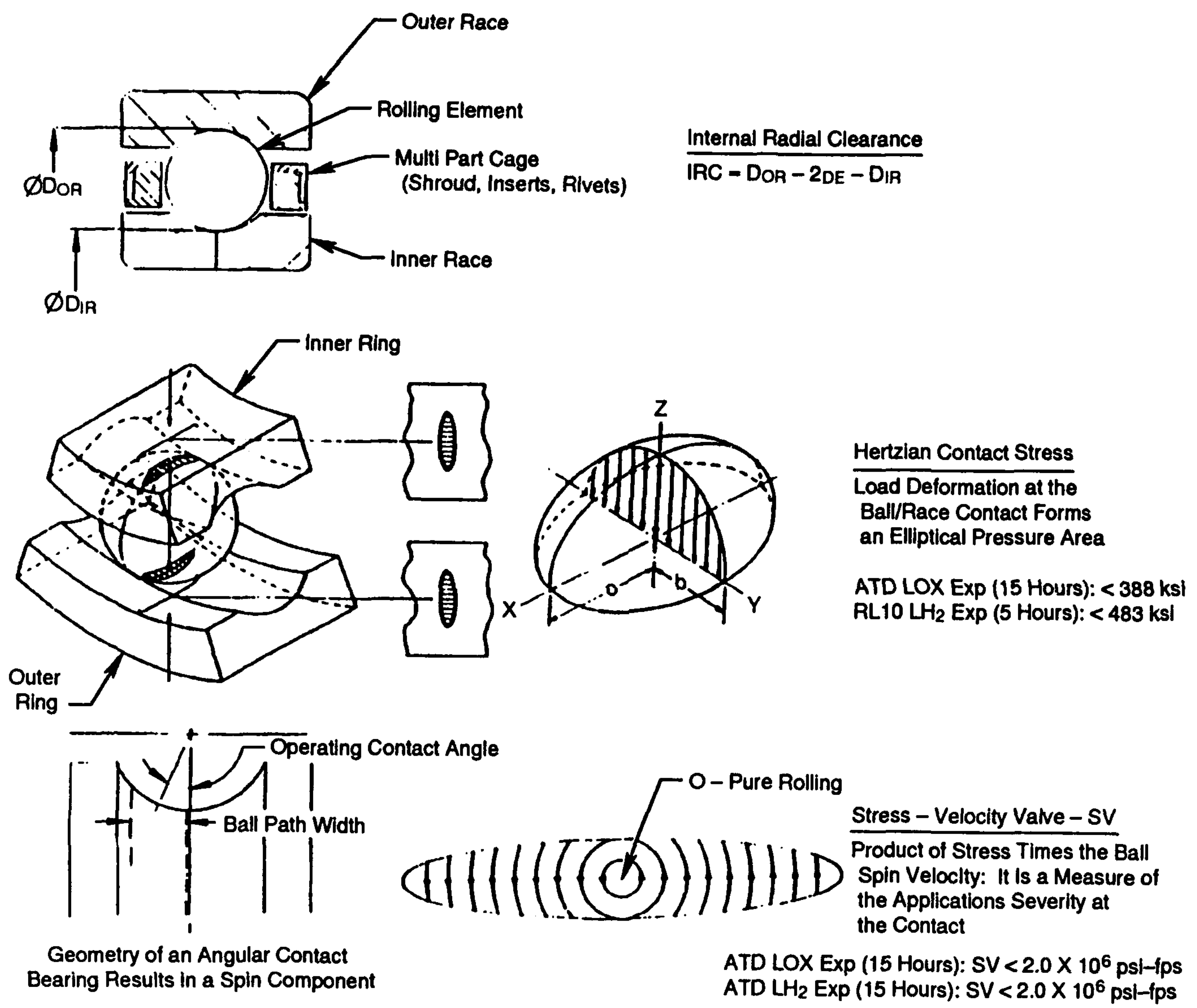

Figure 110. Ball Bearing Nomenclature

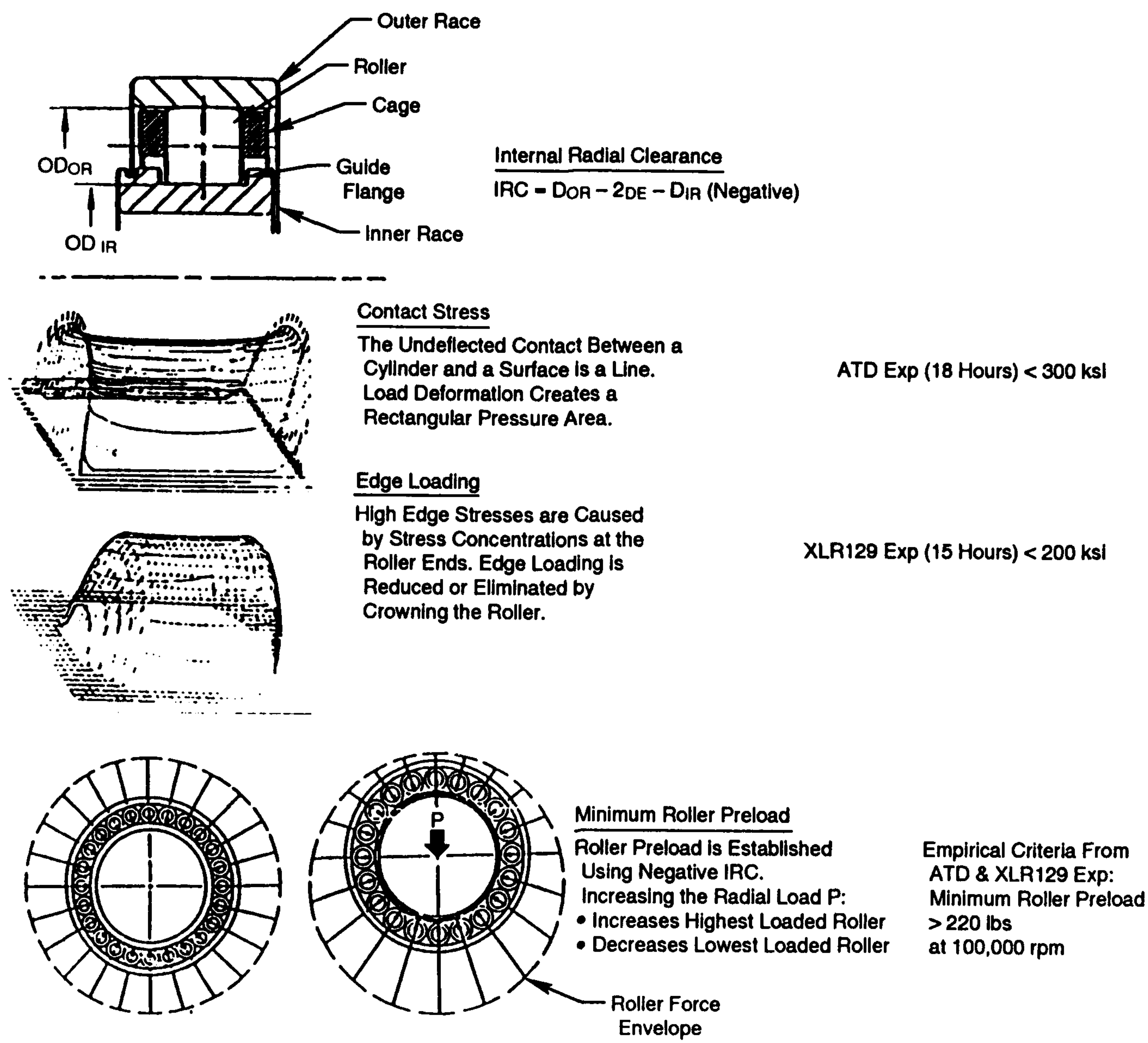

Figure 111. Roller Bearing Nomenclature

RL10 - 35 x 62 mm - 30,000 rpm (1.05 x 10^6 DN)

Endurance
- 1 Brg For 150 Hrs.
- 2 Brg's For 36 Hrs Each
- 5 Brg's For 25 Hrs Each

(Max Stress: 383 ksi)

Axial Overload
- 5 Hrs At 1,000 lbs (Rulon-A Cage)
- 5 Hrs At 1,500 lbs (Salox-M Cage)
- 25 Hrs At 1,300 lbs (Rulon-A Cage)

(Max Stress: 488 ksi @ 1,000 lbs)
(Max Stress: 542 ksi @ 1,500 lbs)

Overspeed
- 1 Brg For 5.8 Hrs At 40,000 rpm
- 1 Brg For 8.5 Hrs At 40,000 rpm
- 1 Brg For 0.5 Hrs At 50,000 rpm
- Several Brg's For Up To 15 Hrs At 48,000 rpm

(Max Stress: 383 ksi)

350K - 55 x 90 mm - 40,000 rpm (2.2 x 10^6 DN)
- 6 Brg's For 10 Hrs Each, Axial Load 500 lbs (Max Stress 305 ksi)

SSME-ATD - 60 x 130 mm - 36,500 rpm (2.2 x 10^6 DN)
- 32 Brg's For 222 Cummulative Hrs
- High Time Brg's - 18.1 Hrs, 56 Cycles
- Two Low Speed Brg's (1.5 x 10^6 DN) Have Run 29 Hrs, 168 Cycles
- Axial Loads 800-2,000 lbs, (Max Stress: 394 ksi)
- Transient Axial Load Test, 11,000 lbs (Max Stress: 555 ksi) - ATD Thrust Brg
- LH_2 Coolant Flows: 0.2 - 0.7 pps

Figure 112. Liquid Hydrogen Ball Bearing Experience at Pratt & Whitney

350K - 50 x 90 mm - 24,000 rpm (1.2 x 10^6 DN)

- 8 Brgs, 10 Hrs Max Time Brg's, Axial Loads: 200-400 lbs (Max Stress: 318 ksi)

SSME-ATD - 60 x 130 mm - 25,000 rpm (1.5 x 10^6 DN)

- 19 Brg's In LN_2 / LOX For 99 Cumulative Hrs
- High Time Brg's - 14.8 Hrs, 88 Cycles
- Axial Loads 1,000 - 2,000 lbs (Max Stress: 388 ksi)
- LOX Coolant Flows: 2.0 - 6.0 pps

Figure 113. Liquid Oxygen Ball Bearing Experience at Pratt & Whitney

XLR129, 55 x 96 mm - 48,000 rpm (2.64 x 10^6 DN)

- 2 Brgs, 15.4 Hrs Each, 305 Cycles
- 11 Brgs Exceeded 7.5 Hrs
- Radial Load 1,700 lbs (Max Stress: 278 ksi)

SSME-ATD 73 x 127 mm - 25,000 rpm (1.8 x 10^6 DN)
73 x 133 mm 36,500 rpm (2.7 x 10^6 DN)

- 5 Brgs For 66.3 Cumulative Hrs
- High Time Brg - 28.7 Hrs, 168 Cycles

1.8 x 10^6 DN

- 12 Brgs For 75.2 Cumulative Hrs
- High Time Brg - 18.1 Hrs, 56 Cycles
- Radial Load 3,800 lbs (Max Stress: 300 ksi)

2.7 x 10^6 DN

Figure 114. Liquid Hydrogen Roller Bearing Experience at Pratt & Whitney

Trade Studies Considered:

- Rolling Element Size & Quantity
- Race Curvatures
- Axial Preload
- IRC
- Larger Bore Dia RL10 Brg

N=49,000 rpm, Axial Load = 300 lbs

△ 27 x 58 mm

○ 35 x 62 mm, RL10

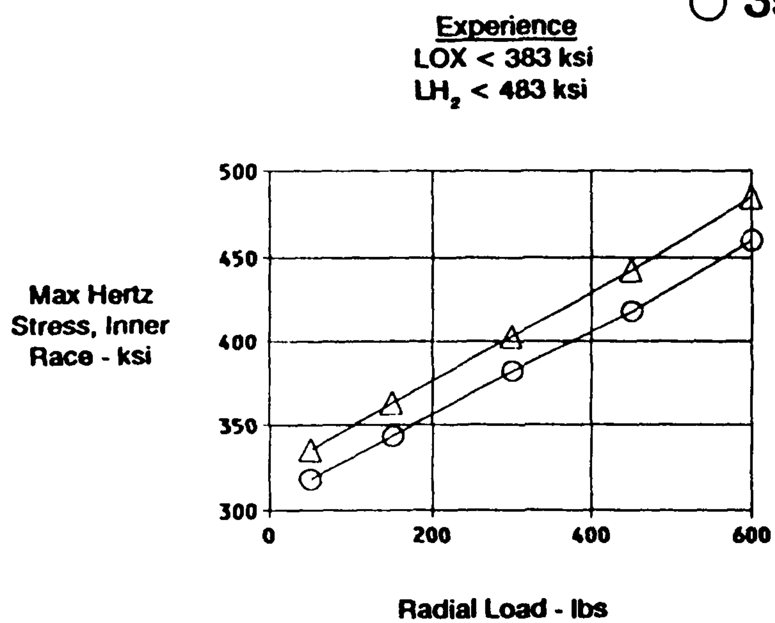

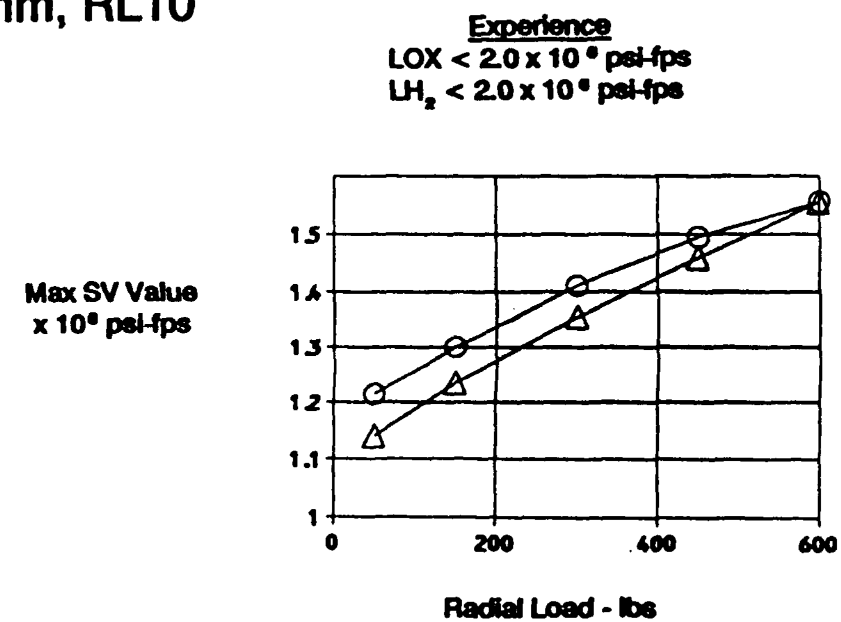

Figure 115. Design Trades for the Ball Bearing Configuration

Selected ——► RL10 Bearing: 35 x 62 mm, 13 - 0.3125 Inch Elements
Proposed AETB Bearing: 27 x 58 mm, 10 - 0.3438 Inch Elements

RL10 Bearing Selection Rationale

Advantages	Concerns
Extensive Test Experience	Higher DN (Within Experience)
Lower Hertz Stress	Higher SV (Within Experience)
Higher Radial Stiffness	
Higher Fatigue Life	
Established Manufacturing	

Figure 116. Design Trades for Selection of the Ball Bearing Configuration

		* LOX Cooled Pump-End Ball	LH2 Cooled Turbine-End Ball
Inner Race		AISI 440C	AISI 9310
Outer Race		AISI 440C	AISI 440C
Rolling Element		AISI 440C	AISI 440C
Cage	- Shroud	K Monel	Aluminum
	- Lubricant	Salox-M-40% Bronze, 60% PTFE	Rulon-A
	- Rivet	AISI 304	Aluminum

* LOX Compatibility Characterization Underway In The ATD Program

Figure 117. Ball Bearing Material Selection

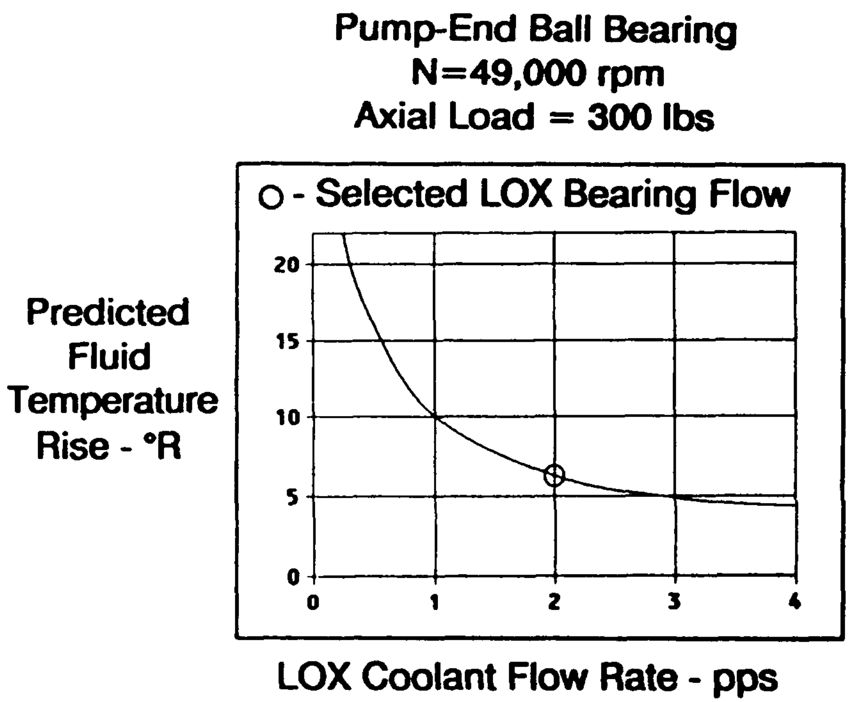

Heat Generation Is Verified In IR&D Test Rig

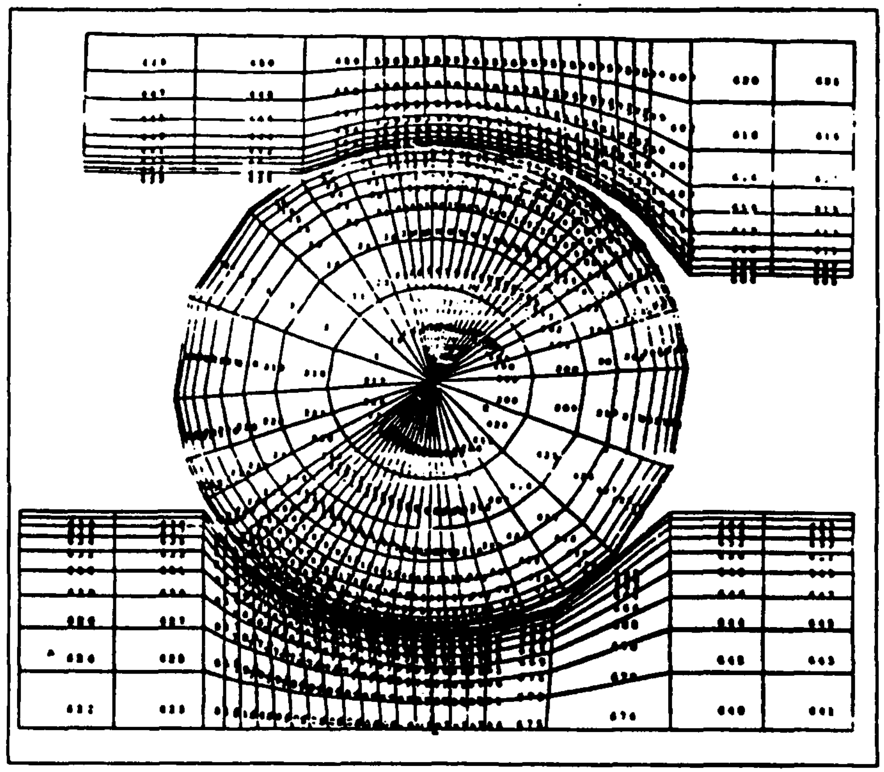

Detailed Thermal Model Of LOX Bearing Planned By CDR

Figure 118. Ball Bearing Heat Generation Analysis

	Pump-End Ball Bearing	LOX Experience	Turbine-End Ball Bearing	LH_2 Experience
Coolant	LOX		LH_2	
Flowrate	2.0 pps		0.1 pps	
Bore x OD	35 x 62 mm		35 x 62 mm	
Rolling Elements	13 - 0.3125 in		13 - 0.3125 in	
Race Curvatures - Inner	58%		58%	
- Outer	52%		52%	
Cage Type	Inner Land Pilot		Inner Land Pilot	
Radial Load	48 lbs		nil	
Axial Load	300 lbs		300 lbs	
IRC	0.0023 - 0.0039 in		0.0027 - 0.0043 in	
Max Hertzian Stress	320 ksi	<383 ksi	300 ksi	<483 ksi
Radial Stiffness	>0.3 x 10^6 lb/in	N/A	>0.3 x 10^6 lb/in	N/A
Max SV	1.2 x 10^6 psi-fps	<2.0 x 10^6 psi-fps	1.1 x 10^6 psi-fps	<2.0 x 10^6 psi-fps
Ball Excursion	0.003 in	<0.025 in	0.001 in	<0.025 in
B1 Life	9 hrs	N/A	9.5 hrs	N/A
*Transient Axial Load	2,500 lbs	N/A	2,500 lbs	2,000 lbs

* Based On Load Containment Criteria

Figure 119. Ball Bearing Design Summary

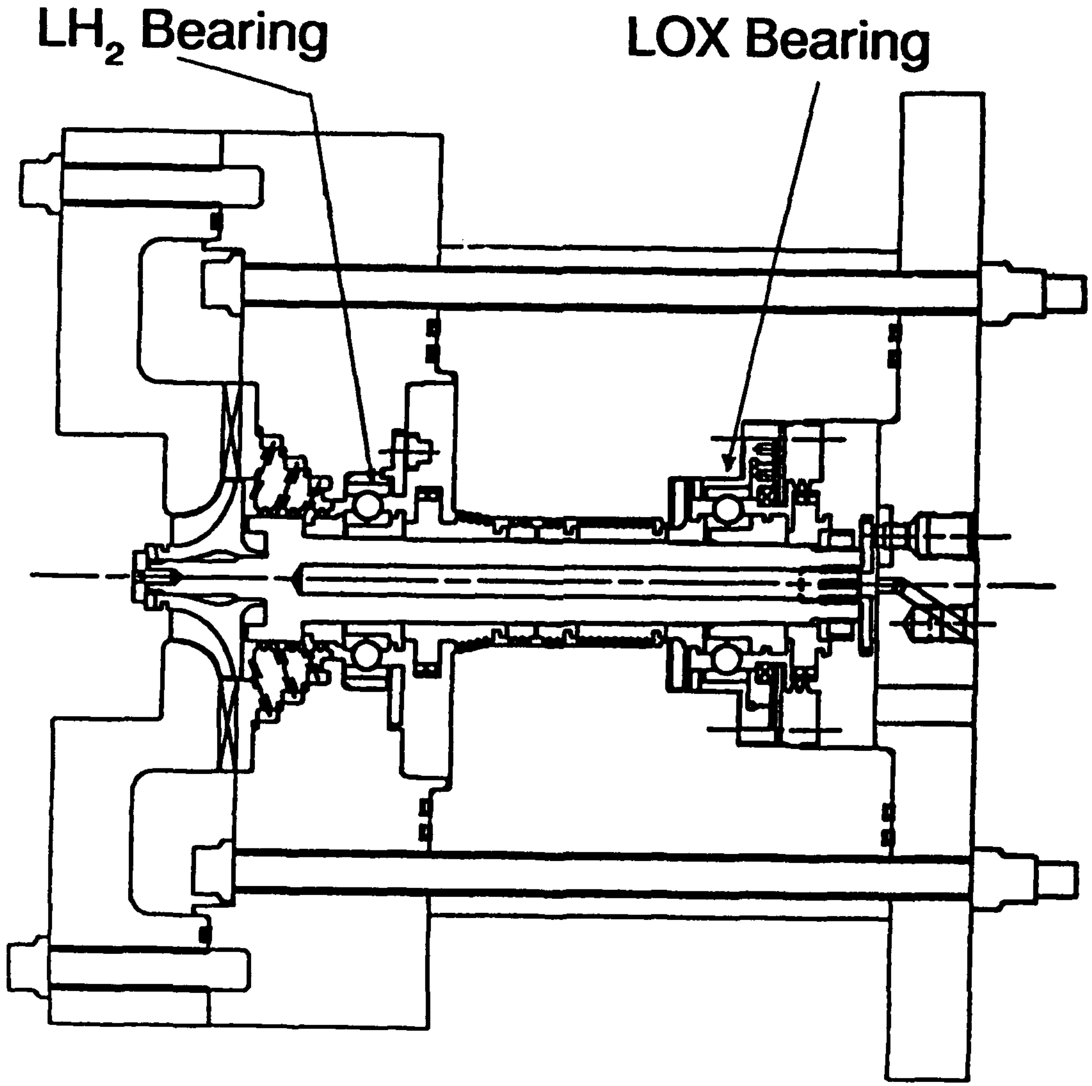

Figure 120. Ball Bearing Test Rig

Trade Studies Considered:
- Rolling Element Size & Quantity
- Race Crown Drop
- Internal Preload (Negative IRC)

N=100,000 rpm, My=-0.0005 in/in, Crown Drop = 0.0006 in

△ IRC = 0.0023 Inches Tight

○ IRC = 0.0026 Inches Tight

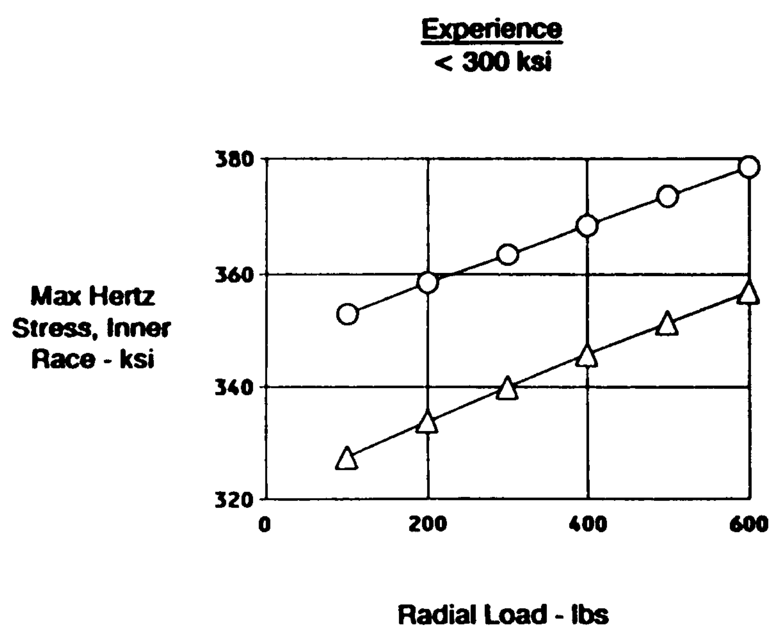

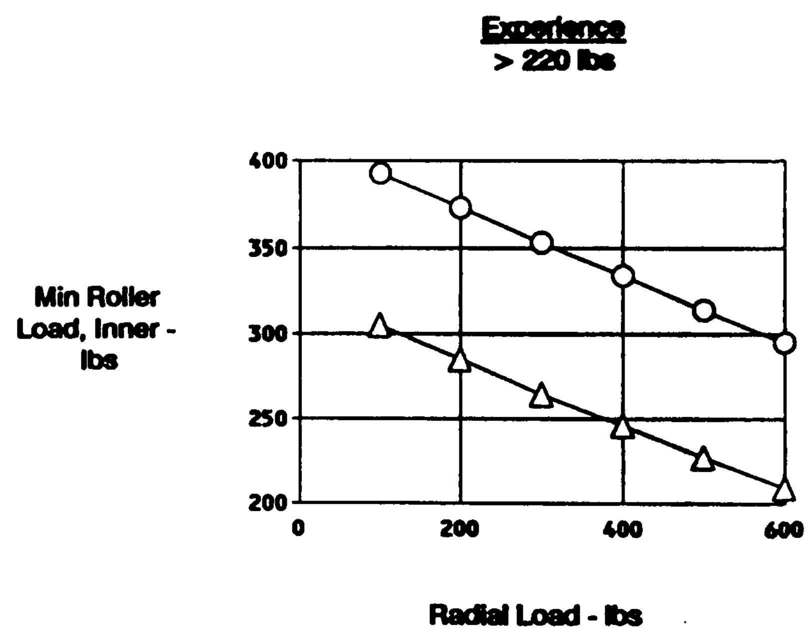

Figure 121. Effects of Radial Load and Negative IRC

Inner Race : AISI 9310
Outer Race : AISI 9310
Rolling Element : AISI 440C
Cage : Armalon, Glass Fabric Filled PTFE

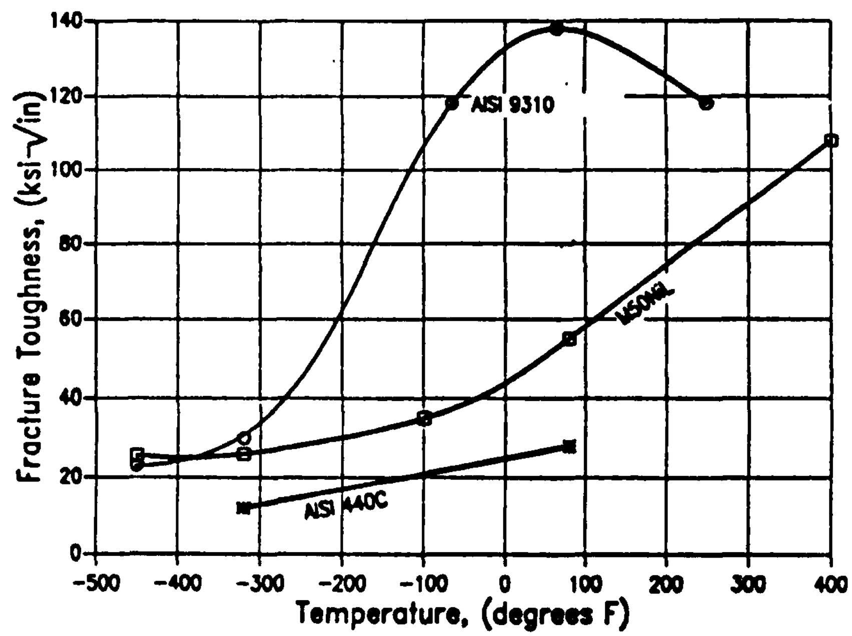

Figure 122. Roller Bearing Material Selection

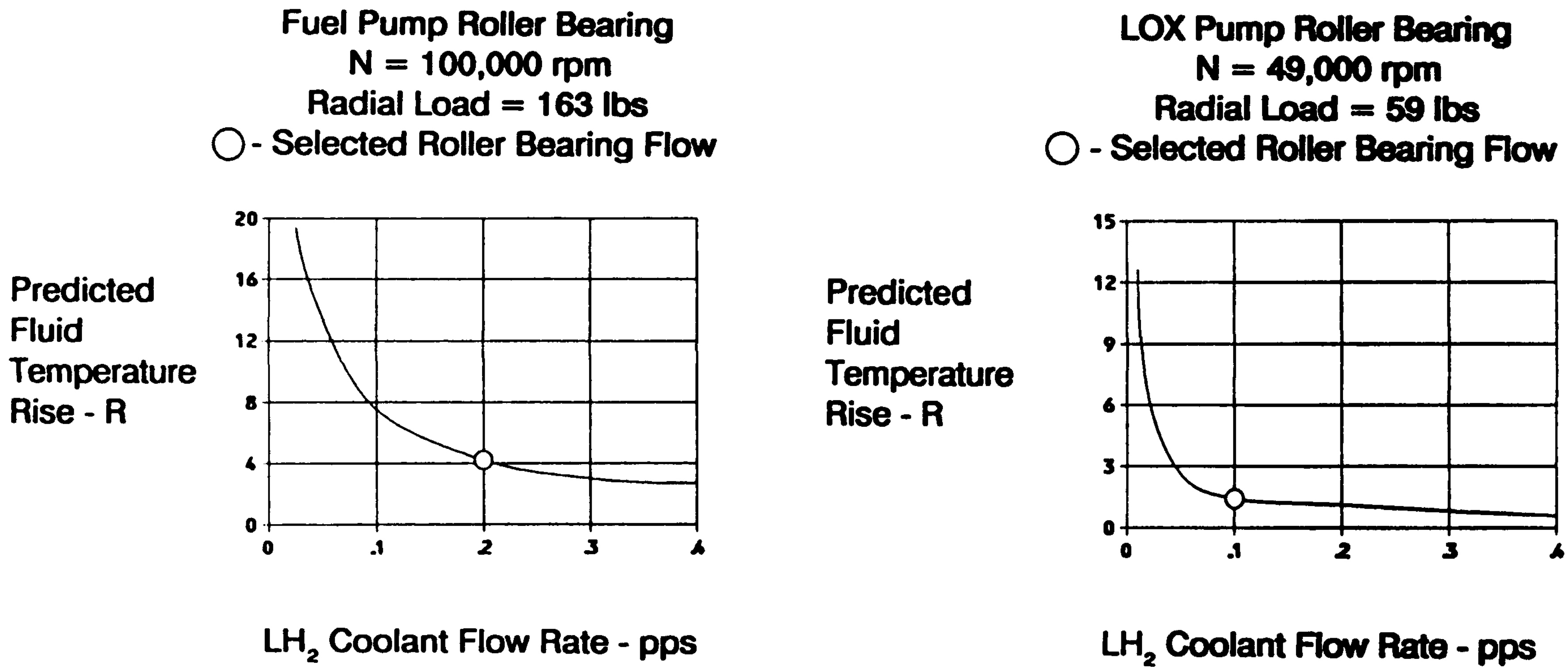

Figure 123. Roller Bearing Heat Generation

	Fuel Pump Roller Bearing	
Coolant	LH_2	
Flowrate	0.2 pps	
Bore x OD	27 x 58 mm	
Rolling Elements	10 - 0.315 Inch	
Cage Type	Outer Land Pilot	
Crown Drop	0.0005 - 0.0007 Inch	
Radial Load	163 lbs (Highest Load, #2 Roller)	
IRC	0.0023 - 0.0026 Inches Tight	
		Experience (18 Hour Life)
Maximum Hertzian Stress	329 - 358	< 300 ksi
Radial Stiffness	$> 1.3 \times 10^6$ lb/inch	N/A
Minimum Roller Preload	270 - 325 lbs	> 220 lbs
Roller Edge Stress	0 - 102 ksi	< 200 ksi
B1 Life	7.5 - 10.5 Hrs	N/A

Figure 124. Roller Bearing Design Parameters

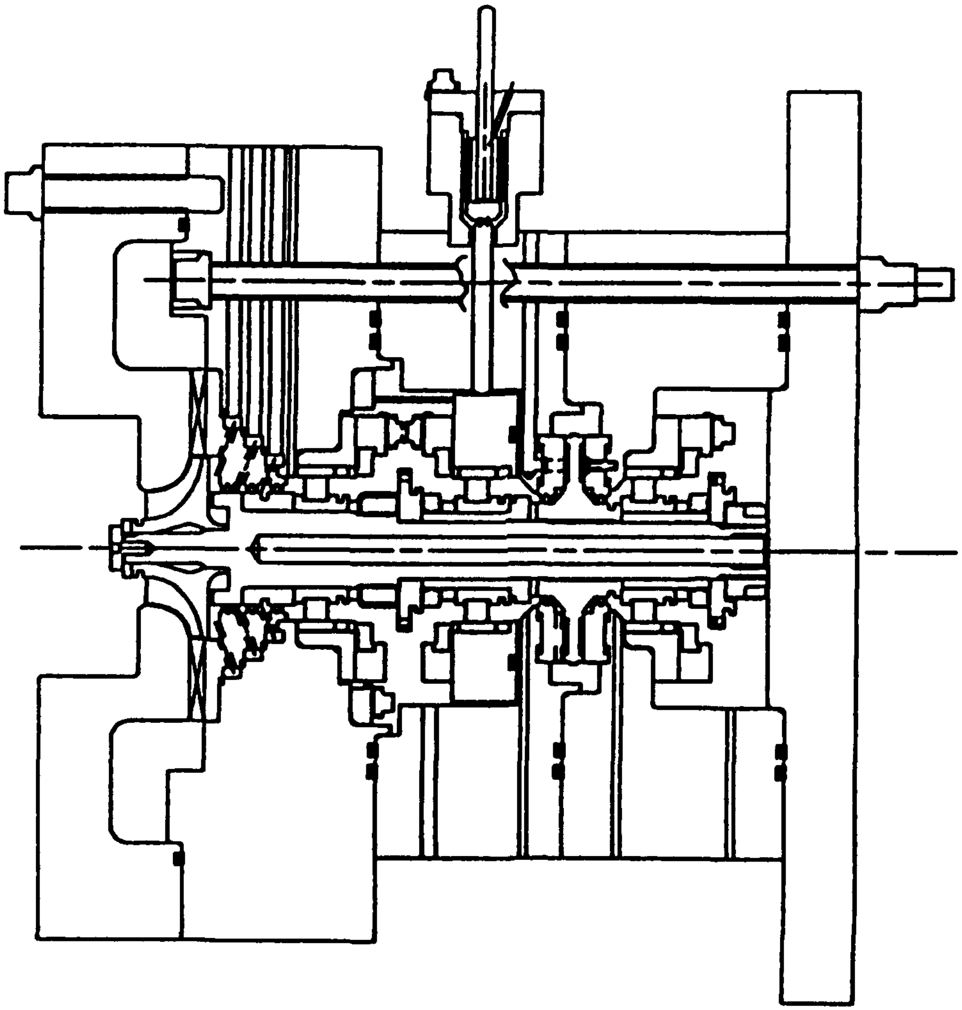

Figure 125. Roller Bearing Test Rig

- LOX Cooled Ball Bearing Uses AISI 440C. AISI 9310 Which Has Superior SCC Resistance Is Not Suitable For LOX Use.
- SCC Failures Occured In The Early Development Stage Of The ATD Program
- Contributors Of SCC Identified:
  - High Inner Ring Hoop Stress
  - Time Mounted On Shaft
  - Grinding Damage
  - Corrosion
  - Non-Optimized Processing & Heat Treat

SCC Addressed For AETB:

- ATD & RL10 AISI 440C Have Improved Processing & Heat Treat Over Early ATD AISI 440C
- RL10 Has Not Had SCC Problems, Maximum Inner Ring Hoop Stress Is 28 ksi
- AETB Inner Ring Hoop Stress < 25 ksi
- ATD Established Eddy Current Procedure Incorporated To Detect Grinding Damage
- Lab Test Underway To Characterize SCC Life Of AISI 440C

Figure 126. Stress Corrosion Cracking Concerns in AISI 440C

Model	Pupose	Verification
A.B. Jones	Contact Stress & Dynamics, Bearing Life	Verified In ATD, Will Be Anchored To AETB In IR&D Rigs
Fit Programs	Bearing Fits, Clearances, And Ring Stresses	Verified In ATD, Will Be Anchored To AETB In IR&D Rigs
→ ADORE	Roller Stability Margin	Will Be Verified And Anchored To AETB In IR&D Rigs
→ Shaberth/Sinda	Heat Generation, Thermal Analysis Thermal Margin	Will Be Verified And Anchored To AETB In IR&D Rigs

Figure 127. Computer Models for Bearing Design

H. Combustion System

The combustion system consists of an injector with igniter, combustion chamber, and a conical nozzle extension as shown in Figure 128. The dual-orifice injector and milled channel liner combustion chamber are based on an existing design completed and detailed under a P&W Space Engine Component Technology Program. Although contract work on the components in preliminary design included only the detailed layout of the exhaust nozzle, the design of all the hot section components is described in the following sections.

1. Injector/Igniter Assembly

The AETB igniter uses the same design approach used in the P&W RL10 engine, SSME-ATD hot gas system preburners, and the Advanced Launch System (ALS) Technology ignition system. Figure 129 shows the H_2-O_2 torch igniter design that will be employed.

The torch igniter consist of a Haynes 230 mount flange housing with a oxygen free high conductivity (OFHC) copper combustion liner and a Haynes 230 structural jacket. The ignition chamber diameter is constricted from 0.500 inch in the chamber to 0.220 inch at the exit to produce adequate igniter chamber pressure for ignition at altitude. The liner operational life is predicted to be adequate with GH_2 cooling. The same design features are incorporated in the SSME-ATD igniter which has over 1000 seconds of operation with no problems to date.

Various ports on the mount flange allow installation of the spark plug, instrumentation, and inlet lines. The igniter is mounted through the center of the injector using stepped studs.

The injector assembly, Figure 130, will be manufactured from ferrite controlled 347 stainless steel (347 SST). It consists primarily of an injector housing with a fuel manifold welded on the outside. In the center of the housing, various cavities are machined to create the internal oxidizer injection manifolds. Sixty-five dual-orifice elements are uniformly spaced in a circular pattern with allowance in the center for the torch igniter. Ferrite controlled 347 SST was chosen for its ease of machining, weldability, brazeability and ductility. The ferrite control helps reduce the risk of post-weld cracks in applications where no filler metal is added to the weld.

A separation plate is brazed in the top of the assembly to separate the primary and secondary oxygen plenums. A welded dome closes the secondary plenum and provides for installation of the igniter. The fuel plenum is created with a porous faceplate welded to the housing and brazed to individual fuel sleeves. The porous plate provides transpiration cooling of the injector face.

The core of the injector consists of the 65 LO_2 elements and fuel sleeves The elements, Figure 131, are of the dual-orifice tangential entry type and are brazed into the top of the housing. Primary LO_2 enters each element through three holes equally spaced, and secondary oxygen enters through three equally spaced axial slots. On the bottom of the housing are nozzles machined from the housing forging prior to the sleeves being brazed to the housing. The annulus created by the nozzle OD and sleeve ID meter the fuel into the combustion chamber.

The injector has been analyzed for acceptable structural integrity at the design point by both conventional calculations and a 2D boundary model, BEASY. The model included both thermal gradients and pressure loads for the injector. Figure 132 summaries the factor of safety for the injector.

A chugging model was created and run at the 5 percent, 10 percent, and 20 percent power levels. The analysis predicts no chugging will occur at these points, as shown in Figure 133. The model represents the propellant feed system in terms of inductance-resistance-capacitance (L-R-C) theory. High frequency combustion stability analyses were also conducted and adequate stability margin is predicted.

2. Combustion Chamber Assembly

The AETB combustion chamber, Figure 134, has a contraction ratio of 3:1 and an expansion ratio of 2:1. The chamber consists of a NASA-Z copper alloy liner with 120 milled coolant channels on the outside surface. Liner cooling channels are a constant 0.040-inch wide with a maximum height-to-width ratio of 5:1. Wall thickness between hydrogen coolant and the hot combustion wall is a constant 0.030-inch thick. The passage height is set to allow a maximum wall temperature of 1460 R without exceeding the allowable budgeted cycle pressure drop. At the normal operating point, the maximum wall temperature is 1355 R. Maximum heat flux at the operating point is 51.7 Btu/in.^{2}-second, occurring 0.50 inch upstream of the throat. This configuration provides a minimum predicted life of 200 cycles. No coolant two-phase flow instabilities are predicted in the liner or nozzle coolant circuit, since coolant pressure remains above the critical pressure of hydrogen over nearly all the thrust range. At 1,000 pounds thrust (20:1 turndown), pressure will drop below critical pressure but not before the hydrogen temperature is well above critical temperature.

The liner has an electroformed copper outer jacket that closes out the milled coolant channels and provides structural support for the chamber. Coolant manifolds are welded to each end of the chamber. Both manifolds, consisting of a ferrite controlled 347 SST material, are welded forming an internal primary distribution manifold with crossover ducts to a minor manifold, which is created when the jacket and manifold are joined.

The inlet manifold of the chamber interfaces with the nozzle extension, and the outlet manifold interfaces with the injector. Both of these joints incorporate a pilot snap fit. The snap is used to control radial movement during operation and to center the mating assemblies. The injector face extends into the chamber 0.7 inch to protect the uncooled portion of the liner.

The liner has been analyzed for acceptable structural integrity and life. The inlet and outlet manifolds have been analyzed by a 2D NASTRAN finite element model. A summary of these analyses with the calculated factors of safety is shown in Figure 135. The proof pressure condition was also examined and found to have acceptable margin when pressurizing the combustion chamber and cooling passages simultaneously. Coolant pressure and combustion pressure will be applied simultaneously during proof pressure tests with the throat area sealed off. The divergent section of the chamber will be exposed to ambient pressure.

3. Exhaust Nozzle Assembly

The conical nozzle extension consists of 160 coolant tubes brazed into a structural jacket containing the inlet and exit manifolds. The nozzle cross section is shown in Figure 136. The base material for the assembly details, Haynes 188, was chosen for its ductility, weldability, and good strength in hot hydrogen. It will also facilitate brazing during nozzle assembly, provide high-temperature capability, and meet heat transfer requirements.

The 160 coolant tubes are brazed into the inlet and exit manifold with a structural jacket joining the two. Each coolant tube is joined to the inlet and exit manifold by a braze joint. On the inlet end the tube will be hooked to fit into the inlet manifold. The tube exit will be an offset square socket joint that will fit into a machined annulus ring. Various combinations of tube attachments were examined and the current tube configuration was selected based on cooling and fabrication considerations. The uncooled portion of the nozzle is protected by being recessed into the inlet manifold of the combustion chamber.

The inlet manifold also contains one end of a spring arm that is used for controlling the radial thermal growth caused by the 600°F temperature differential between the cold chamber inlet and hot nozzle inlet. The spring arm between the two manifolds is designed to accommodate the relative thermal deflections of the manifolds while eliminating seal sliding and maintaining acceptable structural integrity.

A preliminary structural analysis of the spring arm was conducted by first examining the axisymmetric loads, then expanding the analysis to include asymmetric loading caused by transient pressure loads, weight, and interface loads. As shown in Figure 137, a safety factor of 1.24 is indicated. Buckling analysis was completed by evaluating shear forces on the spring arm from axial, transverse, bending, and torsion loads, resulting in a buckling factor greater than 10.

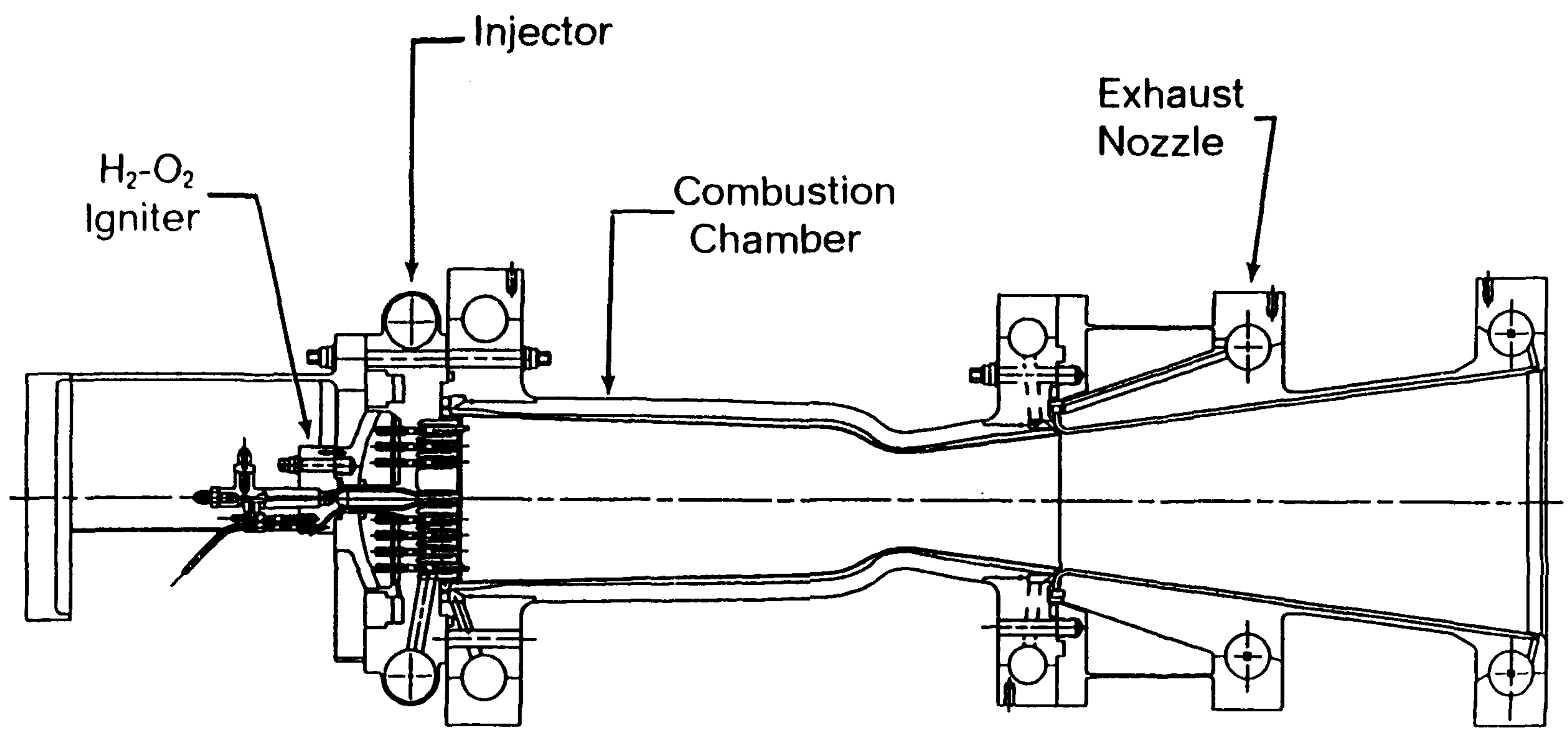

Contraction Ratio = 3.0
Combustion Length = 15 in.
Milled Channel - Copper

Nozzle Expansion Ratio = 7.5
Nozzle Expansion Length = 22 in.
Tubular - Haynes

Figure 128. Thrust Chamber Assembly

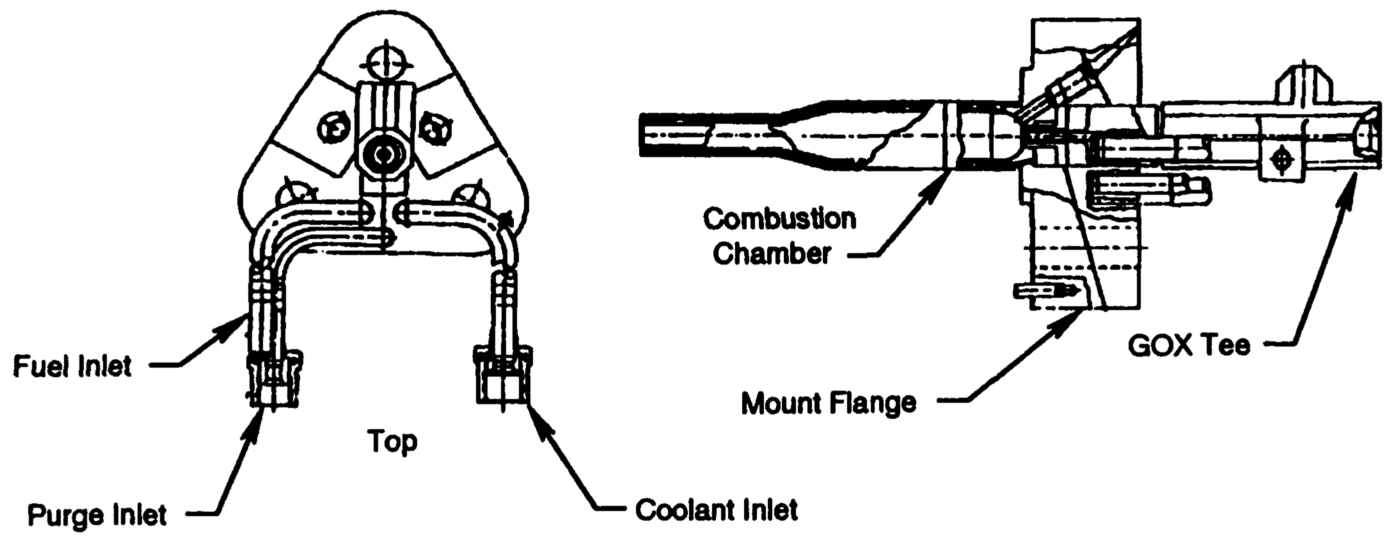

Figure 129. Igniter Assembly

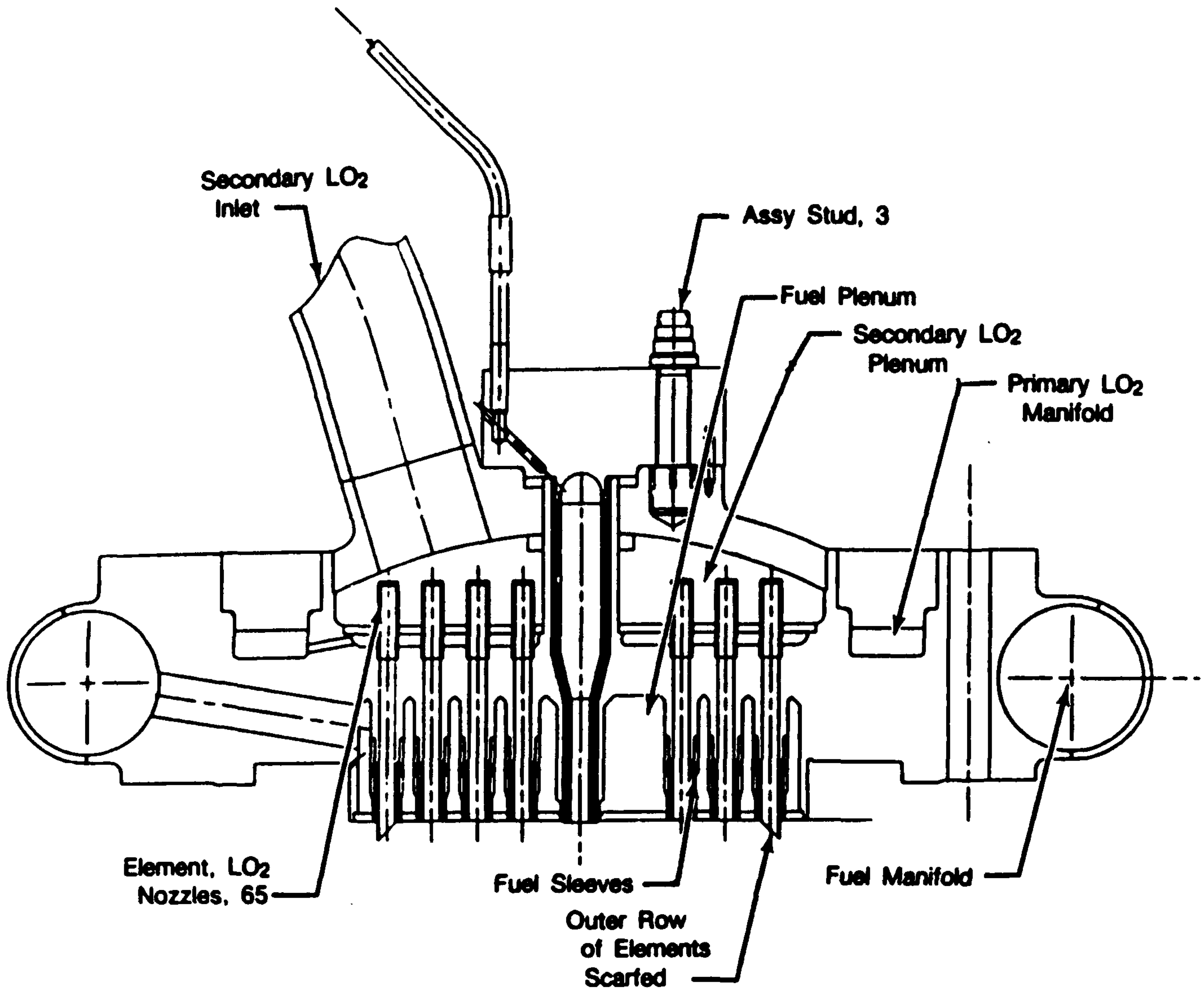

Figure 130. Injector Assembly With Igniter Mounted

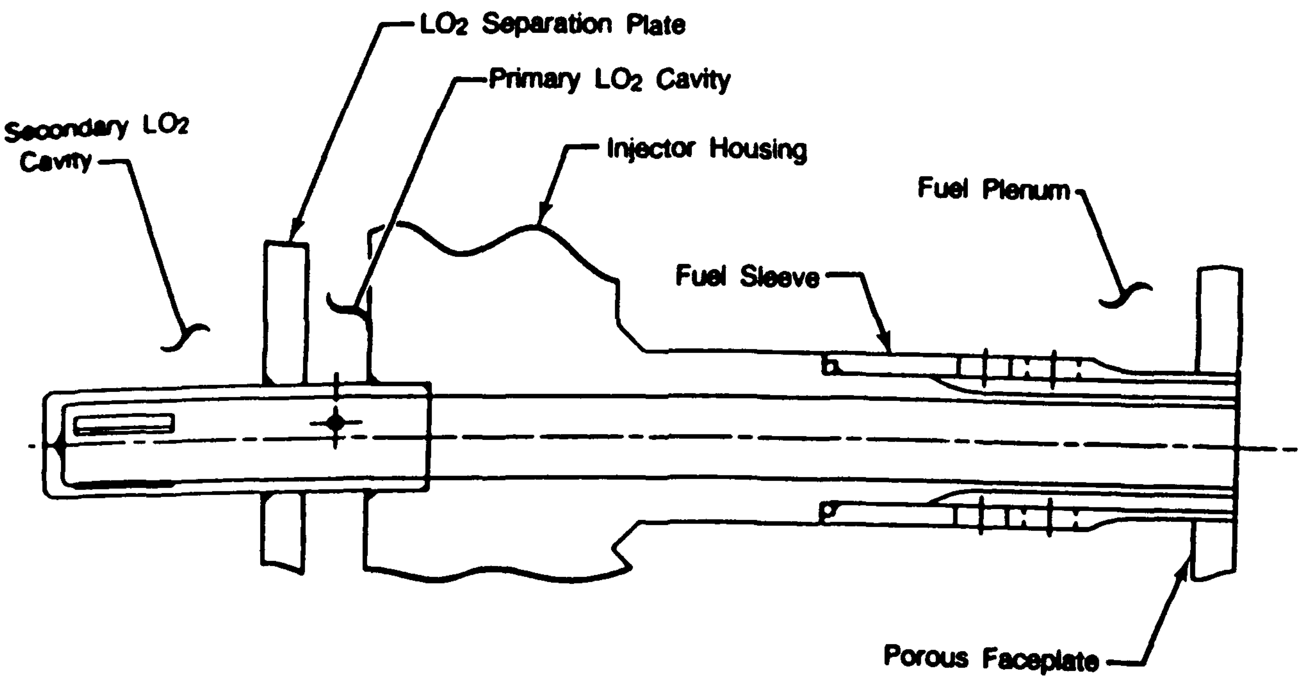

Figure 131. Liquid Oxygen Element and Fuel Sleeve

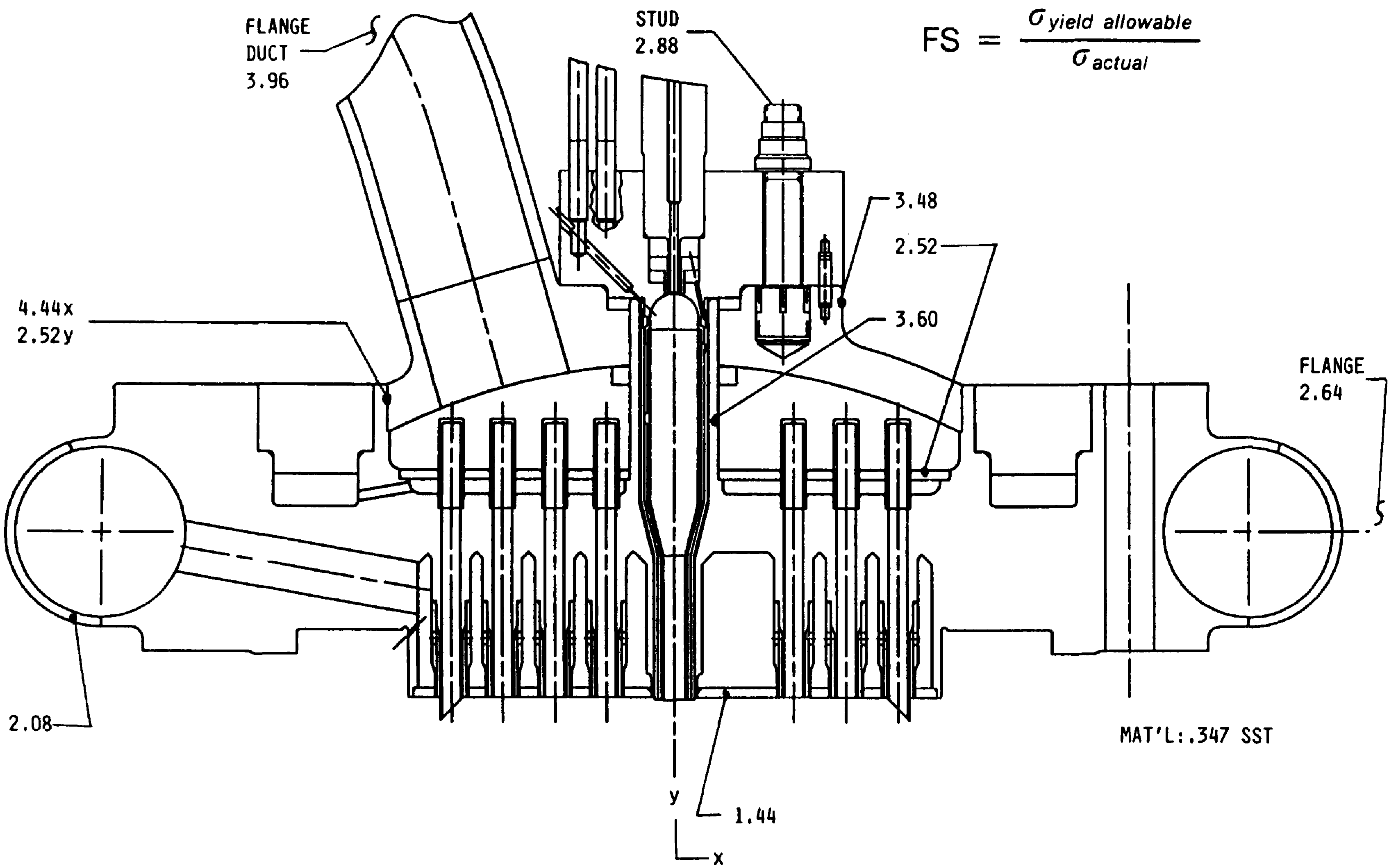

Figure 132. Injector Factors of Safety

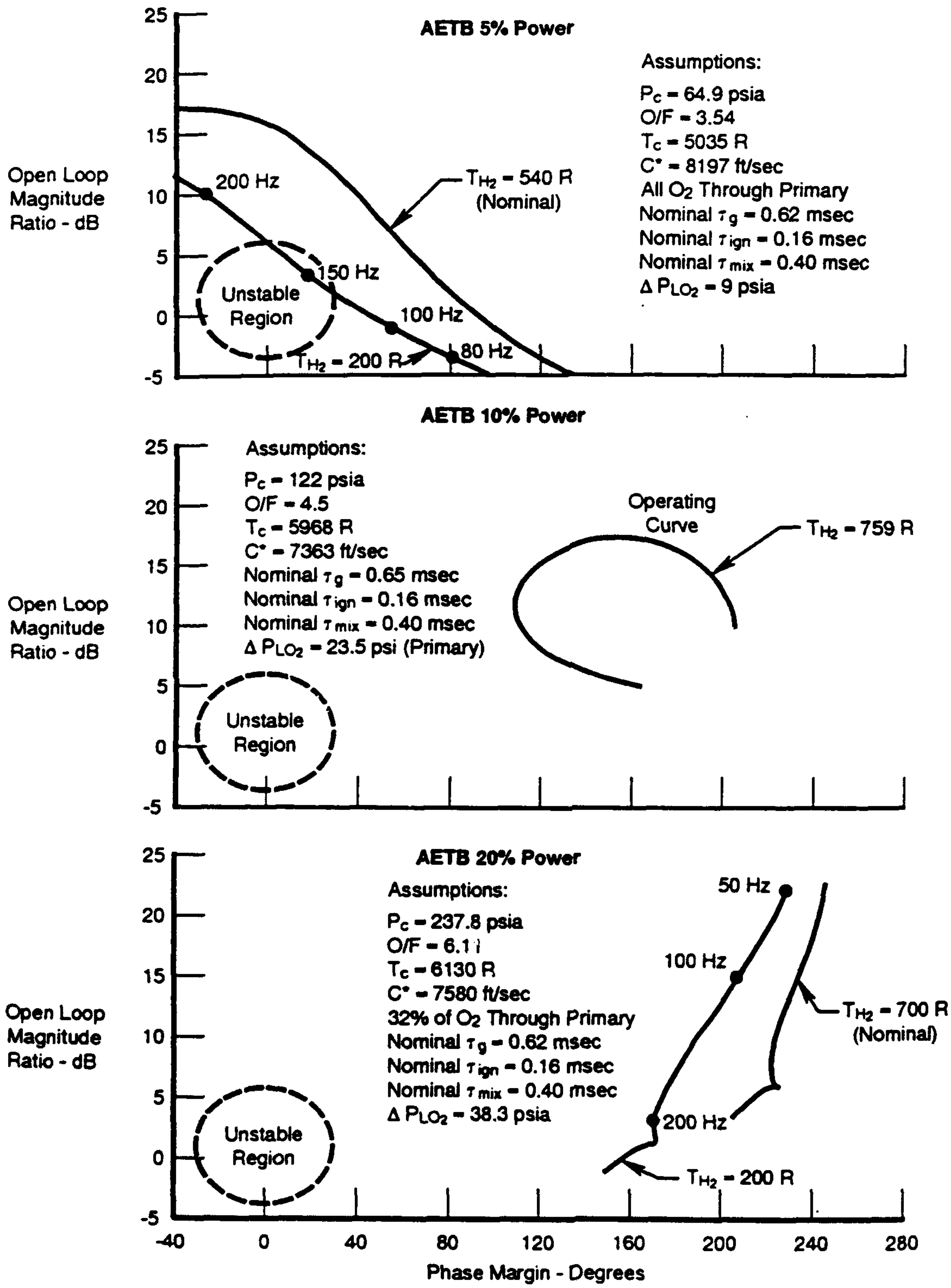

Figure 133. L-R-C Stability Curves at Power Levels of 5%, 10%, and 20%

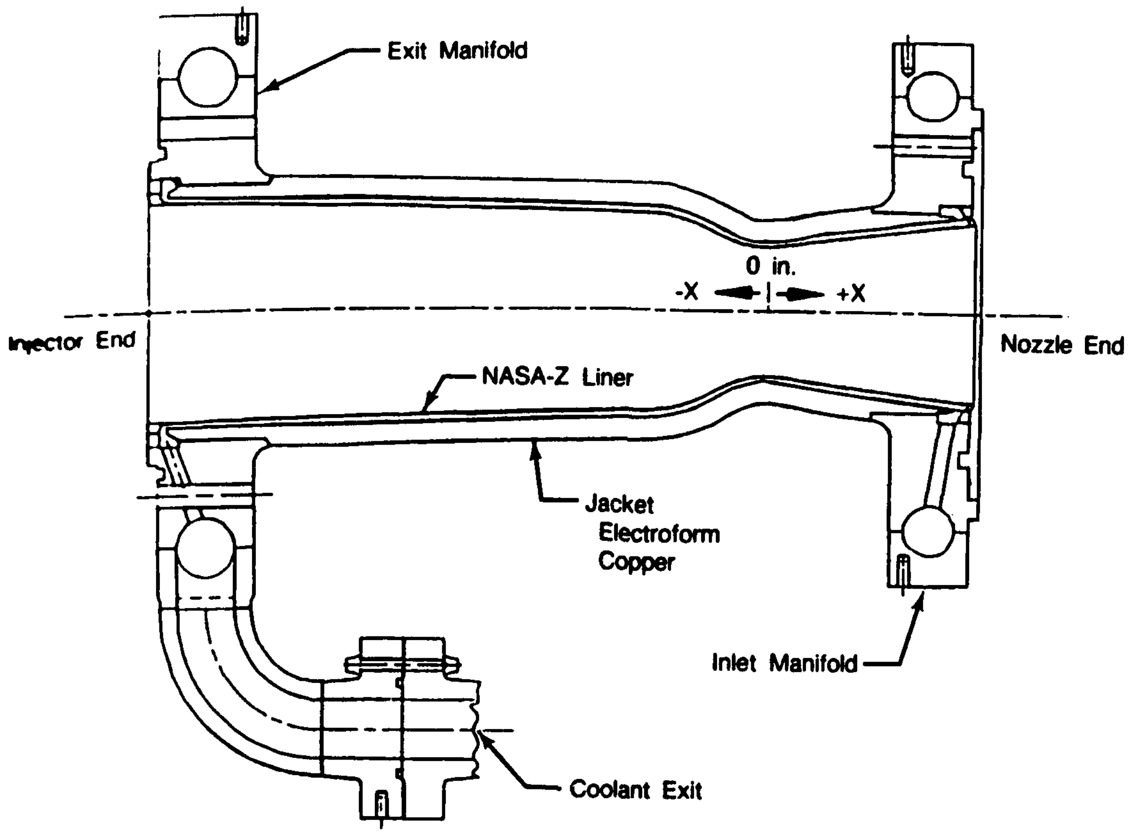

Figure 134. Milled Channel Combustion Chamber

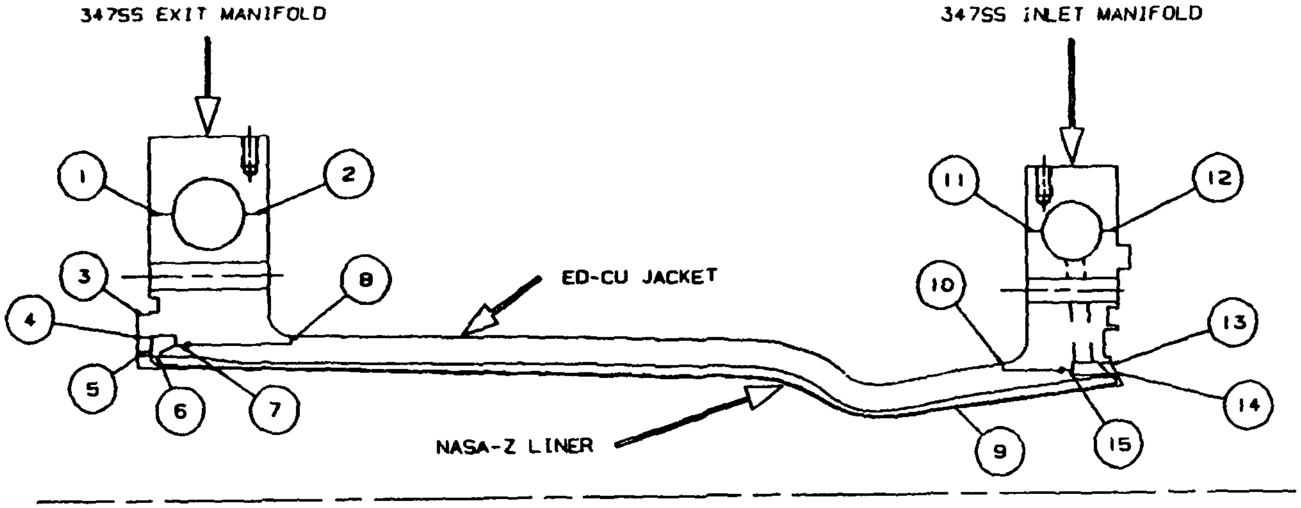

Location	Factors of Safety
1	2.9
2	2.9
3	> 4.0
4	> 4.0
5	2.9
6	1.2
7	1.2
8	1.1 *
9	3.7
10	> 4.0
11	> 4.0
12	> 4.0
13	> 4.0
14	2.0
15	2.5
Goal	1.2

* Acceptable since stress primarily hoop stress driven by flange rolling. Axial load F.S. = 2.6

Figure 135. Chamber Factors of Safety and Life

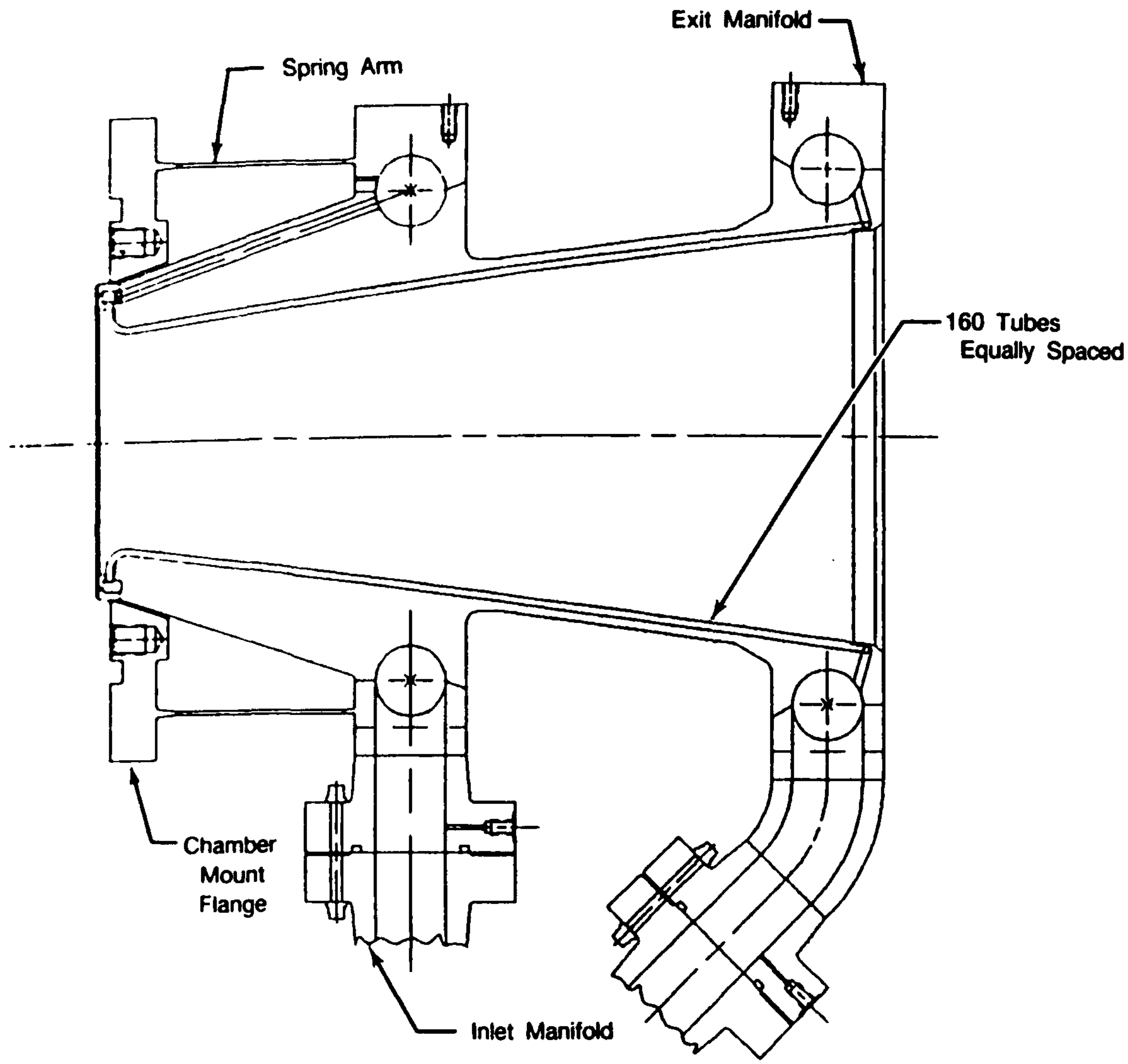

Figure 136. Exhaust Nozzle

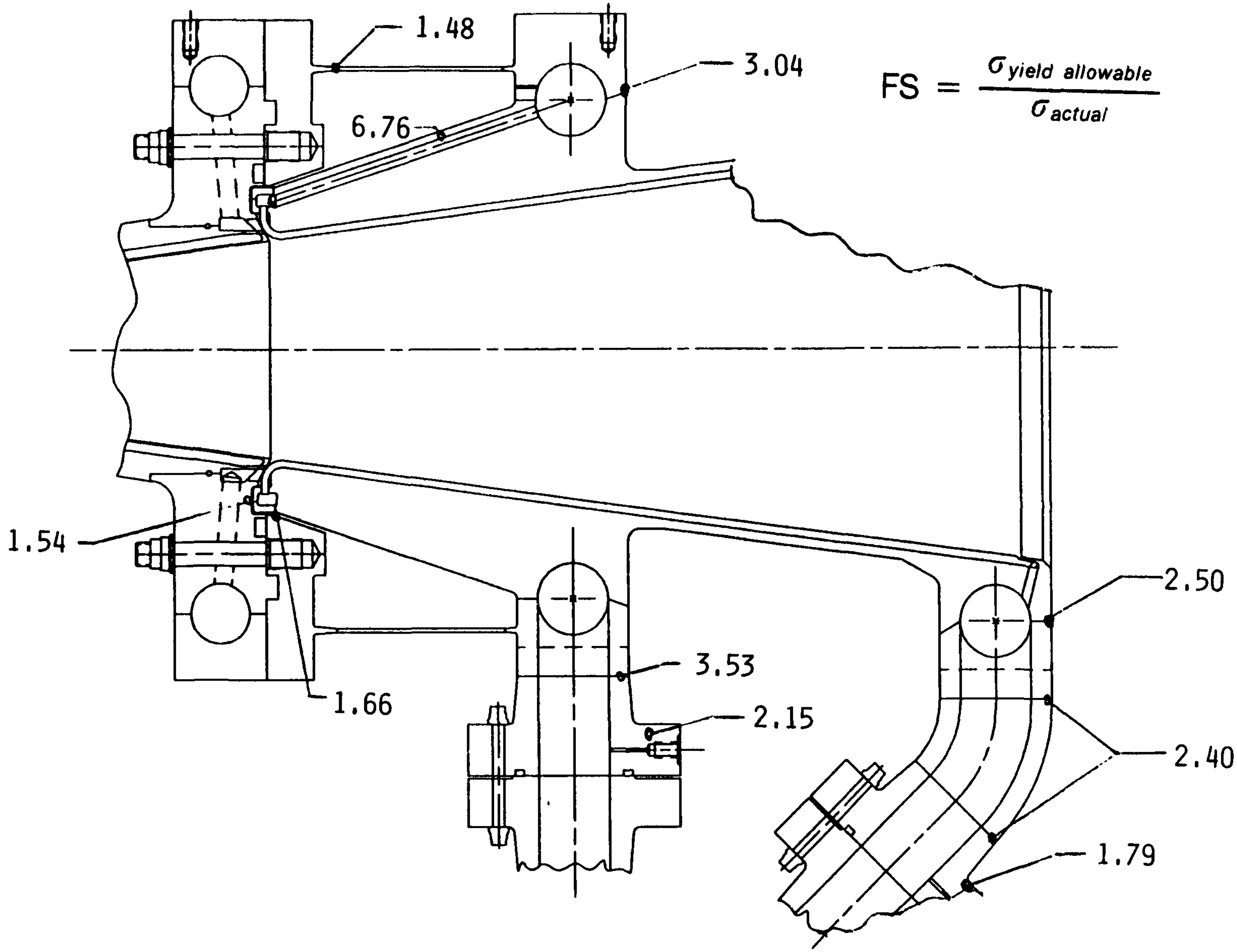

$$FS = \frac{\sigma_{yield\ allowable}}{\sigma_{actual}}$$

Figure 137. Nozzle Factors of Safety at Design Point

I. Hydrogen Mixer

In the split expander cycle, the hydrogen mixer, shown in Figure 138, mixes the warm hydrogen from the turbines with the cold hydrogen from the first-stage fuel pump discharge. The combined flow then enters the main combustor chamber injector fuel manifold. Good mixing of these streams is critical to maintaining stable combustion and uniform flow through the individual fuel elements. At the design point, the flow into the mixer is split 60/40 between the hot and cold lines. The cold hydrogen flow is controlled by means of the fuel jacket bypass valve (FJBV). The percent of cold flow bypassed is lower at lower throttle conditions. For instance, at 20 percent thrust, the FJBV is completely closed so all the flow into the mixer is the warm hydrogen from the turbines. When bypassing cold flow to the mixer, the mixer must effectively mix the hot and cold hydrogen, yet minimize system pressure loss. To achieve the required mixing performance, the AETB will use an in-line mixer similar in concept to the one used by the Space Shuttle Main Engine (SSME) system. The AETB design will use a single tube for the high velocity flow. The Rocketdyne SSME mixer uses seven tubes clustered inside the mixing line.

The mixer works on the same principle as a jet pump, i.e., a high velocity stream imparts momentum to a lower velocity stream. The momentum transfer creates turbulence which promotes mixing of the two streams. The hot hydrogen from the turbine discharge forms the high-velocity stream while the cold hydrogen from the pump is the low-velocity stream. Using the established design procedure for jet pumps, the minimum mixing length for the maximum jet pump efficiency was calculated to be 10 inches at worst case operating conditions. If the AETB mixer had used seven tubes, like the SSME mixer, the required length would be reduced to five inches. The actual mixing length will be 37 inches. There is a relatively high momentum ratio of 28.3 between streams. This compares to the SSME momentum ratio of 1.1. The area ratio of the AETB mixer is 2.5 compared to 2.2 for the SSME. Due to the extended mixing length and high momentum ratio, the mixer design is conservative and will provide uniform flow to the injector.

The mixer design incorporates the following features:

- The two-piece construction nearly eliminates the thermal stress problems that were evident with an earlier welded, one-piece design.
- The hot inflow is a separate piece of hardware, which provides the versatility of changing mixer geometry to evaluate alternative mixer designs.
- The parts are machined entirely from 347 stainless steel using only conventional machining techniques.
- Repairability is built into the design by allowing enough radial clearance around all tapped holes for threaded insert repairs.
- A conservative LCF exceeds 3000 thermal cycles.
- The cantilevered tube natural frequency is 3300 Hz. This is well below the vibration mode of either pump rotor and well above the low energy vortex shedding frequency of 66 Hz.

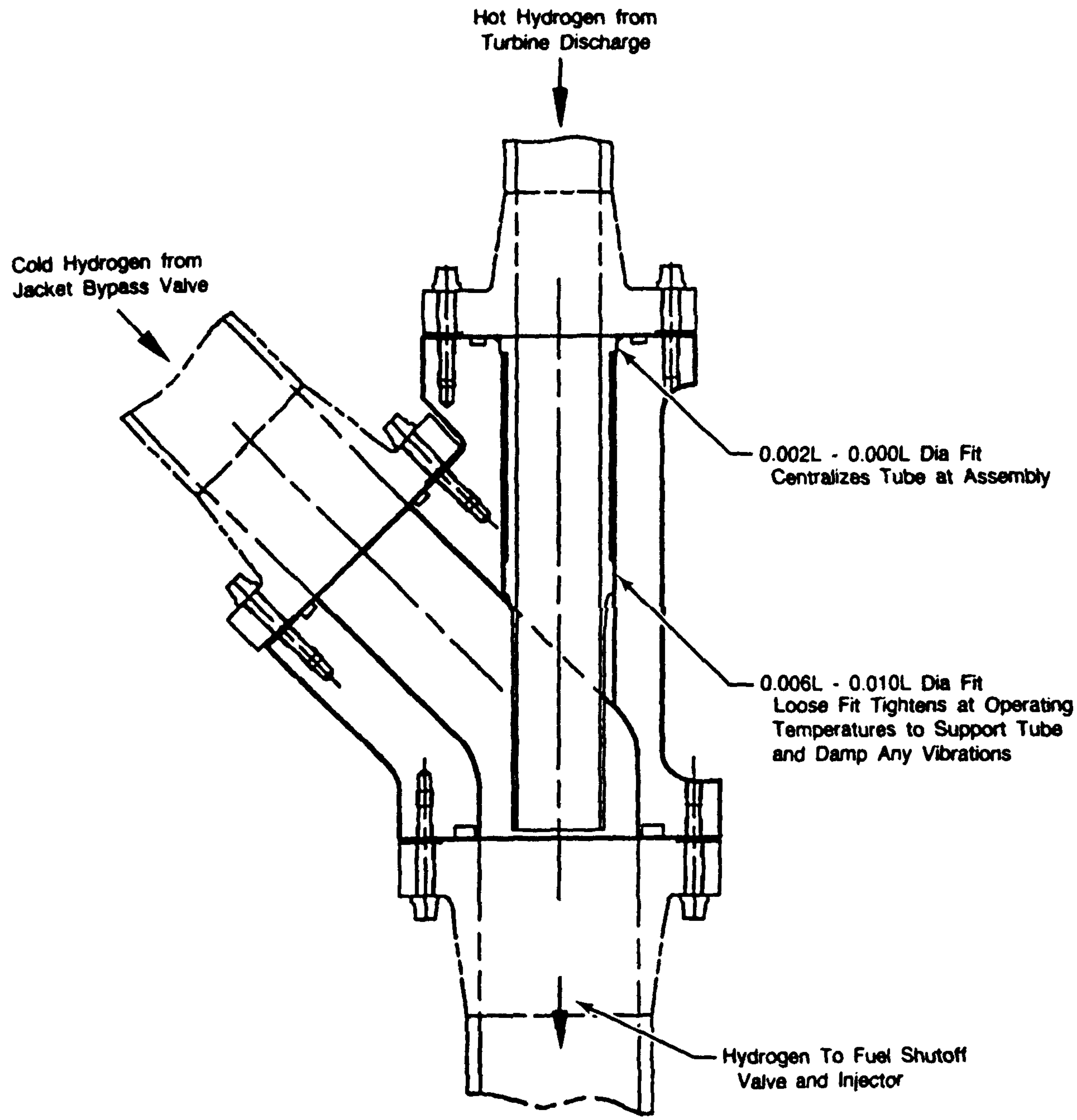

Figure 138. Hydrogen Mixer

J. Control System

1. Requirements

The design of the AETB control system follows a flowdown of requirements from the general to the specific. The system configuration dictates the control mode selection, thrust, and mixture ratio control, which drives the requirements for control valves and sensors. The control mode, sensor and valve requirements, along with hazard analysis and safety input, are used to generate the control logic which will implement the control laws and failure accommodation methods. This approach leads to a control system that will meet all system, hardware and safety requirements. The test bed will be an oxygen/hydrogen split expander cycle of 20,000 lbf thrust at 1200 psia chamber pressure. The test bed will be throttleable to a 20:1 ratio with mixture ratio control of 5 to 7 and operation at a mixture ratio of 12.0. In addition, the test bed will be capable of tank head and pumped idle operation, and will be able to be operated as a full expander engine.

a. System Description

A simplified schematic, Figure 139, is used as a reference to explain the control concepts. It shows the functional arrangement of the valves, plumbing, and turbopumps on the test bed. The igniter and purge valves were omitted for clarity. The turbopumps are shown as separate pump and turbine sections and the nozzle and chamber heat exchangers are shown as separate from the nozzle and chamber.

On the fuel side of the test bed, hydrogen passes through the Engine Fuel Inlet Valve (EFIV) and into the primary fuel pump. At the primary fuel pump discharge some hydrogen is bypassed into the Fuel Jacket Bypass Valve (FJBV) and, if necessary, some is recirculated through the Fuel Pump Recirculation Valve (FPRV) back to the primary pump inlet. The remainder of the flow travels through the two-stage secondary fuel pump. At the pump discharge is the Fuel Cooldown Valve (FCDV) which is used during shutdown and during cooldown. The hydrogen flow passes from pump discharge through the nozzle and chamber heat exchangers where it cools them and picks up energy to power the turbines. For high power full expander operation, some flow is bypassed around the chamber and nozzle heat exchangers through the Chamber Coolant Bypass Valve (CCBV). The hot hydrogen from the heat exchangers expands first through the oxidizer pump turbine and next through the two fuel pump turbines. The Main Turbine Bypass Valve (MTBV) and Fuel Turbine Bypass Valve (FTBV) are used for thrust control and high mixture ratio operation, respectively. Turbine bypass flow and turbine discharge flow are combined with FJBV discharge flow in the hydrogen mixer, passed through the Fuel Shutoff Valve (FSOV) into the injector manifold and into the chamber where it is mixed with oxygen, combusted, and expanded through the exhaust nozzle.

The oxidizer side of the test bed is significantly simpler than the fuel side. Liquid oxygen passes through the Engine Oxidizer Inlet Valve (EOIV) and into the oxidizer pump. At the pump discharge some flow is recirculated back to pump inlet through the Oxidizer Pump Recirculation Valve (OPRV), if necessary. During pump cooldown and test bed shutdown, the Oxidizer Cooldown Valve (OCDV) is opened to provide a flow path when the injector valves are closed. Flow from the pump discharge then passes through the Primary Oxidizer Shutoff Valve (POSV) and the Secondary Oxidizer Control Valve (SOCV), which is used for throttling and to control test bed mixture ratio. From there it passes into the primary and secondary injector manifolds and into the chamber where it is mixed with hydrogen for combustion.

b. Controller Functions

The controller will perform the following functions:

- Perform pre-start diagnostic system checks, purge the lines of moisture and air with inert gas, and chill the pumps to where cavitation is not a problem.

- Start the test bed to the requested thrust level and mixture ratio setting. A goal of <5 seconds has been chosen for the start time. Model simulations indicate that this is achievable.

- For mainstage operation, regulate test bed power setting (throttling) and mixture ratio (O/F). Although no response requirements exist for the test bed, the bandwidth of the thrust control loop will be made as wide as possible within hardware limitations.

- At the termination of a test or if the control or facility declares an abort situation, the test bed will be shutdown in a safe manner.

- Subsequent to shutdown, purge the test bed of fuel, oxidizer, and combustion products to make the test bed safe.

- During all test bed operation, monitor safety parameters and take appropriate action when safety limits are violated. In most cases this will be a test bed shutdown.

c. Thrust Control

Thrust control will be accomplished by closed loop control of chamber pressure (P_c) as shown in Figure 140. Chamber pressure will be sensed and the MTBV will be modulated by the control to achieve the desired thrust, Figure 139. Feedback P_c with lead-lag compensation for overshoot minimization will be compared to a requested reference P_c and the resulting P_c error fed through a proportional plus integral controller. The proportional gain will give fast response to request changes and the integral gain will give good steady-state accuracy. The lead-lag compensator time constants and the proportional and integral gains will be determined through control studies during the final design.

Chamber pressure will be sensed by the controller to control test bed thrust level. A sensor accuracy of three percent of point has been specified. To achieve this accuracy over the wide throttling range and to sense chamber light during engine start without excessive sensor complexity and cost, multirange transducers will be used, Figure 141. Low (<150 psia), medium (<500 psia), and high (<1500 psia) range pressure sensors will be used to cover the entire pressure operating range. The control will gradually phase out the appropriate range sensor in the transition regions to avoid discontinuities. Each sensor will be accurate to one percent of full scale and, as seen in Figure 141, will provide three percent of point accuracy over its range of operation.

Since the chamber pressure sensor performs a critical control function, redundant sensing capabilities will be provided. The high range will have dual pressure sensors, and redundancy in the medium and low ranges will be accomplished by using the sensor in the next higher range as a backup. Some thrust control accuracy in the backup mode will be lost in the medium and low ranges, but redundant pressure sensing will be accomplished with the addition of only one high-range sensor.

The total achievable thrust control accuracy is set not only by P_c sensor accuracy, but also by valve positioning accuracy as well. The MTBV will be positioned by the control until P_c is within the sensor inaccuracy so its contribution to thrust inaccuracy can be neglected. However, the FJBV and the SOCV positioning inaccuracies will contribute to thrust errors. The allowable valve position error is 1.5 percent of stroke. The steady-state model was run to determine the sensitivity of P_c to SOCV and FJBV areas. The total root sum square thrust error for valve position inaccuracy and P_c sensor inaccuracy is shown in Figure 142. The total P_c error is shown for ball-type and linear valves since a determination of the valve type has not been made. Figure 142 is valid for the nominal 6.0 mixture ratio point. Thrust inaccuracy at other mixture ratio points will be determined as part of final design.

d. Mixture Ratio Control

The options for mixture ratio control are to schedule O/F open loop by positioning the SOCV as a function of requested chamber pressure, or use flowmeters to directly measure O/F and position the SOCV so that O/F feedback equals the O/F request.

Open-loop O/F control was chosen because it represents the simplest design, avoids possible thrust and O/F loop coupling problems, and meets the requirements of the test bed. A sensitivity study on O/F error similar to that performed for P_c error was conducted. As seen in Figure 143, the estimated O/F absolute error will be kept within 0.12 for power settings above 15 percent. This study was performed at the 6.0 mixture ratio point and will be repeated at other O/F settings. At this time the effect of open-loop mixture ratio control during throttle transients has not been determined. However, rate limit logic and other control compensation techniques can be implemented should transient inaccuracy prove unacceptable.

Figure 144 shows the operating range of other test bed parameters due to valve positioning inaccuracy. As shown, no system limits will be violated with the chosen control modes.

A schematic of the overall control mode is shown in Figure 145. As discussed above, a thrust request will be transformed into a rate-limited P_c request which will be fed through a proportional plus integral controller with lead-lag compensated P_c feedback to control thrust closed loop. Mixture ratio control will be open loop with the SOCV and FJBV positioned from a bivariate table lookup based on requested P_c and rate-limited O/F request. The FTBV will be positioned as a function of O/F request to achieve the high mixture ratio point. The recirculation valves will be opened, if necessary, as a function of thrust and O/F setting.

e. Component and System Protection

The control must protect the test bed pumps, valves, thrust chamber, and other components from damage and must operate the test bed in a safe manner. To accomplish this, a large portion of the control function is dedicated to execution of fault accommodation and safety monitoring logic.

Prior to engine start, the controller will perform diagnostic self-checks to determine its own state of health and will continuously monitor itself during engine runs. Sensor validity checks will be performed and either sensor redundancy will be provided (for critical parameters), or test bed shutdown will be initiated when out-of-range signals are detected. Limited capability will be present for sensor in-range failures and verification with other parameters will be performed where possible and safe to do so. Valve actuator simulations will be incorporated into the logic to check for slow or stuck modulating valves, and pre-start rate checks will be performed on the discrete valves.

Throughout operation, the control will monitor engine parameters for violation of safety limits, and will shut down the test bed if any violations occur. Monitored parameters include fuel and oxidizer pump metal temperatures during prestart, pump inlet pressures, pump speeds, and pump vibration levels. Pump bearing cooling flow temperatures will also be monitored for excessive heat generation, and interpropellant seal health will be determined by helium inlet pressure and He/H_2 and He/O_2 discharge pressures. Oxidizer turbine inlet temperature will be monitored, and in addition to its control function, sensed main chamber pressure will be monitored for limit violation and the inability of the test bed to achieve requested chamber pressure.

Although not specifically monitored by the control, protection from other system anomalies will be inherently afforded by the design of the control logic. Combustion instability will be avoided by design of the valve schedules to maintain proper primary to secondary LO_2 injector flow split and primary LO_2 injector delta pressure. Because the primary fuel pump is designed for twice as much flow as the secondary fuel pump, the control must also properly position valves to avoid secondary pump choke and primary pump stall. In addition, during test bed shutdown, FJBV positioning is critical to avoid reverse hydrogen flow from the mixer to the secondary pump inlet when the FSOV is shut, Figure 139.

f. Software Development

The control logic software will be developed using the standard industry 'waterfall' process structured to DOD-STD-2167A. The 2167A process starts with an analysis of the system requirements. Next, design of the system proceeds along with software requirements definition. Then, software design and production of source code begins, and finally, test and certification of the software is completed. At this time, analysis of requirements has been accomplished, and a Control System Requirements Document (CSRD) and Software Requirements Specification (SRS) have been published.

The software development process is concurrently engineered with inputs from the customer and various P&W functional groups such as Propulsion Systems Analysis, Controls Engineering, and Safety Engineering. The development proceeds in parallel with hardware development, ending in system integration testing and operational testing and evaluation.

Much of the AETB software will incorporate already proven codes from the National Aero-Space Plane (NASP) program such as system executive, I/O software, and monitor software. Unique to the AETB will be the control law software and bench test simulation software. The control law software will be comprised of the program executive which handles process control, initialization software, monitor support, processor health software, and the actual control laws themselves. The control laws will consist of engineering unit conversions, thrust and mixture ratio control loops, failure detection and accommodation logic, and engine safety monitoring. It is anticipated that the majority of the control law software will be dedicated to the tasks of failure detection and safety monitoring.

g. Valve Requirements

The valve configuration is selected to provide control over thrust and mixture ratio in the split expander, full expander, and tank head idle modes. Additionally, valves are selected to start, shutdown, and inert the test bed prior to and after operation.

The design requirements of the control valves are shown in Table 14. Fuel and oxidizer valves were sized for the 125 percent thrust point with the exception of the OCDV and FCDV which were sized for shutdown flow, the FTBV which is sized for 12.0 O/F operation, and the MTBV which is sized for tank head idle operation. The purge valves have been oversized for commonality and will be provided with downstream orifices for flow control. Position feedback through LVDT's will be provided for fully modulating valves, and position of the solenoid valves will be indicated at the critical position. Fully modulating valve effector loop bandwidths are set to give adequate response so as not to impact upon major loop (thrust control) response. Model studies indicate the system response to MTBV area has a bandwidth of 0.7 Hz. The MTBV effector bandwidth is set at 5 Hz which is sufficiently responsive. The failsafe/depower position of all valves has been chosen at the shutdown or low power setting. Valve slew rates were driven by the abort shutdown requirement.

h. Sensor Requirements

The control sensors have been selected as a result of cycle and throttling studies to sense the operating conditions to meet the performance, operability, and safety requirements of the test bed. Sensor design requirements are given in Tables 15 and 16. A summary explanation of the requirements is presented in Tables 17 and 18. In these tables, signal loss refers to control action if the sensor input has been determined to be invalid. The redline/permissive column refers to the action that the control takes if the sensor input indicates a violation of redline or permissive limits.

2. Electronic Controller

a. Objectives

The brassboard controller design objectives are focused on efficiently supporting test bed operation. During testing at NASA, the brassboard will be used to support test bed demonstrations of the engine cycle and investigations of technologies such as advanced health monitoring and electromechanical actuators. Support of the objectives requires a flexible and expandable design. During preliminary design, several requirements were given to hardware and software designers to meet the test objectives. These requirements included the capability for system growth, adaptability to Input/Output (I/O) modifications or additions, and the ability to easily reconfigure the test setup.

Control system growth will be required to support control changes and investigation of advanced health monitoring sensors. Currently an open loop start schedule with a steady-state closed-loop thrust control and open-loop control of mixture ratio are planned. Changes to the control cycle that increase throughput or I/O changes should be accommodated by the controller.

The controller must be adaptable to I/O modifications. Technologies such as electromechanical actuators that require testing with the brassboard will require that current I/O hardware and software be changed to support the tests. The changes are best accomplished with modular designs of hardware and software components. In the event that processing and I/O changes are significant enough to warrant a growth of two or three times in processing or I/O capacity, the brassboard must have the capability to accept additional channels or functional groups. The level of processing and I/O required for the current design can be accomplished with one 19-inch rack of computer hardware in one functional group.

b. I/O Requirements

Input/Output requirements determined during preliminary design are shown in Table 19. The brassboard design accounts for all required I/O and provides spare channel capability for each of the I/O types. Since the I/O circuit boards are modular in design, further expansion beyond the spare capability is possible by adding additional circuit boards. Five spare slots remain in the baseline system to accommodate additional processor, sensor and effector interfaces.

c. Test Stand Interfaces

Test stand interfaces were designed with safety and test time optimization as the main objectives. Safety considerations determined that abort signals from the brassboard and the facility should have the capability to terminate a test if an unsafe condition is detected. A discrete signal interface will be used to implement abort system communication. Upon assertion of the abort signal, both the facility and the brassboard will take action to shut down the test bed with minimal delay. As a precaution against AC power loss during test, an uninterruptable power source will be required from the stand.

Several features were added to the brassboard system design to optimize the time for test bed operation. Propellants, stand power, test bed hardware and test personnel time are all costs associated with operation of the test bed. The brassboard system design has provisions to perform preprogrammed test sequences based on input from a time code generator and the Monitor System user interface. Predetermined test programs can be loaded into the monitor system to accomplish accurate and repeatable tests. The sequencer function allows verification of test setup parameters prior to actual testing. Data transfer between the brassboard system and the stand computers can be accomplished with an Ethernet Local Area Network using the DECnet protocol.

d. System Description

The brassboard system consists of three major components, the Brassboard, the Monitor System, and a Brassboard Test System (BTS) as shown in Figure 146. The configuration shown depicts the system in the verification configuration, where software and hardware testing is performed prior to engine test. During engine test, the BTS is replaced by the actual test bed.

The brassboard design is based on a functional group concept. A functional group consists of a 20-slot VME card cage, processor board and a full complement of I/O hardware. Up to four functional groups can be used in one system to distribute processing and I/O functions as shown in Figure 147. The brassboard contains 19-inch wide rack mounted hardware with two separate card cages for circuit boards. Each cage holds up to 20 boards and is an industry standard VME design. As shown in Figure 148, five spare slots are provided for expansion capability. The AETB brassboard contains cards in only one of the card cages, the other is provided for expansion capability. Other associated hardware such as power supplies, fans and connector panels are also provided. One processor board and one set of I/O hardware as previously described are included. In addition, a global bus board is used to provide timing functions and a link between functional groups.

The monitor system is a MicroVAX-based computer system with a 1553 interface to communicate with the brassboard. The monitor's two main functions are to provide a vehicle interface simulation and a user interface for brassboard operation as shown in Figure 149. The vehicle interface simulation will send commands to the brassboard that would normally occur during an actual mission. Commands sent to the brassboard include prestart conditioning, start, throttling and shutdown commands. In return, the monitor will receive feedback from commanded parameters and engine sensor data. The data can be stored in the monitor for later graphic analysis. All communication initiated from the vehicle interface simulation can be automated by building command files and storing event sequences prior to test bed operation. The user interface functions of the monitor include storage and downloading of control programs, examination and alteration of control constants and memory, real-time display and bar graphs of engine parameters, parameter versus time plots and other general computer functions.

The BTS provides a real-time simulation of the test bed for hardware and software verification. A complete set of I/O hardware to mirror the brassboard I/O set is provided to simulate sensors and actuators. The sensor and actuator simulations are interfaced with the engine simulation to provide a complete test bed simulation. To the brassboard, the BTS appears and acts like the actual test bed. The BTS will be used extensively during verification at P&W prior to test bed operation. After the first complete set of test bed hardware is used for acceptance testing, the BTS can be used to verify logic changes prior to operation with the test bed.

e. Circuit Board Block Diagrams

The processor board, Figure 150, contains two processors which share the same bus. One processor is used for I/O and the other is used for control laws. A 1553 avionics data bus and VME I/O bus interfaces are also provided.

The global bus board, Figure 151, provides a link between optional functional groups. The board contains global RAM accessed by all functional groups for communication. System functions such as clocks, real-time interrupts and switch discretes are also implemented on this board.

The Linear Variable Differential Transducer (LVDT) board, Figure 152, provides signal conditioning for up to 16 channels. A dual-coil input for each sensor is input through multiplexers and full wave rectifiers to an A/D circuit and the conversions are made available through the VME bus to the I/O processor.

The torque motor board, Figure 153, provides current drive for up to 12 channels. Current commands are received from the I/O processor through the VME bus, converted to a pulse width signal, filtered, and sent to the current drivers. Each channel has wraparound current sensing to detect torque motor or cable faults.

The low level interface board, Figure 154, conditions thermocouples, RTD's and strain gauge pressure signals. The board provides excitation or cold junction compensation for each signal and A/D conversion. A new board will be designed to optimize its use and reduce the number of boards required. Proven circuit board designs will be used in the new board design.

The frequency board, Figure 155, provides pump speed monitoring by measuring the frequency of speed sensor signals. The board is a modification of a commercially available design. The same type board can be configured to condition flowmeter signals if necessary.

The discrete interface boards, Figure 156, condition switch inputs and drive relay/solenoid outputs. Two input boards and two output boards are provided to meet I/O quantity requirements.

The analog input and output board, Figure 157, conditions high-level inputs and drives high-level outputs. The board will be used to measure a conditioned vibration signal from the turbopump sensor.

A processor throughput and memory usage study was performed for the brassboard processor board. The study was based on measurements taken on the NASP controller which uses the same hardware. The control law and I/O processing estimates are based on the I/O channels. As shown in Table 20, 62 percent of the available throughput and 41 percent of the available memory will be used. If throughput or memory requirements grow beyond the current hardware limit, additional modules can be added to share the control and diagnostic tasks. A processor upgrade will be evaluated during the final design phase. This would provide additional capability for anticipated advanced sensors.

3. Valves and Actuators

a. Objectives

The valves and actuators use brassboard controller commands to control the flow of propellants and purge fluids for engine operation from pre-start conditioning through rated power to post-shutdown conditioning and all levels in between. The valve and actuator configurations are being designed to meet the objectives of providing safe, reliable, low-cost flow control and allow component replacement and flexibility to meet the varied test bed operating conditions and configurations.

The valves have been separated into three categories:

1. There are five control valves that control flow of the following fluids:

- Fuel Jacket Bypass Valve, FJBV — cryogenic H_2
- Fuel Pump Recirculation Valve, FPRV — cryogenic H_2
- Secondary Oxidizer Control Valve, SOCV — cryogenic O_2
- Main Turbine Bypass Valve, MTBV — warm gas H_2
- Fuel Turbine Bypass Valve, FTBV — warm gas H_2.

Each of the control valves is modulated by a hydraulic actuator to provide variable flow control as requested by the controller.

2. The main shutoff valves are as follows:

- Engine Oxidizer Inlet Valve, EOIV
- Engine Fuel Inlet Valve, EFIV

- Fuel Shutoff Valve, FSOV
- Fuel Turbine Shutoff Valve, FTSV
- Primary Oxidizer Shutoff Valve, POSV.

3. The ancillary shutoff valves are as follows:

- Oxidizer Pump Recirculation Valve, OPRV
- Oxidizer Igniter Shutoff Valve, OISV
- Fuel Igniter Shutoff Valve, FISV
- Fuel Pump Cooldown Valve, FCDV
- Oxidizer Pump Cooldown Valve, OCDV
- Solenoid Purge Valves, SPV, 7 Per Engine.

The main and ancillary shutoff valves are positioned either full open or full closed by pneumatic actuation as requested by the controller.

b. Control Valve Configurations

Each control valve assembly consists of a control valve element and an actuation element as shown in Figure 158. Based on supplier recommendations, the control valve element is either a common ball or poppet valve design featuring reliable, dual dynamic seals with an interseal leakage drain. The valve is positioned by a hydraulic actuator, which is thermally insulated from the valve element.

The hydraulic actuators are off-the-shelf units which use Electro-Hydraulic Servo Valves (EHSV) for output effector interface with the brassboard and Linear Variable Differential Transformers (LVDT) for valve position input interface with the brassboard. The EHSV is a three-element device which converts the brassboard actuator slew rate command from an electrical signal to a hydraulic flow rate which slews the actuator piston. The first element is a torque motor which uses the brassboard supplied current in the stator to move an armature which positions the first-stage servo device. The first-stage servo, which is the second element, ports high-pressure hydraulic fluid to position the second-stage spool valve, which is the third element. This second stage ports either supply or return pressure to each of the two control pressures to either extend or retract the actuator piston. A feedback spring connected to the second-stage spool valve nulls the first-stage servo device such that a nearly linear current versus second-stage control pressure flow rate is created. Designs of both the LVDT's and EHSV's will be tailored for aerospace applications.

The hydraulic actuators will use 3000 psi MIL-H-22072 operating fluid which is a LO_2-compatible water-glycol mixture. The actuator interface with the control valves will include an insulation device to help ensure that the actuator operating temperature stays within the allowable range.

The actuators will include a failsafe positioning feature within the EHSV's by biasing the second-stage spool valve to create an actuator slew rate in the safe direction. For all cases in which electrical power to the EHSV could be interrupted, the EHSV will provide an actuator slew rate which positions the valve to the preselected normal position of either full closed or full open, as listed in Table 21.

Five supplier proposals for potential control valve configurations were received. Data provided in the proposals show that the AETB valve and actuator requirements can be met.

c. Shutoff Valve Configurations

The shutoff valve assemblies consist of a valve element and an actuator element as shown in Figure 159. Based on supplier proposal data, the valve elements are either common ball or poppet types. The actuation elements use off-the-shelf pneumatic actuators with position switch feedback and solenoid valve interface to the brassboard controller. The solenoid controls the 100 to 1000 psi GHe operating fluid supply to the actuator piston to oppose a preloaded spring element, which positions the valve in the normal position, as listed in Tables 22 and 23. Since solenoid power is required to move the valve from its normal position, any loss of electrical power results in all shutoff valves slewing to their normal position as a failsafe feature.

The EOIV and EFIV applications will use existing RL10 Propellant Inlet Shutoff Valves, as shown in Figure 160. These RL10 valves were ranked against supplier proposals during the proposal evaluation and were determined to have the highest rating. A pressure switch will be added to the RL10 inlet valve actuator helium pressure supply to meet the valve position feedback requirement of the AETB which exceeds normal RL10 inlet valve requirements.

Six supplier proposals for potential shutoff valve configurations were received. Data provided in these proposals shows that the valve requirements, as listed in Tables 22 and 23, can be met within the scope of the AETB program.

d. Ancillary Shutoff Valve Configurations

The ancillary valves, except the S#PV purge valve applications, will use designs similar to the main shutoff valves. Two supplier proposals for ancillary purge valve applications were direct order catalog items. These pneumatically actuated valves are direct-drive solenoid actuated valves which meet the valve requirements listed in Table 23. These direct driven valves are different from the main shutoff valves in that pneumatic supply pressure is not needed as servo pressure to actuate the valve. The electromagnetic force created within the solenoid actuates the valve. A preloaded spring opposes the solenoid and provides failsafe positioning in the event of loss of electrical power.

4. Sensors and Cables

This section is divided into three topics. First, the control and safety sensors are discussed. These sensors are actively used by the electronic controller to operate the test bed or to monitor safety conditions. Delivered as part of the control system, they are required to meet the same life requirements as the test bed. Next, a preliminary list is presented of the performance instrumentation that will be monitored through the test stand data system. If desired, these parameters could be incorporated into the facility abort system. Finally, the cables and electrical interfaces of the control system are discussed.

a. Control and Safety Sensors

A total of 35 control and safety sensors are planned for each test bed. The parameters used for control and safety include 14 pressures, 16 temperatures, 3 pump shaft speeds, 2 pump vibrations, and 22 valve positions. The locations of these sensors are shown on the flow schematic, Figure 161.

Cross sections showing the locations of the hydrogen turbopump sensors, Figure 162, and oxygen turbopump sensors, Figure 163 are included for reference.

The speed sensors are described on Figure 164. The design will be based on the speed sensors used on P&W's SSME-ATD program. However, the AETB speed sensors will be custom designed to meet the required speed and envelope restrictions. The custom design requirement imposes a longer lead time on speed sensors than any of the other sensors, thus their procurement will start first.

The 16 temperature measurements consist of 13 bearing coolant thermocouples (T/C), two pump skin T/C's, and one fluid line bulk temperature at the nozzle coolant exit. The bearing coolant T/C's are described in Figure 165. These T/C's are required to measure small changes in bearing coolant temperature and will be useful in detecting an impending failure. The absolute accuracy of each T/C is not as critical as the T/C-to-T/C variation. To obtain the least sensor-to-sensor variation, the T/C's will be fabricated from a common lot of wire.

The pressure transducers are described in Figure 166. Three types of pressure transducers were selected to meet the system accuracy requirements. To achieve the required accuracy, each type of transducer employs a different temperature compensation method. This approach permits cost effective procurement of these components and uses standard methods of pressure calibration.

Turbopump vibration will be sensed using industry standard accelerometers described in Figure 167. Detail specifications for each sensor are listed in Table 24 (speed sensors), Table 25 (thermocouples), Table 26 (pressure transducers), and Table 27 (accelerometers).

b. Instrumentation

The preliminary performance instrumentation list is shown in Table 28. The list contains 28 pressures, 21 temperatures, 2 flow rates, a voltage and an amperage measurement. These instrumentation sensors are shown on the flow schematic that also contains the control and safety sensors, Figure 168.

c. Cables and Electric Interfaces

A simplified control system interconnection diagram is shown in Figure 169. Fiber optic cables are used between the Control Room and Test Stand Safe Room. This type of cable provides electrical isolation and will thus prevent damage from a difference in electrical potential between the two locations.

The control system shielding and grounding plan, along with a typical cable assembly, are shown in Figures 170 and 171, respectively. The grounding configuration, in conjunction with twisted pair shielded cables, provides protection from radio frequency interference (RFI), electromagnetic interference (EMI), and potential differences caused by lightning.

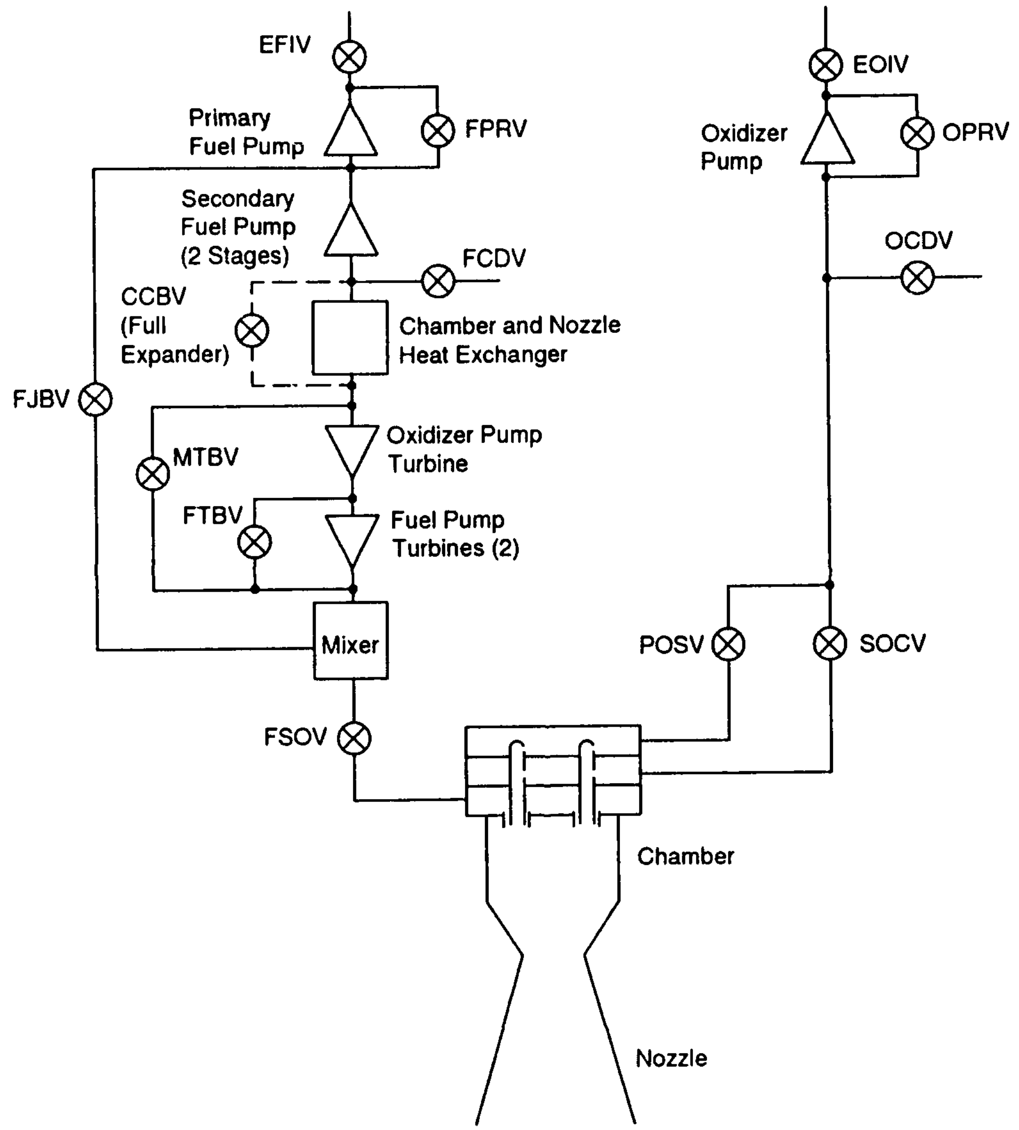

Figure 139. Control System Functional Schematic

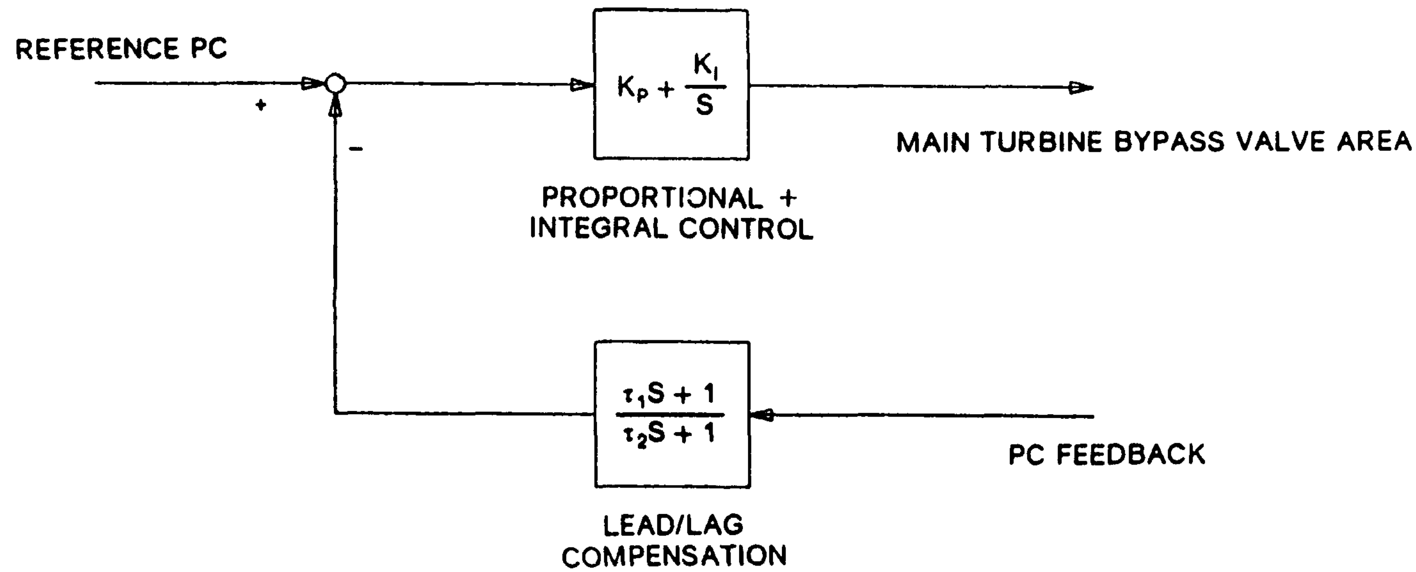

Figure 140. Thrust Control Logic Using Closed Loop Control on Chamber Pressure

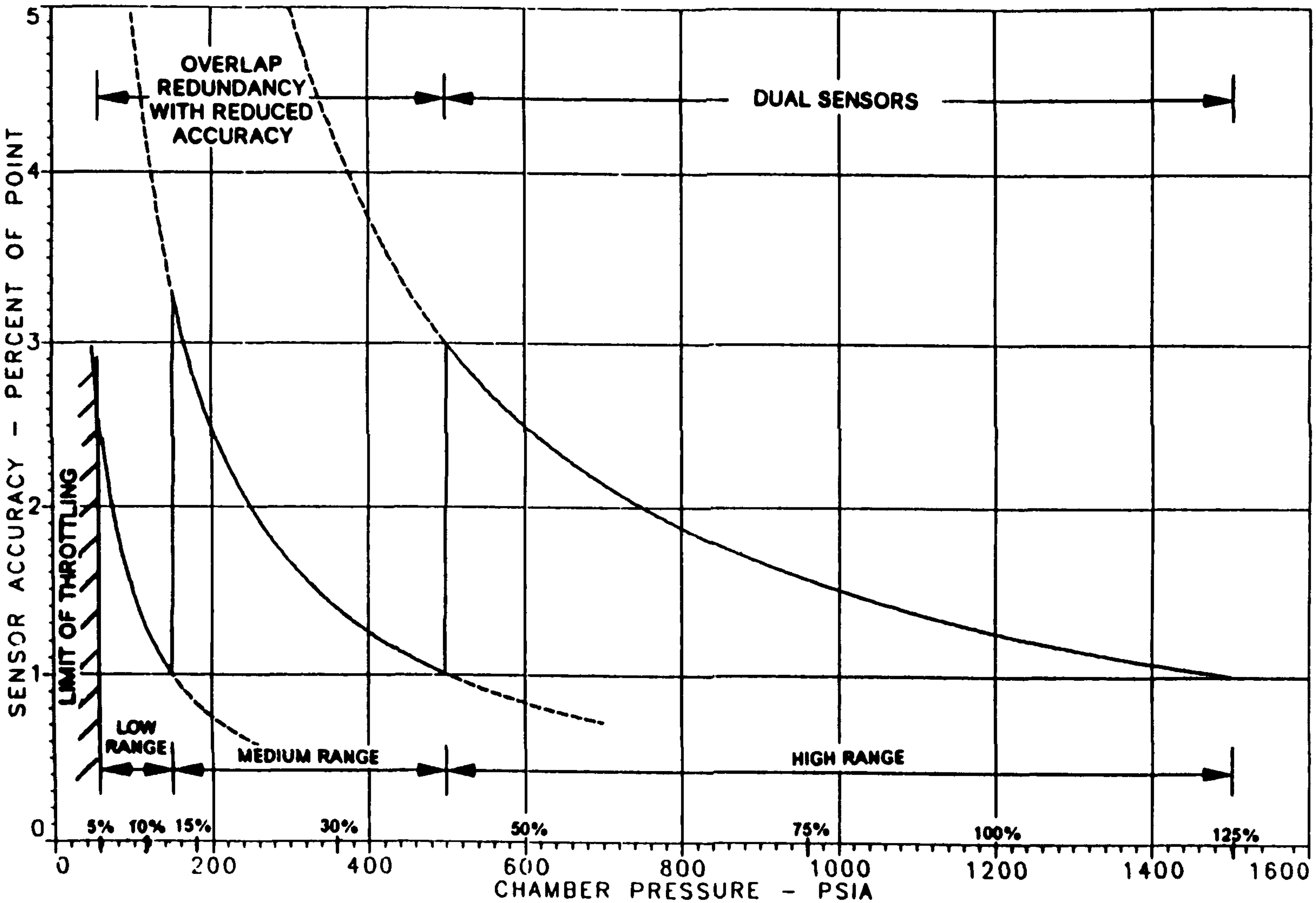

Figure 141. Wide Range of Chamber Pressure Monitored by Three Ranges of Pressure Transducers

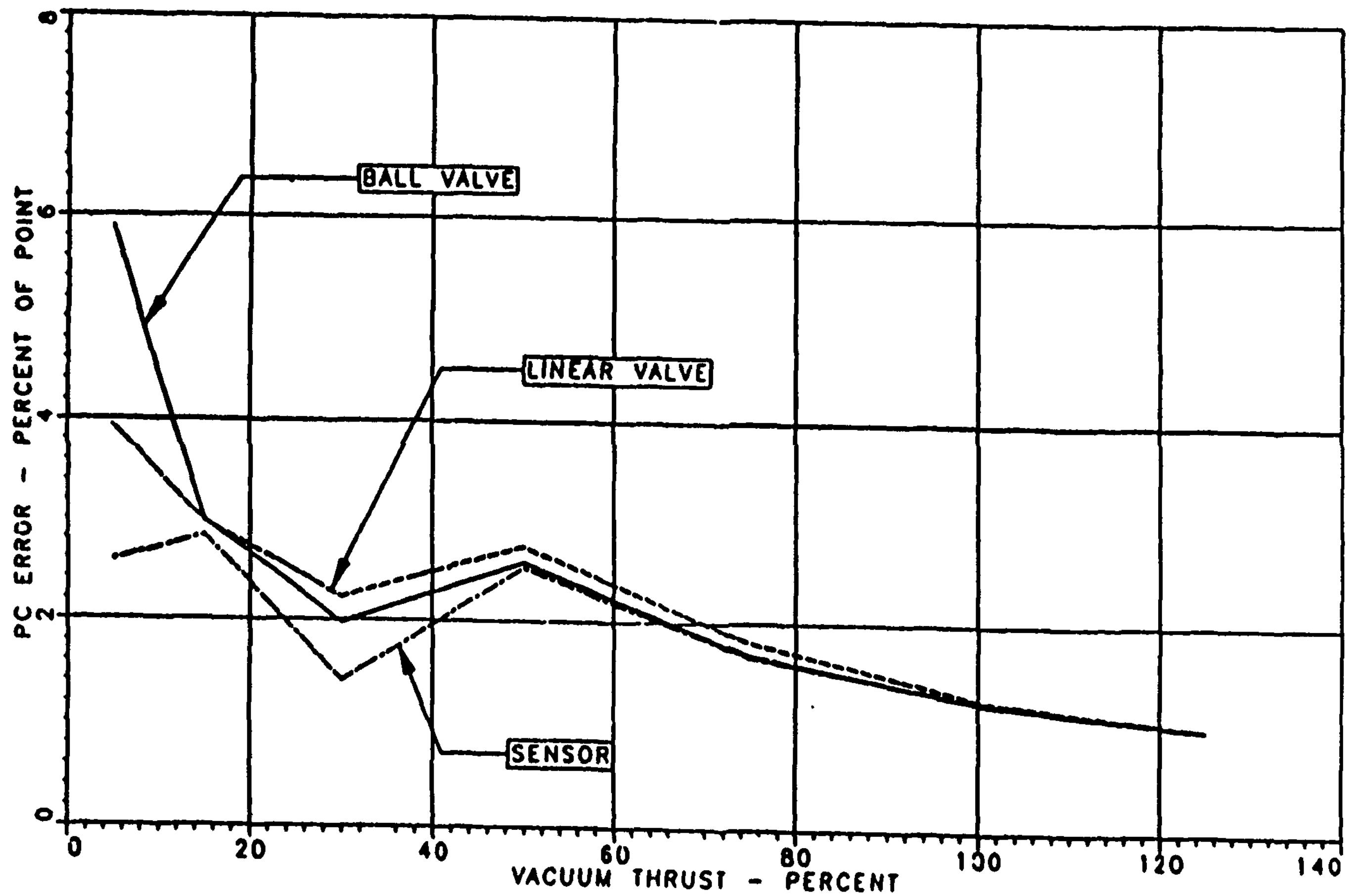

Figure 142. Chamber Pressure Sensitivity Shows Minimal Effect Due to Valve Positioning Inaccuracies

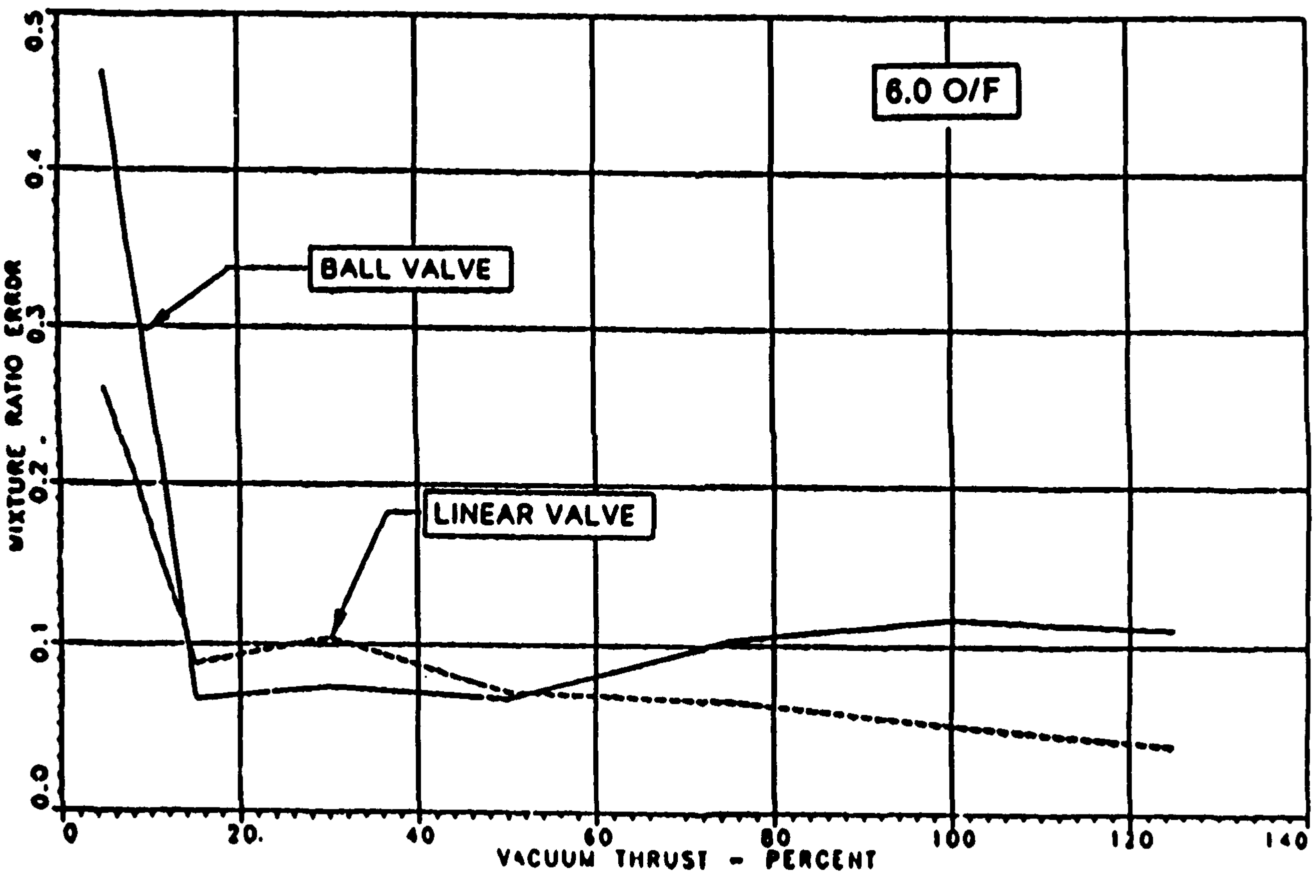

Figure 143. Open-Loop Mixture Ratio Sensitivity Shows Minimal Effect Due to Valve Positioning Inaccuracies

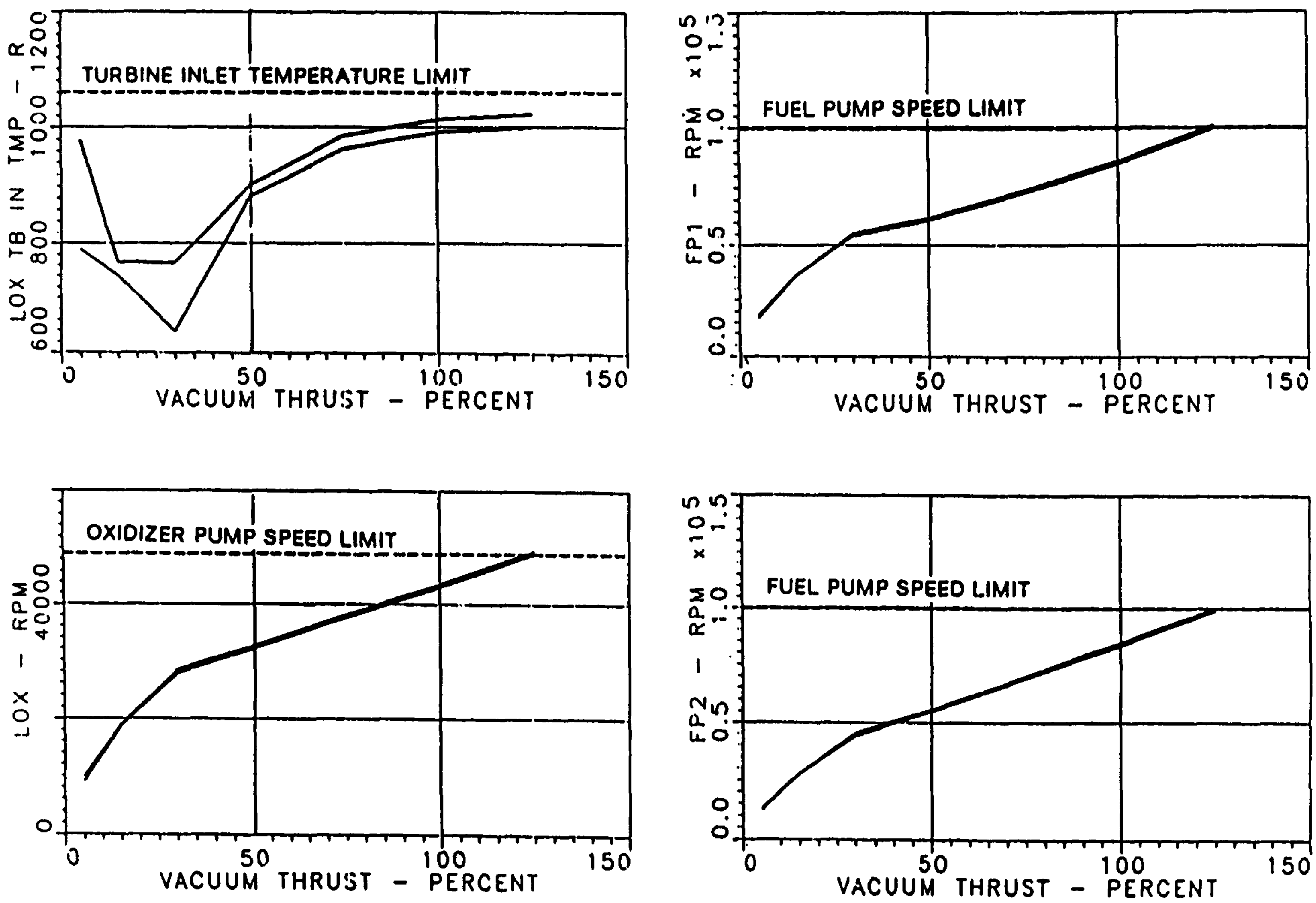

Figure 144. Various Engine Parameters Show Minimal Effect Due to Valve Positioning Inaccuracies

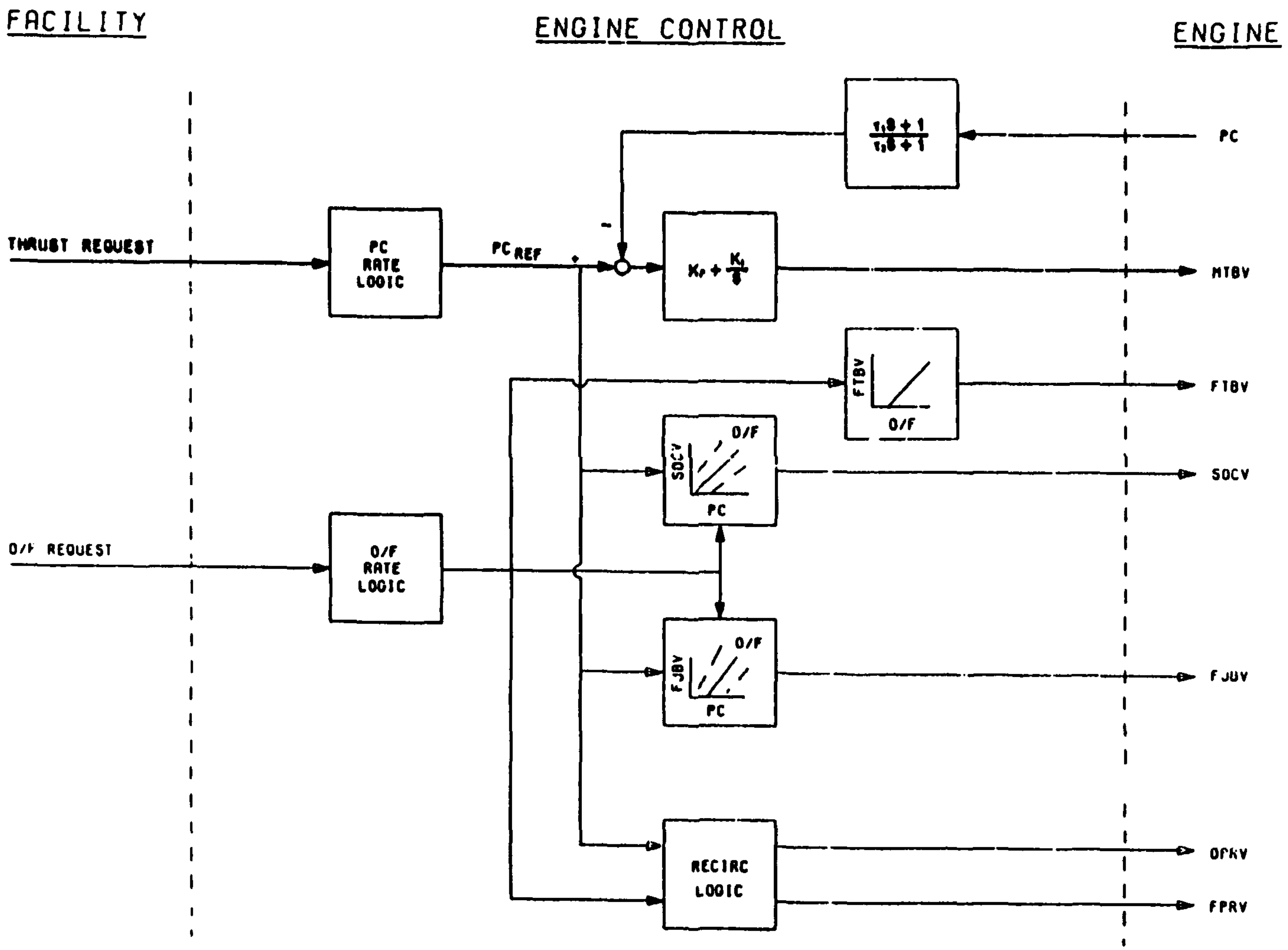

Figure 145. Split Expander Mainstage Control Logic

Table 14. Control Valve Requirements

VALVE Name	FEEDBACK (Indicator: Open/Closed)	REQUIREMENTS					CONTROL MODE
		REDUNDANCY (Failsafe: Open/Closed)	SYSTEM ACCURACY % F.S.	BANDWIDTH Hz	SLEW TIME sec	SAMPLING sec	
FJBV/CCBV	Position	Single (C)	1.5	3	0.200	0.020	Schedule
FTBV/OTBV	Position	Single (O)	1.5	5	0.300	0.010	Closed Loop
MTBV	Position	Single (O)	1.5	5	0.300	0.010	Closed Loop
SOCV	Position	Single (C)	1.5	3	0.300	0.020	Schedule
FPRV	Position	Single (C)	1.5	3	1.000	0.020	f(Pc&OF)
OPRV	Discrete (C)	Single (C)	N/A	N/A	1.000	0.020	f(Pc&OF)
EFIV	Discrete (O)	Single (C)	N/A	N/A	0.500	0.020	f(time)
EOIV	Discrete (O)	Single (C)	N/A	N/A	0.500	0.020	f(time)
FSOV	Discrete (O)	Single (C)	N/A	N/A	0.500	0.020	f(time)
POSV	Discrete (O)	Single (C)	N/A	N/A	0.300	0.020	f(time)
OISV	Discrete (O)	Single (C)	N/A	N/A	0.300	0.020	f(time)
FISV	Discrete (O)	Single (C)	N/A	N/A	0.300	0.020	f(time)
FCDV	Discrete (C)	Single (O)	N/A	N/A	0.400	0.020	f(time)
OCDV	Discrete (C)	Single (O)	N/A	N/A	0.300	0.020	f(time)
FTSV	Discrete (O)	Single (C)	N/A	N/A	0.500	0.020	f(time)
S1PV	Discrete (O)	Single (O)	N/A	N/A	0.100	0.020	f(time)
S2PV	Discrete (O)	Single (O)	N/A	N/A	0.100	0.020	f(time)
S3PV	Discrete (O)	Single (C)	N/A	N/A	0.100	0.020	f(time)
S4PV	Discrete (O)	Single (C)	N/A	N/A	0.100	0.020	f(time)
S5PV	Discrete (O)	Single (C)	N/A	N/A	0.100	0.020	f(time)
S6PV	Discrete (O)	Single (O)	N/A	N/A	0.100	0.020	f(time)
S7PV	Discrete (O)	Single (O)	N/A	N/A	0.100	0.020	f(time)

Table 15. Control Sensor Requirements for the Fuel Turbopump

PARAMETER	REQUIREMENTS						SAFETY	
	REDUN-DANCY	SYSTEM ACCURACY (+/-)	RANGE	UNITS	SAMPLING msec	BAND-WIDTH Hz	PER-MISSIVE	REDLINE
Fuel Pump 1 Metal Temp	Single	10 deg	38-600	Deg R	80	0.2	X	
Fuel Pump 1 Inlet Press	Single	4% FS	0-75	PSIA	80	1.0	X	X
Fuel Pump 1 Speed	Single	0.5% FS	7.5K-110K	RPM	20			X
FP1 Brg. #1 Inlet Temp	Single	(2)	38-180(1)	Deg R	80	1.0		X
FP1 Brg. #1 Exit Temp	Single	(2)	38-180(1)	Deg R	80	1.0		X
FP1 Brg. #2 Inlet Temp	Single	(2)	38-180(1)	Deg R	80	1.0		X
FP1 Brg. #2 Exit Temp	Single	(2)	38-180(1)	Deg R	80	1.0		X
Fuel Pump Assembly Radial Vibration	Single	5% FS	0-20	G's	20			X
Fuel Pump 2 Speed	Single	0.5% FS	7.5K-110K	RPM	20			X
FP2 Brg. #3 Inlet Temp	Single	(2)	38-180(1)	Deg R	80	1.0		X
FP2 Brg. #3 Exit Temp	Single	(2)	38-180(1)	Deg R	80	1.0		X
FP2 Brg. #4 Inlet Temp	Single	(2)	38-180(1)	Deg R	80	1.0		X
FP2 Brg. #4 Exit Temp	Single	(2)	38-180(1)	Deg R	80	1.0		X

NOTE: (1) All cryogenic temp sensors must read up to 600 °R, but accuracy required above listed value may be reduced to ± 15 °R.
(2) Required accuracy is to measure a delta of ± 2 °R across the bearing. The absolute accuracy for the temp readings is ± 10 °R.

Table 16. Control Sensor Requirements for the Oxidizer Turbopump and Thrust Chamber

PARAMETER	REQUIREMENTS						SAFETY	
	REDUNDANCY	SYSTEM ACCURACY (+/-)	RANGE	UNITS	SAMPLING msec	BANDWIDTH Hz	PERMISSIVE	REDLINE
LO2 Turbine Inlet Temp	Single	10 deg	500-1200	Deg R	80	0.5		X
LO2 Pump Metal Temp	Single	10 deg	160-600	Deg R	80	0.2	X	
LO2 Pump Inlet Press	Single	4% FS	0-75	PSIA	80	1.0	X	X
LO2 Pump Speed	Single	0.5% FS	5K-55K	RPM	20			X
LO2 Pump Radial Vibs	Single	5% FS	0-20	G's	20			X
LO2P Brg. #1 Inlet Temp	Single	(2)	160-215(1)	Deg R	80	1.0		X
LO2P Brg. #1 Exit Temp	Single	(2)	160-215(1)	Deg R	80	1.0		X
LO2P Brg. #2 Inlet Temp / Brg. #3 Exit Temp	Single	(2)	38-180(1)	Deg R	80	1.0		X
LO2P Brg. #2 Exit Temp	Single	(2)	38-180(1)	Deg R	80	1.0		X
LO2P Brg. #3 Inlet Temp	Single	(2)	38-180(1)	Deg R	80	1.0		X
IPS He Pressure	Dual	5% FS	15-1000	PSIA	20	1.0		X
IPS He/H2 Disch Press	Single	5% FS	0-300 (3)	PSIA	20	1.0		X
IPS He/O2 Disch Press	Single	5%FS	0-100 (3)	PSIA	20	1.0		X
Main Chamber Press,Low	Single	1% FS (5)	0-150 (4)	PSIA	20	7.0	X	X
Main Chamber Press,Med	Single	1% FS (5)	0-500 (4)	PSIA	20	7.0	X	X
Main Chamber Press,High	Single	1% FS (5)	0-1500	PSIA	20	7.0	X	X
Igniter Chamber Press	Single	1% FS (5)	0-1500	PSIA	20	7.0	X	X
Low Press He Purge	Single	5% FS	15-100	PSIA	80	1.0		X
High Press He Purge	Single	5% FS	15-1500	PSIA	80	1.0		X
Low Press N2 Purge	Single	5% FS	15-100	PSIA	80	1.0		X
High Press N2 Purge	Single	5% FS	15-1000	PSIA	80	1.0		X

(3) Rate transducer for an overpressure of 1000 psia.
(4) Rate transducer for an overpressure of 1500 psia.
(5) Transducer in a controlled temp environment (+/- 25 deg)

Table 17. Explanation of Fuel and Oxidizer Turbopump Sensors

SENSOR	FUNCTION	ACCURACY	SIGNAL LOSS	REDLINE/ PERMISSIVE
Pump Metal Temperature	Monitor Cooldown	Not Critical (10°R)	During/Prior to Start, Abort Start. All Other Times, Continue.	Inhibit Start
Pump Inlet Pressure	Monitor Inlet Pressure to Avoid Cavitation	Not Critical (4% F/S)	Inlet Valves Open and $Pc = Pc_{REF}$, Continue. Otherwise, Shutdown.	Shutdown
Bearing Coolant Inlet and Discharge Temperatures	Monitor Bearing Health	2° Delta T (5° ΔT Good Bearing, 9° ΔT Failing Bearing)	Shutdown	Shutdown
Speed	Monitor Speed for Overspeed	Tight to Prevent False Overspeed Detect (.5% F/S)	Valves Correct and $Pc = Pc_{REF}$, Continue. Otherwise Shutdown.	Shutdown
Vibration	Monitor Rotor Imbalance	5% F/S, ATD Experience	Shutdown	Shutdown

Table 18. Explanation of Oxidizer Turbopump, Thrust Chamber, and Purge Sensors

SENSOR	FUNCTION	ACCURACY	SIGNAL LOSS	REDLINE/ PERMISSIVE
IPS Helium Purge Pressure	Safety: H_2/O_2 Separation	Not Critical (5% F/S)	Redundant, Use Remaining. Shutdown for Total Loss	Shutdown
IPS He/O_2: and He/H_2 Discharge Pressure	Detect Deterioration of IPS Labyrinth Seals	3 - 15 psi to Sense Seal Breakdown (5% F/S)	Shutdown	Shutdown
Oxidizer Turbine Inlet Temperature	Monitor Nozzle and Chamber Cooling	Not Critical (10°R)	Shutdown	Shutdown
Chamber Pressure	Control Loop: Thrust	3% of Point	Redundant, Use Remaining. Shutdown for Total Loss	Shutdown for $Pc > Lim$ or $Pc_{REF} - Pc > TBD$
Lox Manifold N2 Purge Supply Pressure	Monitor Purge Pressure	Not Critical (5% F/S)	Continue with Test, Inhibit Throttling Below TBD Power.	Same as Signal Loss
Fuel and Lox Line He and N2 Purge Supply Pressure	Monitor Purge Pressure	Not Critical (5% F/S)	Prestart and Start, Abort. Otherwise, Continue with Test.	Continue with Test

Table 19. Input/Output Requirements and Spare Capability

DESCRIPTION	REQUIRED QUANTITY	ACTUAL QUANTITY	SPARE QUANTITY
Analog	2	8	6
Discrete Input	17	32	15
Frequency (Magnetic Pickup)	3	4	1
LVDT	5	16	11
Strain Gage	14	TBD	TBD
RTD	2	TBD	TBD
T/C	16	TBD	TBD
Solenoid/Relay	18	24	6
T/M	5	12	7
T/M Wraparound	5	12	7
D/A	0	4	4
Circuit Board Slots	16	20	4

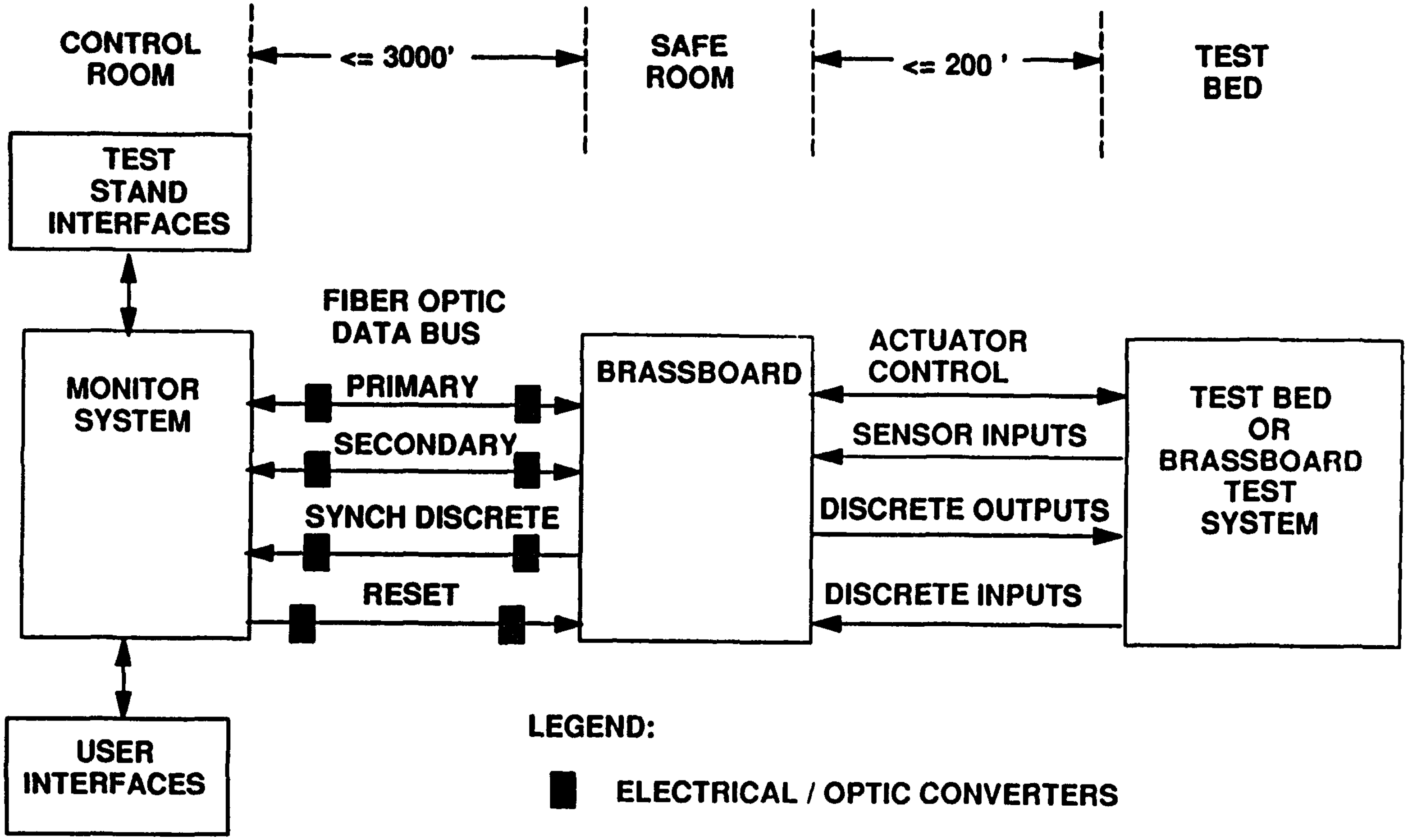

Figure 146. Hardware System Description

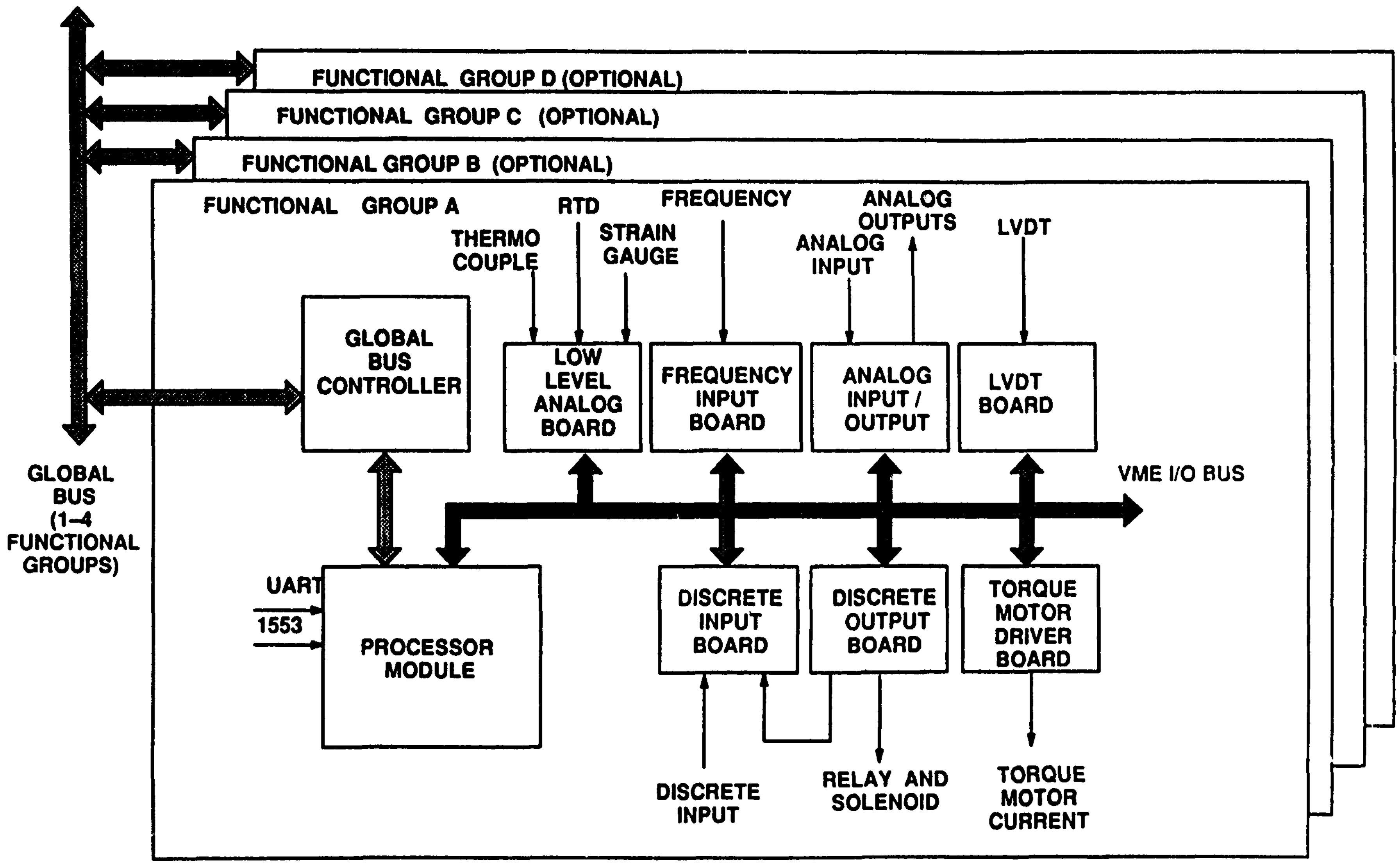

NOTE: EACH CARDCAGE CONTAINS 20 SLOTS , BASELINE SYSTEM HAS FIVE SPARE SLOTS

Figure 147. Brassboard Modular Design Provides Flexibility and Expandability

SLOT	REFERENCE PART #	BOARD NAME
1	SK 114914	PROCESSOR
2	260X2264	LOGIC ANALYZER I/F
3		
4	TBD	LOW LEVEL BOARD
5		
6	SK 114929	DISCRETE INPUT
7	SK 114929	DISCRETE INPUT
8	SK 114930	DISCRETE OUTPUT
9	SK 114930	DISCRETE OUTPUT
10	SK 114913	TORQUE MOTOR
11	SK 114916	LVDT
12	SK 114928	FREQUENCY
13	SK 114931	ANALOG I/O
14		SPARE
15		SPARE
16		SPARE
17		SPARE
18		SPARE
19	SK 114915	GLOBAL BUS CONTROLLER
20		

Figure 148. Brassboard VME Rack Configuration

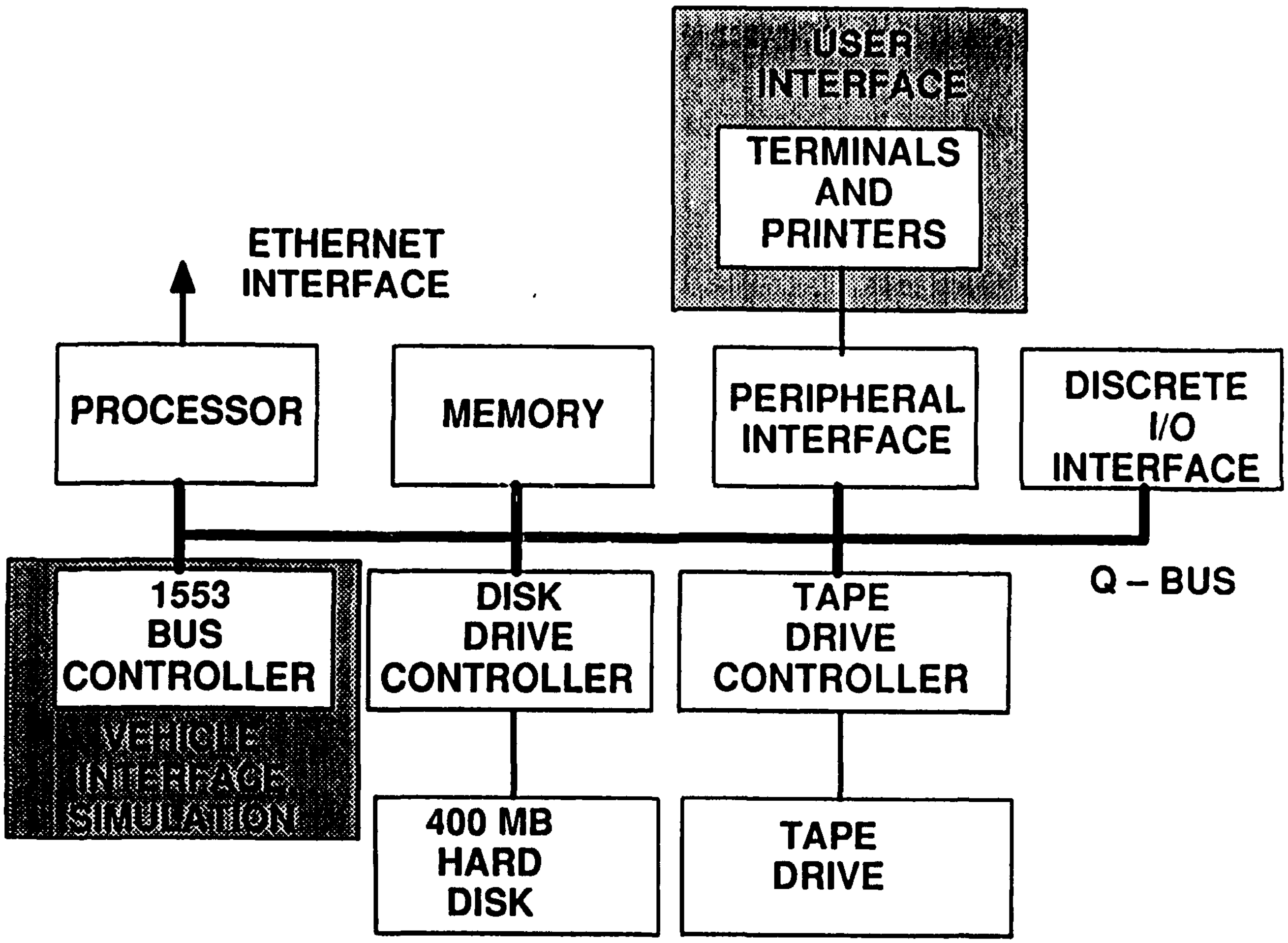

Figure 149. Monitor System Description

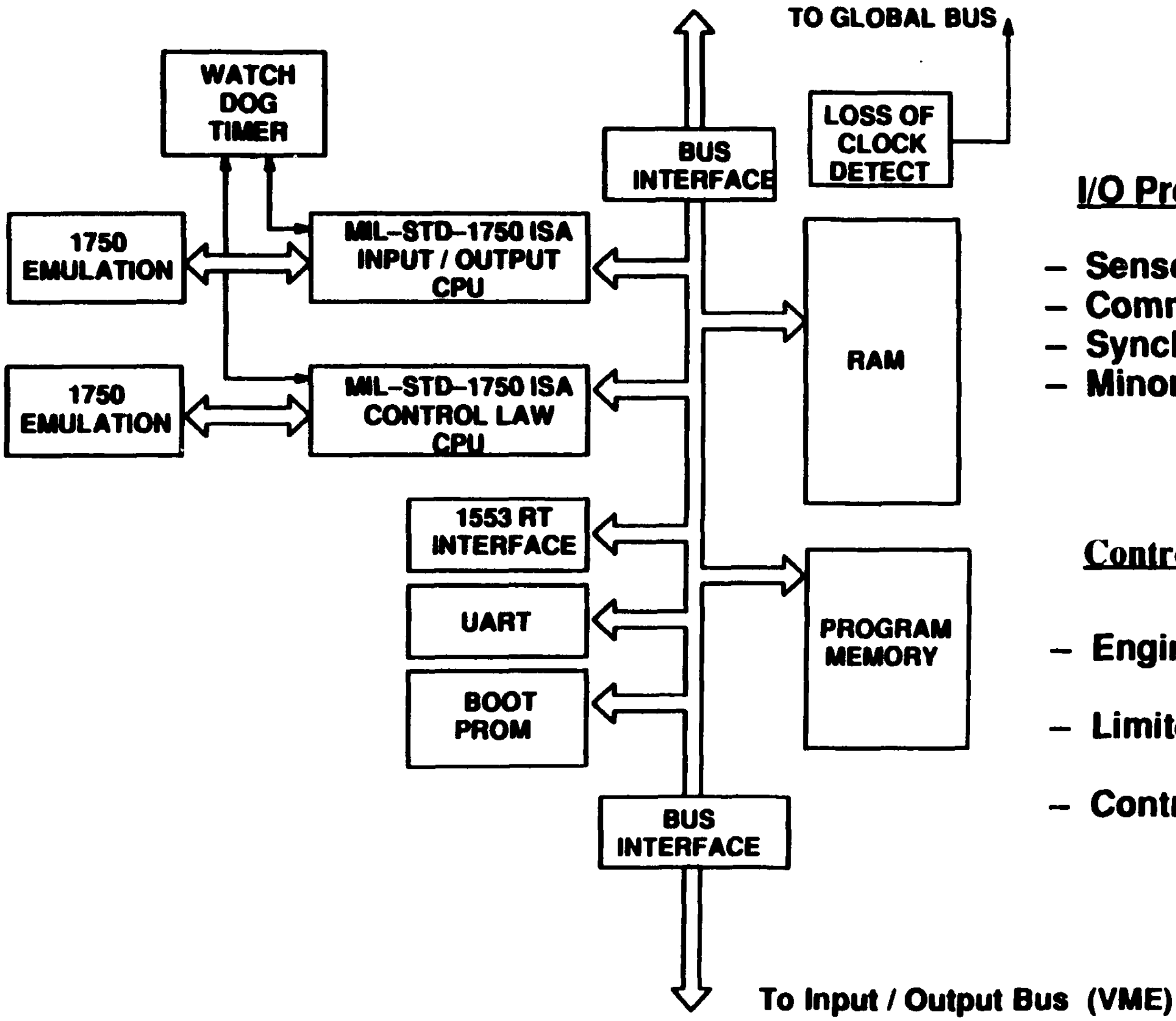

I/O Processor Functions

- Sensor data acquisition
- Communication with 1553 interface
- Synchronization of processors
- Minor Loop Closure

Control Law Processor Functions

- Engine control law algorithm execution
- Limited health monitoring algorithm execution
- Control Monitor Communication

Figure 150. Processor Board Description

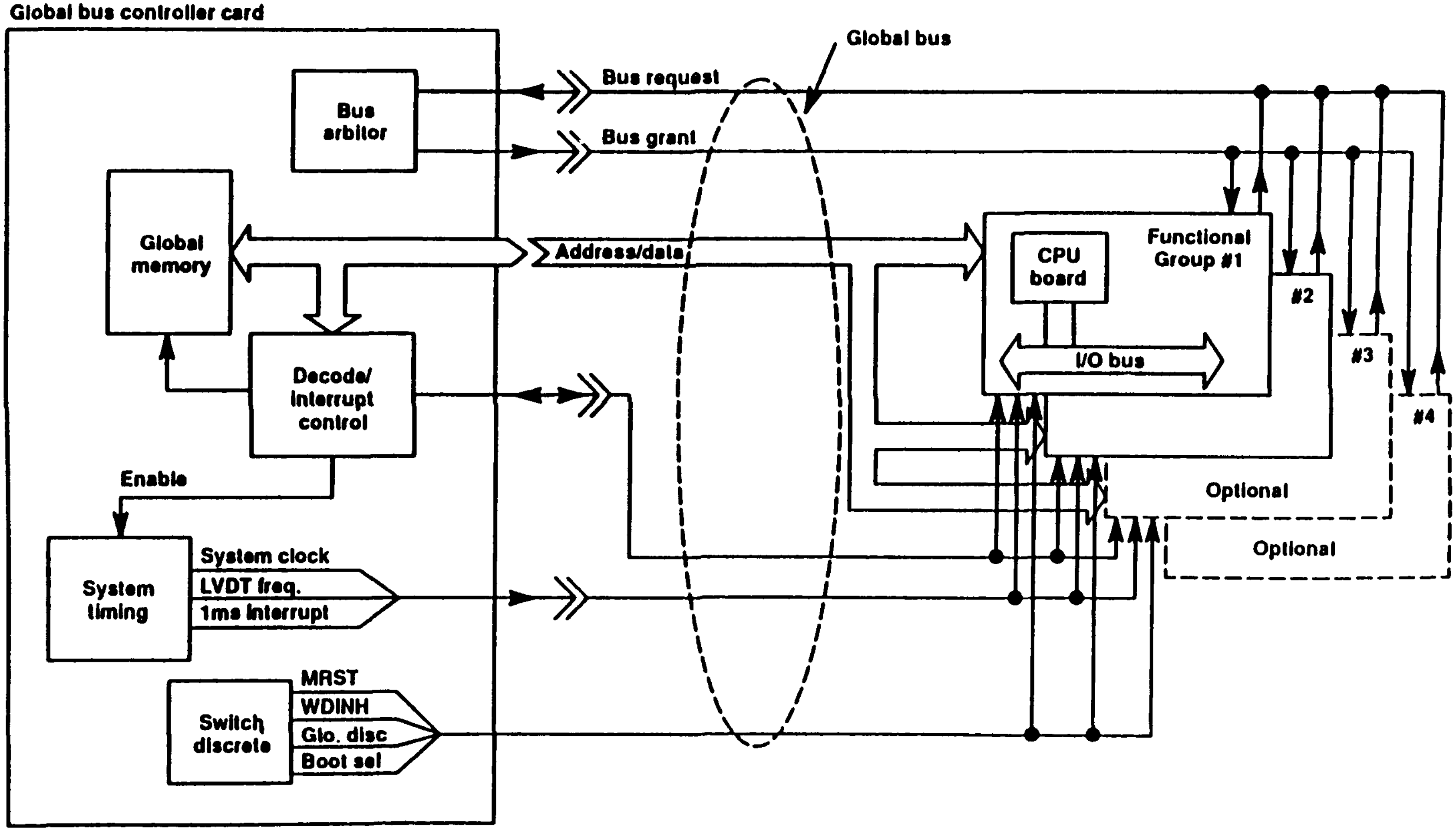

Figure 151. Global Bus Controller Description

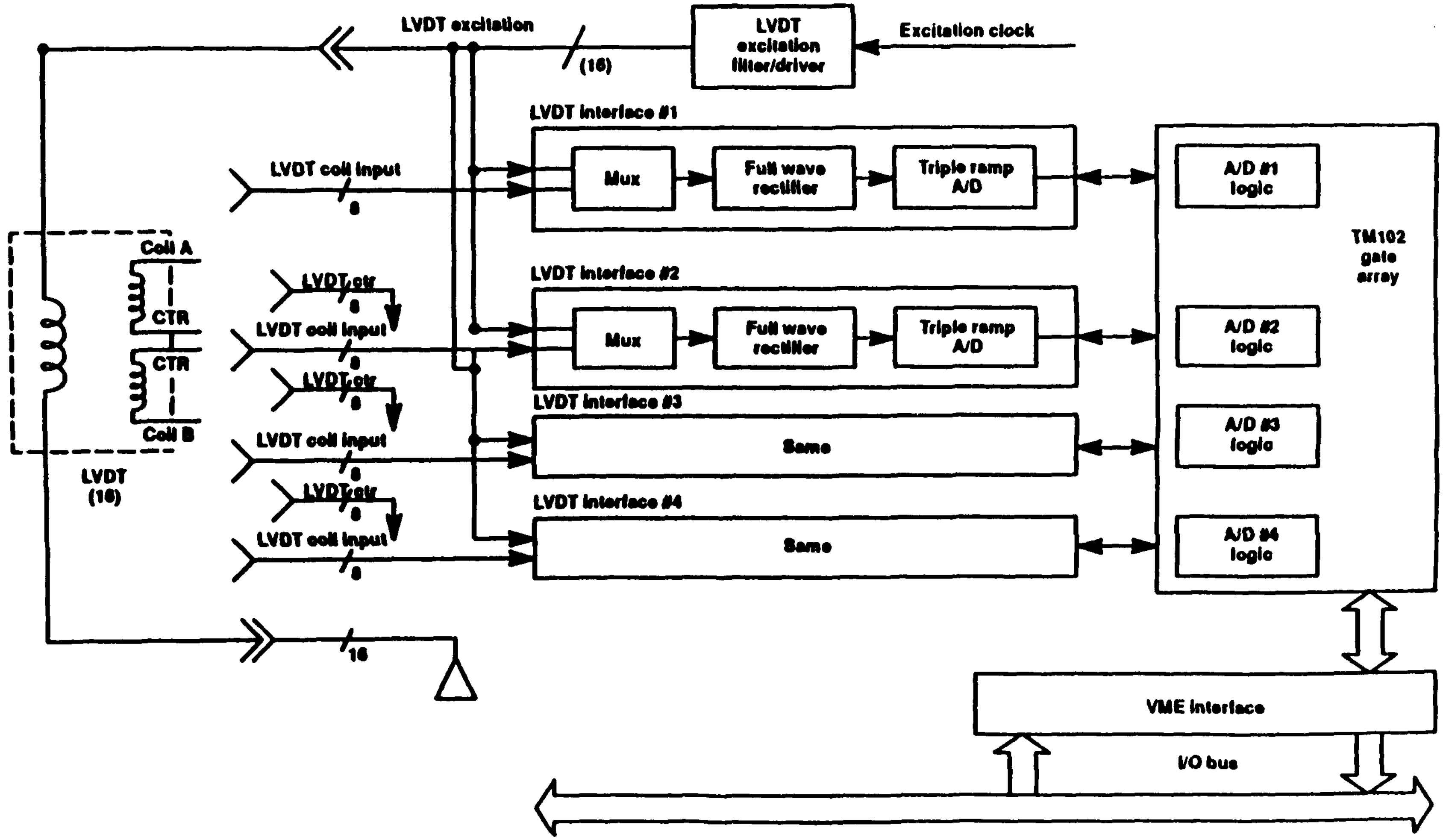

Figure 152. LVDT Board Provides Signal Conditioning for up to 16 Channels

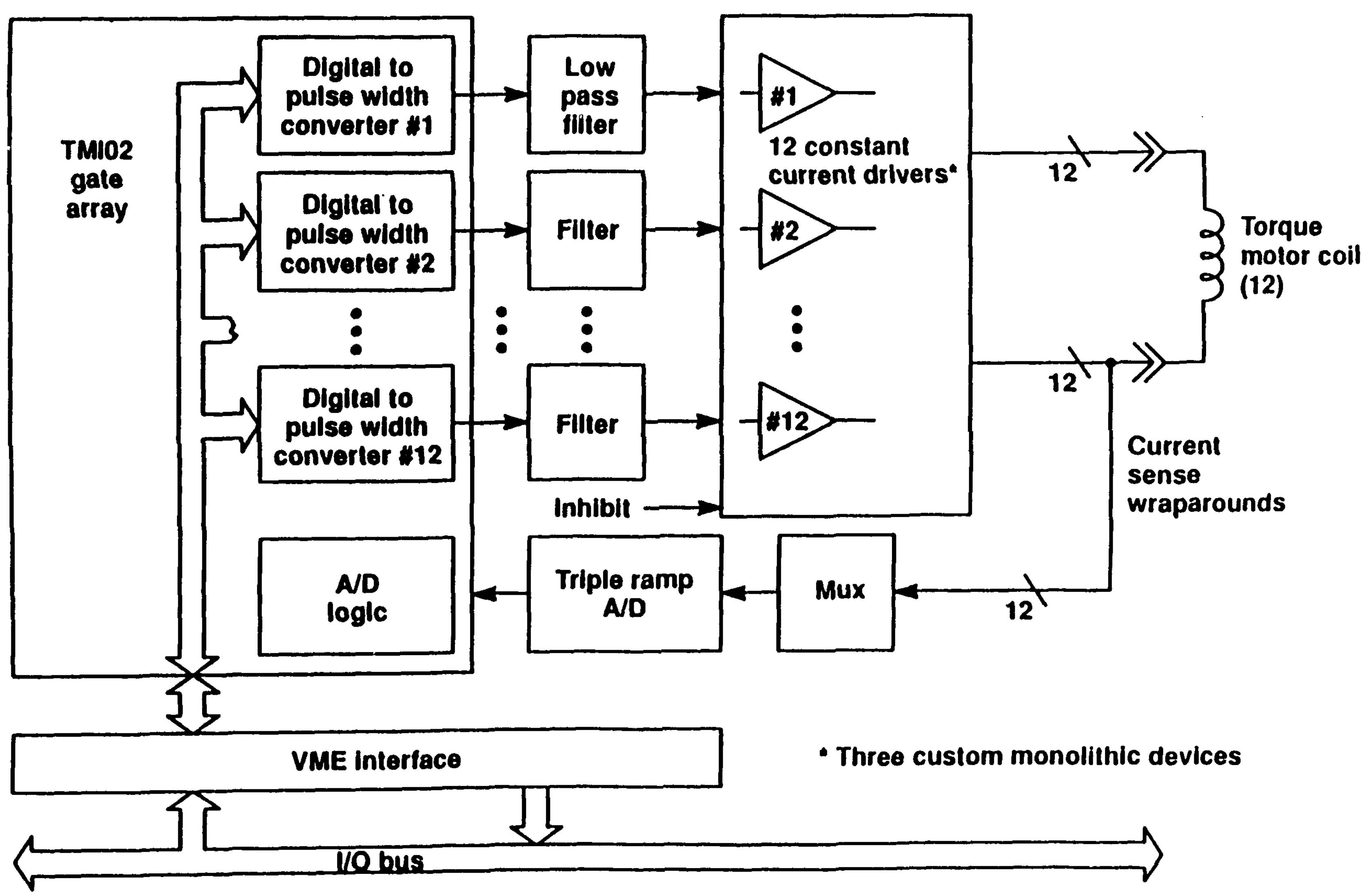

Figure 153. Torque Motor Board Description

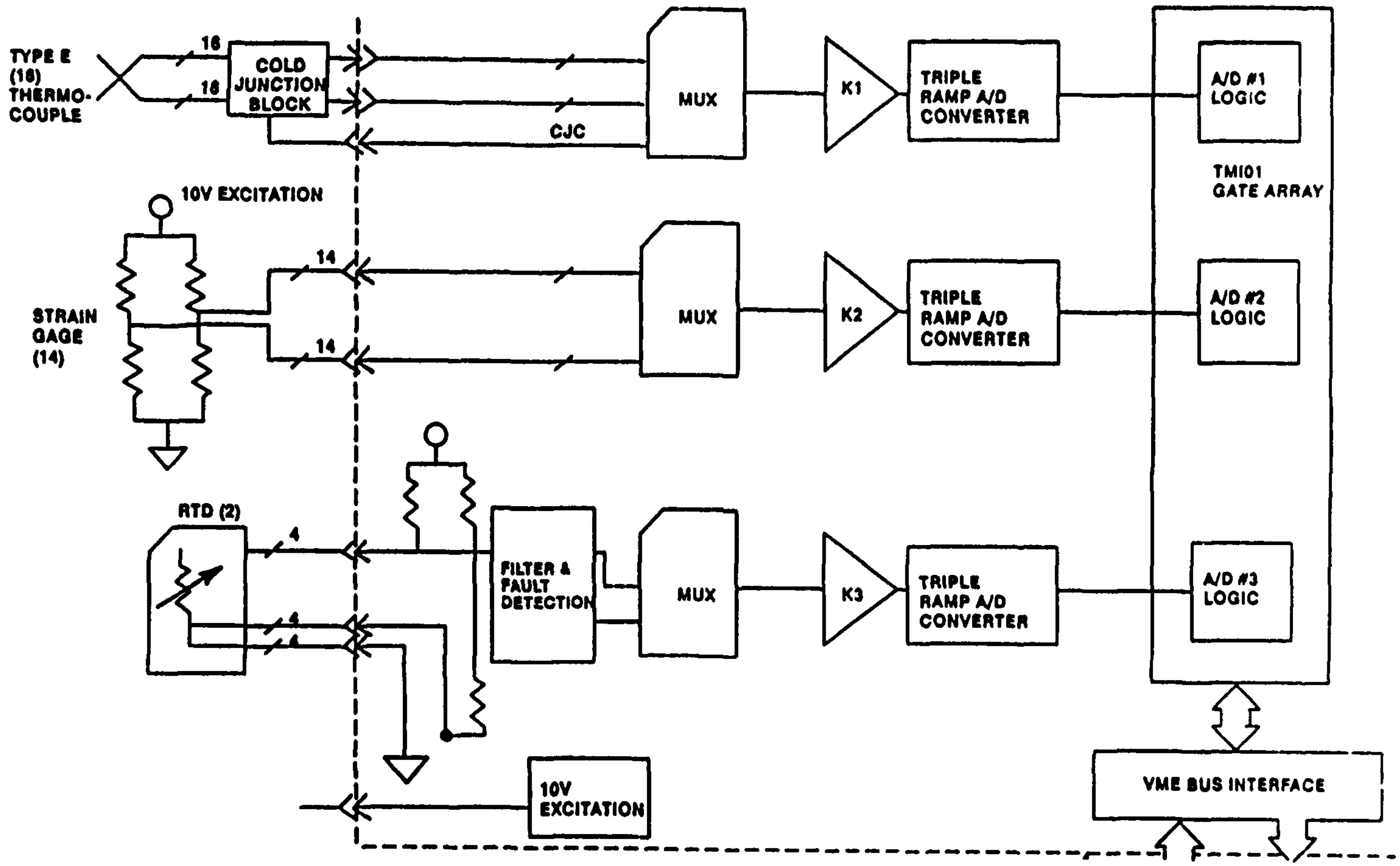

Figure 154. Low Level Interface Board Conditions Thermocouples, RTD and Pressures

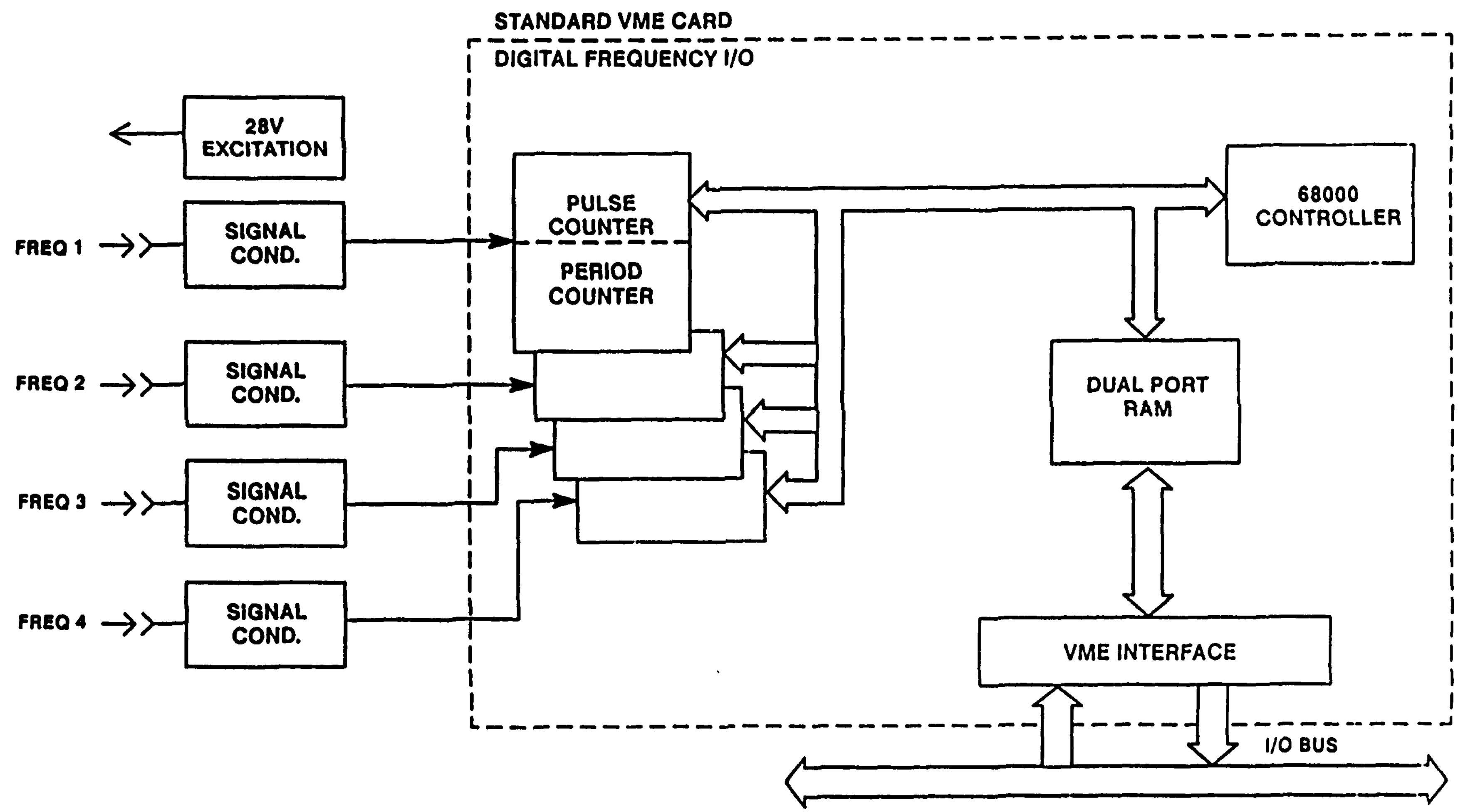

Figure 155. Frequency Board Provides Pump Speed Monitoring

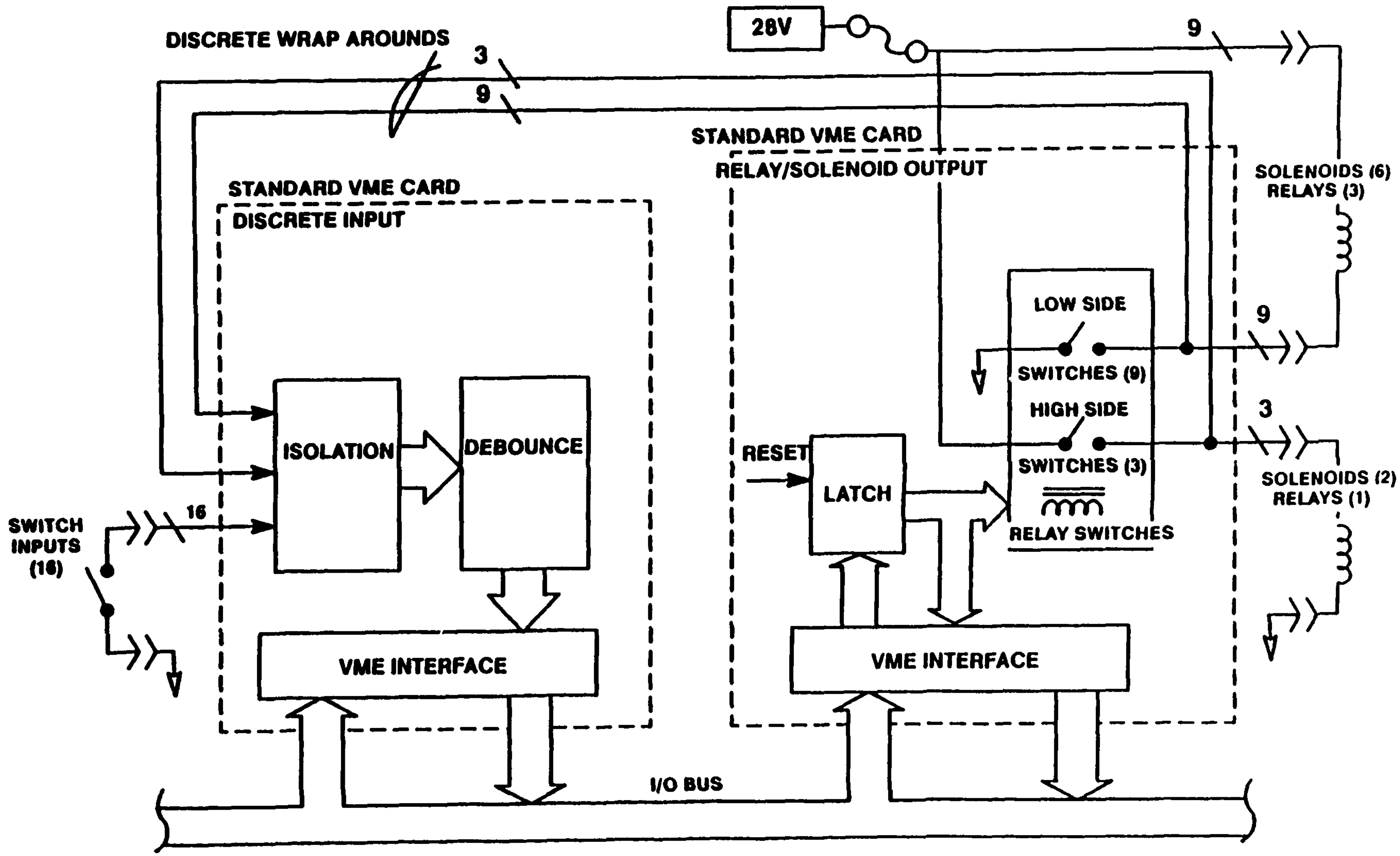

Figure 156. Discrete Interface Board Conditions Switch Inputs and Drives Solenoid Outputs

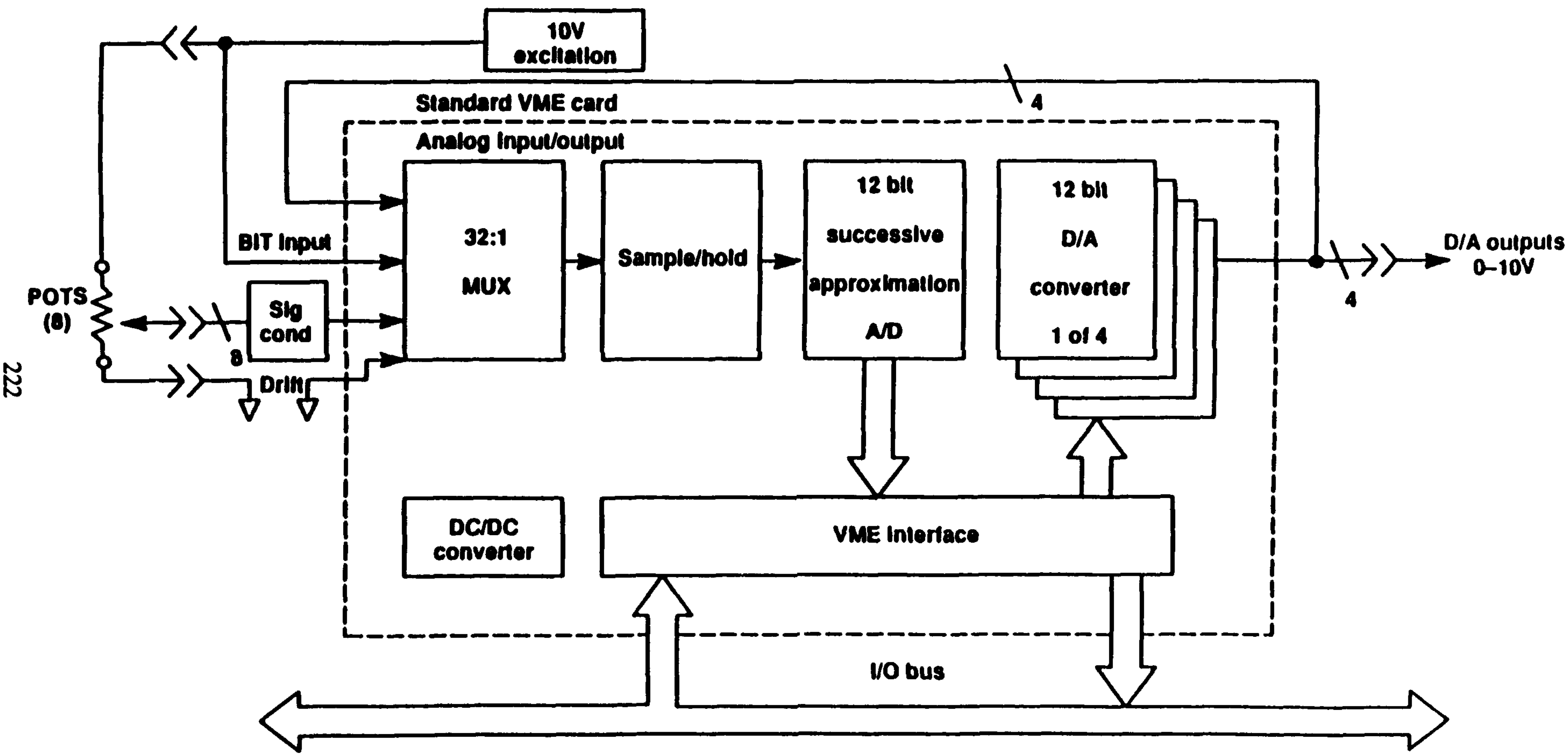

Figure 157. Analog Input/Output Board Used for Vibration Sensors

Table 20. Processor Throughput and Memory Usage

THROUGHPUT

CPU	MIPS USED	MIPS AVAILABLE	% USED
I/O	.48	.70	69%
CLP	.38	.70	55%
TOTAL	.87	1.40	62%

MEMORY

CPU	WORDS USED	WORDS AVAILABLE	% USED
I/O	17404	57344	30%
CLP	29617	57344	52%
TOTAL	47021	114688	41%

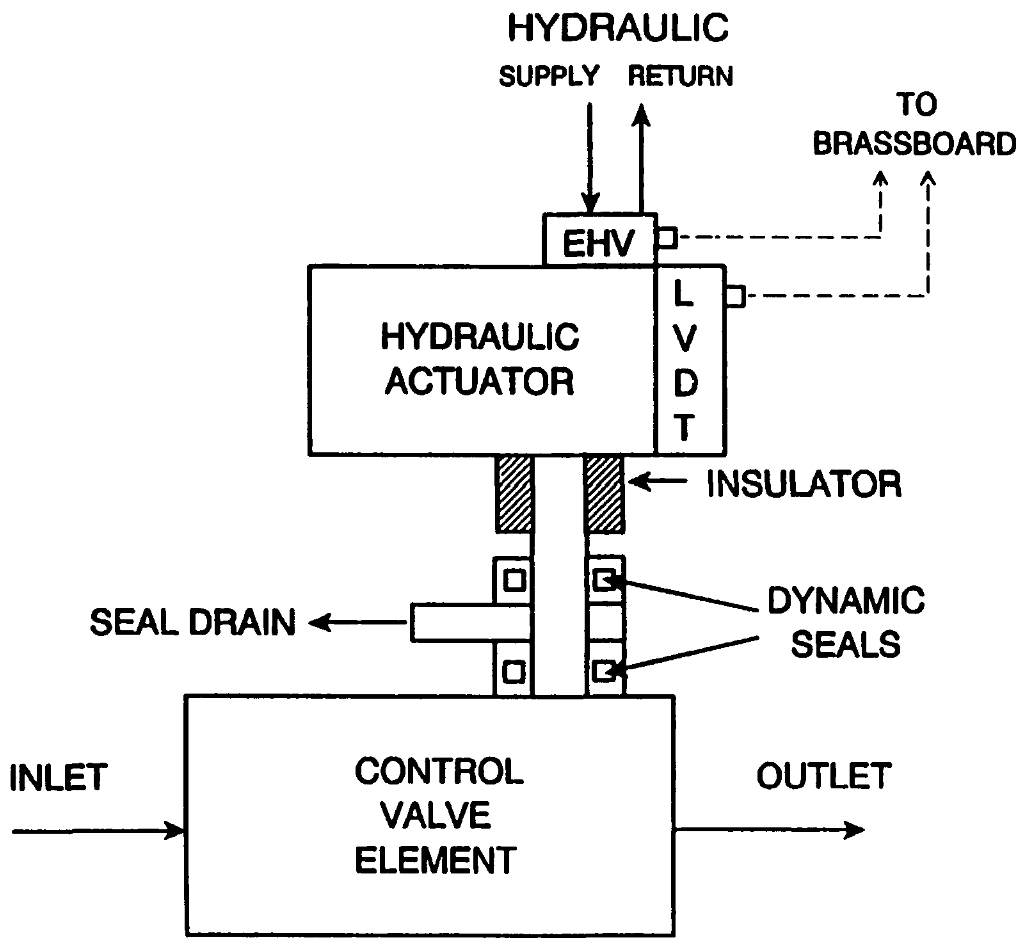

Figure 158. Control Valve Configuration

Table 21. Control Valve Requirements

POSITION	FJBV/CCBV Note (3)		MTBV		FTBV/OTBV Note (3)		SOCV		FPRV	
FLUID	LH2		GH2		GH2		LOX		LH2	
VALVE SIZING POINTS	MIN.	MAX.	MIN.	MAX.	MIN.	MAX.	MIN.	MAX.	MIN.	MAX.
Flow (lbm/sec)	0.35	3.18	0.139	0.042	0.034	0.85	0.4	33.51	0.0	1.60
Inlet Pressure (psia)	945	1566	4043	11.5	1991	2627	144	1490	1917	103
Pressure Drop (psi)	271	171	2248	1.6	820	1360	86	197	1850	33
Inlet Temp. (°R)	54	63	1019	700	739	599	164	169	68	44
Density (lbm/ft³)	4.27	4.30	0.68	0.003	0.48	0.75	71.1	71.4	4.36	4.16
OTHER DESIGN PARAMETERS										
Max. Pressure (psia)	3285		4043		3460		2285		1917	
Pressure Drop (psi)										
Valve Open	171-309		2-2248		820-1360		112-881		32-257	
Valve Closed	0-357		N/A		0-1664		0-2285		(-5)-1850 Note (2)	
Fluid Temp. Range (°R)										
Valve Open	54-98		627-1068		599-744		163-177		42-47	
Valve Closed	37-710 Note (1)		N/A		478-976		162-163		37-69 Note (1)	
Line Size-ID (in.)	1.278		1.338		1.338		1.38		0.18 (1/4 Tube)	
Positive Sealing	YES		NO		YES		YES		YES	
Normal Position	CLOSED		OPEN		CLOSED		CLOSED		CLOSED	
Max. Actuation Time (sec)	0.200		0.300		0.300		0.300		1.000	
Envelope (in.)	11x15x6		11x15x6		11x15x6		11x15x6		11x11x6	

NOTES

(1) Temperatures may occur simultaneously on opposite sides of valve.
(2) (-5) psi pressure drop indicates slight pressure reversal under some operating conditions. Reverse leakage acceptable.
(3) Valves may be installed in alternate positions.

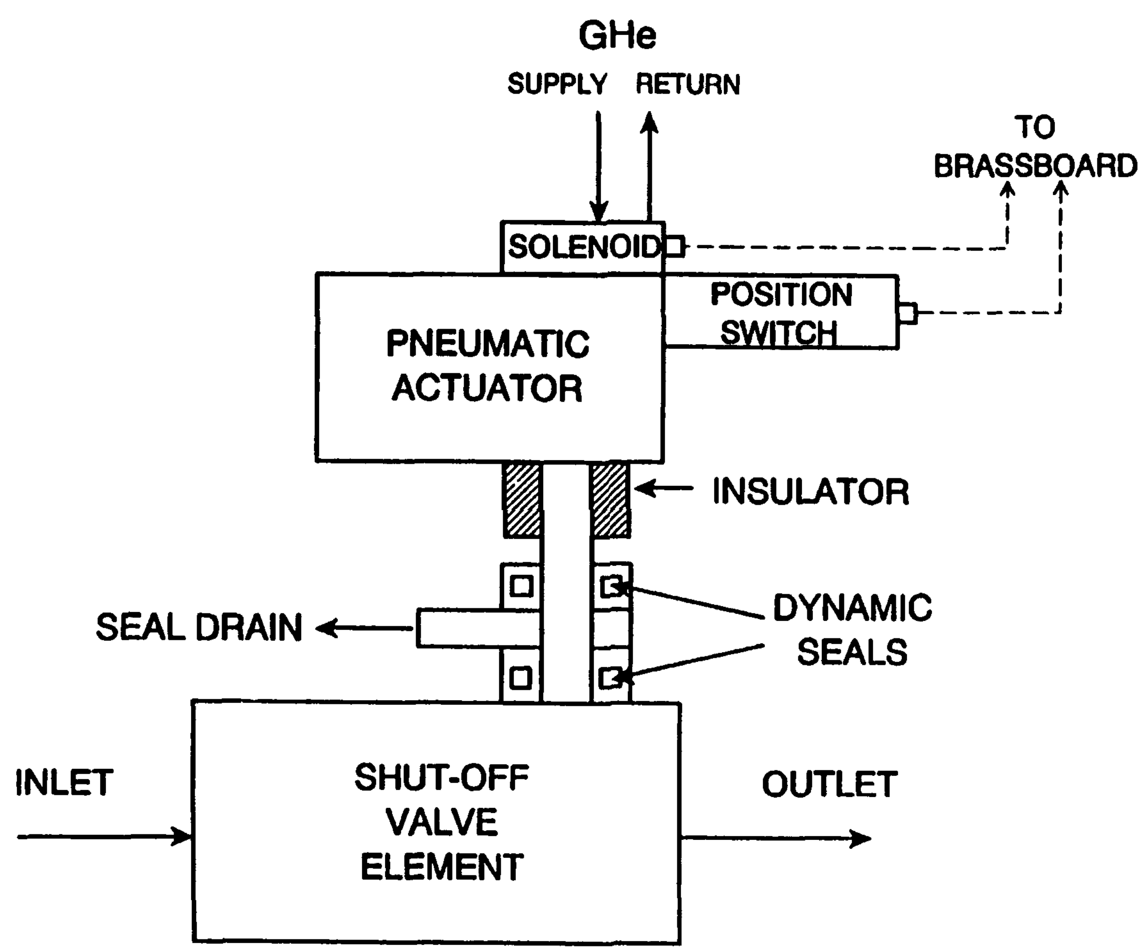

Figure 159. Shutoff Valve Configuration

Table 22. *Main Shutoff Valve Requirements*

POSITION	EFIV	EOIV	FTSV	FSOV	POSV
FLUID	LH2	LOX	GH2	GH2	LOX
VALVE SIZING POINT					
Flow (lb/sec)	7.50	45.0	4.05	7.33	5.58
Inlet Pressure (psia)	70	70	1805	1646	2234
Pressure Drop (psi)	5 Max.	5 Max.	10 Max.	10 Max.	753
Inlet Temp. (°R)	38	162	745	448	173
Density (lbm/ft^3)	4.39	71.38	0.44	0.64	71.47
OTHER DESIGN PARAMETERS					
Max. Pressure (psia)	70	70	1805	1646	2234
Pressure Drop (psi)					
Valve Closed	0-55	0-55	0-55	0-1646	0-2234
Fluid Temp. Range (°R)					
Valve Open	38	163	360-827	387-710	162-176
Valve Closed	38	163	700	387-710	162-176
Line Size-ID (in.)	2.16	2.85	1.338	2.469	0.884
Valve Type	OPEN/CLOSE	OPEN/CLOSE	OPEN/CLOSE	OPEN/CLOSE	OPEN/CLOSE
Normal Position	CLOSED	CLOSED	OPEN	CLOSED	CLOSED
Position Switch Indication	OPEN	OPEN	OPEN	OPEN	OPEN
Max. Actuation Time (sec)	0.200	0.200	0.300	0.500	0.300
Envelope (in.)	4x9x7	4x9x7	10x14x7	10x14x7	9x8x4

Table 23. Ancillary Shutoff Valve Requirements

POSITION	FCDV	FISV	OPRV	OCDV	OISV	S#PV
FLUID	GH2-LH2	GH2	LOX	GOX-LOX	GOX	GHE/GN2
VALVE SIZING POINT						
Flow (lb/sec)	5.0 LH2	Note (1)	1.35	20.0 LOX	Note (1)	Note (4)
Inlet Pressure (psia)	3000	N/A	171	2400	N/A	N/A
Pressure Drop (psi)	3000	N/A	101	2400	N/A	N/A
Inlet Temp. (°R)	115	387-802 (2)	165	175	540	540
Density (lbm/ft^3)	3.63	N/A	70.98	71.49	N/A	N/A
OTHER DESIGN PARAMETERS						
Max. Pressure (psia)	4503	4143	2356	2356	3000	3000
Pressure Drop (psi) Valve Closed	0-4503	0-2650	(-5)-2356 Note (3)	0-2356	3000	3000
Fluid Temp. Range (°R)						
Valve Open	37-111	387-802	161-163	162	540	540
Valve Closed	37-111	387-802 (2)	162-174 (2)	162-174	540	540
Line Size-ID (in.)	0.305 (3/8 Tube)	0.305 (3/8 Tube)	0.18 (1/4 Tube)	0.305 (3/8 Tube)	0.305 (3/8 Tube)	0.305 (3/8 Tube)
Valve Type	OPEN/CLOSE	3-PORT 2 POSITION SELECTOR	OPEN/CLOSE	OPEN/CLOSE	OPEN/CLOSE	OPEN/CLOSE
Normal Position	OPEN	N/A	CLOSED	OPEN	CLOSED	OPEN
Position Switch Indication	CLOSED	TBD	CLOSED	CLOSED	OPEN	OPEN
Max. Actuation Time (sec)	0.200	0.300	1.000	0.200	0.300	0.300
Envelope (in.)	8x5x5	8x10x6	7x4x4	7x4x4	7x4x4	2.5x4x3

NOTES

(1) Flows controlled by separate orifices. Minimum capacity 0.32 equivalent sharp edge orifice diameter (Cd=0.6)

(2) Temperatures may occur simultaneously on opposite sides of valve.

(3) (-5) psi pressure drop indicates slight pressure reversal under some operating conditions. Reverse leakage acceptable.

(4) S#PV (S1PV-S7PV) Seven solenoid valves. Flows controlled by separate orifices. Minimum capacity 0.15 equivalent sharp edge orifice diameter (Cd=0.6)

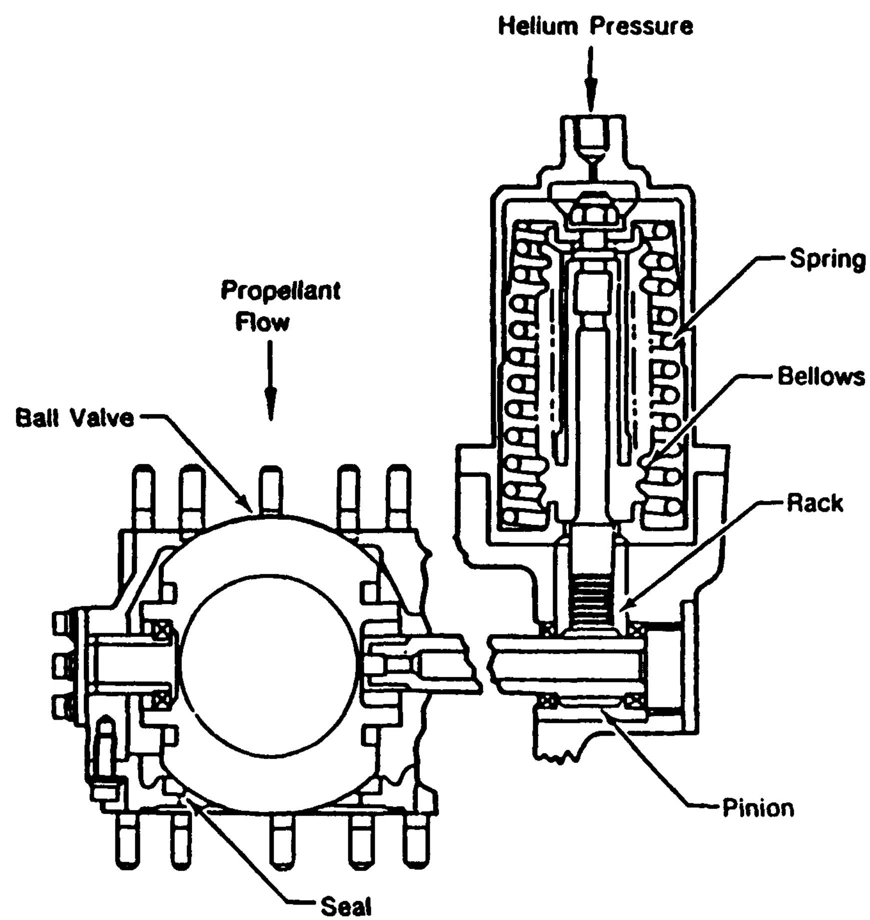

Figure 160. RL10 Inlet Valves Used for Fuel and Oxidizer Inlets

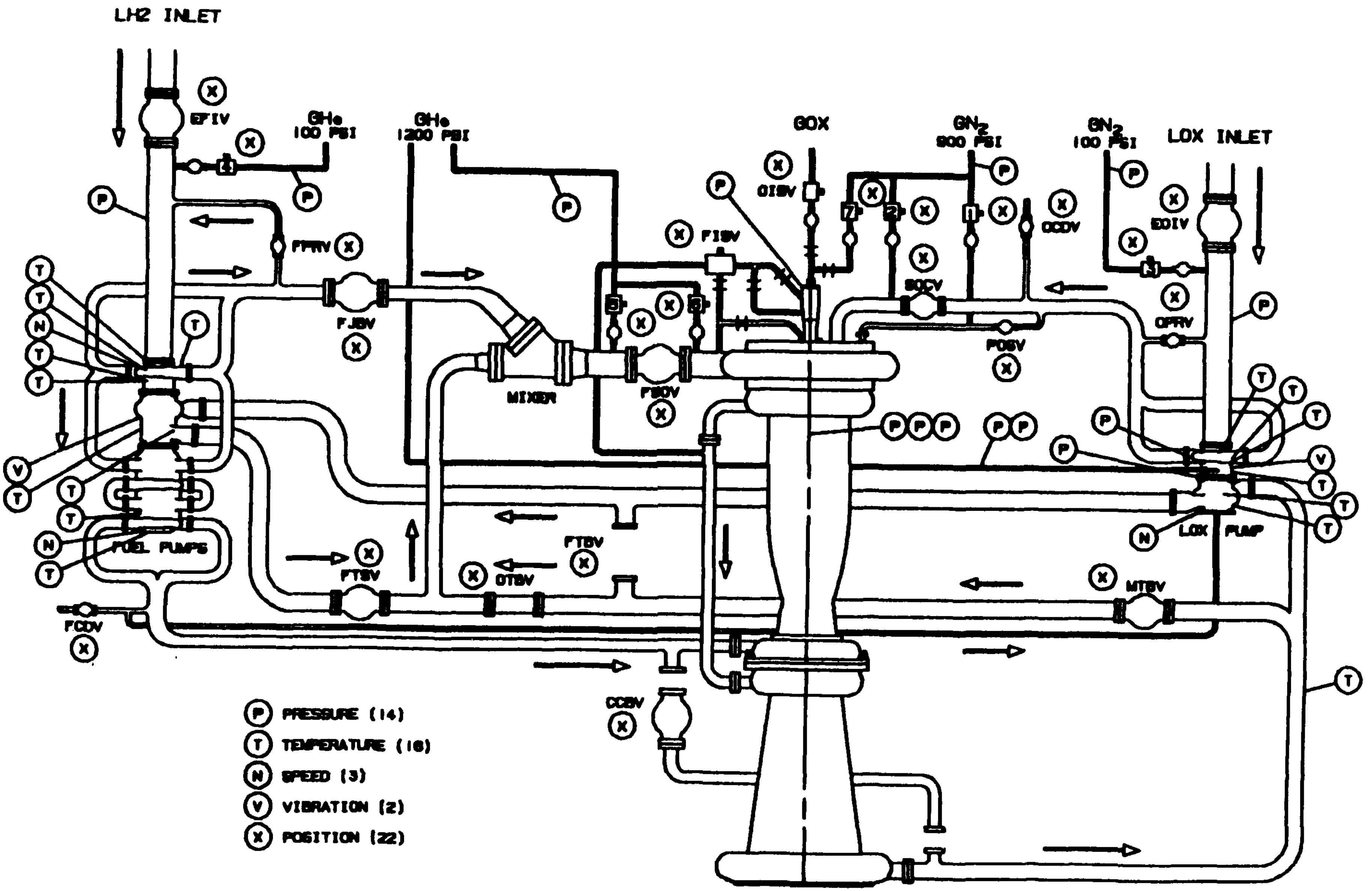

Figure 161. Flow Schematic With Control and Safety Sensors

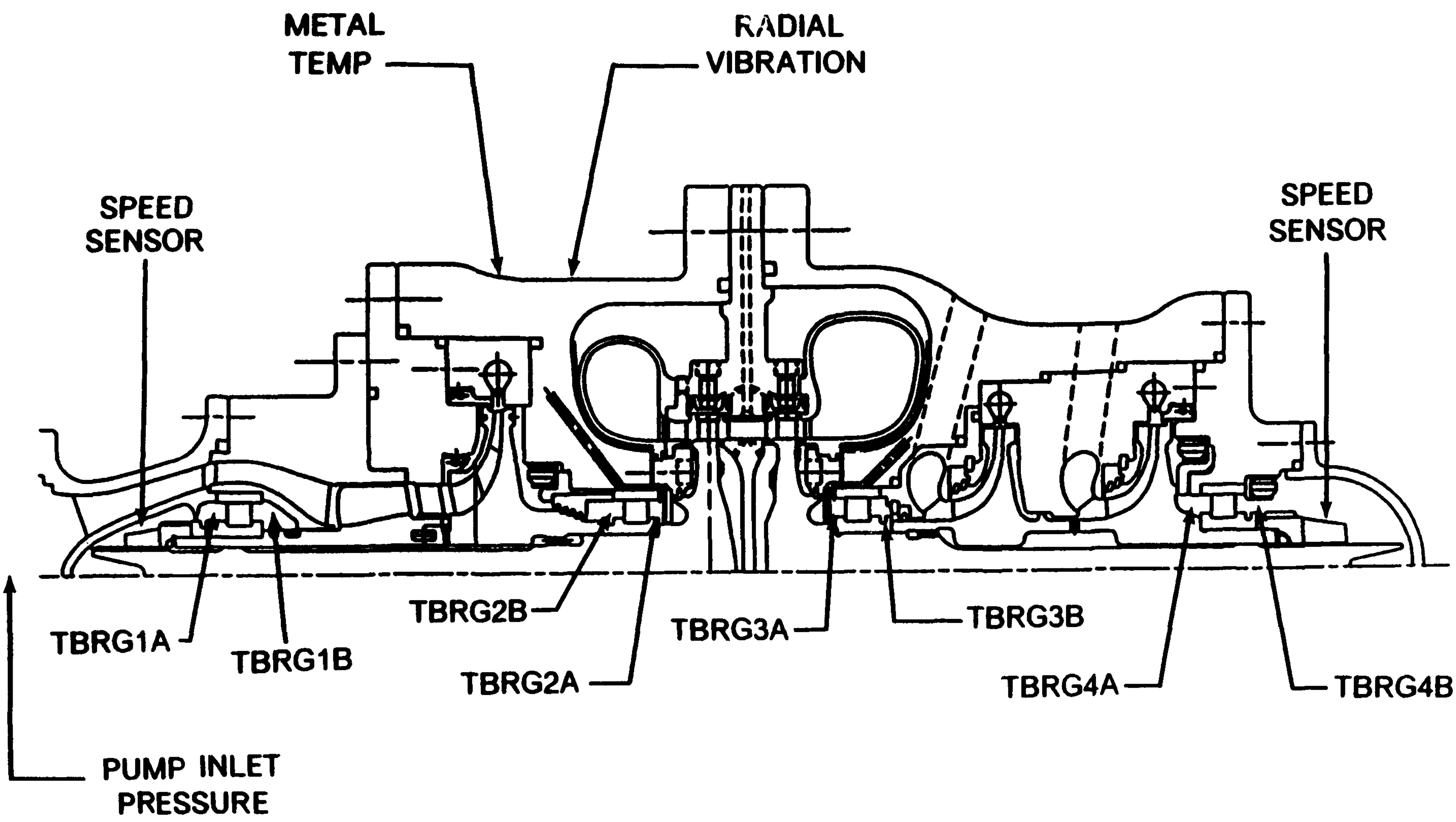

Figure 162. Hydrogen Turbopump Sensors

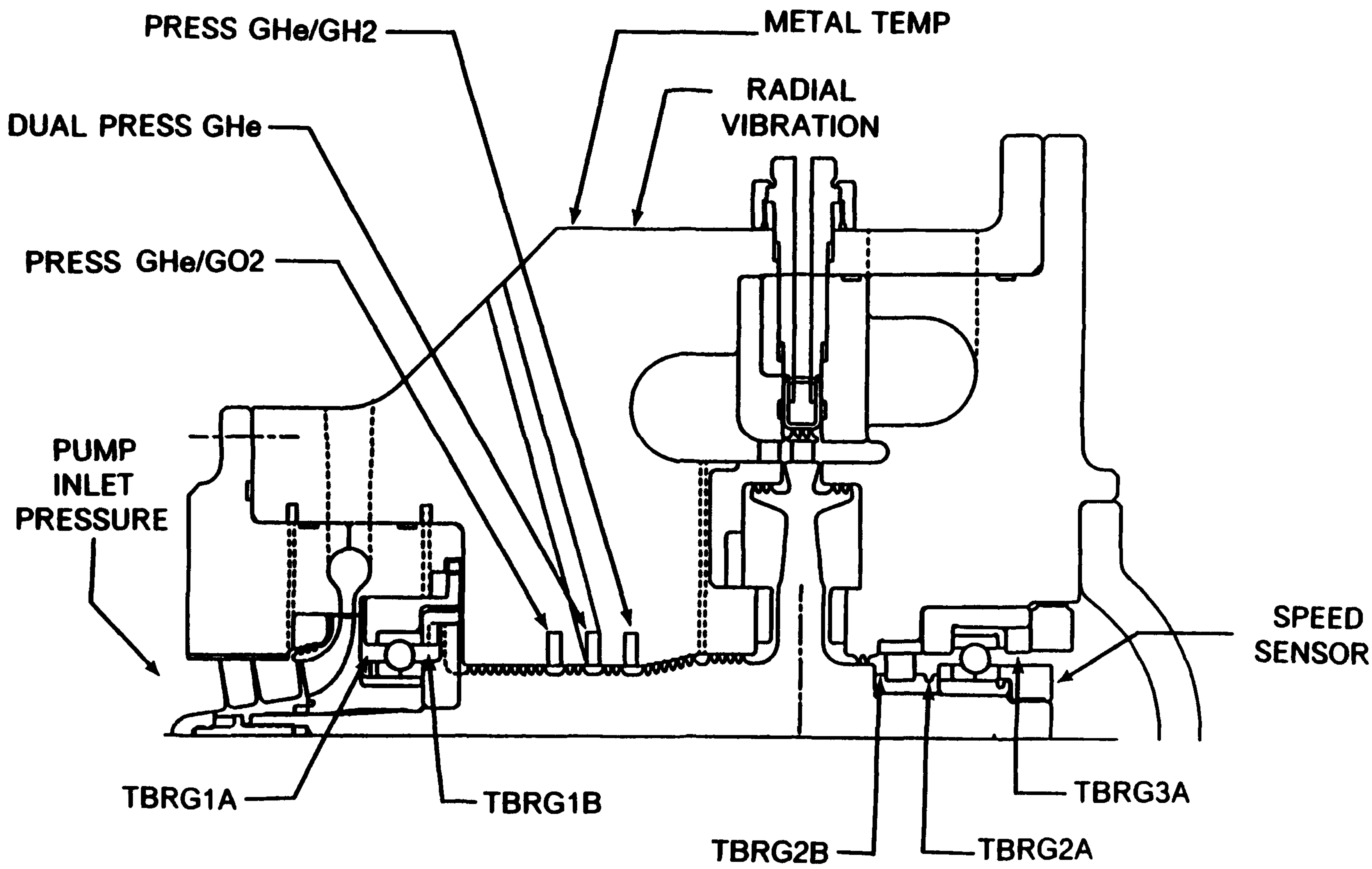

Figure 163. Oxygen Turbopump Sensors

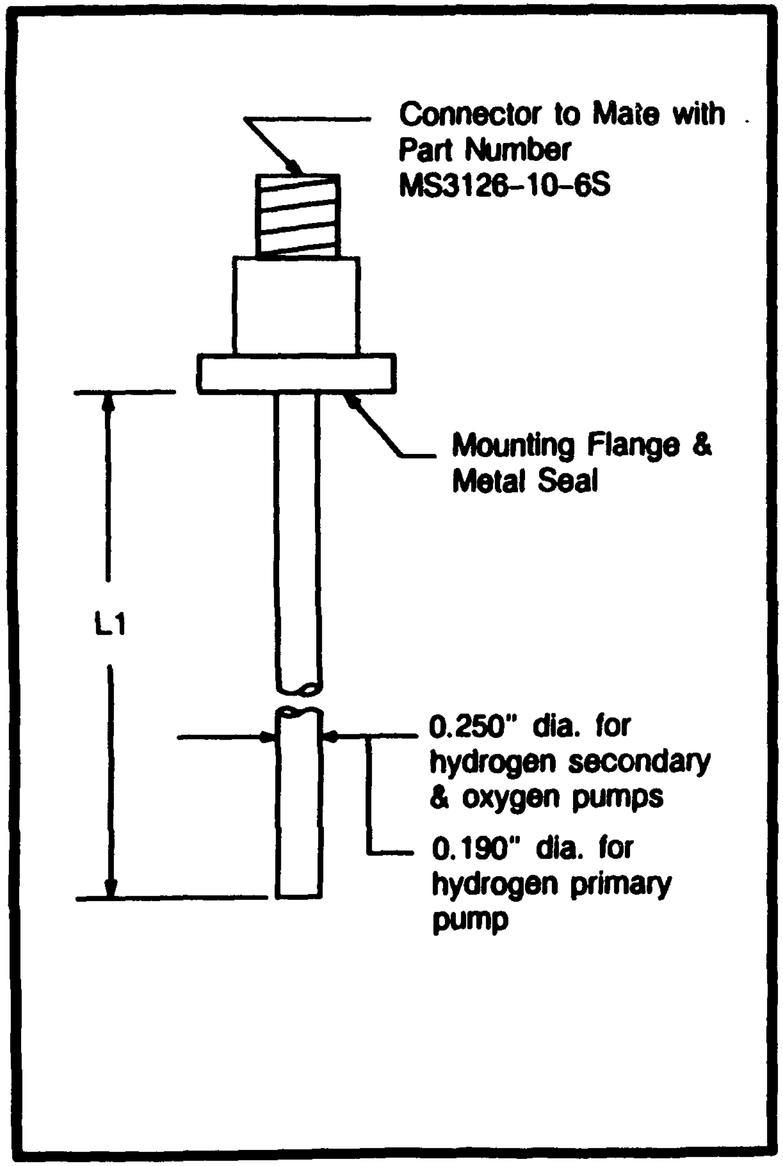

TYPE:
MAGNETIC

PROBABLE SUPPLIER:
ROSEMOUNT

SENSOR ACCURACY:
±0.2% FULL SCALE

SIGNAL CONDITIONER:
PROVIDES TTL OUTPUT

LATENT PERIOD:
20 MILLISECONDS MAXIMUM

MOUNTING FLANGE, METAL SEAL AND PROBE LENGTH(L1) WILL BE DEFINED DURING FINAL DESIGN

Figure 164. Speed Sensors Description

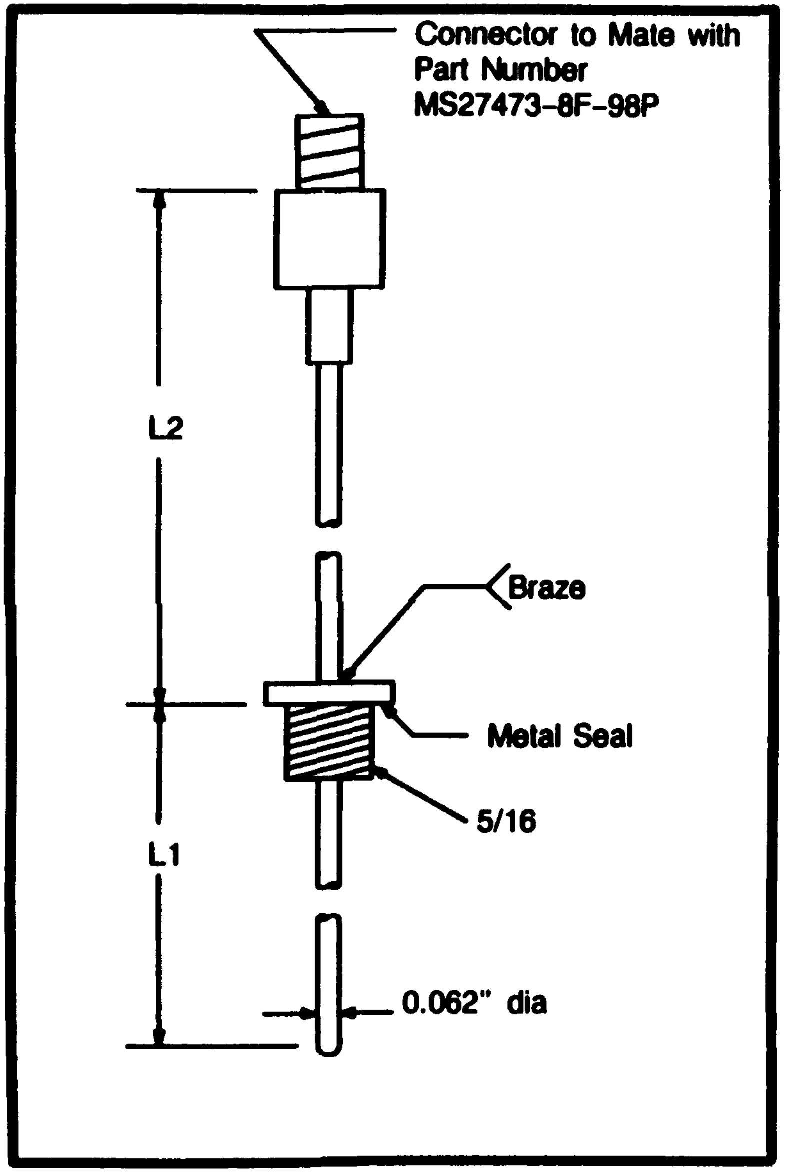

TYPE:
THERMOCOUPLE TYPE 'E'
CHROMEL - CONSTANTINE

PROBABLE SUPPLIER:
C.S. GORDON

ACCURACY:
± 1°R

CALIBRATION:
LH2, 35 to 45°R
LN2 and LAr 140 to 180°R

EXPERIENCE:
SSME ALTERNATE TURBOPUMP

METAL SEAL, LENGTHS L1 & L2 WILL BE DEFINED DURING FINAL DESIGN

Figure 165. Temperature Sensors Description

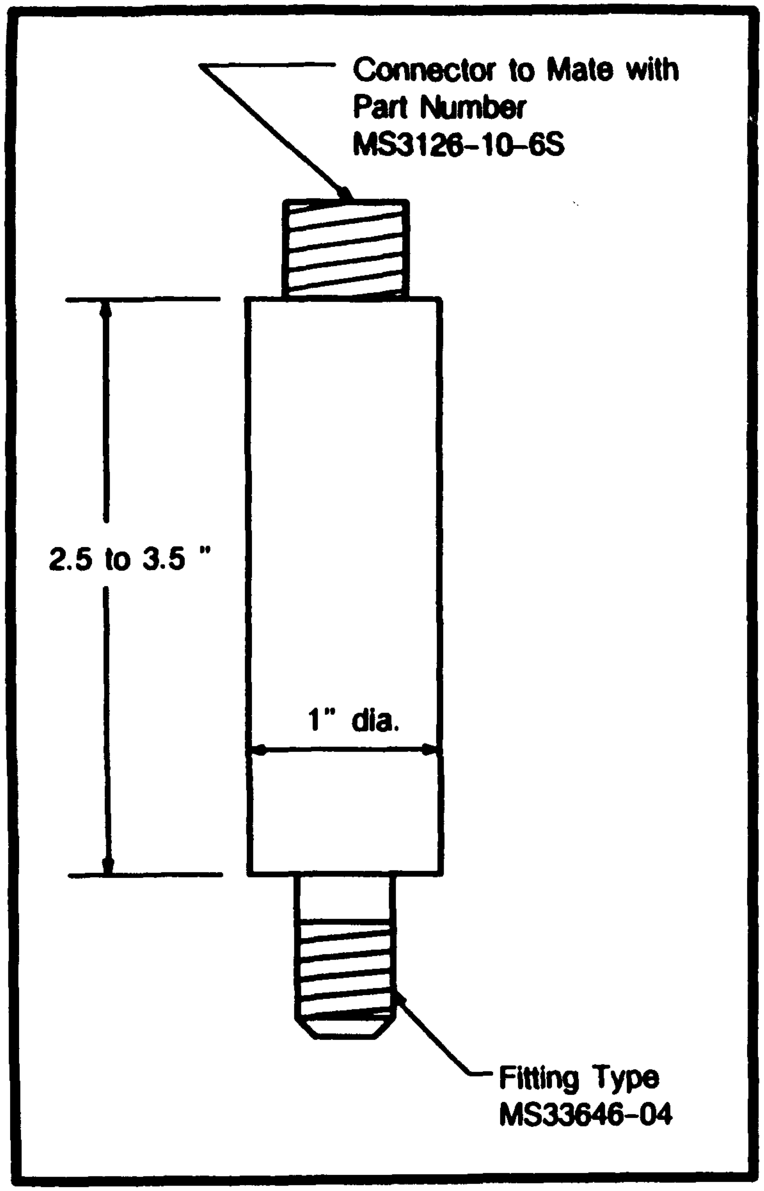

TYPE 1:
- ACCURACY: ± 4% OF FULL SCALE
- TEMPERATURE COMPENSATED – INTERNAL TO THE TRANSDUCER

TYPE 2:
- ACCURACY: ± 0.5% OF FULL SCALE
- TEMPERATURE COMPENSATED – INTERNAL TO THE SENSOR
- MOUNTED IN AN ISOTHERMAL BATH

TYPE 3: (Optional)
- ACCURACY: ± 2% OF FULL SCALE
- TEMPERATURE COMPENSATED WITH EXTERNAL SOFTWARE USING INTERNAL RTD

POTENTIAL SUPPLIERS:
- KULITE, SENSOMETRIC, SENSOTRON STATHAM, TELEDYNE TABER

EXPERIENCE:
- SSME, RL10, NASP, JET ENGINES

Figure 166. Pressure Transducers Description

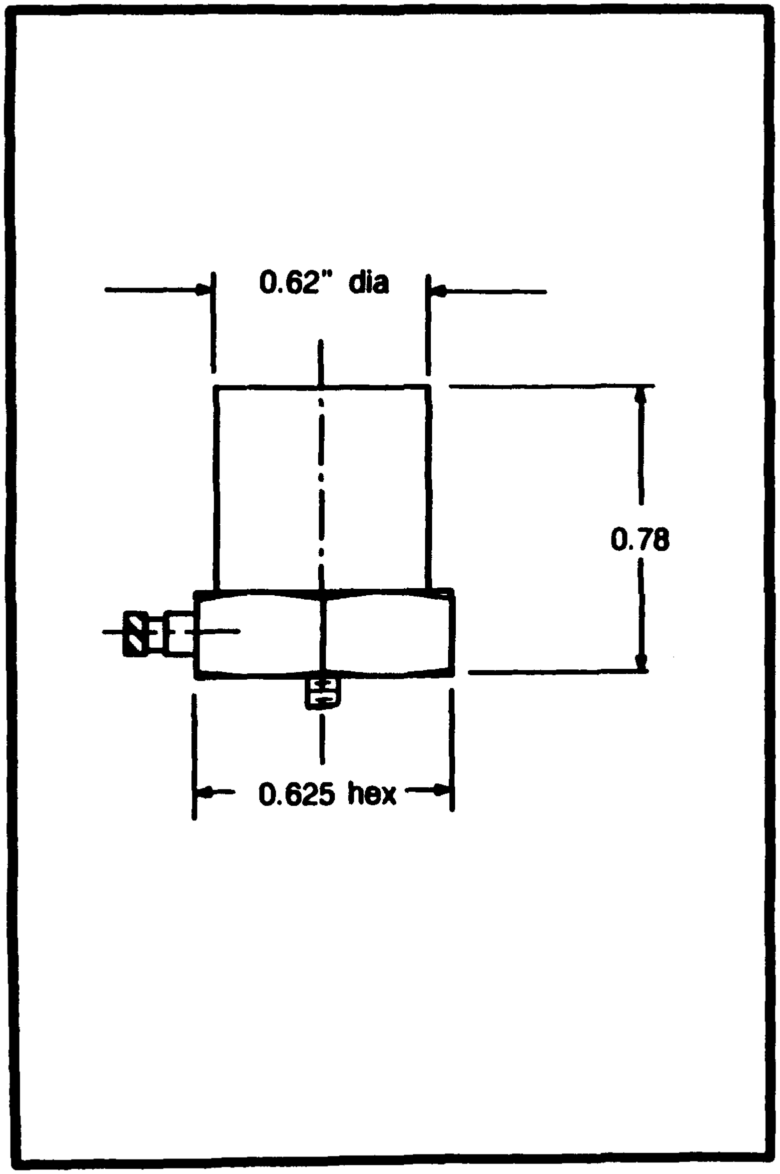

TYPE:
ACCELEROMETER PART NUMBER 2271F

SUPPLIER:
ENDEVCO

ACCURACY:
±2.5% FULL SCALE

OUTPUT SIGNAL:
0.0 TO 10 VOLTS D.C.

EXPERIENCE:
RL10, SSME TURBOPUMPS AND JET ENGINES

Figure 167. Vibration Sensors Description

Table 24. Speed Sensor Details

Sensor	Range RPM	Device Accuracy +/- FS	System Accuracy +/- F.S.	Signal	Connector Mates With / Pump Interface	Environ.	Remarks
Fuel Pump #1 Speed	7500-110,000	0.2%	0.5%	Frequency Modulated 1 V PK to PK	MS3126-10-6S / 0.749+.000/ -.003/8 micro inch surface	LH2, GH2, GHe	Rosemount SSME Type Speed Sensor will meet specification with an amplifier and limiting circuit to shape the output signal to the desired level and range for the controller.
Fuel Pump #2 Speed	7500-110,000	0.2%	0.5%	Frequency Modulated 1 V PK to PK	MS3126-10-6S / 0.749+.000/ -.003/8 micro inch surface	LH2, GH2, GHe	•
LOX Pump Speed	5,000-55,000	0.2%	0.5%	Frequency Modulated 1 V PK to PK	MS3126-10-6S / 0.749+.000/ -.003/8 micro inch surface	LH2, GH2, GHe	•

Table 25. Thermocouple Details

Sensor Parameter	Range DEG R	Target Device Accuracy +/-	System Target Accuracy +/-	Type (See Remarks Note 2)	Signal mv	Connector Mates With / Engine Interface	Environ.	Remarks
Fuel Pump Metal Temperature	38-600	1 Degree	10 Degrees	Type E Nickel Chromium vs. Copper-Nickel	-9.739 to 3.683	MS27473-8F-98SN / Mounted On Stud	Vacuum or Air.	Notes: 1. Required accuracy is to measure a delta of +/- 2R across the bearing. The absolute accuracy for the temperature readings is +/- 10 R for system. 2. Type E thermocouples are nickel-chronium (chromel) vs. copper-nickel (Constantan).
Fuel Pump No. 1 Bearing #1 Inlet Temperature	38-180	1 Degree	See Remarks Note 1	Type E Nickel-Chromium vs. Copper-Nickel	-9.739 to -8.069	MS27473-8F-98SN / 5/16/024-UNFJ	Gaseous Helium; Liquid Hydrogen	
Fuel Pump No. 1 Bearing #2 Inlet Temperature	38-180	1 Degree	See Remarks Note 1	Type E Nickel-Chromium vs Copper-Nickel	-9.739 to -8.069	MS27473-8F-98SN / 5/16-24-UNFJ	Gaseous Helium; Liquid Hydrogen	
Fuel Pump No. 1 Bearing #1 Exit Temperature	38-180	1 Degree	See Remarks Note 1	Type E Nickel-Chromium vs Copper-Nickel	-9.739 to -8.069	MS27473-8F-98SN / 5/16-24-UNFJ	Gaseous Helium; Liquid Hydrogen	
Fuel Pump No. 1 Bearing #2 Exit Temperature	38-180	1 Degree	See Remarks Note 1	Type E Nickel-Chromium vs Copper-Nickel	-9.739 to -8.069	MS27473-8F-98SN / 5/16-24-UNFJ	Gaseous Helium; Liquid Hydrogen	
Fuel Pump No. 2 Bearing #3 Inlet Temperature	38-180	1 Degree	See Remarks Note 1	Type E Nickel-Chromium vs Copper-Nickel	-9.739 to -8.069	MS27473-8F-98SN / 5/16-24-98SN	Gaseous Helium; Liquid Hydrogen	
Fuel Pump No. 2 Bearing #3 Exit Temperature	38-180	1 Degree	See Remarks Note 1	Type E Nickel-Chromium vs Copper-Nickel	-9.739 to -8.069	MS27473-8F-98SN / 5/16-24-UNFJ	Gaseous Helium; Liquid Hydrogen	

(Continued) Table 25. Thermocouple Details

Sensor Parameter	Range DEG R	Target Device Accuracy +/-	System Target Accuracy +/-	Type (See Remarks Note 2)	Signal mv	Connector Mates With / Engine Interface	Environ.	Remarks
Fuel Pump No. 2 Bearing #4 Inlet Temperature	38-180	1 Degree	See Remarks Note 1	Type E Nickel Chromium vs. Nickel-Copper	-9.739 to -8.069	MS27473-8F-98SN / 5/16-24-UNFJ	Gaseous Helium; Liquid Hydrogen	
Fuel Pump No. 2 Bearing #4 Exit Temperature	38-180	1 Degree	See Remarks Note 1	Type E Nickel-Chromium vs. Nickel-Copper	-9.739 to -8.069	MS27473-8F-98SN / 5/16/024-UNFJ	Gaseous Helium; Liquid Hydrogen	
LOX Pump Metal Temp	160-600	1 Degree	10 Degrees	Type E Nickel-Chromium vs Nickel-Copper	-8.401 to 3.683	MS27473-8F-98SN / Mounted On Stud	Vacuum, or Air	
LOX Pump Turbine Inlet Temperature	500-1200	1 Degree	10 Degrees	Type E Nickel-Chromium vs Nickel-Copper	0.262 to 28.409	MS27473-8F-98SN / 5/16-24-UNFJ	Gaseous Hydrogen	
LOX Pump Bearing #1 Inlet Temperature	160-215	1 Degree	See Remarks Note 1	Type E Nickel-Chromium vs Nickel-Copper	-8.401 to -7.418	MS27473-8F-98SN / 5/16-24-UNFJ	Gaseous Helium; Liquid Oxygen	
LOX Pump Bearing #1 Exit Temperature	160-215	1 Degree	See Remarks Note 1	Type E Nickel-Chromium vs Nickel-Copper	-8.401 to -7.418	MS27473-8F-98SN / 5/16-24-98SN	Gaseous Helium; Liquid Oxygen	

(Continued) *Table 25. Thermocouple Details*

Sensor Parameter	Range DEG R	Target Device Accuracy +/-	System Target Accuracy +/-	Type (See Remarks Note 2)	Signal mv	Connector Mates With / Engine Interface	Environ.	Remarks
LOX Fump Bearing #2 Exit Temperature	38-180	1 Degree	See Remarks Note 1	Type E Nickel Chromium vs. Nickel-Copper	-9.739 to -8.069	MS27473-8F-98SN / 5/16-24-UNFJ	Gaseous Helium; Liquid Hydrogen	
LOX Pump Bearing #3 Inlet Temperature	38-180	1 Degree	See Remarks Note 1	Type E Nickel-Chromium vs. Nickel-Copper	-9.739 to -8.069	MS27473-8F-98SN / 5/16/024-UNFJ	Gaseous Helium; Liquid Hydrogen	
LOX Pump Bearing #2 Inlet/ Bearing #3 Exit Temperature	38-180	1 Degree	See Remarks Note 1	Type E Nickel-Chromium vs Nickel-Copper	-9.739 to -8.069	MS27473-8F-98SN / 5/16-24-UNFJ	Gaseous Helium; Liquid Hydrogen	

Table 26. Pressure Transducer Details

Sensor Parameter	Range PSIA	Target Device Accuracy +/-	Target System Accuracy +/-	Excitation VDC +/- mv	Signal* mv	Transducer Elec. Conn. Mate With / Press. Conn	Environ.	Remarks
Igniter Chamber Pressure (Note 3)	0-1500	0.5% of F.S.	1% of F.S.	10+/-3	8 +\-5 To 108 +\-10	MS3126-10-6S / MS33646-E4	Gaseous Oxygen, Hydrogen, Helium, & Nitrogen	Notes: 1. Possible "Off the Shelf" Transducer Models: For Normal Accuracy Transducers (4% Device Target Accuracy) (A) Teledyne Taber Model 2211LT (B) Sensotron Model SEN-102A (C) Kulite Model BM-19-1100HT (D) Statham Model PA 8224 For Medium Accuracy Transducers (Device Accuracy Greater of 2% of Point or +/- 1 psi) (A) Sensotron Model SEN-102B (B) Kulite Model BM-20P-1100HT (C) Statham Model PA9502 For High Accuracy Transducers (Device Accuracy 0.5% of Full Scale (A) Sensotron Model SEN-202B (B) Kistler Model 614B 2 Inter-Propellant Seal Requires Two Transducers 3. Transducer in a Controlled Temperature Environment (+/-25 Degree R).
Main Chamber Pressure Low (Note 3)	0-150	0.5% of F.S	1% of F.S.	10+\-3	8 +\-5 To 108 +\-10	MS3126-10-6S / MS33646-E4	Gaseous Oxygen, Hydrogen, Helium, & Nitrogen	
Main Chamber Pressure Medium (Note 3)	0-500	0.5% of F.S	1% of F.S.	10+\-3	8 +\-5 To 108 +\-10	MS3126-10-6S / MS33646-E4	Gaseous Oxygen, Hydrogen, Helium, & Nitrogen	
Main Chamber Pressure High (Note 3)	0-1500	0.5% of F.S	1% of F.S.	10+\-3	8 +\-5 To 108 +\-10	MS3126-10-6S / MS33646-E4	Gaseous Helium, Hydrogen, Nitrogen & Oxygen.	
Low Pressure Helium Purge	15-1500	4% of F.S	5% of F.S.	10+/-3	8 +\-5 To 108 +\-10	MS3126-10-6S / MS33646-E4	Gaseous Helium	
High Pressure Nitrogen Purge	15-1500	4% of F.S	5% of F.S.	10+/-3	8 +\-5 To 108 +\-10	MS3126-10-6S / MS33646-E4	Gaseous Helium	

(Continued) Table 26. Pressure Transducer Details

Sensor Parameter	Range PSIA	Target Device Accuracy +/-	Target System Accuracy +/-	Excitation VDC +/- mv	Signal* mv	Transducer Elec. Conn. Mate With / Press. Conn	Environ.	Remarks
Low Pressure Nitrogen Purge	15-100	4% of F.S	5% of F.S.	10+/-3	8 +\-5 To 108 +\-10	MS3126-10-6S / MS33646-E4	Gaseous Nitrogen	
High Pressure Nitrogen Purge	15-1000	4% of F.S	5% of F.S.	10+/-3	8 +\-5 To 108 +\-10	MS3126-10-6S / MS33646-E4	Gaseous Nitrogen	
Fuel Pump 1 Inlet Pressure	0-75	Greater of 2% of PT. or 1.0 PSI	4% of F.S.	10+/-3	8 +\-5 To 108 +\-10	MS3126-10-6S / MS33646-E4	Liquid Hydrogen	
LOX Pump Inlet Pressure	0-75	Greater of 2% of PT. or 1.0 PSI	4% of F.S.	10+/-3	8 +\-5 To 108 +\-10	MS3126-10-6S / MS33646-E4	Liquid Oxygen	
IPS He/H2 Discharge Pressure	0-300	4% of F.S.0 PSI	5% of F.S.	10+/-3mv	8 +\-5 To 108 +\-10	MS3126-10-6S / MS33646-E4	Gaseous Oxygen/ Gaseous Hydrogen	
IPS He/02 Discharge Pressure	0-100	4% of F.S.	5% of F.S.	10+/-3mv	8 +\-5 To 108 +\-10	MS3126-10-6S / MS33646-E4	Gaseous Oxygen/ Gaseous Helium	
Inter Propellant Seal Helium	15-1000 (See Remarks, Note 2)	4% of F.S.	5% of F.S.	10+/-3mv	8 +\-5 To 108 +\-10	MS3126-10-6S / MS33646-E4	Gaseous Helium	

Table 27. Accelerometer Details

Sensor Parameter	Range	Target Device Accuracy +/-	Target System Accuracy +/-	Signal	Connector Type Pump Interface	Environ.	Possible Vendor P/N	Remarks
LOX Pump Radial Vibration	0-20G	2.5% of F.S.	5% of F.S.	0-10 mv	BCN 10-32-UNF	VAC/AIR	ENDEVCO 2271A OR KISTLER MODEL 8616A500	ENDEVCO 2271A with 2771A remote charge amp and a 2775A signal conditioner. Or Kistler model 8616A500 with 5023 charge amp with ENDEVCO 2775A cond.
Fuel Pump Assembly Radial Vibration	0-20G	2.5% of F.S.	5% of F.S.	0-10 mv	BCN 10-32-UNF	VAC/AIR	•	

Table 28. Preliminary Instrumentation List

NO.	HEADER	ITEM DESCRIPTION	UNITS	RANGES	LOCATION	NOTES
1	PSFENGIN	Press, Engine Fuel Inlet	psia	0-75	In facility plumbing	
2	TFFENGIN	Temp, Engine Fuel Inlet	°R	35-180	In facility plumbing	
3	WFFENGIN	Flow, Engine Fuel Inlet	lbm/sec	0-7.5	In facility plumbing	
4	TFFWFMIN	Temp, Fuel at Flowmeter	°R	35-180	In facility plumbing at flowmeter	
5	PSFP1IN	Press,Fuel Pump Inlet	psia	0-75	In rig plumbing at pump inlet	
6	TFFP1IN	Temp,Fuel Pump Inlet	°R	35-180	In rig plumbing at pump inlet	
7	TFFP1EX	Temp, 1st Stage Fuel Pump Exit	°R	35-180	In rig plumbing	
8	PSFP2EX	Press, 2nd Stage Fuel Pump Exit	psia	0-3000	In rig plumbing	
9	TFFP2EX	Temp, 2nd Stage Fuel Pump Exit	°R	35-180	In rig plumbing	
10	PSFT1IN	Press, Fuel Pump Turbine Inlet	psia	0-3000	In rig plumbing	
11	TFFT1IN	Temp, Fuel Pump Turbine Inlet	°R	500-1000	In rig plumbing	
12	PSFT1EX	Press, 1st Stage Fuel Pump Turbine Exit	psia	0-2000	In turbine housing	
13	PSFT2EX	Press, 2nd Stage Fuel Pump Turbine Exit	psia	0-2000	In rig plumbing	
14	TFFT2EX	Temp, 2nd Stage Fuel Pump Turbine Exit	°R	500-1000	In rig plumbing	
--						
15	PSFJBVIN	Press, Upstream of FJBV	psia	0-2000	In rig plumbing	
16	PSFJBVEX	Press, Downstream of FJBV	psia	0-2000	In rig plumbing	
17	TFFMXHIN	Temp, Mixer Hot Flow In	°R	500-1000	In rig plumbing	
18	TFFMXCIN	Temp, Mixer Cold Flow In	°R	40-900	In rig plumbing	
19	PSFINJIN	Press, Fuel Injector Manifold	psia	0-1500	In fuel injector manifold	
20	TFFINJIN	Temp, Fuel Injector Manifold	°R	400-900	In fuel injector manifold	

(Continued) Table 28. Preliminary Instrumentation List

NO.	HEADER	ITEM DESCRIPTION	UNITS	RANGES	LOCATION	NOTES
21	PSFCCCIN	Press, Combustion Chamber Coolant Inlet	psia	0-5000	In chamber coolant inlet flange	
22	TFFCCCIN	Temp, Combustion Chamber Coolant Inlet	°R	35-180	In chamber coolant inlet flange	
23	PSFCCCEX	Press, Combustion Chamber Coolant Exit	psia	0-4000	In chamber coolant exit flange	
24	TFFCCCEX	Temp, Combustion Chamber Coolant Exit	°R	300-900	In chamber coolant exit flange	
25	PSNSAC	Press, Nozzle Spring Arm Cavity	psia	0-2000	In nozzle spring arm cavity	
26	TFNSAC	Temp, Nozzle Spring Arm Cavity	°R	300-900	In nozzle spring arm cavity	
27	PSFNOZEX	Press, Nozzle Coolant Exit	psia	0-4000	In nozzle coolant exit flange	
28	TFFNOZEX	Temp, Nozzle Coolant Exit	°R	450-1100	In nozzle coolant exit flange	
29	PHCCAC01	Press, Combustion Chamber, Accoustic	Hz	1000-10,000	Thru face plate, separate port	
30	PHCCAC02	Press, Combustion Chamber, Accoustic	Hz	1000-10,000	Thru face plate, separate port	
31	PCHACC01	Press, Chamber, High Accuracy	psia	0-1500	Thru face plate	
–						
32	PSOENGIN	Press, Engine Oxidizer Inlet	psia	0-75	In facility plumbing	
33	TFOENGIN	Temp, Engine Oxidizer Inlet	°R	150-250	In facility plumbing	
34	WFOENGIN	Flow, Engine Oxidizer Inlet	lbm/sec	0-45	In facility plumbing	
35	TFOWFMIN	Temp, Oxidizer at Flowmeter	°R	150-250	In facility plumbing at flowmeter	
36	PSOPIN	Press, Oxidizer pump inlet	psia	0-75	In rig plumbing at pump inlet	
37	TFOPIN	Temp, Oxidizer Pump inlet	°R	150-250	In rig plumbing at pump inlet	
38	PSOTIN	Press, Oxidizer Pump Turbine Inlet	psia	0-4000	In rig plumbing	
39	TFOTIN	Temp, Oxidizer Pump Turbine Inlet	°R	450-1100	In rig plumbing	
40	PSSOCVIN	Press, Upstream of SOCV	psia	0-2500	In rig plumbing	
41	TFSOCVIN	Temp, Upstream of SOCV	°R	150-250	In rig plumbing	
42	PSPOSVEX	Press, Downstream of POSV	psia	0-2000	In primary LO2 injector manifold	
43	TFPOSVEX	Temp, Downstream of POSV	°R	150-250	In primary LO2 injector manifold	
44	PSSOCVEX	Press, Downstream of SOCV	psia	0-2000	In secondary LO2 injector flange	
45	TFSOCVEX	Temp, Downstream of SOCV	°R	150-250	In secondary LO2 injector flange	

(Continued) Table 28. Preliminary Instrumentation List

NO.	HEADER	ITEM DESCRIPTION	UNITS	RANGES	LOCATION	NOTES
46	PSAMB01	Press, Ambient/ Capsule	psia	0-15	On Facility	
47	PSAMB02	Press, Ambient/ Capsule	psia	0-15	On Facility	
48	VOLSPARK	Volts, Spark Plug Ingiter	volts	0-2000	Across spark plug	
49	AMPSPARK	Amps, Spark Plug Exciter	amps	0-1.5	Across exciter	
50	PSHYDSUP	Press, Hydraulic Supply to Acts.	psia	0-3000	On facility system	
51	PSHYDRTN	Press, Hydraulic Return from Acts.	psia	0-500	On facility system	
52	PSPNUSUP	Press, Pneumatic Supply to Acts.	psia	0-1500	On facility system	
53	PSPNURTN	Press, Pneumatic Return from Acts.	psia	0-250	On facility system	

TOTALS

Pressures	**28**
Temperatures	**21**
Flowmeters	**2**
Voltage	**1**
Amperage	**1**

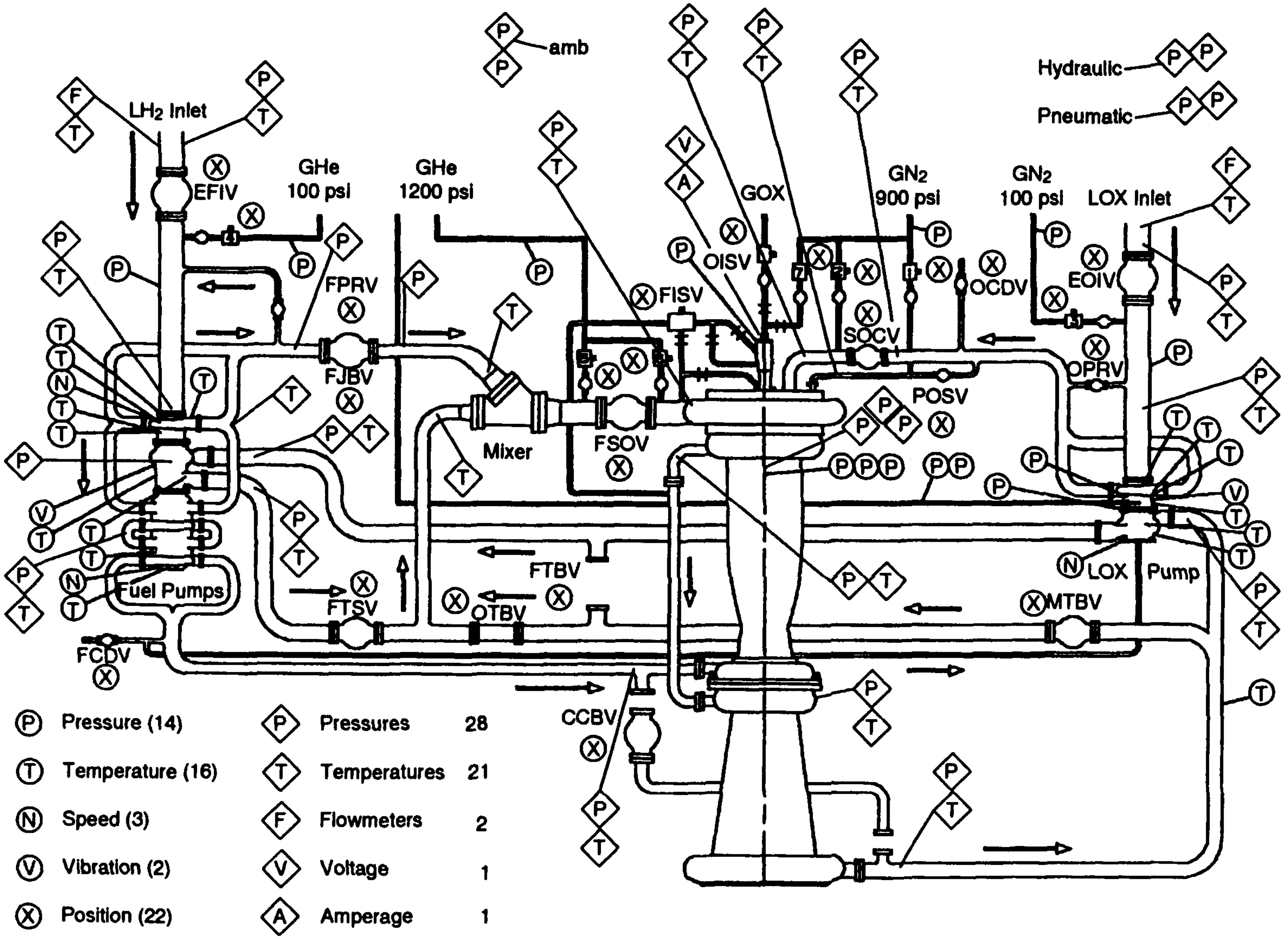

Figure 168. Performance Instrumentation in Addition to Control and Safety Sensors

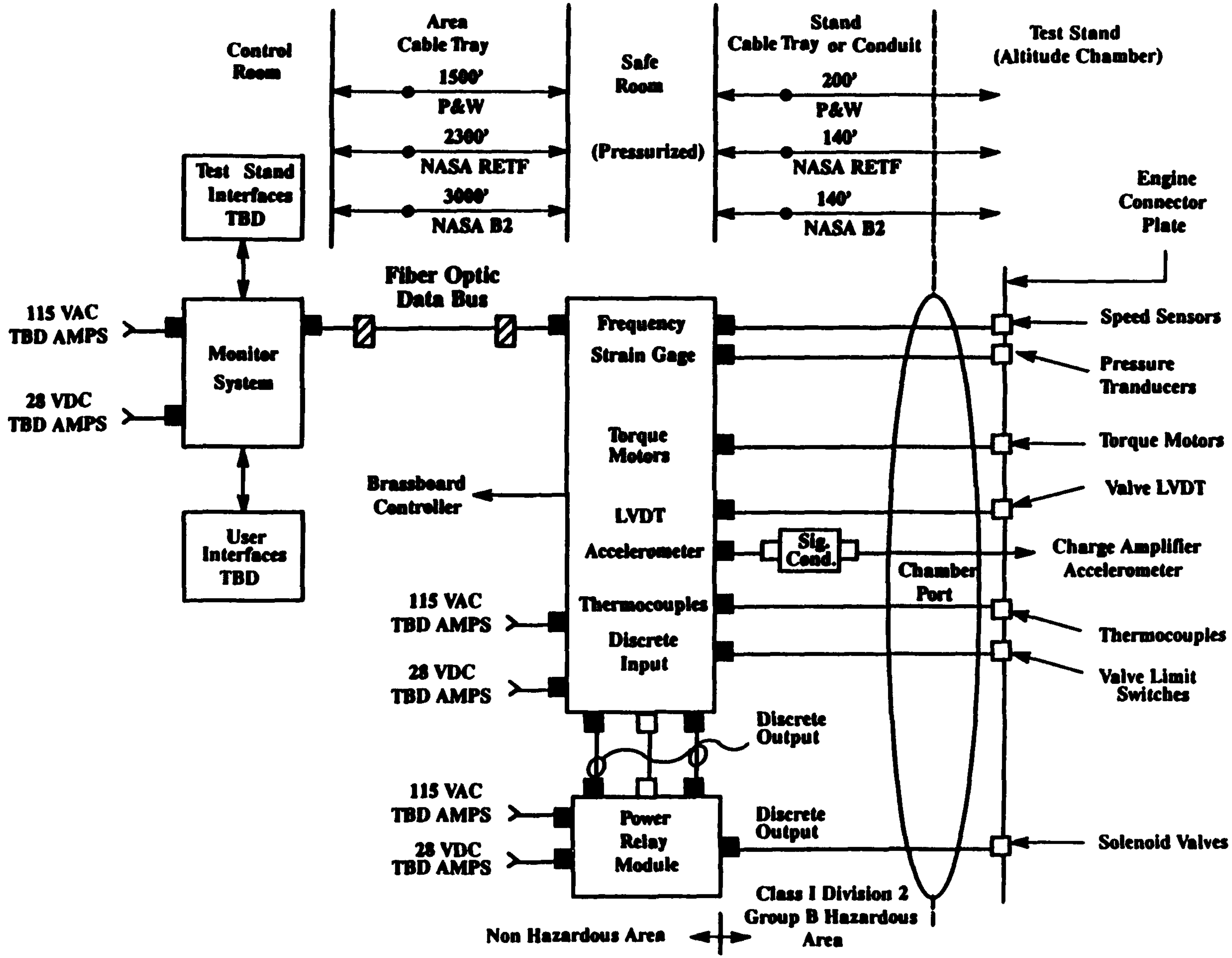

Figure 169. Simplified Control Interconnect Diagram

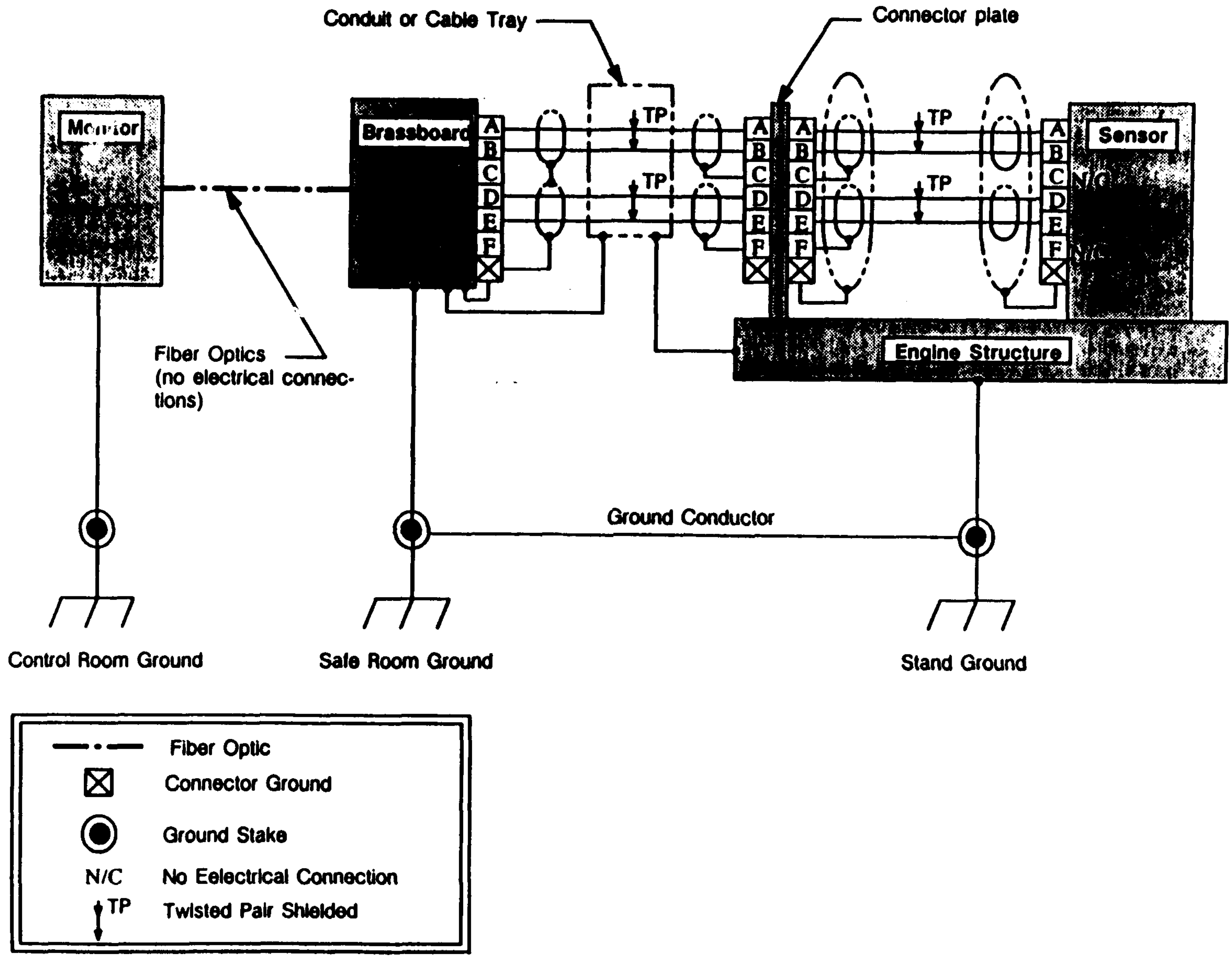

Figure 170. System Shielding and Grounding Plan Provides RFI, EMI and Lightning Protection

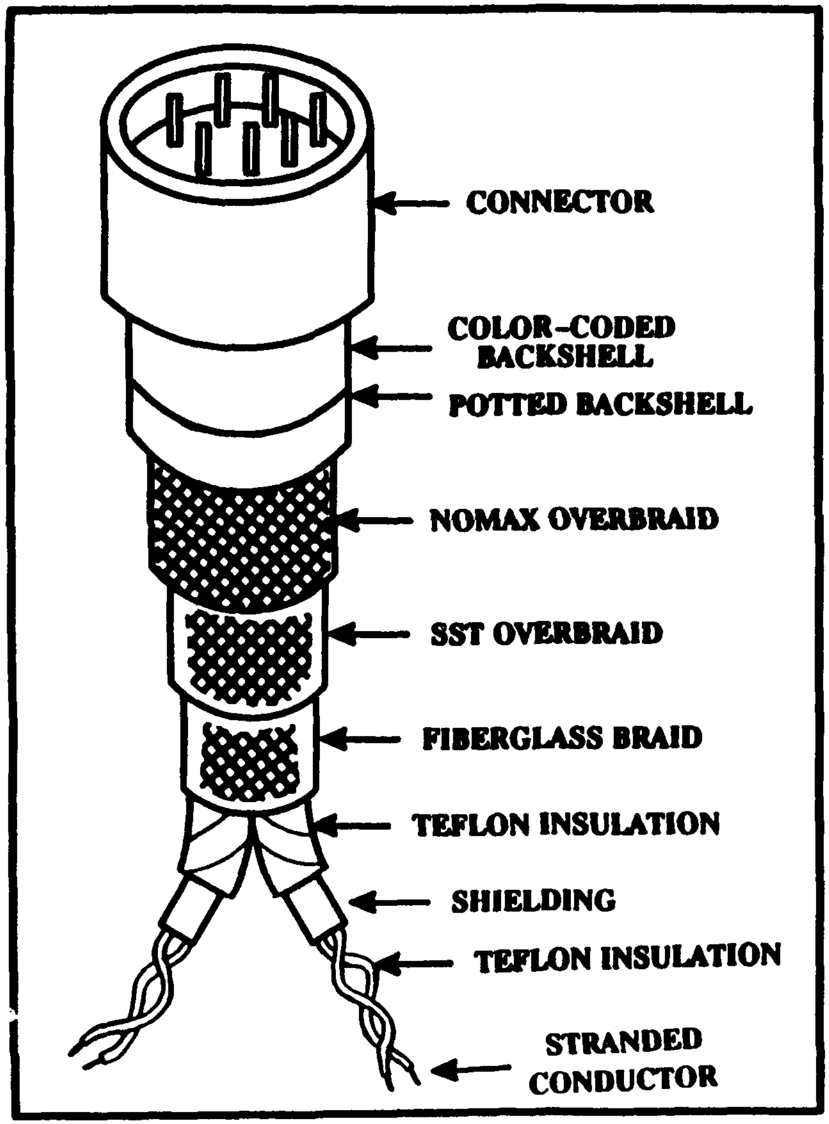

PRIMARY CONNECTOR TYPES:
- MIL-C-38999 SERIES II
- MIL-C-26482 SERIES I

FOOLPROOF INTERCONNECT:
- COLOR CODED SENSOR MOUNTING
- COLOR CODED BACKSHELLS
- CABLE LENGTH
- SENSOR/CABLE LABELS
- CONNECTOR SIZE & TYPE

POSSIBLE SUPPLIERS:
- SCOTT ELECTROKRAFT
- MILCOM

EXPERIENCE:
- SSME AND JET ENGINES

Figure 171. Cable Assembly Details

SECTION V
SYSTEM MECHANICAL INTEGRATION

The system mechanical integration is driven by test cycle configuration versatility and test stand size. The overall dimensional limits are dictated by the configuration of P&W's E6 altitude facility which limits the overall width of the engine to something less than six feet, Figure 172. The NASA testing facilities are larger than E6 and cause no dimensional restrictions on the layout envelope.

A bolted frame assembly is the heart of the system mechanical integration. Figure 173 depicts the frame partially assembled. It consists of a mounting pad configured to mate with E6, a top plate, 8 top rails, 8 side rails provisioned as appropriate with pump and controls mounting features, 8 primary bottom links, and 16 connection links. Completion of the frame assembly occurs as the rest of the engine is assembled. Figure 174 shows the thrust chamber assembly installed. Assembly continues as shown in Figures 175 through 179 with pump mounting provisions, LO_2 and fuel pumps, valves and actuators, mixer, and major plumbing lines installed. Small plumbing lines, wiring harnesses, instrumentation hookups, etc. (omitted for clarity) will be installed during final assembly.

The test cycle configuration versatility is achieved by locating the components most likely to require access on the exterior of the frame. For example, to prepare for the high mixture ratio demonstration, the two flange covers are removed and the fuel turbine bypass valve (FTBV) is installed, Figure 180. To prepare for the full expander cycle demonstration, the FTBV is moved to the oxidizer turbine bypass position and a spool piece is installed where the FTBV was located, Figure 181. The fuel jacket bypass valve (FJBV) can be moved to the combustion chamber bypass location for full expander testing at P_c above 750 psi. As shown in Figure 182, the pumps are also readily accessible for removal. The thrust chamber assembly, while more difficult, is also removable while the engine is still on the test stand, Figure 183. Methods of removing the thrust chamber through the top or bottom of the frame will be considered during the final design phase.

The estimated overall engine weight is 2200 pounds with the breakdown as follows:

	Pounds
Thrust Chamber Assembly	550
Valves, Mixer, etc.	550
Turbopumps	450
Frame	250
Plumbing	200
Miscellaneous	200
TOTAL	2200

The static seals selected will be provided by Furon, Inc. and were selected for their demonstrated high reliability in P&W's SSME-ATD program. Deformable metal seals will be used on all threaded (MS) bosses. The cryogenic seals will be Raco face seals and the hot seals will be Omni face seals. Both the Raco and Omni seals have fluoroloy jackets and MP35N preloading springs, Figure 184.

Configuration control for the AETB will be achieved using the existing P&W configuration management system.

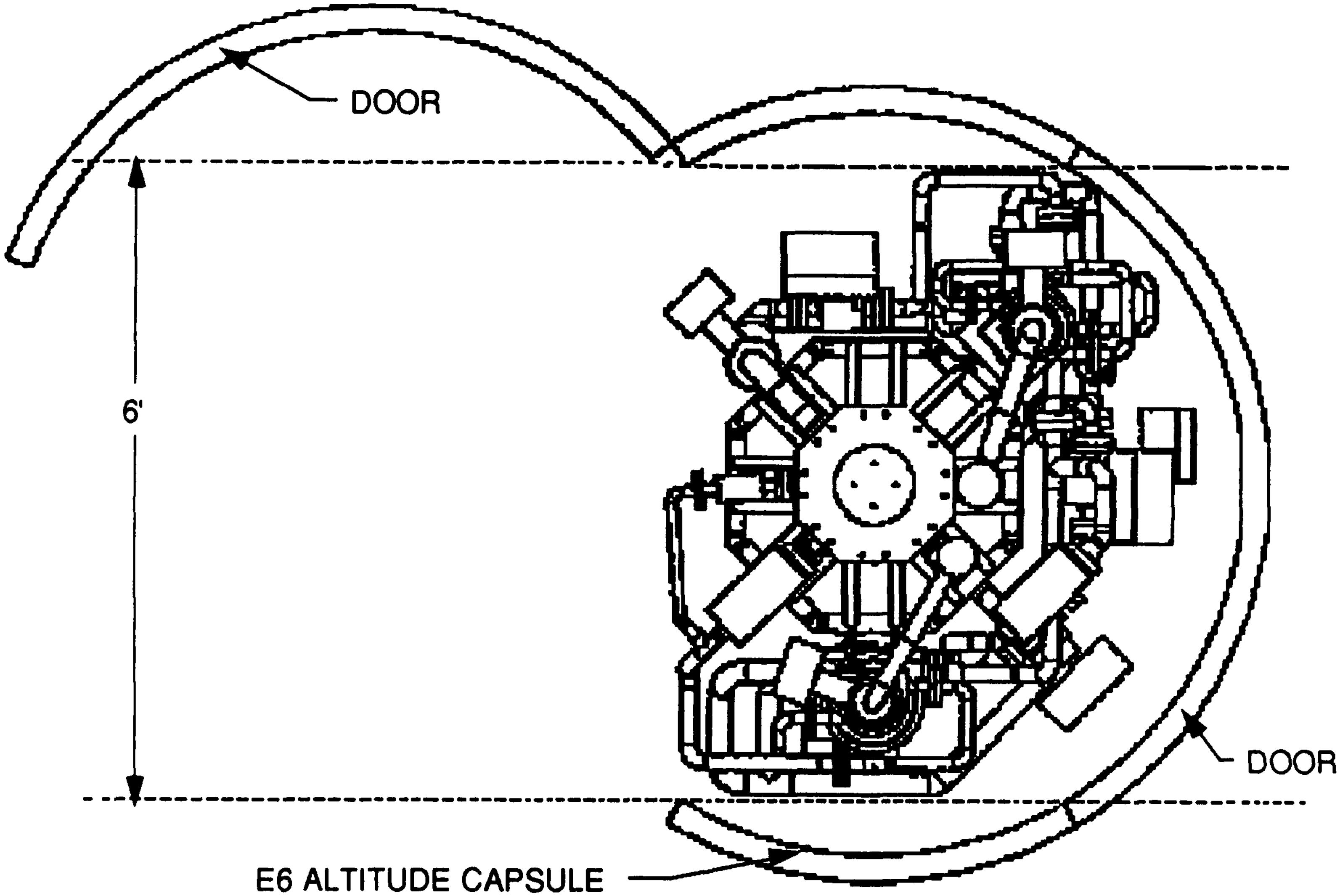

Figure 172. Test Stand Size Limitations on P&W's E6 Stand Establish the Maximum Test Bed Envelope

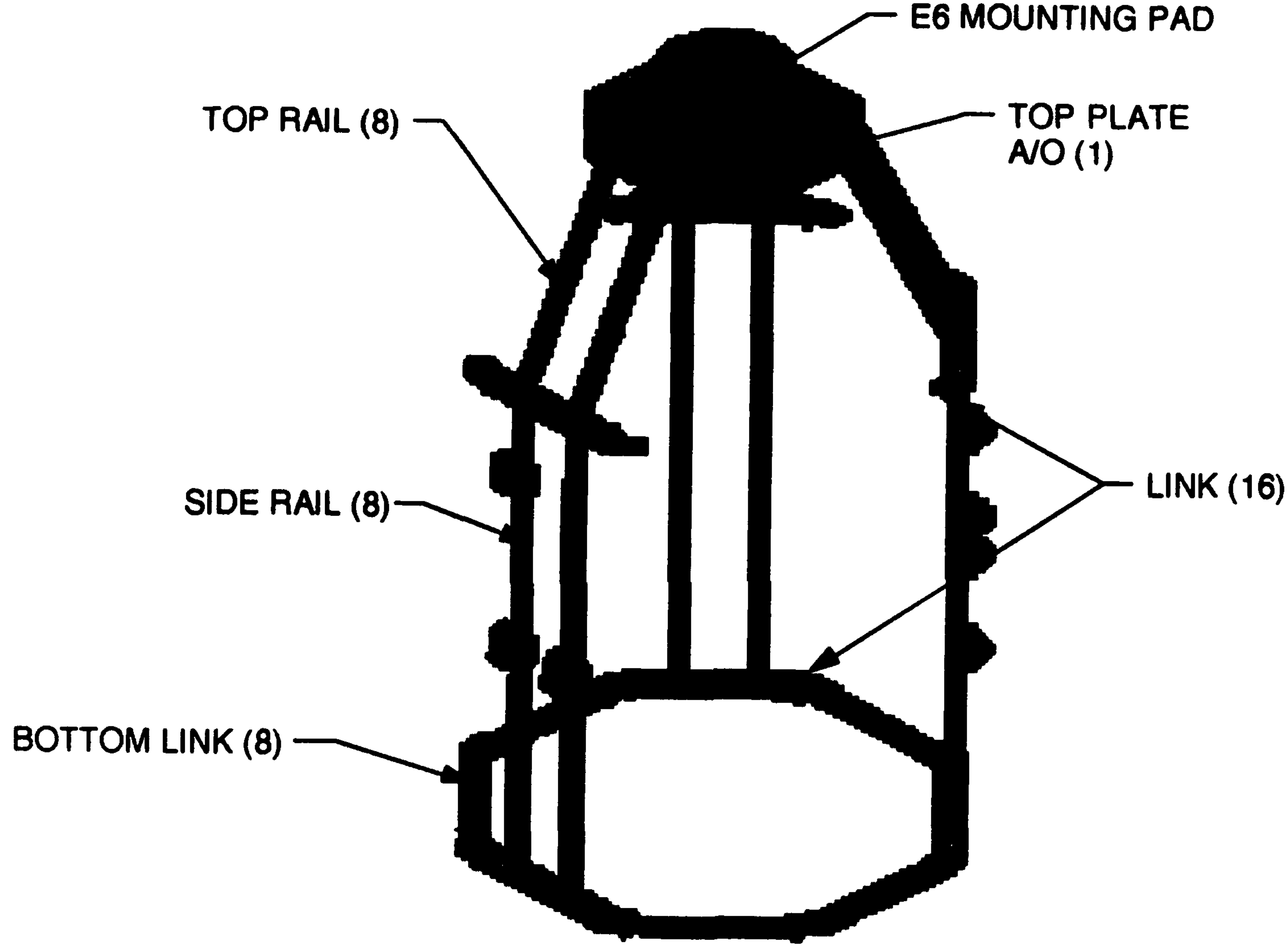

Figure 173. A Bolted Frame is the Heart of System Integration

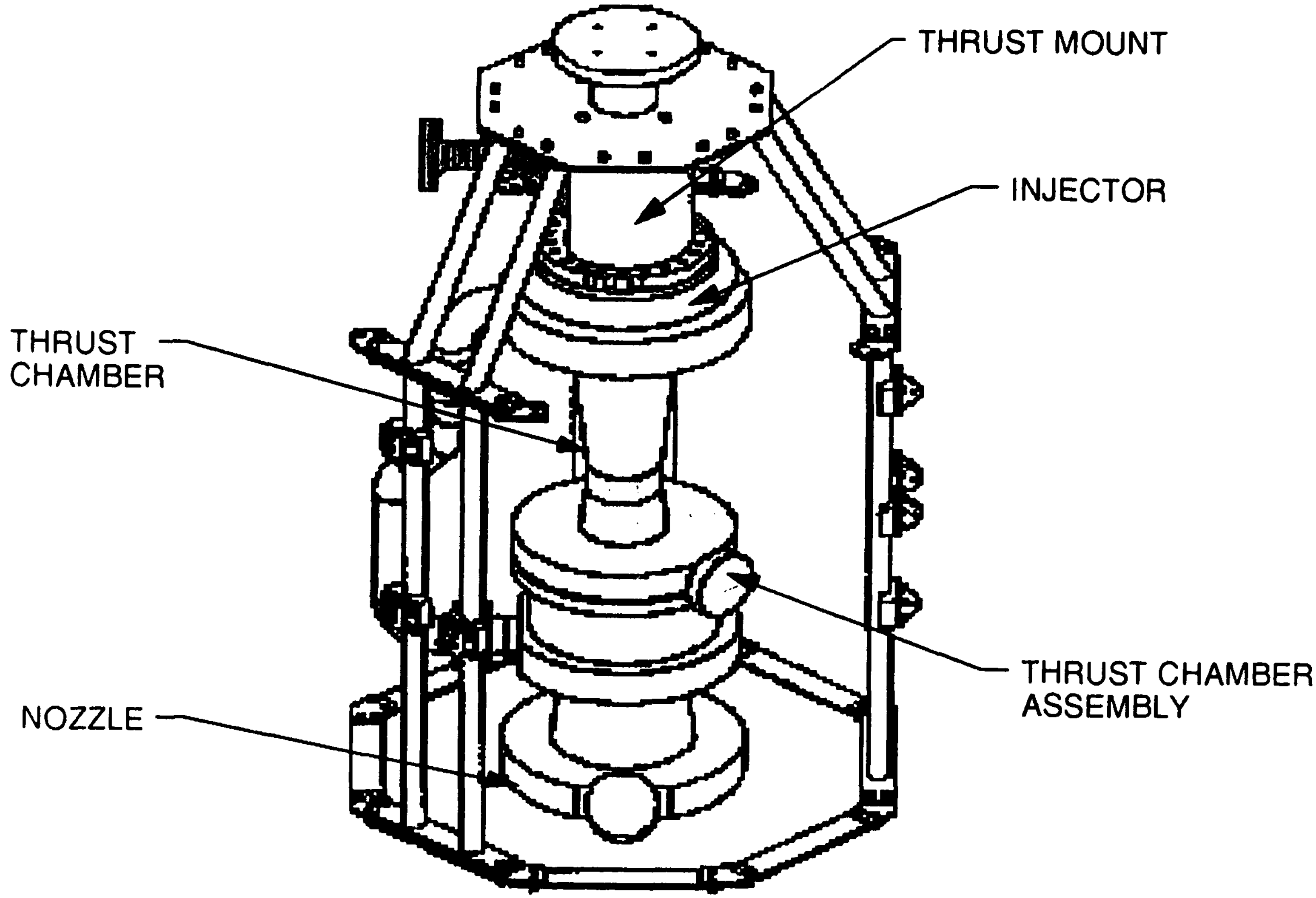

Figure 174. Thrust Chamber Assembly Installed in Partially Assembled Frame

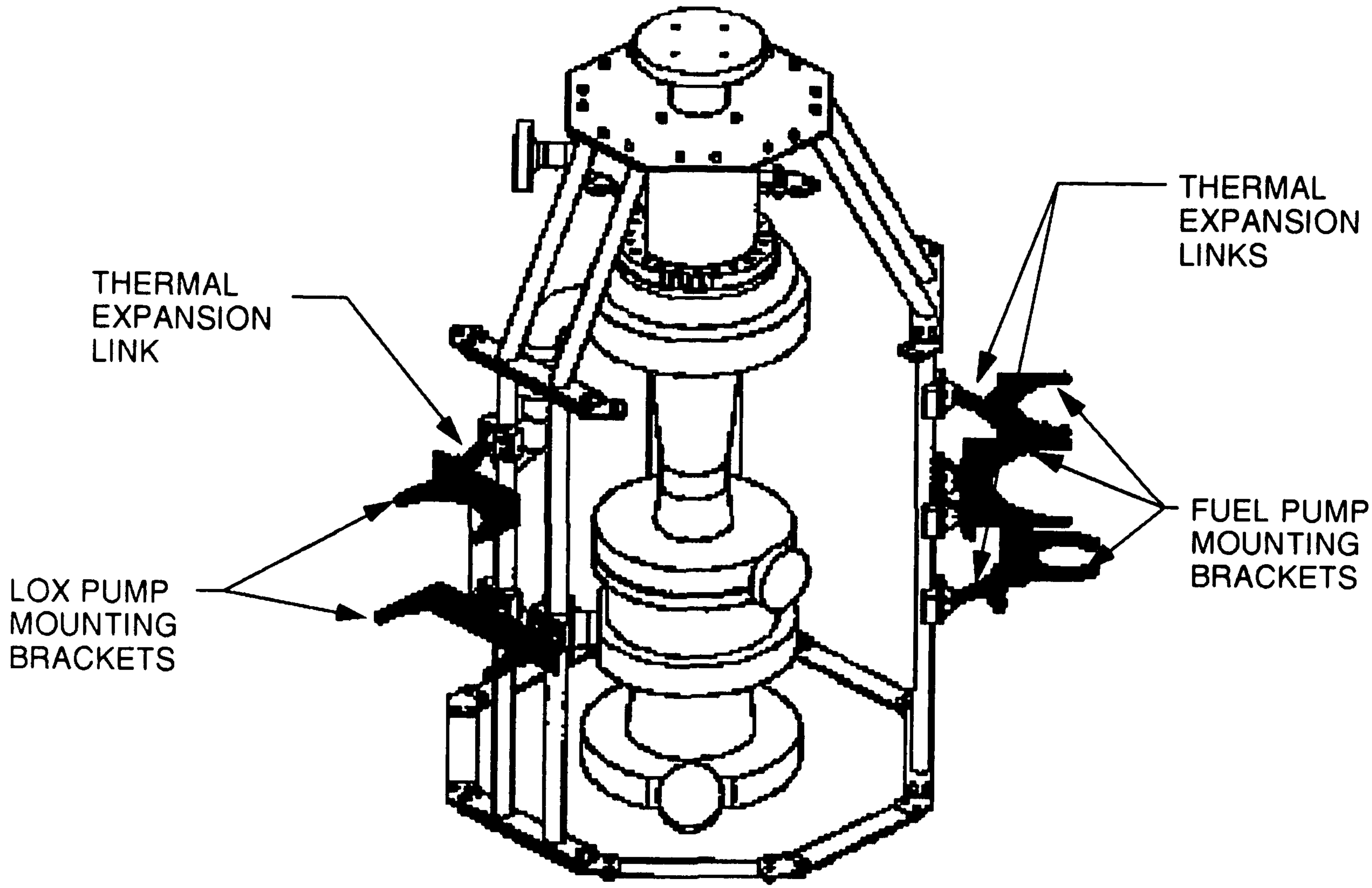

Figure 175. Pump Mounting Brackets Bolted in Place

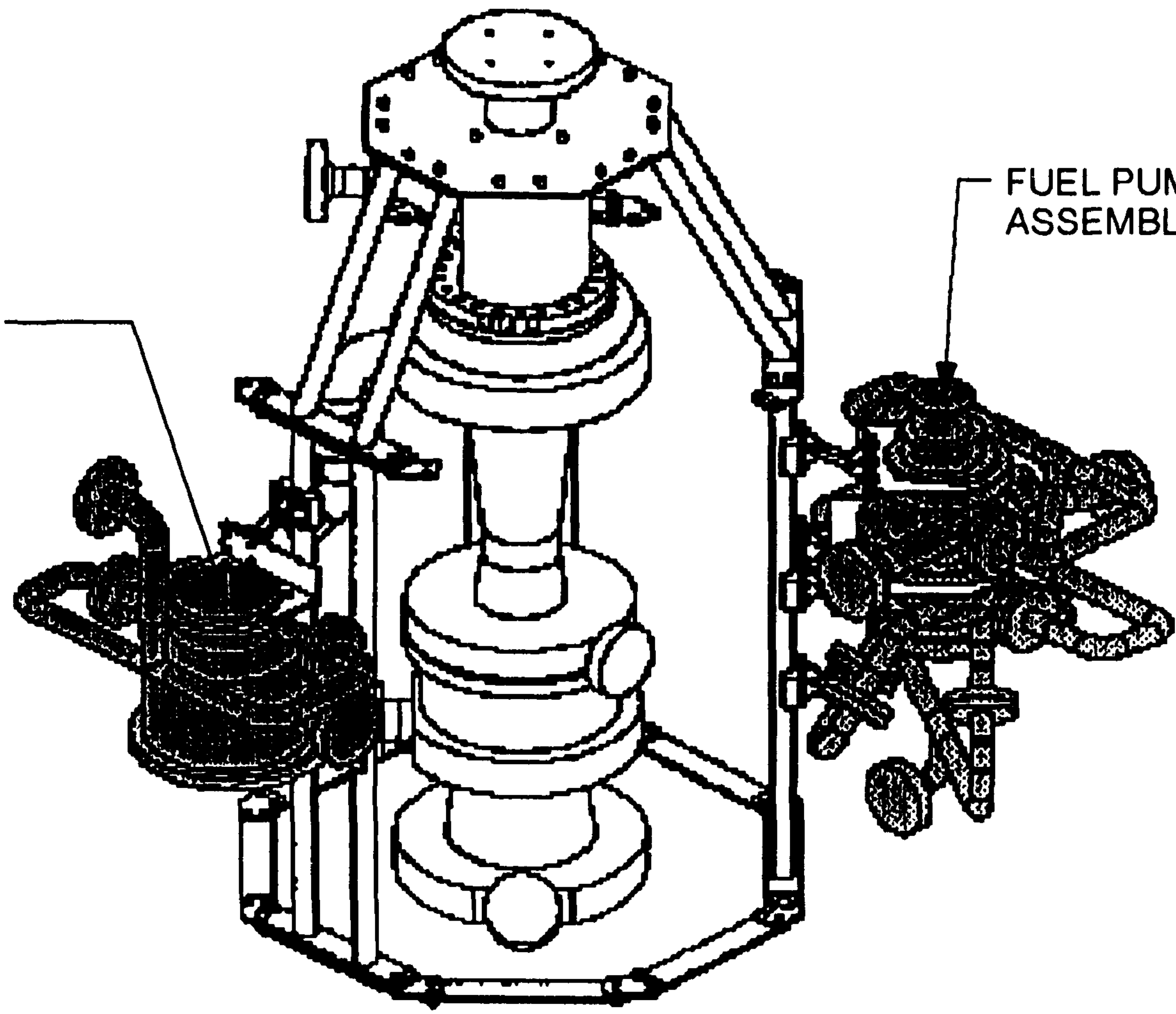

Figure 176. Oxygen and Fuel Pump Assemblies Attached to Frame

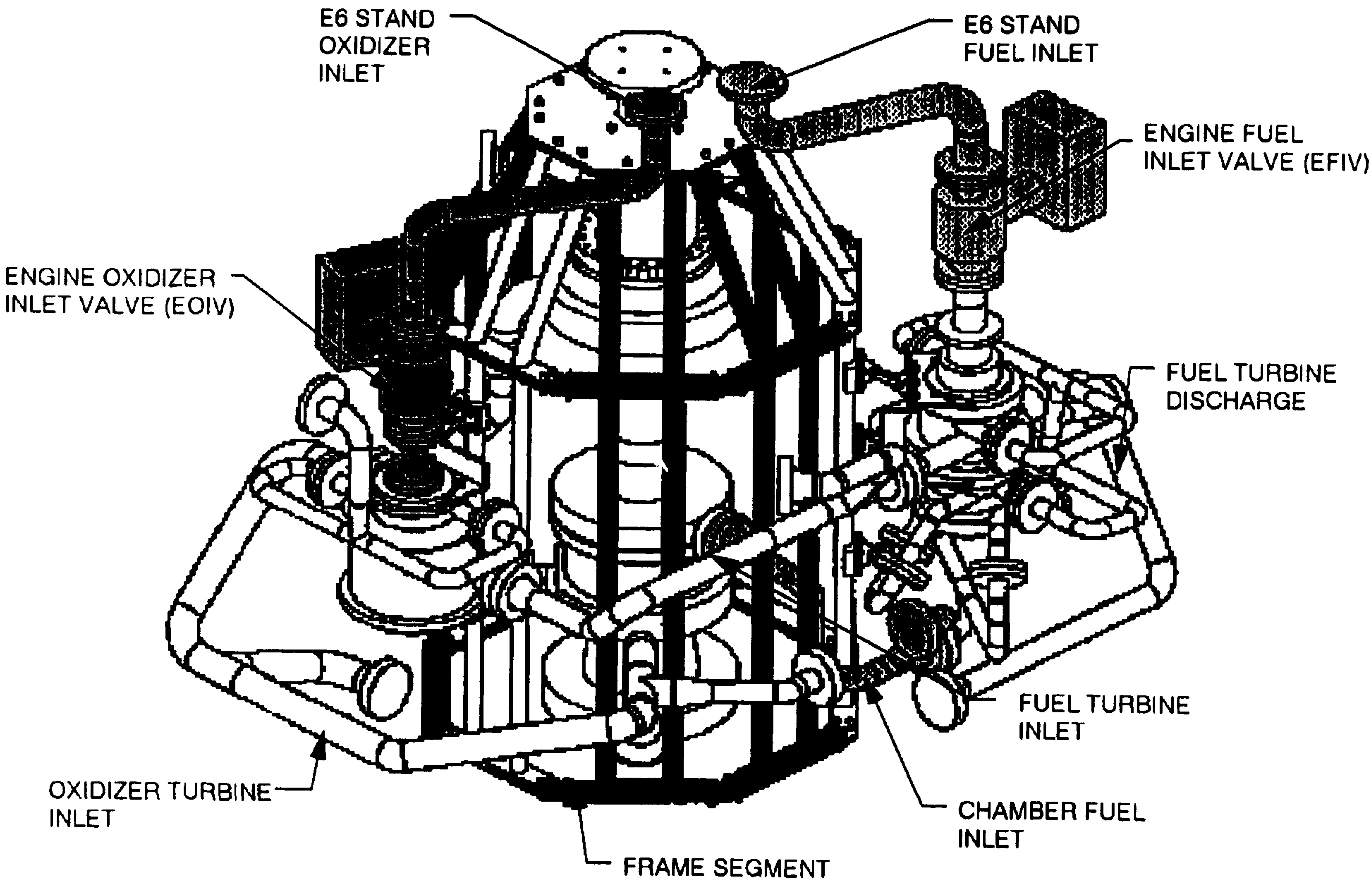

Figure 177. Frame Completed, Initial Plumbing and Valves Added

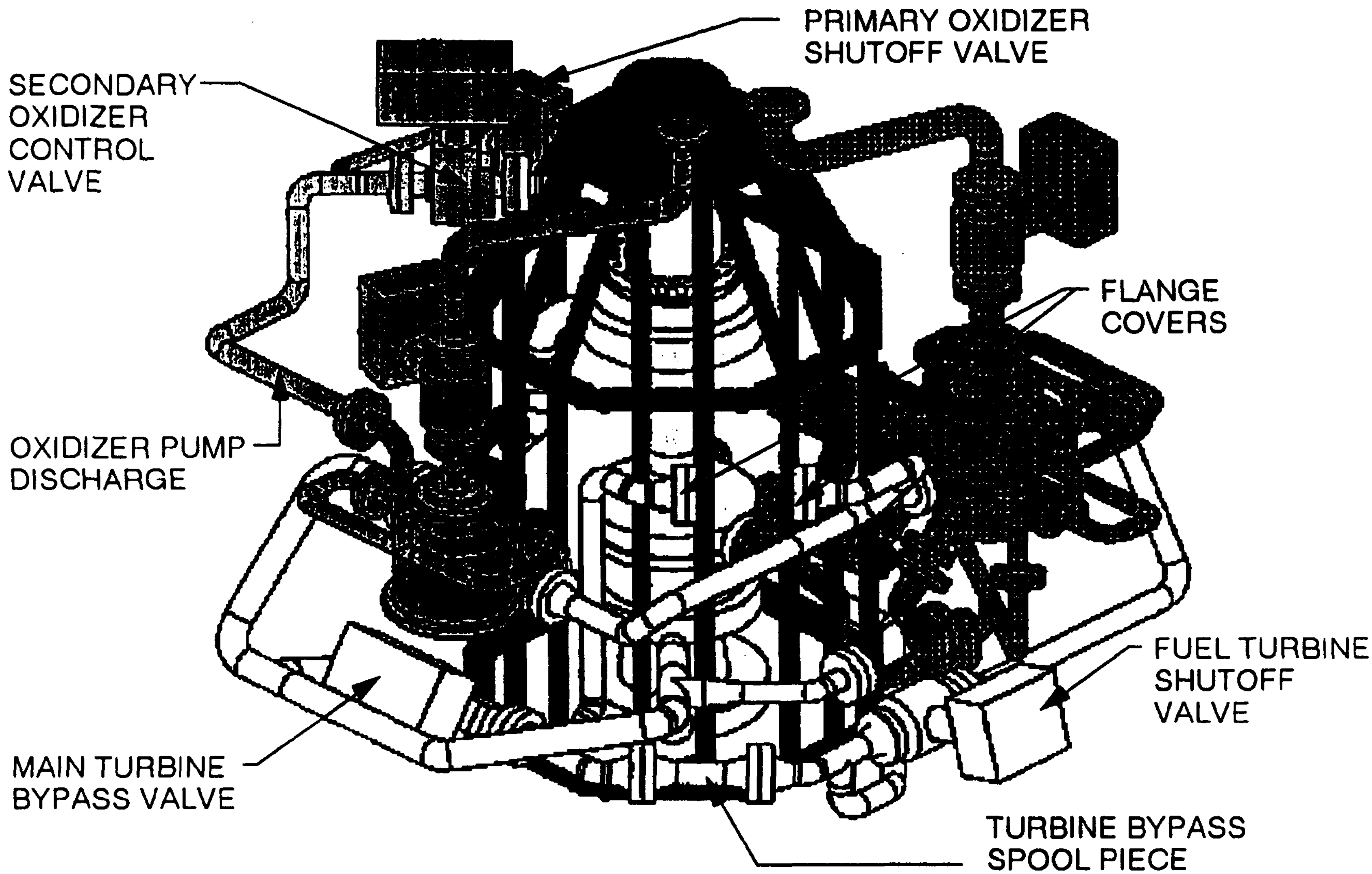

Figure 178. Split Expander Rig Assembly Completed

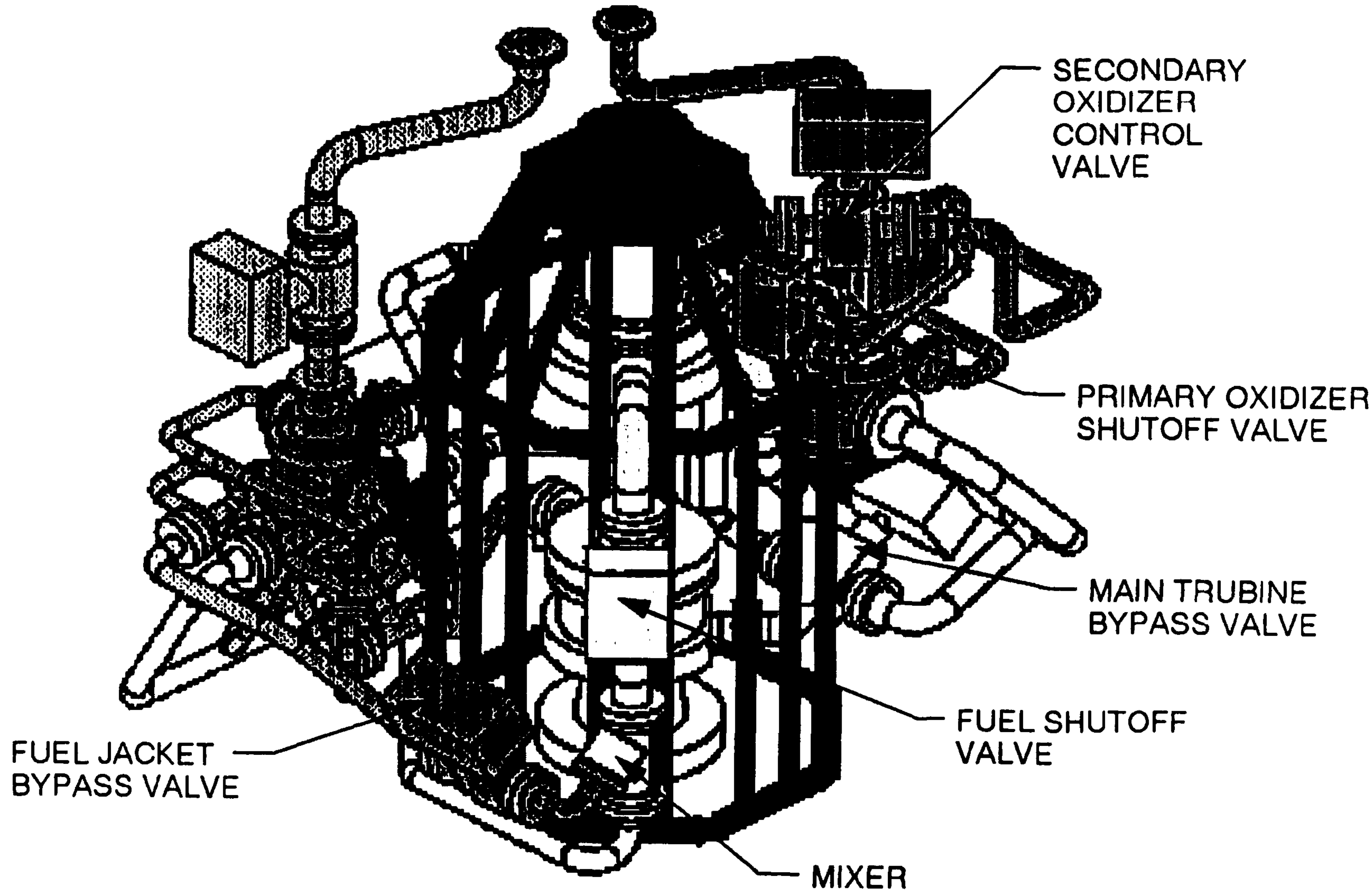

Figure 179. Reverse View of Split Expander Rig Assembly

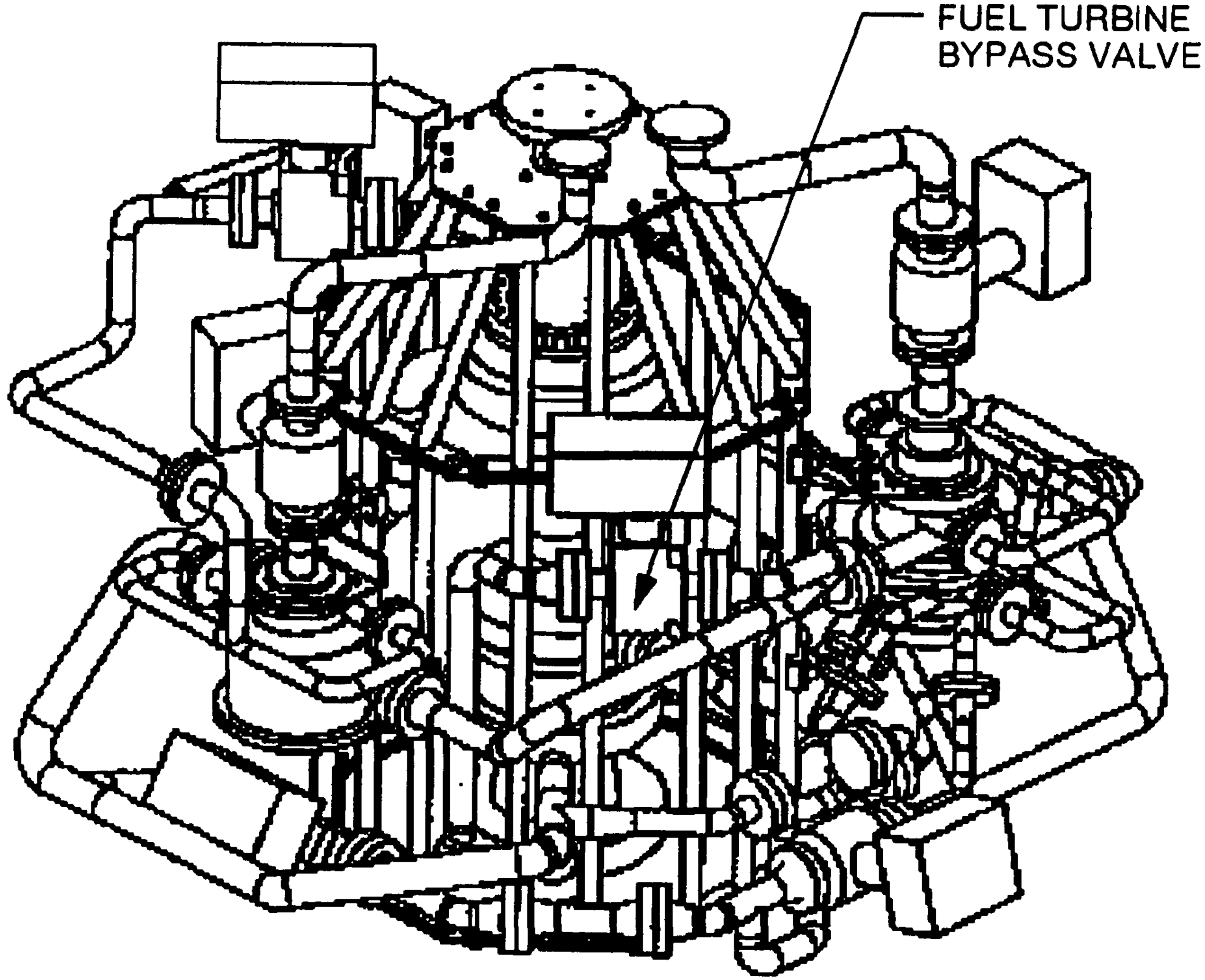

Figure 180. High Mixture Ratio Demonstration Adds Fuel Turbine Bypass Valve

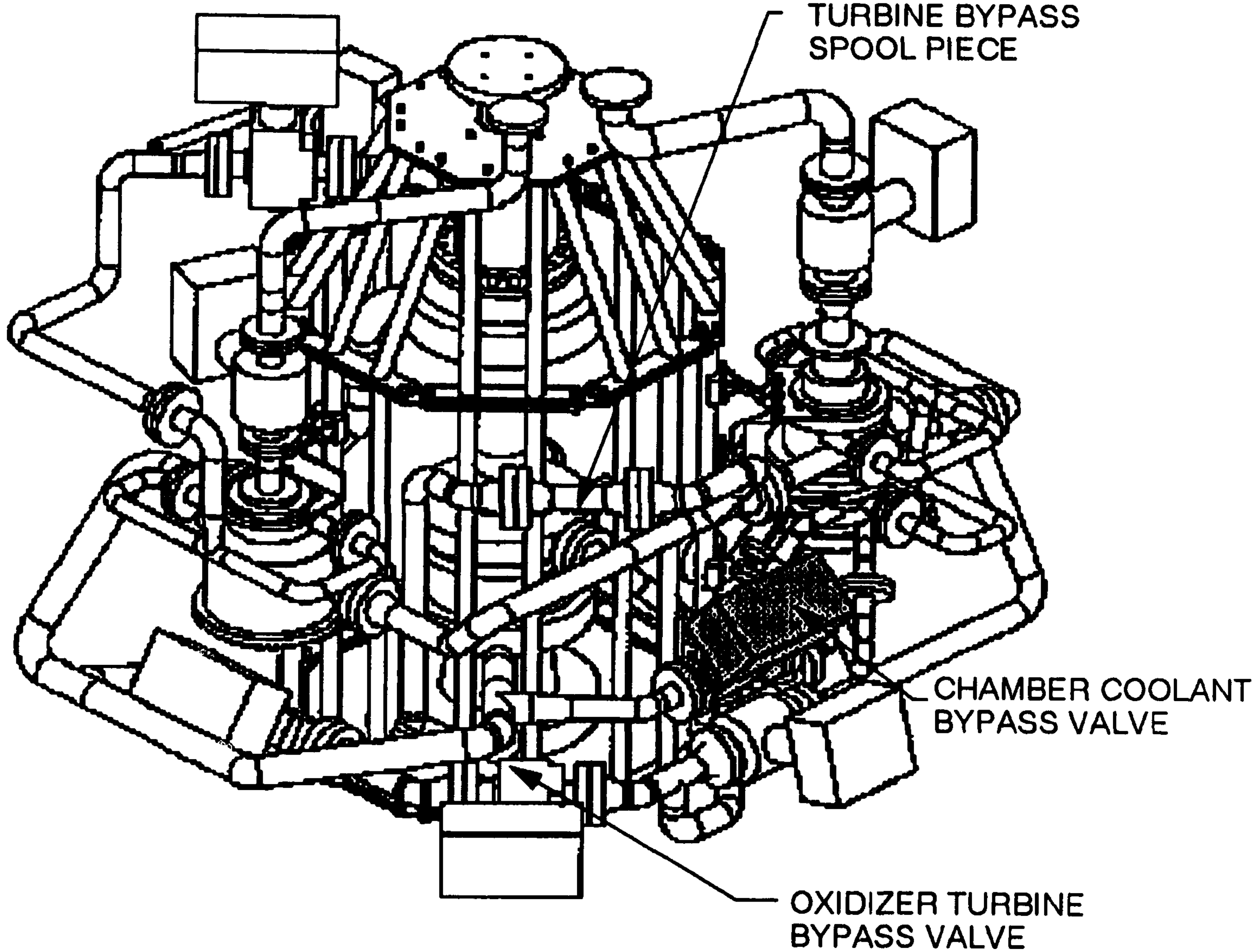

Figure 181. Full Expander Cycle Modifications

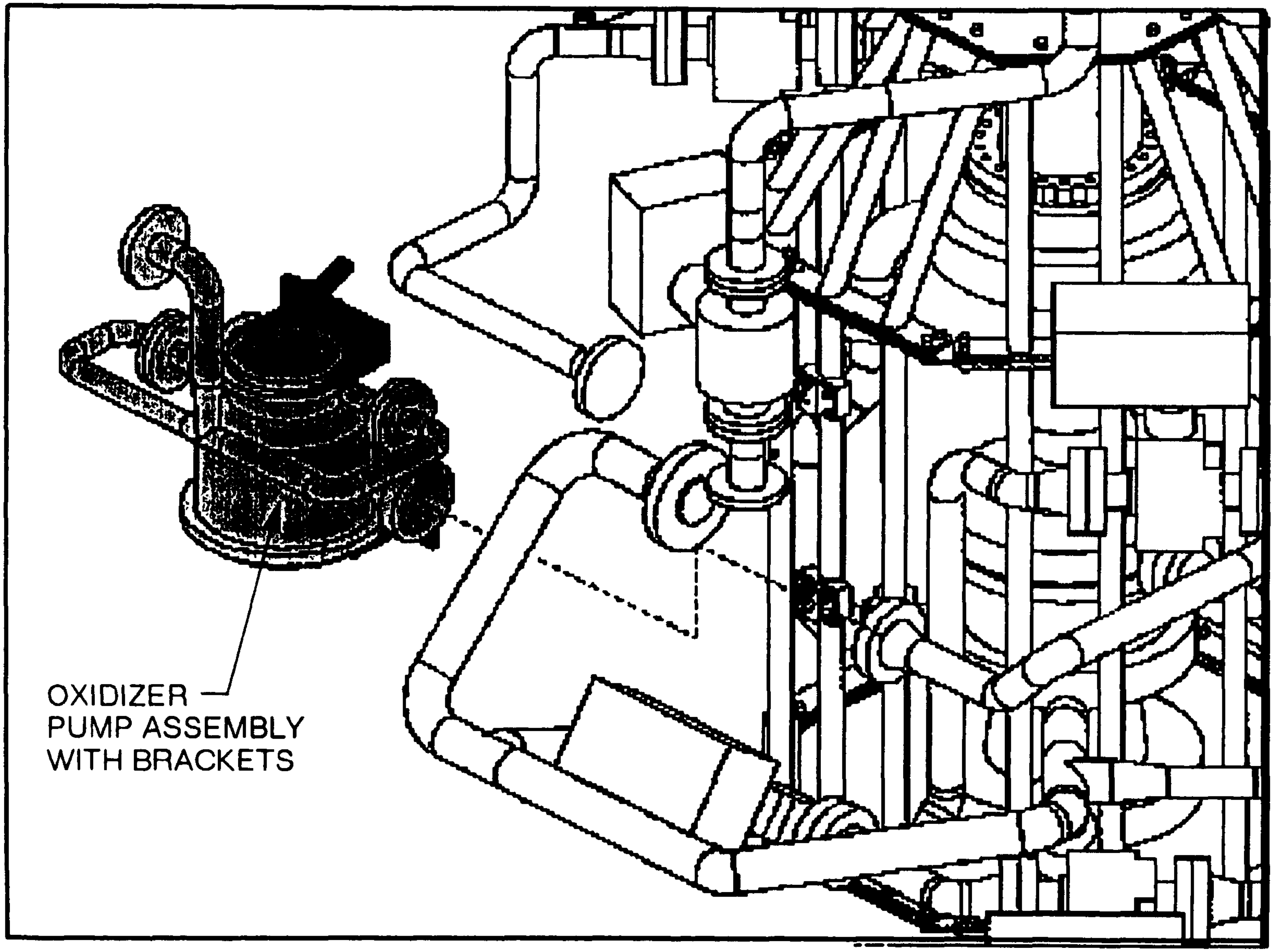

Figure 182. Turbopumps Readily Accessible for Maintenance

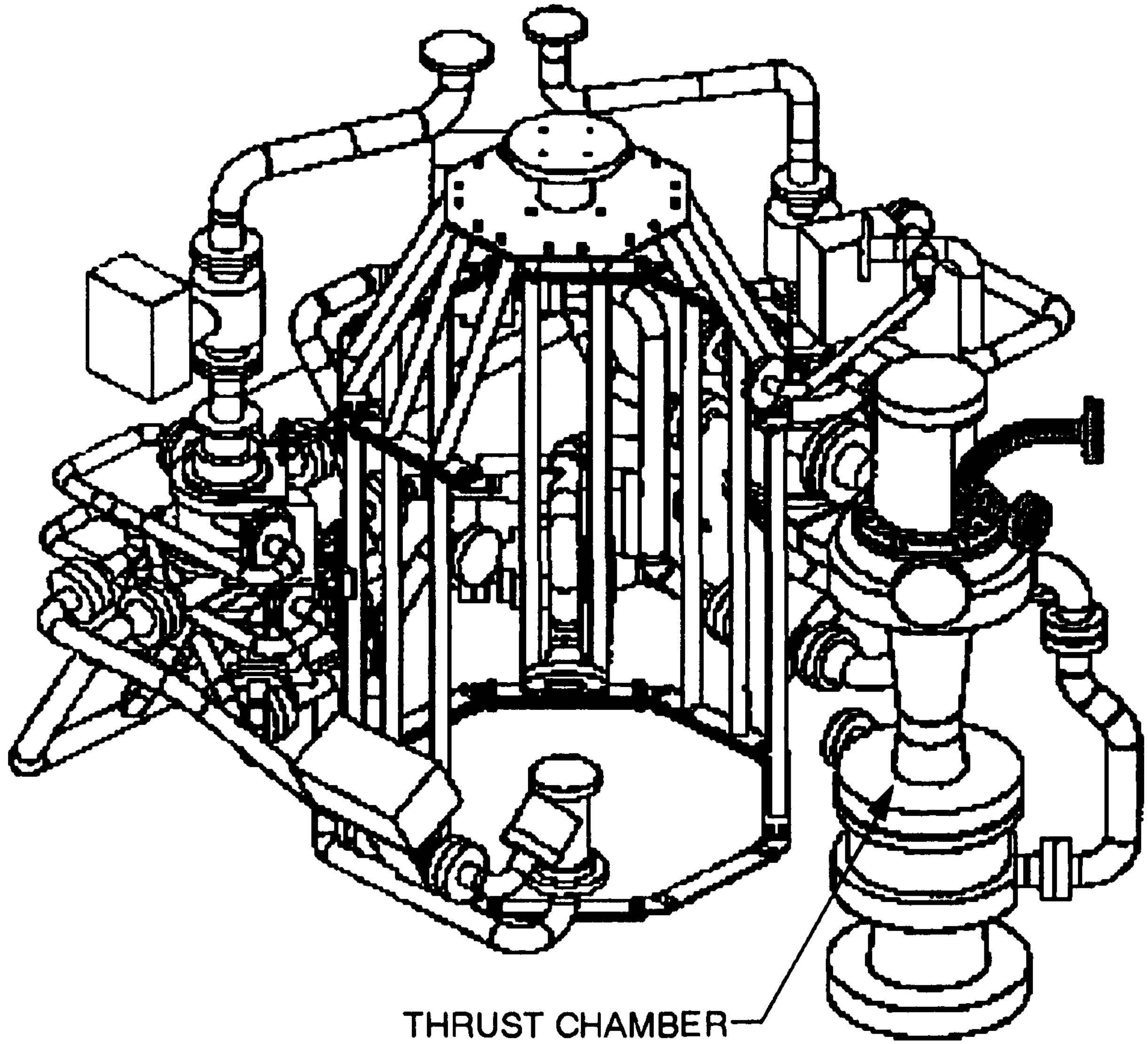

Figure 183. Thrust Chamber Can Be Removed With Some Frame Disassembly

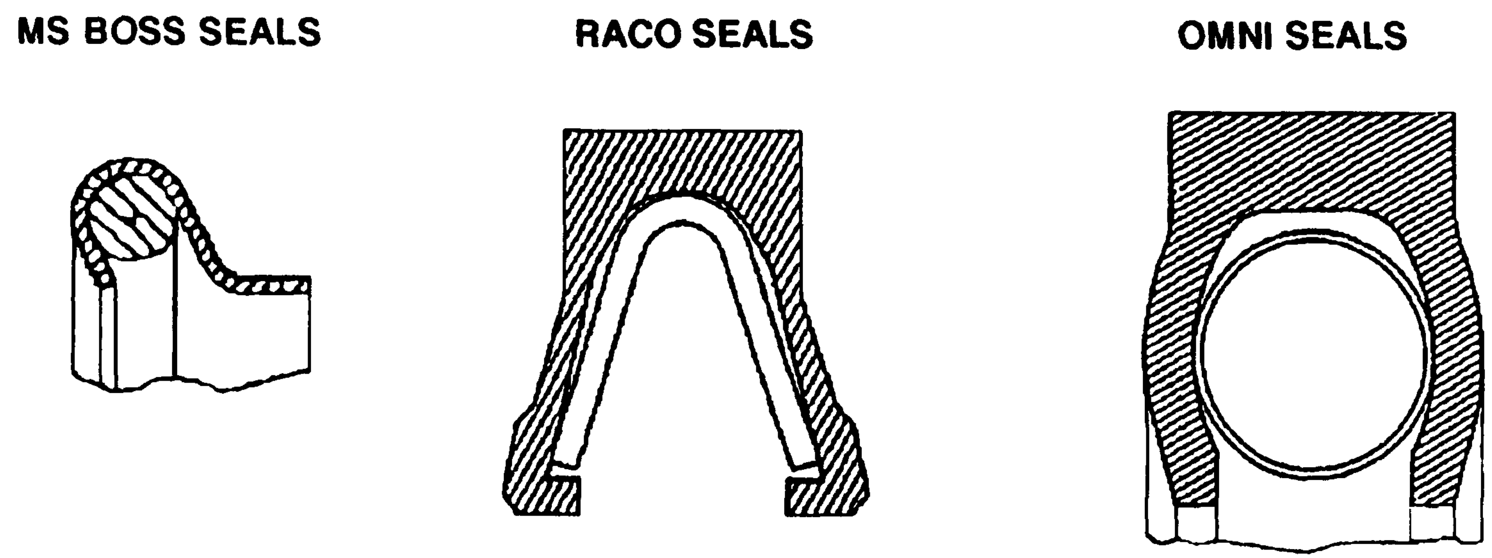

Figure 184. Static Seal Selections

SECTION VI
RELIABILITY AND SYSTEM SAFETY

The Failure Modes and Effects Analysis (FMEA) and the Preliminary Hazard Analysis (PHA) qualify the AETB preliminary design expected hazardous events resulting from an AETB hardware failure or a hazardous condition. To address AETB failure modes and their subsequent effects, P&W reliability established a FMEA team. The team is composed of personnel from Reliability, Manufacturing, Materials, System Safety, Design, and Maintainability. This team worked through the current drawings of each of the AETB components to 'brainstorm' each conceivable failure and the effects of that failure on the system. Using this team concept, the Product Assurance group instilled the concurrent engineering process into the FMEA to ensure each failure was exposed and addressed.

The AETB FMEA ground rules derived for the analysis were as follows:

- Single Point Failures — The FMEA considered only failure effects from a single failure occurrence within each component.

- Bottoms-Up Analysis — The FMEA is derived from investigating failures at the lowest hardware level possible within the current design phase.

- Most Probable Failure Effect — Each failure is investigated considering only the most likely system or subsystem effect.

- Hardware/Functional Mixture — Since the preliminary design was not detailed enough in some areas, the loss of a particular component function was investigated instead of a hardware failure.

- Criticality Classifications — Five criticality classifications were used in the analysis:

  -CRIT 1 — Major loss of AETB hardware

  -CRIT 1R — Loss of a single redundant element, both of which if lost would result in a major loss of AETB hardware

  -CRIT 2 — Loss of mission/test

  -CRIT 2R — Loss of a single redundant element, both of which if lost would result in a mission/test loss

  -CRIT 3 — A posttest hardware repair or unscheduled maintenance action resulting from a hardware failure.

Having established the failures and their effects, the FMEA documentation was then initiated. The documentation began by drawing the reliability functional block diagrams as shown in Figures 185 and 186. The purpose of the diagrams is to document physical and functional interfaces, double check the FMEA system effects by tracing a potential failure to its highest level, and to provide a reference showing correlation of the components addressed in the FMEA to their placement within the AETB system.

The FMEA document provides a full description of the failure modes and effects uncovered by the FMEA. The document is used to provide all the analysis findings to P&W and NASA-LeRC. The documentation format used by P&W provides charts for each failure mode allowing quick and concise evaluation of the failures, their causes, their effects, and the controls in place to prevent the failure or mitigate its effects. A sample page of the document is provided in Figure 187.

The final step in the FMEA documentation is to prepare the Critical Items List (CIL). The CIL provides a summary of all the CRIT 1 and 1R failures uncovered during the FMEA. The purpose of the CIL is to highlight those failures and to generate, as a part of the FMEA process, all rationale for retention justifying why the failure should not be a concern in subsequent AETB testing. The following table summaries the FMEA findings:

	CRIT Classifications				
Component	1	1R	2	2R	3
Injector/Igniter	1	0	3	0	0
MCC/Nozzle	0	0	2	0	0
LO_2 Turbopump	2	0	7	0	4
Hydrogen Turbopump	1	0	6	0	3
Controls	0	0	55	0	0
Ducting/Mixer	0	0	3	0	0
TOTAL	4	0	76	0	7

Of the 87 failure modes analyzed, four have been identified as potential CRIT 1 failures. These four failure modes are within the injector housing, the hydrogen turbopump primary and secondary blisk, the LO_2 turbopump turbine blisk, and the LO_2 turbopump bearing. These failures will be monitored through the design to identify and apply proper design considerations and/or controls.

The FMEA and CIL will be updated throughout the AETB test phases to ensure proper attention is paid to all interfaces. The FMEA and CIL documentation for the AETB preliminary design was delivered to NASA-LeRC in December 1990 as P&W FR-21322.

The PHA was performed by P&W's System Safety Group. The PHA is used within the design process to identify hazards early in the design process, to ensure all identified hazards are recognized and addressed, to aid in the formation of controls for the hazards, and to track all identified hazards to closure. These hazards may be the result of characteristics in the design, a hardware failure, environmental effects, or human error. The PHA also considers the hazardous conditions occurring at various phases of test bed life including handling and transportation, test bed assembly and mounting, test bed operation, and test bed maintenance.

As with the AETB FMEA, ground rules were derived for the PHA prior to initiating the analysis. The ground rules used for the analysis were as follows:

- Reference Document — MIL-STD-882B is the reference document used for the AETB PHA.
- Hazard Groups — The AETB hazards were categorized into the following hazard groups: fire/explosion, projectiles, temperature, pressure, vibratory energy, rotational energy, and electrical energy.
- Worst Credible Hazard Effect — Each failure was investigated considering only the most likely system or subsystem effect.
- Hazard Severities — Four hazard severity classifications, established from MIL-STD-882B, were used in the analysis:

Description	Class	Mishap Definition
Catastrophic	I	Death, or system loss requiring complete replacement of the test facility.
Critical	II	Severe injury or occupational illness requiring hospitalization, or major system damage requiring removal of the AETB to complete repairs.
Marginal	III	Minor injury or occupational illness requiring first aid, or minor system damage which can be repaired with the AETB installed but will require more than two days.
Negligible	IV	Less than minor injury or minor system damage.

- Hazard Probabilities — Five hazard probability ratings, established from MIL-STD-882B, were used in the analysis:

Rating	Probability Definition
A	Likely to occur frequently during testing of the AETB.
B	Will occur more than twice during testing of the AETB.
C	Will occur more than once during testing of the AETB.
D	Unlikely but can reasonably be expected to occur during testing of the AETB.
E	Unlikely to occur, but possible.

Upon qualifying the hazardous events to the lowest level cause, the System Safety Engineer completes a Hazard Control Sheet (HCS) which is part of the Hazard Control and Tracking (HCAT) System. This form, Figure 188, is used to track each event and subsequent cause through a sequential status until the event is closed. Until final closure, the HCAT is in either an Open (acceptable hazard controls have been identified but have not been implemented), or a Closed status.

To close an HCAT event, acceptable hazard controls are identified and proof of their implementation exists, and the appropriate authority accepts the residual risk. The HCAT may also be closed by the appropriate authority accepting the associated risk with no additional controls necessary. The authorization to close the HCAT is derived by the Hazard Risk Index, a combination of the hazard severity and the hazard probability. The following table summarizes the AETB closure authorities.

Hazard Risk Index	Acceptance/Closure Authority
IA, IB, IIA, IIB, IIIA	NASA-LeRC
ID, IIC, IID, IIIB, IIIC	P&W AETB Program Manager
IE, IIE, IIID, IIIE, IVA, IVB	P&W AETB System Safety Manager
IVC, IVD, IVE	P&W AETB System Safety Engineer

The final step of the AETB PHA was to compile all of the HCS forms within the PHA document. This document provides NASA-LeRC and P&W with a listing of all conceivable hazardous events uncovered during the preliminary design phase. The following table summarizes the findings of the PHA.

Component	Category I	II	III	IV
Injector/Igniter	0	6	2	0
MCC/Nozzle	0	3	4	0
LO_2 Turbopump	0	6	5	0
Hydrogen Turbopump	0	3	6	0
Controls	0	5	2	0
Ducting/Mixer	0	3	1	0
TOTAL	0	26	20	0

P&W System Safety group completed the PHA and submitted it to NASA-LeRC as FR-21321 in December ›90. The PHA will be updated as the design progresses, to a Sub-System Hazard Analysis (SSHA) and a ›stem Hazard Analysis (SHA) per the AETB System Safety Program Plan. These documents will be completed ıe month prior to the AETB Critical Design Review.

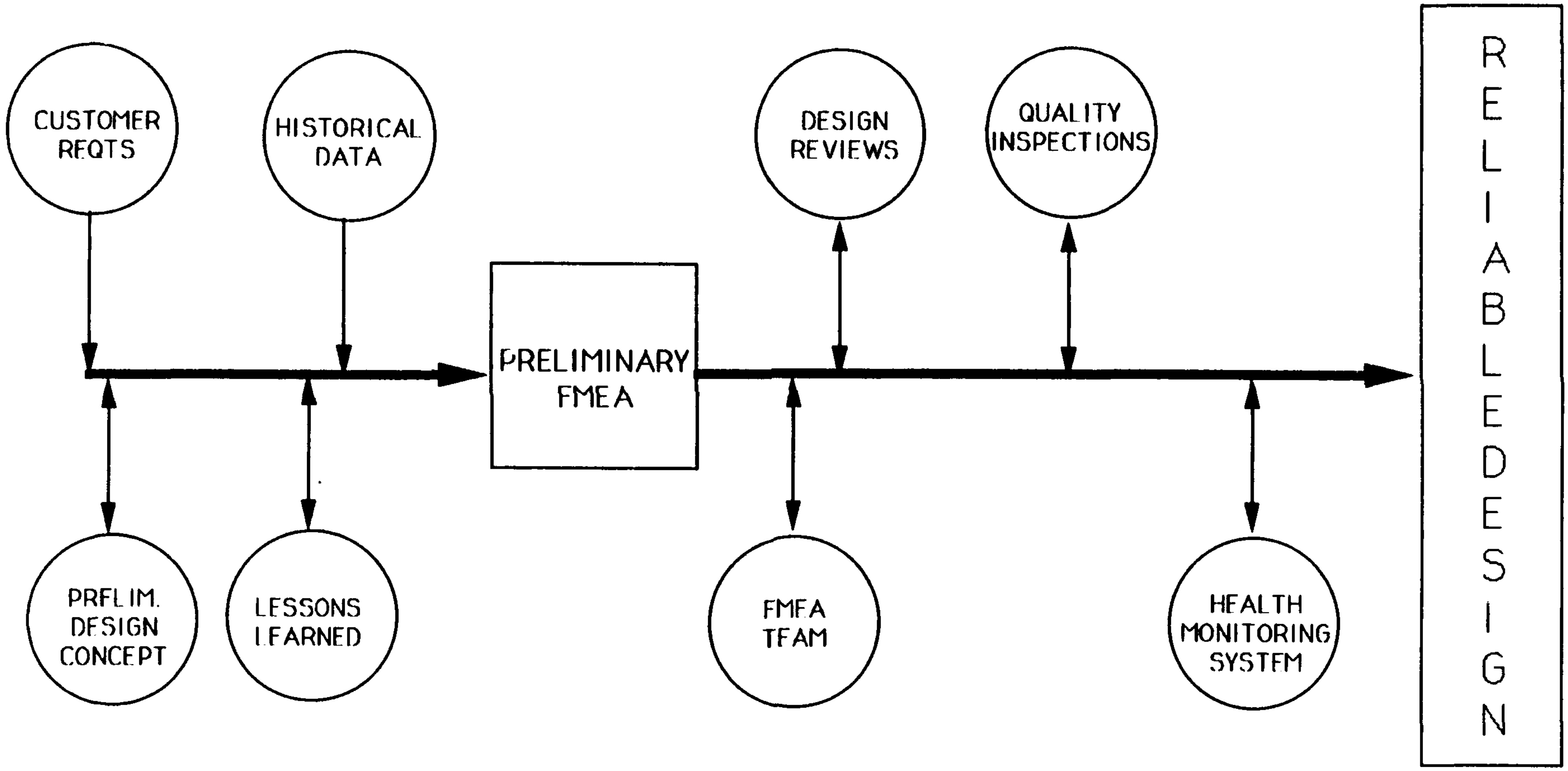

Figure 185. AETB FMEA Process

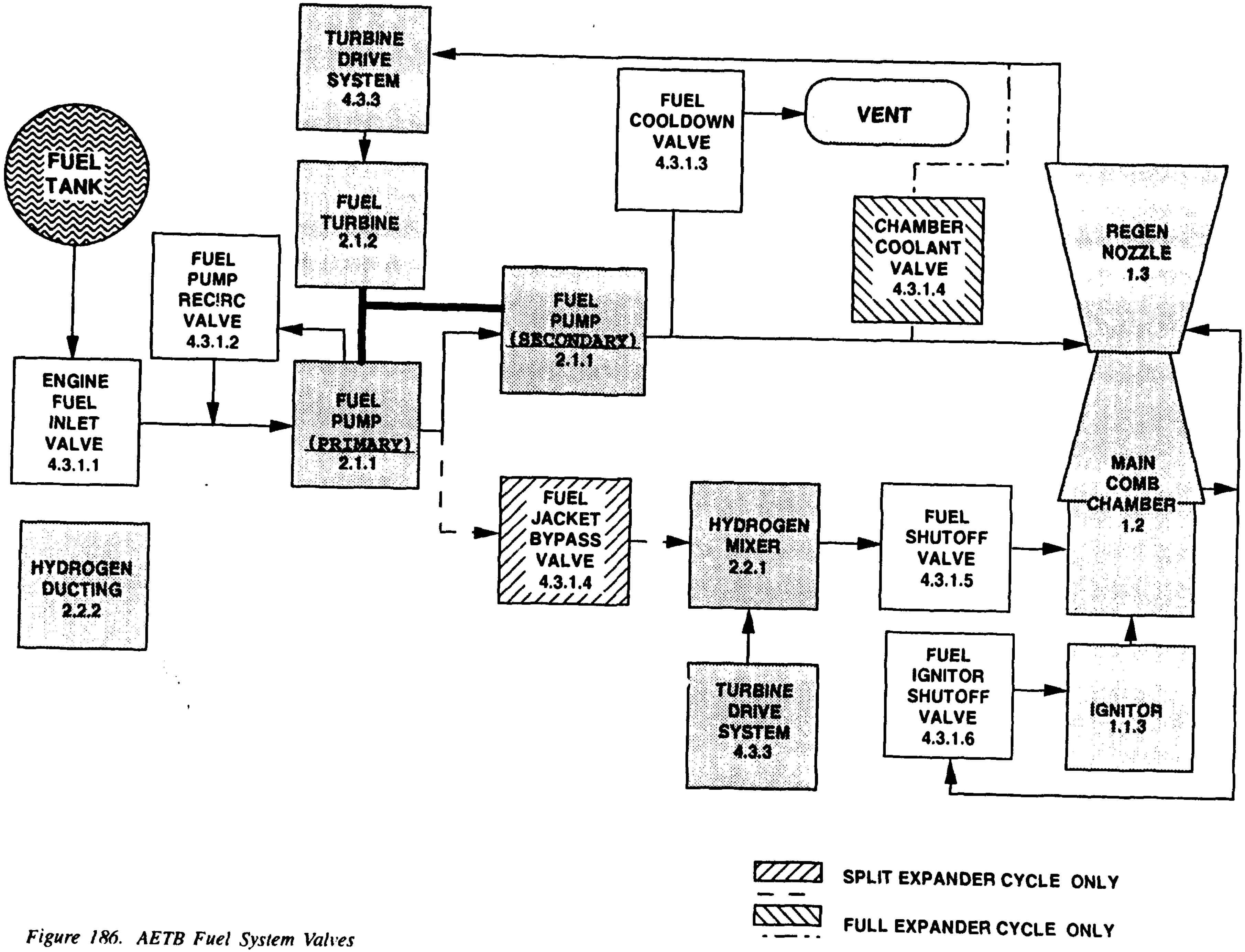

Figure 186. AETB Fuel System Valves

FAILURE MODE AND EFFECTS ANALYSIS

PAGE:

SUBSYSTEM:
FUNCTIONAL ASSY:

PREPARED BY:
APPROVED BY:

ISSUE DATE:
REV. DATE

Item, Function, Failure Mode and Cause	Oper. Phase	Effect of Failure on Subsystem	Cond. Class	Failure React. Time	Failure Detection Method	Hazard Control and Design Considerations/Corrective Action
<u>4.2.14 INTER PROPEL LANT SEAL HELIUM / HYDROGEN DIS CHARGE PRESSURE SENSOR</u> Senses Helium/Hydrogen discharge pressure to assure proper sealing of the Hydrogen side of the IPS. <u>Failure Mode.</u> 1 Fails open/shorted 2. Soft failure, communicates erroneous information 3. Structural failure of sensor/housing <u>Cause.</u> 1. Initial fabrication error, assembly error, or damage from working environment. 2 Same as 1. 3 Same as 1.	p,s,m,c,d	1. No or high reading. The readings will be out of range causing the test bed to shut down 2 Possible action/no action response from the central processor based on the false information 3 Loss of sensor signal.	II	Sec	Processor soft ware will determine loss of function.	<u>Design Considerations:</u> 1. Initial qualification testing to validate the manufacturing quality. Strict adherence to assembly and maintenance procedures. Adequate vibration analysis to verify appropriate cable lengths and clamp positions

Figure 187. AETB FMEA Document

UNITED TECHNOLOGIES PRATT & WHITNEY
Government Engine & Space Propulsion

HAZARD CONTROL SHEET

Hazard Level	Category HRI ____	No.	
Status		Page	1 of 1
Program Phase		Date	

System: Subsystem:

Operation/Phase:

Hazard Group:

References:

Hazard Description:

Potential Effects:

Assumptions/Rationale:

Hazard Control Considerations:	Reference:

Remarks/Disposition:

Closure Classification	Category HRI ____
Originated:	Closed:

Figure 188. Hazard Control Sheet

SECTION VII
APPENDIX A

PRATT & WHITNEY

AETB PRELIMINARY

DESIGN REVIEW

January 29-31, 1991

Detailed Steady State Cycle Sheets

Table 29. Uprated Design Point

AETB ROCETS SIMULATION

THRUST=25000.LB INLET O/F=6.0

OPERATOR - S. CHESLA
CONFIGURATION - SPLIT
VERSION - AETBY4
PROCESS DATE - 1/15/91
PROCESS TIME - 10:23:51

ENGINE PERFORMANCE

THRUST (VACUUM)	(LB)	25000.
THRUST (SEA LEVEL)	(LB)	19074.
SPECIFIC IMPULSE (VACUUM)	(SEC)	480.09
SPECIFIC IMPULSE (S.L. / AR=7.5)	(SEC)	366.28
TOTAL ENGINE INLET FLOW RATE	(LB/SEC)	52.50
MIXTURE RATIO - INLET		6.00

CHAMBER PERFORMANCE

INJECTOR FACE PRESSURE (TOTAL)	(PSIA)	1500.1
THROAT PRESSURE (TOTAL)	(PSIA)	1453.8
MIXTURE RATIO - CHAMBER		6.086
FLOW RATE (THROAT)	(LB/SEC)	52.07
THROAT AREA	(IN2)	8.377
NOZZLE AREA RATIO		1000.0
THEORETICAL CHAR. VELOCITY	(FT/SEC)	7577.2
CHAR ..LOCITY EFFICIENCY		0.993

ENGINE HEAT TRANSFER

CHAMBER/NOZL COOLANT DELTA P	(PSIA)	410.2
CHAMBER/NOZL COOLANT DELTA T	(DEG R)	907.3
CHAMBER/NOZL HEAT TRANSFER	(BTU/SEC)	12489.9

FUEL SYSTEM CONDITIONS

STATION	PRESS (PSIA)	TEMP (DEG R)	FLOW (LB/SEC)	ENTHALPY (BTU/LB)	DENSITY (LB/FT3)
1 ENGINE INLET	70.0	38.0	7.500	-104.8	4.386
2 PUMP A INLET	67.5	38.0	7.500	-104.8	4.383
3 PUMP A EXIT	1916.9	68.3	7.500	17.2	4.356
4 FJBV INLET	1909.2	68.4	3.143	22.3	4.299
5 FJBV EXIT	1664.1	70.2	3.143	22.3	4.124
6 PUMP B INLET	1911.9	69.7	4.765	26.2	4.261
7 PUMP B EXIT	3196.2	90.5	4.765	115.8	4.256
8 PUMP C EXIT	4502.9	111.1	4.499	206.2	4.281
9 CHBR COOL IN	4491.1	111.2	3.710	206.2	4.275
10 INTERFACE	4142.9	777.3	3.710	2730.1	0.890
11 NOZL COOL EX	4080.9	1018.5	3.691	3577.7	0.684
12 MTBV INLET	4043.3	1018.7	0.139	3577.7	0.678
24 MTBV EXIT	1795.6	1034.4	0.139	3577.7	0.312
13 O2 VOLUTE IN	4043.3	1018.7	3.553	3577.7	0.678
14 O2 TURB IN	4034.6	1000.3	3.524	3512.9	0.689
15 O2 TURB EX	3503.0	942.3	3.630	3297.1	0.641
16 O2 VOLUTE EX	3496.1	942.3	3.630	3297.1	0.639
17 FTBV INLET	3459.8	942.6	0.000	3297.1	0.633
24 FTBV EXIT	1795.6	953.8	0.000	3297.1	0.338
18 H2 VOLUTE IN	3459.3	942.6	3.630	3297.1	0.633
19 H2 TURB A IN	3451.4	896.3	3.848	3134.8	0.661
20 H2 TURB A EX	2507.1	815.2	3.848	2826.1	0.540
21 H2 TURB B IN	2507.1	815.2	3.969	2826.1	0.540
22 H2 TURB B EX	1843.1	744.7	4.049	2562.1	0.440
23 H2 VOLUTE EX	1834.0	744.8	4.049	2562.1	0.438
24 FTSV EXIT	1795.6	754.6	4.049	2595.7	0.423
25 MIX. TURB IN	1737.4	754.9	4.187	2595.7	0.410
5 MIX. FJBV IN	1664.1	70.2	3.143	22.3	4.124
26 MIXER EXIT	1646.3	448.4	7.330	1492.3	0.642
27 FSOV INLET	1646.3	448.4	7.330	1492.3	0.642
28 FSOV EXIT	1636.4	448.4	7.330	1492.3	0.638
29 INJ MANIFOLD	1610.6	448.5	7.330	1492.3	0.629
30 INJEC. INLET	1593.5	448.6	7.330	1492.3	0.622
31 INJEC. FACE	1500.1				

OXIDIZER SYSTEM CONDITIONS

STATION	PRESS (PSIA)	TEMP (DEG R)	FLOW (LB/SEC)	ENTHALPY (BTU/LB)	DENSITY (LB/FT3)
32 ENGINE INLET	70.0	161.8	45.000	61.2	71.38
33 PUMP INLET	67.0	162.1	45.815	61.3	71.31
34 PUMP EXIT	2356.0	173.4	45.815	69.5	71.57
35 POSV INLET	2291.7	173.6	4.988	69.5	71.47
36 POSV EXIT	1690.7	176.1	4.988	69.5	70.54
37 SOCV INLET	2285.2	173.7	39.737	69.5	71.46
38 SOCV EXIT	1693.0	176.1	39.737	69.5	70.54
39 PRIM INJ MAN	1690.7	176.1	4.988	69.5	70.54
40 SEC INJ MAN	1686.4	176.1	39.737	69.5	70.53
41 PRIMARY INJ	1681.1	176.1	4.988	69.5	70.52
42 SECONDARY INJ	1679.8	176.1	39.737	69.5	70.52
43 INJECTOR FACE	1499.9				

(Continued) Table 29. Uprated Design Point

AETB ROCETS SIMULATION

THRUST=25000.LB INLET O/F=6.0

OPERATOR - S. CHESLA
CONFIGURATION - SPLIT
VERSION - AETBY4
PROCESS DATE - 1/15/91
PROCESS TIME - 10:23:51

* TURBOMACHINERY PERFORMANCE DATA *

	FUEL PUMP A 1ST STAGE	FUEL PUMP B 1ST STAGE	FUEL PUMP B 2ND STAGE	LOX PUMP
	*********	*********	*********	**********
EFFICIENCY	0.643	0.623	0.626	0.727
HORSEPOWER	1295.	604.	576.	528.
TORQUE (FT-LB)	69.2	32.0	30.5	56.7
SPEED (RPM)	98240.	99221.	99221.	48863.
HEAD RISE (FT)	61034.	43429.	44078.	4605.
DIAMETER (IN)	4.43	3.75	3.75	2.67
TIP SPEED (FT/SEC)	1899.	1624.	1624.	569.
VOLUMETRIC FLOW (GPM)	773.	503.	472.	287.
HEAD COEFFICIENT	0.5442	0.5289	0.5378	0.4559
FLOW COEFFICIENT	0.0908	0.0928	0.0880	0.1401
SUCTION SS	10370.1			23586.0

	FUEL TURBINES TURBINE A	FUEL TURBINES TURBINE B	LOX TURBINE
	*********	*********	*********
EFFICIENCY (T/T)	0.816	0.843	0.822
HORSEPOWER TOTAL	1314.9	1209.7	619.8
HORSEPOWER PUMP	1294.7	1179.4	528.0
TORQUE (FT-LB)	70.3	64.0	66.6
SPEED (RPM)	98240.	99221.	48863.
MEAN DIAMETER (IN)	3.85	3.85	6.75
MEAN TIP SPEED (FT/SEC)	1650.3	1650.3	1439.1
DELTA H (ACTUAL) (BTU/LB)	241.5	215.5	124.3
DELTA H (IDEAL) (BTU/LB)	296.1	255.5	151.3
U/C (IDEAL)	.4285	.4659	.5228
FLOW PARAMETER (IN2)	.0334	.0452	.0276
PRES.RATIO (T/T)	1.377	1.360	1.152
GAMMA	1.398	1.398	1.398

* VALVE DATA *

STATION		DELTA P PSIA	FLOW (LB/SEC)	BYPASS %	AREA (IN2)
JACKET BYPASS VALVE	(FJBV)	245.1	3.14	41.906	0.145
TURBINE BYPASS VALVE	(MTBV)	2247.7	0.14	3.757	0.008
FUEL TURBINE BYPASS	(FTBV)	1664.2	0.00	0.000	0.000
PRI SHUT OFF VALVE	(POSV)	601.0	4.988		0.036
SEC CONTROL VALVE	(SOCV)	592.2	39.737		0.289
FUEL SHUT OFF VALVE	(FSOV)	9.9	7.330		
FUEL TURBINE SHUTOFF	(FTSV)	9.8	4.049		
FUEL PUMP RECIRC.	(FRV)	1849.4	0.000		

* INJECTOR ELEMENT DATA *

STATION	DELTA P PSIA	FLOW (LB/SEC)	AREA (IN2)
FUEL INJECTOR	93.5	7.330	1.435
PRIMARY LOX INJECTOR	181.2	4.988	0.066
SECONDARY LOX INJECTOR	179.7	39.737	0.528

* INTERNAL FLOWS *

		SOURCE STATION	SINK STATION	FLOW (LB/SEC)
********************	********	********	********	********
LOX IPS FLOW	(LO1)	34	AMB	0.275
LOX VAPORIZER RECIRC.	(LO2)	34	33	0.815
LH2 OT DISK COOLANT	(LH2)			
LH2A (LEAKAGE)		8	14	0.070
LH2B (IPS)		8	AMB	0.053
LH2 OT BEARING COOLANT	(LH3)	8	15	0.105
LH2 OT IPS	(LH4)	14	AMB	0.098
FT LH2 2ND BEARING COOL.	(LH5)			
LH5A (LEAKAGE)		8	19	0.061
LH5B (RECIRC)		8	3	0.207
FT LH2 SHROUD COOLANT	(LH6)			
LH6A (COOLANT)		8	19	0.158
LH6B (LEAKAGE)		8	20	0.010
LH6C (LEAKAGE)		8	20	0.011
LH6D (LEAKAGE)		8	22	0.015
FT LH2 DISK COOLANT	(LH7)	8	20	0.100
FT LH2 3RD BRG FLOW	(LH8)			
LH8A (LEAKAGE)		7	22	0.065
LH8B (RECIRC)		7	6	0.201

Table 30. Normal Operating Point, O/F = 6

THRUST=20000.LB INLET O/F=6.0

OPERATOR - S. CHESLA
CONFIGURATION - SPLIT
VERSION - AETBY4
PROCESS DATE - 1/15/91
PROCESS TIME - 10:38:36

ENGINE PERFORMANCE

THRUST (VACUUM)	(LB)	20000.
THRUST (SEA LEVEL)	(LB)	15059.
SPECIFIC IMPULSE (VACUUM)	(SEC)	480.00
SPECIFIC IMPULSE (S.L. / AR=7.5)	(SEC)	361.42
TOTAL ENGINE INLET FLOW RATE	(LB/SEC)	42.01
MIXTURE RATIO - INLET		6.00

CHAMBER PERFORMANCE

INJECTOR FACE PRESSURE (TOTAL)	(PSIA)	1198.0
THROAT PRESSURE (TOTAL)	(PSIA)	1161.0
MIXTURE RATIO - CHAMBER		6.087
FLOW RATE (THROAT)	(LB/SEC)	41.67
THROAT AREA	(IN2)	8.377
NOZZLE AREA RATIO		1000.0
THEORETICAL CHAR. VELOCITY	(FT/SEC)	7563.0
CHAR VELOCITY EFFICIENCY		0.993

ENGINE HEAT TRANSFER

CHAMBER/NOZL COOLANT DELTA P	(PSIA)	354.3
CHAMBER/NOZL COOLANT DELTA T	(DEG R)	843.0
CHAMBER/NOZL HEAT TRANSFER	(BTU/SEC)	10664.4

FUEL SYSTEM CONDITIONS

STATION	PRESS (PSIA)	TEMP (DEG R)	FLOW (LB/SEC)	ENTHALPY (BTU/LB)	DENSITY (LB/FT3)
1 ENGINE INLET	70.0	38.0	6.002	-104.8	4.386
2 PUMP A INLET	68.4	38.0	6.002	-104.8	4.384
3 PUMP A EXIT	1644.2	63.8	6.002	-0.7	4.388
4 FJBV INLET	1640.8	63.8	2.077	3.2	4.312
5 FJBV EXIT	1331.9	66.1	2.077	3.2	4.074
6 PUMP B INLET	1640.2	64.6	4.245	5.4	4.287
7 PUMP B EXIT	2556.9	79.5	4.245	69.2	4.273
8 PUMP C EXIT	3488.5	94.2	4.019	133.4	4.280
9 CHBR COOL IN	3478.9	94.3	3.330	133.4	4.275
10 INTERFACE	3177.9	728.7	3.330	2534.8	0.745
11 NOZL COOL EX	3124.6	957.3	3.313	3340.7	0.568
12 MTBV INLET	3088.2	957.6	0.541	3340.7	0.562
24 MTBV EXIT	1467.5	968.6	0.541	3340.7	0.275
13 O2 VOLUTE IN	3088.2	957.6	2.772	3340.7	0.562
14 O2 TURB IN	3081.8	936.7	2.759	3267.4	0.572
15 O2 TURB EX	2705.1	881.4	2.853	3065.0	0.536
16 O2 VOLUTE EX	2700.1	881.5	2.853	3065.0	0.535
17 FTBV INLET	2673.3	881.6	0.000	3065.0	0.530
24 FTBV EXIT	1467.5	889.5	0.000	3065.0	0.298
18 H2 VOLUTE IN	2673.3	881.6	2.853	3065.0	0.530
19 H2 TURB A IN	2667.1	833.3	3.046	2893.9	0.560
20 H2 TURB A EX	1974.5	759.2	3.046	2615.8	0.460
21 H2 TURB B IN	1974.5	759.2	3.151	2615.8	0.460
22 H2 TURB B EX	1502.0	693.4	3.245	2374.4	0.389
23 H2 VOLUTE EX	1495.4	693.4	3.245	2374.4	0.388
24 FTSV EXIT	1467.5	732.9	3.245	2512.5	0.360
25 MIX. TURB IN	1411.7	733.2	3.786	2512.5	0.347
5 MIX. FJBV IN	1331.9	66.1	2.077	3.2	4.074
26 MIXER EXIT	1323.8	485.0	5.863	1623.7	0.485
27 FSOV INLET	1323.8	485.0	5.863	1623.7	0.485
28 FSOV EXIT	1315.3	485.0	5.863	1623.7	0.482
29 INJ MANIFOLD	1293.5	485.1	5.863	1623.7	0.474
30 INJEQ. INLET	1278.9	485.1	5.863	1623.7	0.469
31 INJEC. FACE	1198.0				

OXIDIZER SYSTEM CONDITIONS

STATION	PRESS (PSIA)	TEMP (DEG R)	FLOW (LB/SEC)	ENTHALPY (BTU/LB)	DENSITY (LB/FT3)
32 ENGINE INLET	70.0	161.8	36.011	61.2	71.38
33 PUMP INLET	68.1	162.1	36.740	61.3	71.32
34 PUMP EXIT	1897.8	171.0	36.740	67.8	71.53
35 POSV INLET	1856.6	171.2	4.550	67.8	71.46
36 POSV EXIT	1356.4	173.2	4.550	67.8	70.67
37 SOCV INLET	1852.6	171.2	31.238	67.8	71.46
38 SOCV EXIT	1317.1	173.4	31.238	67.8	70.61
39 PRIM INJ MAN	1356.4	173.2	4.550	67.8	70.67
40 SEC INJ MAN	1313.0	173.4	31.238	67.8	70.60
41 PRIMARY INJ	1348.5	173.2	4.550	67.8	70.66
42 SECONDARY INJ	1309.0	173.4	31.238	67.8	70.60
43 INJECTOR FACE	1198.0				

(Continued) *Table 30. Normal Operating Point, O/F = 6*

AETB ROCETS SIMULATION

THRUST=20000.LB INLET O/F=6.0

OPERATOR - S. CHESLA
CONFIGURATION - SPLIT
VERSION - AETBY4
PROCESS DATE - 1/15/91
PROCESS TIME - 10:38:36

* TURBOMACHINERY PERFORMANCE DATA *

	FUEL PUMP A 1ST STAGE	FUEL PUMP B 1ST STAGE	FUEL PUMP B 2ND STAGE	LOX PUMP
	*********	*********	*********	**********
EFFICIENCY	0.642	0.621	0.628	0.728
HORSEPOWER	884.	383.	365.	338.
TORQUE (FT-LB)	53.0	23.7	22.6	41.8
SPEED (RPM)	87715.	84786.	84786.	42502.
HEAD RISE (FT)	52007.	30846.	31368.	3683.
DIAMETER (IN)	4.43	3.75	3.75	2.67
TIP SPEED (FT/SEC)	1695.	1387.	1387.	495.
VOLUMETRIC FLOW (GPM)	619.	446.	422.	231.
HEAD COEFFICIENT	0.5817	0.5144	0.5242	0.4819
FLOW COEFFICIENT	0.0814	0.0964	0.0920	0.1292
SUCTION SS	8175.1			18025.7

	FUEL TURBINES TURBINE A	FUEL TURBINES TURBINE B	LOX TURBINE
	*********	*********	*********
EFFICIENCY (T/T)	0.812	0.836	0.812
HORSEPOWER TOTAL	900.4	772.7	407.5
HORSEPOWER PUMP	884.4	748.5	338.0
TORQUE (FT-LB)	53.9	47.9	50.4
SPEED (RPM)	87715.	84786.	42502.
MEAN DIAMETER (IN)	3.85	3.85	6.75
MEAN TIP SPEED (FT/SEC)	1473.5	1473.5	1251.8
DELTA H (ACTUAL)(BTU/LB)	209.0	173.3	104.4
DELTA H (IDEAL) (BTU/LB)	257.3	207.4	128.5
U/C (IDEAL)	.4104	.4419	.4934
FLOW PARAMETER (IN2)	.0330	.0440	.0274
PRES.RATIO (T/T)	1.351	1.315	1.139
GAMMA	1.398	1.398	1.399

* VALVE DATA *

STATION		DELTA P PSIA	FLOW (LB/SEC)	BYPASS %	AREA (IN2)
JACKET BYPASS VALVE	(FJBV)	308.9	2.08	34.600	0.085
TURBINE BYPASS VALVE	(MTBV)	1620.6	0.54	16.334	0.039
FUEL TURBINE BYPASS	(FTBV)	1205.7	0.00	0.000	0.000
PRI SHUT OFF VALVE	(POSV)	500.2	4.550		0.036
SEC CONTROL VALVE	(SOCV)	535.5	31.238		0.239
FUEL SHUT OFF VALVE	(FSOV)	8.5	5.863		
FUEL TURBINE SHUTOFF	(FTSV)	7.1	3.245		
FUEL PUMP RECIRC.	(FRV)	1575.8	0.000		

* INJECTOR ELEMENT DATA *

STATION	DELTA P PSIA	FLOW (LB/SEC)	AREA (IN2)
FUEL INJECTOR	81.0	5.863	1.435
PRIMARY LOX INJECTOR	150.5	4.550	0.066
SECONDARY LOX INJECTOR	111.0	31.238	0.528

* INTERNAL FLOWS *

		SOURCE STATION	SINK STATION	FLOW (LB/SEC)
**************************				
LOX IPS FLOW	(LO1)	34	AMB	0.224
LOX VAPORIZER RECIRC.	(LO2)	34	33	0.729
LH2 OT DISK COOLANT	(LH2)			
LH2A (LEAKAGE)		8	14	0.065
LH2B (IPS)		8	AMB	0.045
LH2 OT BEARING COOLANT	(LH3)	8	15	0.093
LH2 OT IPS	(LH4)	14	AMB	0.078
FT LH2 2ND BEARING COOL.	(LH5)			
LH5A (LEAKAGE)		8	19	0.054
LH5B (RECIRC)		8	3	0.175
FT LH2 SHROUD COOLANT	(LH6)			
LH6A (COOLANT)		8	19	0.139
LH6B (LEAKAGE)		8	20	0.009
LH6C (LEAKAGE)		8	20	0.009
LH6D (LEAKAGE)		8	22	0.013
FT LH2 DISK COOLANT	(LH7)	8	20	0.087
FT LH2 3RD BRG FLOW	(LH8)			
LH8A (LEAKAGE)		7	22	0.081
LH8B (RECIRC)		7	6	0.144

Table 31. Normal Operating Point, O/F = 5

AETB ROCETS SIMULATION

THRUST=20000.LB INLET O/F=5.0

OPERATOR - L. HARTZHEIM
CONFIGURATION - SPLIT
VERSION - AETBY4
PROCESS DATE - 1/15/91
PROCESS TIME - 15:48: 5

ENGINE PERFORMANCE

THRUST (VACUUM)	(LB)	20000.
THRUST (SEA LEVEL)	(LB)	15436.
SPECIFIC IMPULSE (VACUUM)	(SEC)	474.93
SPECIFIC IMPULSE (S.L. / AR=7.8)	(SEC)	366.84
TOTAL ENGINE INLET FLOW RATE	(LB/SEC)	42.51
MIXTURE RATIO - INLET		5.00

CHAMBER PERFORMANCE

INJECTOR FACE PRESSURE (TOTAL)	(PSIA)	1241.1
THROAT PRESSURE (TOTAL)	(PSIA)	1202.6
MIXTURE RATIO - CHAMBER		5.058
FLOW RATE (THROAT)	(LB/SEC)	42.11
THROAT AREA	(IN2)	8.377
NOZZLE AREA RATIO		1000.0
THEORETICAL CHAR. VELOCITY	(FT/SEC)	7791.4
CHAR. VELOCITY EFFICIENCY		0.988

ENGINE HEAT TRANSFER

CHAMBER/NOZL COOLANT DELTA P	(PSIA)	345.4
CHAMBER/NOZL COOLANT DELTA T	(DEG R)	806.8
CHAMBER/NOZL HEAT TRANSFER	(BTU/SEC)	10024.0

FUEL SYSTEM CONDITIONS

STATION	PRESS (PSIA)	TEMP (DEG R)	FLOW (LB/SEC)	ENTHALPY (BTU/LB)	DENSITY (LB/FT3)
1 ENGINE INLET	70.0	38.0	7.085	-104.8	4.386
2 PUMP A INLET	67.8	38.0	7.085	-104.8	4.383
3 PUMP A EXIT	1573.8	63.0	7.085	-5.0	4.353
4 FJBV INLET	1566.0	63.0	3.176	-0.9	4.301
5 FJBV EXIT	1394.8	64.4	3.176	-0.9	4.170
6 PUMP B INLET	1869.8	64.3	4.294	2.7	4.264
7 PUMP B EXIT	2654.0	81.9	4.294	78.3	4.247
8 PUMP C EXIT	3751.9	99.4	4.049	184.7	4.261
9 CHBR COOL IN	3742.3	99.5	3.330	184.7	4.256
10 INTERFACE	3478.8	692.4	3.330	2412.3	0.849
11 NOZL COOL EX	3396.9	906.3	3.313	3168.6	0.645
12 MTBV INLET	3364.8	906.5	0.182	3168.6	0.639
24 MTBV EXIT	1804.3	919.0	0.182	3168.6	0.298
13 O2 VOLUTE IN	3364.8	906.5	3.131	3168.6	0.639
14 O2 TURB IN	3357.6	889.5	3.108	3108.5	0.649
15 O2 TURB EX	2916.2	837.4	3.204	2914.0	0.605
16 O2 VOLUTE EX	2910.5	837.4	3.204	2914.0	0.604
17 FTBV INLET	2880.5	837.6	0.000	2914.0	0.598
24 FTBV EXIT	1504.3	846.3	0.000	2914.0	0.321
18 H2 VOLUTE IN	2880.5	837.6	3.204	2914.0	0.598
19 H2 TURB A IN	2873.5	796.0	3.403	2766.1	0.626
20 H2 TURB A EX	2092.8	724.2	3.403	2494.8	0.510
21 H2 TURB B IN	2092.8	724.2	3.513	2494.8	0.510
22 H2 TURB B EX	1543.5	663.6	3.577	2270.6	0.416
23 H2 VOLUTE EX	1536.0	663.7	3.577	2270.6	0.414
24 FTSV EXIT	1504.3	676.2	3.577	2314.1	0.399
25 MIX. TURB IN	1454.6	676.5	3.759	2314.1	0.386
5 MIX. FJBV IN	1394.8	64.4	3.176	-0.9	4.170
26 MIXER EXIT	1376.8	386.6	6.935	1253.9	0.627
27 FSOV INLET	1376.8	386.6	6.935	1253.9	0.627
28 FSOV EXIT	1367.6	386.7	6.935	1253.9	0.623
29 INJ MANIFOLD	1344.1	386.7	6.935	1253.9	0.613
30 INJEC. INLET	1328.3	386.7	6.935	1253.9	0.606
31 INJEC. FACE	1241.1				

OXIDIZER SYSTEM CONDITIONS

STATION	PRESS (PSIA)	TEMP (DEG R)	FLOW (LB/SEC)	ENTHALPY (BTU/LB)	DENSITY (LB/FT3)
32 ENGINE INLET	70.0	161.8	35.426	61.2	71.38
33 PUMP INLET	68.1	162.2	36.226	61.4	71.30
34 PUMP EXIT	2273.2	173.1	36.226	69.3	71.53
35 POSV INLET	2233.5	173.3	5.582	69.3	71.47
36 POSV EXIT	1480.7	176.3	5.582	69.3	70.29
37 SOCV INLET	2229.9	173.3	29.578	69.3	71.47
38 SOCV EXIT	1348.7	176.8	29.578	69.3	70.07
39 PRIM INJ MAN	1480.7	176.3	5.582	69.3	70.29
40 SEC INJ MAN	1345.0	176.8	29.578	69.3	70.07
41 PRIMARY INJ	1468.8	176.4	5.582	69.3	70.27
42 SECONDARY INJ	1341.3	176.9	29.578	69.3	70.06
43 INJECTOR FACE	1241.0				

(Continued) *Table 31. Normal Operating Point, O/F = 5*

AETB ROCETS SIMULATION

THRUST=20000.LB INLET O/F=5.0

OPERATOR - L. HARTZHEIM
CONFIGURATION - SPLIT
VERSION - AETBY4
PROCESS DATE - 1/15/91
PROCESS TIME - 15:48: 5

* TURBOMACHINERY PERFORMANCE DATA *

		FUEL PUMP A	FUEL PUMP B		LOX PUMP
		1ST STAGE	1ST STAGE	2ND STAGE	
		*********	*********	*********	**********
EFFICIENCY		0.641	0.623	0.626	0.723
HORSEPOWER		1000.	459.	437.	404.
TORQUE	(FT-LB)	58.5	26.6	25.3	46.6
SPEED	(RPM)	89819.	90799.	90799.	45594.
HEAD RISE	(FT)	49729.	36691.	37159.	4439.
DIAMETER	(IN)	4.43	3.75	3.75	2.67
TIP SPEED	(FT/SEC)	1736.	1486.	1486.	531.
VOLUMETRIC FLOW	(GPM)	731.	454.	427.	227.
HEAD COEFFICIENT		0.5304	0.5335	0.5414	0.5046
FLOW COEFFICIENT		0.0939	0.0916	0.0869	0.1188
SUCTION SS		9182.6			19200.6

		FUEL TURBINES		LOX TURBINE
		TURBINE A	TURBINE B	
		*********	*********	*********
EFFICIENCY	(T/T)	0.814	0.842	0.820
HORSEPOWER TOTAL		1016.9	921.9	484.2
HORSEPOWER PUMP		1000.1	896.5	404.3
TORQUE	(FT-LB)	59.5	53.3	55.8
SPEED	(RPM)	89819.	90799.	45594.
MEAN DIAMETER	(IN)	3.85	3.85	6.75
MEAN TIP SPEED	(FT/SEC)	1508.9	1508.9	1342.9
DELTA H (ACTUAL)	(BTU/LB)	211.2	185.5	110.1
DELTA H (IDEAL)	(BTU/LB)	259.5	220.3	134.2
U/C (IDEAL)		.4185	.4591	.5179
FLOW PARAMETER	(IN2)	.0334	.0452	.0276
PRES.RATIO	(T/T)	1.373	1.356	1.151
GAMMA		1.399	1.398	1.399

* VALVE DATA *

STATION		DELTA P PSIA	FLOW (LB/SEC)	BYPASS %	AREA (IN2)
JACKET BYPASS VALVE	(FJBV)	171.2	3.18	44.826	0.175
TURBINE BYPASS VALVE	(MTBV)	1860.5	0.18	5.500	0.012
FUEL TURBINE BYPASS	(FTBV)	1376.2	0.00	0.000	0.000
PRI SHUT OFF VALVE	(POSV)	752.7	5.582		0.036
SEC CONTROL VALVE	(SOCV)	881.2	29.578		0.176
FUEL SHUT OFF VALVE	(FSOV)	9.1	6.935		
FUEL TURBINE SHUTOFF	(FTSV)	8.1	3.577		
FUEL PUMP RECIRC.	(FRV)	1506.0	0.000		

* INJECTOR ELEMENT DATA *

STATION	DELTA P PSIA	FLOW (LB/SEC)	AREA (IN2)
FUEL INJECTOR	87.3	6.935	1.435
PRIMARY LOX INJECTOR	227.8	5.582	0.066
SECONDARY LOX INJECTOR	100.2	29.578	0.528

* INTERNAL FLOWS *

		SOURCE STATION	SINK STATION	FLOW (LB/SEC)
LOX IPS FLOW	(LO1)	34	AMB	0.266
LOX VAPORIZER RECIRC.	(LO2)	34	33	0.800
LH2 OT DISK COOLANT	(LH2)			
LH2A (LEAKAGE)		8	14	0.064
LH2B (IPS)		8	AMB	0.047
LH2 OT BEARING COOLANT	(LH3)	8	15	0.096
LH2 OT IPS	(LH4)	14	AMB	0.087
FT LH2 2ND BEARING COOL.	(LH5)			
LH5A (LEAKAGE)		8	19	0.055
LH5B (RECIRC)		8	3	0.190
FT LH2 SHROUD COOLANT	(LH6)			
LH6A (COOLANT)		8	19	0.144
LH6B (LEAKAGE)		8	20	0.009
LH6C (LEAKAGE)		8	20	0.010
LH6D (LEAKAGE)		8	22	0.014
FT LH2 DISK COOLANT	(LH7)	8	20	0.091
FT LH2 3RD BRG FLOW	(LH8)			
LH8A (LEAKAGE)		7	22	0.050
LH8B (RECIRC)		7	6	0.194

Table 32. Normal Operating Point, O/F = 7

AETB ROCETS SIMULATION
THRUST=20000.LB INLET O/F=7.0

OPERATOR - L. HARTZHEIM
CONFIGURATION - SPLIT
VERSION - AETBY4
PROCESS DATE - 1/15/91
PROCESS TIME - 14:47:36

ENGINE PERFORMANCE

THRUST (VACUUM)	(LB)	20000.
THRUST (SEA LEVEL)	(LB)	14647.
SPECIFIC IMPULSE (VACUUM)	(SEC)	476.86
SPECIFIC IMPULSE (S.L. / AR=7.5)	(SEC)	349.23
TOTAL ENGINE INLET FLOW RATE	(LB/SEC)	42.23
MIXTURE RATIO - INLET		7.00

CHAMBER PERFORMANCE

INJECTOR FACE PRESSURE (TOTAL)	(PSIA)	1157.2
THROAT PRESSURE (TOTAL)	(PSIA)	1121.5
MIXTURE RATIO - CHAMBER		7.112
FLOW RATE (THROAT)	(LB/SEC)	41.94
THROAT AREA	(IN2)	8.377
NOZZLE AREA RATIO		1000.0
THEORETICAL CHAR. VELOCITY	(FT/SEC)	7294.7
CHAR. VELOCITY EFFICIENCY		0.980

ENGINE HEAT TRANSFER

CHAMBER/NOZL COOLANT DELTA P	(PSIA)	344.1
CHAMBER/NOZL COOLANT DELTA T	(DEG R)	967.8
CHAMBER/NOZL HEAT TRANSFER	(BTU/SEC)	11090.0

FUEL SYSTEM CONDITIONS

STATION	PRESS (PSIA)	TEMP (DEG R)	FLOW (LB/SEC)	ENTHALPY (BTU/LB)	DENSITY (LB/FT3)
1 ENGINE INLET	70.0	38.0	5.279	-104.8	4.386
2 PUMP A INLET	68.8	38.0	5.279	-104.8	4.385
3 PUMP A EXIT	1658.6	62.9	5.279	-5.0	4.341
4 FJBV INLET	1556.5	62.9	1.610	-1.4	4.300
5 FJBV EXIT	1281.4	64.9	1.610	-1.4	4.084
6 PUMP B INLET	1555.1	63.6	3.972	0.6	4.277
7 PUMP B EXIT	2359.4	76.8	3.972	56.7	4.263
8 PUMP C EXIT	3175.8	89.8	3.761	113.2	4.265
9 CHBR COOL IN	3167.5	89.8	3.110	113.2	4.261
10 INTERFACE	2919.4	801.8	3.110	2787.8	0.631
11 NOZL COOL EX	2823.4	1057.6	3.094	3684.0	0.470
12 MTBV INLET	2784.9	1057.9	0.742	3684.0	0.464
24 MTBV EXIT	1422.8	1067.5	0.742	3684.0	0.242
13 O2 VOLUTE IN	2784.9	1057.9	2.352	3684.0	0.464
14 O2 TURB IN	2779.4	1030.9	2.350	3589.5	0.474
15 O2 TURB EX	2466.6	969.1	2.438	3366.0	0.450
16 O2 VOLUTE EX	2462.2	969.1	2.438	3365.9	0.450
17 FTBV INLET	2438.9	969.2	0.000	3365.9	0.446
24 FTBV EXIT	1422.8	976.2	0.000	3365.9	0.265
18 H2 VOLUTE IN	2438.9	969.2	2.438	3365.9	0.446
19 H2 TURB A IN	2433.5	908.9	2.621	3154.9	0.472
20 H2 TURB A EX	1849.1	830.2	2.621	2864.7	0.398
21 H2 TURB B IN	1849.1	830.2	2.719	2864.7	0.398
22 H2 TURB B EX	1452.1	763.7	2.803	2620.7	0.342
23 H2 VOLUTE EX	1446.4	763.7	2.803	2620.7	0.340
24 FTBV EXIT	1422.8	826.8	2.803	2843.2	0.311
25 MIX. TURB IN	1366.1	827.2	3.545	2843.2	0.299
5 MIX. FJBV IN	1281.4	64.9	1.610	-1.4	4.084
26 MIXER EXIT	1276.7	576.6	5.155	1954.9	0.396
27 FBOV INLET	1276.7	576.6	5.155	1954.9	0.396
28 FBOV EXIT	1260.6	576.6	5.155	1954.9	0.394
29 INJ MANIFOLD	1247.9	576.7	5.155	1954.9	0.388
30 INJEC. INLET	1234.2	576.8	5.155	1954.9	0.384
31 INJEC. FACE	1157.2				

OXIDIZER SYSTEM CONDITIONS

STATION	PRESS (PSIA)	TEMP (DEG R)	FLOW (LB/SEC)	ENTHALPY (BTU/LB)	DENSITY (LB/FT3)
32 ENGINE INLET	70.0	161.8	36.953	61.2	71.38
33 PUMP INLET	68.0	162.0	37.606	61.3	71.33
34 PUMP EXIT	1538.6	169.2	37.606	66.5	71.49
35 POSV INLET	1495.1	169.4	3.260	66.5	71.42
36 POSV EXIT	1238.2	170.4	3.260	66.5	71.02
37 SOCV INLET	1490.5	169.4	33.511	66.5	71.42
38 SOCV EXIT	1293.3	170.2	33.511	66.5	71.10
39 PRIM INJ MAN	1238.2	170.4	3.260	66.5	71.02
40 SEC INJ MAN	1288.7	170.2	33.511	66.5	71.10
41 PRIMARY INJ	1234.1	170.4	3.260	66.5	71.01
42 SECONDARY INJ	1284.0	170.2	33.511	66.5	71.09
43 INJECTOR FACE	1157.2				

(Continued) *Table 32. Normal Operating Point, O/F = 7*

AETB ROCETS SIMULATION

THRUST=20000.LB INLET O/F=7.0

OPERATOR	- L. HARTZHEIM
CONFIGURATION	- SPLIT
VERSION	- AETBY4
PROCESS DATE	- 1/15/91
PROCESS TIME	- 14:47:36

* TURBOMACHINERY PERFORMANCE DATA *

		FUEL PUMP A	FUEL PUMP B		LOX PUMP
		1ST STAGE	1ST STAGE	2ND STAGE	
		*********	*********	*********	**********
EFFICIENCY		0.635	0.621	0.628	0.725
HORSEPOWER		746.	316.	300.	279.
TORQUE	(FT-LB)	46.7	20.8	19.8	37.2
SPEED	(RPM)	83868.	79517.	79517.	39460.
HEAD RISE	(FT)	49286.	27128.	27571.	2962.
DIAMETER	(IN)	4.43	3.75	3.75	2.67
TIP SPEED	(FT/SEC)	1621.	1301.	1301.	460.
VOLUMETRIC FLOW	(GPM)	546.	418.	396.	236.
HEAD COEFFICIENT		0.6030	0.5143	0.5238	0.4496
FLOW COEFFICIENT		0.0751	0.0964	0.0921	0.1425
SUCTION SS		7304.7			16935.6

		FUEL TURBINES		LOX TURBINE
		TURBINE A	TURBINE B	
		*********	*********	*********
EFFICIENCY	(T/T)	0.808	0.826	0.799
HORSEPOWER TOTAL		760.1	638.0	339.2
HORSEPOWER PUMP		745.5	615.9	279.2
TORQUE	(FT-LB)	47.6	42.1	45.1
SPEED	(RPM)	83868.	79517.	39460.
MEAN DIAMETER	(IN)	3.85	3.85	6.75
MEAN TIP SPEED	(FT/SEC)	1408.9	1408.9	1162.2
DELTA H (ACTUAL)	(BTU/LB)	205.0	165.8	102.0
DELTA H (IDEAL)	(BTU/LB)	253.6	200.8	127.7
U/C (IDEAL)		.3953	.4211	.4594
FLOW PARAMETER	(IN2)	.0325	.0424	.0271
PRES.RATIO	(T/T)	1.316	1.273	1.127
GAMMA		1.398	1.398	1.399

* VALVE DATA *

STATION		DELTA P PSIA	FLOW (LB/SEC)	BYPASS %	AREA (IN2)
JACKET BYPASS VALVE	(FJBV)	275.1	1.61	30.489	0.070
TURBINE BYPASS VALVE	(MTBV)	1362.2	0.74	23.975	0.062
FUEL TURBINE BYPASS	(FTBV)	1016.1	0.00	0.000	0.000
PRI SHUT OFF VALVE	(POSV)	256.9	3.260		0.036
SEC CONTROL VALVE	(SOCV)	197.1	33.511		0.423
FUEL SHUT OFF VALVE	(FSOV)	8.1	5.155		
FUEL TURBINE SHUTOFF	(FTSV)	6.0	2.803		
FUEL PUMP RECIRC.	(FRV)	1489.8	0.000		

* INJECTOR ELEMENT DATA *

STATION	DELTA P PSIA	FLOW (LB/SEC)	AREA (IN2)
FUEL INJECTOR	77.0	5.155	1.435
PRIMARY LOX INJECTOR	76.9	3.260	0.066
SECONDARY LOX INJECTOR	126.8	33.511	0.528

* INTERNAL FLOWS *

		SOURCE STATION	SINK STATION	FLOW (LB/SEC)
LOX IPS FLOW	(LO1)	34	AMB	0.183
LOX VAPORIZER RECIRC.	(LO2)	34	33	0.653
LH2 OT DISK COOLANT	(LH2)			
LH2A (LEAKAGE)		8	14	0.064
LH2B (IPS)		8	AMB	0.042
LH2 OT BEARING COOLANT	(LH3)	8	15	0.089
LH2 OT IPS	(LH4)	14	AMB	0.067
FT LH2 2ND BEARING COOL.	(LH5)			
LH5A (LEAKAGE)		8	19	0.051
LH5B (RECIRC)		8	3	0.164
FT LH2 SHROUD COOLANT	(LH6)			
LH6A (COOLANT)		8	19	0.132
LH6B (LEAKAGE)		8	20	0.008
LH6C (LEAKAGE)		8	20	0.009
LH6D (LEAKAGE)		8	22	0.012
FT LH2 DISK COOLANT	(LH7)	8	20	0.082
FT LH2 3RD BRG FLOW	(LH8)			
LH8A (LEAKAGE)		7	22	0.072
LH8B (RECIRC)		7	6	0.139

Table 33. Thrust = 15,000 Pounds, O/F = 6

AETB ROCETS SIMULATION

THRUST=15000.LB INLET O/F=6.0

OPERATOR - S. CHESLA
CONFIGURATION - SPLIT
VERSION - AETBY4
PROCESS DATE - 1/15/91
PROCESS TIME - 11:44:43

ENGINE PERFORMANCE

THRUST (VACUUM)	(LB)	15000.
THRUST (SEA LEVEL)	(LB)	11049.
SPECIFIC IMPULSE (VACUUM)	(SEC)	479.87
SPECIFIC IMPULSE (S.L. / AR=7.5)	(SEC)	353.46
TOTAL ENGINE INLET FLOW RATE	(LB/SEC)	31.52
MIXTURE RATIO - INLET		6.00

CHAMBER PERFORMANCE

INJECTOR FACE PRESSURE (TOTAL)	(PSIA)	896.5
THROAT PRESSURE (TOTAL)	(PSIA)	848.9
MIXTURE RATIO - CHAMBER		6.086
FLOW RATE (THROAT)	(LB/SEC)	31.26
THROAT AREA	(IN2)	8.377
NOZZLE AREA RATIO		1000.0
THEORETICAL CHAR. VELOCITY	(FT/SEC)	7544.4
CHAR VELOCITY EFFICIENCY		0.993

ENGINE HEAT TRANSFER

CHAMBER/NOZL COOLANT DELTA P	(PSIA)	313.0
CHAMBER/NOZL COOLANT DELTA T	(DEG R)	836.5
CHAMBER/NOZL HEAT TRANSFER	(BTU/SEC)	8593.3

FUEL SYSTEM CONDITIONS

STATION	PRESS (PSIA)	TEMP (DEG R)	FLOW (LB/SEC)	ENTHALPY (BTU/LB)	DENSITY (LB/FT3)
1 ENGINE INLET	70.0	38.0	4.502	-104.8	4.386
2 PUMP A INLET	69.1	38.0	4.502	-104.8	4.385
3 PUMP A EXIT	1246.9	58.0	4.502	-25.4	4.340
4 FJBV INLET	1245.7	58.0	1.221	-22.5	4.304
5 FJBV EXIT	1001.4	59.9	1.221	-22.5	4.099
6 PUMP B INLET	1244.1	58.6	3.546	-21.0	4.288
7 PUMP B EXIT	1875.1	68.9	3.546	23.0	4.269
8 PUMP C EXIT	2514.9	79.2	3.359	67.2	4.266
9 CHBR COOL IN	2508.2	79.2	2.770	67.2	4.262
10 INTERFACE	2242.2	694.7	2.770	2395.9	0.567
11 NOZL COOL EX	2195.2	915.7	2.756	3173.3	0.425
12 MTBV INLET	2161.5	915.9	0.807	3173.3	0.419
24 MTBV EXIT	1127.7	922.8	0.807	3173.3	0.225
13 O2 VOLUTE IN	2161.5	918.9	1.949	3173.3	0.419
14 O2 TURB IN	2187.3	889.2	1.984	3079.5	0.430
15 O2 TURB EX	1920.0	835.7	2.036	2878.6	0.411
16 O2 VOLUTE EX	1916.6	833.7	2.036	2878.6	0.410
17 FTBV INLET	1898.8	833.8	0.000	2878.6	0.406
24 FTBV EXIT	1127.7	838.7	0.000	2878.6	0.245
18 H2 VOLUTE IN	1898.6	833.8	2.036	2878.6	0.406
19 H2 TURB A IN	1894.7	778.5	2.203	2682.5	0.433
20 H2 TURB A EX	1453.9	712.6	2.203	2441.0	0.368
21 H2 TURB B IN	1453.9	712.6	2.291	2441.0	0.368
22 H2 TURB B EX	1150.2	653.6	2.370	2227.7	0.318
23 H2 VOLUTE EX	1145.8	653.6	2.370	2227.7	0.317
24 FTSV EXIT	1127.7	722.1	2.370	2467.8	0.284
25 MIX. TURB IN	1077.9	722.4	3.177	2467.8	0.272
5 MIX. FJBV IN	1001.4	59.9	1.221	-22.5	4.099
26 MIXER EXIT	998.8	528.4	4.397	1776.5	0.341
27 FSOV INLET	998.8	528.4	4.397	1776.5	0.341
28 FSOV EXIT	991.9	528.5	4.397	1776.5	0.339
29 INJ MANIFOLD	974.5	528.5	4.397	1776.5	0.333
30 INJEC. INLET	962.8	528.6	4.397	1776.5	0.329
31 INJEC. FACE	896.5				

OXIDIZER SYSTEM CONDITIONS

STATION	PRESS (PSIA)	TEMP (DEG R)	FLOW (LB/SEC)	ENTHALPY (BTU/LB)	DENSITY (LB/FT3)
32 ENGINE INLET	70.0	161.8	27.015	61.2	71.38
33 PUMP INLET	68.9	162.1	27.638	61.3	71.33
34 PUMP EXIT	1407.7	168.7	27.638	66.1	71.46
35 POSV INLET	1384.5	168.8	3.917	66.1	71.42
36 POSV EXIT	1013.6	170.3	3.917	66.1	70.83
37 SOCV INLET	1382.3	168.8	22.931	66.1	71.42
38 SOCV EXIT	960.6	170.5	22.931	66.1	70.75
39 PRIM INJ MAN	1013.6	170.3	3.917	66.1	70.83
40 SEC INJ MAN	958.4	170.5	22.931	66.1	70.74
41 PRIMARY INJ	1007.8	170.3	3.917	66.1	70.82
42 SECONDARY INJ	956.2	170.5	22.931	66.1	70.74
43 INJECTOR FACE	896.5				

(Continued) Table 33. Thrust = 15,000 Pounds, O/F = 6

AETB ROCETS SIMULATION

THRUST=15000.LB INLET O/F=6.0

OPERATOR - S. CHESLA
CONFIGURATION - SPLIT
VERSION - AETBY4
PROCESS DATE - 1/15/91
PROCESS TIME - 11:44:43

* TURBOMACHINERY PERFORMANCE DATA *

		FUEL PUMP A	FUEL PUMP B		LOX PUMP
		1ST STAGE	1ST STAGE	2ND STAGE	
		*********	*********	*********	**********
EFFICIENCY		0.631	0.621	0.628	0.721
HORSEPOWER		506.	221.	210.	188.
TORQUE	(FT-LB)	35.9	16.4	15.6	27.9
SPEED	(RPM)	74067.	70510.	70510.	35411.
HEAD RISE	(FT)	38964.	21247.	21590.	2698.
DIAMETER	(IN)	4.43	3.75	3.75	2.67
TIP SPEED	(FT/SEC)	1432.	1154.	1154.	413.
VOLUMETRIC FLOW	(GPM)	466.	373.	353.	174.
HEAD COEFFICIENT		0.6112	0.5123	0.5217	0.5085
FLOW COEFFICIENT		0.0726	0.0969	0.0928	0.1168
SUCTION SS		5927.6			12949.8

		FUEL TURBINES		LOX TURBINE
		TURBINE A	TURBINE B	
		*********	*********	*********
EFFICIENCY	(T/T)	0.805	0.819	0.795
HORSEPOWER TOTAL		517.0	447.8	236.2
HORSEPOWER PUMP		505.6	430.6	188.0
TORQUE	(FT-LB)	36.7	33.4	35.0
SPEED	(RPM)	74067.	70510.	35411.
MEAN DIAMETER	(IN)	3.85	3.85	6.75
MEAN TIP SPEED	(FT/SEC)	1244.2	1244.2	1042.9
DELTA H (ACTUAL)	(BTU/LB)	165.9	138.2	85.4
DELTA H (IDEAL)	(BTU/LB)	206.1	168.8	107.5
U/C (IDEAL)		.3872	.4074	.4494
FLOW PARAMETER	(IN2)	.0324	.0421	.0270
PRES.RATIO	(T/T)	1.303	1.264	1.124
GAMMA		1.398	1.398	1.398

* VALVE DATA *

STATION		DELTA P PSIA	FLOW (LB/SEC)	BYPASS %	AREA (IN2)
JACKET BYPASS VALVE	(FJBV)	244.3	1.22	27.110	0.056
TURBINE BYPASS VALVE	(MTBV)	1033.9	0.81	29.270	0.081
FUEL TURBINE BYPASS	(FTBV)	771.1	0.00	0.000	0.000
PRI SHUT OFF VALVE	(POSV)	370.9	3.917		0.036
SEC CONTROL VALVE	(SOCV)	421.8	22.931		0.198
FUEL SHUT OFF VALVE	(FSOV)	6.9	4.397		
FUEL TURBINE SHUTOFF	(FTSV)	4.6	2.370		
FUEL PUMP RECIRC.	(FRV)	1177.8	0.000		

* INJECTOR ELEMENT DATA *

STATION	DELTA P PSIA	FLOW (LB/SEC)	AREA (IN2)
FUEL INJECTOR	66.3	4.397	1.435
PRIMARY LOX INJECTOR	111.3	3.917	0.066
SECONDARY LOX INJECTOR	59.7	22.931	0.528

* INTERNAL FLOWS *

		SOURCE STATION	SINK STATION	FLOW (LB/SEC)
LOX IPS FLOW	(LO1)	34	AMB	0.168
LOX VAPORIZER RECIRC.	(LO2)	34	33	0.623
LH2 OT DISK COOLANT	(LH2)			
LH2A (LEAKAGE)		8	14	0.061
LH2B (IPS)		8	AMB	0.036
LH2 OT BEARING COOLANT	(LH3)	8	15	0.081
LH2 OT IPS	(LH4)	14	AMB	0.056
FT LH2 2ND BEARING COOL.	(LH5)			
LH5A (LEAKAGE)		8	19	0.047
LH5B (RECIRC)		8	3	0.145
FT LH2 SHROUD COOLANT	(LH6)			
LH6A (COOLANT)		8	19	0.121
LH6B (LEAKAGE)		8	20	0.007
LH6C (LEAKAGE)		8	20	0.008
LH6D (LEAKAGE)		8	22	0.011
FT LH2 DISK COOLANT	(LH7)	8	20	0.073
FT LH2 3RD BRG FLOW	(LH8)			
LH8A (LEAKAGE)		7	22	0.068
LH8B (RECIRC)		7	6	0.119

Table 34. Thrust = 10,000 Pounds, O/F = 6

AETB ROCETS SIMULATION

THRUST=10000.LB INLET O/F=6.0

OPERATOR - S. CHEBLA
CONFIGURATION - SPLIT
VERSION - AETBY4
PROCESS DATE - 1/15/91
PROCESS TIME - 14: 0:48

ENGINE PERFORMANCE

THRUST (VACUUM)	(LB)	10000.
THRUST (SEA LEVEL)	(LB)	7065.
SPECIFIC IMPULSE (VACUUM)	(SEC)	476.39
SPECIFIC IMPULSE (S.L. / AR=7.5)	(SEC)	336.57
TOTAL ENGINE INLET FLOW RATE	(LB/SEC)	21.17
MIXTURE RATIO - INLET		6.00

CHAMBER PERFORMANCE

INJECTOR FACE PRESSURE (TOTAL)	(PSIA)	597.4
THROAT PRESSURE (TOTAL)	(PSIA)	578.9
MIXTURE RATIO - CHAMBER		6.090
FLOW RATE (THROAT)	(LB/SEC)	20.99
THROAT AREA	(IN2)	8.377
NOZZLE AREA RATIO		1000.0
THEORETICAL CHAR. VELOCITY	(FT/SEC)	7515.8
CHAR ..LOCITY EFFICIENCY		0.989

ENGINE HEAT TRANSFER

CHAMBER/NOZL COOLANT DELTA P	(PSIA)	266.7
CHAMBER/NOZL COOLANT DELTA T	(DEG R)	773.0
CHAMBER/NOZL HEAT TRANSFER	(BTU/SEC)	6367.7

FUEL SYSTEM CONDITIONS

STATION	PRESS (PSIA)	TEMP (DEG R)	FLOW (LB/SEC)	ENTHALPY (BTU/LB)	DENSITY (LB/FT3)
1 ENGINE INLET	70.0	38.0	3.025	-104.8	4.386
2 PUMP A INLET	69.6	38.0	3.025	-104.8	4.385
3 PUMP A EXIT	945.2	54.4	3.025	-41.7	4.295
4 FJBV INLET	945.1	54.4	0.352	-39.7	4.269
5 FJBV EXIT	674.3	56.3	0.352	-39.7	4.013
6 PUMP B INLET	943.4	54.7	2.848	-39.1	4.260
7 PUMP B EXIT	1318.5	60.9	2.848	-12.7	4.246
8 PUMP C EXIT	1699.0	67.1	2.704	13.7	4.240
9 CHBR COOL IN	1694.8	67.1	2.216	13.7	4.237
10 INTERFACE	1468.2	632.3	2.216	2158.0	0.415
11 NOZL COOL EX	1428.0	840.1	2.205	2890.4	0.307
12 MTBV INLET	1398.2	840.3	0.933	2890.4	0.301
24 MTBV EXIT	788.2	844.2	0.933	2890.4	0.172
13 O2 VOLUTE IN	1398.2	840.3	1.272	2890.4	0.301
14 O2 TURB IN	1395.7	806.2	1.290	2769.6	0.313
15 O2 TURB EX	1256.8	749.4	1.360	2566.2	0.303
16 O2 VOLUTE EX	1254.8	749.4	1.360	2566.2	0.303
17 FTBV INLET	1244.0	749.5	0.000	2566.2	0.300
24 FTBV EXIT	788.2	752.2	0.000	2566.2	0.192
18 H2 VOLUTE IN	1244.3	749.5	1.360	2566.2	0.300
19 H2 TURB A IN	1241.5	686.5	1.503	2344.9	0.328
20 H2 TURB A EX	979.0	628.4	1.503	2135.3	0.284
21 H2 TURB B IN	979.0	628.4	1.575	2135.3	0.284
22 H2 TURB B EX	802.0	571.3	1.664	1928.2	0.256
23 H2 VOLUTE EX	799.3	571.3	1.664	1928.2	0.255
24 FTSV EXIT	788.2	668.7	1.664	2273.9	0.216
25 MIX. TURB IN	744.4	669.0	2.597	2273.9	0.204
5 MIX. FJBV IN	674.3	56.3	0.352	-39.7	4.013
26 MIXER EXIT	674.1	591.2	2.950	1997.5	0.208
27 FSOV INLET	674.1	591.2	2.950	1997.5	0.208
28 FSOV EXIT	668.9	591.2	2.950	1997.5	0.207
29 INJ MANIFOLD	656.1	591.3	2.950	1997.5	0.203
30 INJEC. INLET	647.5	591.3	2.950	1997.5	0.200
31 INJEC. FACE	597.3				

OXIDIZER SYSTEM CONDITIONS

STATION	PRESS (PSIA)	TEMP (DEG R)	FLOW (LB/SEC)	ENTHALPY (BTU/LB)	DENSITY (LB/FT3)
32 ENGINE INLET	70.0	161.8	18.150	61.2	71.38
33 PUMP INLET	69.5	162.0	18.667	61.3	71.33
34 PUMP EXIT	991.9	166.9	18.667	64.7	71.37
35 POSV INLET	981.5	166.9	3.474	64.7	71.35
36 POSV EXIT	689.4	168.1	3.474	64.7	70.89
37 SOCV INLET	980.6	166.9	14.557	64.7	71.35
38 SOCV EXIT	623.2	168.4	14.557	64.7	70.78
39 PRIM INJ MAN	689.4	168.1	3.474	64.7	70.89
40 SEC INJ MAN	622.3	168.4	14.557	64.7	70.78
41 PRIMARY INJ	684.8	168.1	3.474	64.7	70.88
42 SECONDARY INJ	621.4	168.4	14.557	64.7	70.77
43 INJECTOR FACE	597.4				

(Continued) Table 34. Thrust = 10,000 Pounds, O/F = 6

AETB ROCETS SIMULATION

THRUST=10000.LB INLET O/F=6.0

OPERATOR - S. CHESLA
CONFIGURATION - SPLIT
VERSION - AETBY4
PROCESS DATE - 1/15/91
PROCESS TIME - 14: 0:48

* TURBOMACHINERY PERFORMANCE DATA *

		FUEL PUMP A	FUEL PUMP B		LOX PUMP
		1ST STAGE	1ST STAGE	2ND STAGE	
		*********	*********	*********	*********
EFFICIENCY		0.594	0.619	0.626	0.693
HORSEPOWER		270.	106.	101.	91.
TORQUE	(FT-LB)	22.8	10.1	9.6	16.8
SPEED	(RPM)	62300.	55196.	55196.	28497.
HEAD RISE	(FT)	29171.	12703.	12913.	1861.
DIAMETER	(IN)	4.43	3.75	3.75	2.67
TIP SPEED	(FT/SEC)	1204.	903.	903.	332.
VOLUMETRIC FLOW	(GPM)	316.	301.	286.	117.
HEAD COEFFICIENT		0.6467	0.4999	0.5092	0.5417
FLOW COEFFICIENT		0.0586	0.1000	0.0960	0.0981
SUCTION SS		4079.8			8463.4

		FUEL TURBINES		LOX TURBINE
		TURBINE A	TURBINE B	
		*********	*********	*********
EFFICIENCY	(T/T)	0.796	0.792	0.776
HORSEPOWER TOTAL		278.1	219.9	122.3
HORSEPOWER PUMP		270.0	207.7	91.1
TORQUE	(FT-LB)	23.4	20.9	22.5
SPEED	(RPM)	62300.	55196.	28497.
MEAN DIAMETER	(IN)	3.85	3.85	6.75
MEAN TIP SPEED	(FT/SEC)	1046.6	1046.6	839.3
DELTA H (ACTUAL)	(BTU/LB)	130.7	98.7	67.0
DELTA H (IDEAL)	(BTU/LB)	164.3	124.6	86.3
U/C (IDEAL)		.3648	.3711	.4036
FLOW PARAMETER	(IN2)	.0317	.0403	.0262
PRES.RATIO	(T/T)	1.268	1.221	1.110
GAMMA		1.397	1.396	1.398

* VALVE DATA *

STATION		DELTA P PSIA	FLOW (LB/SEC)	BYPASS %	AREA (IN2)
JACKET BYPASS VALVE	(FJBV)	270.9	0.35	11.648	0.016
TURBINE BYPASS VALVE	(MTBV)	610.0	0.93	42.310	0.138
FUEL TURBINE BYPASS	(FTBV)	455.8	0.00	0.000	0.000
PRI SHUT OFF VALVE	(POSV)	292.0	3.474		0.036
SEC CONTROL VALVE	(SOCV)	357.4	14.557		0.136
FUEL SHUT OFF VALVE	(FSOV)	5.2	2.950		
FUEL TURBINE SHUTOFF	(FTSV)	2.8	1.664		
FUEL PUMP RECIRC.	(FRV)	875.6	0.000		

* INJECTOR ELEMENT DATA *

STATION	DELTA P PSIA	FLOW (LB/SEC)	AREA (IN2)
FUEL INJECTOR	50.2	2.950	1.435
PRIMARY LOX INJECTOR	87.5	3.474	0.066
SECONDARY LOX INJECTOR	24.0	14.557	0.528

* INTERNAL FLOWS *

		SOURCE STATION	SINK STATION	FLOW (LB/SEC)
**				
LOX IPS FLOW	(LO1)	34	AMB	0.119
LOX VAPORIZER RECIRC.	(LO2)	34	33	0.517
LH2 OT DISK COOLANT	(LH2)			
LH2A (LEAKAGE)		8	14	0.056
LH2B (IPS)		8	AMB	0.027
LH2 OT BEARING COOLANT	(LH3)	8	15	0.070
LH2 OT IPS	(LH4)	14	AMB	0.038
FT LH2 2ND BEARING COOL.	(LH5)			
LH5A (LEAKAGE)		8	19	0.040
LH5B (RECIRC)		8	3	0.111
FT LH2 SHROUD COOLANT	(LH6)			
LH6A (COOLANT)		8	19	0.103
LH6B (LEAKAGE)		8	20	0.006
LH6C (LEAKAGE)		8	20	0.006
LH6D (LEAKAGE)		8	22	0.009
FT LH2 DISK COOLANT	(LH7)	8	20	0.060
FT LH2 3RD BRG FLOW	(LH8)			
LH8A (LEAKAGE)		7	22	0.080
LH8B (RECIRC)		7	6	0.064

Table 35. Thrust = 6,000 Pounds, O/F = 6

AETB ROCETS SIMULATION

THRUST=6000.LB INLET O/F=6.0

OPERATOR - S. CHESLA
CONFIGURATION - SPLIT
VERSION - AETBY4
PROCESS DATE - 1/15/91
PROCESS TIME - 14:14:45

ENGINE PERFORMANCE

THRUST (VACUUM)	(LB)	6000.
THRUST (SEA LEVEL)	(LB)	3867.
SPECIFIC IMPULSE (VACUUM)	(SEC)	473.71
SPECIFIC IMPULSE (S.L. / AR=7.5)	(SEC)	305.28
TOTAL ENGINE INLET FLOW RATE	(LB/SEC)	12.77
MIXTURE RATIO - INLET		6.00

CHAMBER PERFORMANCE

INJECTOR FACE PRESSURE (TOTAL)	(PSIA)	357.6
THROAT PRESSURE (TOTAL)	(PSIA)	346.5
MIXTURE RATIO - CHAMBER		6.090
FLOW RATE (THROAT)	(LB/SEC)	12.67
THROAT AREA	(IN2)	8.377
NOZZLE AREA RATIO		1000.0
THEO.‾ ..L CHAR. VELOCITY	(FT/SEC)	7478.7
CHAR. VELOCITY EFFICIENCY		0.986

ENGINE HEAT TRANSFER

CHAMBER/NOZL COOLANT DELTA P	(PSIA)	165.0
CHAMBER/NOZL COOLANT DELTA T	(DEG R)	765.7
CHAMBER/NOZL HEAT TRANSFER	(BTU/SEC)	4244.0

FUEL SYSTEM CONDITIONS

STATION	PRESS (PSIA)	TEMP (DEG R)	FLOW (LB/SEC)	ENTHALPY (BTU/LB)	DENSITY (LB/FT3
1 ENGINE INLET	70.0	38.0	1.824	-104.8	4.386
2 PUMP A INLET	69.9	38.0	1.824	-104.8	4.386
3 PUMP A EXIT	555.7	48.4	1.824	-67.0	4.288
4 FJBV INLET	555.7	48.4	0.000	-65.7	4.269
5 FJBV EXIT	555.7	48.4	0.000	-65.7	4.269
6 PUMP B INLET	554.8	48.5	1.960	-65.3	4.262
7 PUMP B EXIT	755.0	51.9	1.960	-51.3	4.254
8 PUMP C EXIT	957.6	55.2	1.854	-37.2	4.248
9 CHBR COOL IN	955.7	55.2	1.493	-37.2	4.246
10 INTERFACE	821.5	612.3	1.493	2075.3	0.846
11 NOZL COOL EX	790.7	820.9	1.486	2808.4	0.177
12 MTBV INLET	767.2	821.1	0.814	2808.4	0.172
24 MTBV EXIT	493.9	822.8	0.814	2808.4	0.112
13 O2 VOLUTE IN	767.2	821.1	0.672	2808.4	0.172
14 O2 TURB IN	765.9	771.1	0.695	2632.3	0.182
15 O2 TURB EX	706.5	706.5	0.748	2404.4	0.184
16 O2 VOLUTE EX	705.5	706.5	0.748	2404.4	0.184
17 FTBV INLET	700.2	706.5	0.000	2404.4	0.183
24 FTBV EXIT	493.9	7.7.7	0.000	2404.4	0.130
18 H2 VOLUTE IN	700.2	706.5	0.748	2404.4	0.183
19 H2 TURB A IN	698.9	627.2	0.856	2125.8	0.205
20 H2 TURB A EX	584.0	578.4	0.856	1949.8	0.185
21 H2 TURB B IN	584.0	578.4	0.908	1949.8	0.185
22 H2 TURB B EX	500.7	529.0	0.965	1771.5	0.174
23 H2 VOLUTE EX	499.4	529.0	0.965	1771.5	0.174
24 FTSV EXIT	493.9	662.3	0.965	2245.8	0.138
25 MIX. TURB IN	461.7	662.5	1.779	2245.8	0.129
5 MIX. FJBV IN	555.7	48.4	0.000	-65.7	4.269
26 MIXER EXIT	409.5	662.8	1.779	2245.8	0.115
27 FSOV INLET	409.5	662.8	1.779	2245.8	0.115
28 FSOV EXIT	406.0	662.8	1.779	2245.8	0.114
29 INJ MANIFOLD	397.5	662.8	1.779	2245.8	0.111
30 INJEC. INLET	391.8	662.9	1.779	2245.8	0.110
31 INJEC. FACE	357.6				

OXIDIZER SYSTEM CONDITIONS

STATION	PRESS (PSIA)	TEMP (DEG R)	FLOW (LB/SEC)	ENTHALPY (BTU/LB)	DENSITY (LB/FT3)
32 ENGINE INLET	70.0	161.8	10.945	61.2	71.38
33 PUMP INLET	69.8	161.9	11.312	61.3	71.35
34 PUMP EXIT	535.6	164.6	11.312	63.1	71.33
35 POSV INLET	531.8	164.6	2.340	63.1	71.32
36 POSV EXIT	399.2	165.2	2.340	63.1	71.11
37 SOCV INLET	531.5	164.6	8.540	63.1	71.32
38 SOCV EXIT	366.4	165.3	8.540	63.1	71.05
39 PRIM INJ MAN	399.2	165.2	2.340	63.1	71.11
40 SEC INJ MAN	366.1	165.3	8.540	63.1	71.05
41 PRIMARY INJ	397.1	165.2	2.340	63.1	71.10
42 SECONDARY INJ	365.8	165.3	8.540	63.1	71.05
43 INJECTOR FACE	357.6				

(Continued) *Table 35. Thrust = 6,000 Pounds, O/F = 6*

AETB ROCETS SIMULATION

THRUST=6000.LB INLET O/F=6.0

OPERATOR - S. CHESLA
CONFIGURATION - SPLIT
VERSION - AETBY4
PROCESS DATE - 1/15/91
PROCESS TIME - 14:14:45

* TURBOMACHINERY PERFORMANCE DATA *

		FUEL PUMP A	FUEL PUMP B		LOX PUMP
		1ST STAGE	1ST STAGE	2ND STAGE	
		*********	*********	*********	**********
EFFICIENCY		0.550	0.621	0.628	0.661
HORSEPOWER		98.	39.	37.	29.
TORQUE	(FT-LB)	11.2	5.1	4.9	7.7
SPEED	(RPM)	45795.	39603.	39603.	19921.
HEAD RISE	(FT)	16194.	6767.	6864.	940.
DIAMETER	(IN)	4.43	3.75	3.75	2.67
TIP SPEED	(FT/SEC)	885.	648.	648.	232.
VOLUMETRIC FLOW	(GPM)	191.	207.	196.	71.
HEAD COEFFICIENT		0.6645	0.5173	0.5257	0.5600
FLOW COEFFICIENT		0.0481	0.0957	0.0916	0.0851
SUCTION SS		2322.0			4607.1

		FUEL TURBINES		LOX TURBINE
		TURBINE A	TURBINE B	
		*********	*********	*********
EFFICIENCY	(T/T)	0.778	0.742	0.730
HORSEPOWER TOTAL		102.0	82.3	44.5
HORSEPOWER PUMP		97.7	75.7	29.3
TORQUE	(FT-LB)	11.7	10.9	11.7
SPEED	(RPM)	45795.	39603.	19921.
MEAN DIAMETER	(IN)	3.85	3.85	6.75
MEAN TIP SPEED	(FT/SEC)	769.3	769.3	586.7
DELTA H (ACTUAL)	(BTU/LB)	84.3	64.1	45.3
DELTA H (IDEAL)	(BTU/LB)	108.3	86.3	62.1
U/C (IDEAL)		.3303	.3199	.3328
FLOW PARAMETER	(IN2)	.0307	.0374	.0252
PRES.RATIO	(T/T)	1.197	1.166	1.084
GAMMA		1.395	1.392	1.397

* VALVE DATA *

STATION		DELTA P PSIA	FLOW (LB/SEC)	BYPASS %	AREA (IN2)
JACKET BYPASS VALVE	(FJBV)	0.1	0.00	0.000	0.000
TURBINE BYPASS VALVE	(MTBV)	273.3	0.81	54.768	0.223
FUEL TURBINE BYPASS	(FTBV)	206.3	0.00	0.000	0.000
PRI SHUT OFF VALVE	(POSV)	132.5	2.340		0.036
SEC CONTROL VALVE	(SOCV)	165.0	8.540		0.118
FUEL SHUT OFF VALVE	(FSOV)	3.5	1.779		
FUEL TURBINE SHUTOFF	(FTSV)	1.4	0.965		
FUEL PUMP RECIRC.	(FRV)	485.9	0.000		

* INJECTOR ELEMENT DATA *

STATION	DELTA P PSIA	FLOW (LB/SEC)	AREA (IN2)
FUEL INJECTOR	34.2	1.779	1.435
PRIMARY LOX INJECTOR	39.6	2.340	0.066
SECONDARY LOX INJECTOR	8.2	8.540	0.528

* INTERNAL FLOWS *

		SOURCE STATION	SINK STATION	FLOW (LB/SEC)
LOX IPS FLOW	(LO1)	34	AMB	0.065
LOX VAPORIZER RECIRC.	(LO2)	34	33	0.367
LH2 OT DISK COOLANT	(LH2)			
LH2A (LEAKAGE)		8	14	0.044
LH2B (IPS)		8	AMB	0.017
LH2 OT BEARING COOLANT	(LH3)	8	15	0.053
LH2 OT IPS	(LH4)	14	AMB	0.021
FT LH2 2ND BEARING COOL.	(LH5)			
LH5A (LEAKAGE)		8	19	0.030
LH5B (RECIRC)		8	3	0.081
FT LH2 SHROUD COOLANT	(LH6)			
LH6A (COOLANT)		8	19	0.078
LH6B (LEAKAGE)		8	20	0.004
LH6C (LEAKAGE)		8	20	0.005
LH6D (LEAKAGE)		8	22	0.006
FT LH2 DISK COOLANT	(LH7)	8	20	0.043
FT LH2 3RD BRG FLOW	(LH8)			
LH8A (LEAKAGE)		7	22	0.051
LH8B (RECIRC)		7	6	0.054

Table 36. Thrust = 4,000 Pounds, O/F = 6

AETB ROCETS SIMULATION

THRUST=4000.LB INLET O/F 6.0

OPERATOR - S. CHEBLA
CONFIGURATION - SPLIT
VERSION - AETBY4
PROCESS DATE - 1/18/91
PROCESS TIME - 9:23:34

ENGINE PERFORMANCE

THRUST (VACUUM)	(LB)	4000.
THRUST (SEA LEVEL)	(LB)	2266.
SPECIFIC IMPULSE (VACUUM)	(SEC)	472.51
SPECIFIC IMPULSE (S.L. / AR=7.5)	(SEC)	267.72
TOTAL ENGINE INLET FLOW RATE	(LB/SEC)	8.53
MIXTURE RATIO - INLET		6.00

CHAMBER PERFORMANCE

INJECTOR FACE PRESSURE (TOTAL)	(PSIA)	237.8
THROAT PRESSURE (TOTAL)	(PSIA)	230.5
MIXTURE RATIO - CHAMBER		6.087
FLOW RATE (THROAT)	(LB/SEC)	8.47
THROAT AREA	(IN2)	8.377
NOZZLE AREA RATIO		1000.0
THEORETICAL CHAR. VELOCITY	(FT/SEC)	7448.9
CHAR VELOCITY EFFICIENCY		0.985

ENGINE HEAT TRANSFER

CHAMBER/NOZL COOLANT DELTA P	(PSIA)	120.2
CHAMBER/NOZL COOLANT DELTA T	(DEG R)	834.4
CHAMBER/NOZL HEAT TRANSFER	(BTU/SEC)	3015.6

FUEL SYSTEM CONDITIONS

STATION	PRESS (PSIA)	TEMP (DEG R)	FLOW (LB/SEC)	ENTHALPY (BTU/LB)	DENSITY (LB/FT3)
1 ENGINE INLET	70.0	38.0	1.219	-104.8	4.386
2 PUMP A INLET	69.9	42.1	1.919	-94.3	4.205
3 PUMP A EXIT	326.5	46.8	1.919	-76.1	4.192
4 FJBV INLET	326.5	46.8	0.000	-75.3	4.179
5 FJBV EXIT	326.5	46.8	0.000	-75.3	4.179
6 PUMP B INLET	326.1	47.0	1.364	-74.7	4.169
7 PUMP B EXIT	476.2	49.6	1.364	-63.9	4.163
8 PUMP C EXIT	626.7	52.2	1.274	-53.0	4.156
9 CHBR COOL IN	625.9	52.3	0.979	-53.0	4.155
10 INTERFACE	523.0	613.8	0.979	2075.4	0.158
11 NOZL COOL EX	505.7	886.7	0.974	3033.0	0.106
12 MTBV INLET	488.7	886.8	0.583	3033.0	0.102
24 MTBV EXIT	334.3	887.8	0.583	3033.0	0.070
13 O2 VOLUTE IN	488.7	886.8	0.391	3033.0	0.102
14 O2 TURB IN	488.0	810.3	0.415	2764.3	0.112
15 O2 TURB EX	455.9	726.5	0.458	2469.5	0.117
16 O2 VOLUTE EX	455.3	726.5	0.458	2469.5	0.116
17 FTBV INLET	452.2	726.5	0.000	2469.5	0.116
24 FTBV EXIT	334.3	777.2	0.000	2469.5	0.086
18 H2 VOLUTE IN	452.2	726.5	0.458	2469.5	0.116
19 H2 TURB A IN	451.4	621.4	0.546	2101.0	0.135
20 H2 TURB A EX	387.9	571.1	0.546	1921.0	0.126
21 H2 TURB B IN	387.9	571.1	0.587	1921.0	0.126
22 H2 TURB B EX	338.3	539.1	0.607	1805.8	0.116
23 H2 VOLUTE EX	337.5	539.1	0.607	1805.8	0.116
24 FTSV EXIT	334.3	709.2	0.607	2406.8	0.088
25 MIX. TURB IN	311.7	709.4	1.190	2406.8	0.082
5 MIX. FJBV IN	326.5	46.8	0.000	-75.3	4.179
26 MIXER EXIT	275.0	709.6	1.190	2406.8	0.072
27 FSOV INLET	275.0	709.6	1.190	2406.8	0.072
28 FSOV EXIT	272.5	709.6	1.190	2406.8	0.072
29 INJ MANIFOLD	266.8	709.6	1.190	2406.8	0.070
30 INJEC. INLET	262.4	709.7	1.190	2406.8	0.069
31 INJEC. FACE	237.8				

OXIDIZER SYSTEM CONDITIONS

STATION	PRESS (PSIA)	TEMP (DEG R)	FLOW (LB/SEC)	ENTHALPY (BTU/LB)	DENSITY (LB/FT3)
32 ENGINE INLET	70.0	161.8	7.314	61.2	71.38
33 PUMP INLET	69.9	161.9	7.601	61.2	71.36
34 PUMP EXIT	354.8	163.7	7.601	62.4	71.31
35 POSV INLET	353.1	163.7	1.904	62.4	71.31
36 POSV EXIT	265.3	164.0	1.904	62.4	71.16
37 SOCV INLET	353.0	163.7	5.367	62.4	71.31
38 SOCV EXIT	241.3	164.1	5.367	62.4	71.12
39 PRIM INJ MAN	265.3	164.0	1.904	62.4	71.16
40 SEC INJ MAN	241.2	164.1	5.367	62.4	71.12
41 PRIMARY INJ	264.0	164.1	1.904	62.4	71.16
42 SECONDARY INJ	241.0	164.1	5.367	62.4	71.12
43 INJECTOR FACE	237.8				

(Continued) Table 36. Thrust = 4,000 Pounds, O/F = 6

AETB ROCETS SIMULATION

THRUST=4000.LB INLET O/F 6.0

OPERATOR - S. CHESLA
CONFIGURATION - SPLIT
VERSION - AETBY4
PROCESS DATE - 1/15/91
PROCESS TIME - 9:23:34

* TURBOMACHINERY PERFORMANCE DATA *

		FUEL PUMP A	FUEL PUMP B		LOX PUMP
		1ST STAGE	1ST STAGE	2ND STAGE	
		*********	*********	*********	*********
EFFICIENCY		0.622	0.618	0.615	0.623
HORSEPOWER		49.	21.	20.	13.
TORQUE	(FT-LB)	7.4	3.3	3.1	4.4
SPEED	(RPM)	34842.	33087.	33087.	15411.
HEAD RISE	(FT)	8804.	5188.	5210.	575.
DIAMETER	(IN)	4.43	3.75	3.75	2.67
TIP SPEED	(FT/SEC)	673.	541.	541.	180.
VOLUMETRIC FLOW	(GPM)	205.	147.	138.	48.
HEAD COEFFICIENT		0.6240	0.5682	0.5717	0.5727
FLOW COEFFICIENT		0.0681	0.0815	0.0769	0.0740
SUCTION SS		2249.9			2903.9

		FUEL TURBINES		LOX TURBINE
		TURBINE A	TURBINE B	
		*********	*********	*********
EFFICIENCY	(T/T)	0.739	0.695	0.685
HORSEPOWER TOTAL		51.9	44.2	21.9
HORSEPOWER PUMP		49.4	40.4	12.8
TORQUE	(FT-LB)	7.8	7.0	7.5
SPEED	(RPM)	34842.	33087.	15411.
MEAN DIAMETER	(IN)	3.85	3.85	6.75
MEAN TIP SPEED	(FT/SEC)	585.3	585.3	453.9
DELTA H (ACTUAL)	(BTU/LB)	67.2	53.3	37.3
DELTA H (IDEAL)	(BTU/LB)	90.9	76.7	54.4
U/C (IDEAL)		.2743	.2836	.2749
FLOW PARAMETER	(IN2)	.0302	.0362	.0242
PRES.RATIO	(T/T)	1.164	1.147	1.070
GAMMA		1.394	1.391	1.396

* VALVE DATA *

STATION		DELTA P PSIA	FLOW (LB/SEC)	BYPASS %	AREA (IN2)
JACKET BYPASS VALVE	(FJBV)	0.1	0.00	0.000	0.000
TURBINE BYPASS VALVE	(MTBV)	154.5	0.58	59.825	0.268
FUEL TURBINE BYPASS	(FTBV)	117.9	0.00	0.000	0.000
PRI SHUT OFF VALVE	(POSV)	87.8	1.904		0.036
SEC CONTROL VALVE	(SOCV)	111.7	5.367		0.090
FUEL SHUT OFF VALVE	(FSOV)	2.5	1.190		
FUEL TURBINE SHUTOFF	(FTSV)	0.8	0.607		
FUEL PUMP RECIRC.	(FRV)	256.6	0.700		

* INJECTOR ELEMENT DATA *

STATION	DELTA P PSIA	FLOW (LB/SEC)	AREA (IN2)
FUEL INJECTOR	24.6	1.190	1.435
PRIMARY LOX INJECTOR	26.2	1.904	0.066
SECONDARY LOX INJECTOR	3.3	5.367	0.528

* INTERNAL FLOWS *

		SOURCE STATION	SINK STATION	FLOW (LB/SEC)
**************************				
LOX IPS FLOW	(LO1)	34	AMB	0.043
LOX VAPORIZER RECIRC.	(LO2)	34	33	0.287
LH2 OT DISK COOLANT	(LH2)			
LH2A (LEAKAGE)		8	14	0.037
LH2B (IPS)		8	AMB	0.011
LH2 OT BEARING COOLANT	(LH3)	8	15	0.043
LH2 OT IPS	(LH4)	14	AMB	0.013
FT LH2 2ND BEARING COOL.	(LH5)			
LH5A (LEAKAGE)		8	19	0.024
LH5B (RECIRC)		8	3	0.070
FT LH2 SHROUD COOLANT	(LH6)			
LH6A (COOLANT)		8	19	0.063
LH6B (LEAKAGE)		8	20	0.003
LH6C (LEAKAGE)		8	20	0.004
LH6D (LEAKAGE)		8	22	0.005
FT LH2 DISK COOLANT	(LH7)	8	20	0.034
FT LH2 3RD BRG FLOW	(LH8)			
LH8A (LEAKAGE)		7	22	0.015
LH8B (RECIRC)		7	6	0.075

Table 37. Thrust = 1,000 Pounds, O/F = 3.5

AETB ROCETS SIMULATION

THRUST=1000.LB INLET O/F=3.5

OPERATOR - S. CHESLA
CONFIGURATION - SPLIT
VERSION - AETBY4
PROCESS DATE - 1/15/91
PROCESS TIME - 9:46:17

ENGINE PERFORMANCE

THRUST (VACUUM)	(LB)	1000.
SPECIFIC IMPULSE (VACUUM)	(SEC)	465.07
TOTAL ENGINE INLET FLOW RATE	(LB/SEC)	2.18
MIXTURE RATIO - INLET		3.50

CHAMBER PERFORMANCE

INJECTOR FACE PRESSURE (TOTAL)	(PSIA)	65.0
THROAT PRESSURE (TOTAL)	(PSIA)	62.9
MIXTURE RATIO - CHAMBER		3.531
FLOW RATE (THROAT)	(LB/SEC)	2.15
THROAT AREA	(IN2)	8.377
NOZZLE AREA RATIO		1000.0
THEORETICAL CHAR. VELOCITY	(FT/SEC)	7946.0
CHAR. VELOCITY EFFICIENCY		0.993

ENGINE HEAT TRANSFER

CHAMBER/NOZL COOLANT DELTA P	(PSIA)	93.8
CHAMBER/NOZL COOLANT DELTA T	(DEG R)	698.4
CHAMBER/NOZL HEAT TRANSFER	(BTU/SEC)	901.0

FUEL SYSTEM CONDITIONS

STATION	PRESS (PSIA)	TEMP (DEG R)	FLOW (LB/SEC)	ENTHALPY (BTU/LB)	DENSITY (LB/FT3)
1 ENGINE INLET	70.0	38.0	0.404	-104.8	4.386
2 PUMP A INLET	70.0	42.5	2.081	-93.0	4.182
3 PUMP A EXIT	102.6	43.6	2.081	-89.4	4.157
4 FJBV INLET	102.6	43.6	0.000	-89.1	4.152
5 FJBV EXIT	102.6	43.6	0.000	-89.1	4.152
6 PUMP B INLET	102.5	43.9	0.594	-88.4	4.139
7 PUMP B EXIT	177.5	45.5	0.594	-82.2	4.122
8 PUMP C EXIT	251.3	47.1	0.531	-75.9	4.103
9 CHBR COOL IN	251.2	47.1	0.346	-75.9	4.103
10 INTERFACE	171.2	559.8	0.346	1877.2	0.057
11 NOZL COOL EX	157.5	745.5	0.345	2529.7	0.040
12 MTBV INLET	151.8	745.5	0.226	2529.7	0.038
24 MTBV EXIT	104.1	745.8	0.226	2529.7	0.026
13 O2 VOLUTE IN	151.8	745.5	0.119	2529.7	0.038
14 O2 TURB IN	151.6	590.4	0.146	1985.5	0.048
15 O2 TURB EX	142.5	478.3	0.180	1584.6	0.056
16 O2 VOLUTE EX	142.3	478.3	0.180	1584.6	0.056
17 FTBV INLET	141.2	478.3	0.000	1584.6	0.055
24 FTBV EXIT	104.1	478.3	0.000	1584.6	0.041
18 H2 VOLUTE IN	141.2	478.3	0.180	1584.6	0.055
19 H2 TURB A IN	141.0	404.8	0.222	1314.6	0.065
20 H2 TURB A EX	122.1	374.9	0.222	1201.8	0.061
21 H2 TURB B IN	122.1	374.9	0.242	1201.8	0.061
22 H2 TURB B EX	105.5	359.9	0.247	1143.9	0.055
23 H2 VOLUTE EX	105.2	359.9	0.247	1143.9	0.055
24 FTSV EXIT	104.1	540.0	0.247	1805.0	0.036
25 MIX. TURB IN	95.4	540.0	0.473	1805.0	0.033
5 MIX. FJBV IN	102.6	43.6	0.000	-89.1	4.152
26 MIXER EXIT	81.0	540.1	0.473	1805.0	0.028
27 FSOV INLET	81.0	540.1	0.473	1805.0	0.028
28 FSOV EXIT	80.0	540.1	0.473	1805.0	0.028
29 INJ MANIFOLD	77.5	540.1	0.473	1805.0	0.027
30 INJEC. INLET	75.8	540.1	0.473	1805.0	0.026
31 INJEC. FACE	64.9				

OXIDIZER SYSTEM CONDITIONS

STATION	PRESS (PSIA)	TEMP (DEG R)	FLOW (LB/SEC)	ENTHALPY (BTU/LB)	DENSITY (LB/FT3)
32 ENGINE INLET	70.0	161.8	1.695	61.2	71.38
33 PUMP INLET	70.0	161.9	1.851	61.3	71.35
34 PUMP EXIT	154.4	163.0	1.851	61.8	71.25
35 POSV INLET	154.4	163.0	1.676	61.8	71.25
36 POSV EXIT	86.3	163.2	1.676	61.8	71.14
37 SOCV INLET	154.4	163.0	0.000	61.8	71.25
38 SOCV EXIT	65.0	163.3	0.000	61.8	71.10
39 PRIM INJ MAN	86.3	163.2	1.676	61.8	71.14
40 SEC INJ MAN	65.0	163.3	0.000	61.8	71.10
41 PRIMARY INJ	85.2	163.2	1.676	61.8	71.14
42 SECONDARY INJ	65.0	163.3	0.000	61.8	71.10
43 INJECTOR FACE	65.0				

(Continued) *Table 37. Thrust = 1,000 Pounds, O/F = 3.5*

AETB ROCETS SIMULATION

THRUST=1000.LB INLET O/F=3.5

OPERATOR - S. CHESLA
CONFIGURATION - SPLIT
VERSION - AETBY4
PROCESS DATE - 1/15/91
PROCESS TIME - 9:46:17

* TURBOMACHINERY PERFORMANCE DATA *

		FUEL PUMP A	FUEL PUMP B		LOX PUMP
		1ST STAGE	1ST STAGE	2ND STAGE	
		*********	*********	*********	**********
EFFICIENCY		0.404	0.546	0.524	0.389
HORSEPOWER		11.	5.	5.	1.
TORQUE	(FT-LB)	2.9	1.2	1.1	0.9
SPEED	(RPM)	18921.	22275.	22275.	8241.
HEAD RISE	(FT)	1125.	2616.	2585.	171.
DIAMETER	(IN)	4.43	3.75	3.75	2.67
TIP SPEED	(FT/SEC)	366.	364.	364.	96.
VOLUMETRIC FLOW	(GPM)	225.	65.	58.	12.
HEAD COEFFICIENT		0.2704	0.6321	0.6258	0.5947
FLOW COEFFICIENT		0.1371	0.0532	0.0482	0.0337
SUCTION SS		1323.8			766.6

		FUEL TURBINES		LOX TURBINE
		TURBINE A	TURBINE B	
		*********	*********	*********
EFFICIENCY	(T/T)	0.638	0.611	0.562
HORSEPOWER TOTAL		11.3	11.1	4.1
HORSEPOWER PUMP		10.5	9.9	1.5
TORQUE	(FT-LB)	3.1	2.6	2.6
SPEED	(RPM)	18921.	22275.	8241.
MEAN DIAMETER	(IN)	3.85	3.85	6.75
MEAN TIP SPEED	(FT/SEC)	317.8	317.8	242.7
DELTA H (ACTUAL)	(BTU/LB)	36.0	32.3	19.8
DELTA H (IDEAL)	(BTU/LB)	56.4	52.9	35.3
U/C (IDEAL)		.1891	.2299	.1825
FLOW PARAMETER	(IN2)	.0316	.0383	.0234
PRES.RATIO	(T/T)	1.155	1.158	1.064
GAMMA		1.360	1 352	1.391

* VALVE DATA *

STATION		DELTA P PSIA	FLOW (LB/SEC)	BYPASS %	AREA (IN2)
JACKET BYPASS VALVE	(FJBV)	0.0	0.00	0.000	0.000
TURBINE BYPASS VALVE	(MTBV)	47.7	0.23	65.447	0.307
FUEL TURBINE BYPASS	(FTBV)	37.2	0.00	0.000	0.000
PRI SHUT OFF VALVE	(POSV)	68.1	1.676		0.036
SEC CONTROL VALVE	(SOCV)	89.4	0.000		0.000
FUEL SHUT OFF VALVE	(FSOV)	1.0	0.473		
FUEL TURBINE SHUTOFF	(FTSV)	0.3	0.247		
FUEL PUMP RECIRC.	(FRV)	32.6	1.597		

* INJECTOR ELEMENT DATA *

STATION	DELTA P PSIA	FLOW (LB/SEC)	AREA (IN2)
FUEL INJECTOR	10.9	0.473	1.435
PRIMARY LOX INJECTOR	20.3	1.676	0.066
SECONDARY LOX INJECTOR	0.1	0.000	0.528

* INTERNAL FLOWS *

		SOURCE STATION	SINK STATION	FLOW (LB/SEC)
********************************				
LOX IPS FLOW	(LO1)	34	AMB	0.019
LOX VAPORIZER RECIRC.	(LO2)	34	33	0.156
LH2 OT DISK COOLANT	(LH2)			
LH2A (LEAKAGE)		8	14	0.031
LH2B (IPS)		8	AMB	0.005
LH2 OT BEARING COOLANT	(LH3)	8	15	0.034
LH2 OT IPS	(LH4)	14	AMB	0.005
FT LH2 2ND BEARING COOL.	(LH5)			
LH5A (LEAKAGE)		8	19	0.012
LH5B (RECIRC)		8	3	0.049
FT LH2 SHROUD COOLANT	(LH6)			
LH6A (COOLANT)		8	19	0.030
LH6B (LEAKAGE)		8	20	0.002
LH6C (LEAKAGE)		8	20	0.003
LH6D (LEAKAGE)		8	22	0.003
FT LH2 DISK COOLANT	(LH7)	8	20	0.015
FT LH2 3RD BRG FLOW	(LH8)			
LH8A (LEAKAGE)		7	22	0.002
LH8B (RECIRC)		7	6	0.061

Table 38. Tank Head Idle Operating Point

AETB ROCETS SIMULATION

THRUST= 88. LB INLET O/F=3.5

OPERATOR	- S. CHESLA
CONFIGURATION	- THI
VERSION	- AETBY4
PROCESS DATE	- 1/16/91
PROCESS TIME	- 9:49:22

ENGINE PERFORMANCE

THRUST (VACUUM)	(LB)	88.
SPECIFIC IMPULSE (VACUUM)	(SEC)	467.77
TOTAL ENGINE INLET FLOW RATE	(LB/SEC)	0.19
MIXTURE RATIO - INLET		3.50

CHAMBER PERFORMANCE

INJECTOR FACE PRESSURE (TOTAL)	(PSIA)	5.7
THROAT PRESSURE (TOTAL)	(PSIA)	5.5
MIXTURE RATIO - CHAMBER		3.500
FLOW RATE (THROAT)	(LB/SEC)	0.19
THROAT AREA	(IN2)	8.377
NOZZLE AREA RATIO		1000.0
THEORETICAL CHAR. VELOCITY	(FT/SEC)	7884.9
CHAR. VELOCITY EFFICIENCY		1.000

ENGINE HEAT TRANSFER

CHAM ...ZL COOLANT DELTA P	(PSIA)	6.8
CHAMBER/NOZL COOLANT DELTA T	(DEG R)	662.0
CHAMBER/NOZL HEAT TRANSFER	(BTU/SEC)	103.0

* VALVE DATA *

STATION	DELTA P PSIA	FLOW (LB/SEC)	BYPASS %	AREA (IN2)
TURBINE BYPASS VALVE (MTBV)	1.6	0.04	100.000	0.969
PRI SHUT OFF VALVE (POSV)	3.2	0.146		0.036
FUEL SHUT OFF VALVE (FSOV)	0.1	0.042		
FUEL TURBINE SHUTOFF (FTSV)	1.6	0.000		

* INJECTOR ELEMENT DATA *

STATION	DELTA P PSIA	FLOW (LB/SEC)	AREA (IN2)
FUEL INJECTOR	1.3	0.042	1.435
PRIMARY LOX INJECTOR	7.1	0.146	0.066

FUEL SYSTEM CONDITIONS

STATION	PRESS (PSIA)	TEMP (DEG R)	FLOW (LB/SEC)	ENTHALPY (BTU/LB)	DENSITY (LB/FT3)
1 ENGINE INLET	19.0	37.6	0.042	-104.8	3.615
2 PUMP A INLET	19.0	37.6	0.042	-104.8	3.615
3 PUMP A EXIT	19.0	37.6	0.042	-104.8	3.615
4 FJBV INLET	19.0	37.6	0.000	-104.8	3.615
5 FJBV EXIT	7.5	699.6	0.000	2366.5	0.002
6 PUMP B INLET	19.0	37.6	0.042	-104.8	3.615
7 PUMP B EXIT	19.0	37.6	0.042	-104.8	3.615
8 PUMP C EXIT	19.0	37.6	0.042	-104.8	3.615
9 CHBR COOL IN	19.0	37.6	0.042	-104.8	3.614
10 INTERFACE	13.5	522.3	0.042	1740.4	0.005
11 NOZL COOL EX	12.5	699.6	0.042	2366.5	0.003
12 MTBV INLET	11.5	699.6	0.042	2366.5	0.003
24 MTBV EXIT	9.9	699.6	0.042	2366.5	0.003
24 FTBV EXIT	9.9	699.6	0.000	2366.5	0.003
28 MIX. TURB IN	9.0	699.6	0.042	2366.5	0.002
5 MIX. FJBV IN	7.8	37.6	0.000	-104.8	3.615
26 MIXER EXIT	7.5	699.6	0.042	2366.5	0.002
27 FBOV INLET	7.8	699.6	0.042	2366.5	0.002
28 FBOV EXIT	7.4	699.6	0.042	2366.5	0.002
29 INJ MANIFOLD	7.1	6 9.6	0.042	2366.5	0.002
30 INJEC. INLET	6.9	699.6	0.042	2366.5	0.002
31 INJEC. FACE	5.7				

OXIDIZER SYSTEM CONDITIONS

STATION	PRESS (PSIA)	TEMP (DEG R)	FLOW (LB/SEC)	ENTHALPY (BTU/LB)	DENSITY (LB/FT3)
32 ENGINE INLET	16.0	162.0	0.146	61.2	71.29
33 PUMP INLET	16.0	162.0	0.146	61.2	71.29
34 PUMP EXIT	16.0	162.0	0.146	61.2	71.29
35 POSV INLET	16.0	162.0	0.146	61.2	71.29
36 POSV EXIT	12.8	159.4	0.146	61.2	16.31
39 PRIM INJ MAN	12.8	159.4	0.146	61.2	16.31
41 PRIMARY INJ	12.8	159.4	0.146	61.2	16.09
43 INJECTOR FACE	5.7				

Table 39. Accelerometer Details

AETB ROCETS SIMULATION

THRUST=16419.LB INLET O/F=6.0

OPERATOR - S. CHESLA
CONFIGURATION - FULL
VERSION - AETBV4
PROCESS DATE - 1/18/91
PROCESS TIME - 17: 6:11

ENGINE PERFORMANCE

THRUST (VACUUM)	(LB)	16419.
THRUST (SEA LEVEL)	(LB)	12173.
SPECIFIC IMPULSE (VACUUM)	(SEC)	479.95
SPECIFIC IMPULSE (S.L. / AR=7.5)	(SEC)	355.83
TOTAL ENGINE INLET FLOW RATE	(LB/SEC)	34.54
MIXTURE RATIO - INLET		6.00

CHAMBER PERFORMANCE

INJECTOR FACE PRESSURE (TOTAL)	(PSIA)	980.6
THROAT PRESSURE (TOTAL)	(PSIA)	950.3
MIXTURE RATIO - CHAMBER		6.129
FLOW RATE (THROAT)	(LB/SEC)	34.21
THROAT AREA	(IN2)	8.577
NOZZLE AREA RATIO		1000.0
THEORETICAL CHAR. VELOCITY	(FT/SEC)	7539.6
CHAR. VELOCITY EFFICIENCY		0.993

ENGINE HEAT TRANSFER

CHAMBER/NOZL COOLANT DELTA P	(PSIA)	238.5
CHAMBER/NOZL COOLANT DELTA T	(DEG R)	531.4
CHAMBER/NOZL HEAT TRANSFER	(BTU/SEC)	8800.9

FUEL SYSTEM CONDITIONS

STATION	PRESS (PSIA)	TEMP (DEG R)	FLOW (LB/SEC)	ENTHALPY (BTU/LB)	DENSITY (LB/FT3)
1 ENGINE INLET	70.0	38.0	4.934	-104.8	4.386
2 PUMP A INLET	68.9	38.0	4.934	-104.8	4.385
3 PUMP A EXIT	1844.1	68.8	4.934	18.6	4.293
4 FJBV INLET	1844.1	68.8	0.000	22.0	4.257
5 FJBV EXIT	1844.1	68.8	0.000	22.0	4.257
6 PUMP B INLET	1837.9	69.1	5.139	22.6	4.247
7 PUMP B EXIT	2561.4	82.5	5.139	78.1	4.193
8 PUMP C EXIT	3301.1	95.7	4.940	133.4	4.180
9 CBV INLET	3284.6	95.8	1.676	133.4	4.171
9 CHBR COOL IN	3284.6	95.8	2.640	133.4	4.171
10 INTERFACE	3108.3	787.2	2.627	2633.8	0.703
11 NOZL COOL EX	3046.1	999.0	2.627	3404.8	0.533
11 CBV EXIT	3046.1	97.8	1.676	133.4	4.041
12 MTBV INLET	3003.7	627.4	1.138	2171.0	0.811
17 MTBV EXIT	2627.2	629.0	1.138	2171.0	0.717
13 O2 VOLUTE IN	3003.7	627.4	3.166	2171.0	0.811
14 O2 TURB IN	2997.9	617.8	3.128	2136.0	0.822
15 O2 TURB EX	2655.4	587.6	3.212	2019.5	0.769
16 O2 VOLUTE EX	2650.9	587.6	3.212	2019.5	0.768
17 OTBV INLET	2627.2	5.8.7	0.847	2059.1	0.750
24 OTBV EXIT	1266.8	605.6	0.847	2059.1	0.376
18 H2 VOLUTE IN	2627.2	598.7	3.502	2059.1	0.750
19 H2 TURB A IN	2620.6	576.7	3.676	1979.1	0.773
20 H2 TURB A EX	1848.8	525.4	3.676	1778.0	0.614
21 H2 TURB B IN	1848.8	525.4	3.777	1778.0	0.614
22 H2 TURB B EX	1306.8	468.4	3.938	1562.7	0.495
23 H2 VOLUTE EX	1299.1	468.5	3.938	1562.7	0.493
24 FTSV EXIT	1266.8	492.6	3.938	1650.6	0.458
25 MIX. TURB IN	1196.7	492.9	4.786	1650.6	0.434
26 MIXER EXIT	1084.4	493.3	4.786	1650.6	0.395
27 FSOV INLET	1084.4	493.3	4.786	1650.6	0.395
28 FSOV EXIT	1077.4	493.3	4.786	1650.6	0.392
29 INJ MANIFOLD	1059.5	493.3	4.786	1650.6	0.386
30 INJEC. INLET	1047.7	493.4	4.786	1650.6	0.382
31 INJEC. FACE	980.6				

OXIDIZER SYSTEM CONDITIONS

STATION	PRESS (PSIA)	TEMP (DEG R)	FLOW (LB/SEC)	ENTHALPY (BTU/LB)	DENSITY (LB/FT3)
32 ENGINE INLET	70.0	161.8	29.605	61.2	71.38
33 PUMP INLET	68.7	162.1	30.278	61.3	71.32
34 PUMP EXIT	1628.0	169.8	30.278	66.9	71.48
35 POSV INLET	1600.1	169.9	4.412	66.9	71.44
36 POSV EXIT	1129.5	171.8	4.412	66.9	70.69
37 SOCV INLET	1597.5	169.9	25.000	66.9	71.43
38 SOCV EXIT	1056.9	172.1	25.000	66.9	70.57
39 PRIM INJ MAN	1129.5	171.8	4.412	66.9	70.69
40 SEC INJ MAN	1054.3	172.1	25.000	66.9	70.57
41 PRIMARY INJ	1122.1	171.8	4.412	66.9	70.68
42 SECONDARY INJ	1051.7	172.1	25.000	66.9	70.56
43 INJECTOR FACE	980.6				

(Continued) Table 39. Accelerometer Details

AETB ROCETS SIMULATION

THRUST=16419.LB INLET O/F=6.0

OPERATOR - S. CHESLA
CONFIGURATION - FULL
VERSION - AETBY4
PROCESS DATE - 1/15/91
PROCESS TIME - 17: 6:11

* TURBOMACHINERY PERFORMANCE DATA *

		FUEL PUMP A	FUEL PUMP B		LOX PUMP
		1ST STAGE	1ST STAGE	2ND STAGE	
		*********	*********	*********	**********
EFFICIENCY		0.617	0.572	0.591	0.723
HORSEPOWER		861.	404.	387.	239.
TORQUE	(FT-LB)	50.3	24.9	23.9	32.8
SPEED	(RPM)	90000.	84994.	84994.	38314.
HEAD RISE	(FT)	59209.	24699.	25443.	3141.
DIAMETER	(IN)	4.43	3.75	3.75	2.67
TIP SPEED	(FT/SEC)	1740.	1391.	1391.	446.
VOLUMETRIC FLOW	(GPM)	516.	550.	530.	190.
HEAD COEFFICIENT		0.6290	0.4099	0.4231	0.5057
FLOW COEFFICIENT		0.0662	0.1186	0.1155	0.1182
SUCTION SS		7600.5			14662.9

		FUEL TURBINES		LOX TURBINE
		TURBINE A	TURBINE B	
		*********	*********	*********
EFFICIENCY	(T/T)	0.822	0.845	0.832
HORSEPOWER TOTAL		878.0	815.8	295.8
HORSEPOWER PUMP		861.1	790.3	239.3
TORQUE	(FT-LB)	51.2	50.4	40.5
SPEED	(RPM)	90000.	84994.	38314.
MEAN DIAMETER	(IN)	3.85	3.85	6.75
MEAN TIP SPEED	(FT/SEC)	1511.9	1511.9	1128.6
DELTA H (ACTUAL)	(BTU/LB)	168.8	152.6	66.8
DELTA H (IDEAL)	(BTU/LB)	205.4	180.7	80.4
U/C (IDEAL)		.4714	.4746	.5624
FLOW PARAMETER	(IN2)	.0337	.0468	.0259
PRES.RATIO	(T/T)	1.417	1.415	1.129
GAMMA		1.399	1.395	1.400

* VALVE DATA *

STATION		DELTA P PSIA	FLOW (LB/SEC)	BYPASS %	AREA (IN2)
JACKET BYPASS VALVE	(FJBV)	1.1	0.00	0.000	0.000
TURBINE BYPASS VALVE	(MTBV)	376.0	1.14	26.435	0.099
OX. TURBINE BYPASS	(OTBV)	1360.4	0.85	-9.029	0.056
PRI SHUT OFF VALVE	(POSV)	470.6	4.412		0.036
SEC CONTROL VALVE	(SOCV)	540.6	25.000		0.190
CHAMBER BYPASS VALVE	(CBV)	238.5	1.676		0.080
FUEL SHUT OFF VALVE	(FSOV)	7.0	4.786		
FUEL TURBINE SHUTOFF	(FTSV)	8.2	3.938		
FUEL PUMP RECIRC.	(FRV)	1775.2	0.000		

* INJECTOR ELEMENT DATA *

STATION	DELTA P PSIA	FLOW (LB/SEC)	AREA (IN2)
FUEL INJECTOR	67.0	4.786	1.435
PRIMARY LOX INJECTOR	141.5	4.412	0.066
SECONDARY LOX INJECTOR	71.1	25.000	0.528

* INTERNAL FLOWS *

		SOURCE STATION	SINK STATION	FLOW (LB/SEC)
LOX IPS FLOW	(LO1)	34	AMB	0.193
LOX VAPORIZER RECIRC.	(LO2)	34	33	0.672
LH2 OT DISK COOLANT	(LH2)			
LH2A (LEAKAGE)		8	14	0.055
LH2B (IPS)		8	AMB	0.043
LH2 OT BEARING COOLANT	(LH3)	8	15	0.084
LH2 OT IPS	(LH4)	14	AMB	0.093
FT LH2 2ND BEARING COOL.	(LH5)			
LH5A (LEAKAGE)		8	19	0.048
LH5B (RECIRC)		8	3	0.154
FT LH2 SHROUD COOLANT	(LH6)			
LH6A (COOLANT)		8	19	0.125
LH6B (LEAKAGE)		8	20	0.008
LH6C (LEAKAGE)		8	20	0.009
LH6D (LEAKAGE)		8	22	0.013
FT LH2 DISK COOLANT	(LH7)	8	20	0.085
FT LH2 3RD BRG FLOW	(LH8)			
LH8A (LEAKAGE)		7	22	0.148
LH8B (RECIRC)		7	6	0.051

Table 40. High Mixture Ratio Operating Point

AETB ROCETS SIMULATION

THRUST=17000.LB INLET O/F=12.

OPERATOR	- S. CHESLA
CONFIGURATION	- SPLIT
VERSION	- AETBY4
PROCESS DATE	- 1/15/91
PROCESS TIME	- 15:16:44

ENGINE PERFORMANCE

THRUST (VACUUM)	(LB)	17000.
THRUST (SEA LEVEL)	(LB)	12491.
SPECIFIC IMPULSE (VACUUM)	(SEC)	391.74
SPECIFIC IMPULSE (S.L. / AR=7.5)	(SEC)	287.85
TOTAL ENGINE INLET FLOW RATE	(LB/SEC)	43.67
MIXTURE RATIO - INLET		12.00

CHAMBER PERFORMANCE

INJECTOR FACE PRESSURE (TOTAL)	(PSIA)	1001.3
THROAT PRESSURE (TOTAL)	(PSIA)	970.4
MIXTURE RATIO - CHAMBER		12.318
FLOW RATE (THROAT)	(LB/SEC)	43.40
THROAT AREA	(IN2)	8.377
NOZZLE AREA RATIO		1000.0
THEORETICAL CHAR. VELOCITY	(FT/SEC)	6149.9
CHAR. VELOCITY EFFICIENCY		0.980

ENGINE HEAT TRANSFER

CHAMBER/NOZL COOLANT DELTA P	(PSIA)	272.3
CHAMBER/NOZL COOLANT DELTA T	(DEG R)	718.5
CHAMBER/NOZL HEAT TRANSFER	(BTU/SEC)	7536.9

FUEL SYSTEM CONDITIONS

STATION	PRESS (PSIA)	TEMP (DEG R)	FLOW (LB/SEC)	ENTHALPY (BTU/LB)	DENSITY (LB/FT3)
1 ENGINE INLET	70.0	38.0	3.360	-104.8	4.384
2 PUMP A INLET	69.5	38.0	3.360	-104.8	4.385
3 PUMP A EXIT	1484.5	66.3	3.360	3.2	4.195
4 FJBV INLET	1484.5	66.3	0.000	6.7	4.155
5 FJBV EXIT	1484.5	66.3	0.000	6.7	4.155
6 PUMP B INLET	1481.5	66.6	3.566	7.5	4.144
7 PUMP B EXIT	2070.4	76.7	3.566	50.1	4.136
8 PUMP C EXIT	2669.9	86.8	3.388	93.0	4.139
9 CHBR COOL IN	2663.0	86.8	2.799	93.0	4.135
10 INTERFACE	2461.7	614.2	2.799	2112.0	0.691
11 NOZL COOL EX	2390.7	805.4	2.785	2788.6	0.522
12 MTBV INLET	2362.7	805.8	0.287	2788.6	0.517
24 MTBV EXIT	1170.7	812.9	0.287	2788.6	0.262
13 O2 VOLUTE IN	2362.7	805.8	2.498	2788.6	0.517
14 O2 TURB IN	2357.0	788.9	2.489	2729.6	0.588
15 O2 TURB EX	2019.8	739.0	2.873	2548.6	0.483
16 O2 VOLUTE EX	2015.2	739.0	2.573	2545.5	0.482
17 FTBV INLET	1991.0	739.2	0.336	2545.5	0.477
24 FTBV EXIT	1170.7	744.0	0.336	2545.5	0.288
18 H2 VOLUTE IN	1991.0	739.2	2.237	2545.5	0.477
19 H2 TURB A IN	1986.7	693.9	2.410	2386.0	0.507
20 H2 TURB A EX	1510.5	635.8	2.410	2171.6	0.424
21 H2 TURB B IN	1510.5	635.8	2.500	2171.6	0.424
22 H2 TURB B EX	1194.2	577.3	2.621	1956.1	0.371
23 H2 VOLUTE EX	1189.7	577.3	2.621	1956.1	0.370
24 FTSV EXIT	1170.7	615.0	2.621	2090.9	0.344
25 MIX. TURB IN	1127.7	615.2	3.244	2090.9	0.332
5 MIX. FJBV IN	1484.5	66.3	0.000	6.7	4.155
26 MIXER EXIT	1060.2	615.6	3.244	2090.9	0.313
27 FSOV INLET	1060.2	615.6	3.244	2090.9	0.313
28 FSOV EXIT	1056.1	615.6	3.244	2090.9	0.311
29 INJ MANIFOLD	1045.7	615.6	3.244	2090.9	0.308
30 INJEC. INLET	1038.9	615.7	3.244	2090.9	0.306
31 INJEC. FACE	1001.3				

OXIDIZER SYSTEM CONDITIONS

STATION	PRESS (PSIA)	TEMP (DEG R)	FLOW (LB/SEC)	ENTHALPY (BTU/LB)	DENSITY (LB/FT3)
32 ENGINE INLET	70.0	161.8	40.315	61.2	71.38
33 PUMP INLET	67.6	162.0	40.959	61.3	71.34
34 PUMP EXIT	1497.6	169.1	40.959	66.5	71.46
35 POSV INLET	1445.8	169.3	3.737	66.5	71.38
36 POSV EXIT	1107.9	170.7	3.737	66.5	70.84
37 SOCV INLET	1440.3	169.4	36.400	66.5	71.37
38 SOCV EXIT	1162.3	170.5	36.400	66.5	70.93
39 PRIM INJ MAN	1107.9	170.7	3.737	66.5	70.84
40 SEC INJ MAN	1156.8	170.5	36.400	66.5	70.92
41 PRIMARY INJ	1102.6	170.7	3.737	66.5	70.84
42 SECONDARY INJ	1151.3	170.5	36.400	66.5	70.91
43 INJECTOR FACE	1001.3				

(Continued) Table 40. High Mixture Ratio Operating Point

AETB ROCETS SIMULATION

THRUST=17000.LB INLET O/F=12.

CONFIGURATION - SPLIT
VERSION - AETBY4
PROCESS DATE - 1/15/91
PROCESS TIME - 15:16:44

* TURBOMACHINERY PERFORMANCE DATA *

		FUEL PUMP A	FUEL PUMP B		LOX PUMP
		1ST STAGE	1ST STAGE	2ND STAGE	
		*********	*********	*********	**********
EFFICIENCY		0.571	0.618	0.626	0.716
HORSEPOWER		513.	215.	205.	300.
TORQUE	(FT-LB)	34.0	16.0	15.3	39.2
SPEED	(RPM)	79179.	70346.	70346.	40151.
HEAD RISE	(FT)	47983.	20486.	20865.	2881.
DIAMETER	(IN)	4.43	3.75	3.75	2.67
TIP SPEED	(FT/SEC)	1530.	1151.	1151.	468.
VOLUMETRIC FLOW	(GPM)	359.	387.	367.	257.
HEAD COEFFICIENT		0.6586	0.4963	0.5065	0.4224
FLOW COEFFICIENT		0.0524	0.1008	0.0967	0.1526
SUCTION SS		5536.7			18102.9

		FUEL TURBINES		LOX TURBINE
		TURBINE A	TURBINE B	
		*********	*********	*********
EFFICIENCY	(T/T)	0.816	0.831	0.802
HORSEPOWER TOTAL		526.2	440.0	361.6
HORSEPOWER PUMP		513.2	420.3	299.6
TORQUE	(FT-LB)	34.9	32.9	47.3
SPEED	(RPM)	79179.	70346.	40151.
MEAN DIAMETER	(IN)	3.85	3.85	6.75
MEAN TIP SPEED	(FT/SEC)	1330.1	1330.1	1182.5
DELTA H (ACTUAL)	(BTU/LB)	154.3	124.4	102.7
DELTA H (IDEAL)	(BTU/LB)	189.0	149.7	128.1
U/C (IDEAL)		.4322	.4315	.4669
FLOW PARAMETER	(IN2)	.0320	.0417	.0297
PRES.RATIO	(T/T)	1.315	1.265	1.167
GAMMA		1.398	1.398	1.398

* VALVE DATA *

STATION		DELTA P PSIA	FLOW (LB/SEC)	BYPASS %	AREA (IN2)
JACKET BYPASS VALVE	(FJBV)	0.5	0.00	0.000	0.000
TURBINE BYPASS VALVE	(MTBV)	1192.0	0.29	10.315	0.025
FUEL TURBINE BYPASS	(FTBV)	820.3	0.34	13.075	0.033
PRI SHUT OFF VALVE	(POSV)	337.8	3.737		0.036
SEC CONTROL VALVE	(SOCV)	278.0	36.400		0.387
FUEL SHUT OFF VALVE	(FSOV)	4.1	3.244		
FUEL TURBINE SHUTOFF	(FTSV)	4.8	2.621		
FUEL PUMP RECIRC.	(FRV)	1415.0	0.000		

* INJECTOR ELEMENT DATA *

STATION	DELTA P PSIA	FLOW (LB/SEC)	AREA (IN2)
FUEL INJECTOR	37.6	3.244	1.435
PRIMARY LOX INJECTOR	101.3	3.737	0.066
SECONDARY LOX INJECTOR	150.0	36.400	0.528

* INTERNAL FLOWS *

		SOURCE STATION	SINK STATION	FLOW (LB/SEC)
LOX IPS FLOW	(LO1)	34	AMB	0.178
LOX VAPORIZER RECIRC.	(LO2)	34	33	0.644
LH2 OT DISK COOLANT	(LH2)			
LH2A (LEAKAGE)		8	14	0.056
LH2B (IPS)		8	AMB	0.036
LH2 OT BEARING COOLANT	(LH3)	8	15	0.084
LH2 OT IPS	(LH4)	14	AMB	0.065
FT LH2 2ND BEARING COOL.	(LH5)			
LH5A (LEAKAGE)		8	19	0.048
LH5B (RECIRC)		8	3	0.138
FT LH2 SHROUD COOLANT	(LH6)			
LH6A (COOLANT)		8	19	0.125
LH6B (LEAKAGE)		8	20	0.007
LH6C (LEAKAGE)		8	20	0.008
LH6D (LEAKAGE)		8	22	0.011
FT LH2 DISK COOLANT	(LH7)	8	20	0.075
FT LH2 3RD BRG FLOW	(LH8)			
LH8A (LEAKAGE)		7	22	0.110
LH8B (RECIRC)		7	6	0.068

NASA
National Aeronautics and Space Administration

Report Documentation Page

1. Report No. CR-187081	2. Government Accession No.	3. Recipient's Catalog No.
4. Title and Subtitle ADVANCED EXPANDER TEST BED ENGINE Preliminary Design Report		5. Report Date May 1991
		6. Performing Organization Code
7. Author(s) A. I. Masters, J. C. Mitchell, et. al.		8. Performing Organization Report No. FR- 21329
		10. Work Unit No. 593-12-41
9. Performing Organization Name and Address Pratt & Whitney P. O. Box 109600 West Palm Beach, FL 33410-9600		11. Contract or Grant No. NAS3-25960
12. Sponsoring Agency Name and Address NASA Lewis Research Center 21000 Brookpark Road Cleveland, OH 44135		13. Type of Report and Period Covered Preliminary Design 27 April, '90 - 31 Jan. '91
		14. Sponsoring Agency Code

15. Supplementary Notes

Program Manager: W. K. Tabata

16. Abstract

The Advanced Expander Test Bed (AETB) is a key element in NASA's Space Chemical Engine Technology Program for development and demonstration of expander cycle oxygen/hydrogen engine technology and component technology for the next space engine. The AETB will be used to validate the high-pressure expander cycle concept, investigate system interactions, and conduct investigations of advanced mission focused components and new health monitoring techniques. The split-expander cycle AETB will operate at combustion chamber pressures up to 1200 psia with propellant flow rates equivalent to 20,000 lbf vacuum thrust.

Work under the contract began 27 April 1990. Effort during Preliminary Design focused on: (1) definition of the key methodologies to be applied to the test bed design and to be verified as part of the AETB program, (2) development of transient and steady state AETB models, and (3) preparation of the AETB preliminary design of major components and systems.

17. Key Words (Suggested by Author(s)) Space Propulsion, Expander Cycle Engines, Oxygen/Hydrogen Engines, Liquid Propellant Rockets, Rocket Design, Rocket Test Run	18. Distribution Statement General Release

19. Security Classif. (of this report) Unclassified	20. Security Classif. (of this page) Unclassified	21. No of pages 301	22. Price*

NASA FORM 1626 OCT 86

*For sale by the National Technical Information Service, Springfield, Virginia 22161